frontiers | Research Topics

New progress of nutritional immunity on aquatic animals by functional feed additives under the condition of low fish meal

Edited by
Hongyu Liu, Samad Rahimnejad and Qun Zhao

Published in
Frontiers in Immunology
Frontiers in Nutrition

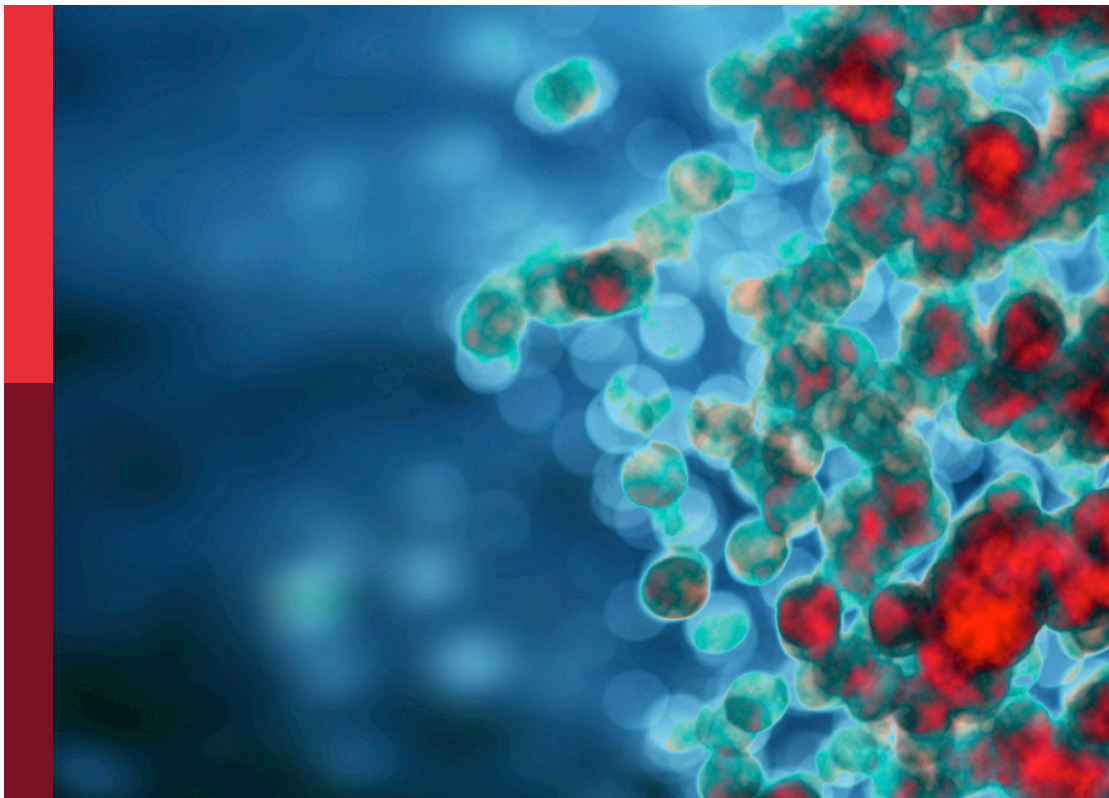

ISSN 1664-8714
ISBN 978-2-8325-6469-1
DOI 10.3389/978-2-8325-6469-1

About Frontiers

Frontiers is more than just an open access publisher of scholarly articles: it is a pioneering approach to the world of academia, radically improving the way scholarly research is managed. The grand vision of Frontiers is a world where all people have an equal opportunity to seek, share and generate knowledge. Frontiers provides immediate and permanent online open access to all its publications, but this alone is not enough to realize our grand goals.

Frontiers journal series

The Frontiers journal series is a multi-tier and interdisciplinary set of open-access, online journals, promising a paradigm shift from the current review, selection and dissemination processes in academic publishing. All Frontiers journals are driven by researchers for researchers; therefore, they constitute a service to the scholarly community. At the same time, the *Frontiers journal series* operates on a revolutionary invention, the tiered publishing system, initially addressing specific communities of scholars, and gradually climbing up to broader public understanding, thus serving the interests of the lay society, too.

Dedication to quality

Each Frontiers article is a landmark of the highest quality, thanks to genuinely collaborative interactions between authors and review editors, who include some of the world's best academicians. Research must be certified by peers before entering a stream of knowledge that may eventually reach the public - and shape society; therefore, Frontiers only applies the most rigorous and unbiased reviews. Frontiers revolutionizes research publishing by freely delivering the most outstanding research, evaluated with no bias from both the academic and social point of view. By applying the most advanced information technologies, Frontiers is catapulting scholarly publishing into a new generation.

What are Frontiers Research Topics?

Frontiers Research Topics are very popular trademarks of the *Frontiers journals series*: they are collections of at least ten articles, all centered on a particular subject. With their unique mix of varied contributions from Original Research to Review Articles, Frontiers Research Topics unify the most influential researchers, the latest key findings and historical advances in a hot research area.

Find out more on how to host your own Frontiers Research Topic or contribute to one as an author by contacting the Frontiers editorial office: frontiersin.org/about/contact

New progress of nutritional immunity on aquatic animals by functional feed additives under the condition of low fish meal

Topic editors

Hongyu Liu — Guangdong Ocean University, China
Samad Rahimnejad — University of Murcia, Spain
Qun Zhao — Hainan University, China

Citation

Liu, H., Rahimnejad, S., Zhao, Q., eds. (2025). *New progress of nutritional immunity on aquatic animals by functional feed additives under the condition of low fish meal*. Lausanne: Frontiers Media SA. doi: 10.3389/978-2-8325-6469-1

Table of contents

frontiers | Frontiers in Animal Science

TYPE Original Research
PUBLISHED 13 November 2023
DOI 10.3389/fanim.2023.1281722

OPEN ACCESS

EDITED BY
Samad Rahimnejad,
University of Murcia, Spain

REVIEWED BY
Heba Mahboub,
Zagazig University, Egypt
Mansour Torfi Mozanzadeh,
South Iran Aquaculture Research Center, Iran

*CORRESPONDENCE
Darci Carlos Fornari
darci.peixegen@gmail.com
D. Allen Davis
davisda@auburn.edu

RECEIVED 04 September 2023
ACCEPTED 26 October 2023
PUBLISHED 13 November 2023

CITATION
Fornari DC, Peixoto S, Ksepka SP, Bullard SA, Rossi W, Nuzback DE and Davis DA (2023) Effects of dietary mycotoxins and mycotoxin adsorbent additives on production performance, hematological parameters, and liver histology in juvenile Nile tilapia (*Oreochromis niloticus*). *Front. Anim. Sci.* 4:1281722. doi: 10.3389/fanim.2023.1281722

Effects of dietary mycotoxins and mycotoxin adsorbent additives on production performance, hematological parameters, and liver histology in juvenile Nile tilapia (*Oreochromis niloticus*)

Darci Carlos Fornari[1,2*], Silvio Peixoto[2,3], Steven P. Ksepka[4], Stephen A. Bullard[4], Waldemar Rossi[5], Dennis E. Nuzback[6] and D. Allen Davis[2*]

[1]AQUAM, Animal Science Research Program, Federal University of Rio Grande do Sul – UFRGS, Porto Alegre, RS, Brazil, [2]School of Fisheries, Aquaculture, and Aquatic Science, Auburn University, Auburn, AL, United States, [3]Department of Fisheries and Aquaculture, Federal Rural University of Pernambuco, Recife, PE, Brazil, [4]Southeastern Cooperative Fish Parasite and Disease Laboratory, School of Fisheries, Aquaculture and Aquatic Sciences, College of Agriculture, Auburn University, Auburn, AL, United States, [5]School of Aquaculture and Aquatic Sciences, College of Agriculture, Community, and the Sciences, Kentucky State University, Frankfort, KY, United States, [6]Phibro Animal Health Corporation, Teaneck, NJ, United States

Mycotoxins are fungal secondary metabolites that can adversely affect animals consuming contaminated feeds. This 71-day feeding trial was conducted to assess the effects of dietary deoxynivalenol plus zearalenone (DON+ZEN = 1.6 + 0.3 ppm), and fumonisins (FUM = 15 ppm), and three adsorbent additives on the production performance, hematological parameters, and liver histology of juvenile Nile tilapia. A mycotoxin-free diet (Control) formulated to contain 35% protein and 8% lipid was spiked with either DON+ZEN or FUM using contaminated corn meals replacing portions of non-spiked corn. Subsequently, three out of four DON+ZEN- and FUM-spiked diets were supplemented (0.5%) with an adsorbent. The research was carried out in a recirculating water system (2,500 L) with a controlled temperature of (25.9 $\pm$ 1.1°C), feeding was carried out twice a day at rates ranging from 5 to 8%. The experiment included nine treatments with five replications, each experimental unit consisting of an aquarium with a useful volume of 75-L and fifteen juvenile Nile tilapia (average initial weight of 4.0 $\pm$ 0.1 g). Mycotoxin-spiked diets without added adsorbent supported lower final biomass and survival of Nile tilapia relative to control and adsorbent containing diets ($P \leq 0.05$). Histological examinations revealed liver inflammation evidenced by lymphocytic infiltration adjacent to pancreatic tissue in fish fed mycotoxin-spiked diets without added adsorbent. Mycotoxin contamination significantly increased HSI (hepato somatic index), which was reverted to the Control value or reduced further by adsorbent addition. Lowest and intermediate hematocrit values were observed in groups

fed mycotoxin-spiked diets without and with added adsorbents, respectively. Our results reinforce the importance of using adsorbents and the need to investigate the effect of sub-lethal concentrations of mycotoxins in aquaculture feeds.

KEYWORDS

fumonisins, deoxynivalenol, zearalenone, adsorbents, productive performance

Introduction

Diet influences the behavior, health, physiological functions, reproduction, and growth of aquatic organisms (National Research Council (NRC), 2011). While maintaining the quality of raw materials and feeds from point of origin to end use is a complex task (Patriarca and Pinto, 2017; Nogueira et al., 2020; Taroncher et al., 2021), evidences of mycotoxin contamination of feedstuffs and aquaculture feeds in recent years have been alarming, drawing increased attention worldwide (Anater et al., 2016; Gonçalves et al., 2020; Oliveira and Vasconcelos, 2020; Bashorun et al., 2023). Heightened concerns over mycotoxin contamination of feed (and food) have coincided with climate changes including higher temperatures, which are expected to favor growth of mycotoxigenic fungi leading to increased contamination of crops (both before harvest and during storage) and finished feeds (Paterson and Lima, 2010; Battilani et al., 2016; Bashorun et al., 2023).

Mycotoxins are toxic secondary metabolites produced by a diversity of fungi that contaminate agricultural crops and feeds (Zychowski et al., 2013; Marroquín-Cardona et al., 2014; Guan et al., 2023). The mycotoxin-producing fungi Aspergillus, Penicillium and Fusarium produce fumonisins (FUM), deoxynivalenol (DON), zearalenone (ZEN) and aflatoxins (AFL), all mycotoxins that are common in aquaculture feeds and that represent the greatest risks for aquaculture (Anater et al., 2016; Nogueira et al., 2020; Taroncher et al., 2021). Research reports on these mycotoxins highlight reduction of protein synthesis, modification of lipid metabolism and mitochondrial activity, and due weakening of the immune system in orally exposed animals (Wang et al., 1991; Döll et al., 2010; Tola et al., 2015; Patriarca and Pinto, 2017; Abdel-Tawwab et al., 2020; Zahran et al., 2020; Ahmed et al., 2022; Smaoui et al., 2023).

Efforts to control feed-driven mycotoxicosis in animals include management strategies that begin before crop establishment and extend to rigorous testing for mycotoxins in feed mills and adoption of mycotoxin mitigation additives for use in feeds (Boudergue et al., 2009; Zhu et al., 2016; Ahmed et al., 2022). Some of the most widely used additives for mycotoxin detoxification of feeds consist of adsorbents based on clays, micronized yeast, plant fibers, and polymers, which alleviate adverse effects of ingested mycotoxins by preventing absorption into blood and organs by complexation. One common adsorbent is bentonite, a clay with a wide variety of industrial uses (Chestnut et al., 1992; Avantaggiato et al., 2005; Hussain et al., 2017). The use of clays is a viable technical and economical solution, as they are abundantly available and can be obtained at reasonable costs. There is considerable interest in validating the efficacy of these products in aquaculture feeds, as well as evaluating the effect of different mycotoxin types on fish health (Nogueira et al., 2020; Oliveira and Vasconcelos, 2020; Smaoui et al., 2023).

In general, warm-water fish are considered more tolerant to dietary mycotoxins than cold-water counterparts, notably rainbow trout (Halver and Goldblatt, 1969; Hooft et al., 2019; Koletsi et al., 2023). However, herbivorous and omnivorous warm water fish are likely more exposed to dietary mycotoxins because are fed diets with higher levels of plant-based ingredients, especially cereal-grain by-products that usually contain higher levels of mycotoxins. In addition, species produced in tropical regions might have higher risks of exposure to mycotoxin contaminated feeds given the more suitable environmental conditions for fungal growth. Tilapia (*Oreochromis* spp.), particularly the Nile tilapia (*O. niloticus*), is one of such species largely produced in tropical and temperate regions.

Although Nile tilapia is a hardy fish in many aspects including tolerance to mycotoxins, dietary concentrations of DON/ZEN (< 0.1 to ~ 1 ppm each; Tola et al., 2015) and FUM (40 - 150 ppm; Tuan et al., 2003) have been found to adversely affect growth performance of juvenile fish. Therefore, considering the need for additional information on the potentially harmful effects of dietary mycotoxins on chronically exposed fish, the objectives of this study were to evaluate the responses of juvenile Nile tilapia to practical diets spiked with DON + ZEN or FUM and the potential beneficial effects of mycotoxin adsorbent additives.

Materials and methods

This study followed a completely randomized design including nine dietary treatments with five replicates each (Table 1). Mycotoxin-contaminated corn and mycotoxin adsorbents were sourced from Phibro Animal Health Corporation, Teaneck, NJ, USA.

TABLE 1 Outline of the nine-treatment experimental design evaluating dietary deoxynivalenol + zearalenone (DON+ZEN), fumonisins (FUM), and absorbents AA, AB, and AC.

Diet (Treatment)	Mycotoxin and absorbent combination
1 (Control)	Non-spiked, adsorbent unsupplemented (local corn)
	Corn with DON+ZEN (DZ)
2 (DZ)	DON 1.5ppm + ZEN 0.3 ppm without absorbent
3 (DZ+AA)	DON 1.5 ppm + ZEN 0.3 ppm + 0.5% Adsorbent AA
4 (DZ+AB)	DON 1.5 ppm + ZEN 0.3 ppm + 0.5% Adsorbent AB
5 (DZ+AC)	DON 1.5 ppm + ZEN 0.3 ppm + 0.5% Adsorbent AC
	Corn with FUM (F)
6 (F)	FUM 15 ppm without absorbent
7 (F+AA)	FUM 15ppm + 0.5% Adsorbent AA
8 (F+AB)	FUM 15ppm + 0.5% Adsorbent AB
9 (F+AC)	FUM 15 ppm + 0.5% Adsorbent AC

Experimental diets

All experimental diets were formulated to contain 35% crude protein and 8% lipids and meet the nutritional requirements of Nile tilapia (National Research Council (NRC), 2011; Table 2). Two batches of corn contaminated with mycotoxins were used, one spiked with deoxynivalenol and zearalenone (DON+ZEN; DZ), and another with fumonisins (FUM; F). Inclusion of the contaminated corn in the experimental diets was performed by replacing a portion or the entirety of a locally sourced, non-spiked corn in the overall control (Control) diet. Three different types of commercial adsorbents (designated as adsorbent A (AA), adsorbent B (AB) and adsorbent C (AC)) were evaluated. AA and AB were sodium bentonites containing hydrated calcium aluminosilicates mined from two different locations, while AC consisted of a proprietary blend of adsorbent AB with Saccharomyces cerevisiae beer yeast. Inclusion of mycotoxins and adsorbents in the Control diet originated eight test diets (Table 2): two adsorbent unsupplemented and mycotoxin-contaminated control diets (DZ = 1.5 ppm of DON + 0.3 ppm of ZEN; and F = 15 ppm of FUM), each supplemented with one of the adsorbents evaluated (DZ +AA, AB, or AC; F+AA, AB, or AC). The inclusion levels of DON +ZEN and FUM in the experimental diets were based on reported sub-lethal concentrations for Nile tilapia juveniles (Tuan et al., 2003; Oliveira and Vasconcelos, 2020, respectively), while the adsorbents were included following the manufacturer's recommended levels.

All diets were prepared at the Auburn University E.W. Shell Fisheries Center, Auburn, AL, USA where the research was conducted. In short, pre-ground dry ingredients and oil were weighed and then mixed in a food mixer (Hobart Corporation, Troy, OH, USA) for 15 min. Hot water was added while mixing for the diet to attain a consistency appropriate for pelleting. Each diet was screw pressed through a 3-mm die plate. After pelleting, diets were dried using standard procedures to a moisture content of <10% and stored at 4 °C until fed.

Levels of mycotoxins in the finished diets (Table 3) were analyzed using liquid chromatography-mass spectrometry (LC/MS) and/or liquid chromatography coupled to sequential mass spectrometry LC/MS/MS following AOAC 2008.02 (Midwest Laboratories in Omaha, Nebraska). As expected, concentrations of DON (1.6 ppm) and ZEN (0.289 to 0.347 ppm) in the DZ diets and of FUM in the F diets were close to the target levels. Trace amounts of DON, FUM, ochratoxin, and ZEN were detected in the Control diet, while AFL was detected in DZ and F diets and FUM in all DZ diets. This was also expected since trace amounts of mycotoxins are usually present in ingredients (specially cereal-grains) used in practical formulations (Tola et al., 2015; Hooft and Bureau, 2017). However, these levels were much lower than those generally considered as safe for farmed animals, including fish (Tuan et al., 2002; Manning et al., 2003; Tuan et al., 2003; Hooft et al., 2019), making potential influences on the responses of the Nile tilapia to the Control and mycotoxin-spiked diets in this study very unlikely.

Fish and rearing conditions

Sex-reversed Nile tilapia were acquired from Spring Genetics, Miami, FL, USA. Following conditioning to local conditions, groups of fifteen tilapia juveniles (mean initial weight 4.0 ± 0.1 g) were stocked into forty-four 75-L aquaria connected to a 2,500-L indoor recirculating system. Rearing water temperature and dissolved oxygen were monitored daily. Water temperature (mean ± standard deviation = 25.9 ± 1.1 oC) was maintained using a submerged 3,600-W heater (Aquatic Eco-Systems Inc., Apopka, FL, USA). An airline connected to a central regenerative blower was used to maintain the dissolved oxygen near saturation (5.94 ± 1.09 mg/L) using air stones in each aquarium and sump tank. The pH (7.93 ± 0.58), total ammonia nitrogen (TAN; 0.089 ± 0.105 mg/L) and nitrite nitrogen (0.063 ± 0.087 mg/L) were measured twice per week and also maintained within optimum ranges for Nile tilapia. Timer-controlled photoperiod was set at 14 h light and 10 h dark. To prevent potential buildups of mycotoxins in the recirculating water, filter backwashes and water exchanges were performed on a regular basis.

During the experimental period (71 days), fish in each aquarium were fed one of the randomly assigned experimental diets twice daily at fixed rates ranging from 5 to 8% of body weight/day. Daily rations were adjusted every 15 days by group weighing fish in each aquarium. The glass aquaria allowed feeding activity to be monitored at each feeding, and no leftover feed was observed during the experimental period.

Sampling and data acquisition

Production performance metrics

At the end of the growth trial all fish from each aquarium were counted and group weighed after an overnight fasting to determine biomass gain, weight gain, survival, and feed conversion ratio using the following equations:

10.3389/fanim.2023.1281722

TABLE 2 Formulations of the experimental diets (g/100g as is).

		DON 1.5 ppm + ZEN 0.3 ppm				FUM 15 ppm			
	Control	DZ	DZ+AA	DZ+AB	DZ+AC	F	F +AA	F +AB	F +AC
Poultry by-product meal	6.00	6.00	6.00	6.00	6.00	6.00	6.00	6.00	6.00
Soybean meal	56.40	56.40	56.40	56.40	56.40	56.4	56.4	56.4	56.4
Menhaden fish oil	2.57	2.57	2.57	2.57	2.57	2.57	2.57	2.57	2.57
Local corn	31.00	26.04	26.04	26.04	26.04	–	–	–	–
Corn (DON+ZEN)[a]	–	4.96	4.96	4.96	4.96	–	–	–	–
Corn (FUM)[a]	–	–	–	–	–	31.0	31.0	31.0	31.0
Corn Starch	0.23	0.23	0.08	0.08	0.08	0.23	0.08	0.08	0.08
Mineral premix[b]	0.50	0.50	0.50	0.50	0.50	0.50	0.50	0.50	0.50
Vitamin premix[c]	0.80	0.80	0.80	0.80	0.80	0.80	0.80	0.80	0.80
Choline chloride	0.20	0.20	0.20	0.20	0.20	0.20	0.20	0.20	0.20
$CaPO_4$, dibasic	0.10	0.10	0.10	0.10	0.10	0.10	0.10	0.10	0.10
Rovimix Stay-C 35%	1.85	1.85	1.85	1.85	1.85	1.85	1.85	1.85	1.85
Adsorbent A[a]	–	–	0.50	–	–	–	0.50	–	–
Adsorbent B[a]	–	–	–	0.50	–	–	–	0.50	–
Adsorbent C[a]	–	–	–	–	0.50	–	–	–	0.50
Cellulose	0.35	0.35	–	–	–	0.35	–	–	–

Dashes indicate no inclusion of an ingredient.
[a]Sourced from Phibro Animal Health Corporation, Teaneck, NJ, USA.
[b]Trace mineral (g/100g premix): Cobalt chloride, 0.004; Cupric sulfate pentahydrate, 0.250; Ferrous sulfate, 4.000; Magnesium sulfate anhydrous, 13.862; Manganous sulfate monohydrate, 0.650; Potassium iodide, 0.067; Sodium selenite, 0.010; Zinc sulfate heptahydrate, 13.193; Alpha-cellulose, 67.964.
[c]Vitamin (g/kg premix): Thiamin HCl, 0.44; Riboflavin, 0.63; Pyridoxine HCl, 0.91; DL pantothenic acid, 1.72; Nicotinic acid, 4.58; Biotin, 0.21; Folic acid, 0.55; Inositol, 21.05; Menadione sodium bisulfite, 0.89; Vitamin A acetate, 0.68; Vitamin D_3, 0.12; DL alpha-tocopherol acetate, 12.63; Alpha-cellulose, 955.59.
DON - deoxynivalenol; ZEN – zearalenone; FUM - fumonisins;

TABLE 3 Analyzed mycotoxin concentration (ppm) of the experimental diets.

Treatment	DON	ZEN	FUM	AFL	OTA
Control	0.2	0.053	1.0	n.d.	0.0029
DON+ZEN (DZ)					
DZ	1.6	0.347	1.2	0.0186	n.d.
DZ+AA	1.6	0.318	1.0	0.0138	n.d.
DZ+AB	1.6	0.289	1.1	n.d.	n.d.
DZ+AC	1.6	0.321	1.0	n.d.	n.d.
FUM (F)					
F	n.d.	n.d.	16.0	n.d.	n.d.
F+AA	n.d.	n.d.	15.9	0.003	n.d.
F+AB	n.d.	n.d.	14.9	0.003	n.d.
F+AC	n.d.	n.d.	15.7	0.003	n.d.

DON, deoxynivalenol; ZEN, zearalenone; FUM, fumonisins; AFL, aflatoxin; OTA, ochratoxin;. n.d., not detected.

Biomass gain (g) = final fish biomass – initial fish biomas;

Weight gain (%) = [(final body weight – initial body weight)/(initial body weight)] × 100;

Survival (%) = final population/initial population × 100;

Feed conversion ratio (FCR) = feed fed/weight gain.

Additionally, four fish per aquarium were randomly sampled and sedated using 100 ppm buffered tricaine methanesulfonate (MS-222) for the collection of blood, and determination of length and weight of each fish. After this procedure, fish were euthanized and their livers dissected and weighed. The liver weight was used to compute hepatosomatic index (HSI) as follows:

HSI (%) = [liver weight/body weight] × 100.

Hematological analyses

Blood from four fish per aquarium was drawn from the caudal vasculature using 1-mL syringes with 21-gauge needles, then aliquoted into two 3-mL microtubes. The first aliquot was collected with 10% EDTA anticoagulant to measure hematocrit, as described by Reitman and Frankel (1957). The second aliquot, without anticoagulant, was centrifuged at 3,000 × g for 10 min and the serum was collected into 1.5 mL microtubes and stored at -80°C pending the following analyses performed using a VetScan Diagnostic Profile II (Abaxis, Inc., Union City, CA): alkaline phosphatase (ALP); alanine aminotransferase (ALT); bile acids (BA); total bilirubin (TBIL); albumin (ALB); urea nitrogen (BUN), and cholesterol (CHOL).

Liver histology

The intact liver of one fish per aquarium was excised immediately after spinal severance. After fixation in 10% neutral buffered formalin for 48 h, the dissected livers were transferred to 70% ethanol until processed for histological examination. A 0.5 cm long portion of liver tissue was cut from each sample to fit into tissue processing cassettes, yielding 44 portions of tissue that were rinsed in distilled water for 2 h, dehydrated in an ethanol, sectioned at 4 μm, and stained with Gill's 2 hematoxylin and eosin (Luna, 1968). Ten slides with approximately 20 sections per slide were cut from each block, yielding >8,800 sections on 440 slides. Five slides per block were evaluated for pathology. Slides were evaluated by comparing histological features of the treatment groups to that of the Control diet-fed groups.

Statistical analysis

Due to discrepant production performance relative to the other four replicates, data from one replicate each of treatments DZ+AA and DZ+AB were flagged as outliers and were excluded from the analyzed data. All remaining data were subjected to an one-way ANOVA. When significant ($P < 0.05$) treatment effects were detected, the Student-Newman-Keuls multiple comparison test was used to identify differences among treatment means. All statistical analyses were conducted using the Statistical Analysis System for windows (SAS Institute, Cary, NC).

Results

Production performance

There were significant differences for biomass gain, percentage survival and HSI among fish in different dietary treatments (Table 4). Survival and biomass gain significantly decreased in fish fed the DZ diet when compared to the Control-fed fish. Addition of the adsorbents AA, AB and AC to DZ supported biomass gain and survival similar to the Control-fed fish ($P > 0.05$). Feeding the DZ diet significantly increased HSI of Nile tilapia relative to Control-fed fish, whereas a significant reduction in HSI was observed when adsorbent AC was included in the DZ diet. Inclusion of FUM in the F diet significantly reduced biomass gain and survival of the Nile tilapia relative to Control-fed groups, whereas addition of the adsorbents AB and AC, or all absorbents to the F diet supported biomass gain and survival similar to Control-fed groups, respectively ($P > 0.05$). The HSI of tilapia fed the F+AC diet was significantly lower than groups fed other F diets and the Control. The final weight, weight gain and FCR of Nile tilapia were unaffected by the experimental diets.

Hematological parameters

Of all hematological analyses performed in the experimental fish, significant dietary effects were only found for hematocrit (Table 5). While all test diets supported lower hematocrit in comparison to the Control diet, the addition of the adsorbents in DZ and F diets significantly increased it from 34.9 and 35.1% to as high as 38.8%, respectively.

Liver histology

Histological sections of livers from all Nile tilapia from the Control groups (Figure 1A) displayed normal histological features (Ferguson, 2006) and served as references for comparison to the treatment groups. Contrastingly, fish fed all F diets (regardless of adsorbent inclusion) and the DZ diet, displayed liver inflammation characterized by lymphocytic infiltration adjacent to exocrine pancreatic tissues (Figure 1B). No lympoocytic infiltration or any pathological changes were observed in fish fed the Control and DZ diets with added adsorbents, showing similar histological appearance to Control-fed groups (Figure 1A).

Discussion

In recent years, contamination of feedstuffs and aquaculture feeds with mycotoxins and their effects in farmed fish have received considerable attention (Vila-Donat et al., 2018; Gonçalves et al., 2020; Oliveira and Vasconcelos, 2020), and so have ways of attenuating their harmful effects (Olokkaran and Mathew, 2020; Zahran et al., 2020). Despite great research efforts worldwide,

TABLE 4 Production performance and hepatosomatic index (HSI) of the Nile tilapia[†] fed the experimental diets for 71 days.

Treatment	Biomass Gain (g)	Final Weight (g)	Weight Gain (g)	Weight Gain (%)	FCR	Survival (%)	HSI (%)
DON+ZEN (DZ)							
Control	975.6[a]	68.7	64.7	1623.9	1.04	94.67[a]	0.80[b]
DZ	773.5[b]	65.7	61.8	1569.4	1.08	78.67[b]	0.94[a]
DZ+AA*	966.6[a]	68.0	63.9	1575.7	1.07	95.00[a]	0.67[bc]
DZ+AB*	992.1[a]	67.3	63.3	1591.0	1.03	98.33[a]	0.80[b]
DZ+AC	964.4[a]	68.0	64.0	1618.3	1.04	94.67[a]	0.58[c]
P value	<0.0001	0.9056	0.8927	0.638	0.8152	0.0002	<0.0001
PSE	8.390	1.760	1.900	10.390	0.020	2.578	0.478
FUM (F)							
Control	975.6[a]	68.7	64.7	1623.9	1.04	94.67[a]	0.80[b]
F	809.8[c]	66.4	62.4	1545.2	1.08	81.3[b]	0.89[a]
F+AA	888.9[bc]	63.9	62.4	1570.1	1.07	89.3[a]	0.79[b]
F+AB	912.0[ab]	69.0	65.0	1628.3	1.03	88.3[a]	0.82[b]
F+AC	944.4[ab]	67.5	63.5	1566.6	1.04	93.3[a]	0.54[c]
P value	<0.0001	0.731	0.725	0.638	0.461	0.0006	<0.0001
PSE	8.030	1.900	1.940	9.990	0.022	2.450	0.470

[†] Mean initial weight = 3.99 g; * One replicate was excluded (n = 4). Means with different superscript letters in the same column within a treatment group (DON+ZEN and FUM) are significantly different (P ≤ 0.05). DON, deoxynivalenol; ZEN, zearalenone; FUM, fumonisins; PSE, pooled standard error.

TABLE 5 Hematological parameters of the Nile tilapia fed the experimental diets for 71 days.

Treatment	Hct (%)	ALP (U/L)	ALT (U/L)	BA (umol/L)	TBIL (mg/dL)	ALB (g/dL)	BUN (mg/dL)	CHOL (mg/dL)
DON+ZEN (DZ)								
Control	43.0[a]	29.6	22.0	10.6	0.50	1.84	2.40	185.0
DZ	34.9[c]	38.8	25.4	7.4	0.44	1.60	2.20	189.4
DZ+AA*	38.2[b]	32.8	26.0	8.3	0.43	1.65	2.00	184.3
DZ+AB*	37.4[b]	27.8	32.8	10.0	0.43	1.83	2.25	182.5
DZ+AC	38.8[b]	29.8	22.2	11.0	0.40	1.75	2.00	183.0
P value	<0.001	0.442	0.556	0.905	0.160	0.514	0.481	0.988
PSE	1.746	3.090	3.204	2.609	0.247	0.497	0.625	4.608
FUM (F)								
Control	43.0[a]	29.6	22.0	10.6	0.50	1.84	2.40	185.0
F	35.1[c]	36.2	28.2	11.6	0.40	1.60	2.00	165.6
F+AA	38.5[b]	28.0	36.4	36.8	0.40	1.80	2.20	166.4
F+AB	36.1[b]	34.0	24.3	14.3	0.42	1.63	2.50	172.5
F+AC	38.8[b]	31.6	27.2	8.8	0.40	1.64	2.00	165.6
P value	<0.001	0.415	0.647	0.355	0.201	0.533	0.237	0.733
PSE	1.744	2.677	3.913	4.886	0.274	0.520	0.630	5.119

* One replicate was excluded (n = 4). Means with different superscript letters in the same column within a treatment group (DON+ZEN and FUM) are significantly different (P ≤ 0.05). Hct, hematocrit; ALP, alkaline phosphatase; ALT, alanine aminotransferase; BA, bile acids; TBIL, total bilirubin; ALB, albumin; BUN, urea nitrogen; CHOL, cholesterol; DON, deoxynivalenol; ZEN, zearalenone; FUM, fumonisins; PSE, pooled standard error.

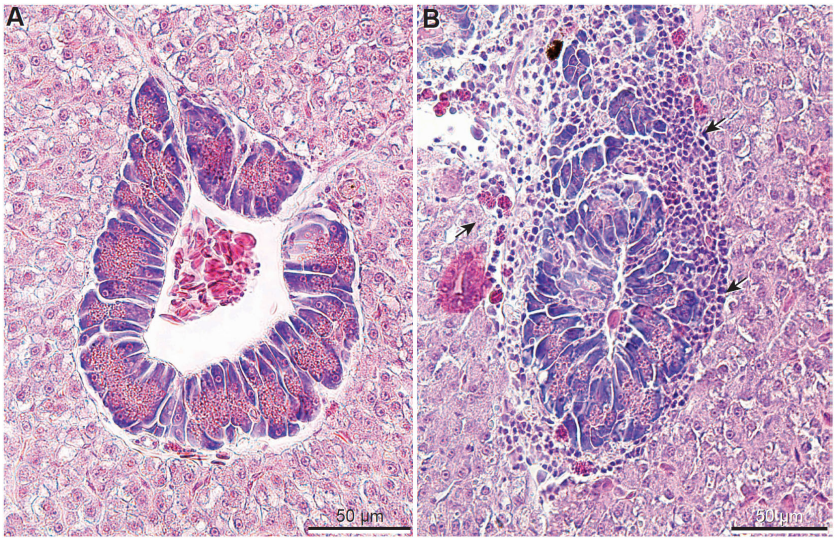

FIGURE 1
Liver histological sections (hematoxylin and eosin) of the Nile tilapia: **(A)** Liver from fish fed the Control diet showing normal structure of hepatocytes and exocrine pancreatic tissue; **(B)** Example of liver from fish fed DZ (DON 1.5 ppm + ZEN 0.3 ppm, without absorbent) and F (FUM = 15 ppm, without absorbent; shown above) diets showing lymphocytes adjacent exocrine pancreatic tissue (arrows).

several aspects of mycotoxin contaminations and strategies for preventing/mitigating mycotoxicosis in farmed fish, such as upper dietary limits for different mycotoxins and effectiveness of mycotoxin mitigating additives, remain undefined for several species. Nevertheless, it is a reality that mycotoxin-contaminated diets can adversely affect the production performance and health of fish (Greeff-Laubscher et al., 2020), which is corroborated by the findings of the present study demonstrating significant reductions in final biomass and survival of Nile tilapia fed diets contaminated with sub-lethal levels of some of the most economically relevant mycotoxins, especially in the absence of adsorbent additives.

Adverse effects of dietary DON+ZEN on the performance and of Nile tilapia were observed in the present study. Accordingly, Gonçalves et al. (2018) reported decreases in growth performance of rainbow trout (*Oncorhynchus mykiss*) fed diets containing 1.1 and 2.7 ppm of DON for 50 days or 0.3 ppm of DON for 168 days. Döll et al. (2010) also found that dietary DON concentrations above 0.3 ppm negatively affected the performance of Atlantic salmon (*Salmo salar*). Hooft et al. (2019) tested the effects of DON at concentrations of 0.1, 0.7 and 1.3 ppm in diets for Nile tilapia and rainbow trout, reporting deleterious effects on trout performance at all concentrations but only at 1.3 ppm for Nile tilapia. As with other warm-water species such as channel catfish (*Ictalurus punctatus*; Jantrarotai and Lovell, 1990), Nile tilapia displays relatively higher tolerance to dietary mycotoxins (Tuan et al., 2002; Hooft et al., 2019) than rainbow trout (Halver and Goldblatt, 1969; Hooft et al., 2011).

Similarly to the effects of DON+ZEN, the responses of Nile tilapia fed FUM-contaminated diets in this study are in agreement with previous findings by Tuan et al. (2003), who verified negative effects in performance parameters of Nile tilapia fry fed diets containing FUM at 10 ppm. Similar effects were observed in other fish species including channel catfish (*Ictalurus punctatus*) and common carp (*Cyprinus carpio*), whereby dietary FUM at ~ 10 and 20 ppm (respectively) adversely affected performance (Lumlertdacha et al., 1995). The adverse effects of FUM in animals has been associated with alterations in sphingolipid biosynthesis. The mechanism of action seems to be linked to the enzyme N-acyltransferase which, when inhibited by FUM in the endoplasmic reticulum, leads to the toxic accumulation of free sphinganine and sphingosine in cells (Wang et al., 1991).

Adsorbents directly bind mycotoxins decreasing their absorption in the gastrointestinal tract (Huwig et al., 2001), but adsorbent efficiency varies among different adsorbing materials as well as among different mycotoxins. Inorganic and/or yeast-based mycotoxin sequestering additives show relatively lower efficiency against DON when compared to the adsorption of AFL, ZEA, and FUM (Avantaggiato et al., 2005; Kong et al., 2014; Holanda and Kim, 2021). However, even when inorganic adsorbents were tested in DON contaminated feeds, improvements in growth, feed intake, and feed efficiency were observed in pigs (Holanda and Kim, 2021), corroborating the results of this study. In addition, it is possible that a more efficient adsorption of ZEA in the DZ diets contributed to the positive effects observed in Nile tilapia in this study. Overall, our findings indicate that the adsorbents attenuated the negative effects of these mycotoxins on juvenile Nile tilapia, in agreement with findings of Zychowski et al. (2013) and Hussain et al. (2017) when a clay-based adsorbent was tested in diets contaminated with AFL-B1. The efficacy of mycotoxin adsorbents have also been demonstrated in other animals and *in vitro* assays, showing an overall decrease in adverse effects (Solfrizzo et al., 2001; Avantaggiato et al., 2005; Di Gregorio et al., 2014; Selim et al., 2014; Vila-Donat et al., 2018). Further studies covering economic analyses of the economic and

environmental impacts of using mycotoxin adsorbents in commercial feeds are warranted.

The HSI is a somatic index commonly used to indicate differences in dietary nutrient/energy partitioning, as well as adverse effects including liver inflammation caused by mycotoxins (Mommsen, 2001). Accordingly, in this study we found a greater HSI in tilapia fed the DZ and F diets, whereas the addition of the adsorbents in both diets lowered HSI values, especially for adsorbent AC (Table 4). Tuan et al. (2003) found that after eight weeks feeding Nile tilapia (2.7 g) FUM-containing diets, concentrations above 40 ppm caused substantial changes in the liver. Lumlertdacha et al. (1994) also observed altered livers in catfish after 10 weeks of exposure to dietary FUM at 20 ppm. In the present study, changes in the liver of Nile tilapia were found after 71 days of consuming the DZ (DON+ZEN = 1.6 ppm and 0.3 ppm, respectively) and F (FUM = 15 ppm) diets. However, addition of any of the adsorbents in the DZ diets prevented noticeable pathological changes in the livers based on the liver histology of Control-fed fish, indicating the effectiveness of these additives in reducing/preventing absorption of mycotoxins in the gut.

As with other animals, hematological and biochemical parameters are widely used in the evaluation of nutritional and health status, as well as adaptation to challenging environmental conditions (Fazio et al., 2013; Faggio et al., 2014; Abdel-Tawwab et al., 2015; Sehonova et al., 2018; Burgos-Aceves et al., 2019). In the present study, neither dietary mycotoxins nor adsorbents affected the assessed hematological parameters ($P>0.05$), but the observed differences in hematocrit indicate deleterious effects of the dietary mycotoxins. Similar observations of reduced hematocrit in Nile tilapia after receiving diets containing FUM and moniliformin for eight weeks were reported by Tuan et al. (2003). Abdel-Tawwab et al. (2020) also reported decreased hematocrit values in European sea bass (*Dicentrarchus labrax*) fed diets with ZEN. The mycotoxin toxicity might have induced a hypochromic macrocytic anemia, which inhibits red blood cell enlargement (Abdel-Tawwab et al., 2020). Other parameters, such as BUN analysis, are mainly associated with gill and liver diseases (Stoskopf, 1993), but there were no statistical differences between the treatments in this experiment.

In the present study, the dietary concentrations of mycotoxins were well above those reported for commercial feeds for both DON +ZEN and FUM. Pietsch et al. (2014) reported a wide variation of DON (0.066 to 0.825 ppm) and ZEN (0.003 to 0.051 ppm), and ~3.42 ppm of FUM in commercial feeds. Therefore, our study not only highlight the deleterious effects of the evaluated mycotoxins, but also demonstrate the potential benefits of using commercially available additives for prevention of potential mycotoxicosis. In addition, adverse effects arising from chronic exposure to relatively lower levels of dietary mycotoxin may also occur as aspects such as health status, environmental conditions, and exposure period to contaminated feeds may influence the fish's responses to the toxins (Gonçalves et al., 2020; Oliveira and Vasconcelos, 2020).

In summary, exposure of juvenile Nile tilapia to dietary DON +ZEN and FUM at 1.6 + 0.3 ppm and 15 ppm, respectively, during a 71-day period adversely affects production performance and survival of the fish. Inclusion of adsorbent additives in the diets may help in attenuating/preventing adverse effects driven by mycotoxin contamination.

Data availability statement

The raw data supporting the conclusions of this article will be made available by the authors, without undue reservation.

Ethics statement

The animal study was approved by School of Fisheries, Aquaculture, and Aquatic Science, Auburn University, complying with regulations on the use of animals (approval code 20183337). The study was conducted in accordance with the local legislation and institutional requirements.

Author contributions

DF: Conceptualization, Data curation, Formal Analysis, Investigation, Methodology, Project administration, Resources, Software, Writing – original draft, Writing – review & editing. SP: Conceptualization, Data curation, Formal Analysis, Methodology, Writing – review & editing. SK: Conceptualization, Formal Analysis, Investigation, Writing – review & editing. SB: Conceptualization, Data curation, Investigation, Methodology, Writing – review & editing. WR: Conceptualization, Methodology, Writing – review & editing. DN: Funding acquisition, Methodology, Resources, Supervision, Writing – review & editing. DD: Conceptualization, Data curation, Investigation, Methodology, Project administration, Resources, Supervision, Validation, Writing – review & editing.

Funding

The author(s) declare financial support was received for the research, authorship, and/or publication of this article. This research was funded by the Alabama Agricultural Experiment Station, the Hatch program (ALA016-08027) of the National Institute of Food and Agriculture, U.S. Department of Agriculture and Phibro Animal Health Corporation. Scholarships for DF and SP were provided by the National Council for Scientific and Technological Development (CNPq; CNPq-204884/2018-7) and the Brazilian Federal Foundation for Support and Evaluation of Graduate Education (CAPES; CAPES-PRINT-88887.368344/2019-00), respectively.

Acknowledgments

The authors thank those who have taken time to critically review this manuscript as well as those who helped support research at the E.W. Shell Research Station, School of Fisheries, Aquaculture

and Aquatic Sciences, Auburn University. Special thanks to students and staff who helped maintain the daily management during the trials. Mention of trademark or proprietary product does not constitute an endorsement of the product by Auburn University and does not imply its approval to the exclusion of other products that may also be suitable.

Conflict of interest

Author DN was employed by the company Phibro Animal Health Corporation, who assisted in sourcing mycotoxin loaded ingredients.

The remaining authors declare that the research was conducted in the absence of any commercial or financial relationships that could be construed as a potential conflict of interest.

Publisher's note

All claims expressed in this article are solely those of the authors and do not necessarily represent those of their affiliated organizations, or those of the publisher, the editors and the reviewers. Any product that may be evaluated in this article, or claim that may be made by its manufacturer, is not guaranteed or endorsed by the publisher.

References

Abdel-Tawwab, M., Khalifa, E., Diab, A. M., Khallaf, M. A., Abdel-Razek, N., and Khalil, R. H. (2020). Dietary garlic and chitosan alleviated zearalenone toxic effects on performance, immunity, and challenge of European sea bass, *Dicentrarchus labrax*, to *Vibrio alginolyticus* infection. *Aquacult. Int.* 28, 493–510. doi: 10.1007/s10499-019-00477-0

Abdel-Tawwab, M., Sharafeldin, K. M., Mosaad, M. N. M., and Ismaiel, N. E. M. (2015). Coffee bean in common carp, *Cyprinus carpio* L. diets: effect on growth performance, biochemical status, and resistance to waterborne zinc toxicity. *Aquaculture* 448, 207–213. doi: 10.1016/j.aquaculture.2015.06.010

Ahmed, S. A. A., Nada, H. S., Elsheshtawy, H. M., Ibrahim, S. M., Fahmy, E. M., Khedr, M. H. E., et al. (2022). Comparative antitoxic potency of honey and natamycin-supplemented diets against aflatoxicosis and their influences on growth, serum biochemistry, immunohistochemistry, and residual deposition in Nile tilapia (*Oreochromis niloticus*). *Aquaculture* 551, 01–09. doi: 10.1016/j.aquaculture.2022.737934

Anater, A., Manyes, L., Meca, G., Ferrer, E., Luciano, F. B., Pimpão, C. T., et al. (2016). Mycotoxins and their consequences in aquaculture: A review. *Aquaculture* 451, 1–10. doi: 10.1016/j.aquaculture.2015.08.022

Avantaggiato, G., Solfrizzo, M., and Visconti, A. (2005). Recent advances on the use of adsorbent materials for detoxification of *fusarium* mycotoxins. *Food Addit. Contam* 22, 379–388. doi: 10.1080/02652030500058312

Bashorun, A., Hassan, Z. U., Al-Yafei, M. A., and Jaoua, S. (2023). Fungal contamination and mycotoxins in aquafeed and tissues of aquaculture fishes and their biological control. *Aquaculture* 576, 01–08. doi: 10.1016/j.aquaculture.2023.739892

Battilani, P., Toscano, P., van der Fels-Klerx, H. J., Moretti, A., Leggieri Camardo, M., Brera, C., et al. (2016). Aflatoxin B_1 contamination in maize in Europe increases due to climate change. *Sci. Rep.* 6, 24328. doi: 10.1038/srep24328

Boudergue, C., Burel, C., Dragacci, S., Favrot, M.-C., Fremy, J.-M., Massimi, C., et al. (2009). *Review of mycotoxin-detoxifying agents used as feed additives: mode of action, efficacy and fee/food safety* Vol. 6 (European Union: EFSA Supporting Publication), 192. EN-22.

Burgos-Aceves, M. A., Lionetti, L., and Faggio, C. (2019). Multidisciplinary haematology as prognostic device in environmental and xenobiotic stress-induced response in fish. *Sci. Total Environ.* 670, 1170–1183. doi: 10.1016/j.scitotenv.2019.03.275

Chestnut, A. B., Anderson, P. D., Cochran, M. A., Fribourg, H. A., and Gwinn, K. D. (1992). Effects of hydrated sodium calcium aluminosilicate on fescue toxicosis and mineral absorption. *J. Anim. Sci.* 70, 2838–2846. doi: 10.2527/1992.7092838x

Di Gregorio, M. C., de Neeff, D. V., Jager, A. V., Corassin, C. H., de Pinho Carão, A. C., de Albuquerque, R., et al. (2014). Mineral adsorbents for prevention of mycotoxins in animal feeds. *Toxin Rev.* 33, 125–135. doi: 10.3109/15569543.2014.905604

Döll, S., Baardsen, G., Koppe, W., Stubhaug, I., and Dänicke, S. (2010). "Effects of increasing concentrations of the mycotoxins deoxynivalenol, zearalenone or ochratoxin A in diets for Atlantic salmon (*Salmo salar*) on growth performance and health," in *The 14th International Symposium on Fish Nutrition and Feeding*, (Qingdao, China). 120.

Faggio, C., Fedele, G., Arfuso, F., Panzera, M., and Fazio, F. (2014). Haematological and biochemical response of *Mugil cephalus* after acclimation to captivity. *Cah. Biol. Mar.* 55, 31–36.

Fazio, F., Marafioti, S., Torre, A., Sanfilippo, M., Panzera, M., and Faggio, C. (2013). Haematological and serum protein profiles of *Mugil cephalus*: effect of two different habitats. *Ichthyol. Res.* 60, 36–42. doi: 10.1007/s10228-012-0303-1

Ferguson, H. W. (2006). "Liver," in *Systemic pathology of fish, 2nd edition*. Ed. H. W. Ferguson (London: Scotian Press), 201–216.

Gonçalves, R. A., Navarro-Guillén, C., Gilannejad, N., Dias, J., Schatzmayr, D., Bichl, G., et al. (2018). Impact of deoxynivalenol on rainbow trout: growth performance, digestibility, key gene expression regulation and metabolism. *Aquaculture* 490, 362–372. doi: 10.1016/j.aquaculture.2018.03.001

Gonçalves, R. A., Schatzmayr, D., Albalat, A., and Mackenzie, S. (2020). Mycotoxins in aquaculture: feed and food. *Aquaculture* 12, 145–175. doi: 10.1111/raq.12310

Greeff-Laubscher, M. R., Beukes, I., Marais, G. J., and Jacobs, K. (2020). Aflatoxin detoxification using microorganisms and enzymes. *Mycology.* 11, 105–117. doi: 10.1080/21501203.2019.1604575

Guan, Y., Chen, J., Nepovimova, E., Long, M., Wu, W., and Kuca, K. (2023). Mycotoxin production by three different toxigenic fungi genera on formulated abalone feed and the effect of an aquatic environment on fumonisins. *Toxins* 13 (46), 01–17. doi: 10.3390/toxins13010046

Halver, J. E., and Goldblatt, L. A. (1969). "Aflatoxicosis and trout hepatoma," in *Aflatoxin: scientific background, control, and implications* (New York, New York, USA: Academic Press), 265–306.

Holanda, D. M., and Kim, S. W. (2021). Mycotoxin occurrence, toxicity, and detoxifying agents in pig production with emphasis on deoxynivalenol. *Toxins* 13, 171. doi: 10.3390/toxins13020171

Hooft, J. M., and Bureau, D. P. (2017). Evaluation of the efficacy of a commercial feed additive against adverse effects of feed-borne deoxynivalenol (DON) on the performance of rainbow trout (*Oncorhynchus mykiss*). *Aquaculture* 473, 237–245. doi: 10.1016/j.aquaculture.2017.02.019

Hooft, J. M., Elmor, A. E. H. I., Encarnaçao, P., and Bureau, D. P. (2011). Rainbow trout (*Oncorhynchus mykiss*) is extremely sensitive to the feed-borne *Fusarium* mycotoxin deoxynivalenol (DON). *Aquaculture* 311, 224–232. doi: 10.1016/j.aquaculture.2010.11.049

Hooft, J. M., Wu, P., Powell, C. D., Lou, Y., Squires, E. J., Cant, J. P., et al. (2019). A comparative investigation of the effects of feed-borne deoxynivalenol (DON) on growth performance, nutrient utilization and metabolism of detoxification in rainbow trout (*Oncorhynchus mykiss*) and Nile tilapia (*Oreochromis niloticus*) fed diets containing different levels of digestible carbohydrates. *Aquaculture* 505, 306–318. doi: 10.1016/j.aquaculture.2019.02.019

Hussain, D., Mateen, A., and Gatlin, D. M. (2017). Alleviation of aflatoxin B_1 (AFB_1) toxicity by calcium bentonite clay: Effects on growth performance, condition indices and bioaccumulation of AFB_1 residues in Nile tilapia (*Oreochromis niloticus*). *Aquaculture* 475, 8–15. doi: 10.1016/j.aquaculture.2017.04.003

Huwig, A., Freimund, S., Käppeli, O., and Dutler, H. (2001). Mycotoxin detoxication of animal feed by different adsorbents. *Toxicol. Lett.* 122, 179–188. doi: 10.1016/s0378-4274(01)00360-5

Jantrarotai, W., and Lovell, R. T. (1990). Acute and subchronic toxicity of cyclopiazonic acid to channel catfish. *J Aquat Anim Health* 2, 255–260. doi: 10.1577/1548-8667(1990)002<0255:AASTOC>2.3.CO;2

Koletsi, P., Graat, E. A. M., Lyons, P., and Wiegertjes, G. F. (2023). Are the effects of Deoxynivalenol (DON) on performance, liver and gastrointestinal tract health of rainbow trout (*Oncorhynchus mykiss*) influenced by dietary composition? *Aquaculture.* 32, 01–14. doi: 10.1016/j.aqrep.2023.101740

Kong, C., Shin, S. Y., and Kim, B. G. (2014). Evaluation of mycotoxin sequestering agents for aflatoxin and deoxynivalenol: an in *vitro* approach. *SpringerPlus* 3, 346. doi: 10.1186/2193-1801-3-346

Lumlertdacha, S., Lovell, R. T., Shelby, R. A., Lenz, S. D., and Kemppainen, B. W. (1994). Growth, hematology, and histopathology of channel catfish, *Ictalurus punctatus*, fed toxins from *Fusarium moniliforme*. *Aquaculture* 130, 201–218. doi: 10.1016/0044-8486(94)00219-E

Luna, L. G. (1968). *Manual of histologic staining methods of the armed forces institute of pathology, third ed* (New York: McGraw–Hill).

Manning, B. B., Ulloa, R. B., Li, M. H., Robinson, E. H., and Rottinghaus, G. E. (2003). Ochratoxin A fed to channel catfish (*Ictalurus punctatus*) causes reduced growth and lesions of hepatopancreatic tissue. *Aquaculture* 219, 739–750. doi: 10.1016/S0044-8486(03)00033-4

Marroquín-Cardona, A. G., Johnson, N. M., Phillips, T. D., and Hayes, A. W. (2014). Mycotoxins in a changing global environment: A review. *Food Chem. Toxicol.* 69, 220–230. doi: 10.1016/j.fct.2014.04.025

Mommsen, T. P. (2001). Paradigms of growth in fish. *Comp. Biochem. Physiol.* 129, 207–219. doi: 10.1016/S1096-4959(01)00312-8

National Research Council (NRC) (2011). *Nutrient requirements of fish and shrimp* (Washington D.C., USA: National Academies Press).

Nogueira, W. V., de Oliveira, F. K., Marimón Sibaja, K. V., de Oliveira Garcia, S., Kupski, L., de Souza, M. M., et al. (2020). Occurrence and bioacessibility of mycotoxins in fish feed. *Food Addit. Contam. Part B* 13, 244–251. doi: 10.1080/19393210.2020.1766577

Oliveira, M., and Vasconcelos, V. (2020). Occurrence of mycotoxins in fish feed and its effects: a review. *Toxins* 12, 160. doi: 10.3390/toxins12030160

Olokkaran, R., and Mathew, S. (2020). *In vitro* detoxification of aflatoxin B1 by calcium bentonite clay supplementation in aflatoxigenic mould contaminated feeds for Nile tilapia, *Oreochromis niloticus* (Linnaeus 1758). *Asian J. Fish. Aquat. Res.* 10, 1–18. doi: 10.9734/ajfar/2020/v10i130169

Paterson, R. R. M., and Lima, N. (2010). How will climate change affect mycotoxins in food? *Food Res. Int.* 43, 1902–1914. doi: 10.1016/j.foodres.2009.07.010

Patriarca, A., and Pinto, V. F. (2017). Prevalence of mycotoxins in foods and decontamination. *Curr. Opin. Food Sci.* 14, 50–60. doi: 10.1016/j.cofs.2017.01.011

Pietsch, C., Michel, C., Kersten, S., Valenta, H., Dänicke, S., Schulz, C., et al. (2014). *In vivo* effects of deoxynivalenol (DON) on innate immune responses of carp (*Cyprinus carpio* L.). *Food Chem. Toxicol.* 68, 44–52. doi: 10.1016/j.fct.2014.03.012

Reitman, S., and Frankel, S. (1957). *In vitro* determination of transaminase activity in serum. *Am. J. Clin. Pathol.* 28, 56–63. doi: 10.1093/ajcp/28.1.56

Sehonova, P., Svobodova, Z., Dolezelova, P., Vosmerova, P., and Faggio, C. (2018). Effects of water borne antidepressant son non-target animals living in the aquatic environment: a review. *Sci. Total Environ.* 631, 789–794. doi: 10.1016/j.scitotenv.2018.03.076

Selim, K. M., El-hofy, H., and Khalil, R. H. (2014). The efficacy of three mycotoxin adsorbents to alleviate aflatoxin B1 - induced toxicity in *Oreochromis niloticus*. *Aquacult. Int.* 22, 523–540. doi: 10.1007/s10499-013-9661-6

Smaoui, S., D´Amore, T., Agriopoulou, S., and Khaneghah, A. M. (2023). Mycotoxins in seafood: occurrence, recent development of analytical techniques and future challenges. *Separations* 22, 523–540. doi: 10.3390/separations10030217

Solfrizzo, M., Carratu, M. R., Avantaggiato, G., Galvano, F., Pietri, A., and Visconti, A. (2001). Ineffectiveness of activated carbon in reducing the alteration of sphingolipid metabolism in rats exposed to fumonisin contaminated diets. *Food Chem. Toxicol.* 10, 217. doi: 10.1016/s0278-6915(00)00160-5

Stoskopf, M. K. (1993). "Clinical pathology," in *Fish medicine*. Ed. M. K. Stoskopf (Philadelphia: W.B. Saunders Company), 113–131.

Taroncher, M., Rodríguez-Carrasco, Y., Aspevik, T., Kousoulaki, K., Barba, F. J., and Ruiz, M. J. (2021). Cytoprotective effects of fish protein hydrolysates against H_2O_2-induced oxidative stress and mycotoxins in caco-2/TC7 cells. *Fish Physiol. Biochem.* 47, 515–532. doi: 10.1007/s10695-021-00929-6

Tola, S., Bureau, D. P., Hooft, J. M., Beamish, F. W. H., Sulyok, M., Krska, R., et al. (2015). Effects of wheat naturally contaminated with *Fusarium* mycotoxins on growth performance and selected health in dices of red tilapia (Oreochromis niloticus × O. mossambicus). *Toxins* 7, 1929–1944. doi: 10.3390/toxins7061929

Tuan, N. A., Grizzle, J. M., Lovell, R. T., Manning, B. B., and Rottinghaus, G. E. (2002). Growth and hepatic lesions of Nile tilapia (*Oreochromis niloticus*) fed diets containing aflatoxin B_1. *Aquaculture* 212, 311–319. doi: 10.1016/S0044-8486(02)00021-2

Tuan, N. A., Manning, B. B., Lovell, R. T., and Rottinghaus, G. E. (2003). Responses of Nile tilapia (*Oreochromis niloticus*) fed diets containing different concentrations of moniliformin or fumonisin B_1. *Aquaculture* 217, 515–528. doi: 10.1016/S0044-8486(02)00268-5

Vila-Donat, P., Marín, S., Sanchis, V., and Ramos, A. J. (2018). A review of the mycotoxin adsorbing agents, with an emphasis on their multi-binding capacity, for animal feed decontamination. *Food Chem. Toxicol.* 114, 246–259. doi: 10.1016/j.fct.2018.02.044

Wang, E., Norred, W. P., Bacon, C. W., Riley, R. T., and Merril, A. H. Jr. (1991). Inhibition of sphingolipid biosynthesis by fumonisins; Implications for diseases associated with *Fusarium moniliforme*. *J. Biol. Chem.* 226, 1486–1490. doi: 10.1016/S0021-9258(18)98712-0

Zahran, E., Risha, E., Hamed, M., Ibrahim, T., and Palić, D. (2020). Dietary mycotoxicosis prevention with modified zeolite (Clinoptilolite) feed additive in Nile tilapia (*Oreochromis niloticus*). *Aquaculture* 515, 734562. doi: 10.1016/j.aquaculture.2019.734562

Zhu, Y., Hassan, Y. I., Watts, C., and Zhou, T. (2016). Innovative technologies for the mitigation of mycotoxins in animals feed and ingredients – A review of recent patents. *Anim. Feed Sci. Technol.* 2016, 19–29. doi: 10.1016/j.anifeedsci.2016.03.030

Zychowski, K. E., Hoffmann, A. R., Ly, H. J., Ponhlenz, C., Buentello, A., Romoser, A., et al. (2013). The effect of aflatoxin-B1 on red drum (*Sciaenops ocellatus*) and assessment of dietary supplementation of NovaSil for the prevention of aflatoxicosis. *Toxins* 5, 1555–1573. doi: 10.3390/toxins5091555

frontiers | Frontiers in Immunology

TYPE Original Research
PUBLISHED 22 November 2023
DOI 10.3389/fimmu.2023.1301033

OPEN ACCESS

EDITED BY
Andrew R. Williams,
University of Copenhagen, Denmark

REVIEWED BY
Xuan Wang,
Ocean University of China, China
Xiuzhen Sheng,
Ocean University of China, China
Jianchun Shao,
Fujian Agriculture and Forestry University, China

*CORRESPONDENCE
Shuyan Chi
chishuyan77@163.com
Beiping Tan
bptan@126.com

RECEIVED 24 September 2023
ACCEPTED 06 November 2023
PUBLISHED 22 November 2023

CITATION
He Y, Dong X, Yang Q, Liu H, Zhang S, Xie S, Chi S and Tan B (2023) An integrated study of glutamine alleviates enteritis induced by glycinin in hybrid groupers using transcriptomics, proteomics and microRNA analyses.
Front. Immunol. 14:1301033.
doi: 10.3389/fimmu.2023.1301033

An integrated study of glutamine alleviates enteritis induced by glycinin in hybrid groupers using transcriptomics, proteomics and microRNA analyses

Yuanfa He[1,2], Xiaohui Dong[1,3], Qihui Yang[1,3], Hongyu Liu[1,3], Shuang Zhang[1,3], Shiwei Xie[1,3], Shuyan Chi[1,3]* and Beiping Tan[1,3]*

[1]Laboratory of Aquatic Animal Nutrition and Feed, College of Fisheries, Guangdong Ocean University, Zhanjiang, China, [2]College of Fisheries, Southwest University, Chongqing, China, [3]Key Laboratory of Aquatic, Livestock and Poultry Feed Science and Technology in South China, Ministry of Agriculture and Rural Affair, Zhanjiang, China

Glutamine has been used to improve intestinal development and immunity in fish. We previously found that dietary glutamine enhances growth and alleviates enteritis in juvenile hybrid groupers (*Epinephelus fuscoguttatus*♀ × *Epinephelus lanceolatus*♂). This study aimed to further reveal the protective role of glutamine on glycinin-induced enteritis by integrating transcriptome, proteome, and microRNA analyses. Three isonitrogenous and isolipidic trial diets were formulated: a diet containing 10% glycinin (11S group), 10% glycinin diet supplemented with 2% alanine-glutamine (Gln group), and a diet containing neither glycinin nor alanine-glutamine (fishmeal, FM group). Each experimental diet was fed to triplicate hybrid grouper groups for 8 weeks. The analysis of intestinal transcriptomic and proteomics revealed a total of 570 differentially expressed genes (DEGs) and 169 differentially expressed proteins (DEPs) in the 11S and FM comparison group. Similarly, a total of 626 DEGs and 165 DEPs were identified in the Gln and 11S comparison group. Integration of transcriptome and proteome showed that 117 DEGs showed consistent expression patterns at both the transcriptional and translational levels in the Gln and 11S comparison group. These DEGs showed significant enrichment in pathways associated with intestinal epithelial barrier function, such as extracellular matrix (ECM)-receptor interaction, tight junction, and cell adhesion molecules ($P < 0.05$). Further, the expression levels of genes (*myosin-11*, *cortactin*, *tenascin*, *major histocompatibility complex class I* and *II*) related to these pathways above were significantly upregulated at both the transcriptional and translational levels ($P < 0.05$). The microRNA results showed that the expression levels of miR-212 (target genes *colla1* and *colla2*) and miR-18a-5p (target gene *colla1*) in fish fed Gln group were significantly lower compared to the 11S group fish ($P < 0.05$). In conclusion, ECM-receptor interaction, tight junction, and cell adhesion molecules pathways play a key role in glutamine alleviation of hybrid grouper enteritis induced by

high-dose glycinin, in which miRNAs and target mRNAs/proteins participated cooperatively. Our findings provide valuable insights into the RNAs and protein profiles, contributing to a deeper understanding of the underlying mechanism for fish enteritis.

KEYWORDS

amino acid, anti-nutritional factor, intestinal inflammation, multi-omics, signaling pathway

Introduction

Soya glycinin, accounting for 40% of the total protein in soy seed, has been identified as a major anti-nutritional factor and has a hexameric structure consisting of six subunits with the basic structure A-S-S-B (disulfide bond, where A and B represent the acidic and basic subunits, respectively) (1). Its antigenicities are relatively stable and are not easily destroyed at 100°C temperature treatment. Nowadays, the methods of mitigating soya glycinin-induced enteritis or antigenicity are physical (2), chemical (3), biological (4), and the application of innovative feed additives (5). However, in-depth research is still needed to completely remove the immunogenicity of soya glycinin. High-dose glycinin can impair intestinal immune function, cause inflammation response, and ultimately inhibit growth performance in fish (5–8). In general, soya glycinin-induced intestinal inflammation is accompanied by mRNA levels of *zonula occludin-1* (*zo-1*), *occludin* and *claudin-4* reduced as well as *interleukin-1β* and *tumor necrosis factor-α* increased (5, 9). Transcriptomic techniques have been employed to investigate the differential expression of soybean meal-induced enteritis (SBMIE) and affect its immune system-related pathways including cytokine-cytokine receptor interactions, intestinal immune network for immunoglobulin A (IgA) production, nuclear factor NF-κB signaling pathway, Jak (Janus kinase)-STAT (Signal transducers and activators of transcription) signaling pathway, T-cell receptor signaling pathway and tumor necrosis factor (TNF) signaling pathway, which play key roles in responding to soybean meal stress in fish (10, 11). The utilization of proteomics has provided valuable insights into the intricate molecular mechanisms by which fish respond to external stimuli such as feed additives. The influences of dietary tryptophan on the growth and physiology of snapper (*Sparus aurata*) were studied previously, and its proteomic data showed that dietary tryptophan did not affect growth but stimulated immunity in the fish (12). However, the integrated transcriptomic and proteomics analyses have been less studied in fish, and the integration of transcriptomic and proteomics analysis can provide more complete information compared to single omics, as well as the two can mutually validate the reliability of the data.

Although transcriptomic and proteomics technologies can provide a comprehensive understanding of overall molecular level changes, inconsistent expression levels may exist between mRNAs and proteins (13, 14). In addition to deficiencies in high-throughput omics technology and incompleteness of mRNA/protein databases, the complex regulatory mechanisms underlying the translation of mRNAs into mature proteins may also lead to inconsistent results. MicroRNAs (miRNAs) are major regulators of cellular function (15), prominently contributing to post-transcriptional and translational gene expression through various mechanisms (16). In addition, miRNAs have been found to have important roles in regulating intestinal functions such as epithelial cell growth (17), mucosal barrier function (18), and the development of gastrointestinal disease (19–21). As an important aspect, mRNA expression levels in fish can be regulated by miRNA targeting. A miRNAome study on the intestinal immune function of turbot (*Scophthalmus maximus* L.) showed that differentially expressed miRNAs contribute to the enhancement of intestinal immune response and the prevention of host infection, where their target genes are implicated in diverse immune functions and inflammatory responses (22). Meanwhile, fish composition influences the expression levels of intestinal miRNAs and their target genes, as well as some pathways, such as cell adhesion molecules, ECM-receptor interaction, apoptotic signaling pathway, and cytokine-cytokine receptor interaction, were identified by small RNA sequencing (11, 23).

The nutritional strategies of feed additives for aquatic animals have been studied separately at the mRNA, protein, or miRNA molecules. However, these molecules are interconnected and can mutually influence. mRNAs are transcribed from genes and act as templates for protein synthesis, while miRNAs exert regulatory control over protein translation or mRNA stability (24). This genetic information flow ultimately leads to the synthesis of proteins, which play various roles in biological processes. Thus, the integration of these three components (mRNAs, proteins, and miRNAs) is essential for a comprehensive study of fish intestinal health.

The national production of grouper is at 205,816 tons in 2022, which has become the third most productive species among marine economic fish species (25). Our previous study reported that the addition of purified high-dose glycinin to the diet reduced growth performance and caused enteritis in juvenile hybrid groupers (*Epinephelus fuscoguttatus*♀ × *Epinephelus lanceolatus*♂) (26). We also found that feed supplementation with 2% alanyl-glutamine enhanced growth performance and alleviated enteritis induced by glycinin in the same species (27). However, the potential protective mechanisms for glutamine to alleviate enteritis in fish based on

multi-omics techniques have not been studied. This experiment aimed to further reveal the potential protective role of glutamine (Gln) against glycinin-induced enteritis in hybrid groupers by integrating transcriptomics, proteomics, and miRNA analyses. In addition, because Gln tends to become hot and less soluble during feed processing, a feed substitute for Gln, alanyl-glutamine, was used for the study (28–30).

Materials and methods

Grouping and sample collection

Three experimental diets were prepared with equal levels of protein (48% crude protein) and lipid (12% crude lipid): a diet based on fishmeal (referred to as Group FM), a diet containing 10% glycinin (referred to as Group 11S), and glycinin diet supplemented with 2% alanine-glutamine (referred to as Group Gln). The feed formulation is based on our published articles (24). Juvenile hybrid groupers used in this experiment were obtained from a local commercial hatchery (Zhanjiang, Guangdong, China). Healthy and vigorous hybrid groupers (8.50 ± 0.01 g) were fed each diet for 8 weeks. After the feeding trial finished, distal intestine (DI) samples from the three groups were obtained to determine transcriptome, proteome, and miRNA levels.

Transcriptome sequencing and *de novo* assembly

A total of 1 μg of RNA from FM, 11S, and Gln experimental groups was utilized for the preparation of transcriptome library. Initial steps involved the generation of first-strand cDNA through PCR, followed by the subsequent generation of second-strand cDNA. Subsequent to PCR amplification of cDNA fragments along with adapters, the resulting products underwent purification using AMPure XP Beads. Subsequently, the purified double-stranded cDNA underwent end-repaired, A-tailing, and ligation to sequencing junctions. Ultimately, PCR enrichment yielded the final cDNA library. The library's quality was then assessed using the Agilent Technologies 2100 bioanalyzer, followed by sequencing on the Illumina platform. Raw data underwent filtration to eliminate adapter sequences and low-quality reads, resulting in a collection of high-quality clean reads, which was assembled to obtain a Unigene library for the species. Once high-quality sequencing data has been obtained, it needs to be assembled using Trinity software (31). Trinity-derived transcripts served as reference sequences (Ref), against which clean reads from each sample were aligned and compared. Finally, reliable transcripts were obtained by filtering the low-expression transcripts. Following the assembly process, the assembled All-Unigenes were subjected to comprehensive annotation against the publicly accessible protein databases, which encompassed GO (Gene Ontology), KOG (EuKaryotic Orthologous Groups), Swiss-prot, Nt (non-redundant nucleotide sequences), and Nr (non-redundant protein sequences). The quantification of gene expression level relied on the expected number of fragments per kilobase of transcript per million mapped reads (FPKM). Differentially expressed genes (DEGs) between the two groups were pinpointed using a criterion of fold change (FC) ≥ 1.5 and a false discovery rate (FDR) of < 0.05. The process of pathway assignments involved utilizing sequences to query the KEGG database, with KEGG terms having corrected *P*-values (*Q*-values) of ≤ 0.05 deemed significant. Transcriptome (*de novo* assembly) sequencing data have been *submitted to* the NCBI SRA database with the accession number PRJNA1008292.

Proteome sequencing and analysis

The quantitative proteomic analysis of gut tissues from hybrid groupers was carried out using a 4D-label-free approach at Jingjie PTM Biolabs Inc. (Hangzhou, China). As previously described by Jiang et al. (32), the gut samples were initially ground, lysed, and subjected to centrifugation to yield the supernatant. The protein concentration of the supernatant was measured. Following trichloroacetic acid precipitation and acetone washing, protein samples were dissolved in triethylamine borane and digested with trypsin to yield peptides. Subsequently, peptides were desalted through Strata X SPE column, separated using NanoElute ultra-high-performance liquid system, and introduced into the capillary ion source for ionization. The mass spectrometry analysis was carried out using the timsTOF Pro (tims: trapped ion mobility spectrometry; TOF: time of flight) manufactured by Bruker in United States.

We employed the Maxquant search engine (v1.6.15.0) to process raw data from mass spectrometry. The transcriptome database of hybrid grouper (fasta format) was utilized as a reverse decoy database to facilitate the identification of matching proteins from the tandem mass spectra. Additionally, a reverse database was integrated to estimate the false discovery rate (FDR) resulting from random matches. Contaminated proteins within the identified list were excluded to minimize their impact. Cleavage enzyme specificity was designated as Trypsin/P, allowing for a maximum of 2 missing cleavages. Peptides were required to have a minimum length of seven amino acid residues, and a maximum of 5 modifications were considered. Precursor ion mass tolerance was set as 20 ppm for both the First search and Main search phases. Similarly, a mass tolerance of 20 ppm was applied to fragment ions. Fixed modifications encompassed carbamidomethyl on cysteine, while variable modifications encompassed methionine oxidation and protein N-terminal acetylation. To ensure robust identification quality, an FDR of 1% was maintained for protein and peptide identification. Differential proteins were identified after sample qualification. Their relative quantification differences between the two groups were assessed through a T-test, yielding the corresponding p-value. Furthermore, utilizing a p-value criterion of ≤ 0.05, protein ratios exceeding 1.2 was considered up-regulated, while a ratio less than 1/1.2 was considered down-regulated. Using the list of identified proteins, we conducted a subcellular localization analysis through the WoLF-PSORT database. The pathway analysis was executed utilizing the KEGG database. Furthermore, we employed a two-tailed test to analyze enriched pathways and ascertain the enrichment of differentially expressed proteins. A significance threshold of *P*-

value ≤ 0.05 was applied. The MS proteomics data have been *submitted to* the ProteomeXchange Consortium via the iProX partner repository with the dataset identifier PXD044757.

miRNA qPCR analysis

Screening of miRNAs regulating key genes associated with the intestinal barrier pathways based on a small RNA sequencing database in hybrid groupers. Small RNA transcriptome data were submitted to the SRA database under the accession number SUB7175134. Isolation of miRNA from the intestinal tract was conducted utilizing the RNAiso from small RNA Kit (Takara, China). Subsequently, mature miRNA's first-strand cDNA was conducted using the Mir-X^{TM} miRNA First-Strand Synthesis Kit (Takara, China). Quantitative analysis used the miRNA SYBR Green RT-qPCR Kit (Takara, China) with the provided miRNA reference gene (U6). The specific primers for the target miRNA used in this study are detailed in Supplementary Table 1. Relative quantitative was determined by the $2^{-\Delta\Delta CT}$ method (33).

Transcriptome and proteome validation

The identical samples employed for transcriptome analysis underwent RT-qPCR validation (n = *3). Primers were designed using Premier 5.0 and subsequently validated using the online Primer-BLAST program. Primer sequences are provided in* Supplementary Table 1. For mRNA sequencing, 1 μg of RNA was subjected to reverse transcribed to generate cDNA. Real-time PCR assays were conducted using the CFX96 real-time PCR Detection System. The reference gene β-Actin was chosen based on a prior study (34). Similarly, relative quantitative was determined by the $2^{-\Delta\Delta CT}$ method (33).

Protein abundance levels were validated through the quantification of eight selected proteins using parallel reaction monitoring-mass spectrometry (PRM-MS) analysis conducted by Jingjie PTM BioLab Co., Ltd. (Hangzhou, China). Relative quantification using the PRM approach was employed, utilizing signature peptides derived from the target proteins identified based on the 4D-label-free data. Quantification was established with a minimum peptide count of 2, encompassing both unique and razor peptides. Protein extraction and trypsin digestion were conducted as previously outlined. Following the approach outlined in the earlier study (35), peptides were dissolved and then subjected to tandem mass spectrometry in conjunction with liquid chromatography (LC-MS/MS). Subsequently, the acquired MS data underwent processing utilizing Skyline software (v.3.6), which included the setting of several parameters.

Statistics analysis

Analysis of miRNA expression level was evaluated using a two-tailed t-test (GraphPad Prism 8.0). For significant differences, * $0.01<P<0.05$ and ** $0.001<P<0.01$ between the two groups. The software GraphPad Prism 8.0 was used to generate the histograms.

Results

mRNA sequencing analysis

A total of nine qualified libraries were subjected to sequencing, distributed across the FM, 11S, and Gln groups, with each group consisting of three biological replicates. Table 1 provides a concise overview of the sequencing and assembly details. The FM, 11S, and Gln groups yielded approximately 19.94, 18.05, and 18.26 Gb of clean reads, respectively. Over 91.72% of the reads exhibited Q-scores at the Q30 level, and over 63.22% of the clean reads were successfully aligned.

Differentially expressed genes and KEGG pathway analysis

As shown in Figure 1, 570 DEGs were identified in the 11S and FM comparison group, with 266 upregulation and 304

TABLE 1 Overview of mRNA sequencing datasets from the intestine (9 samples).

Data type	BaseSum	GC(%)	Q20(%)	Q30(%)	Total_Reads	Mapped_Reads	Mapped_Ratio
FM_1	6,284,606,100	43.59%	96.34%	91.12%	20948687	13278452	63.39%
FM_2	6,619,536,600	42.13%	96.67%	91.89%	22065122	14276743	64.70%
FM_3	6,590,311,200	42.01%	96.20%	90.99%	21967704	13669264	62.22%
11S_1	6,591,993,000	43.58%	96.98%	92.27%	21973310	14859914	67.63%
11S_2	5,596,750,200	44.06%	97.32%	92.99%	18655834	12999383	69.68%
11S_3	5,859,667,500	43.58%	96.88%	92.37%	20362363	13610968	66.84%
Gln_1	5,801,036,700	42.44%	96.39%	91.31%	19336789	12502238	64.66%
Gln_2	6,165,045,300	42.18%	96.69%	92.04%	20550151	12499831	60.83%
Gln_3	6,289,937,700	41.07%	95.87%	90.48%	20966459	10283714	49.05%

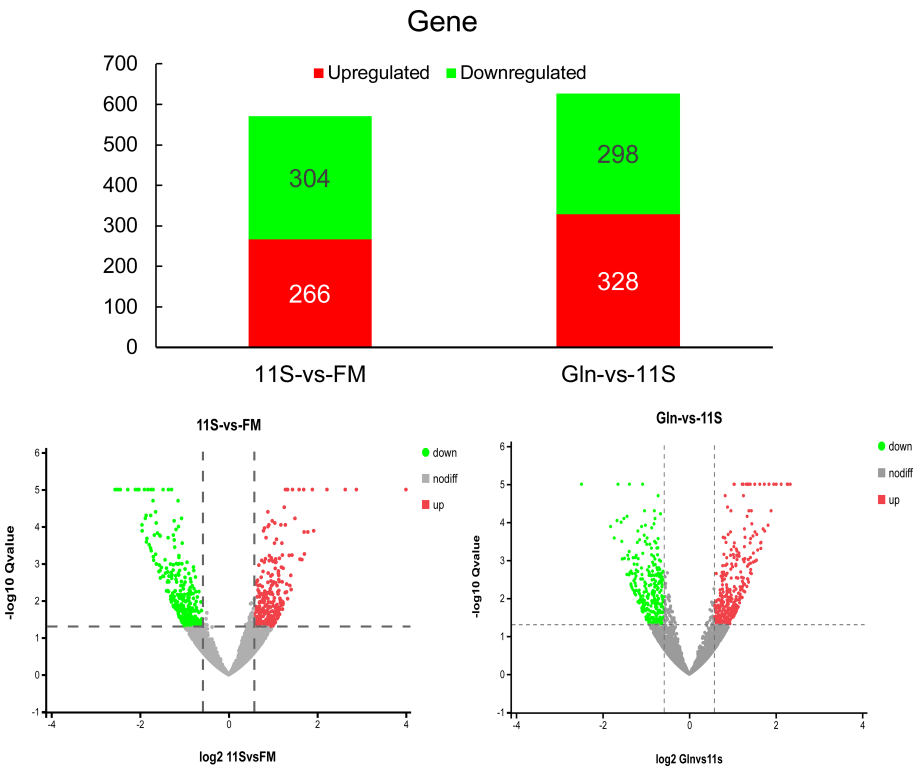

FIGURE 1
Analysis of histogram and volcano plot of differentially expressed genes (DEGs) in both 11S-vs-FM and Gln-vs-11S comparison groups. The horizontal and vertical axis in the volcano plot represents the DEGs value and -log10 p-value, respectively. In this visualization, upregulated DEGs are marked by red dots. Conversely, downregulated DEGs are indicated by green dots. Genes displaying no significant difference in expression are marked by gray dots.

downregulation genes (FC > 1.5). Likewise, 626 DEGs were identified in the Gln and 11S comparison group, with 328 upregulation and 298 downregulation genes. Principal component analysis (PCA) was used to assess the similarities within samples and whether the samples could be grouped well (Supplementary Figure 1).

In the comparison of 11S and FM groups, 570 DEGs were enriched in 153 pathways, with the counts of DEGs within each enriched pathway ranging from 3 to 18 (Figure 2A). Among these, the prominent KEGG pathways comprised immune system- and human disease-related pathways such as phagosome (ko04145) and herpes simplex infection (ko05168), and intestinal epithelial barrier-related pathways such as tight junction (ko04530) and focal adhesion (ko04510). Additionally, pathways linked to cell growth and death, such as apoptosis (ko04215) and necroptosis (k04217) were also significantly enriched ($P < 0.05$, Figure 2A). Furthermore, upregulated genes showed significant enrichment in ribosome (ko03010), PPAR signaling pathway (ko03320), ferroptosis (ko04216), primary bile acid biosynthesis (ko00120), glutathione metabolism (ko00480), FoxO signaling pathway (ko04068) and peroxisome (ko04146, $P < 0.05$, Figure 2B). Downregulated genes showed significant enrichment in intestinal epithelial barrier-related pathways such as ECM-receptor interaction (ko04512), tight junction, focal adhesion, and cell adhesion molecules (ko04514; $P < 0.05$, Figure 2C).

In the comparison of Gln and 11S groups, 626 DEGs were enriched in 133 pathways, with the counts of DEGs within each enriched pathway ranging from 2 to 28 (Figure 3A). Among them, the leading 20 KEGG pathways showed significant enrichment in immune system- and human disease-related pathways, including NOD-like receptor signaling pathway (ko04621), C-type lectin receptor signaling pathway (ko04625), RIG-I-like receptor signaling pathway (ko04622), intestinal immune network for IgA production (ko04672), toll-like receptor signaling pathway (ko04620), salmonella infection (ko05132) and cardiac muscle contraction (ko04260). Additionally, pathways associated with intestinal epithelial barriers, including tight junction, focal adhesion and ECM-receptor interaction (ko04512), were also notably enriched ($P < 0.05$, Figure 3A). Upregulated genes showed significant enrichment in pathways linked to the immune system, including toll-like receptor signaling pathway, NOD-like receptor signaling pathway, C-type lectin receptor signaling pathway, RIG-I-like receptor signaling pathway, intestinal immune network for IgA production and MAPK signaling pathway (ko04010; $P < 0.05$, Figure 3B). Additionally, they were significantly enriched in intestinal epithelial barrier-related pathways such as focal adhesion, regulation of actin cytoskeleton, ECM-receptor interaction, tight junction, and cell adhesion molecules (CAMs; $P < 0.05$). *Downregulated genes showed significant enrichment in the ribosome, oxidative phosphorylation (ko00190)*, PPAR signaling pathway (ko03320), and cardiac muscle contraction (ko04260; $P < 0.05$, Figure 3C).

10.3389/fimmu.2023.1301033

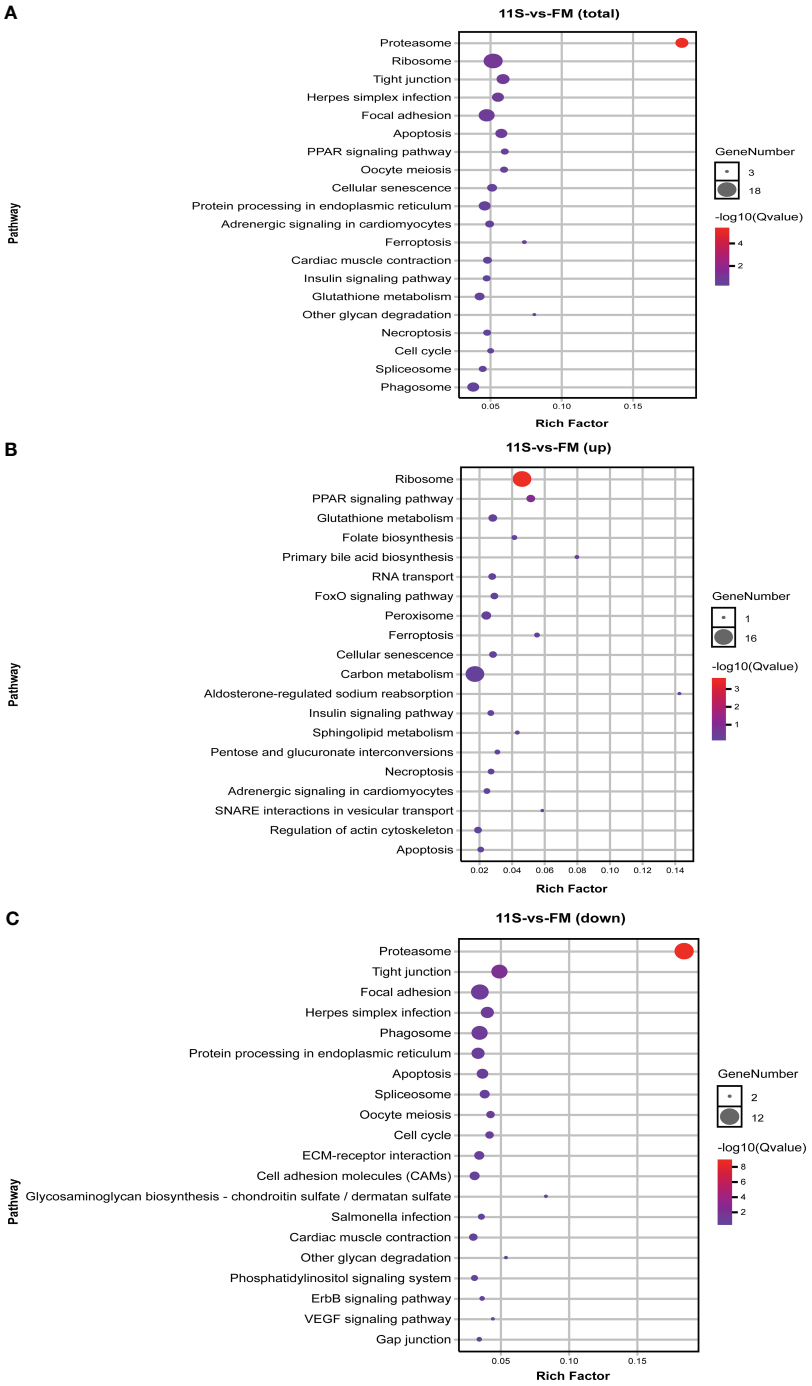

FIGURE 2
KEGG pathways enrichment analysis for differentially expressed genes (DEGs) in 11S-vs-FM comparison group. **(A)** Enrichment by total DEGs. **(B)** Enrichment by upregulated DEGs. **(C)** Enrichment by downregulated DEGs.

Differentially expressed proteins and subcellular localization analysis

As shown in Figure 4, a total of 169 DEPs were found in the 11S and FM comparison group, with 106 upregulated proteins and 63 downregulated proteins (FC >1.2). A total of 165 DEPs were found in the Gln and 11S comparison group, including 74 upregulated proteins and 91 downregulated proteins. Subcellular localization analysis showed that 78 proteins were situated in the cytoplasm (46.15%, Supplementary Figure 2A); 32 proteins were located in the mitochondria (18.93%); 19 proteins were localized in extracellular (11.24%); 17 proteins were localized in the nucleus (10.06%). Similarly, of the 165 DEPs in the Gln and 11S comparison group: 77 proteins were localized in the cytoplasm (46.67%); 32 proteins were localized in the mitochondria (19.39%); 19 proteins were localized in the nucleus (11.52%); 10 proteins were localized in

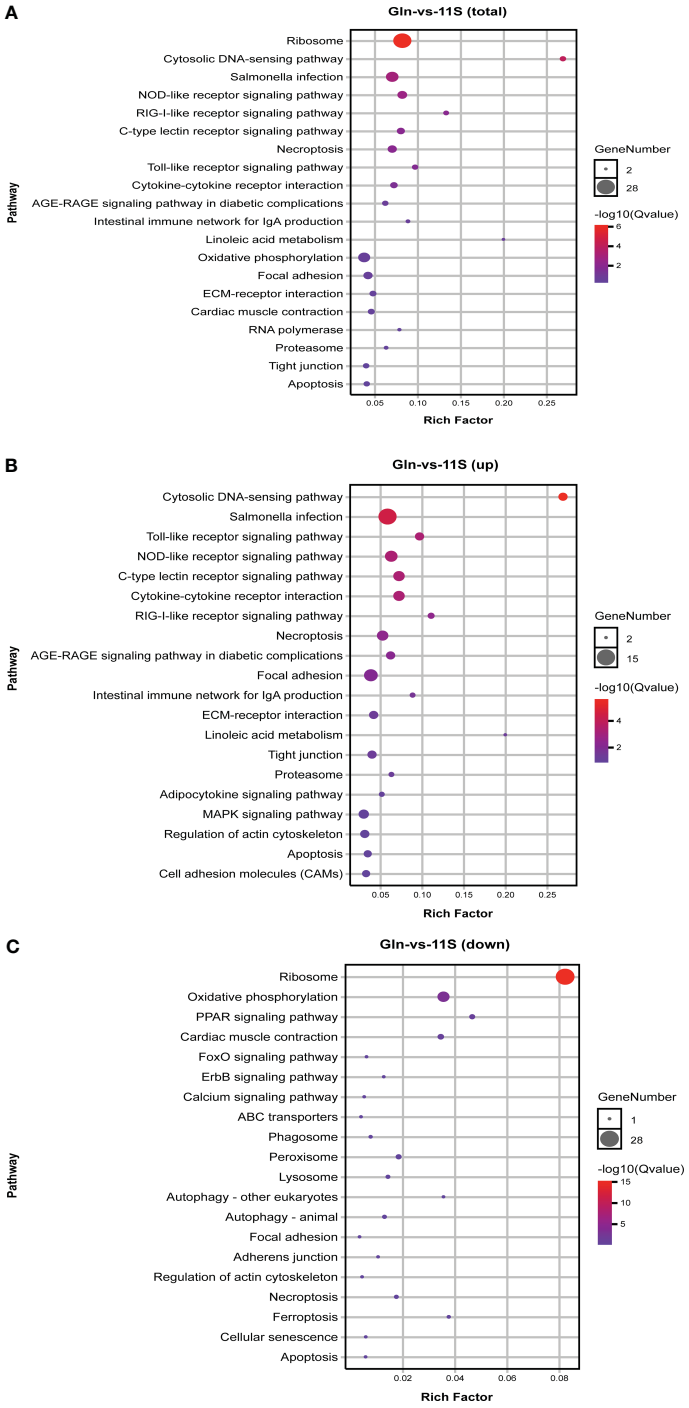

FIGURE 3
KEGG pathways enrichment analysis for differentially expressed genes (DEGs) in Gln-vs-11S comparison group. **(A)** Enrichment by total DEGs. **(B)** Enrichment by upregulated DEGs. **(C)** Enrichment by downregulated DEGs.

the plasma membrane (6.06%); as well as 8 proteins were localized in the cytoplasm and nucleus (4.85%; Supplementary Figure 2B).

KEGG pathway analysis for differentially expressed proteins

In the 11S and FM comparison group, 169 DEPs were functionally annotated using KEGG analysis. Among these, upregulated proteins showed significant enrichment pathways related to immune system- and human disease, such as NOD-like receptor signaling pathway, natural killer cell-mediated cytotoxicity, chronic myeloid leukemia (ko05220), renal cell carcinoma (ko05211), and acute myeloid leukemia (ko05221, $P < 0.05$, Figure 5A). Down-regulated proteins showed significant enrichment in pathways, such as alcoholism (ko05034), N-glycan biosynthesis (ko00510), drug metabolism-cytochrome P450

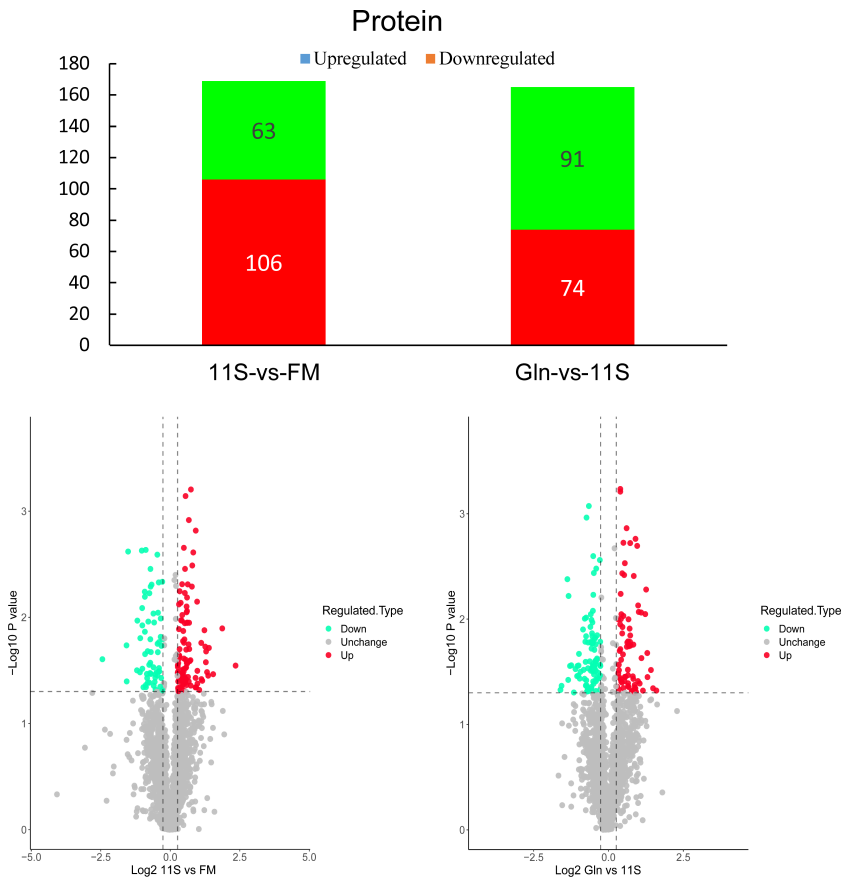

FIGURE 4
Analysis of histogram and volcano plot of differentially expressed proteins (DEPs) in both 11S-vs-FM and Gln-vs-11S comparison groups. The horizontal and vertical axis in the volcano plot represents the DEPs value and -log10 p-value, respectively. In this visualization, upregulated DEPs are denoted by red dots. Conversely, downregulated DEPs are denoted by green dots. Proteins displaying no significant difference in expression are marked by gray dots.

(ko00982), mRNA surveillance pathway (ko03015), various types of N-glycan biosynthesis (ko00513), amphetamine addiction (ko05031), sphingolipid metabolism (ko00600), and protein export (ko03060; P < *0.05*, Figure 5B).

In the Gln and 11S comparison group, up-regulated proteins showed significant enrichment in pathways associated with immune system- and human disease, such as Th1 and Th2 cell differentiation (ko04658), platelet activation (04611), JAK-STAT signaling pathway (ko04630), Th17 cell differentiation (ko04659), primary immunodeficiency (ko05340), inflammatory bowel disease (IBD, ko05321), and leishmaniasis (ko05140; *P* < 0.05, Figure 6A). They also demonstrated significant enrichment in pathways associated with the intestinal epithelial barrier function, such as tight junction and cell adhesion molecules (*P*<0.05). Down-regulated proteins showed significant enrichment in pathways, such as oocyte meiosis (ko04114), pentose and glucuronate interconversions (ko00040), hippo signaling pathway (ko04391), hepatitis C (ko05160), cell cycle (ko04110), folate biosynthesis (ko00790), and pentose phosphate pathway (ko00030; P < *0.05*, Figure 6B).

Integration analysis of the DEGs and DEPs

We performed a nine-quadrant plot classification of DEGs and DEPs (Figures 7A, C), quadrants 1 and 9 indicate that the mRNA is inconsistent with the corresponding protein differential expression pattern; quadrants 2 and 8 indicate that the mRNA is differentially expressed and the corresponding protein is unchanged; quadrants 3 and 7 suggest concordance between mRNA and corresponding protein differential expression; quadrant 4 and 6 indicate differential expression of protein and no change in corresponding mRNA; quadrant 5 indicates that both co-expressed mRNA and protein are non-differentially expressed. Then, KEGG enrichment pathway analysis was performed on differentially expressed mRNAs and proteins consistent with quadrants 3 and 7 in the 11S and FM comparison group (Figure 7B). The results showed that spliceosome (ko03040), NOD-like receptor signaling pathway, carbon metabolism (ko01200), protein export, necroptosis, pyruvate metabolism (ko00620), C-type lectin receptor signaling pathway and pentose phosphate pathway were significantly enriched in the TOP 20 pathways (P < 0.05). Similarly, KEGG enrichment pathway

10.3389/fimmu.2023.1301033

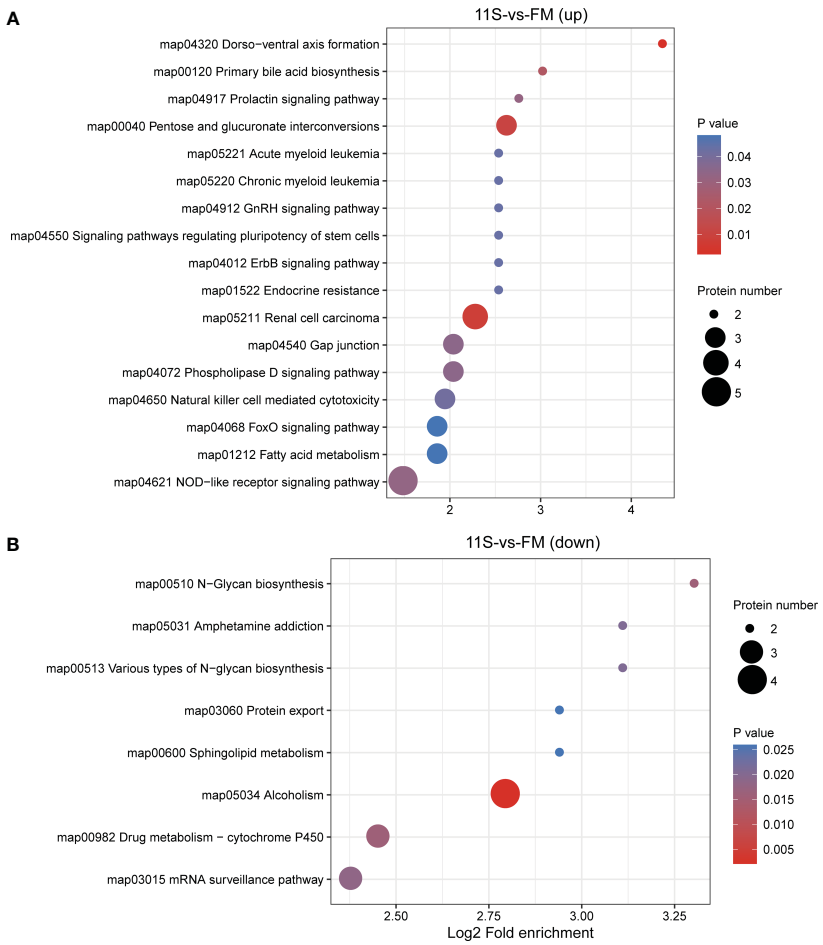

FIGURE 5
Enrichment analysis of KEGG pathway for differentially expressed protein (DEPs) in 11S-vs-FM comparison group. Log2 Fold enrichment is displayed on the horizontal axis, while the vertical axis denotes KEGG pathway names. Bubble size signifies protein counts within each pathway. The enriched *P*-value is represented by a color. **(A)** Enrichment by upregulated DEPs. **(B)** Enrichment by downregulated DEPs.

analysis of differential mRNAs and proteins consistently expressed in quadrants 3 and 7 in the Gln and 11S comparison group showed that pathways such as glycosaminoglycan biosynthesis (ko00532), NOD-like receptor signaling pathway, necroptosis, phagosome, sphingolipid mem, C-type lectin receptor signaling pathway, and ferroptosis and proteasome showed significant enrichment ($P < 0.05$, Figure 7D). Furthermore, the leading 20 KEGG pathways showed enrichment in immune system-related pathways, including NOD-like receptor signaling pathway and phagosome, along with intestinal barrier-related pathways including tight junction, adherens junction, and cell adhesion molecules.

mRNAs and proteins associated with the intestinal epithelial barrier

Myosin-1, Tubulin alpha-2, Actin (alpha skeletal muscle B), Major histocompatibility complex class II (MHC-II), Mucin-3B, Mucosal pentraxin, Leiomodin-1, Cytoplasmic dynein 1 heavy chain 1, Lysozyme, Eukaryotic translation initiation factor 5B, and Pyruvate kinase were significantly downregulated at both mRNA and protein levels in Group 11S than in Group FM ($P < 0.05$, Table 2). In the Gln and 11S comparison group, Ras-related C3 botulinum toxin substrate 2, Myosin-1, Cortactin, Wiskott-Aldrich syndrome protein, tenascin, Cluster of differentiation 4 (CD4), MHC-I, MHC-I -II, lysozyme, and NF-kappa-B inhibitor showed significant upregulation at both mRNA and protein levels ($P < 0.05$).

miRNAs and their target genes involved in the intestinal epithelial barrier

We also focused on genes with inconsistent mRNA and corresponding protein differential expression patterns and further screened the genes and proteins associated with the intestinal epithelial barrier function in the first quadrant (Table 3). MHC-I showed an upregulation at the mRNA level and a downregulation at the protein level in the 11S and FM comparison group. As shown by the miRNA target gene profile, miR-143_2, miR-222, miR-192-3p_2, miR-34a-5p_2, and miR-21b_3p were able to target the *mhc-I* gene. Similarly, the Gln and 11S comparison group found that

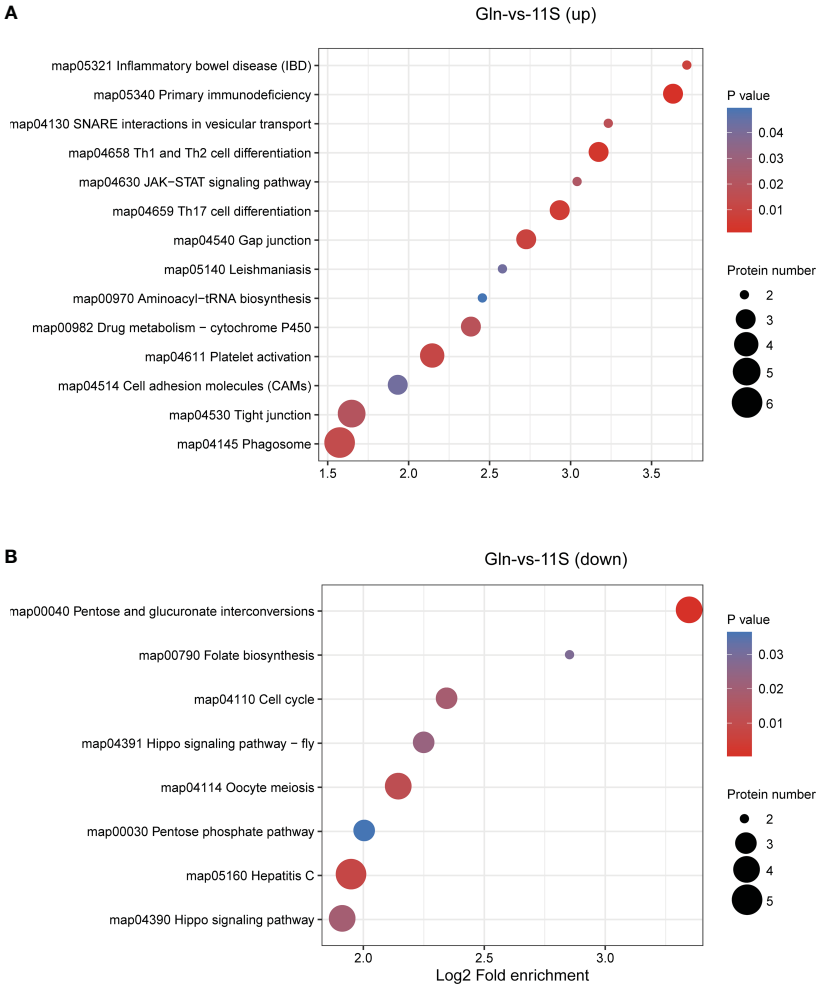

FIGURE 6
Enrichment analysis of KEGG pathway for differentially expressed protein (DEPs) in Gln-vs-11S comparison group. Log2 Fold enrichment is displayed on the horizontal axis, while the vertical axis denotes KEGG pathway names. Bubble size signifies protein count within each pathway. The enriched *P*-value is represented by color. **(A)** Enrichment by upregulated DEPs. **(B)** Enrichment by downregulated DEPs.

Colla1 and Col1a2 exhibited an upregulation at the mRNA level and a downregulation at the protein level. Moreover, miR-24, miR-212, and miR-18a-5p were able to target the *colla1* gene, and miR-205a, miR-29a-3p, and miR-212 were able to target the *colla2* gene. In addition, the expression levels of miR-18a-5p and miR-212 in the intestine of the Gln group were notably lower than those in Group 11S ($P < 0.05$, Figure 8), while miR-24 expression between Groups 11S and Gln showed no significant difference ($P > 0.05$).

Transcriptome and proteome validation

To validate the precision of the transcriptome findings of FM, 11S, and Gln groups. Ten genes (5 upregulation and 5 downregulation) were selected for qPCR validation in this experiment (Supplementary Figure 3). The agreement between RT-qPCR and transcriptome sequencing results underscores the enhanced accuracy of transcriptome sequencing. To validate the precision of the results of the three proteome groups (FM, 11S, and Gln), the DEPs validation analysis was then performed by PRM quantitative proteomics (Supplementary Figure 4). The results showed that the ribosomal protein L32 (RPL32), ribosomal protein S7 (RPS7), macrophage migration inhibitory factor (MMIF), malate dehydrogenase (MDH), and beta-hydroxysteroid dehydrogenase (β-HSD) proteins in the 11S and FM comparison group showed consistent expression levels between PRM and 4D-LFQ analyses (Supplementary Figure 4A). Moreover, the expression levels of CD45, RPL19, histone, annexin, and annexin max3 proteins in the Gln and 11S comparison group were consistent with the results of the 4D-LFQ analysis (Supplementary Figure 4B).

Discussion

We previously found that dietary Gln improved growth performance and alleviated intestinal inflammation induced by glycinin in hybrid grouper juveniles (27). However, the potential protective mechanism by which Gln alleviates enteritis in hybrid grouper remains unclear. On this basis, we further revealed its protective mechanism against soybean glycinin-induced hybrid

10.3389/fimmu.2023.1301033

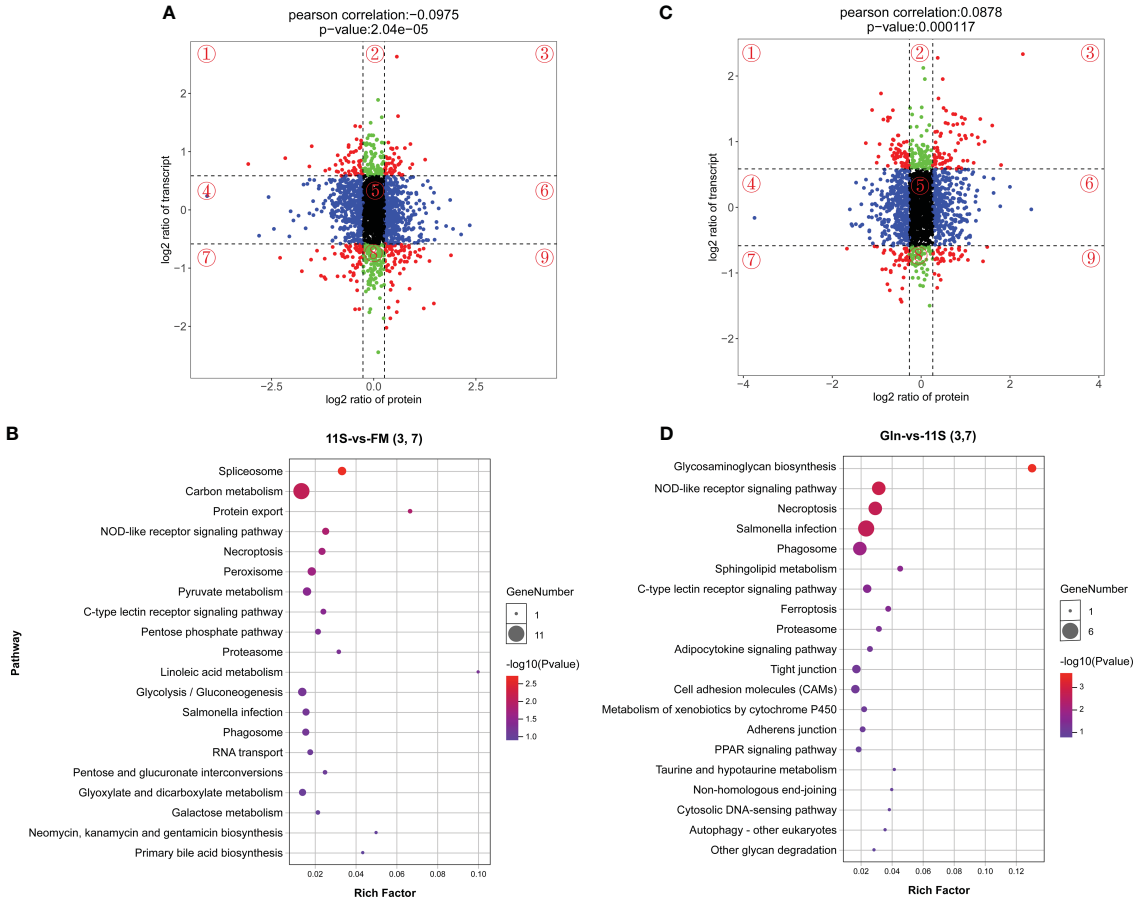

FIGURE 7
Top 20 KEGG enrichment analysis with differential mRNAs consistent with the corresponding differential protein expression (quadrants 3 and 7) in both the 11S-vs-FM and Gln-vs-11S group. The horizontal axis **(A, C)** represents the log2 ratio of protein, and the vertical axis **(A, C)** denotes the log2 ratio of transcript. The horizontal axis **(B, D)** indicates the rich factor, and the vertical axis **(B, D)** denotes the name of the KEGG pathway. Bubble size **(B, D)** indicates protein counts within each pathway. Enriched-log 10 *P*-value is represented by a color **(B, D)**.

TABLE 2 Differential genes and proteins associated with the intestinal epithelial barrier in quadrants 3 or 7.

Groups	Gene/Protein name	log2FC.x	log2FC.y	Group	Pathway
11S vs FM	*myh11*/Myosin-11	-0.76	-0.79	7	Tight junction
	α-tub/Tubulin alpha-2	-0.67	-0.62	7	Tight junction
	acta1b/Actin, alpha skeletal muscle B	-0.33	-0.71	7	Tight junction
	mhc-II/Major histocompatibility complex class II	-0.26	-0.73	7	Cell adhesion molecules (CAMs)
	muc3b/Mucin-3B	-1.75	-1.05	7	ECM-receptor interaction
	mptx/Mucosal pentraxin	-1.20	-0.84	7	—-
	lmod1/Leiomodin-1	-0.37	-0.69	7	—-
	dync1h1/Cytoplasmic dynein 1 heavy chain 1	-0.33	-0.67	7	Phagosome
	lys/Lysozyme	-1.21	-1.16	7	NOD-like receptor signaling pathway
	eif5b/Eukaryotic translation initiation factor 5B	-0.45	-0.66	7	TOR signaling pathway
	pk/Pyruvate kinase	-0.35	-0.92	7	TCA cycle
Gln vs 11S	*myh11*/Myosin-11	0.40	0.82	3	tight junction

(Continued)

10.3389/fimmu.2023.1301033

TABLE 2 Continued

Groups	Gene/Protein name	log2FC.x	log2FC.y	Group	Pathway
	cttn1/Cortactin	0.60	0.71	3	tight junction
	tnc/Tenascin	0.37	2.28	3	ECM-receptor interaction/Focal adhesion
	cd36/Cluster of differentiation 4	0.91	0.60	3	ECM-receptor interaction
	mhc-I/Major histocompatibility complex class I	0.39	1.66	3	Cell adhesion molecules (CAMs)
	mhc-II/Major histocompatibility complex class II	0.51	1.51	3	Cell adhesion molecules (CAMs)
	ptprc, *cd45*/Receptor-type tyrosine-protein phosphatase C	0.84	0.62	3	Cell adhesion molecules (CAMs)
	lys/Lysozyme	2.29	2.33	3	NOD-like receptor signaling pathway
	iκB/NF-kappa-B inhibitor	0.30	0.90	3	NF-κB signaling pathway

The fold change (FC) thresholds for the transcriptome and proteome were ≥1.5 and ≥1.2, respectively. Log2FC.x represents proteins and log2FC.y represents genes.

grouper enteritis by integrating transcriptomic, proteomics, and miRNAs analyses. In the 11S and FM comparison group, the foremost 20 KEGG pathways involved in the immune system- and disease processes-related pathways, such as phagosomes and herpes simplex infection, as well as involved in the intestinal epithelial barrier-related pathways, such as tight junction, focal adhesion, apoptosis, and necroptosis, were significantly enriched. Analogous pathways have been identified in carnivorous fish that experience SBMIE, such as Atlantic salmon (*Salmo salar*) (10, 36) and turbot (37, 38). We also reported that these pathways above in hybrid groupers were enriched in the soybean meal substituted 50% of fishmeal (SBM50) and fishmeal comparison group (39). In addition, the downregulated genes were involved in intestinal epithelial barrier-related pathways such as tight junction, focal adhesion, ECM-receptor *interaction*, and cell adhesion molecules (CAMs), suggesting impaired intestinal development and increased intestinal permeability in fish fed 11S diet alone. When Gln was added to the 11S diet, the upregulated genes exhibited a pronounced enrichment in pathways associated with the immune system. These included the toll-like receptor signaling pathway, NOD-like receptor signaling pathway, C-type lectin receptor signaling pathway, RIG-I-like receptor signaling pathway, intestinal immune network for IgA production, and MAPK signaling pathway. Furthermore, there was significant enrichment in pathways related to the intestinal epithelial barrier, including focal adhesion, ECM-receptor interaction, tight junction, regulation of actin cytoskeleton, and cell adhesion molecules (CAMs). The above results suggested that Gln enhanced intestinal immune and intestinal epithelial barrier functions and reduced the occurrence of hybrid grouper enteritis induced by soybean 11S. Similar results have been observed in various fish species, showing that the addition of Gln in the feed was effective in alleviating the clinical symptoms of trinitrobenzene sulfonic acid-induced enteritis in grass carp (*Ctenopharyngodon idella*) (40) and soybean antigenic protein-induced enteritis in Jian carp (*Cyprinus carpio var* Jian) (9, 41), and in promoting intestinal barrier function and hindgut morphology of soybean meal-induced enteritis in turbot (30, 38).

Proteins are the direct function executors of myriad life activities. Proteomics enables population assessment of protein expression levels, composition, and modification status in samples through high-throughput analysis, which in turn reveals protein functions, potential relationships between proteins, and the mining

TABLE 3 miRNAs targeting genes and proteins related to the intestinal barrier function.

Groups	miRNA	Target Gene/Protein name	log2FC.x	log2FC.y	Group
11S vs FM	miR-143_2	*mhc-I*/ Major histocompatibility complex class I	-0.36	0.77	1
	miR-222				
	miR-192-3p_2				
	miR-34a-5p_2				
	miR-21b-3p				
Gln vs 11S	miR-24	*colla1*/Collagen alpha-1(I)	-0.75	1.37	1
	miR-212				
	miR-18a-5p				
	miR-205a	*col1a2*/Collagen alpha-2(I)	-0.85	1.34	1
	miR-29a-3p				
	miR-212				

Log2FC.x represents proteins and log2FC.y represents genes.

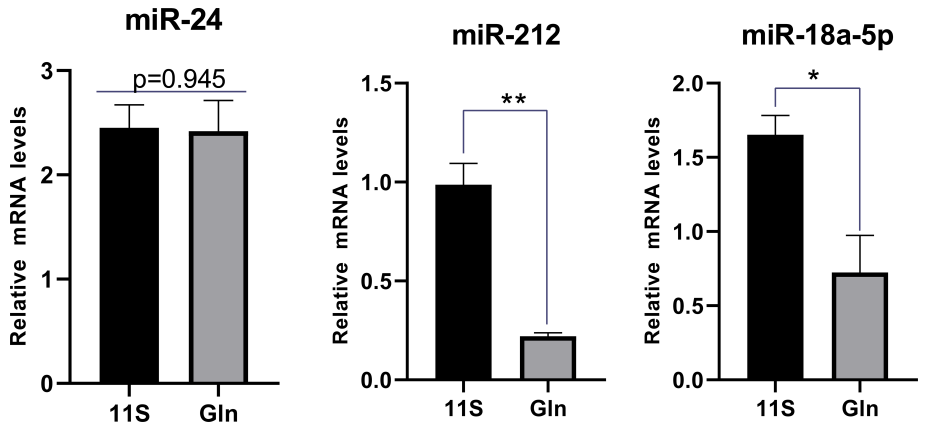

FIGURE 8
Targeted miRNA levels were analyzed by quantitative PCR (qPCR) in 11S and Gln groups. Screening of miRNAs regulating key genes associated with the intestinal barrier pathways based on a small RNA sequencing database in hybrid groupers. *0.01<P<0.05 and ** 0.001<P<0.01.

of new proteins. The proteomics data of this study showed that a total of 169 DEPs were found in the comparison of the 11S and FM group, and 165 DEPs were found in the Gln and 11S comparison group. These DEPs of the two comparison groups were mainly distributed in the cytoplasm, with a percentage of 46.15% and 46.67%, respectively, suggesting that the DEPs may mainly play important functions in the cytoplasm. In addition, KEGG functional annotation was performed on these DEPs. In the Gln and 11S comparison group, the expression of upregulated proteins displayed significant enrichment in pathways associated with the immune system and human disease pathways, including NOD-like receptor signaling pathway, natural killer cell-mediated cytotoxicity, renal cell carcinoma, chronic myeloid leukemia, and acute myeloid leukemia, implying that these signaling pathways above may play an important role in glycinin-induced enteritis in hybrid groupers. When soybean 11S feeds were supplemented with Gln, the up-regulated DEPs showed significant enrichment in intestinal epithelial barrier-related pathways including tight junction and cell adhesion molecules (CAMs). Similar results have been observed in the jejunum of maternal and piglets, demonstrating that dietary Gln increased the translation levels of intestinal tight junction and cell adhesion molecule proteins (42). Notably, immune system- and human disease-related pathways, including Th1 and Th2 cell proliferation, Th17 cell proliferation, platelet activation, JAK-STAT signaling pathway, primary immunodeficiency, inflammatory bowel disease, and leishmaniasis were also significantly enriched in Gln and 11S comparison group, suggesting a close link between intestinal epithelial barrier function and immune system pathways in hybrid grouper with Gln supplementation in soya 11S feed.

Correlation analysis of transcriptomic and proteomics data offers a more complete insight compared to single omics, and the two can mutually validate the reliability of the data. In this study, 2,057 genes were associated with the mRNA and protein levels in the FM, 11S, and Gln groups. The correlation coefficients of gene expression associated with the 11S-vs-FM and Gln-vs-11S comparison groups at the mRNA and protein levels were -0.10 and 0.09, respectively, indicating that the mRNA-protein correlation in this study was low. Huang et al. (43) correlated the transcriptome and proteome of *Cyanobacteria* at two points of time (24 h and 48 h) under nitrogen starvation and found correlation coefficients of 0.04 and -0.001, respectively. The process of translation from mRNA to protein is subject to complicated regulation, such as post-transcriptional regulation and protein translation modification, resulting in a weak correlation between transcriptome and proteome (44). In order to clarify the mechanism of protective effect of Gln in alleviating soybean 11S-induced grouper enteritis, differential expressed mRNAs and consistently expressed proteins were further analyzed for KEGG enrichment pathway. Genes such as *myosin-1*, *tubulin alpha-2*, *alpha-actin*, *major histocompatibility complex class II* (*mhc-II*), *mucin-3B*, *mucosal pentraxin*, *leiomodin-1*, *cytoplasmic dynein 1 heavy chain 1*, *lysozyme*, and *eukaryotic translation initiation factor 5B* were down-regulated at both mRNA and protein levels in the 11S and FM comparison group. In addition, *myosin-1*, *cortactin*, *Wiskott-Aldrich syndrome protein*, *ras-related C3 botulinum toxin substrate 2*, *tenascin*, *cd4*, *mhc-I*, *mhc-II*, *lysozyme*, and *iκBα* were upregulated at both the transcriptional and translational levels in the Gln and 11S comparison group. These genes participate in intestinal epithelial barrier pathways, including tight junction, adhesion junction, cell adhesion molecules (CAMs) and ECM-receptor interaction, as well as NOD-like receptor signaling pathway and NF-κB signaling pathway. Tight junctions are essential for animal organisms to establish a selective permeability barrier between neighboring cells. Myosin in tight junctions is the most important component of fish muscle proteins responsible for the contractile function of myogenic fibers and has ATPase activity, which binds actin and forms fibers under physiological conditions of low ionic strength (45). In addition, cortactin is associated with a variety of complex cellular processes, including cell motility, invasiveness, synaptogenesis, phagocytosis, tumorigenesis, and metastasis formation (46). Overexpression of cortactin could contribute to the emergence of invasive tumor phenotypes in a variety of ways, including enhanced actin polymerization, down-regulated

epidermal growth factor receptor, and molecule interactions between cyclin D1 and CD44 proteins (46). The extracellular matrix (ECM) is a complex blend of structural and functional macromolecules, which hold a vital role in the development of tissues and organs, and the preservation of cells and tissue (47). The tenascin involved in the ECM was also reported in Gln on mouse mesangial cells (48), showing that the mRNA expression level of tenascin was not affected after treating the cells with 2 mM Gln compared to the control group (no Gln was added), which was inconsistent with the results of the present experiments, probably due to the differences in the different species, *in vitro* and *in vivo* experiments. After infection of bone marrow-derived macrophages (BMDMs) using the bacterium *Leishmania donovani*, supplementation with Gln can significantly increase the gene expression of *mhc-II* (49), which is similar to the results of the present experiment. The MHC also comprises the most polymorphic genes in the vertebrate genomes that are closely related to immune response (50). IκB is an inhibitor of NF-κB, and NF-κB activity is inhibited when it is present. The IKK complexes, encompassing IKKα, IKKβ, and IKKγ, are capable of initiating the phosphorylation of IκB. The phosphorylation event prompts the degradation of IκB, subsequently culminating in the activation of NF-κB. This activation involves various subunits of NF-κB, including NF-κB p52, NF-κB p65, and c-Rel. As a result, there is an up-regulation in the expression of pro-inflammatory cytokines like tnf-α (51). The present study and our previous results (27) also found that dietary Gln down-regulated *ikkβ*, *nf-κb*, *tnf-α*, *il-1β*, *ifn-α*, and *hsp70* mRNA expression levels as well as up-regulated IκB expression at both mRNA and protein levels and ultimately reduced the occurrence of inflammation in hybrid groupers. Similar results were found for another amino acid, Met-Met, showing that suitable dietary Met-Met down-regulated the gene levels of *nf-κb p65*, *c-rel*, *ikkβ*, and *ikkγ* and up-regulated the gene levels of *iκBα* in the intestinal tract of juvenile grass carp (52). In addition, lysozyme can remove the residual cell wall after the action of antibacterial factors, enhance the antibacterial sensitivity of other immune factors, synergize with other immune factors to resist the invasion of foreign pathogens, which increases the activity of serum lysozyme and improve its immunity accordingly (53). Our previous results also showed that soybean 11S reduced the intestinal lysozyme activity of hybrid grouper at both the transcriptional and protein levels, whereas the supplementation of Gln in the 11S feed increased the lysozyme activity at both mRNA and protein levels. This suggests a potential enhancement in the intestinal immune function of the hybrid grouper.

The primary factor contributing to the limited correlation between transcriptome and proteome data arises from the intricate regulation occurring at multiple stages of gene expression. This includes transcription of DNA into mRNA and subsequent translation of mRNA into protein. Diverse factors exert control over these processes, encompassing both transcriptional and translational levels, as well as post-translational modifications. These multifaceted regulatory mechanisms lead to variations in mRNA transcript numbers, protein localization, abundance, and functionality. Consequently, these dynamic changes disrupt the alignment between mRNA and its corresponding protein, resulting in the observed reduced correlation between the two. We next focused on the role of miRNAs in post-transcriptional and translational control of gene expression from the miRNA level (16) to further explain genes that are inconsistent at the mRNA and protein levels. The intestinal miRNA expression profile and their target genes were obtained from the previous experiment, showing that the *mhc-I* gene (up-regulated at transcriptional level and down-regulated at translational level) could be regulated by miR-143_2, miR-222, miR-192-3p_2, miR-34a-5p_2, and miR-21b-3p. The result implied that these miRNAs likely have a significant role in regulating the target mRNA/protein (MHC-I). In addition, the target genes of miR-24, miR-24-3p, miR-18a-5p, and miR-212 in the Gln and 11S comparison group were *type I collagen α1*; the target genes of miR-205a, miR-29a-3p, and miR-212 were *type I collagen α2*. Collagen has strong biological activity and function and plays a crucial role in mediating cell migration, differentiation, and proliferation (54). In this experiment, *collagen α1* and *collagen α2 genes* were up-regulated at transcriptional level and down-regulated at translational level, suggesting that these miRNAs above may inhibit the translational level of *collagen α1* and *collagen α2* genes. The qPCR results of miRNA further confirmed that miR-18a-5p and miR-212 expression levels were significantly affected in the Gln and 11S groups. Notably, the down-regulation of miR-212 expression targeted *collagen α1* and *collagen α* genes. Our early miRNA data showed that miR-212 had significantly higher expression levels ($log_2FC=2.182$) in the SBM50 and FM comparison group (39). MiR-212 is a potent therapeutic target in mouse intestinal epithelial cells, where it affects a variety of T cells. Inhibition of miR-212/132 led to the induction of Treg1 and CD4+ cells and caused a decrease in Th17 cells (55). During chronic HIV/SIV infection, the disrupted expression of miR-212 in colonic epithelial cells can contribute to the disruption of the epithelial barrier by down-regulating the expression of occludin and PPARγ (56). The increased expression levels of Collagen α1 and Collagen α2 proteins, miR-18a-5p and miR-212 will be a key point. Notably, further validation of the targeting relationship of these miRNAs with target genes by dual luciferase reporter is needed.

In conclusion, enteritis induced by soybean glycinin was affected by mRNA and protein levels. By integrated transcriptome and proteome, 117 genes showed consistent expression patterns at both the transcriptional and translational levels in the Gln and 11S comparison group. Further found that the intestinal epithelial barrier pathways mediated the molecular mechanism in Gln alleviation of grouper enteritis induced by soybean glycinin. In addition, some miRNAs such as miR-212 and miR-18a-5 play key regulatory roles in Gln alleviation of hybrid grouper enteritis. Our findings provide valuable insights into the RNAs and protein profiles, contributing to a deeper understanding of the underlying mechanism for fish enteritis.

Data availability statement

The datasets presented in this study can be found in online repositories. The names of the repository/repositories and accession number(s) can be found below: NCBI via accession ID

PRJNA1008292 and ProteomeXchange Consortium via the iProX partner repository with the dataset identifier PXD044757.

Ethics statement

The animal study underwent review and approval by the Animal Research and Ethics Committees of Guangdong Ocean University, China. The study was conducted in accordance with the local legislation and institutional requirements.

Author contributions

YH: Methodology, Software, Writing – original draft, Writing – review & editing. XD: Writing – review & editing, Formal Analysis. QY: Formal Analysis, Writing – review & editing. SZ: Formal Analysis, Writing – review & editing. HL: Formal Analysis, Writing – review & editing. SX: Formal Analysis, Writing – review & editing. SC: Writing – review & editing, Conceptualization, Funding acquisition. BT: Conceptualization, Funding acquisition, Writing – review & editing.

Funding

The author(s) declare financial support was received for the research, authorship, and/or publication of this article. This study was financially supported by the National Key R&D Program of China (2019YFD0900200), the China Agriculture Research System of MOF and MARA (CARS-47), and Guangdong Provincial Higher Education Key Field Special Project (2020ZDZX1034).

Conflict of interest

The authors declare that the research was conducted in the absence of any commercial or financial relationships that could be construed as a potential conflict of interest.

Publisher's note

All claims expressed in this article are solely those of the authors and do not necessarily represent those of their affiliated organizations, or those of the publisher, the editors and the reviewers. Any product that may be evaluated in this article, or claim that may be made by its manufacturer, is not guaranteed or endorsed by the publisher.

Supplementary material

The Supplementary Material for this article can be found online at: https://www.frontiersin.org/articles/10.3389/fimmu.2023.1301033/full#supplementary-material

References

1. Mujoo R, Trinh DT, Ng PK. Characterization of storage proteins in different soybean varieties and their relationship to tofu yield and texture. *Food Chem* (2003) 82 (2):265–73. doi: 10.1016/S0308-8146(02)00547-2

2. Xi J, Yao L, Chen H. The effects of thermal treatments on the antigenicity and structural properties of soybean glycinin. *J Food Biochem* (2021) 45(9):e13874. doi: 10.1111/jfbc.13874

3. Bu G, Zhu T, Chen F. Effects of glycation modification on soybean protein antigenicity and structural properties. *J Chin Cereals Oils Assoc* (2017) 32(1):34–9.

4. Wang Z, Li L, Yuan D, Yuan D, Zhao X, Cui S, et al. Reduction of the allergenic protein in soybean meal by enzymatic hydrolysis. *Food Agr Immunol* (2014) 25(3):301–10. doi: 10.1080/09540105.2013.782268

5. Zhu R, Li L, Li M, Yu Z, Wang HH, Quan YN, et al. Effects of dietary glycinin on the growth performance, immunity, hepatopancreas and intestinal health of juvenile *Rhynchocypris lagowskii* Dybowski. *Aquaculture* (2021) 544:737030. doi: 10.1016/j.fsi.2022.08.063

6. Li Y, Yang P, Zhang Y, Ai Q, Xu W, Zhang W, et al. Effects of dietary glycinin on the growth performance, digestion, intestinal morphology and bacterial community of juvenile turbot, *Scophthalmus maximus* L. *Aquaculture* (2017) 479:125–33. doi: 10.1016/j.aquaculture.2017.05.008

7. Li M, Li L, Kong YD, Zhu R, Yu Z, Wang JY, et al. Effects of glycinin on growth performance, immunity and antioxidant capacity in juvenile golden crucian carp, *Cyprinus carpio*× *Carassius auratus*. *Aquac Res* (2020) 51(2):465–79. doi: 10.1111/are.14390

8. Yin B, Liu H, Tan B, Dong X, Chi S, Yang Q, et al. MHC II-PI3K/Akt/mTOR signaling pathway regulates intestinal immune response induced by soy glycinin in hybrid grouper (Epinephelus fuscoguttatus♀ × E. lanceolatus♂): protective effects of sodium butyrate. *Front Immunol* (2020) 11:615980. doi: 10.3389/fimmu.2020.615980

9. Jiang WD, Hu K, Zhang JX, Liu Y, Jiang J, Wu P, et al. Soyabean glycinin depresses intestinal growth and function in juvenile Jian carp (*Cyprinus carpio var* Jian): protective effects of glutamine. *Brit J Nutr* (2015) 114(10):1569–83. doi: 10.1017/S0007114515003219

10. De Santis C, Bartie KL, Olsen RE, Taggart JB, Tocher DR. Nutrigenomic profiling of transcriptional processes affected in liver and distal intestine in response to a soybean meal-induced nutritional stress in Atlantic salmon (*Salmo salar*). *Comp Biochem Phys D* (2015) 15:1–11. doi: 10.1016/j.cbd.2015.04.001

11. Wu N, Wang B, Cui ZW, Zhang XY, Cheng YY, Xu X, et al. Integrative transcriptomic and microRNAomic profiling reveals immune mechanism for the resilience to soybean meal stress in fish gut and liver. *Front Physiol* (2018) 9:1154. doi: 10.3389/fphys.2018.01154

12. Cerqueira M, Schrama D, Silva TS, Colen R, Engrola SA, Conceição LE, et al. How tryptophan levels in plant-based aquafeeds affect fish physiology, metabolism and proteome. *J Proteomics* (2020) 221:103782. doi: 10.1016/j.jprot.2020.103782

13. Lu XY, Huang Y, Yu YD, Yang YM. Application of genomics/proteomics technologies in the research of biocompatibility of biomaterials. *J Inorg Mater* (2013) 28:21–8. doi: 10.3724/SP.J.1077.2013.12269

14. Tian Q, Stepaniants SB, Mao M, Weng L, Feetham MC, Doyle MJ, et al. Integrated genomic and proteomic analyses of gene expression in mammalian cells. *Mol Cell Proteomics* (2004) 3(10):960–9. doi: 10.1074/mcp.M400055-MCP200

15. Bartel DP. MicroRNAs: target recognition and regulatory functions. *Cell* (2009) 136(2):215–33. doi: 10.1016/j.cell.2009.01.002

16. Morozova N, Zinovyev A, Nonne N, Pritchard L-L, Gorban AN, Harel-Bellan A. Kinetic signatures of microRNA modes of action. *RNA* (2012) 18(9):1635–55. doi: 10.1261/rna.032284.112

17. Nguyen HTT, Dalmasso G, Yan Y, Laroui H, Dahan S, Mayer L, et al. MicroRNA-7 modulates CD98 expression during intestinal epithelial cell differentiation. *J Biol Chem* (2010) 285(2):1479–89. doi: 10.1074/jbc.M109.057141

18. McKenna LB, Schug J, Vourekas A, McKenna JB, Bramswig NC, Friedman JR, et al. MicroRNAs control intestinal epithelial differentiation, architecture, and barrier function. *Gastroenterology* (2010) 139(5):1654–64. doi: 10.1053/j.gastro.2010.07.040

19. Biton M, Levin A, Slyper M, Alkalay I, Horwitz E, Mor H, et al. Epithelial microRNAs regulate gut mucosal immunity via epithelium–T cell crosstalk. *Nat Immunol* (2011) 12(3):239. doi: 10.1038/ni.1994

20. Goto Y, Kiyono H. Epithelial cell microRNAs in gut immunity. *Nat Immunol* (2011) 12(3):195. doi: 10.1038/ni0311-195

21. Monzo M, Navarro A, Bandres E, Artells R, Moreno I, Gel B, et al. Overlapping expression of microRNAs in human embryonic colon and colorectal cancer. *Cell Res* (2008) 18(8):823. doi: 10.1038/cr.2008.81

22. Gao C, Cai X, Fu Q, Yang N, Song L, Su B, et al. Dynamics of miRNA transcriptome in turbot (*Scophthalmus maximus* L.) intestine following *Vibrio Anguillarum* infection. *Mar Biotechnol (N Y)* (2019) 21(4):550–64. doi: 10.1007/s10126-019-09903-z

23. Miao LH, Lin Y, Pan WJ, Huang X, Ge XP, Ren MC, et al. Identification of differentially expressed microRNAs associate with glucose metabolism in different organs of blunt snout bream (*Megalobrama amblycephala*). *Int J Mol Sci* (2017) 18(6): E1161. doi: 10.3390/ijms18061161

24. Takane K, Kanai A. Vertebrate virus-encoded microRNAs and their sequence conservation. *Jpn J Infect Dis* (2011) 64(5):357–66. doi: 10.7883/yoken.64.357

25. Fisheries Bureau of Agriculture Ministry of China. *2022 China Fisheries Statistical Yearbook*. Beijing, China: China Agriculture Press (2023). p. 25.

26. He Y, Liang J, Dong X, Liu H, Yang Q, Zhang S, et al. Soybean β-conglycinin and glycinin reduced growth performance and the intestinal immune defense and altered microbiome in juvenile pearl gentian groupers *Epinephelus fuscoguttatus*♀× *Epinephelus lanceolatus*♂. *Anim Nutr* (2022) 9:193–203. doi: 10.1016/j.aninu.2021.11.001

27. He Y. *Study on the protective mechanism of glutamine against β-conglycinin and glycinin induced enteritis in pearl gentian grouper (Epinephelus fuscoguttatus*♀ × *Epinephelus lanceolatus*♂*) [Doctoral Degree]*. Zhanjiang, China: Guangdong Ocean University (2021).

28. Fürst P, Pogan K, Stehle P. Glutamine dipeptides in clinical nutrition. *Nutrition* (1997) 13(7-8):731–7. doi: 10.1016/s0899-9007(97)83035-3

29. Wu G, Meier SA, Knabe DA. Dietary glutamine supplementation prevents jejunal atrophy in weaned pigs. *J Nutr* (1996) 126(10):2578–84. doi: 10.1093/jn/126.10.2578

30. Liu Y, Chen Z, Dai J, Yang P, Hu H, Ai Q, et al. The protective role of glutamine on enteropathy induced by high dose of soybean meal in turbot, *Scophthalmus maximus* L. *Aquaculture* (2018) 497:510–9. doi: 10.1016/j.aquaculture.2018.08.021

31. Grabherr MG, Haas BJ, Yassour M, Levin JZ, Thompson DA, Amit I, et al. Full-length transcriptome assembly from RNA-Seq data without a reference genome. *Nat Biotechnol* (2011) 29(7):644. doi: 10.1038/nbt.1883

32. Jiang L, Yin X, Chen YH, Chen Y, Jiang W, Zheng H, et al. Proteomic analysis reveals ginsenoside Rb1 attenuates myocardial ischemia/reperfusion injury through inhibiting ROS production from mitochondrial complex I. *Theranostics* (2021) 11(4):1703. doi: 10.7150/thno.43895

33. Schefe JH, Lehmann KE, Buschmann IR, Unger T, Funke-Kaiser H. Quantitative real-time RT-PCR data analysis: current concepts and the novel "gene expression's C_T difference" formula. *J Mol Med* (2006) 84(11):901–10. doi: 10.1007/s00109-006-0097-6

34. An W, Dong X, Tan B, Yang Q, Chi S, Zhang S, et al. Effects of dietary n-3 highly unsaturated fatty acids on growth, non-specific immunity, expression of some immune-related genes and resistance to Vibrio harveyi in hybrid grouper (female symbol *Epinephelus fuscoguttatus* x male symbol *Epinephelus lanceolatu*). *Fish Shellfish Immunol* (2019) 96:86–96. doi: 10.1016/j.fsi.2019.11.072

35. Ma C, Wang W, Wang Y, Sun Y, Kang L, Zhang Q, et al. TMT-labeled quantitative proteomic analyses on the *longissimus dorsi* to identify the proteins underlying intramuscular fat content in pigs. *J Proteomics* (2020) 213:103630. doi: 10.1016/j.jprot.2019.103630

36. Kortner TM, Skugor S, Penn MH, Mydland LT, Djordjevic B, Hillestad M, et al. Dietary soyasaponin supplementation to pea protein concentrate reveals nutrigenomic interactions underlying enteropathy in Atlantic salmon (*Salmo salar*). *BMC Vet Res* (2012) 8(1):101. doi: 10.1186/1746-6148-8-101

37. Liu Y, Chen Z, Dai J, Yang P, Xu W, Ai Q, et al. Sodium butyrate supplementation in high-soybean meal diets for turbot (*Scophthalmus maximus* L.): Effects on inflammatory status, mucosal barriers and microbiota in the intestine. *Fish Shellfish Immunol* (2019) 88:65–75. doi: 10.1016/j.fsi.2019.02.064

38. Gu M, Bai N, Xu B, Xu X, Jia Q, Zhang Z. Protective effect of glutamine and arginine against soybean meal-induced enteritis in the juvenile turbot (*Scophthalmus maximus*). *Fish Shellfish Immunol* (2017) 70:95–105. doi: 10.1016/j.fsi.2017.08.048

39. He Y, Ye G, Chi S, Tan B, Dong X, Yang Q, et al. Integrative transcriptomic and small RNA sequencing reveals immune-related miRNA–mRNA regulation network for soybean meal-induced enteritis in hybrid grouper, *Epinephelus fuscoguttatus*♀ × *Epinephelus lanceolatus*♂. *Front Immunol* (2020) 11:1502. doi: 10.3389/fimmu.2020.01502

40. Yu D, Chang J, Liu J. Effect of glutamine supplement in diet on intestinal morphology and disease resistance of grass carp. *Feed Ind Magzine* (2017) 38(14):14–6.

41. Zhang JX, Guo LY, Feng L, Jiang WD, Kuang SY, Liu Y, et al. Soybean β-conglycinin induces inflammation and oxidation and causes dysfunction of intestinal digestion and absorption in fish. *PloS One* (2013) 8(3):e58115. doi: 10.1371/journal.pone.0058115

42. Zhu Y. *Regulation of glutamine on the small intestinal development in IUGR pigs via suppressing intestinal microRNA-29a and autophagy activity*. Beijing: China Agricultural University (2017). [Doctoral Thesis].

43. Huang S, Chen L, Te R, Qiao J, Wang J, Zhang W. Complementary iTRAQ proteomics and RNA-seq transcriptomics reveal multiple levels of regulation in response to nitrogen starvation in *Synechocystis* sp. PCC 6803. *Mol Biosyst* (2013) 9(10):2565–74. doi: 10.1039/c3mb70188c

44. Vogel C, de Sousa Abreu R, Ko D, Le SY, Shapiro BA, Burns SC, et al. Sequence signatures and mRNA concentration can explain two-thirds of protein abundance variation in a human cell line. *Mol Syst Biol* (2010) 6(1):400. doi: 10.1038/msb.2010.59

45. Yu KF, Yuan CH, Chen SS, Wang XC, Konno K. Biochemical properties of muscle proteins between summer and winter silver carp by chymotryptic digestion. *J Fish Chin* (2011) 35(6):940–7. doi: 10.3724/SP.J.1231.2011.17334

46. Zhao G, Zhang HY. Advances in the study of the role of cortactin in tumor progression. *Chin J Curr Adv Gen Surg* (2009) 12(2):135–8.

47. Faury G. Role of the elastin-laminin receptor in the cardiovascular system. *Pathol Biol* (1998) 46(7):517–26.

48. Pithon-Curi T. Glutamine causes overexpression of glomerulosclerosis markers in cultured mesangial cells. *Eur J Biochem* (2001) 268(S1):189–43.

49. Ferreira C, Mesquita I, Barbosa AM, Osório NS, Torrado E, Beauparlant CJ, et al. Glutamine supplementation improves the efficacy of miltefosine treatment for *visceral leishmaniasis*. *PloS Negl Trop D* (2020) 14(3):e0008125. doi: 10.1371/journal.pntd.0008125

50. Rauta PR, Nayak B, Das S. Immune system and immune responses in fish and their role in comparative immunity study: a model for higher organisms. *Immunol Lett* (2012) 148(1):23–33. doi: 10.1016/j.imlet.2012.08.003

51. Baltimore D. NF-κB is 25. *Nat Immunol* (2011) 12(8):683–5. doi: 10.1038/ni.2072

52. Su YN, Wu P, Feng L, Jiang WD, Jiang J, Zhang YA, et al. The improved growth performance and enhanced immune function by DL-methionyl-DL-methionine are associated with NF-κB and TOR signalling in intestine of juvenile grass carp (*Ctenopharyngodon idella*). *Fish Shellfish Immunol* (2018) 74:101–18. doi: 10.1016/j.fsi.2017.12.051

53. Zheng QM, Wu RQ, Ye X. The research advance of lysozyme in aquatic animals. *J Shanghai Fish Univ* (2006) 15(4):483–7.

54. Zhang J, Duan R, Tian Y, Konno K. Characterisation of acid-soluble collagen from skin of silver carp (*Hypophthalmichthys molitrix*). *Food Chem* (2009) 116(1):318–22. doi: 10.1016/j.foodchem.2009.02.053

55. Chinen I, Nakahama T, Kimura A, Nguyen NT, Takemori H, Kumagai A, et al. The aryl hydrocarbon receptor/microRNA-212/132 axis in T cells regulates IL-10 production to maintain intestinal homeostasis. *Int Immunol* (2015) 27(8):405–15. doi: 10.1093/intimm/dxv015

56. Kumar V, Mansfield J, Fan R, MacLean A, Li J, Mohan M. miR-130a and miR-212 disrupt the intestinal epithelial barrier through modulation of PPARγ and occludin expression in chronic simian immunodeficiency virus–infected. *Rhesus Macaques. J Immunol* (2018) 200(8):2677–89. doi: 10.4049/jimmunol.1701148

frontiers | Frontiers in Immunology

TYPE Original Research
PUBLISHED 08 December 2023
DOI 10.3389/fimmu.2023.1296848

OPEN ACCESS

EDITED BY
Samad Rahimnejad,
University of Murcia, Spain

REVIEWED BY
Xiuzhen Sheng,
Ocean University of China, China
Qiyou Xu,
Huzhou University, China

*CORRESPONDENCE
Ligai Wang
wligaikuaile@126.com
Dongdong Xu
xudong0580@163.com

RECEIVED 19 September 2023
ACCEPTED 17 November 2023
PUBLISHED 08 December 2023

CITATION
Ma S, Wang L, Zeng Y, Tan P, Chen R, Hu W, Xu H and Xu D (2023) Reparative effect of different dietary additives on soybean meal-induced intestinal injury in yellow drum (*Nibea albiflora*). *Front. Immunol.* 14:1296848. doi: 10.3389/fimmu.2023.1296848

Reparative effect of different dietary additives on soybean meal-induced intestinal injury in yellow drum (*Nibea albiflora*)

Shipeng Ma[1], Ligai Wang[2*], Yanqing Zeng[1], Peng Tan[2], Ruiyi Chen[2], Weihua Hu[2], Hanxiang Xu[1] and Dongdong Xu[2*]

[1]Fisheries College, Zhejiang Ocean University, Zhoushan, China, [2]Key Laboratory of Mariculture and Enhancement, Zhejiang Marine Fisheries Research Institute, Zhoushan, China

Soybean meal (SBM) is an acceptable replacement for unsustainable marine fish meal (FM) in aquaculture. However, we previously reported that high dietary SBM supplementation causes intestinal inflammatory injury in yellow drum (*Nibea albiflora*). Accordingly, a 4-week SBM-induced enteritis (SBMIE) in yellow drum trial was conducted first, followed by a 4-week additive-supplemented reparative experiment to evaluate the reparative effect of five additives on SBMIE in yellow drum. The control diet comprised 50% FM protein substituted with SBM. The additive-supplemented diet was added with 0.02% curcumin (SBMC), 0.05% berberine (SBM-BBR), 0.5% tea polyphenols (SBM-TPS), 1% taurine (SBM-TAU), or 0.8% glutamine (SBM-GLU) based on the control diet, respectively. The weight gain (WG), specific growth rate (SGR), feed efficiency ratio (FER), and survival rate (SR) of fish fed the additive-supplemented diets were significantly higher than those of fish fed the SBM diet. The WG, SGR, and FER of fish fed the SBMC, SBM-GLU and SBM-TAU diets were significantly higher than those of fish fed other diets. Moreover, fish fed the additive-supplemented diets SBMC and SBM-GLU, exhibited significantly increased intestinal villus height (IVH), intestinal muscular thickness (IMRT), and intestinal mucosal thickness (IMLT) and significantly decreased crypt depth (CD) in comparison with those fed the SBM diets. The relative expression of intestinal tight junction factors (*ocln, zo1*), cytoskeletal factors (*f-actin, arp2/3*), and anti-inflammatory cytokines *(il10, tgfb)* mRNA was remarkably elevated in fish fed additive-supplemented diets than those of fish fed the SBM diet. Whereas, the relative expression of intestinal myosin light chain kinase (*mlck*) and pro-inflammatory cytokines (*il1, il6, tnfa*) mRNA was markedly lower in fish fed the additive-supplemented diets. The highest relative expression of intestinal *ocln*, *f-actin*, and *arp2/3* and the lowest relative expression of intestinal *mlck* were found in fish fed the SBMC diet. Hence, all five dietary additives effectively repaired the intestinal injury induced by SBM, with curcumin exhibiting the strongest repair effect for SBMIE in yellow drum.

KEYWORDS

***Nibea albiflora*, soybean meal, dietary additive, intestinal injury, reparative effect**

1 Introduction

Soybean meal (SBM) is a good-quality plant protein source commonly used as a substitution to unsustainable fish meal (FM) in aquaculture feed because of its reasonable price, security of supply, and sustainability (1). However, the various anti-nutritional factors and unbalanced amino acid content in SBM in fish feed (2) could lead to a pro-inflammatory response in the distal intestine of carnivorous fish (3–7). Similarly, we previously reported that substituted of 45% FM protein with SBM protein reduced growth performance and induced intestinal inflammation in yellow drum (*Nibea albiflora*) (8). The primary associated manifestations include shortened intestinal mucosal folds, swollen of the lamina propria and subepithelial mucosa, and intense infiltration of inflammatory cells, which, collectively, can reduce the nutrient absorption capacity of the intestine and decrease growth performance (5, 9). Hence, it is particularly important to develop strategies to minimize intestinal injury caused by high proportions of SBM supplementation in marine fish.

Countermeasures, including enhancing processing technology and cultivating soybean protein-tolerant fish varieties, have been implemented for the widely use of SBM in cultivated fish varieties (10). Functional feed additives have also been served to alleviate SBM-induced enteropathy (SBMIE) in fish (11). These additives are nutritional/non-nutritional compounds provided in fish diets that enhance the physicochemical properties of diets or the performance of the target species (12, 13). Previous research suggests that a myriad of additives exhibit beneficiary properties such as anti-inflammatory, antioxidant, and immunomodulatory and may thus have the capacity to relieve SBMIE symptoms by strengthening the anti-inflammatory and immune responses of fish (14–16). Curcumin and berberine are both traditional herbal extracts, which can enhance intestinal villus development in Nile tilapia (*Oreochromis niloticus*) (17) and protect the intestinal barrier function of fish by regulating the intestinal microbiota (18). Meanwhile, tea polyphenols are plant extracts, which can attenuate the impairment of intestinal barrier function in fish by upregulating the expression of tight junction proteins and adhesion junction proteins (19). Taurine and glutamine are important functional amino acids, which has immune-enhancing and systemic nitrogen balance maintaining properties. Besides, taurine can improve intestinal homeostasis by regulating intestinal microbiota in mouse (20). Glutamine enhanced the intestinal tissue oxygenation and/or brush barrier function, as well as altered inflammatory processes in red drum (*Sciaenops ocellatus)* (21). Hence, all of these additives have great potential in the treatment of intestine injury in fish.

Yellow drum (*N. albiflora*) has become an important species for marine aquaculture in the East China Sea region due to its taste, rich nutrient content, and rapid growth (22). The successful artificial breeding of yellow drums has enabled their intensive cultivation, particularly in the coastal provinces of eastern China. We previously found that high dietary SBM supplementation causes intestinal inflammatory injury in yellow drum (8). Hence, in this study, we evaluated the effects of curcumin, berberine, tea polyphenols, glutamine, and taurine as potential feed additives on growth performance, whole-body nutritional composition, intestinal structure, and immune-related gene expression in yellow drum fed a high proportion of SBM diets. Collectively, this study can provide an effective solution for repairing intestinal injuries induced by SBM in marine fish.

2 Materials and methods

2.1 Experimental diets

In the current study, six isonitrogenous (49.95%) and isolipid (12.50%) diets were formulated using FM and SBM as the primary protein sources, fish oil and soybean oil as the primary lipid sources, and wheat flour as the carbohydrate source, according to the formulas described by Wang et al. (2016) (23). In the control diet, 50% of the FM protein was substituted with SBM protein (Table 1), whereas the other five treatment diets were supplemented with 0.02% curcumin (SBMC), 0.05% berberine (SBM-BBR), 0.5% tea polyphenols (SBM-TPS), 1% taurine (SBM-TAU), or 0.8% glutamine (SBM-TAU) based on the control diet.

2.2 Experimental fish and feeding management

Juvenile yellow drums obtained from the research station of the Marine Fisheries Institute of Zhejiang Province (Xixuan Island, Zhoushan, Zhejiang Province, China) were acclimated in an indoor flow-through aquaculture system for two weeks before initiating the feeding trial. A total of 450 yellow drum juveniles (initial weight: 6.65 ± 0.02 g) were transferred to 18 cylindrical fiberglass tanks (capacity: 1000 L) with 25 individuals per tank. Diets were randomly assigned to tanks in triplicates. The experiment was divided into two stages: week 1–4, when all fish were fed the SBM diet to induce intestinal inflammation; and week 4–8, when all fish, excluding the control group, were fed the additive-supplemented diets. All fish were fed twice daily at 7:00 and 14:00. The following parameters were maintained throughout the experimental period: temperature, 26–28 °C; salinity, 27.0 ± 1.0 g/L; unionized ammonia nitrogen< 0.05 mg/L; dissolved oxygen > 6.0 mg/L. The fish tanks were cleaned every two weeks, at which point the fish were removed and weighed to adjust the feeding amount.

2.3 Sample collection

After the feeding experiment, the fish were fasted for 24 h, the total number of fish in each tank was counted, and the survival rate (SR) was calculated. The weight of each tank fish was measured and then the weight gain rate (WG) and specific growth rate (SGR) of the fish were calculated. Fish were anesthetized with MS-222, and 12 individuals were randomly selected from each tank, and their total length, body length, and body weight were measured to calculate the condition factor (CF). Appropriately sized posterior intestinal tissue was cleaned with phosphate-buffered saline (PBS),

10.3389/fimmu.2023.1296848

TABLE 1 Ingredients and composition of the experimental diets (%, dry-matter basis).

Ingredients	Experimental diets					
	SBM [1]	SBMC [2]	SBM-BBR [3]	SBM-TPS [4]	SBM-GLU [5]	SBM-TAU [6]
Fish meal [7]	25.00	25.00	25.00	25.00	25.00	25.00
Soybean meal	28.59	28.59	28.59	28.59	28.59	28.59
Soy protein concentrate	8.00	8.00	8.00	8.00	8.00	8.00
Wheat gluten meal	11.00	11.00	11.00	11.00	11.00	11.00
Wheat flour	4.75	4.75	4.75	4.75	4.75	4.75
Fish oil	4.75	4.75	4.75	4.75	4.75	4.75
Soybean oil	1.00	1.00	1.00	1.00	1.00	1.00
Soybean lecithin	2.00	2.00	2.00	2.00	2.00	2.00
Premix for marine fish [8]	0.30	0.30	0.30	0.30	0.30	0.30
Choline chloride	0.50	0.50	0.50	0.50	0.50	0.50
Monocalcium phosphate	0.50	0.50	0.50	0.50	0.50	0.50
Additive	0.00	0.02	0.05	0.50	0.80	1.00
Feeding attractant [9]	0.10	0.10	0.10	0.10	0.10	0.10
Mildew preventive [10]	0.20	0.20	0.20	0.20	0.20	0.20
DL-Methionine	0.10	0.10	0.10	0.10	0.10	0.10
L-Lysine	1.50	1.50	1.50	1.50	1.50	1.50
Sodium carboxymethyl cellulose	3.72	3.70	3.66	3.21	2.91	2.71
Cellulose	96.28	96.30	96.34	96.79	97.09	97.29
Total	100.00	100.00	100.00	100.00	100.00	100.00
nutrient level (dry matter basis)						
Crude protein	49.95	50.22	49.93	49.93	50.34	50.56
Crude lipid	12.50	12.24	12.51	12.40	12.82	12.37
Crude ash	7.92	7.75	7.95	8.12	7.98	8.25

[1]SBM: As control diet, 50% of the fish meal protein was replaced by soybean meal.
[2-6]The additive-supplemented diets: Supplemented with 0.02% curcumin (SBMC), 0.05% berberine (SBM-BBR), 0.5% tea polyphenols (SBM-TPS), 1% taurine (SBM-TAU), or 0.8% glutamine (SBM-GLU) based on the control diet.
[7]Fish meal: Peruvian steamed fishmeal, Peru.
[8]Premix for marine fish: includes vitamin premix and mineral premix. vitamin premix (mg kg^{-1} diet); VB_1, 25; VB_2, 36.7; VA, 32; VE, 120; VD, 35; VK_3, 5.1; VC, 142; VB_6, 20; VB_{12}, 0.1; VH, 1.2; VB_5, 60; VB_9, 20; VB_3, 200; inositol, 792. mineral premix (mg kg^{-1} diet): magnesium sulfate, 1826; ferrous sulfate, 119; zinc sulfate, 76; manganese sulfate, 44; cobalt chloride, 2; potassium iodide, 0.8; copper sulfate, 1; sodium chloride, 100; monopotassium phosphate, 233.2; monosodium phosphate, 137.0.
[9]Feeding attractant: glycine:betaine = 1:3.
[10]Mildew preventive: fumaric acid:calcium propionate = 1:1.

and excess connective tissue was removed and fixed in 4% paraformaldehyde solution. Hindgut tissues were immersed in lyophilized vials containing RNA preservation solution (Solarbio, Beijing, China), flash-frozen in liquid nitrogen, and subsequently transferred to a −80°C refrigerator for storage. In addition, three fish were selected from each tank for the whole-body analysis.

2.4 Chemical analysis

The nutritional compositions of the experimental diets and whole fish were determined using the AOAC (1995) method. The samples were dried to a constant weight at 105 °C in a drying oven to measure the moisture content. Crude protein content was determined using a Kjeldahl nitrogen tester (BUCHI, KjeIFIex K-360, Switzerland). The crude fat content was determined using a Soxhlet extractor (FOSS Soxtec-2055, Sweden); the samples were heated in an electric furnace until they were smokeless and then cauterized to constant weight (4 h) using a Muffle furnace at 550°C to determine the ash content.

2.5 Histological analysis

The intestines and liver of three fish from each tank were collected for histometric evaluation. The fixed hindgut and liver

samples were collected and dehydrated using a fully automated dehydrator. The dehydrated tissues were paraffin-embedded, and transversely cut into 5–6 μm tissue sections with a microtome and dried overnight.

The H&E (hematoxylin and eosin) staining process was divided into the following steps: dewaxing, staining, dehydration, transparency, and sealing. The sealed sections were imaged using a 250 FLASH digital pathology system (3DHISTECH, Hungary). Image-Pro Plus 6.0 software (Media Cybernetics) was used to analyze the intestinal villus height (IVH), intestinal muscle thickness (IMRT), intestinal mucosal thickness (IMLT), and crypt depth (CD) in each group (7, 24, 25).

2.6 RNA extraction and real-time quantitative polymerase chain reaction

Total RNA was extracted and purified from distal intestinal tissue samples (approximately 50 mg) using the R1200 Total RNA Extraction Kit (Solarbio, Beijing, China) according to the manufacturer's instructions. RNA concentration and purity were determined using an ND-2000 spectrophotometer (NanoDrop 2000; Wilmington, DE, USA). OD260/280 values between 1.8 and 2.0 indicated high-quality RNA samples, and the relative amounts of RNA and its integrity were detected by electrophoresis. The cDNA was synthesized with the PrimeScript RT reagent Kit with gDNA Eraser Kit (TaKaRa, Japan) and stored at −20°C for future use.

Primers were designed using Primer 3 (https://primer3.ut.ee/) based on the sequences of yellow drum-related genes in the yellow drum transcriptome (the target genes are shown in Table 2), and the primers were synthesized by the Zhejiang Shangya Biological Company. RT-qPCR was performed using TransStart Tip Green qPCR SuperMix (All Style Gold, Beijing, China) on a StepOnePlus real-time PCR system (Thermo Fisher Scientific, USA). The constitutively expressed ribosomal protein *actb*, which was shown to be stably expressed in the yellow drum, was selected as the housekeeping gene for sample normalization. After the values were normalized to *actb*, the fold change in transcript levels was determined by the relative quantitative method ($2^{-\Delta\Delta CT}$).

2.7 Calculations and statistical analysis

The following variables were calculated:
Survival rate (SR, %).

$$SR = N_t \times 100/N_0$$

Weight gain (WG, %).

$$WG = 100 \times (W_t - W_0)/W_0$$

Specific growth rate (SGR per day, %/d).

$$SGR = 100 \times (Ln\ \ W_t - Ln\ \ W_0)/t$$

Feed efficiency ratio (FER, %).

$$FER = 100 \times weight\ \ gain/total\ \ amount\ \ of\ \ food\ \ consumed$$

Hepatosomatic index HSI (%).

$$HSI = 100 \times (liver\ \ weight/W_t)$$

Viscerosomatic index (VSI, %).

$$VSI = 100 \times (visceral\ \ weight/W_t)$$

Condition factor CF (g/cm^3).

$$CF = 100 \times (body\ \ weight,\ g)/(body\ \ lenght, cm)^3$$

where W_t and W_0 represent the final and initial fish weights, respectively; N_t and N_0 are the final and initial numbers of fish in each tank, respectively; and t represents the trial period in days.

Data were analyzed by one-way analysis of variance (ANOVA) using SPSS23.0 software, Duncan's multiple comparisons were

TABLE 2 Primers used for qRT-PCR.

Target gene	Forward primer (5′–3′)	Reverse primer (5′–3′)
actb	CCAACTCATTGGCATGGCTT	GATGCAACTGCAGAACCCTG
f-actin	AGGACAGCTACGTGGGAGAT	TGTTGGCTTTGGGGTTGAGT
Arp2/3	TACCCGGTGCTGTTTGTGTA	TGCACTGGTTTCTTCCTCCT
il1	TACTGTGCACCTGCCAAGAC	CTCTGTGCCCTTGTCCACTT
il6	TGAAGGCTCCGACGAAATG	GTCCAGTAGGCTAAACTGCTATC
tnfa	TGAAGAAGATGGTGCCCTTAC	GCCTGGAATCGAGCTCTAAAT
il10	CACTTTGTGGGCTACATCCA	GTTGAGGTATGCTGTGGTAGTC
tgfb	CGTCGCAGAACGCATCTATAA	CACGGCTATGATGTCCTGTATT
ocln	CCAGGCTACCAGGTGAAGAA	CTTCGGACAGGCGTGAAATC
zo1	TCACTCACCATGTTCCTCCC	CAGAAACACAGTTGGCTCCC
mlck	AGATGTGGAGGTGGTGGAAG	CGTGTATTTGGCATCGTCGT

actb, β-actin internal reference gene; f-actin, filamentous actin; arp2/3, arp2/3 complex; il1, interleukin 1; il6, interleukin 6; tnfa, tumor necrosis factor alpha; il10, interleukin 10; tgfb, transforming growth factor β; ocln, occludin; zo1, tight junction protein; mlck, myosin light chain kinase.

performed when the data were normally distributed within groups, and a $P< 0.05$ was considered statistically significant. The experimental results were expressed as mean ± standard error (mean ± SEM).

3 Results

3.1 Growth, survival, and morphological indices

The fish fed additive-supplemented diets had remarkably elevated WG, SGR, SR, and FER than those of fish fed the SBM diet. The WG and SGR of fish fed SBM-TPS or SBM-BBR were remarkably lower than those of fish fed SBMC, SBM-GlU, or SBM-TAU($P< 0.05$; Table 3).

The HSI and VSI differed significantly among the diets. The HSI of fish fed the SBM-BBR, SBM-TPS, and SBM-TAU diets were remarkably lower than that of fish fed the SBM diet ($P< 0.05$), whereas the HSI of fish fed the SBMC and SBM-GLU diets did not differ significantly from that of fish fed the SBM diet ($P > 0.05$). The VSI was significantly higher in fish fed the SBM-GLU diet than in those fed the SBM diet, and fish fed the SBM-TAU diet had significantly lower VSI than those fed the SBM diet.There were no significant differences between fish fed SBMC, SBM-BBR, or SBM-TPS diets and those fed SBM diets. The CF was not significantly different among the groups. ($P< 0.05$; Table 3).

3.2 Fish body composition

Excluding the fish in the SBM-GLU group, the fish fed the additive-supplemented diets had a remarkably lower moisture content than that of fish fed the SBM diet. The crude protein and lipid contents of fish fed the additive-supplemented diets, excluding the SBMC diet, were remarkably higher than those fed the control diet ($P< 0.05$; Table 4), whereas the crude lipid content of fish fed the SBMC diet did not differ significantly from that of fish fed the SBM diet ($P > 0.05$). Moreover, there was no significant difference in crude ash content between fish fed the additive-supplemented diets and those fed the SBM diet ($P > 0.05$).

3.3 Muscle amino acid composition analysis

The fish fed the additive-supplemented diets (except for the SBMC diet) had remarkably increased essential amino acid (EAA),

TABLE 3 Analysis of growth performance, survival rate and morphological indicators.

Parameter	Group					
	SBM	SBMC	SBM-BBR	SBM-TPS	SBM-GLU	SBM-TAU
IBW (g)	6.67 ± 0.02	6.66 ± 0.02	6.65 ± 0.02	6.65 ± 0.01	6.66 ± 0.02	6.65 ± 0.02
MBW (g)	24.51 ± 0.34	25.54 ± 0.75	25.40 ± 0.68	25.06 ± 0.38	25.47 ± 0.59	25.44 ± 1.04
FBW (g)	53.37 ± 1.42^{a}	61.16 ± 1.41^{c}	57.18 ± 0.72^{b}	56.44 ± 0.98^{b}	60.29 ± 0.53^{c}	60.28 ± 2.60^{c}
WG (%)	700.65 ± 20.52^{a}	817.74 ± 20.18^{c}	759.51 ± 8.63^{b}	748.24 ± 14.64^{b}	805.46 ± 5.45^{c}	806.12 ± 40.68^{c}
SGR (%/d)	4.16 ± 0.05^{a}	4.43 ± 0.04^{c}	4.30 ± 0.02^{b}	4.28 ± 0.03^{b}	4.41 ± 0.01^{c}	4.41 ± 0.09^{c}
SR (%)	90.67 ± 2.31^{a}	97.33 ± 2.31^{b}	98.67 ± 2.31^{b}	100.00 ± 0.00^{b}	98.67 ± 2.31^{b}	100.00 ± 0.00^{b}
FER(%)	100.57 ± 10.01^{a}	119.27 ± 2.04^{b}	114.93 ± 2.99^{b}	115.15 ± 1.15^{b}	118.66 ± 2.46^{b}	114.58 ± 4.61^{b}
HSI (%)	1.65 ± 0.15^{c}	1.64 ± 0.27^{c}	1.54 ± 0.28^{b}	1.41 ± 0.26^{a}	1.62 ± 0.23^{c}	1.39 ± 0.25^{a}
VSI (%)	5.11 ± 0.32^{b}	5.00 ± 0.62^{b}	5.05 ± 0.29^{b}	5.04 ± 0.69^{b}	5.40 ± 0.52^{c}	4.74 ± 0.51^{a}
CF (g/cm^{3})	1.89 ± 0.11	1.97 ± 0.13	1.92 ± 0.10	1.91 ± 0.11	1.92 ± 0.14	1.94 ± 0.13

Data represent mean ± SEM (n = 3). Based on one-way ANOVA, values in the same row with different superscript letters are significantly different (P< 0.05). IBW, initial body weight; MBW (28d): metaphase body weight; FBW, final body weight; WG, weight gain rate; SGR, specific growth rate; SR, survival rate; FER, feed efficiency ratio; HIS, hepatosomatic index; VSI, viscerosomatic index; CF, condition factor.

TABLE 4 Whole fish body composition analysis.

Parameter	Group					
	SBM	SBMC	SBM-BBR	SBM-TPS	SBM-GLU	SBM-TAU
Moisture (%)	73.83 ± 0.27^{b}	73.24 ± 0.38^{a}	73.02 ± 0.94^{a}	72.88 ± 0.13^{a}	73.64 ± 0.81^{ab}	73.06 ± 0.73^{a}
Crude protein (%)	15.15 ± 0.20^{a}	16.02 ± 0.30^{bc}	16.51 ± 0.36^{c}	16.00 ± 1.01^{bc}	16.64 ± 0.19^{c}	15.77 ± 0.26^{b}
Crude lipid (%)	6.07 ± 0.38^{a}	5.95 ± 0.13^{a}	6.39 ± 2.00^{b}	6.33 ± 1.23^{b}	6.37 ± 0.37^{b}	6.67 ± 1.67^{b}
Ash (%)	3.43 ± 0.17	3.58 ± 0.14	3.54 ± 0.17	3.65 ± 0.21	3.43 ± 0.10	3.60 ± 0.27

Data represent mean ± SEM (n = 3). Based on one-way ANOVA, values in the same row with different superscript letters are significantly different (P< 0.05).

non-essential amino acid (NEAA), and total amino acid (TAA) contents than in those fed the SBM diet ($P< 0.05$; Table 5). The TAA contents of fish fed the SBM-GLU and SBM-BBR diets were the highest.

3.4 Distal intestinal and liver micromorphology

Yellow drums fed the SBM diet exhibited intestinal fold atrophy and shortening, breakage, and detachment, enlargement of the intrinsic layer in the intestinal folds, and deepen the crypt depth, typical of SBMIE in the end of 8-week feeding trial. However, the intestinal morphology of the yellow drum significantly improved after consumption of the additive-supplemented diet (Figure 1). IVH, IMRT, and IMLT were significantly increased, and CD was remarkably decreased in fish fed an additive-supplemented diet, particularly the SBMC or SBM-GLU diets ($P< 0.05$; Table 6).

A proportion of the hepatocytes from fish fed the SBM diet exhibited irregular geometry, severe vacuolization, intracellular localized nuclei, and solidification, whereas others lacked nuclei and exhibited broken cellular structures (Figure 2A). In contrast, fish fed the additive-supplemented diets exhibited markedly improved liver morphology, as evidenced by reduced cellular vacuolization, with most nuclei being centrally located and with intact cellular structures (Figures 2B–F). The repair effect was the most significant in the SBMC group.

3.5 Distal intestinal physical barrier-related gene expression

Overall, the expression of *il1*, *il6*, and *tnfa* mRNAs was significantly downregulated, whereas that of *il10* and *tgfb* was significantly upregulated in the distal intestines of fish fed the additive-supplemented diets than that of fish fed the SBM diet ($P< 0.05$; Figures 3A, B). Whereas, no significant difference was observed in *il6* expression or a decrease in *il10* mRNA expression in fish fed SBM-BBR. Moreover, there was an elevated expression levels of *tnfa* mRNA but no significant different expression level of *il10* mRNA in the SBM-TPS diet than those of fish fed the SBM diet (Figures 3A, B).

The mRNA expression levels of filamentous actin (*f-actin*), arp2/3 complex (*arp2/3*), and occludin (*ocln*) were remarkably higher in fish fed the additive-supplemented diets ($P< 0.05$; Figure 3C) than in the SBM-fed group. In particular, the increase in *ocln* expression was more significant in fish fed SBMC, SBM-GLU, and SBM-TAU diets. Moreover, the zonula occludens-1 (*zo1*) mRNA expression was significantly higher, whereas that of myosin light-chain kinase (*mlck*) was remarkably lower in fish fed the

TABLE 5 Muscle amino acid composition analysis.

Parameter	Group					
	SBM	SBMC	SBM-BBR	SBM-TPS	SBM-GLU	SBM-TAU
Threonine (%)	3.49 ± 0.69^{ab}	3.56 ± 0.17^{abc}	4.12 ± 0.10^{bc}	3.96 ± 0.09^{bc}	4.69 ± 0.12^{c}	3.67 ± 0.19^{abc}
Valine (%)	3.72 ± 0.73^{ab}	3.79 ± 0.21^{ab}	4.37 ± 0.13^{b}	4.17 ± 0.10^{b}	4.40 ± 0.14^{b}	3.90 ± 0.22^{ab}
Methionine (%)	2.28 ± 0.26^{ab}	2.52 ± 0.17^{b}	2.89 ± 0.18^{c}	2.84 ± 0.14^{c}	3.00 ± 0.11^{c}	2.54 ± 0.09^{b}
Isoleucine (%)	3.49 ± 0.66^{ab}	3.56 ± 0.21^{abc}	4.11 ± 0.12^{bc}	3.92 ± 0.12^{bc}	4.15 ± 0.14^{c}	3.66 ± 0.20^{abc}
Leucine (%)	6.12 ± 1.19^{ab}	6.23 ± 0.33^{abc}	7.21 ± 0.26^{bc}	6.94 ± 0.16^{bc}	7.28 ± 0.24^{c}	6.47 ± 0.36^{abc}
Phenylalanine (%)	3.44 ± 0.66^{ab}	3.52 ± 0.19^{ab}	4.00 ± 0.18^{b}	3.89 ± 0.10^{b}	4.04 ± 0.13^{b}	3.62 ± 0.17^{ab}
Histidine (%)	1.57 ± 0.34^{ab}	1.60 ± 0.07^{abc}	1.89 ± 0.02c	1.79 ± 0.03bc	1.91 ± 0.08c	1.69 ± 0.11abc
Lysine (%)	7.26 ± 1.38^{ab}	7.41 ± 0.41^{abc}	8.50 ± 0.29^{bc}	8.24 ± 0.18^{bc}	8.63 ± 0.31^{c}	7.68 ± 0.41^{abc}
Arginine (%)	4.70 ± 0.92^{ab}	4.78 ± 0.20^{abc}	5.48 ± 0.15^{bc}	5.33 ± 0.11b^{c}	5.60 ± 0.13^{c}	4.97 ± 0.25^{abc}
EAA (%)	36.07 ± 6.81^{a}	36.97 ± 1.92^{a}	42.58 ± 1.31^{c}	41.08 ± 1.01^{c}	43.17 ± 1.39^{c}	38.19 ± 1.99^{b}
Serine (%)	3.22 ± 0.63^{ab}	3.31 ± 0.16^{abc}	3.87 ± 0.15^{cd}	3.75 ± 0.10^{bcd}	3.98 ± 0.11^{d}	3.46 ± 0.18^{abcd}
Glutamic acid (%)	12.61 ± 2.40^{ab}	12.78 ± 0.64^{ab}	14.89 ± 0.52^{bc}	14.46 ± 0.38^{bc}	15.29 ± 0.46^{c}	13.44 ± 0.72^{abc}
Glycine (%)	4.34 ± 0.88^{ab}	4.50 ± 0.09^{abc}	4.93 ± 0.29^{bc}	5.05 ± 0.03^{bc}	5.24 ± 0.18^{c}	4.03 ± 0.06^{a}
Alanine (%)	4.78 ± 0.90^{ab}	4.89 ± 0.22^{abc}	5.57 ± 0.22^{bc}	5.48 ± 0.10^{bc}	5.68 ± 0.16^{c}	5.05 ± 0.20^{abc}
Tyrosine (%)	2.75 ± 0.53^{ab}	2.79 ± 0.16^{ab}	3.21 ± 0.10^{b}	3.08 ± 0.07^{b}	3.25 ± 0.11^{b}	2.89 ± 0.17^{ab}
Asparagine (%)	8.13 ± 1.54^{ab}	8.27 ± 0.45^{abc}	9.53 ± 0.36^{bc}	9.25 ± 0.23^{bc}	9.69 ± 0.34^{c}	8.57 ± 0.45^{abc}
NEAA (%)	35.83 ± 6.86^{a}	36.54 ± 1.63^{a}	42.01 ± 1.64^{b}	41.08 ± 0.89^{b}	43.14 ± 1.17^{c}	37.42 ± 1.75^{ab}
TAA (%)	71.90 ± 13.67^{a}	73.51 ± 3.52^{a}	84.59 ± 2.95^{c}	82.16 ± 1.90^{b}	86.31 ± 2.55^{c}	75.61 ± 3.74^{ab}

Data represent mean ± SEM (n = 3). Based on one-way ANOVA, values in the same row with different superscript letters are significantly different ($P< 0.05$). EAA, essential amino acid; NEAA, non-essential amino acid; TAA, total amino acid.

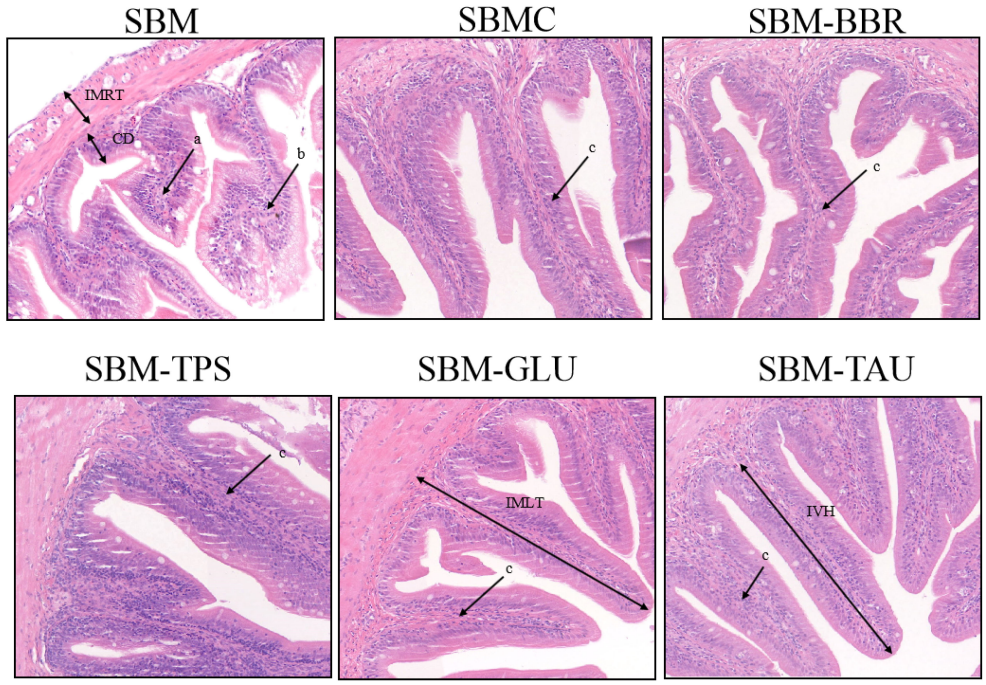

FIGURE 1
Representative histomorphological images from hematoxylin and eosin (H&E)-stained sections of the distal intestine. Scale Bar: 50 μm; (a) Widening of the lamina propria of the intestinal villi; (b) Intestinal villi atrophied, shortened; (c) intestinal villi are elongated and the lamina propria is thin; IVH, Intestinal villus height; IMRT, Intestinal muscular thickness; IMLT, Intestinal mucosal thickness; CD, Crypt depth.

additive-supplemented diets than that of fish fed the SBM diet ($P< 0.05$; Figure 3D).

4 Discussion

In the present study, we evaluated the effectiveness of five feed additives on the repair of SBMIE in yellow drums by assessing the growth performance, intestinal histological morphology, and mRNA expression levels of intestinal barrier-related factors. High levels of SBM in feed can induce intestinal inflammation and injury in carnivorous fish, reducing the ability of the intestinal epithelium to uptake nutrients, and ultimately decreasing fish growth performance (2). However, the growth and survival of fish fed a high proportion of soybean meal diet can be significantly improved through the supplementation of functional feed additives (26, 27). In this study, the growth performance of fish fed diets provided with various additives were remarkably improved compared to those fed the SBM diet. The WG, SGR, and FER of the yellow drum fed SBMC, SBM-GlU, and SBM-TAU diets were the highest. This may be due to the additives reducing intestinal inflammation and increasing intestinal villus length and absorption area. Long villus are related to fine intestinal fitness, nutrient beneficiation, and uptake efficiency, thus improving growth performance (28, 29). This is further corroborated by the histomorphometric measurements of the intestinal tract from this study.

Replacing a significant proportion of FM protein with plant proteins can affect fish intestinal health and reduce crude protein and lipid contents, effectively diminishing the nutritional value of fish (30, 31). However, previous research has indicated that additives supplemented in high plant protein replacing fish meal diet can significantly improve fish body composition (21, 32). In the

TABLE 6 Distal intestine tissue variable scores of the yellow drum fed the experimental diets.

Parameter	Group					
	SBM	SBMC	SBM-BBR	SBM-TPS	SBM-GLU	SBM-TAU
IVH (μm)	343.48 ± 6.94^{a}	449.22 ± 3.40^{c}	349.10 ± 13.31^{a}	436.2 ± 7.70a^{b}	455.03 ± 10.66^{c}	405.37 ± 16.45^{a}
IMLT(μm)	389.74 ± 3.05^{a}	583.91 ± 19.40^{c}	415.79 ± 22.04^{ab}	540.65 ± 16.82^{c}	532.57 ± 20.26^{c}	465.81 ± 16.22^{b}
IMRT(μm)	45.77 ± 2.54^{a}	108.53 ± 7.15^{d}	78.13 ± 1.52^{c}	74.73 ± 3.88^{c}	73.59 ± 2.01^{c}	59.62 ± 2.18^{b}
CD (μm)	77.84 ± 6.35^{b}	46.14 ± 3.82^{a}	46.31 ± 4.85^{a}	50.78 ± 4.77^{a}	48.78 ± 1.34^{a}	48.67 ± 2.66^{a}

Data represent mean ± SEM (n = 3). Based on one-way ANOVA, values in the same row with different superscript letters are significantly different ($P< 0.05$). IVH, intestinal villus height (μm); IMLT, Intestinal mucosal thickness; IMRT, Intestinal muscular thickness; CD, crypt depth (μm).

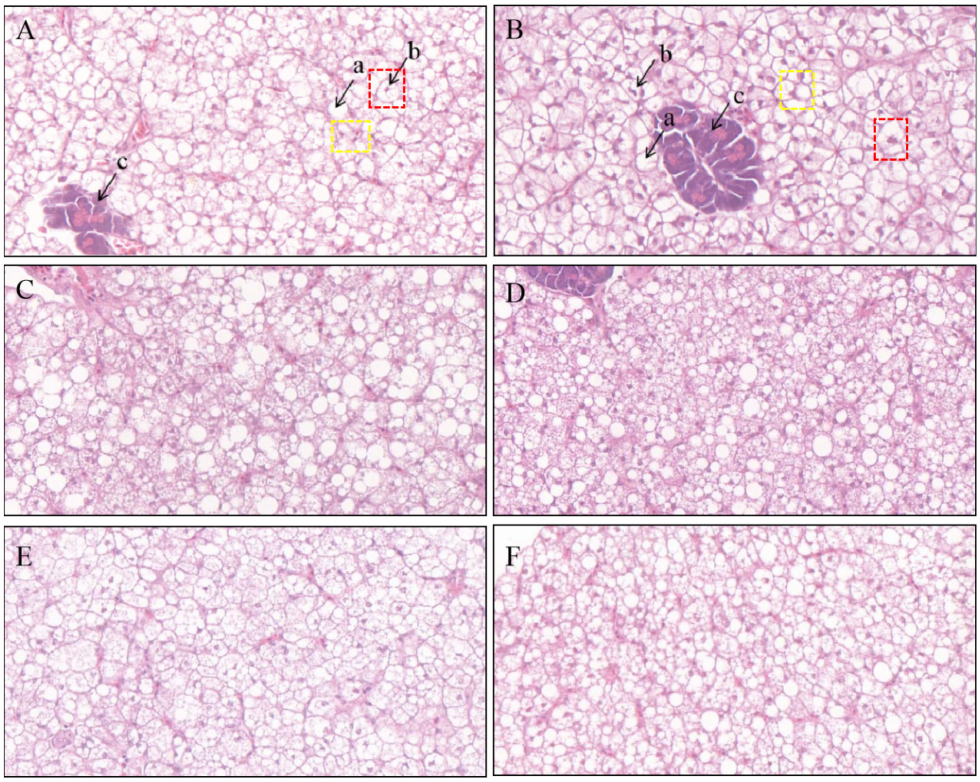

FIGURE 2
Representative histomorphological images from hematoxylin and eosin (H&E) stained sections of the liver. Scale Bar: 20 μm; **(A)** SBM; **(B)** SBMC; **(C)** SBM-BBR; **(D)** SBM-TPS; **(E)** SBM-GLU; **(F)** SBM-TAU; a: vacuolation; b: nucleus; c: portal vein; Red box: Normal liver cells; Yellow box: Liver cells with shifted nuclei.

present study, the whole-body crude protein and crude lipid contents of fish fed the additive-supplemented diets were remarkably higher, whereas the moisture content was significantly lower than that of fish fed the SBM diet. This is likely due to additives that enhance the conversion of ingested food into whole-body proteins and lipids by improving intestinal morphology.

Assessing the changes in intestinal morphology is the most common and direct method for evaluating intestinal barrier function (33). Dietary SBM-induced pro-inflammatory responses are caused by injury to the physical barrier of the intestinal mucosa, subsequently exposing the otherwise protected layers of the mucosa to luminal ingredients, including pathogenic bacteria or other food antigens, thereby exacerbating the enteritis (34). Moreover, the intestine is intricately connected to the liver in terms of immunity and digestion; hence, intestinal injury can lead to liver injury, following the intestine's exposure to harmful bacteria and metabolites (35–37). Nonetheless, the physical barrier of the intestinal mucosa can be improved by the ingestion of dietary additives that serve to repair intestinal injury (38, 39). As evidenced by the intestinal morphological indicators, the additives selected for this study significantly improved the intestinal integrity of yellow drums, which was characterized by increases in IVH, IMRT, IMLT, and CD. Similar results have been observed in *Epinephelus lanceolatus* (40) and *Oreochromis niloticus* (14), corroborating that additive-supplemented diets elicit reparative effects on the intestine injury of the yellow drum. Additionally, the degree of liver injury in fish was markedly ameliorated by the feed additives, which may be related to the repair of the intestinal physical barrier.

To further explore the reparative effects of the five selected additives on SBMIE, we assessed the mRNA expression levels of the intestinal barrier and immune-related genes. Intestinal tight junction proteins and cytoskeletal factors are crucial for protecting the integrity and function of the intestinal barrier, acting as epithelial barriers, and protecting the intestinal tract from viruses and harmful bacteria (41). Hence, intestinal tight junction injury increases the chance of intestinal inflammation. Multiprotein tight junction complexes include occludin, claudin, and ZOs (42–44). In the present study, the additives remarkably increased the mRNA expression levels of tight junction factors (*ocln, zo1*) in the intestine of yellow drum, while reducing that of *mlck*. Notably, *mlck* phosphorylates MLC and regulates tight junction permeability (45, 46). Hence, *mlck* downregulation likely reduced intestinal permeability and improved the symptoms of SBMIE. The cytoskeleton is central to maintaining cellular function and structure, and regulating adherens junctions (AJ) (47, 48). In this study, the mRNA expression of cytoskeletal factors (*f-actin* and *arp2/3*) increased in the intestines of yellow drums fed additive-supplemented diets. The upregulation of intestinal tight junctions and cytoskeletal factors suggests that intestinal barrier injury is repaired, thereby reducing the risk of intestinal inflammation (49). This is consistent with findings in other marine fish (50).

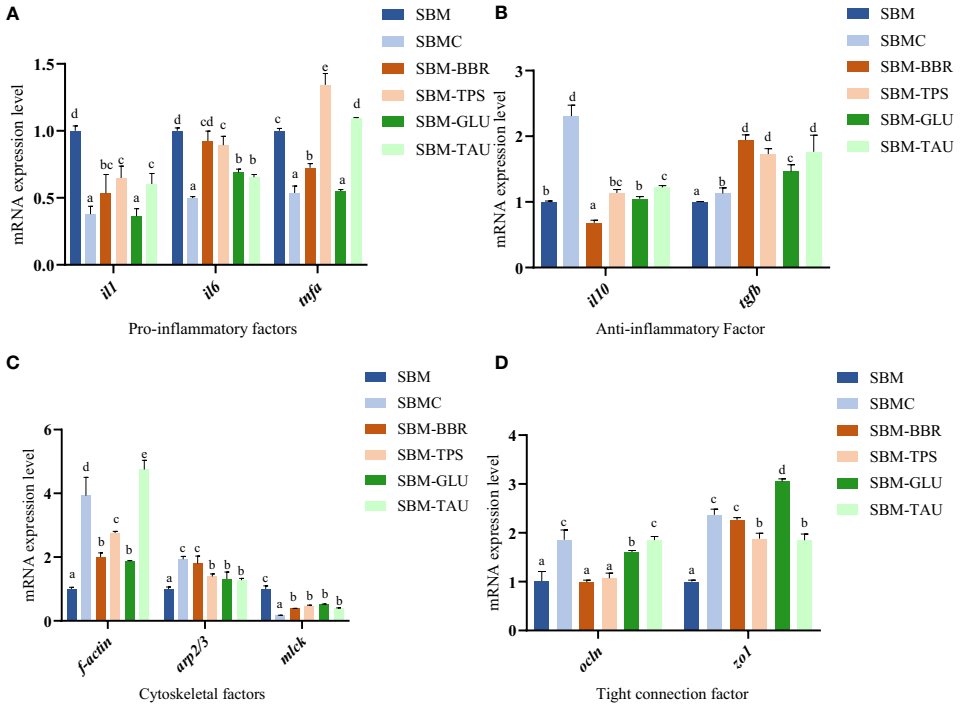

FIGURE 3
Relative mRNA expression of intestinal mucosal immunological barrier-related proteins in the distal intestine. Data represent as mean ± SEM (n = 3). According to the one-way ANOVA, values in the same row with different superscripts were significantly different (P< 0.05). SEM: standard error of the mean. il1, interleukin 1; il6, interleukin 6; tnfa, tumor necrosis factor alpha; il10, interleukin 10; tgfb, transforming growth factor β; f-actin, filamentous actin; arp2/3, arp2/3 complex; mlck, myosin light chain kinase; ocln, occludin; zo1, tight junction protein.

Inflammatory and anti-inflammatory cytokines secreted by the intestinal immune effector cells mediate the intestinal inflammatory response. Although proinflammatory cytokines boost the differentiation of T and B cells, leading to inflammation (51), anti-inflammatory cytokines may also reduce the probability of intestinal inflammation (52). The pro-inflammatory factors Il-1 and Tnf-α act as upstream signals for other pro-inflammatory factors, promoting their production. In contrast, Il-10 and Tgf-β are key factors in preventing enteritis development (53). The results of the current study indicated that the expression of *il1*, *il6*, and *tnfa* mRNA was remarkably downregulated, and *il10* and *tgfb* were remarkably upregulated in fish fed the additive-supplemented diets compared to those fed the SBM diet. This may be due to the additives regulating immune response signaling pathways (Liu et al., 2018), which is in line with the findings of Giri et al. (2019) and Cheng et al. (2011) (26, 54, 55). However, fish fed the SBM-BBR and SBM-TPS diets did not exhibit significant changes in anti-inflammatory or pro-inflammatory cytokine levels, potentially due to the limited repair effect of berberine and tea polyphenols on yellow drum SBMIE, which resulted in incomplete intestinal injury repair.

In summary, the additives selected for this study elicited reparative effects on SBMIE symptoms in yellow drum. The SBMC diet (supplemented with curcumin) had the most reparative effect on growth performance, intestinal morphology, and gene expression of yellow drum. It is speculated that the selected additives enhance the immune function of yellow drum by regulating anti-inflammatory and pro-inflammatory factors, and improve intestinal morphology and nutrient absorption by elevating the expression of intestinal barrier related genes in yellow drum, thereby enhancing the growth performance of yellow drum and increasing its tolerance to high-level soybean meal feed. However, the specific mechanism of the reparative effects of dietary additives in treating SBMIE in yellow drum should be studied further.

Data availability statement

The original contributions presented in the study are included in the article/supplementary material. Further inquiries can be directed to the corresponding authors.

Ethics statement

The animal studies were approved by Zhejiang Ocean University's Committee on Ethics of Animal Experiments. The studies were conducted in accordance with the local legislation and institutional requirements. Written informed consent was obtained from the owners for the participation of their animals in this study.

Author contributions

SM: Writing – original draft, Writing – review & editing. LW: Writing – original draft, Writing – review & editing. YZ: Writing – original draft. PT: Writing – original draft. RC: Writing – original draft. WH: Writing – original draft. DX: Writing – review & editing, Writing – original draft. HX: Writing – review & editing.

Funding

The author(s) declare financial support was received for the research, authorship, and/or publication of this article. This research was supported by grants from the National Natural Science Foundation of China (No. 31972785), the Distinguished Youth Fund of Zhejiang Province (No. LR21C190001), the Science and Technology Planning Project of ZhouShan city (No.2023C31040) and the Science and Technology Planning Project of Zhejiang Marine Fisheries Research Institute (No.HYS-CZ-202305).

Conflict of interest

The authors declare that the research was conducted in the absence of any commercial or financial relationships that could be construed as a potential conflict of interest.

Publisher's note

References

1. Sumon H, Rukshana KS, Subroto S, Sheikh MB, Mohammad LA, Jewel H, et al. Effects of dietary replacement of fish meal by soybean meal on growth, feed utilization, and health condition of stinging catfish, Heteropneustes fossilis. *Saudi J Biol Sci* (2023) 30:3. doi: 10.1016/j.sjbs.2023.103601

2. Buttle LG, Burrells AC, Good JE, Williams PD, Southgate PJ, Burrells C. The binding of soybean agglutinin (SBA) to the intestinal epithelium of Atlantic salmon, *Salmo salar* and rain-bow trout, *Oncorhynchus mykiss*, fed high levels of soybean meal. *Vet Immunol Immunopathol* (2001) 80:237–44. doi: 10.1016/S0165-2427(01)00269-0

3. Urán PA, Gonçalves AA, Taverne-Thiele JJ, Schrama JW, Verreth JAJ, Rombout JHWM. Soybean meal induces intestinal inflammation in common carp (*Cyprinus carpio* L.). *Fish Shellfish Immunol* (2008) 25:751–60. doi: 10.1016/j.fsi.2008.02.013

4. Lim SJ, Lee KJ. Partial replacement of fish meal by cotton-seed meal and soybean meal with iron and phytase supplementation for parrot fish Oplegnathus fasciatus. *Aquaculture* (2009) 290:283–9. doi: 10.1016/j.aquaculture.2009.02.018

5. Inderjit SM, Elvis MC, Elin CV, Åshild K, Anne MB. Transcriptional regulation of IL-17A and other inflammatory markers during the development of soybean meal-induced enteropathy in the distal intestine of Atlantic salmon (*Salmo salar* L.). *Cytokine* (2012) 60:186–96. doi: 10.1016/j.cyto.2012.05.027

6. Hedrera MI, Galdames JA, Jimenez-Reyes MF, Reyes AE, Avendaño-Herrera R, Romero J, et al. Soybean meal induces intestinal inflammation in zebrafish larvae. *PloS One* (2013) 8:e69983. doi: 10.1371/journal.pone.0069983

7. Gu M, Bai N, Zhang YQ, Åshild K. Soybean meal induces enteritis in turbot *Scophthalmus maximus* at high supplementation levels. *Aquaculture* (2016) 464:286–95. doi: 10.1016/j.aquaculture.2016.06.035

8. Wu X, Wang LG, Xie QP, Tan P. Effects of dietary sodium butyrate on growth, diet conversion, body chemical compositions and distal intestinal health in yellow drum (*Nibea albiflora*, Richardson). *Aquacult Res* (2020) 51:69–79. doi: 10.1111/are.14348

9. Deng J, Mai K, Ai QH, Zhang WB, Wang Xj, Xu W, et al. Effects of replacing fish meal with soy protein concentrate on feed intake and growth of juvenile Japanese flounder, Paralichthys Olivaceus. *Aquaculture* (2006) 258:503–13. doi: 10.1016/j.aquaculture.2006.04.004

10. Chen ZC, Liu Y, Li YX, Yang P, Hu HB, Yu GJ, et al. Dietary arginine supplementation mitigates the soybean meal induced enteropathy in juvenile turbot, *Scophthalmus maximus* L. *Aquacult Res* (2018) 49:1535–45. doi: 10.1111/are.13608

11. Jinho B, Ali H, Seonghun W, Wonsuk C, Sang-Gu L, Kang-Woong K, et al. Evaluation of seven different functional feed additives in a low fish meal diet for olive flounder, Paralichthys olivaceus. *Aquaculture* (2020) 525:735333. doi: 10.1016/j.aquaculture.2020.735333

12. NRC. *Nutrient requirements of fish and shrimp*. Washinghton: The National Academy Press (2011).

13. Bai SC, Katya K, Yun H. Additives in aquafeed: an overview. In: Davis DA, editor. *Feed and feeding practices in aquaculture*. UK,Cambridge: Woodhead Publishing (2015). p. 171–91.

14. Zhu F. A review on the application of herbal medicines in the disease control of aquatic animals. *Aquaculture* (2020) 526:735422. doi: 10.1016/j.aquaculture.2020.735422

15. Luo QH, Qian RD, Qiu ZS, Yamamoto FY, Du YY, Lin XW, et al. Dietary α-ketoglutarate alleviates glycinin and β-conglycinin induced damage in the intestine of mirror carp (*Cyprinus carpio*). *Front Immunol* (2023) 14:1140012. doi: 10.3389/fimmu.2023.1140012

16. Luo QH, Zhou ZL, Zhao JH, Xu H, Limbu SM, Xu QY. Dietary β-conglycinin induces intestinal enteritis and affects glycerophospholipid and arginine metabolism in mirror carp (*Cyprinus carpio*). *Aquaculture* (2023) 567:739257. doi: 10.1016/j.aquaculture.2023.739257

17. Abdel-Tawwab M, Eissa ESH, Tawfik WA, Abd Elnabi HE, Saadony S, Bazina WK, et al. Dietary curcumin nanoparticles promoted the performance, antioxidant activity, and humoral immunity, and modulated the hepatic and intestinal histology of Nile tilapia fingerlings. *Fish Physiol Biochem* (2022) 48:585–601. doi: 10.1007/s10695-022-01066-4

18. Yu CB, Zhang J, Qin Q, Liu J, Xu JX, Xu W. Berberine improved intestinal barrier function by modulating the intestinal microbiota in blunt snout bream (*Megalobrama amblycephala*) under dietary high-fat and high-carbohydrate stress. *Fish Shellfish Immunol* (2020) 102:336–49. doi: 10.1016/j.fsi.2020.04.052

19. Ma YB, Jiang WD, Wu P, Liu Y, Jiang J, Kuang SY, et al. Tea polyphenol alleviate Aeromonas hydrophila - induced intestinal physical barrier damage in grass carp (*Ctenopharyngodon idella*). *Aquaculture* (2021) 544:737067. doi: 10.1016/j.aquaculture.2021.737067

20. Fang H, Meng FP, Piao FY, Jin B, Li M and Li WZ. Effect of taurine on intestinal microbiota and immune cells in peyer's patches of immunosuppressive mice. *Adv Exp Med Biol* (2019) 1155:13–24. doi: 10.1007/978-981-13-8023-5_2

21. Cheng ZY, Buentello A, Gatlin DM. Effects of dietary arginine and glutamine on growth performance, immune responses and intestinal structure of red drum, Sciaenops ocellatus. *Aquaculture* (2011) 319:247–52. doi: 10.1016/j.aquaculture.2011.06.025

22. Han ZF, Xiao SJ, Li WB, Ye K, Wang ZY. The identification of growth, immune related genes and marker discovery through transcriptome in the yellow drum (*Nibea albiflora*). *Genes Genomics* (2018) 40:881–91. doi: 10.1007/s13258-018-0697-x

23. Wang LG, Lu Q, Luo SY, Zhan W, Chen RY, Lou B, et al. Effect of dietary lipid on growth performance, body composition, plasma biochemical parameters and liver fatty acids content of juvenile yellow drum *Nibea albiflora*. *Aquacult Rep* (2016) 4:10–6. doi: 10.1016/j.aqrep.2016.05.002

24. Huang JB, Zhou CP, Xu F, Luo XB, Huang XL, Huang Z, et al. Effects of partial replacement of fish meal with porcine meat meal on growth performance, antioxidant status, intestinal morphology, gut microflora and immune response of juvenile golden pompano (*Trachinotus ovatus*). *Aquaculture* (2022) 561:738646. doi: 10.1016/j.aquaculture.2022.738646

25. Femi JF, Rihanat OY, Oluwole OJ, Ibrahim A, Akeem OA, Benjamin OE. Effect of dietary polyherbal mixture on growth performance, haemato-immunological

indices, antioxidant responses, and intestinal morphometry of african catfish, clarias gariepinus. *Aquacult Nutr* (2022) 2022:11. doi: 10.1155/2022/5502796

26. Cheng ZY, Alejandro B, Delbert MG. Effects of dietary arginine and glutamine on growth performance, immune responses and intestinal structure of red drum, Sciaenops ocellatus. *Aquaculture* (2011) 319:247–52. doi: 10.1016/j.aquaculture.2011.06.025

27. Sahlmann C, Sutherland BJG, Kortner TM, Koop BF, Krogdahl A, Bakke AM. Early response of gene expression in the distal intestine of Atlantic salmon (*Salmo salar* L.) during the development of soybean meal induced enteritis. *Fish Shellfish Immunol* (2013) 34:599–609. doi: 10.1016/j.fsi.2012.11.031

28. Sklan D, Prag T. Lupatsch I.Structure and function of the small intestine of the tilapia *Oreochromis niloticus*× *Oreochromis aureus* (Teleostei, Cichlidae). *Aquacult Res* (2004) 35:350–7. doi: 10.1111/j.1365-2109.2004.01020.x

29. Huerta-Aguirre G, Paredes-Ramos KM, Becerra-Amezcua MP, Hernández-Calderas I, Matadamas-Guzman M, Guzmán-García X. Histopathological analysis of the intestine from Mugil cephalus on environment reference sites. In: Gómez-Oliván L, editor. *Pollution of water bodies in latin america*. Cham: Springer Press (2019). p. 319–28.

30. Regost C, Arzel J, Kaushik SJ. Partial or totalreplacementof fishmeal by corngluten meal in diet for turbot (*Psetta maxima*). *Aquaculture* (1999) 180:99–117. doi: 10.1016/S0044-8486(99)00026-5

31. Fournier V, Huelvan C, Desbruyeres E. Incorporation of a mixture of plant feedstuffs as substitute for fish meal in diets of juvenile turbot (*Psetta maxima*). *Aquaculture* (2004) 236:451–65. doi: 10.1016/j.aquaculture.2004.01.035

32. Cheng ZY, Dmi G, Buentello A. Dietary supplementation of arginine and/or glutamine influences growth performance, immune responses and intestinal morphology of hybrid striped bass (*Morone chrysops*×*Morone saxatilis*). *Aquaculture* (2012) 362-363:39–43. doi: 10.1016/j.aquaculture.2012.07.015

33. Chamorro S, Romero C, Brenes A, Sanchez-Patan F, Bartolome B, Viveros A, et al. Impact of a sustained consumption of grape extract on digestion, gut microbial metabolism and intestinal barrier in broiler chickens. *Food Funct* (2019) 10:1444–54. doi: 10.1039/C8FO02465K

34. Romarheim OH, Øverland M, Mydland LT, Skrede A, Landsverk T. Bacteria grown on natural gas prevent soybean meal-in-duced enteritis in Atlantic salmon. *J Nutr* (2011) 141:124–30. doi: 10.3945/jn.110.128900

35. Zhang XL, Chen JJ, Wang GD, Chen HX, Cao JL, Xie LT, et al. Interactive effects of fluoride and seleno-l-methionine at environmental related concentrations on zebrafish (*Danio rerio*) liver via the gut-liver axis. *Fish Shellfish Immunol* (2022) 127:690–702. doi: 10.1016/j.fsi.2022.07.006

36. Miao ZY, Miao ZR, Teng XH, Xu SW. Melatonin alleviates lead-induced fatty liver in the common carps (*Cyprinus carpio*) via gut-liver axis. *Environ Pollution* (2022) 317:120730. doi: 10.1016/j.envpol.2022.120730

37. Shan JW, Wang GX, Li H, Zhao XY, Ye WD, Su L, et al. The immunoregulatory role of fish specific type II SOCS via inhibiting metaflammation in the gut-liver axis. *Water Biol Secur* (2023) 2:100131. doi: 10.1016/j.watbs.2022.100131

38. Torrecillas S, Montero D, Caballero MJ, Robaina L, Zamorano MJ, Sweetman J, et al. Effects of dietary concentrated mannan oligosaccharides supplementation on growth, gut mucosal immune system and liver lipid metabolism of European sea bass (*Dicentrarchus labrax*) juveniles. *Fish Shellfish Immunol* (2015) 42:508–16. doi: 10.1016/j.fsi.2014.11.033

39. Duan Y, Zhang Y, Dong H, Wang Y, Zheng X, Zhang J. Effect of dietary Clostridium butyricum on growth, intestine health status and resistance to ammonia stress in Pacific white shrimp Litopenaeus vannamei. *Fish Shellfish Immunol* (2017) 65:25–33. doi: 10.1016/j.fsi.2017.03.048

40. Lin Y, Cheng M. Effects of dietary organic acid supplementation on the growth, nutrient digestibility and intestinal histology of the giant grouper *Epinephelus lanceolatus* fed a diet with soybean meal. *Aquaculture* (2017) 469:106–11. doi: 10.1016/j.aquaculture.2016.11.032

41. Ulluwishew D, Anderson RC, McNabb WC, Moughan PJ, Wells JM, Roy NC. Regulation of tight junction permeability byintestinal bacteria and dietary components. *J Nutr* (2011) 141:769–76. doi: 10.3945/jn.110.135657

42. Tsukita S, Furuse M, Itoh M. Multifunctional strands in tight junctions. *Nat Rev Mol Cell Biol* (2001) 2:285–93. doi: 10.1038/35067088

43. Schneeberger EE. The tight junction: a multifunctional complex. *Cell Physiol* (2004) 286:1213–28. doi: 10.1152/ajpcell.00558.2003

44. Chen Q, Chen O, Martins IM, Hou H, Zhao X, Blumberg JB, et al. Collagen peptides ameliorate intestinal epithelial barrier dysfunction in immunostimulatory Caco-2 cell monolayers via enhancing tight junctions. *Food Funct* (2017) 8:1144–51. doi: 10.1039/C6FO01347C

45. Turner JR. Intestinal mucosal barrier function in health and dis-ease. *Nat Rev Immunol* (2009) 9:799–809. doi: 10.1038/nri2653

46. Marchiando AM, Shen L, Graham WV, Edelblum KL, Duckworth CA, Guan Y, et al. The epithelial barrier is main-tained by in vivo tight junction expansion during pathologic intestinal epithelial shedding. *Gastroenterology* (2011) 140:1–2. doi: 10.1053/j.gastro.2011.01.004

47. Turner JR. 'Putting the squeeze' on the tight junction: understanding cytoskeletal regulation. *Semin Cell Dev Biol* (2000) 11:301–8. doi: 10.1006/scdb.2000.0180

48. Weis WI, Nelson WJ. Re-solving the cadherin-catenin-actin conundrum. *J Biol Chem* (2006) . 281:35593–7. doi: 10.1074/jbc.R600027200

49. Rimoldi S, Finzi G, Ceccotti C, Girardello R, Grimaldi A, Ascione C, et al. Butyrate and taurine exert a mitigating effect on the inflamed distal intestine of European sea bass fed with a high percentage of soybean meal. *Fisheries Aquat Sci* (2016) 19:40–53. doi: 10.1186/s41240-016-0041-9

50. Terova G, Díaz N, Rimoldi S, Ceccotti C, Gliozheni E, Piferrer F. Effects of sodium butyrate treatment on histone mod-ifications and the expression of genes related to epigenetic reg-ulatory mechanisms and immune response in European sea bass (*Dicentrarchus Labrax*) fed a plant - based diet. *PloS One* (2016) 11:e0160332. doi: 10.1371/journal.pone.0160332

51. Secombes CJ, Wang T, Hong S, Peddie S, Crampe M, Laing KJ, et al. Cytokines and innate immunity of fish. *Dev Comp Immunol* (2001) 25:713–23. doi: 10.1016/S0145-305X(01)00032-5

52. Savan R, Sakai M. Genomics of fish cytokines. *Comp Biochem Physiol Part D: Genomics Proteomics* (2006) 1:89–101. doi: 10.1016/j.cbd.2005.08.005

53. Kelly A, Houston SA, Sherwood E, Casulli J, Travis MA. Regulation of innate and adaptive immunity by TGFβ. *Adv Immunol* (2017) 134:137–233. doi: 10.1016/bs.ai.2017.01.001

54. Liu Y, Chen ZC, Dai JH, Yang P, Hu HB, Ai QH, et al. The protective role of glutamine on enteropathy induced by high dose of soybean meal in turbot, *Scophthalmus maximus* L. *Aquaculture* (2018) 497:510–9. doi: 10.1016/j.aquaculture.2018.08.021

55. Giri SS, Sukumaran V, Park SC. Effects of bioactive substance from turmeric on growth, skin mucosal immunity and antioxidant factors in common carp, cyprinus carpio. *Fish Shellfish Immunol* (2019) 92:612–20. doi: 10.1016/j.fsi.2019.06.053

frontiers | Frontiers in Immunology

TYPE Original Research
PUBLISHED 22 January 2024
DOI 10.3389/fimmu.2024.1342210

OPEN ACCESS

EDITED BY
Hongyu Liu,
Guangdong Ocean University, China

REVIEWED BY
Peng Tan,
Marine Fishery Institute of Zhejiang Province, China
Katerina Kousoulaki,
Fisheries and Aquaculture Research (Nofima), Norway
Yanjiao Zhang,
Ocean University of China, China

*CORRESPONDENCE
Chenglong Wu
wuchenglong007@163.com

RECEIVED 21 November 2023
ACCEPTED 08 January 2024
PUBLISHED 22 January 2024

CITATION
Zhang H, Zhao L, Zhang P, Xie Y, Yao X, Pan X, Fu Y, Wei J, Bai H, Shao X, Ye J and Wu C (2024) Effects of selenoprotein extracts from *Cardamine hupingshanensis* on growth, selenium metabolism, antioxidant capacity, immunity and intestinal health in largemouth bass *Micropterus salmoides*. *Front. Immunol.* 15:1342210. doi: 10.3389/fimmu.2024.1342210

Effects of selenoprotein extracts from *Cardamine hupingshanensis* on growth, selenium metabolism, antioxidant capacity, immunity and intestinal health in largemouth bass *Micropterus salmoides*

Hao Zhang[1,2], Long Zhao[1,2], Penghui Zhang[1,2], Yuanyuan Xie[1,2], Xinfeng Yao[1,2], Xuewen Pan[1,2], Yifan Fu[1,2], Jiao Wei[1,2], Hongfeng Bai[1,2], Xianping Shao[1,2], Jinyun Ye[1,2] and Chenglong Wu[1,2]*

[1]National-Local Joint Engineering Laboratory of Aquatic Animal Genetic Breeding and Nutrition (Zhejiang), School of Life Science, Huzhou University, Huzhou, China, [2]Zhejiang Provincial Key Laboratory of Aquatic Resources Conservation and Development, School of Life Science, Huzhou University, Huzhou, China

This study aimed to assess the impact of dietary selenoprotein extracts from *Cardamine hupingshanensis* (SePCH) on the growth, hematological parameters, selenium metabolism, immune responses, antioxidant capacities, inflammatory reactions and intestinal barrier functions in juvenile largemouth bass (*Micropterus salmoides*). The base diet was supplemented with four different concentrations of SePCH: 0.00, 0.30, 0.60 and 1.20 g/Kg (actual selenium contents: 0.37, 0.59, 0.84 and 1.30 mg/kg). These concentrations were used to formulate four isonitrogenous and isoenergetic diets for juvenile largemouth bass during a 60-day culture period. Adequate dietary SePCH (0.60 and 1.20 g/Kg) significantly increased weight gain and daily growth rate compared to the control groups (0.00 g/Kg). Furthermore, 0.60 and 1.20 g/Kg SePCH significantly enhanced amounts of white blood cells, red blood cells, platelets, lymphocytes and monocytes, and levels of hemoglobin, mean corpuscular volume and mean corpuscular hemoglobin in the hemocytes. In addition, 0.60 and 1.20 g/Kg SePCH increased the mRNA expression levels of selenocysteine lyase, selenophosphate synthase 1, 15 kDa selenoprotein, selenoprotein T2, selenoprotein H, selenoprotein P and selenoprotein K in the fish liver and intestine compared to the controls. Adequate SePCH not only significantly elevated the activities of antioxidant enzymes (Total superoxide dismutase, catalase, glutathione reductase, glutathione peroxidase), the levels of total antioxidant capacity and glutathione, while increased mRNA transcription levels of NF-E2-related factor 2, Cu/Zn-superoxide dismutase, catalase, glutathione reductase and glutathione peroxidase. However, adequate SePCH significantly decreased levels of malondialdehyde and H_2O_2 and the mRNA expression levels of kelch-like ECH-associated protein 1a and kelch-like ECH-associated protein 1b in the fish liver and intestine compared to the controls.

10.3389/fimmu.2024.1342210

Meanwhile, adequate SePCH markedly enhanced the levels of immune factors (alkaline phosphatase, acid phosphatase, lysozyme, complement component 3, complement component 4 and immunoglobulin M) and innate immune-related genes (lysozyme, hepcidin, liver-expressed antimicrobial peptide 2, complement component 3 and complement component 4) in the fish liver and intestine compared to the controls. Adequate SePCH reduced the levels of pro-inflammatory cytokines (tumour necrosis factor-α, interleukin 8, interleukin 1β and interferon γ), while increasing transforming growth factor β1 levels at both transcriptional and protein levels in the liver and intestine. The mRNA expression levels of mitogen-activated protein kinase 13 (MAPK 13), MAPK14 and nuclear factor kappa B p65 were significantly reduced in the liver and intestine of fish fed with 0.60 and 1.20 g/Kg SePCH compared to the controls. Histological sections also demonstrated that 0.60 and 1.20 g/Kg SePCH significantly increased intestinal villus height and villus width compared to the controls. Furthermore, the mRNA expression levels of tight junction proteins (zonula occludens-1, zonula occludens-3, Claudin-1, Claudin-3, Claudin-5, Claudin-11, Claudin-23 and Claudin-34) and Mucin-17 were significantly upregulated in the intestinal epithelial cells of 0.60 and 1.20 g/Kg SePCH groups compared to the controls. In conclusion, these results found that 0.60 and 1.20 g/Kg dietary SePCH can not only improve growth, hematological parameters, selenium metabolism, antioxidant capacities, enhance immune responses and intestinal functions, but also alleviate inflammatory responses. This information can serve as a useful reference for formulating feeds for largemouth bass.

KEYWORDS

***Micropterus salmoides*, selenoprotein extracts from *Cardamine hupingshanensis*, hematology, antioxidant capacities, immune and inflammatory responses**

1 Introduction

As an essential trace element, selenium (Se) has garnered significant attention for its diverse biological functions, encompassing the enhancement of growth, promotion of normal development and provision of antioxidant and anti-inflammatory activities in both humans and animals (1–3). Selenium sources are classified into two categories based on their composition and origin: inorganic Se (such as Sodium Selenite) and organic Se compounds like selenomethionine (SeMet), selenoyeast, selenocysteine (SeCys) and methylselenocysteine (4, 5). It is widely recognized that Se fulfills its biological roles by becoming integrated into various selenoproteins, including selenocysteine lyase (SCLY), selenophosphate synthase 1 (SPS1), selenoprotein P (SEPP), selenoprotein T (SEPT), selenoprotein W (SEPW), selenoprotein H (SEPH), selenoprotein K (SEPK), 15kDa selenoprotein (SEP15) and glutathione peroxidase (GPx), among others (2, 5). Depending on the dosage at which it is administered, Se assumes distinct physiological functions in both humans and animals (2, 6). Numerous studies have substantiated that Se deficiency or excess can lead to growth retardation, oxidative stress, compromised immunity and dysfunction of the intestinal barrier in animals (1–3, 6). Consequently, organic Se is often included in diets to satisfy the physiological requirements for normal growth and health in animals due to its superior bioavailability and reduced toxicity (1, 2, 6, 7). Nevertheless, limited information is available regarding the utilization of organic Se from plants, which are widely available and more cost-effective, in animals.

Numerous studies have identified the potential of organic selenium (Se) to exhibit antioxidant and immune regulatory effects in both humans and animals (4, 8, 9). Excessive production or content of reactive oxygen species (ROS) during metabolic imbalances and immune stimulation and/or responses can lead to oxidative stress and disruption of physiological functions, which is often indicated by the antioxidant response in animals under ROS overload (10, 11). Selenium is involved in the formation of a range of selenoproteins (SPS1, SEP15, SEPT, SEPH, SEPK and GPx), where it exists in the form of SeCys and SeMet, playing pivotal antioxidant roles in animals (5). It is widely recognized that Se is an essential and integral component of selenoproteins (2). These selenoproteins play crucial roles in antioxidant defense by catalyzing the reduction of peroxides with the assistance of glutathione, thus counteracting peroxidation processes (8, 11). Studies have consistently demonstrated that Se

deficiency can disrupt the antioxidant system, diminish the capacity to eliminate ROS and induce cellular damage in organisms (1, 12). Adequate Se levels can modulate intracellular redox status by regulating the expression and activities of redox-targeted proteins and enzymes, including superoxide dismutase (SOD), thioredoxin (Trx), catalase (CAT), GPx, glutathione reductase (GR), peroxiredoxin (Prx), glutathione S-transferase (GST), SEPH and SEPK, among others (4, 7). These regulatory mechanisms are primarily governed by the well-established Nrf2/Keap1 signaling pathway in human, mammals, and other animals (1, 13).

Furthermore, there exists a close relationship between the immune status of animals and hematological parameters, including white blood cells (WBC), neutrophils (NEU), red blood cells (RBC), hemoglobin (HGB), monocytes (MON), platelets (PLT), lymphocytes (LYM), mean corpuscular hemoglobin (MCH), mean corpuscular volume (MCV), mean corpuscular hemoglobin concentration (MCHC) and others (14, 15). Previous studies have highlighted that elevated levels of RBC, WBC, HGB and LYM can serve as indicators of improved immunity and can effectively enhance fish health by promoting the hematopoietic system through the provision of adequate nutrients (3, 16). Furthermore, immune capacities are intricately linked to antibacterial peptides, immune factors, immunoglobulins (Igs) and selenoproteins found in these immune tissues or organs of animals and fish (8, 17). Among these parameters, selenoproteins can enhance the immune process by regulating the synergistic interactions among these immune cells and inhibiting the expression and contents of inflammatory factors, include tumour necrosis factor-α (TNF-α), interleukins (ILs) and interferons (IFNs), etc. (10, 11). Previous research has proved Se deficiency can impair immune functions by reducing the production or contents of antibacterial compounds and immunoglobulins, as well as mRNA expression levels of antimicrobial peptides and selenoproteins (12, 17). Despite the numerous reports on the antioxidant and immune capacities mediated by sodium selenite and Se yeast, limited information is available concerning the comprehensive relationship between hematological parameters, antioxidant capacities, immune functions and dietary organic Se derived from plant sources in animals and fish species.

Moreover, previous studies have demonstrated Se deficiency can exacerbate inflammatory responses in humans and animals by modulating the levels of pro-inflammatory cytokines and anti-inflammatory cytokines, which include ILs, IFNs, TNF-α, transforming growth factor β1 (TGF-β1) and others (11, 12). Consequently, the overproduction of these inflammatory cytokines (e.g. TNF-α, IL-8, IL-1β and IFN-γ) can lead to cell damage and a decline in immune function in various tissues (10, 11). The content or production of these cytokines is primarily regulated by the p38 MAPK/NF-kB signaling transduction pathway in both humans and animals (4, 18, 19). However, these inflammatory processes can typically be mitigated by elevating the levels or contents of anti-inflammatory cytokines, such as TGF-β1 and IL-10 (11, 20). Furthermore, Se deficiency can severely impair the structure of mucosal cells and the physical barrier of the intestine, thereby limiting digestion and absorption and increasing the risk of disease in animals (21, 22). It is well-established that the intestinal integrity and functions are closely linked to the increased expression levels of tight junction proteins (TJs), including occludin (OCLN), zonula occludens (ZOs) and claudins (CLDNs) in the epithelial cells of the intestines in both humans and animals (23, 24). These proteins play a vital role in forming a protective gel that maintains the integrity and function of the intestinal barrier, accomplished through mucin-linked carbohydrates (22). Furthermore, as the key component of intestinal mucus, mucins (MUCs) are mainly produced by goblet cells to protect the epithelium from bacteria or hazardous materials (25). Consequently, MUCs serve critical structural and functional roles within the intestinal epithelial tissue and are essential for preserving intestinal health and immune function (26). Despite the fact that adequate inorganic Se and yeast-Se have been shown to alleviate inflammatory responses, protect the integrity of the intestinal structure and enhance intestinal barrier functions in animals (9, 24), there is limited information available about the effects of organic plant-derived Se on inflammatory responses and intestinal barrier functions in fish up to this point.

Cardamine hupingshanensis, a member of the cruciferous plant genus, is a distinctive organic Se source known for its elevated Se content across all its tissues (27–29). The primary bioactive compound within *C. hupingshanensis* is selenocysteine, which plays a pivotal role in selenoprotein synthesis, thereby contributing to a range of physiological functions (28, 29). Consequently, selenoprotein extracts from *C. hupingshanensis* (SePCH) constitute an innovative organic Se source endowed with robust antioxidant and immune-enhancing properties. However, there has been limited exploration into the use of SePCH as a dietary organic Se supplement in fish feed. As a carnivorous fish species, largemouth bass (*Micropterus salmoides*) has gained widespread cultivation in China owing to its rapid growth, robust adaptability and superior meat quality, thus establishing itself as one of the foremost commercial freshwater species in the country, with an output of 0.8 million tons in 2022 (30). While yeast-Se requirements have been studied in largemouth bass (1), the current knowledge landscape lacks insights into the SePCH requirements for this economically significant species in freshwater aquaculture. Consequently, this experiment is designed to evaluate the impacts of SePCH on largemouth bass, focusing on gene expression and protein production. Furthermore, we aim to elucidate the underlying mechanisms through which dietary SePCH influences intestinal barrier functions and the immune system, accomplished by analyzing hematological parameters, inflammation, oxidative stress and the transcription variations of TJs and MUCs. These findings provide valuable information for optimizing the formulation of compound feeds tailored to largemouth bass.

2 Materials and methods

The care and ethical treatment of the experimental animals strictly adhered to the "Guidance of the Care and Use of Laboratory Animals." The research protocol involving the experimental subjects received approval from the National-Local Joint

Engineering Laboratory of Aquatic Animal Genetic Breeding and Nutrition (Zhejiang).

2.1 Feed composition and experimental diets

The primary protein sources in these artificial diets were casein and fish meal, while rapeseed oil served as the principal lipid source. The base diet was supplemented with 0.00, 0.30, 0.60 and 1.20 g/Kg of SePCH to form four isonitrogenous and isoenergetic diets (see Table 1 for details). The actual selenium contents are 0.37, 0.59, 0.84 and 1.30 mg/kg in these four different diets, respectively, measured with iCAPRQ ICP-MS (thermo, USA). All components underwent filtration using a 60-μm mesh and were blended according to the specifications provided in Table 1. Subsequently, these mixture underwent processing using a F-26 dual-screw extruder (Machinery Factory of South China University of Technology, Guangzhou, China), and made into pellets with 1.5 × 2.5 mm following the procedures outlined by Wu et al. (16) and Jia et al. (31). These pellets were dried at 35°C in one airflow drying oven for at least 24 hours and stored at -20°C until further use.

2.2 Fish and feeding trial

The feeding trial took place at the Aquatic animal culture center, Huzhou University. Healthy juvenile largemouth bass were procured from Zhejiang Deqing Longshengli Aquatic Hatchery (Huzhou, China) and acclimated in a recirculating aquaculture tanks for a period of two weeks prior to the experiment. During this acclimation period, they were provided with a basal diet devoid of SePCH. A total of 300 juvenile largemouth bass, initially weighing (5.04 ± 0.02)g, were selected and randomly allocated to 12 aquaculture tanks. There were 4 different experimental groups in these tanks, each with 3 replicates. Within each replicate, 25 fish were reared for a duration of 60 days. The daily feed intake during the culture period was maintained at 3% of the total fish weight and was administered at 8:00 and 17:00, respectively. Tank water was exchanged every other day, and

TABLE 1 Ingredient and proximate composition of basal diet (on dry weight basis).

Ingredients	Feed Diets (g/Kg)			
	0.00	0.30	0.60	1.20
Casein [a]	350.00	350.00	350.00	350.00
Soybean meal [b]	100.00	100.00	100.00	100.00
Gelatinized tapioca starch [c]	100.00	100.00	100.00	100.00
Fish meal [d]	200.00	200.00	200.00	200.00
Rapeseed oil [e]	65.00	65.00	65.00	65.00
Microcrystalline cellulose [f]	131.00	130.70	130.40	129.80
Mineral premix [g]	20.00	20.00	20.00	20.00
Vitamin premix [h]	10.00	10.00	10.00	10.00
Lecithin [i]	20.00	20.00	20.00	20.00
Choline chloride [j]	4.00	4.00	4.00	4.00
Selenoprotein extracts from *C. hupingshanensis* [k]	0.00	0.30	0.60	1.20
Nutrient levels (g/kg dry matter basis)				
Crude protein	494.67	490.10	491.30	482.31
Crude lipid	114.7	117.7	118.0	118.0
Moisture	36.86	33.86	35.73	37.45
Crude Ash	59.91	60.23	60.29	60.41

[a]Casein, obtained from Gansu Hualing Dairy Co., Ltd., Lanzhou, China; crude protein 80.56%.
[b]Soybean meal, obtained from Ningbo Food Co., Ltd., Zhejiang, China.
[c]Gelatinized tapioca starch, obtained from Xinxin biochemical technology Co., Ltd., Zhejiang, China.
[d]Fish meal, Pesquera Diamante S.A. crude protein 66.7%; crude lipid 9.8%.
[e]Rapeseed oil, produced using oil press.
[f]Microcrystalline cellulose, obtained from Sinopharm Chemical Reagent Co., Ltd., Shanghai, China.
[g]Mineral premix (mg/kg) Mineral mixture: KI 0.4mg, $CoCl_2$-$6H_2O$ 52 mg, $CuSO_4$-$5H_2O$ 16 mg, $FeSO_4$-$7H_2O$ 200 mg, $ZnSO_4$-H_2O 280 mg, $MnSO_4$-H_2O 45 mg, $MgSO_4$-$7H_2O$ 1200 mg, $Ca(H_2PO_4)_2$ 12000 mg, NaCl 60 mg.
[h]Vitamin premix (mg/kg) Vitamin premix: vitamin A, 20 mg; vitamin D3, 3 mg; vitamin C, 300 mg; vitamin E, 300 mg; thiamin, 20 mg; riboflavin, 10 mg; pyridoxine HCl, 20 mg; vitamin B12, 0.2 mg; vitamin K3, 5 mg; inositol, 1000 mg; pantothenic acid, 30 mg; folic acid, 3 mg; niacin acid, 50 mg; biotin, 1 mg.
[i]lecithin, Jiangsu Yuanshengyuan Biological Engineering Co., Ltd., Nanjing, China.
[j]Choline chloride, obtained from Xinxin biotechnology Co., Ltd., Shandong, China.
[k]Purchased from Hubei Shengxi Biotechnology Co Ltd: The selenium content in the Selenium-enriched C. hupingshanensis was 764 mg/kg.

thorough suctioning was performed to ensure water quality. Throughout the experimental period, water temperature was mainly stayed at 26.5-28.5°C, with natural lighting conditions and dissolved oxygen levels exceeding 5.8 mg/L.

2.3 Sample collection and detection of growth performances

After a 24-hour fasting period, fish from these 12 tanks were counted at the end of feeding trial. Subsequently, they were weighed to evaluate weight gain (WG) and daily growth rate (DGR) after being anesthetized with tricaine methane sulfonate (100 ppm) (MS-222, Sigma, St. Louis, MO, USA). Samples were then collected on ice for further analyses. Blood for hematological analysis was obtained from the caudal tail veins of fifteen fish randomly selected from each tank. Approximately 0.3 mL of blood was selected in 2 ml heparinized Eppendorf tubes. Liver and intestine specimens were also collected and promptly flash-frozen in liquid nitrogen and then deposited at -80 °C for the next measurements and analysis of relative enzyme activity and gene transcription variations.

2.4 Hematological analyses

TEK 8500VET automatic blood analyzer provided by Jiangxi Tekang Technology (Nanchang, China) was employed for hematological analysis, which encompassed assessments of total cell counts and various cell categories. Parameters examined included counts of WBC, RBC, HGB, PLT, MCV, MCH, MCHC, MON, LYM and NEU. Fifteen duplicate blood samples from each group were subjected to analysis

2.5 Measurements of antioxidant enzyme activities and immunological parameters

To assess antioxidant enzyme activities' variation in these fish liver and intestine, frozen tissue samples were initially pulverized using liquid nitrogen. Subsequently, the samples were homogenized with a 0.9% NaCl solution at a volume ratio of 1:9 (w/v) at 4°C. Following homogenization, the suspensions were subjected to centrifugation at 3000 rpm for 20 minutes at 4°C, and the resulting supernatants were collected. Coomassie Brilliant Blue technique was used to determine the protein concentrations of these supernatants. Activities or contents of SOD, CAT, GPx, GST, GR, glutathione (GSH), malondialdehyde (MDA), hydrogen peroxide (H_2O_2), total antioxidant capacity (T-AOC) and Kelch-like ECH-associated protein 1a (Keap1a) were determined with commercially available kits in accordance with these corresponding instructions provided by Jiancheng Bioengineering (Jiancheng, Nanjing, China). The activities or the levels of lysozyme, complement component 3 (C3), C4, acid phosphatase (ACP), IgM, alkaline phosphatase (ALP), TNF-α, IL-1β, IL-8, IFN-γ and TGF-β1 were also measured using diagnostic assay kits following these corresponding instructions provided by Henyuan Biotech (Shanghai, China). Each measurement was carried out in triplicate.

2.6 Measurements of genes expression

The total RNA were extracted from fish liver and intestine samples using the TRIzol reagent (Invitrogen, USA). The concentration and integrity of these RNA samples were detected through spectrophotometry and electrophoresis following the procedures outlined by Wu et al. (32). After treatment with DNase I treatment (Takara, Dalian, China), 10 μg of total RNA samples were reverse transcribed with SuperScript™ II RT (Takara, Dalian, China) in 75 μL reactions. Primers for quantitative real-time PCR were designed according to largemouth bass genes (Table 2). Primer synthesis was carried out by Biosune Co. (Shanghai, China). β-actin was served as the internal reference. Quantitative PCR (qPCR) assays were conducted following the methods described by Wu et al. (16) and Yang et al. (33). Each analysis was performed carried out in at least triplicate.

2.7 Measurements of histomorphometry

Posterior intestine samples were firstly rinsed with 0.6% saline and then fixed in 4% paraformaldehyde for 48 hours. Subsequently, the samples underwent dehydration in a series of ethanol solutions with increasing concentrations, clearing with xylene and embedding in paraffin wax. The hematoxylin and eosin (H&E) staining method was used to generate and stain histological sections. Photographic documentation of the intestine was carried out by capturing micrographs at a final magnification of 100× using a digital camera. These acquired images were then subjected to analysis using K-Viewe 1.5 software (https://kv.kintoneapp.com/en/user/, accessed on 16 June 2023) to quantify villus height, villi width, muscle thickness and crypt depth. All measurements were performed with a minimum of three replicates.

2.8 Statistical analyses

The following equations were used to calculate animal-specific parameters:

$$\text{Weight gain (WG, \%)} = [(\text{final body weight (FBW)} - \text{initial body weight (IBW)})/\text{initial body weight (IBW)}] \times 100.$$

$$\text{Daily growth rate (DGR, \%)} = [(\text{final body weight (FBW)} - \text{initial body weight (IBW)})/\text{initial body weight (IBW)} * 60\ \text{days}] \times 100.$$

The results derived from the analysis were presented as mean ± standard deviation (SD). To compare these various groups, a one-way analysis of variance (ANOVA) was performed with SPSS 22.0 software (IBM, Chicago, IL, USA). For additional comparisons

10.3389/fimmu.2024.1342210

TABLE 2 Primer sequences for real-time PCR analysis.

Gene	Forward (5′– 3′)	Reverse (5′– 3′)	Reference
SCLY	GTGCCGCCTGCCACTCAAA	TCCTGCCCACGCTCAACCT	XM_038716707.1
SPS1	CGACATCACAGGGTTTGGC	TTGGCTAGGACTGGGAGGTTA	XM_038705397.1
SEP15	GGAGTGAAAAGCCGAAGATGT	CTTCAGCGATGTTCCCGTTA	XM_038718375.1
SEPT2	AGAGCCTGGACCTGGAGT	TCGTTTAGCGTGACTTCG	XM_038699855.1
SEPH	AGGCTGATGAGGAGAAAG	GCATTACGCCCATACACT	XM_038699684.1
SEPP	CTCACACACCACATTTCAC	ATCAGCTTTCTCTTTGCAC	XM_038702803.1
SEPK	TGCTTCGTCACGCTTCACT	TCATCCTCCTCCACCCATT	XM_038723206.1
Cu/Zn-SOD	TGAGCAGGAGGGCGATTC	GCACTGATGCACCCATTTGTA	XM_038708943.1
Mn-SOD	CAGGGATCTACAGGTCTCATT	ACGCTCGCTCACATTCTC	XM_038727054.1
CAT	ACCTATTGCTGTCCGCTTCTC	TCCCAGTTGCCCTCCTCA	XM_038704976.1
GPx1	TTTGGAGTCCCGTCTGTA	CTGCCTCAATGTCAATGGT	XM_038697220.1
GPx3	CCCTCCAGTTGGAAACGA	ACTTGGGTGCCACCTCAT	XM_038699914.1
GR	ATCACGAGCAGGAAGAGTCAG	CATCTCATCACAGCCCAAGC	XM_038700350.1
GST	GAGCCCATCAGAACACCC	ACCCAAATAGCACCCAAC	XM_038729946.1
Keap1a	GTGGTGGGAAGACTTATTG	TCCAGGTGCTTAGTGAGG	XM_038728593.1
Keap1b	CCTTACTCCAGGCTGTCCG	GAAATTACTTTGGTGGGTTTGT	XM_038713665.1
Nrf2	CAAAGACAAGCGTAAGAAGC	CAGGCAGATTGATAATCATAGA	XM_038720536.1
C3	CCACTATGCCACGAGAAC	GAGCGTAATACAGCGACAC	XM_038714039.1
C4	TGGTGGTCGTCCTGCGTC	CCCTCCTGGTTGGTGGTG	XM_038711699.1
lysozyme	CTCTCATTGCTGCCATCA	TGTGTCCACCTCCGTTTG	XM_038713808.1
HEPC	CTCTGCCGTCCCATTCAC	GCATCATCCACGATTCCATT	XM_038710826.1
LEAP-2	AAGGAAAGCAGCAGTAGCG	CTGCCTTCTGGTCAGAGTTG	XM_038731861.1
TGF-β1	CCCGCTTCATCACTAATA	GTTGGAAACCCTTCTCAT	XM_038693206.1
IL-10	CCAGCAGCATCATTACCA	CAGAACCAGGACGGACAG	XM_038696252.1
IL-1β	CGACCGCAGTAAGAAAGA	TCGATGTACCTCGAAAGT	XM_038733429.1
IL-8	TGGCACTCCTGGTCATCC	GCACCTCCACCTGTCCTAT	XM_038713529.1
TNF-α	CAACGGCAAGTGTCAAACCC	TCTTGTCCTGAGCCCTTGGTAT	XM_038723994.1
IFN-γ	GAGTTGCTTTGGCGTTTG	TGTTGATGCTCCTGGTGA	XM_038709291.1
NF-κB p65	GCACAGGACGAGGATGGA	CAGGCAGGGCAGAGACAA	XM_038699792.1
MAPK13	GATGCTGGTTCTGGATGG	TAGGCTCAGGAAAGTCGT	XM_038723459.1
MAPK14	CCACGTTCAGTTCCTTATCTAC	CTCGCAGTCTTCATTCACAG	XM_038696748.1
ZO-1	TTCTAACGGTGGTGTCCTG	TTGTCAAGTGGTGGCAAG	XM_038701018.1
ZO-3	GGACCCCCAGACTTTGTA	AGAGCGAGCCTGTTGTAA	XM_038716281.1
OCLN	ATTCCTGGTTGTCATCGC	AGAGGCTCATCCCAGTAGA	XM_038715419.1
CLDN-1	CTCTGTGGCTGTGGGAACT	GAACATGGTGTCGCTGTAAGT	XM_038713307.1
CLDN-3	CCCGTGCCCTCACCGTTAT	TTGGATGCCTCGTCGTCA	XM_038693400.1
CLDN-11	CCAAGAACAAACGCACCA	TAGAGGGAGAAGCCGAAT	XM_038729166.1
CLDN-5	AGGTGCCCGCATCCCAGAA	AGGGACAGGAGCAGCACAGC	XM_038704228.1
CLDN-23	TGTCTTCACTGCCGCTAT	CCCTGACCTTTCACTCCT	XM_038729173.1

(Continued)

TABLE 2 Continued

Gene	Forward (5′– 3′)	Reverse (5′– 3′)	Reference
CLDN-34	GGAACGTCTACTTTGGGA	GGAACTTGATGGTCTGAT	XM_038715311.1
MUC-2	CTGTATGCCCAGAAGATAAGC	TGGTAGCACGTTCCCAAA	XM_038706114.1
MUC-5AC	ATGGACAACAGACTGATCTTCG	GGTTATCGTCGTCGTAGGG	XM_038731574.1
MUC-17	ATGAAACCATAACCGTAC	TATCACCACAATGAGCAG	XM_038725272.1
β-actin	TCCTGCGTCTTGACTTGG	GATTTCCCTTTCGGCTGT	XM_038695351.1

SCLY, selenocysteine lyase; SPS1, selenophosphate synthase 1; SEP15, 15 kDa selenoprotein; SEPT2, selenoprotein T2; SEPH, selenoprotein H; SEPP, selenoprotein P; SEPK, selenoprotein K; Cu/Zn-SOD, Cu/Zn-Superoxide dismutase; Mn-SOD, Mn-Superoxide dismutase; CAT, catalase; GPx3, glutathione peroxidase 3; GPx1, glutathione peroxidase 1; GR, glutathione reductase; GST, glutathione S-transferase; Keap1a, kelch-like ECH-associated protein 1a; Keap1b, kelch-like ECH-associated protein 1b; Nrf2, NF-E2-related factor 2; C3, complement component 3; C4, complement component 4; lysozyme; HEPC, hepcidin; LEAP-2, liver-expressed antimicrobial peptide 2; IL-10, interleukin 10; TGF-β1, transforming growth factor β1; IL-1β, interleukin-1β; IL-8, interleukin 8; TNF-α, tumour necrosis factor-α; IFN-γ, interferon-γ; NF-κB, nuclear factorkappa B; MAPK13, mitogen-activated protein kinase 13; MAPK14, mitogen-activated protein kinase 14; ZO-1, zonula occludens-1; ZO-3, zonula occludens-3; OCLN, Occludin; CLDN-1, Claudin-1; CLDN-3, Claudin-3; CLDN-11, Claudin-11; CLDN-5, Claudin-5; CLDN-23, Claudin-23; CLDN-34, Claudin-34; MUC-2, Mucin-2; MUC-5AC, Mucin-5AC; MUC-17, Mucin-17.

among the diverse dietary treatments, Duncan's multiple range test was employed with a multiple comparison test. Additionally, to investigate any significant linear or quadratic effects, orthogonal polynomial comparisons were conducted. $p< 0.05$ was utilized to determine the presence of statistical differences.

3 Results

3.1 Growth performance and hematological indices

Following an 8-week cultivation period, the dietary inclusion of SePCH exhibited a beneficial impact on the growth parameters of largemouth bass. Evaluation of the growth parameters revealed that supplementation with 0.60 and 1.20 g/Kg SePCH markedly increased both WG and DGR compared to the control groups (0.00 g/Kg SePCH) ($p< 0.05$) (Figure 1). Furthermore, several hematological indicators showed significant improvements in the 0.60 and 1.20 g/Kg SePCH groups compared to the SePCH deficient groups or control groups ($p< 0.05$). Specifically, counts or levels of WBC, MCV, MCH and MON were markedly enhanced in 0.60 and 1.20 g/Kg SePCH groups compared to the control groups ($p< 0.05$). Additionally, LYM counts notably increased in 0.30, 0.60 and 1.20 g/Kg SePCH groups compared to the controls ($p< 0.05$). As the levels of SePCH supplementation increased, RBC, HGB and PLT levels also increased significantly, reaching their highest levels in the 0.60 g/Kg SePCH groups ($p< 0.05$), although no marked difference was observed between the 0.60 and 1.20 g/Kg SePCH groups. Moreover, no significant changes were obtained in terms of MCHC and NEU values across these four experimental groups (Table 3).

3.2 Analyses of antioxidants and oxidants in fish liver and intestine

Significant variations were observed in the antioxidative indices among the different test groups of fish. In comparison to the 0.00 and 0.30 g/Kg groups, the activities of T-SOD, CAT, GPx and GR were markedly higher in the fish liver of 0.60 and 1.20 g/Kg SePCH groups ($p< 0.05$), with no notable difference in 0.60 and 1.20 g/Kg groups. Conversely, MDA contents exhibited a significant reduction in the 0.60 and 1.20 g/Kg SePCH groups ($p< 0.05$) compared to the controls ($p< 0.05$). The contents of H_2O_2 showed a significant decrease in the 0.60 and 1.20 g/Kg SePCH groups compared to the

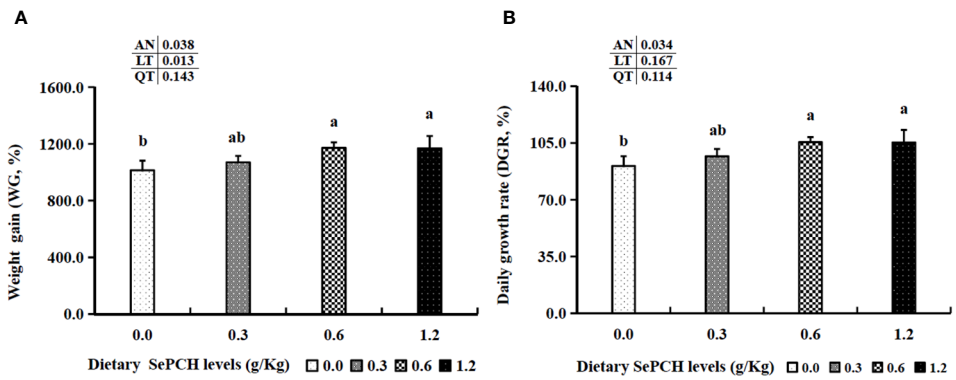

FIGURE 1
Effect of dietary SePCH on weight gain (%) **(A)** and daily growth rate (%) **(B)** of juvenile largemouth bass. Bars with different letters indicate significant differences ($p< 0.05$), while that with the same letter or no letter superscripts indicate no significant differences ($p > 0.05$), AN, ANOVA; LT, linear trend; QT, quadratic trend. The same as the following Figures.

10.3389/fimmu.2024.1342210

TABLE 3 Haematological parameters of juvenile largemouth bass fed diet trials.

	Supplemental levels of SePCH (g/Kg)						
Parameters	0.00	0.30	0.60	1.20	AN	LT	QT
WBC (10^9/L)	158.93 ± 2.27 ^{b}	159.33 ± 1.70 ^{b}	170.54 ± 1.56 ^{a}	167.94 ± 5.56 ^{a}	0.004	0.017	0.150
RBC (10^{12}/L)	2.76 ± 0.08 ^{c}	3.01 ± 0.05 ^{bc}	3.32 ± 0.05 ^{a}	3.08 ± 0.23 ^{ab}	0.001	0.005	0.023
HGB (g/L)	93.67 ± 2.08 ^{c}	105.33 ± 1.53 ^{bc}	114.33 ± 5.86 ^{a}	112.33 ± 4.16 ^{ab}	0.001	0.004	0.004
PLT (10^9/L)	105.00 ± 3.61 ^{b}	125.67 ± 7.64 ^{ab}	140.33 ± 15.04 ^{a}	133.33 ± 21.20 ^{ab}	0.620	0.360	0.640
MCV (fL)	182.53 ± 2.21 ^{b}	186.13 ± 1.70 ^{b}	199.57 ± 3.51 ^{a}	199.90 ± 3.36 ^{a}	0.000	0.001	0.056
MCH (pg)	33.20 ± 1.23 ^{b}	34.67 ± 0.95 ^{ab}	35.80 ± 0.46 ^{a}	36.30 ± 0.70 ^{a}	0.003	0.001	0.419
MCHC (pg)	186.00 ± 1.00	187.67 ± 3.06	188.00 ± 1.73	188.00 ± 2.00	0.613	0.287	0.393
NEU (10^9/L)	6.29 ± 0.74	6.32 ± 0.66	6.49 ± 0.82	6.13 ± 0.58	0.941	0.774	0.614
LYM (10^9/L)	135.90 ± 7.12 ^{b}	145.00 ± 2.27 ^{a}	149.83 ± 1.20 ^{a}	146.45 ± 4.31 ^{a}	0.018	0.300	0.046
MON (10^9/L)	4.53 ± 0.38 ^{b}	4.60 ± 0.10 ^{b}	5.50 ± 0.26 ^{a}	5.10 ± 0.10 ^{a}	0.004	0.057	0.660

$^{a–c}$ Values in the same row with different letters indicate significant differences ($p< 0.05$), while that with the same letter or no letter superscripts indicate no significant differences ($p > 0.05$). AN, ANOVA; LT, linear trend; QT, quadratic trend. The same as the following Tables.

0.00 and 0.30 g/Kg SePCH groups ($p< 0.05$), with no significant difference between 0.00 and 0.30 g/Kg SePCH groups. Compared to the 0.00 and 0.30 g/Kg groups, the contents of Keap1a were markedly decreased in the 0.60 and 1.20 g/Kg SePCH groups ($p< 0.05$), with no significant difference between the two groups. However, the contents of T-AOC and GSH were markedly increased with the increase in SePCH addition, reached the highest levels in the 0.60 g/Kg SePCH groups ($p< 0.05$), and no marked difference was obtained between the 0.60 g/Kg and 1.20 g/Kg SePCH groups. However, GST activities presented no notable difference among all these four fish groups (Table 4).

Activities of T-SOD and CAT were markedly enhanced in the fish intestine of 0.60 and 1.20 g/Kg SePCH groups in comparison with the controls ($p< 0.05$), although there were no notable difference between these two groups. Meanwhile, GPx activities and T-AOC contents significantly increased in the 0.60 and 1.20 g/Kg SePCH groups compared to the 0.00 and 0.30 g/Kg SePCH groups ($p< 0.05$), although no marked difference was observed between the 0.60 and 1.20 g/Kg SePCH groups. The activities of GR and GST exhibited a progressive rise that was positively linked to the doses of SePCH ($p< 0.05$), reaching its maximum in the 1.20 g/Kg SePCH groups with no significant difference between the 0.60 and 1.20 g/Kg SePCH groups. Compared to the 0.00 g/Kg SePCH groups, the contents of GSH significantly increased in the 0.60 and 1.20 g/Kg SePCH groups ($p< 0.05$), with no marked difference between 0.60 and 1.20 g/Kg groups. However, in comparison to the 0.00 g/Kg SePCH groups, the contents of MDA were significantly decreased in the 0.30, 0.60 and 1.20 g/Kg SePCH groups ($p< 0.05$), and there were no marked difference between these three groups. Meanwhile, the 0.60 g/Kg SePCH groups exhibited the lowest Keap1a levels ($p< 0.05$) compared to the 0.00 and 0.30 g/Kg SePCH groups, although there was no notable difference between the 0.60 and 1.20 g/Kg SePCH groups. H_2O_2 contents in the intestine of 0.60 and 1.20 g/Kg SePCH groups were markedly lowed in comparison with those in the 0.00 and 0.30 g/Kg SePCH groups (Table 4).

3.3 Analysis of immune parameters in fish liver and intestine

Lysozyme activities and IgM contents in the fish liver of 0.60 and 1.20 g/Kg SePCH groups were significantly heightened in comparison with the controls ($p< 0.05$), with no noticeable difference compared to the 0.30 g/Kg SePCH groups (Table 5). The activities of ACP reached the maximum in the 1.20 g/Kg SePCH groups and noticeably higher than those in the SePCH deficient groups ($p< 0.05$). The activities of ALP were significantly higher in the 0.60 g/Kg SePCH groups than these in other three groups ($p< 0.05$). Meanwhile, the levels of C3 and C4 in the 0.60 and 1.20 g/Kg SePCH groups were markedly higher than those in the 0.00 and 0.30 g/Kg SePCH groups ($p< 0.05$), although no marked difference was shown between the 0.60 and 1.20 g/Kg SePCH groups.

Regarding anti-inflammatory factors, the levels of TGF-β1 displayed a significant increase in the fish liver of 0.60 and 1.20 g/Kg SePCH groups compared to the 0.00 and 0.30 g/Kg SePCH groups ($p< 0.05$), although no notable difference was presented between the 0.60 and 1.20 g/Kg SePCH groups (Table 5). However, concerning pro-inflammatory factors, the contents of IL-1β, IL-8 and IL-12 significantly decreased in the 0.60 and 1.20 g/Kg SePCH groups compared to the 0.00 g/Kg SePCH groups ($p< 0.05$), although there were no noticeable differences in 0.00 and 0.30 g/Kg SePCH groups. The levels of TNF-α showed a significant reduction in the 0.60 and 1.20 g/Kg SePCH groups compared to the 0.00 and 0.30 g/Kg SePCH groups ($p< 0.05$), although no marked difference was shown between the 0.60 and 1.20 g/Kg SePCH groups. Meanwhile, compared to the control groups, the contents of IFN-γ were noticeably reduced in the 0.30, 0.60 and 1.20

10.3389/fimmu.2024.1342210

TABLE 4 Effects of dietary SePCH on the antioxidative and oxidative indices in the liver and intestine of largemouth bass.

	Supplemental levels of SePCH (g/Kg)						
Parameters	0.00	0.30	0.60	1.20	AN	LT	QT
Liver							
T-SOD (U/mg prot)	9.27 ± 1.59 ^{c}	10.82 ± 0.35 ^{bc}	13.98 ± 0.78 ^{a}	12.44 ± 0.61 ^{ab}	0.002	0.029	0.007
CAT (U/mg prot)	5.47 ± 1.32 ^{b}	7.11 ± 0.99 ^{b}	17.53 ± 0.78 ^{a}	15.61 ± 0.66 ^{a}	0.000	0.002	0.310
GPx (U/mg prot)	45.81 ± 2.17 ^{b}	49.84 ± 1.47 ^{b}	126.98 ± 7.39 ^{a}	125.61 ± 4.27 ^{a}	0.000	0.001	0.111
GR (U/g prot)	11.25 ± 1.53 ^{b}	12.56 ± 0.98 ^{b}	15.37 ± 1.78 ^{a}	15.17 ± 0.71 ^{a}	0.013	0.007	0.090
GST (U/mg prot)	206.93 ± 1.72	205.20 ± 2.99	202.33 ± 1.00	204.05 ± 4.98	0.372	0.258	0.199
GSH (μmol/g prot)	107.36 ± 1.09 ^{b}	112.52 ± 5.19 ^{ab}	118.96 ± 0.65 ^{a}	118.09 ± 4.53 ^{a}	0.012	0.009	0.380
T-AOC (mmol/g prot)	36.23 ± 1.45 ^{c}	40.88 ± 0.62 ^{a}	42.22 ± 0.59 ^{a}	38.68 ± 0.36 ^{b}	0.000	0.435	0.000
MDA (mmol/g prot)	1.25 ± 0.07 ^{a}	1.18 ± 0.05 ^{ab}	1.05 ± 0.08 ^{b}	1.10 ± 0.60 ^{b}	0.320	0.045	0.045
Keap1a (ng/l)	154.57 ± 9.96 ^{a}	143.89 ± 2.67 ^{a}	116.97 ± 6.45 ^{b}	115.21 ± 14.70 ^{b}	0.002	0.001	0.085
H_2O_2 (mmol/g prot)	30.60 ± 0.98 ^{a}	27.29 ± 0.97 ^{b}	23.18 ± 0.42 ^{c}	21.68 ± 0.31 ^{c}	0.000	0.000	0.001
Intestine							
T-SOD (U/mg prot)	11.68 ± 1.05 ^{c}	13.17 ± 1.16 ^{bc}	14.92 ± 0.05 ^{ab}	16.53 ± 0.88 ^{a}	0.001	0.000	0.248
CAT (U/mg prot)	32.39 ± 4.65 ^{c}	36.75 ± 6.48 ^{bc}	47.81 ± 0.85 ^{a}	44.97 ± 6.58 ^{ab}	0.022	0.022	0.079
GPx (U/mg prot)	1.92 ± 0.14 ^{b}	2.00 ± 0.30 ^{b}	2.90 ± 0.17 ^{a}	3.01 ± 0.30 ^{a}	0.000	0.000	0.161
GR (U/g prot)	19.03 ± 1.88 ^{c}	31.76 ± 1.87 ^{b}	35.20 ± 1.86 ^{ab}	37.18 ± 1.77 ^{a}	0.000	0.001	0.000
GST (U/mg prot)	38.73 ± 1.15 ^{c}	41.26 ± 0.67 ^{b}	42.19 ± 0.46 ^{ab}	43.54 ± 1.21 ^{a}	0.001	0.000	0.630
GSH (μmol/g prot)	62.04 ± 1.19 ^{b}	65.57 ± 3.55 ^{ab}	69.24 ± 1.42 ^{a}	66.57 ± 0.72 ^{a}	0.016	0.086	0.008
T-AOC (mmol/g prot)	16.35 ± 0.43 ^{b}	18.50 ± 3.41 ^{b}	26.73 ± 1.59 ^{a}	24.67 ± 1.02 ^{a}	0.001	0.007	0.310
MDA (mmol/g prot)	1.97 ± 0.02 ^{a}	1.35 ± 0.02 ^{b}	1.36 ± 0.01 ^{b}	1.32 ± 0.01 ^{b}	0.000	0.009	0.001
Keap1a (ng/l)	160.13 ± 21.18 ^{a}	134.49 ± 16.06 ^{ab}	101.58 ± 3.70 ^{c}	110.66 ± 6.02 ^{bc}	0.003	0.009	0.010
H_2O_2 (mmol/g prot)	10.90 ± 0.16 ^{a}	10.76 ± 0.11 ^{a}	9.48 ± 0.22 ^{b}	9.23 ± 0.23 ^{b}	0.000	0.000	0.203

TABLE 5 Effect of dietary SePCH on the immune parameters and the anti-inflammatory and pro-inflammatory cytokines in the liver of juvenile largemouth bass.

	Supplemental levels of SePCH (g/Kg)						
Parameters	0.00	0.30	0.60	1.20	AN	LT	QT
lysozyme (U/mg prot)	47.57 ± 4.07 ^{b}	51.97 ± 1.39 ^{ab}	59.70 ± 4.86 ^{a}	57.73 ± 4.48 ^{a}	0.020	0.019	0.054
ACP (U/g prot)	4.41 ± 0.16 ^{c}	6.62 ± 0.31 ^{ab}	6.02 ± 0.05 ^{b}	7.01 ± 0.75 ^{a}	0.000	0.006	0.116
ALP (U/g prot)	124.87 ± 2.81 ^{c}	125.17 ± 1.08 ^{c}	150.93 ± 1.43 ^{a}	133.90 ± 1.14 ^{b}	0.000	0.173	0.020
C3 (μg/ml)	57.27 ± 0.72 ^{b}	57.94 ± 5.78 ^{b}	61.65 ± 1.44 ^{a}	66.85 ± 2.37 ^{a}	0.023	0.001	0.656
C4 (μg/ml)	59.58 ± 1.50 ^{b}	69.47 ± 3.18 ^{b}	88.36 ± 1.64 ^{a}	90.80 ± 14.45 ^{a}	0.002	0.001	0.074
IgM (μg/ml)	269.18 ± 15.30 ^{b}	284.56 ± 9.04 ^{ab}	299.70 ± 7.03 ^{a}	300.49 ± 4.59 ^{a}	0.014	0.006	0.054
TGF-β1 (U/mg prot)	3.67 ± 0.52 ^{b}	3.84 ± 0.54 ^{b}	7.41 ± 0.40 ^{a}	7.06 ± 0.26 ^{a}	0.000	0.002	0.105
IL-1β (U/g prot)	18.03 ± 1.82 ^{a}	16.94 ± 1.19 ^{ab}	14.12 ± 0.70 ^{bc}	13.10 ± 1.90 ^{c}	0.011	0.001	0.333
TNF-α (U/mg prot)	31.03 ± 3.13 ^{a}	30.61 ± 2.03 ^{a}	24.01 ± 2.44 ^{b}	22.92 ± 3.52 ^{b}	0.014	0.004	0.465
IFN-γ (ng/L)	41.91 ± 5.14 ^{a}	37.25 ± 1.85 ^{b}	31.43 ± 3.33 ^{b}	31.86 ± 4.90 ^{b}	0.038	0.015	0.094
IL-8 (pg/L)	31.89 ± 0.30 ^{a}	28.17 ± 1.76 ^{ab}	21.96 ± 5.37 ^{b}	23.91 ± 4.71 ^{b}	0.042	0.035	0.068
IL-12 (ng/L)	24.06 ± 0.58 ^{a}	22.93 ± 1.11 ^{ab}	21.61 ± 0.71 ^{b}	21.61 ± 0.47 ^{b}	0.011	0.005	0.050

g/Kg SePCH groups ($p< 0.05$), and no marked differences were observed among those three groups.

Immunological parameters were also evaluated in the intestinal tissues of our experimental fish (Table 6). In comparison to the 0.00 and 0.30 g/Kg SePCH groups, the activities of lysozyme and IgM showed a noticeable increase in the 0.60 and 1.20 g/Kg SePCH groups ($p< 0.05$), and no marked difference was presented between the 0.60 and 1.20 g/Kg groups. Meanwhile, compared to the 0.00 g/Kg SePCH groups, the activities of ACP and ALP were markedly enhanced in the 0.60 and 1.20 g/Kg SePCH groups ($p< 0.05$), although no marked differences were obtained among the 0.30, 0.60 and 1.20 g/Kg SePCH groups. The contents of C3 in the intestine were markedly elevated in the 0.30 g/Kg to 1.20 g/Kg SePCH groups in comparison with the controls ($p< 0.05$). At the SePCH additive levels of 1.20 g/Kg, the levels of C4 were notably higher than these in other three groups ($p< 0.05$).

Regarding intestinal anti-inflammatory factors, the levels of TGF-β1 in the 0.60 and 1.20 g/Kg SePCH groups were noticeably higher than those in the 0.00 and 0.30 g/Kg SePCH groups ($p< 0.05$), and no difference was shown in the 0.60 and 1.20 g/Kg groups (Table 6). However, in comparison to the controls, the contents of IL-8 and TNF-α were markedly decreased in the 0.60 and 1.20 g/Kg SePCH groups in comparison to the controls ($p< 0.05$), and no marked difference was presented among the 0.30, 0.60 and 1.20 g/Kg SePCH groups. The contents of IFN-γ and IL-1β in the 0.60 and 1.20 g/Kg SePCH groups exhibited significant reductions compared to the 0.00 and 0.30 g/Kg SePCH groups ($p< 0.05$), with no notable difference between the 0.60 and 1.20 g/Kg groups. Similarly, compared to the controls, the contents of IL-12 significantly decreased with SePCH addition from 0.30 g/Kg to 1.20 g/Kg ($p< 0.05$), and no marked difference was presented among these three groups.

3.4 Analysis of genes expression changes in fish liver

The mRNA expression levels of these functional genes involved in Se metabolism, such as SCLY and SEP15, were significantly up-regulated in the 0.60 and 1.20 g/Kg SePCH groups compared to the 0.00 and 0.30 g/Kg groups ($p< 0.05$), with no marked difference between 0.60 and 1.20 g/Kg SePCH groups. Moreover, the transcription levels of SEPH in the liver of fish fed with 0.60 and 1.20 g/Kg SePCH were significantly increased in comparation with the controls ($p< 0.05$), and no marked difference was observed compared to the 0.30 g/Kg SePCH groups. With the dosage of SePCH increased, there was a gradual increase in the mRNA transcriptional expression levels of SPS1, SEPT2, SEPP and SEPK. Additionally, the 0.60 and 1.20 g/Kg SePCH markedly increased the mRNA expression levels of SPS1, SEPT2, SEPP and SEPK compared to the 0.00 and 0.30 g/Kg SePCH groups ($p< 0.05$), and there was no significant difference between the 0.60 and 1.20 g/Kg SePCH (Figure 2A).

Furthermore, the transcription levels of antioxidant-associated genes, such as Cu/Zn-SOD and GR, in the 0.60 g/Kg SePCH group were notably higher than these in the 0.00 and 0.30 g/Kg SePCH groups ($p< 0.05$), although there was no marked difference compared to the 1.20 g/Kg SePCH groups (Figure 3A). The mRNA expression levels of Mn-SOD in the 1.20 g/Kg SePCH groups were markedly higher than that in other three groups ($p< 0.05$), although there were no marked difference among the 0.00, 0.30 and 0.60 SePCH groups. Similarly, the mRNA levels of CAT and GPx1 were notably heightened in the 0.60 and 1.20 g/Kg dietary SePCH groups compared to the 0.00 and 0.30 g/Kg SePCH groups ($p< 0.05$), with no significant difference between the 0.60 and 1.20 g/Kg SePCH groups. The transcription levels of GPx3 in the 0.60 and 1.20 g/Kg SePCH groups were also notably increased

TABLE 6 Effect of dietary SePCH on the immune parameters and the anti-inflammatory and pro-inflammatory cytokines in the intestine of juvenile largemouth bass.

	Supplemental levels of SePCH (g/Kg)						
Parameters	0.00	0.30	0.60	1.20	AN	LT	QT
lysozyme (U/mg prot)	236.01 ± 17.82 ^{b}	254.02 ± 27.10 ^{b}	369.77 ± 27.10 ^{a}	349.20 ± 20.42 ^{a}	0.920	0.004	0.059
ACP (U/g prot)	21.06 ± 1.28 ^{b}	22.05 ± 0.43 ^{ab}	23.58 ± 0.29 ^{a}	23.14 ± 0.77 ^{a}	0.017	0.020	0.040
ALP (U/g prot)	3.01 ± 0.15 ^{b}	3.15 ± 0.01 ^{ab}	3.23 ± 0.06 ^{a}	3.28 ± 0.07 ^{a}	0.026	0.005	0.142
C3 (μg/ml)	85.15 ± 11.57 ^{b}	127.14 ± 2.18 ^{a}	142.51 ± 16.38 ^{a}	142.60 ± 5.32 ^{a}	0.000	0.004	0.001
C4 (μg/ml)	17.48 ± 1.53 ^{d}	21.15 ± 1.00 ^{c}	25.48 ± 1.53 ^{b}	29.15 ± 1.00 ^{a}	0.000	0.000	0.053
IgM (μg/ml)	177.02 ± 3.54 ^{b}	179.01 ± 4.03 ^{b}	219.90 ± 8.72 ^{a}	222.39 ± 5.24 ^{a}	0.000	0.000	0.185
TGF-β1 (U/mg prot)	39.18 ± 1.33 ^{c}	45.69 ± 2.78 ^{b}	57.67 ± 0.65 ^{a}	56.80 ± 1.97 ^{a}	0.000	0.001	0.002
IL-1β (U/g prot)	82.96 ± 2.10 ^{a}	41.65 ± 1.99 ^{b}	36.44 ± 1.70 ^{c}	35.64 ± 0.70 ^{c}	0.000	0.005	0.000
TNF-α (U/mg prot)	70.36 ± 1.93 ^{a}	61.64 ± 4.44 ^{ab}	49.85 ± 6.11 ^{b}	47.54 ± 8.67 ^{b}	0.004	0.001	0.690
IFN-γ (ng/L)	90.20 ± 5.95 ^{a}	88.24 ± 1.48 ^{a}	55.88 ± 7.78 ^{b}	62.50 ± 5.84 ^{b}	0.000	0.006	0.087
IL-8 (pg/L)	63.91 ± 3.98 ^{a}	58.39 ± 3.20 ^{ab}	50.80 ± 5.37 ^{b}	51.15 ± 4.04 ^{b}	0.836	0.007	0.630
IL-12 (ng/L)	38.90 ± 2.32 ^{a}	32.18 ± 3.57 ^{b}	27.96 ± 3.49 ^{b}	27.84 ± 1.60 ^{b}	0.005	0.005	0.014

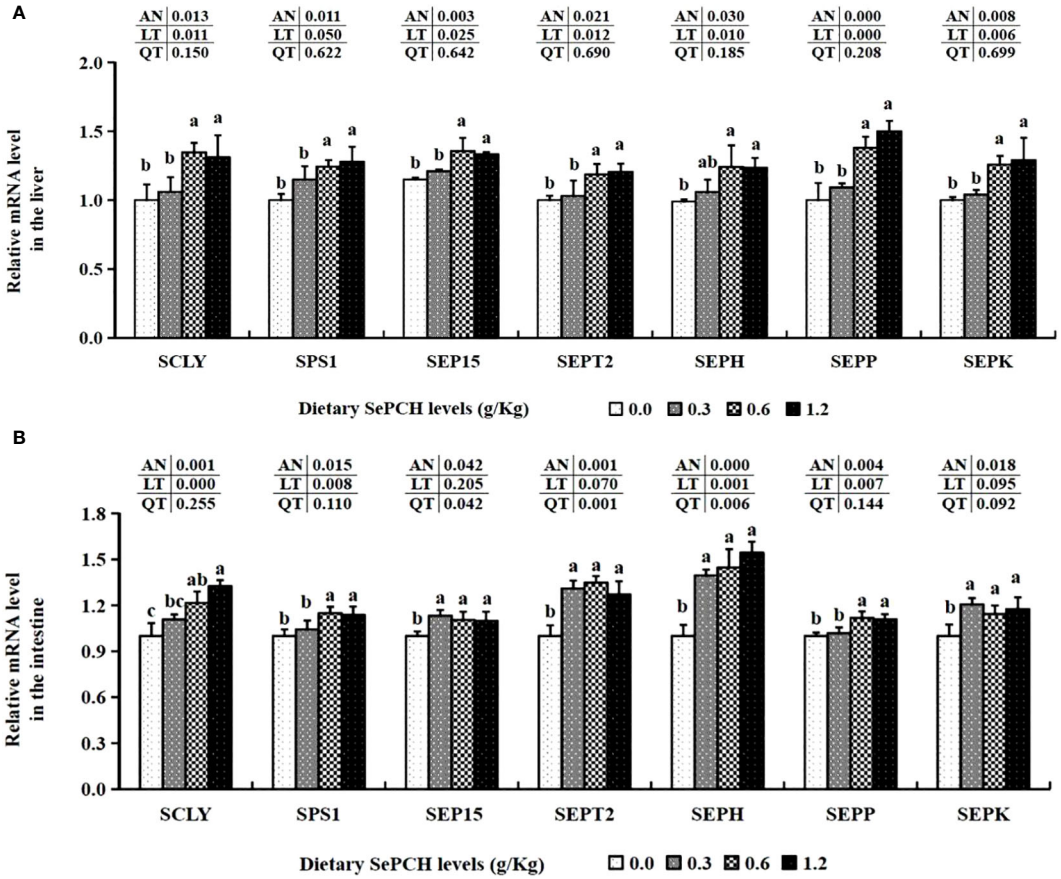

FIGURE 2
Effect of dietary SePCH on expression levels of selenium metabolism related genes in the liver **(A)** and intestine **(B)** of juvenile largemouth bass.

compared to the SePCH deficient groups, although there were no marked difference compared to the 0.30 g/Kg SePCH groups. However, no statistical differences on GST mRNA levels were showed among these four SePCH groups ($p > 0.05$). Moreover, the mRNA levels of Nrf2 were notably up-regulated in the 0.60 and 1.20 g/Kg SePCH diets compared to the 0.00 and 0.30 g/Kg SePCH groups ($p< 0.05$). Conversely, the mRNA levels of Keap1a decreased notably in the 0.60 and 1.20 g/Kg SePCH groups compared to the 0.00 and 0.30 g/Kg SePCH groups ($p< 0.05$). Keap1b also showed a gradual decrease from the 0.30 g/Kg to 1.20 g/Kg SePCH groups and reached its lowest levels in the 0.60 g/Kg SePCH groups, which was notably lower than the control groups (Figure 3A).

The transcription levels of TGF-β1 were notably elevated in the 0.60 and 1.20 g/Kg SePCH groups compared to the 0.00 and 0.30 g/Kg SePCH groups ($p< 0.05$), with no marked difference between the 0.60 and 1.20 g/Kg groups (Figure 4). Additionally, the mRNA expression levels of IL-10 increased notably in the 0.30 g/Kg to 1.20 g/Kg SePCH groups in comparison with the SePCH deficient groups ($p< 0.05$), and there were no marked differences among these three groups. Nonetheless, 0.60 and 1.20 g/Kg SePCH exhibited a notable reduction in the transcription levels of IL-12 and IFN-γ compared to the 0.00 and 0.30 g/Kg SePCH groups ($p< 0.05$), and no marked difference was presented between the 0.60 and 1.20 g/Kg SePCH groups. While the transcription levels of IL-1β showed a declining trend with increasing doses of SePCH, their levels were significantly reduced only at 1.20 g/Kg SePCH compared with the other groups ($p< 0.05$). Compared to the controls, the transcription levels of IL-8 were significantly reduced in the 0.60 and 1.20 g/Kg SePCH groups, although no marked difference was observed between the 0.60 and 1.20 g/Kg SePCH groups ($p > 0.05$). At the same time, compared to the 0.00 and 0.30 g/Kg SePCH groups, the transcription levels of IFN-γ were notably reduced in the 0.60 and 1.20 g/Kg SePCH groups ($p< 0.05$), and there were no marked difference between the 0.60 and 1.20 g/Kg SePCH groups. Additionally, the transcription levels of NF-κB p65 and MAPK14 were notably reduced in the 0.60 an0 g/Kg SePCH groups compared to the controls ($p< 0.05$), and there were no statistical differences between the 0.60 and 1.20 g/Kg SePCH groups (Figure 4). With the increase of SePCH dose, MAPK13 levels showed a decreasing trend and were statistically lower than these in 0.60 g/Kg SePCH groups.

In terms of immune-related factors, in the 0.00 to 0.60 g/Kg SePCH groups, the expression levels of lysozyme were statistically increased with the increase of SePCH dose ($p< 0.05$) and reached the maximum value in the 0.60 g/Kg SePCH groups, with no marked difference between the 0.60 and 1.20 g/Kg SePCH groups. When the SePCH supplementation was 0.60 and 1.20 g/Kg, the transcription levels of hepcidin (HEPC) and liver-expressed

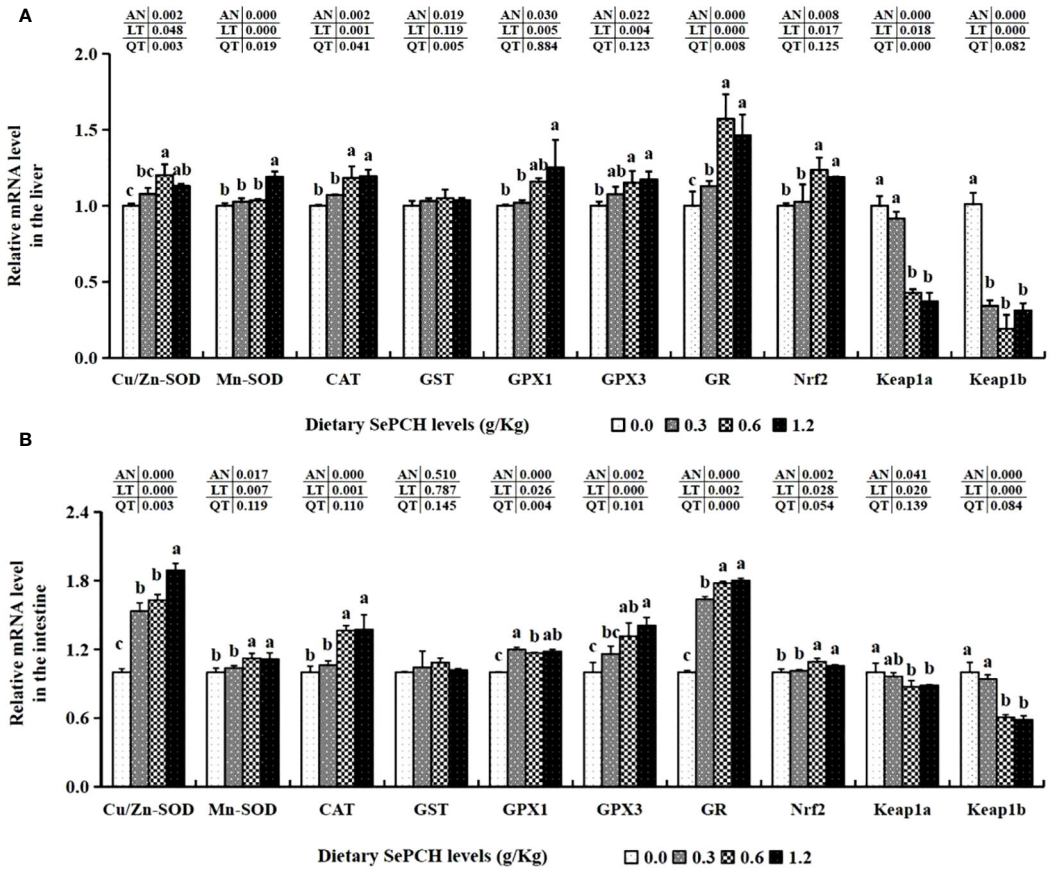

FIGURE 3
Effect of dietary SePCH on expression levels of antioxidant-related genes in the liver **(A)** and intestine **(B)** of juvenile largemouth bass.

antimicrobial peptide 2 (LEAP-2) were markedly higher than those in the SePCH deficient groups ($p< 0.05$), with no statistical difference between them and the 0.30 g/Kg groups. Furthermore, the transcription levels of C3 and C4 were significantly up-regulated in the 0.60 and 1.20 g/Kg SePCH groups compared to those in the 0.00 and 0.30 g/Kg SePCH groups ($p< 0.05$), and no statistical difference was observed between 0.60 and 1.20 g/Kg SePCH groups (Figure 5A).

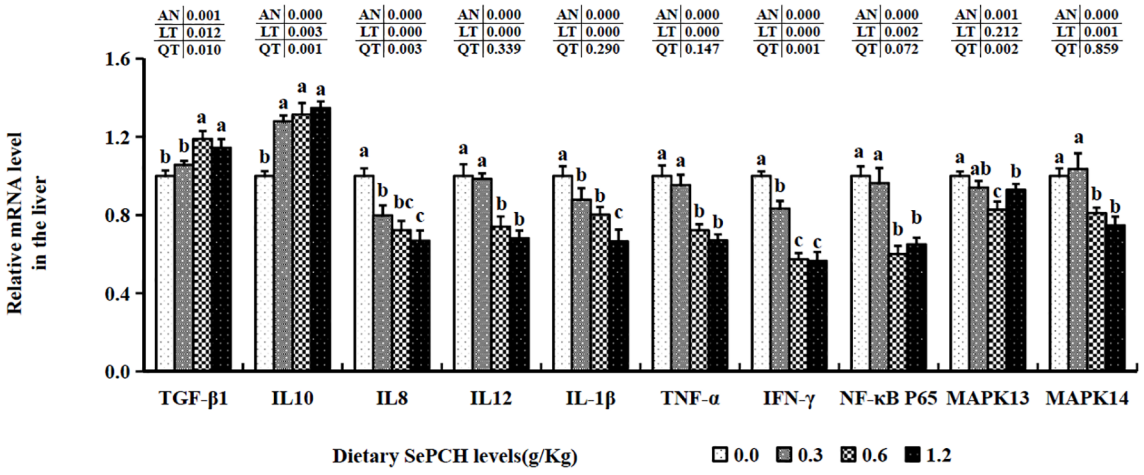

FIGURE 4
Effect of dietary SePCH on relative gene expression levels of anti-inflammatory, pro-inflammatory cytokines and p38 MAPK/NF-κB signaling pathway in the liver of juvenile largemouth bass.

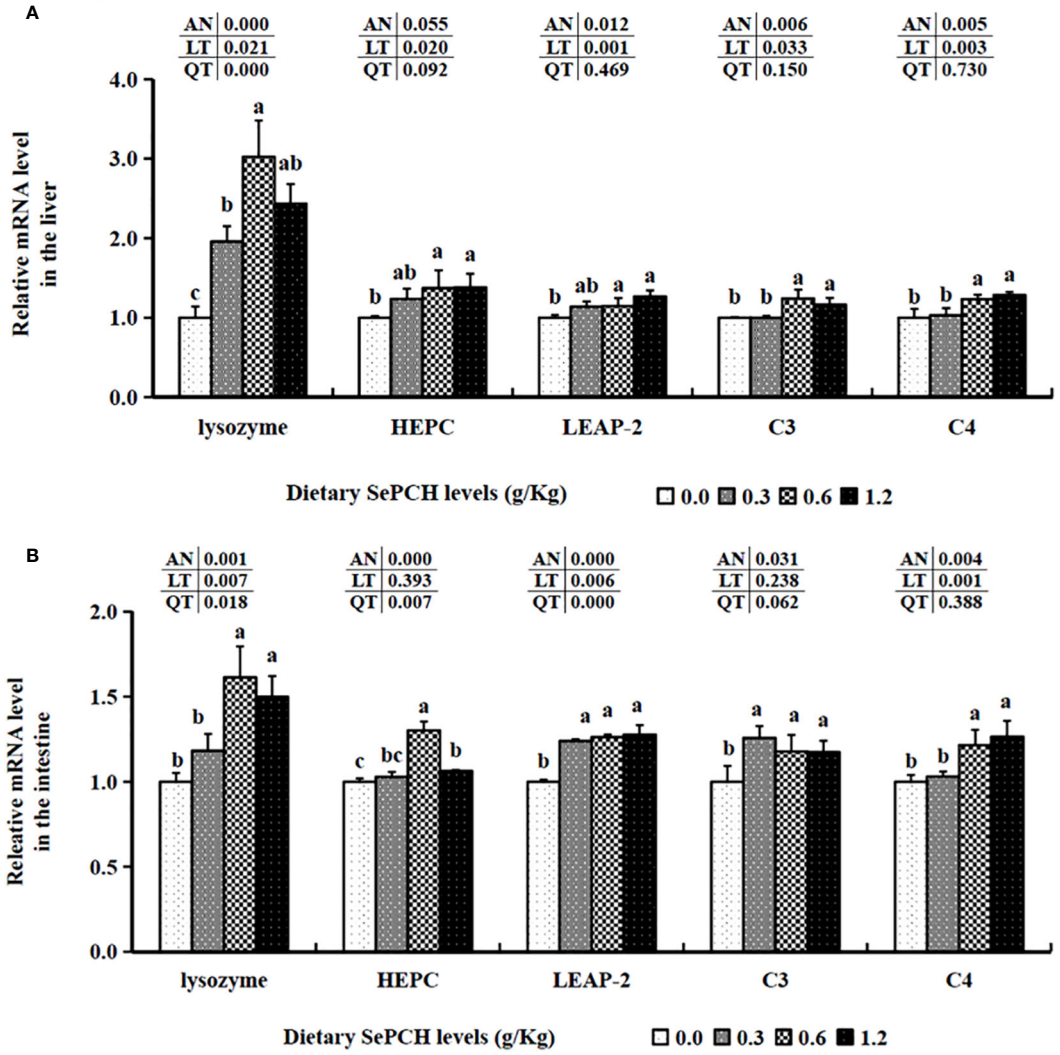

FIGURE 5
Effect of dietary SePCH on relative gene expression levels of immune-related factors in the liver **(A)** and intestine **(B)** of juvenile largemouth bass.

3.5 Genes expression analysis in the intestine

The transcription levels of SCLY in the intestine were significantly elevated and showed a positive correlation with the dietary SePCH levels, with the highest expression observed in the 1.20 g/Kg SePCH groups, significantly surpassing that of the control groups. Furthermore, diets containing 0.60 and 1.20 g/Kg SePCH significantly increased the expression of SPS1 and SEPP in comparison with the controls ($p< 0.05$), with no statistical difference between the 0.60 and 1.20 g/Kg SePCH groups. Simultaneously, diets ranging from 0.30 g/Kg to 1.20 g/Kg SePCH significantly elevated the mRNA expression of SEP15, SEPT2, SEPH and SEPK compared to the SePCH deficient groups ($p< 0.05$), and there were no marked difference among the 0.30, 0.60 and 1.20 g/Kg SePCH groups (Figure 2B).

Gene expression assays related to antioxidants in the intestine of our experimental fish revealed a significant increase in Mn-SOD, CAT and GR at dietary SePCH levels of 0.60 and 1.20 g/Kg in comparison with the controls ($p< 0.05$). The transcription levels of GPx3 and Cu/Zn-SOD exhibited a constant increasing trend and reached their peak in the groups fed with 1.20 g/Kg SePCH, significantly exceeding the SePCH deficient groups ($p< 0.05$). Nevertheless, there were not discernible difference in GST mRNA levels in the fish intestine samples in these four experimental groups. The transcription levels of GPx1 exhibited a noteworthy increase in the 0.60 and 1.20 g/Kg SePCH groups ($p< 0.05$) in comparison with the controls, although there were no marked differences between the 0.60 and 1.20 g/Kg SePCH groups. The transcription levels of Nrf2 markedly increased in the groups fed with 0.60 and 1.20 g/Kg SePCH in comparison with the 0.00 and 0.30 g/Kg SePCH groups. The levels of Keap1a and Keap1b significantly decreased in 0.60 and 1.20 g/Kg dietary SePCH in comparison with the SePCH deficient groups ($p< 0.05$), and there were no statistical difference between the 0.60 and 1.20 g/Kg SePCH groups (Figure 3B).

The 0.60 and 1.20 g/Kg SePCH groups exhibited a marked increase in the expression levels of TGF-β1 and IL-10 in

comparison with the SePCH deficient groups ($p< 0.05$). Importantly, the 0.60 and 1.20 g/Kg SePCH groups showed notable reductions in the transcription levels of IL-8 and IFN-γ in comparison with the SePCH deficient groups ($p< 0.05$). Diets containing 0.30 g/Kg to 1.20 g/Kg SePCH significantly decreased the transcription levels of TNF-α in comparison with the controls ($p< 0.05$), with no marked difference among the 0.30, 0.60 and 1.20 g/Kg SePCH groups. While the transcription levels of IL-12 and IL-1β declined with higher doses of SePCH, the most significant reduction occurred at 1.20 g/Kg SePCH compared to the controls, with no marked difference between the 0.60 and 1.20 g/Kg SePCH groups (Figure 6). Additionally, in the 0.60 and 1.20 g/Kg SePCH groups, the transcription levels of NF-κB p65 were considerably reduced in comparison with the SePCH deficient groups ($p< 0.05$). In the 0.30-1.20 g/Kg SePCH groups, the transcription levels of MAPK13 and MAPK14 were all considerably reduced in comparison with the SePCH deficient groups (Figure 6).

The transcription levels of HEPC were markedly elevated at the 0.60 g/Kg SePCH groups, significantly higher than in the 0.00, 0.30 and 1.20 g/Kg SePCH groups (Figure 5B). Additionally, in the 0.60 and 1.20 g/Kg SePCH groups, the transcription levels of lysozyme and C4 notably increased in comparison with the SePCH deficient groups ($p< 0.05$), with no statistical difference between the 0.60 and 1.20 g/Kg groups ($p > 0.05$). In the 0.30 g/Kg -1.20 g/Kg SePCH groups, the transcription levels of LEAP-2 and C3 were significantly up-regulated in comparison with the control groups ($p< 0.05$). All the transcription levels of CLDN-1, CLDN-11 and CLDN-34 in the intestine showed a discernible increase in the SePCH-treated groups compared to the control groups, although there were no marked differences among these three SePCH treatment groups ($p > 0.05$) (Figure 7). Meanwhile, the transcription levels of ZO-1, OCLN, CLDN-3 and CLDN-5 were all significantly increased at 0.60 and 1.20 g/Kg SePCH in comparison with the SePCH deficient groups. In the 0.60 g/Kg SePCH groups, the transcription levels of ZO-3 were markedly raised compared to the 0.00 and 0.30 g/Kg SePCH groups, with no discernible difference in comparison with the 1.20 g/Kg SePCH groups. In addition, mRNA expression levels of CLDN-23 exhibited a consistent increase and were notably higher in the 1.20 g/Kg SePCH groups in comparison with other three groups ($p< 0.05$) (Figure 7). While mRNA levels of MUC-2 and MUC-5AC consistently improved with increasing doses of SePCH, there was a significant up-regulation of MUC-2 and MUC-5AC transcription levels only in the 1.20 g/Kg SePCH groups in comparison with the SePCH deficient groups, with no statistical difference between the 0.60 and 1.20 g/Kg groups. The 0.60 and 1.20 g/Kg SePCH groups significantly up-regulated the intestinal MUC-17 genes expressions in comparison with the 0.00 and 0.30 g/Kg SePCH groups ($p< 0.05$) (Figure 7).

3.6 Histomorphometric analysis of the intestine

Our investigation of the experimental fish involved the analysis of histological characteristics in intestinal sections (Figure 8). The villus height values in the 0.30 g/Kg to 1.20 g/Kg SePCH groups were notably greater than that in the SePCH deficient groups. Meanwhile, the intestinal morphology in the 0.30 g/Kg to 1.20 g/Kg groups showed robust development, characterized by an increased villus height, reaching its peak in the 1.20 g/Kg SePCH groups ($p< 0.05$). In the 0.60 and 1.20 g/Kg SePCH groups, there was a noticeable increase in villus width compared to the 0.00 g/Kg and 0.30 g/Kg groups, and there was no statistical difference between the 0.60 and 1.20 g/Kg SePCH groups ($p > 0.05$). However, there were no marked differences in muscle thickness and crypt depth among these four groups (Table 7 and Figure 8).

4 Discussion

As an essential micronutrient, dietary Se plays crucial roles in promoting growth and maintaining normal physiological functions in different organisms (2, 34). Numerous studies have demonstrated that dietary selenium can influence the growth and development of

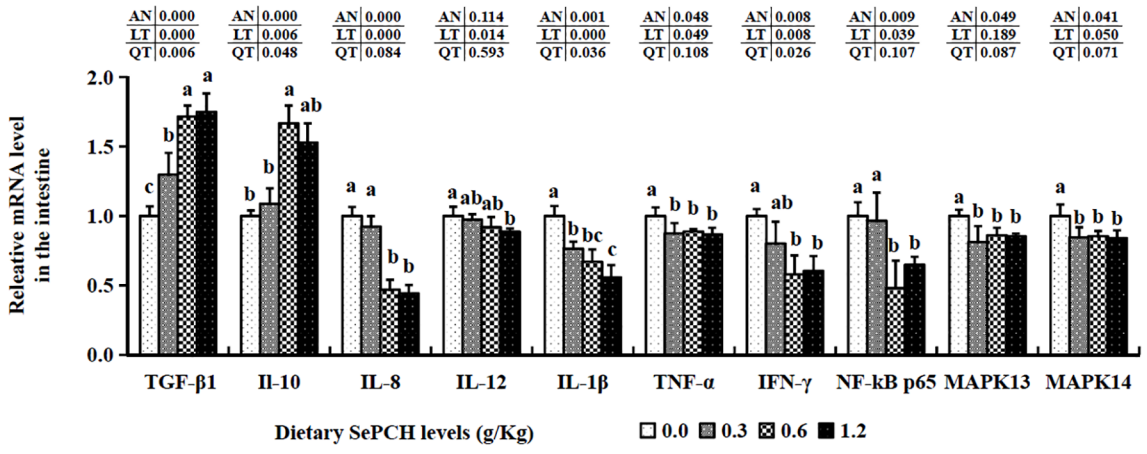

FIGURE 6
Effect of dietary SePCH on relative gene expression levels of anti-inflammatory, pro-inflammatory cytokines and p38 MAPK/NF-κB signaling pathway in the intestine of juvenile largemouth bass.

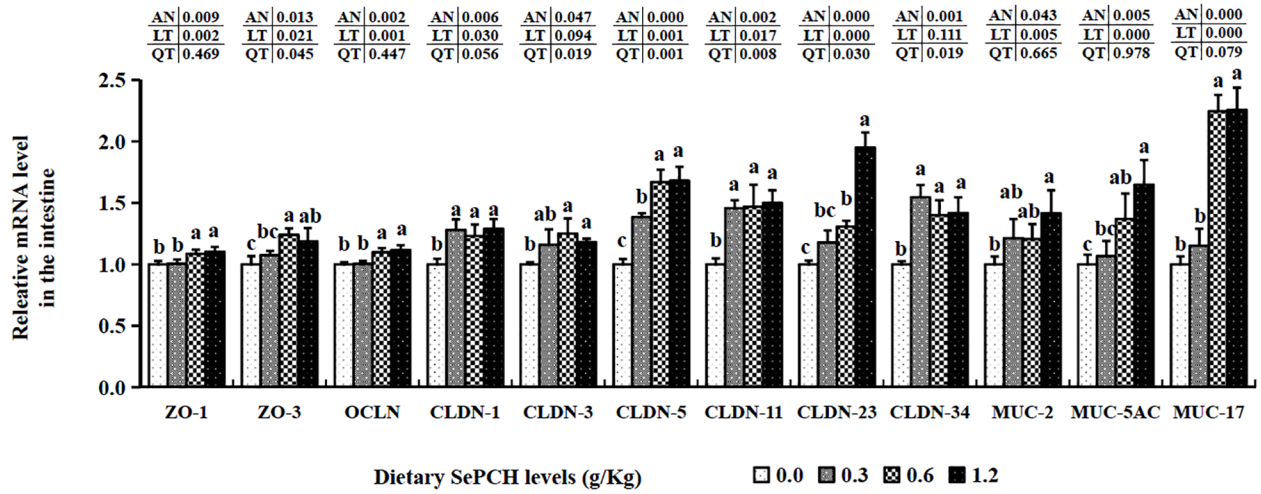

FIGURE 7
Effects of dietary SePCH on intestinal tight junction-related and intestinal mucins gene expression levels of juvenile largemouth bass.

various aquatic and terrestrial animal species, including largemouth bass (1), European seabass (*Dicentrarchus labrax*) (3), rainbow trout (*Oncorhynchus mykiss*) (7), common carp (*Cyprinus carpio*) (35), grass carp (*Ctenopharyngodon idellus*) (36) and chicken (37). In line with these findings, our results also presented that 0.60 and 1.20 g/Kg SePCH (equivalent to 0.84-1.30 mg/kg) notably heightened WG and DGR, highlighting the role of adequate SePCH (0.60 and 1.20 g/Kg) could enhance the growth performance of largemouth bass (1, 3). As reliable indicators, hematology parameters has been used to evaluate the healthy status and nutritional conditions in many aquatic animals (15, 16). Previous research has shown that higher levels of WBC, MON and LYM can contribute to improved immunity in animals under non-stress conditions (14, 38). In agreement with findings in common carp (39) and Nile tilapia (*Oreochromis niloticus*) (40), our results found that SePCH at concentrations of 0.60 and 1.20 g/Kg increased the counts of WBC, MON and LYM in the blood, suggesting enhanced cellular immune responses in largemouth bass fed with adequate SePCH. Moreover, elevated amounts of RBC, HGB and PLT can enhance oxygen-carrying capacity in animals (41). Similar with results in Nile tilapia (42), African catfish (*Clarias gariepinus*) (43) and European seabass (44), our study found that RBC, HGB, PLT, MCV and MCH levels were also increased by 0.60 and 1.20 g/Kg SePCH, indicating that adequate SePCH can improve

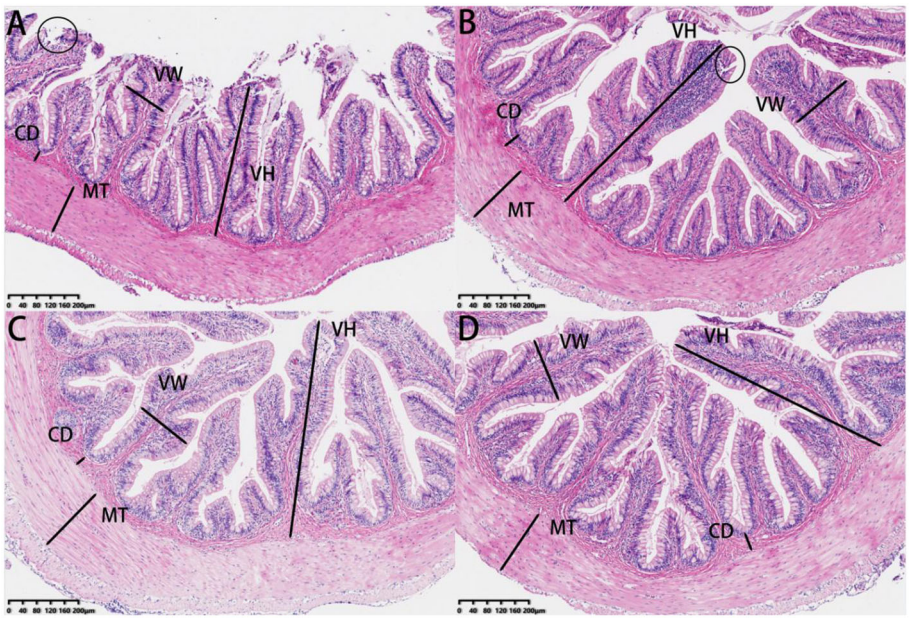

FIGURE 8
HE staining of the intestine sections of juvenile largemouth bass fed with diets containing 0.00 g/Kg **(A)**, 0.30 g/Kg **(B)**, 0.60 g/Kg **(C)** and 1.20 g/Kg **(D)** SePCH (magnification × 100). VH: villus height, VW, villus width; MT, muscular thickness; CD, crypt depth. Circles represent intestinal villi fall off.

TABLE 7 The effects of SePCH on the intestinal morphology of juvenile largemouth bass.

	Supplemental levels of SePCH (g/Kg)						
Parameters	0.00	0.30	0.60	1.20	AN	LT	QT
Villi height (μm)	297.94 ± 4.06 ^{b}	596.46 ± 65.71 ^{a}	619.70 ± 26.30 ^{a}	649.44 ± 11.07 ^{a}	0.000	0.004	0.001
Villi width (μm)	94.12 ± 6.12 ^{b}	104.73 ± 7.02 ^{b}	170.98 ± 19.16 ^{a}	179.98 ± 11.23 ^{a}	0.000	0.000	0.139
Muscular thickness (μm)	155.76 ± 13.25	154.53 ± 28.96	180.35 ± 26.11	185.89 ± 17.16	0.263	0.065	0.801
Crypt depth (μm)	53.81 ± 10.13	53.80 ± 4.20	47.30 ± 8.93	48.59 ± 12.02	0.751	0.382	0.394

$^{a–c}$ Values in the same row with different letters indicate significant differences ($p < 0.05$), while that with the same letter or no letter superscripts indicate no significant differences ($p > 0.05$).

oxygen-carrying capacity and cellular immune responses in largemouth bass.

As the primary form of Se found in SePCH (8), selenocysteine can undergo catalysis by SCLY to yield selenide and alanine (45). Subsequently, selenide, in combination with adenosine triphosphate (ATP), can be enzymatically converted into selenophosphate by SPS1 (8, 45). Selenophosphate plays a direct role in the synthesis of various selenoproteins, thus facilitating Se metabolism within organisms (2). Our results shown that 0.60 and 1.20 g/Kg SePCH increased the expression levels of SCLY and SPS1. This observation aligns with previous studies in black carp (*Mylopharyngodon piceus*) (46), Nile tilapia (47) and mice (48). It suggests that elevated SCLY and SPS1 levels induced by sufficient SePCH can enhance the synthesis of selenoproteins and then promote Se metabolism in largemouth bass. SEPP, the sole selenoprotein containing multiple selenocysteine residues, predominantly resides in the plasma, where it acts as a transporter of Se to various tissues (8, 49). Consistent with previous research in triploid rainbow trout (7) and Nile tilapia (47), our study also found higher expression levels of SEPP in fish fed with adequate SePCH, which suggested that dietary SePCH can improve Se transport via SEPP in largemouth bass. SEP15 is localized within the endoplasmic reticulum (ER) lumen, where it can assist in oxidative folding and structural maturation of N-glycosylated proteins for its oxidoreductase activity (50, 51). On the other hand, SEPH can not only play an crucial role in organ development, but also function as a regulator of redox homeostasis for suppressing DNA damage caused by oxidative stress in the nucleus (52, 53). Additionally, as a DNA-binding protein for redox response, SEPH could heighten the expression of functional genes involved in *de novo* GSH synthesis and phase II detoxification for maintaining cellular redox status (54, 55). SEPT is anchored to the membrane of endoplasmic reticulum (ER), where it exerts selenosulfide oxidoreductase activity via its thioredoxin-like domain, serving as a guardian of ER homeostasis (56, 57). Our results demonstrate higher levels of SEP15, SEPT2 and SEPH in fish fed with 0.60 and 1.20 g/Kg SePCH, which aligns with findings in black carp (46), rainbow trout (58) and yellow catfish (*Pelteobagrus fulvidraco*) (59). These findings suggest that adequate SePCH can help maintain ER redox homeostasis by increasing the levels of SEP15, SEPT2 and SEPH in largemouth bass (60). Furthermore, SEPK, an endoplasmic reticulum-membrane protein, plays a crucial role in facilitating effective Ca^{2+} flux during immune cell activation induced by dietary Se (61). In our study, SEPK expression levels were enhanced in the 0.60 and 1.20 g/Kg SePCH groups, consistent with findings in Nile tilapia (47), rainbow trout (58), yellow catfish (59), grass carp (62) and pig (63). These results collectively suggest that adequate SePCH can improve Se metabolism and immune activation by up-regulating the expression of these selenoproteins in largemouth bass.

As is well known, ROS are continually generated during the metabolic processes for all nutrients and can affect changes on the variations of antioxidant enzymes activities in animals and fish (64, 65). Adequate Se can mitigate excessive ROS levels and play vital antioxidant roles through numerous selenoproteins, including Se-dependent glutathione peroxidase (8, 65). In present study, the activities of T-SOD in the liver and intestine were enhanced in fish groups that received sufficient SePCH. These findings are consistent with results reported in largemouth bass (1), European seabass (3), common carp (35) and grass carp (36). Taken together, these results indicate that the higher T-SOD activities induced by adequate SePCH can catalyze the conversion of O_2^- to H_2O_2, thus mitigating oxidative stress mediated by O_2^- in largemouth bass. CAT and GSH-Px are the primary antioxidant enzymes responsible for decomposing oxygen radicals by catalyzing the conversion of H_2O_2 to H_2O and O_2 in animals and fish (8, 9). Similar to previous findings in largemouth bass (1), European seabass (3), Wuchang bream (*Megalobrama amblycephala*) (9) and common carp (35), our results shown that adequate SePCH not only increased the enzyme activities of CAT and GSH-Px but also reduced H_2O_2 contents compared to the control groups. This suggests that a sufficient dietary intake of SePCH can promote the breakdown of H_2O_2 in largemouth bass. As a dimeric disulfide oxidoreductase, GR can catalyze the reduction of GSH disulfide (GSSG) to GSH for resisting oxidative stress. This process helps maintain the redox environment in human and animal cells (66). Consistent with previous findings in various fish species (46), our study demonstrates higher GR activities and GSH levels in fish fed with adequate SePCH, indicating that sufficient SePCH can enhance cellular redox homeostasis and increase antioxidant capacities by boosting GSH synthesis in the liver and intestine of largemouth bass. Numerous studies have found that the expression of these antioxidant enzymes is primarily regulation by the classical Nrf2/Keap1 signaling transduction pathway (1, 13, 16). Nrf2 can bind Keap1 for maintaining redox homeostasis or antioxidant responses. However, when this balance is disrupted, Nrf2 translocates to the nucleus, where it activates downstream genes related to antioxidant enzymes (13, 67). In this study, we observed up-regulation of Nrf2

and its target molecules, including Cu/Zn-SOD, CAT, GPx1, GPx3 and GR, with a positive correlation to SePCH dosage. However, the expression of Keap1a and Keap1b showed the opposite trend. Similar results were also reported in largemouth bass (1), black carp (46) and chicken (13). Therefore, adequate dietary SePCH can help maintain a better redox status by promoting the transcription levels of antioxidant-related genes through the classical Nrf2/Keap1 signaling transduction pathway in largemouth bass.

ALP and ACP are two essential non-specific phosphohydrolases that can play vital roles in the immune defense through activating immune cells in animals and fish species (5, 17). Similar to findings in grass carp (17), common carp (39) and rainbow trout (68), this investigation observed elevations in ALP and ACP levels in the groups receiving adequate SePCH. Combined with the higher amounts of WBC, MON and LYM in the 0.60 and 1.20 g/Kg SePCH groups, it suggests that adequate SePCH can enhance ALP and ACP activities, thereby stimulating innate immune responses through the activation of these immune cells in largemouth bass. As an antimicrobial enzyme, lysozyme can not only catalyze the hydrolysis of glycosidic bonds in peptidoglycans in the cell walls of gram-positive bacteria, but also acts as an opsonin and play vital roles in facilitating innate immunity by activating the complement system and phagocytes (31). As key constituents in the complement system, C3 and C4 always contribute to both innate and adaptive immunity, making them crucial for host defense against pathogens (16). In this study, the levels of lysozyme, C3 and C4 were all increased in the liver and intestine of fish groups treated with adequate SePCH. These results are consistent with previous findings in black carp (46) and grass carp (17), indicating that adequate SePCH can enhance innate immunity by elevating the levels of lysozyme, C3, and C4 in largemouth bass. As a key element in the humoral immune system, IgM is the primary immunoglobulin present in fish (17). In agreement with results in Wuchang bream (9), common carp (39) and grass carp (17), the contents of IgM were significantly increased in the liver and intestine of fish fed with 0.60 and 1.20 g/Kg SePCH. This suggests that adequate SePCH can enhance humoral immunity via elevating the IgM levels in largemouth bass. HEPC and LEAP-2 are two key antimicrobial proteins expressed in the liver, and they play crucial roles in enhancing immunity by providing the first defense line against many pathogens, including bacteria, fungi, viruses and protozoans (16, 31). Similar to previous results in black carp (46) and largemouth bass (16), our study also found that the transcription levels of HEPC and LEAP-2 were both elevated in the main metabolic and immune tissues of fish fed with adequate dietary SePCH. This indicates the enhanced first-line defense properties mediated by HEPC and LEAP-2 could be enhanced by adequate dietary SePCH in largemouth bass. Taken together, these findings suggest that adequate SePCH can maintain the immunological function homeostasis and provide protective roles for the organism by up-regulating the above defense factors in largemouth bass.

The inflammatory response is a defensive reaction of the immune system to various stimuli such as injury, infection and malnutrition (11). Furthermore, there is a close relationship between the immunological status and the corresponding inflammatory responses, which are primarily controlled by proinflammatory factors (IL-1, IL-8, TNF-α and IFN-γ, etc.) and anti-inflammatory factors (TGF-β1 and IL-10, etc.) (16). In the current study, we observed that adequate SePCH reduced the levels of IL-1β, TNF-α, IL-12, IFN-γ and IL-8 and increased the levels of TGF-β1, along with changes in the transcription levels of these cytokines and IL-10 in the fish liver and intestine. These findings are consistent with previous results in grass carp (24), carp (*C. carpio* var. *specularis*) (69) and European seabass (44). Combined these above findings, it suggest that sufficient dietary SePCH can inhibit the inflammatory response by down-regulating pro-inflammatory genes in the liver and intestine of largemouth bass. It is well-known that the variations in pro-inflammatory and anti-inflammatory cytokines are primarily regulated by the classical p38 MAPK/NF-κB signaling transduction pathway in mammals and animals (4, 11). The p38 MAPK/NF-κB signaling transduction pathway has been illustrated as a crucial pathway involved in various physiological processes, including immune responses, cell survival and inflammation (70). Previous research has shown that inhibiting the p38 MAPK/NF-κB pathways can effectively decrease the transcription and expression levels of pro-inflammatory cytokines, leading to a reduction in inflammatory responses (16, 70). In this study, we observed that the transcription levels of key regulatary elements (MAPK13, MAPK14 and NF-κB p65) were all notably reduced in the liver and intestine of largemouth bass fed with 0.60 and 1.20 g/Kg SePCH in comparison with the SePCH deficient groups, which is similar to earlier studies in grass carp (24), calve (12) and common carp (*C. carpio* L) (71). Collectively, these results indicate that an adequate dietary SePCH can alleviate inflammatory responses by modulating the transcription levels of these pro- and anti-inflammatory genes (IL-1β, TNF-α, IFN-γ, IL-8, IL-12, TGF-β1 and IL-10) through inhibiting the p38 MAPK/NF-κB signaling transduction pathway and thus maintaining immune homeostasis in largemouth bass.

Except as a digestive organ, the intestine also functions as a crucial immune organ, playing vital roles in barrier functions and serving as the first defense line against pathogens' invasion in fish (31). Previous studies have demonstrated that well-developed intestinal structures are characterized by enhanced villus height and villi width (16). Our research similarly revealed that an adequate supply of SePCH could increase both villus height and villi width in largemouth bass. This suggests that a sufficient dietary intake of SePCH can promote intestinal development and growth (24). As known, the intestinal immune defense relies on the physical barrier integrity formed by the TJ complex, which includes proteins like OCLN, CLDNs and ZOs (22, 31). These proteins serve as crucial indicators for assessing the functional integrity of the intestinal barrier (16, 31). TJ proteins are crucial for maintaining the structural integrity and permeability of the intestinal lining, which is closely linked to the absorption of external nutrients (72). For instance, OCLN functions by penetrating tight junctions, lowering membrane permeability and selectively filtering certain molecules in the animal intestine (73). Meanwhile, as two peripheral membrane functional proteins, ZO-1 and ZO-3 play essential roles for establishing and maintaining tight junctions between endothelial and epithelial cells in the animal intestine

(31, 74). Additionally, CLDNs, as transmembrane proteins in cellular tight junctions, are critical for maintaining cell-cell barriers, regulating intercellular communication and preserving cell polarity (22, 75). Consistent with previous findings in largemouth bass (16), grass carp (24), zebrafish (*Danio rerio*) (26), rainbow trout (76) and broiler (77), our results also demonstrate that SePCH at concentrations of 0.60 and 1.20 g/Kg enhances the transcription levels of OCLN, ZO-1, ZO-3, CLDN-1, CLDN-3, CLDN-5, CLDN-11, CLDN-23 and CLDN-34 in the intestine of largemouth bass. This indicates that adequate SePCH can reduce intestinal permeability and bolster the structural integrity of the intestinal barrier (16, 24, 74, 76). Furthermore, MUCs, which are mucosal surface-enriched glycoproteins, play pivotal roles in forming, maintaining and regulating the intestinal barrier and immune responses (78). In our research, we observed an increase in the transcription levels of MUCs (MUC-2, MUC-5AC and MUC-17) in largemouth bass receiving 0.60 and 1.20 g/Kg SePCH. This finding aligns with earlier results in largemouth bass (16), zebrafish (25) and turbot (23), suggesting that adequate SePCH can enhance the mucus barrier, protect the integrity and functionality of the intestinal barrier and maintain health (79). In conclusion, our results indicated that a sufficient dietary intake of SePCH (0.60 and 1.20 g/Kg) can improve intestinal structural integrity and enhance physical barrier function by up-regulating the levels of OCLN, CLDNs and ZOs in largemouth bass.

5 Conclusion

In summary, our results found that SePCH at concentrations of 0.60 and 1.20 g/Kg can present several positive effects on largemouth bass. These effects include improvements in growth, hematological indices, Se metabolism and antioxidant capacities through the Nrf2/Keap1 pathway. Additionally, SePCH enhances immunity by increasing the levels of direct defensive factors and mitigates inflammatory responses via the classical p38 MAPK/NF-κB signaling transduction pathway. Moreover, adequate dietary SePCH positively influences intestinal structural integrity and physical barrier function by modulating TJs and MUCs in largemouth bass.

Data availability statement

The original contributions presented in the study are included in the article/supplementary material. Further inquiries can be directed to the corresponding author.

Ethics statement

The animal studies were approved by the Experimental Animal Ethics Committee of Huzhou University. The studies were conducted in accordance with the local legislation and institutional requirements. Written informed consent was obtained from the owners for the participation of their animals in this study.

Author contributions

HZ: Conceptualization, Data curation, Formal analysis, Investigation, Methodology, Software, Validation, Visualization, Writing – original draft, Writing – review & editing. LZ: Data curation, Investigation, Methodology, Validation, Visualization, Writing – original draft, Writing – review & editing. PZ: Formal analysis, Methodology, Software, Validation, Visualization, Writing – original draft, Writing – review & editing, Data curation, Investigation. YX: Data curation, Formal analysis, Investigation, Methodology, Software, Validation, Writing – original draft, Writing – review & editing. XY: Data curation, Formal analysis, Investigation, Methodology, Software, Validation, Writing – original draft. XP: Data curation, Formal analysis, Investigation, Methodology, Software, Writing – original draft. YF: Data curation, Formal analysis, Investigation, Methodology, Software, Writing – original draft. JW: Formal analysis, Investigation, Methodology, Writing – original draft. HB: Resources, Writing – original draft. XS: Supervision, Writing – original draft, Writing – review & editing. JY: Supervision, Writing – review & editing. CW: Conceptualization, Funding acquisition, Methodology, Project administration, Resources, Supervision, Writing – review & editing, Data curation.

Funding

The author(s) declare financial support was received for the research, authorship, and/or publication of this article. This research was financially supported by the Key Research and Development Program of Zhejiang Province (2019C02046).

Conflict of interest

The authors declare that the research was conducted in the absence of any commercial or financial relationships that could be construed as a potential conflict of interest.

Publisher's note

References

1. Xu Z, Hu J, Zhang Y, Bai L. Evaluation of largemouth bass (*Micropterus salmoide*) fed selenium yeast diets: growth, histopathology, antioxidant ability, and apoptosis. *Aquaculture Rep* (2023) 29:101505. doi: 10.1016/j.aqrep.2023.101505

2. Roman M, Jitaru P, Barbante C. Selenium biochemistry and its role for human health. *Metallomics* (2014) 6:25–54. doi: 10.1039/c3mt00185g

3. Abd El-Kader MF, Fath El-Bab AF, Shoukry M, Abdel-Warith AA, Younis EM, Moustafa EM, et al. Evaluating the possible feeding strategies of selenium nanoparticles on the growth rate and wellbeing of European seabass (*Dicentrarchus labrax*). *Aquaculture Rep* (2020) 18:100539. doi: 10.1016/j.aqrep.2020.100539

4. Ojeda ML, Nogales F. Dietary selenium and its antioxidant properties related to growth, lipid and energy metabolism. *Antioxidants* (2022) 11:1402. doi: 10.3390/antiox11071402

5. Khalil HS, Maulu S, Verdegem M, Abdel Tawwab M. Embracing nanotechnology for selenium application in aquafeeds. *Rev Aquacult* (2023) 15:112–29. doi: 10.1111/raq.12705

6. Rayman MP. Selenium intake, status, and health: a complex relationship. *Hormones* (2020) 19:9–14. doi: 10.1007/s42000-019-00125-5

7. Teng Z, Zhang F, Wang L, Wang L, Huang T, Zhang X. Dietary selenium requirement of triploid rainbow trout (*Oncorhynchus mykiss*) based on selenium yeast supplementation. *Aquac Res* (2022) 53:3365–78. doi: 10.1111/are.15844

8. Avery J, Hoffmann P. Selenium, selenoproteins, and immunity. *Nutrients* (2018) 10:1203. doi: 10.3390/nu10091203

9. Guo H, Lin W, Wang L, Zhang D, Wu X, Li L, et al. The supplementation of dietary selenium yeast and green tea-derived polyphenols improves antioxidant capacity and immune response in juvenile Wuchang bream (*Megalobrama amblycephala*) under ammonia stress. *Aquac Res* (2020) 51:3790–803. doi: 10.1111/are.14724

10. Barrett CW, Short SP, Williams CS. Selenoproteins and oxidative stress-induced inflammatory tumorigenesis in the gut. *Cell Mol Life Sci* (2017) 74:607–16. doi: 10.1007/s00018-016-2339-2

11. Nettleford S, Prabhu K. Selenium and selenoproteins in gut inflammation—A review. *Antioxidants* (2018) 7:36. doi: 10.3390/antiox7030036

12. Wang S, Liu X, Lei L, Wang D, Liu Y. Selenium deficiency induces apoptosis, mitochondrial dynamic imbalance, and inflammatory responses in calf liver. *Biol Trace Elem Res* (2022) 200:4678–89. doi: 10.1007/s12011-021-03059-5

13. Li P, Li K, Zou C, Tong C, Sun L, Cao Z, et al. Selenium yeast alleviates ochratoxin a-induced hepatotoxicity via modulation of the PI3K/AKT and Nrf2/Keap1 signaling pathways in chickens. *Toxins* (2020) 12:143. doi: 10.3390/toxins12030143

14. Amira KI, Rahman MR, Sikder S, Khatoon H, Afruj J, Haque ME, et al. Data on growth, survivability, water quality and hemato-biochemical indices of Nile tilapia (*Oreochromis niloticus*) fry fed with selected marine microalgae. *Data Brief* (2021) 38:107422. doi: 10.1016/j.dib.2021.107422

15. Witeska M, Kondera E, Lugowska K, Bojarski B. Hematological methods in fish - Not only for beginners. *Aquaculture* (2022) 547:737498. doi: 10.1016/j.aquaculture.2021.737498

16. Wu J, Yang W, Song R, Li Z, Jia X, Zhang H, et al. Dietary soybean lecithin improves growth, immunity, antioxidant capability and intestinal barrier functions in largemouth bass (*Micropterus salmoides*) juveniles. *Metabolites* (2023) 13:512. doi: 10.3390/metabo13040512

17. Zheng L, Feng L, Jiang W, Wu P, Tang L, Kuang S, et al. Selenium deficiency impaired immune function of the immune organs in young grass carp (*Ctenopharyngodon idella*). *Fish Shell Fish Immun* (2018) 77:53–70. doi: 10.1016/j.fsi.2018.03.024

18. Lange A, Lange J, Jaskuła E. Cytokine overproduction and immune system dysregulation in alloHSCT and COVID-19 patients. *Frontimmunol* (2021) 12:658896. doi: 10.3389/fimmu.2021.658896

19. Lu C, Gao S, Xu G. Withdrawn: Geraniin inhibits TNF-α induced impairments of osteogenesis through NF-κB and p38 MAPK signalling pathways in bone marrow stem cells. *Stroke Vasc Neurol* (2017) 2:47–52. doi: 10.1136/svn-2016-000046

20. Yi P, Xu X, Qiu B, Li H. Impact of chitosan membrane culture on the expression of pro- and anti-inflammatory cytokines in mesenchymal stem cells. *Exp Ther Med* (2020) 20:3695–702. doi: 10.3892/etm.2020.9108

21. He X, Lin Y, Lian S, Sun D, Guo D, Wang J, et al. Selenium deficiency in chickens induces intestinal mucosal injury by affecting the mucosa morphology, SIgA secretion, and GSH-Px activity. *Biol Trace Elem Res* (2020) 197:660–6. doi: 10.1007/s12011-019-02017-6

22. Xie S, Liu B, Ye H, Li Q, Pan L, Zha X, et al. Dendrobium huoshanense polysaccharide regionally regulates intestinal mucosal barrier function and intestinal microbiota in mice. *Carbohyd Polym* (2019) 206:149–62. doi: 10.1016/j.carbpol.2018.11.002

23. Yang P, Hu H, Liu Y, Li Y, Ai Q, Xu W, et al. Dietary stachyose altered the intestinal microbiota profile and improved the intestinal mucosal barrier function of juvenile turbot (*Scophthalmus maximus L.*). *Aquaculture* (2018) 486:98–106. doi: 10.1016/j.aquaculture.2017.12.014

24. Liu S, Yu H, Li P, Wang C, Liu G, Zhang X, et al. Dietary nano-selenium alleviated intestinal damage of juvenile grass carp (*Ctenopharyngodon idella*) induced by high-fat diet: Insight from intestinal morphology, tight junction, inflammation, anti-oxidization and intestinal microbiota. *Anim Nutr* (2022) 8:235–48. doi: 10.1016/j.aninu.2021.07.001

25. Chen J, Wu S, Wu R, Ai H, Lu X, Wang J, et al. Essential oil from Artemisia argyi alleviated liver disease in zebrafish (*Danio rerio*) via the gut-liver axis. *Fish Shellfish Immun* (2023) 140:108962. doi: 10.1016/j.fsi.2023.108962

26. Zhang X, Chen J, Wang G, Chen H, Cao J, Xie L, et al. Interactive effects of fluoride and seleno-l-methionine at environmental related concentrations on zebrafish (*Danio rerio*) liver via the gut-liver axis. *Fish Shellfish Immun* (2022) 127:690–702. doi: 10.1016/j.fsi.2022.07.006

27. Zhang Z, Huang X, Li S, Zhang C, Luo K. Preparation and characterization of Zein-sulfated *Cardamine hupingshanensis* polysaccharide composite films. *Food Sci Nurt* (2021) 9:6737–45. doi: 10.1002/fsn3.2625

28. Cheng Y, Huang Y, Liu K, Pan S, Qin Z, Wu T, et al. *Cardamine hupingshanensis* aqueous extract improves intestinal redox status and gut microbiota in Se-deficient rats. *J Sci Food Agr* (2021) 101:989–96. doi: 10.1002/jsfa.10707

29. Shao S, Deng G, Mi X, Long S, Zhang J, Tang J. Accumulation and speciation of selenium in cardamine sp. in yutangba Se mining field, Enshi, China. *Chin J Geochemistry* (2014) 33:357–64. doi: 10.1007/s11631-014-0698-7

30. Wang D, Wu FX, Song DD, Gao HQ. *China fishery statistical yearbook* Vol. 25. Beijing, China: Article in China; China Agriculture Press (2022).

31. Jia XW, Qian PC, Wu CL, Xie YY, Yang WX, Song R, et al. Effects of dietary pantothenic acid on growth, antioxidant ability and innate immune response in juvenile black carp. *Aquac. Rep* (2022) 24:101131. doi: 10.1016/j.aqrep.2022.101131

32. Wu C, Ye J, Gao J, Chen L, Lu Z. The effects of dietary carbohydrate on the growth, antioxidant capacities, innate immune responses and pathogen resistance of juvenile Black carp *Mylopharyngodon piceus*. *FISH SHELLFISH Immun* (2016) 49:132–42. doi: 10.1016/j.fsi.2015.12.030

33. Yang W, Wu J, Song R, Li Z, Jia X, Qian P, et al. Effects of dietary soybean lecithin on growth performances, body composition, serum biochemical parameters, digestive and metabolic abilities in largemouth bass *Micropterus salmoides*. *Aquaculture Rep* (2023) 29:101528. doi: 10.1016/j.aqrep.2023.101528

34. Genchi G, Lauria G, Catalano A, Sinicropi MS, Carocci A. Biological activity of selenium and its impact on human health. *Int J Mol Sci* (2023) 24:2633. doi: 10.3390/ijms24032633

35. Saffari S, Keyvanshokooh S, Zakeri M, Johari SA, Pasha-Zanoosi H. Effects of different dietary selenium sources (sodium selenite, selenomethionine and nanoselenium) on growth performance, muscle composition, blood enzymes and antioxidant status of common carp (*Cyprinus carpio*). *Aquac Nutr* (2017) 23:611–7. doi: 10.1111/anu.12428

36. Liu LW, Liang XF, Li J, Fang JG, Yuan XC, Li J, et al. Effects of dietary selenium on growth performance and oxidative stress in juvenile grass carp (*Ctenopharyngodon idellus*). *Aquacult Nutr* (2018) 24:1296–303. doi: 10.1111/anu.12428

37. Mohammadi E, Janmohammadi H, Olyayee M, Helan JA, Kalanaky S. Nano selenium improves humoral immunity, growth performance and breast-muscle selenium concentration of broiler chickens. *Anim Prod Sci* (2020) 60:1902. doi: 10.1071/AN19581

38. Petrera F, Abeni F. Hematological and iron-related parameters in a dual-purpose local cattle breed compared to the specialized Italian Friesian breed during transition and lactation periods. *Comp Clin Pathol* (2018) 27:869–78. doi: 10.1007/s00580-018-2675-8

39. Saffari S, Keyvanshokooh S, Zakeri M, Johari SA, Pasha-Zanoosi H, Mozanzadeh MT. Effects of dietary organic, inorganic, and nanoparticulate selenium sources on growth, hemato-immunological, and serum biochemical parameters of common carp (*Cyprinus carpio*). *Fish Physiol BiochemI* (2018) 44:1087–97. doi: 10.1007/s10695-018-0496-y

40. Neamat-Allah ANF, Mahmoud EA, Abd El Hakim Y. Efficacy of dietary Nano-selenium on growth, immune response, antioxidant, transcriptomic profile and resistance of Nile tilapia (*Oreochromis niloticus*) against Streptococcus iniae infection. *Fish Shellfish Immun* (2019) 94:280–7. doi: 10.1016/j.fsi.2019.09.019

41. Morel N, Moisan M. Blood components are essential to regulate microcirculatory blood flow. *Crit Care* (2017) 21:49. doi: 10.1186/s13054-017-1621-5

42. Rathore SS, Murthy HS, Mamun MA, Nasren S, Rakesh K, Kumar BTN, et al. Nano-selenium supplementation to ameliorate nutrition physiology, immune response, antioxidant system and disease resistance against aeromonas hydrophila in monosex Nile Tilapia (*Oreochromis niloticus*). *Biol Trace Elem Res* (2021) 199:3073–88. doi: 10.1007/s12011-020-02416-0

43. Owolabi OD, Babarinsa MK. Assessment of growth performance, nutrient utilization and haematological profile of African catfish (*Clarias gariepinus*) fed with nanoselenium formulated diets. *IOP Conf series. Materials Sci Eng* (2020) 805:12014. doi: 10.1088/1757-899X/805/1/012014

44. Abd El-Kader MF, Fath El-Bab AF, Abd-Elghany MF, Abdel-Warith AA, Younis EM, Dawood MAO. Selenium nanoparticles act potentially on the growth performance,

hemato-biochemical indices, antioxidative, and immune-related genes of European seabass (*Dicentrarchus labrax*). *Biol Trace Elem Res* (2021) 199:3126–34. doi: 10.1007/s12011-020-02431-1

45. Scortecci JF, Serro VHB, Fernandes AF, Basso LGM, Gutierrez RF, Araujo APU, et al. Initial steps in selenocysteine biosynthesis: The interaction between selenocysteine lyase and selenophosphate synthetase. *Int J Biol Macromol* (2020) 156:18–26. doi: 10.1016/j.ijbiomac.2020.03.241

46. Zhang C, Jia XW, Qian PC, Chen YT, Wu CL, Ye JY. Selenium-rich *cardamine hupingshanensis* on growth, biochemical indices, selenium metabolism, antioxidant capscities and innate immunities in juvenile black carp (*mylopharyngodon piceus*). *Acta Hydrobiologica Sin* (2022) 47:523–34. doi: 10.7541/2023.2022.0063

47. Rathore SS, Murthy HS, Girisha SK, Nithin MS, Nasren S, Mamun MAA, et al. Supplementation of nano-elenium in fish diet: Impact on selenium assimilation and immune-regulated selenoproteome expression in monosex Nile tilapia (*Oreochromis niloticus*). *Comp Biochem Physiol Part C: Toxicol Pharmacol* (2021) 240:108907. doi: 10.1016/j.cbpc.2020.108907

48. Kremer PM, Torres DJ, Hashimoto AC, Berry MJ. Disruption of selenium handling during puberty causes sex-specific neurological impairments in mice. *Antioxidants* (2019) 8:110. doi: 10.3390/antiox8040110

49. Schomburg L. Selenoprotein P - Selenium transport protein, enzyme and biomarker of selenium status. *Free Radical Bio Med* (2022) 191:150–63. doi: 10.1016/j.freeradbiomed.2022.08.022

50. Addinsall AB, Wright CR, Andrikopoulos S, van der Poel C, Stupka N. Emerging roles of endoplasmic reticulum-resident selenoproteins in the regulation of cellular stress responses and the implications for metabolic disease. *Biochemj* (2018) 475:1037–57. doi: 10.1042/bcj20170920

51. Labunskyy VM, Yoo M, Hatfield DL, Gladyshev VN. Sep15, a thioredoxin-like selenoprotein, is involved in the unfolded protein response and differentially regulated by adaptive and acute ER stresses. *Biochemistry-us* (2009) 48:8458–65. doi: 10.1021/bi900717p

52. Wu RT, Cao L, Chen BP, Cheng WH. Selenoprotein H suppresses cellular senescence through genome maintenance and redox regulation. *J Biol Chem* (2014) 289:34378–88. doi: 10.1074/jbc.m114.611970

53. Cui J, Zhou J, He W, Ye J, Westlake T, Medina R, et al. Targeting selenoprotein H in the nucleolus suppresses tumors and metastases by Isovalerylspiramycin I. *J Exp Clin Canc Res* (2022) 41:126. doi: 10.1186/s13046-022-02350-0

54. Panee J, Stoytcheva ZR, Liu W, Berry MJ. Selenoprotein H is a redox-sensing high mobility group family DNA-binding protein that up-regulates genes involved in glutathione synthesis and Phase II Detoxification*. *J Biol Chem* (2007) 282:23759–65. doi: 10.1074/jbc.m702267200

55. Cao L, Pechan T, Lee S, Cheng W. Identification of selenoprotein H isoforms and impact of selenoprotein H overexpression on protein but not mRNA levels of 2 other selenoproteins in 293T Cells. *J Nutr* (2021) 151:3329–38. doi: 10.1093/jn/nxab290

56. Anouar Y, Lihrmann I, Falluel-Morel A, Boukhzar L. Selenoprotein T is a key player in ER proteostasis, endocrine homeostasis and neuroprotection. *Free Radical Bio Med* (2018) 127:145–52. doi: 10.1016/j.freeradbiomed.2018.05.076

57. Pothion H, Jehan C, Tostivint H, Cartier D, Bucharles C, Falluel-Morel A, et al. Selenoprotein T: an essential oxidoreductase serving as a guardian of endoplasmic reticulum homeostasis. *Antioxid Redox Sign* (2020) 33:1257–75. doi: 10.1089/ars.2019.7931

58. Wang L, Zhang X, Wu L, Liu Q, Zhang D, Yin J. Expression of selenoprotein genes in muscle is crucial for the growth of rainbow trout (*Oncorhynchus mykiss*) fed diets supplemented with selenium yeast. *Aquaculture* (2018) 492:82–90. doi: 10.1016/j.aquaculture.2018.03.054

59. Ke J, Zhang D, Lei X, Liu G, Luo Z. Characterization and tissue expression of twelve selenoproteins in yellow catfish (*Pelteobagrus fulvidraco*) fed diets varying in oxidized fish oil and selenium levels. *J Trace Elem Med Bio* (2023) 79:127204. doi: 10.1016/j.jtemb.2023.127204

60. Zhang Y, Roh YJ, Han S, Park I, Lee HM, Ok YS, et al. Role of selenoproteins in redox regulation of signaling and the antioxidant system: A review. *Antioxidants* (2020) 9:383. doi: 10.3390/antiox9050383

61. Lv L, Chai L, Wang J, Wang M, Qin D, Song H, et al. Selenoprotein K enhances sting oligomerization to facilitate antiviral response. *PloS Pathog* (2023) 19:1011314. doi: 10.1371/journal.ppat.1011314

62. Chen F, Zhang Z, Wang L, Yu H, Zhang X, Rong K. Dietary selenium requirement for on-growing grass carp (*Ctenopharyngodon idellus*). *Aquaculture* (2023) 573:739572. doi: 10.1016/j.aquaculture.2023.739572

63. Lu Z, Wang P, Teng T, Shi B, Shan A, Lei XG. Effects of dietary selenium deficiency or excess on selenoprotein gene expression in the spleen tissue of pigs. *Animals* (2019) 9:1122. doi: 10.3390/ani9121122

64. Tolmacheva AS, Nevinsky GA. Essential protective role of catalytically active antibodies (Abzymes) with redox antioxidant functions in animals and humans. *Int J Mol Sci* (2022) 23:3898. doi: 10.3390/ijms23073898

65. Lennicke C, Cocheme HM. Redox metabolism: ROS as specific molecular regulators of cell signaling and function. *Mol Cell* (2021) 81:3691–707. doi: 10.1016/j.molcel.2021.08.018

66. Chai Y, Mieyal JJ. Glutathione and glutaredoxin—key players in cellular redox homeostasis and signaling. *Antioxidants* (2023) 12:1553. doi: 10.3390/antiox12081553

67. Liang H, Wu L, Hamunjo Chama MK, Ge X, Ren M, Chen X, et al. Culture salinity modulates Nrf2 antioxidant signaling pathway and immune response of juvenile genetically improved farmed tilapia (*Oreochromis niloticus*) under different dietary protein levels. *Fish Shellfish Immun* (2021) 117:220–7. doi: 10.1016/j.fsi.2021.08.014

68. Harsij M, Gholipour Kanani H, Adineh H. Effects of antioxidant supplementation (nano-selenium, vitamin C and E) on growth performance, blood biochemistry, immune status and body composition of rainbow trout (*Oncorhynchus mykiss*) under sub-lethal ammonia exposure. *Aquaculture* (2020) 521:734942. doi: 10.1016/j.aquaculture.2020.734942

69. Shang X, Wang B, Sun Q, Zhang Y, Lu Y, Liu S, et al. Selenium-enriched bacillus subtilis reduces the effects of mercury-induced on inflammation and intestinal microbes in carp (*Cyprinus carpio* var. *specularis*). *Fish Physiol Biochem* (2022) 48:215–26. doi: 10.1007/s10695-022-01046-8

70. Wang H, Bi C, Wang Y, Sun J, Meng X, Li J. Selenium ameliorates staphylococcus aureus-induced inflammation in bovine mammary epithelial cells by inhibiting activation of TLR2, NF-κB and MAPK signaling pathways. *BMC Vet Res* (2018) 14:197. doi: 10.1186/s12917-018-1508-y

71. Xu R, Cao J, Xu T, Liu T, Zhu M, Guo M. Selenium deficiency induced inflammation and apoptosis via NF-κB and MAPKs pathways in muscle of common carp (*Cyprinus carpio L.*). *Fish Shellfish Immun* (2023) 138:108847. doi: 10.1016/j.fsi.2023.108847

72. Heinemann U, Schuetz A. Structural features of tight-junction proteins. *Int J Mol Sci* (2019) 20:6020. doi: 10.3390/ijms20236020

73. Suzuki T. Regulation of intestinal epithelial permeability by tight junctions. *Cell Mol Life Sci* (2013) 70:631–59. doi: 10.1007/s00018-012-1070-x

74. Islas S, Vega J, Ponce L, Gonzalez-Mariscal L. Nuclear localization of the tight junction protein ZO-2 in epithelial cells. *Exp Cell Res* (2002) 274:138–48. doi: 10.1006/excr.2001.5457

75. Tamura A, Kitano Y, Hata M, Katsuno T, Moriwaki K, Sasaki H, et al. Megaintestine in claudin-15-eficient mice. *Gastroenteroligy* (2008) 134:523–34. doi: 10.1053/j.gastro.2007.11.040

76. Li L, Liu Z, Quan J, Sun J, Lu J, Zhao G. Dietary nano-selenium alleviates heat stress-induced intestinal damage through affecting intestinal antioxidant capacity and microbiota in rainbow trout (*Oncorhynchus mykiss*). *Fish Shellfish Immun* (2023) 133:108537. doi: 10.1016/j.fsi.2023.108537

77. Chen S, Xue Y, Shen Y, Ju H, Zhang X, Liu J, et al. Effects of different selenium sources on duodenum and jejunum tight junction network and growth performance of broilers in a model of fluorine-induced chronic oxidative stress. *Poultry Sci* (2022) 101:101664. doi: 10.1016/j.psj.2021.101664

78. Yang S, Yu M. Role of goblet cells in intestinal barrier and mucosal immunity. *J Inflammation Res* (2021) 14:3171–83. doi: 10.2147/jir.s318327

79. Canter JA, Ernst SE, Peters KM, Carlson BA, Thielman NRJ, Grysczyk L, et al. Selenium and the 15kDa selenoprotein impact colorectal tumorigenesis by modulating intestinal barrier integrity. *Int J Mol Sci* (2021) 22:10651. doi: 10.3390/ijms221910651

frontiers | Frontiers in Immunology

TYPE Original Research
PUBLISHED 06 February 2024
DOI 10.3389/fimmu.2024.1333469

OPEN ACCESS

EDITED BY
Samad Rahimnejad,
University of Murcia, Spain

REVIEWED BY
Cristobal Espinosa Ruiz,
University of Murcia, Spain
Jingguang Wei,
South China Agricultural University, China

*CORRESPONDENCE
Zhongbao Li
lizhongbao@jmu.edu.cn

RECEIVED 06 November 2023
ACCEPTED 04 January 2024
PUBLISHED 06 February 2024

CITATION
Liu L, Zhao Y, Huang Z, Long Z, Qin H, Lin H, Zhou S, Kong L, Ma J and Li Z (2024) Effects of *Lycium barbarum* polysaccharides supplemented to high soybean meal diet on immunity and hepatic health of spotted sea bass *Lateolabrax maculatus*. *Front. Immunol.* 15:1333469. doi: 10.3389/fimmu.2024.1333469

Effects of *Lycium barbarum* polysaccharides supplemented to high soybean meal diet on immunity and hepatic health of spotted sea bass *Lateolabrax maculatus*

Longhui Liu[1,2], Yanbo Zhao[1,2], Zhangfan Huang[1,2], Zhongying Long[1,2], Huihui Qin[1,2], Hao Lin[1,2], Sishun Zhou[1,2], Lumin Kong[1,2], Jianrong Ma[1,2] and Zhongbao Li[1,2]*

[1]Fisheries College, Jimei University, Xiamen, China, [2]Fujian Provincial Key Laboratory of Marine Fishery Resources and Eco-environment, Xiamen, China

High soybean meal diet (HSBMD) decreased the immunity and damaged the liver health of spotted sea bass; in this study, *Lycium barbarum* polysaccharides (LBP) was added to HSBMD to explore its effects on the immunity and liver health. The diet with 44% fish meal content was designed as a blank control. On this basis, soybean meal was used to replace 50% fish meal as HSBMD, and LBP was added in HSBMD in gradient (1.0, 1.5, 2.0 g/kg) as the experimental diet. 225-tailed spotted sea bass with initial body weight of 44.52 ± 0.24 g were randomly divided into 5 groups and fed the corresponding diet for 52 days, respectively. The results show that: after ingestion of HSBMD, the immunity of spotted sea bass decreased slightly and hepatic tissue was severely damaged. And the addition of LBP significantly improved the immune capacity and protected the hepatic health. Specifically, the activities of serum lysozyme (LZM), immunoglobulin M (IgM), liver acid phosphatase (ACP) and alkaline phosphatase (AKP) were increased, and serum alanine aminotransferase (ALT) and aspartate aminotransferase (AST) activities were significantly decreased, and hepatic morphology was improved. In the analysis of transcriptome results, it was found that toll-like receptor 3 (TLR3) and toll-like receptor 5 (TLR5) were down-regulated in toll-like receptor signaling pathway. And LBP may protect hepatic health by regulating Glycolysis/Gluconeogenesis, Insulin signaling pathway, Steroid biosynthesis and other glucolipid-related pathways. In conclusion, the addition of LBP in HSBMD can improve the immunity and protect the hepatic health of spotted sea bass, and its mechanism may be related to glucose and lipid metabolism.

KEYWORDS

***Lycium barbarum* polysaccharides, high soybean meal diet, spotted sea bass, Immunity, hepatic health**

1 Introduction

The continuous growth of aquaculture production to meet the growing demand for seafood in the world is necessary (1). Over the past three decades, aquaculture has produced about half of the aquatic products consumed by humans, and fish have provided at least 15% of the per capita animal protein intake for more than 4.5 billion people (2, 3). Aquaculture is particularly dependent on fishmeal, especially carnivorous Marine fish farming (4). Unfortunately, aquaculture that relies on fishmeal as its main protein source is not sustainable due to high demand and unstable sources (5). At present, soybean meal, a renewable plant protein with high protein content and relatively balanced amino acid composition, is regarded as the most promising protein source to replace fish meal (6). However, many studies have reported various disadvantages of a diet with varying amounts of soybean meal for fish (7–9). For example, high soybean meal diet (HSBMD) can cause a series of problems in turbot (*Scophthalmus maximus*), including slower growth, tissue degeneration, inflammation and other physiological and metabolic disorders (10). It is worth mentioning that the above symptoms are particularly obvious in carnivorous fish (11, 12).

Lycium barbarum is a plant in the Solanaceae family (*Solanaceae Juss*) that is widely distributed in northwestern China; and it was also introduced in North and South America and Western Europe (13). *Lycium barbarum* is a common tonic and traditional Chinese medicine in China, because it is rich in nutrients and active substances, including polysaccharides, polyphenols, amino acids, trace elements and vitamins (14). In past studies, *Lycium barbarum* polysaccharides (LBP) had been identified as one of the active ingredients responsible for the biological activities (15). Many pharmacological and phytochemical studies have shown that LBP has antioxidant (16), immunomodulatory (17), hypoglycemic (18), anti-inflammatory (19) and liver protection (20). Meanwhile, in our previous study, LBP was found to have excellent effects in regulating hepatic lipid metabolism (21). Thus, LBP may be able to mitigate the adverse effects of HSBMD on the body through the aforementioned effects.

Spotted sea bass (*Lateolabrax maculatus*) is a widely farmed economic fish which is loved by people because of its delicious meat and rich nutrition. According to statistics, the yield of spotted sea bass in 2022 was 21.81 ten thousand tons, and the number of breeding was huge (22). Spotted sea bass is a typical carnivorous fish. As a matter of course, HSBMD causes it to produce a series of related discomfort reactions (23). Therefore, this experiment explored the effects of LBP supplemented to HSBMD on immunity and hepatic health of spotted sea bass. It also provides a theoretical basis for LBP as a feed additive to protect the hepatic health of aquaculture animals.

2 Materials and methods

2.1 LBP preparation and characterization

LBP was purchased from Xi'an Shengqing Biotechnology Co., LTD, China. The total sugar content is 80.90% (phenol-sulfuric acid method). The sample were degreased and decolorized refer to the methods of Cui (24) and Wu (25). Two compositions were isolated from LBP. The molecular weight and yield of composition 1 were 11.343 kDa and 31.4%, respectively, and including galactose (0.08%), mannuronic acid (5.19%), arabinose (0.21%), guluronic acid (7.04%), galacturonic acid (16.57%) glucuronic acid (9.36%) and glucose (61.55%). The molecular weight and yield of composition 2 were 35.508 kDa and 20.9%, respectively, and including glucose (96.59%), galactose (1.01%), arabinose (1.69%), mannose (0.44%), and xylose (0.27%). More detailed results on the preparation and characterization of LBP can be found in previous report (21).

2.2 Experimental diets

Five dietary formulations with crude protein about 45% and crude fat about 12% were designed according to the nutritional requirements of spotted sea bass (26). 44% fish meal (0% soybean meal) was taken as healthy control and labeled as LS group. In addition, half of the fishmeal was replaced with 40% soybean meal and labeled as HS group; accordingly, on the basis of HS group, LBP was added (1.0, 1.5, 2.0 g/kg) and labeled as HL1, HL2, HL3, respectively. Flour was used for balancing among the groups (Table 1).

The raw feed materials were thoroughly crushed in the crusher. According to the principle of mixing from small to large, the various ingredients in the formula were fully mixed, and then the fish oil and soybean oil were mixed, and finally the appropriate amount of water (about 35% of the weight of the feed) was added, and the particles were squeezed into 5 mm particle size through the granulator. In particular, LBP was completely soluble in water when added. The prepared feed was dried to a moisture content of 10% in a constant temperature oven at 55°, subsequently cooled to room temperature, and finally stored at -20° for future utilization.

2.3 Experimental fish and feeding management

This experiment was approved by the Animal Ethics Committee of Jimei University (Grant No. JMU202103009). The fish were purchased from commercial fisheries in Fujian, China. The culture experiment was carried out in the seawater test field of Jimei University, Xiamen, China. And the experiment period was 52 days. Before the start of the study, the experiment site, temporary fish tank (1700 L) and experimental fish tank (160 L) were washed, disinfected and aerated, and the fish were temporarily raised for two weeks to adapt to the environment. During the temporary rearing, fish were fed to apparent satiety twice a day at 8:30 and 17:30. In addition, about 35% of the water was changed half an hour after the evening feeding was completed.

At the end of the temporary culture, the experimental fish was anesthetized with 150 mg/L eugenol after fasting for 24 hours (27). A total of 225 fish with similar size (44.52 ± 0.24 g) were randomly

TABLE 1 Nutritional composition of experimental diet (Dry matter basis).

Ingredients	Group/Contents (g/kg)				
	LS	HS	HL1	HL2	HL3
Fish meal	440	220	220	220	220
Soybean meal	0	400	400	400	400
Casein	110	110	110	110	110
Flour	345	149	148	147.5	147
Fish oil	35	50	50	50	50
Soybean oil	25	25	25	25	25
Mineral premix[a]	6	6	6	6	6
Antioxidant	3	3	3	3	3
$Ca(H_2PO_4)_2$	12	12	12	12	12
Vitamin premix[b]	8	8	8	8	8
Choline	6	6	6	6	6
Methionine	0	1.0	1.0	1.0	1.0
Lecithin	10	10	10	10	10
LBP	0	0	1.0	1.5	2.0
Total	1000				

The proportion of nutrients of the main ingredients in the feed: Soybean meal: Crude fat, 1.9%, Crude protein, 44.2%; Flour: Crude fat, 3%, Crude protein, 13%; Fish meal: Crude fat, 8.4%, Crude protein, 67%.

[a]Mineral premix: $MnSO_4{\cdot}4H_2O$ 50 mg/kg, $MgSO_4{\cdot}H_2O$ 4000 mg/kg, KI 100 mg/kg, $CoCl_2$(1%) 100 mg/kg, $CuSO_4{\cdot}5H_2O$ 20 mg/kg, $FeSO_4{\cdot}H_2O$ 260 mg/kg, $ZnSO_4{\cdot}H_2O$ 150 mg/kg, Na_2SeO_3(1%) 50 mg/kg.

[b]Vitamin premix: thiamine 25 mg/kg, riboflavin 45 mg/kg, pyridoxine hydrochloride 20 mg/kg, Vitamin B12 0.1 mg/kg, Vitamin K3 10 mg/kg, inositol 800 mg/kg, pantothenic acid 60 mg/kg, nicotinic acid 200 mg/kg, folic acid 20 mg/kg, biotin 1.2 mg/kg, vitamin A acetate 32 mg/kg, Vitamin D3 5 mg/kg, α-tocopherol 120 mg/kg, ethoxyquin 150 mg/kg.

assigned to 15 fish tanks and divided into 5 groups with three replicates per group.

Feeding management during the breeding experiment was roughly the same as that of temporary rearing, and each group was fed the corresponding labeled feed separately. All tanks were connected, the temperature of the water controlled by the hot cycle heater was 27.0 ± 0.2°C, the dissolved oxygen was maintained at 7 mg/L, and the PH was maintained between 7.8 and 8.2.

2.4 Sample collection

Similarly, the experimental fish was fasted for 24 hours and anesthetized with 150 mg/L eugenol. Eleven fish were randomly selected from each tank, serum samples were collected by tail vein sampling method, and the serum was separated by centrifugation (836×g, 10min, 4°C) after 16 hours at 4°C, and stored at -80°C for later use. After that, the fish were humanely killed, the livers were collected, and 9 liver samples were briefly stored in liquid nitrogen, and then stored at -80°C. Among them, 5 liver samples were used for the detection of related enzyme activities, and 4 liver samples were used for transcriptome analysis. The remaining 2 samples were fixed with 4% paraformaldehyde for histological observation.

2.5 Analysis of immune parameters

In this study, the immune-related indicators included serum lysozyme (LZM), serum acid phosphatase (ACP), alkaline phosphatase (AKP), immunoglobulin M (IgM), and hepatic ACP and AKP. The principle of LZM activity detection is that LZM exhibited the ability to enzymatically degrade peptidoglycan present on the bacterial cell wall, resulting in bacterial lysis. This concentration gradually decreased while light transmittance increased (28). ACP and AKP can decompose phenylene disodium phosphate to produce free phenol and phosphoric acid, phenol reacts with 4-amino-antipyrine in alkaline solution to oxidize red quinone derivatives. So, the enzyme activities were determined by colorimetry (29). The principle of IgM activity detection is that competition method. In short, samples were added to the enzyme-labeled pore pre-coated with antibodies, and biotin-labeled recognition antigen was added. The two compete with solid phase antibodies to form an immune complex. After the unbound biotin antigen was washed away, avidin-HRP was added to bind to the biotin antigen, and color changes were generated under certain conditions. The light absorption values are negatively correlated with the antigen concentration (30). All kits were provided by Nanjing Jiancheng Biotechnology Co., LTD. (Item No: LZM: A050-1-1, ACP: A060, AKP: A059-2).

2.6 Analysis of related parameters of hepatic injury

In this study, hepatic injury related indexes included serum Alanine aminotransferase (ALT), Aspartate aminotransferase (AST) and liver ALT, AST, as well as observation and analysis of hepatic morphology. Both ALT and AST activities were operated as instructed, color reactions occurred, absorbances were measured at specific wavelengths, and enzyme activity was calculated (31). (Item No: ALT: C009-2-1, AST:C010-2-1).

2.6.1 Hepatic morphological analysis

The hepatic morphology was observed by hematoxylin-eosin staining. In short, samples were fixed in 4% paraformaldehyde for 24 h after collection, fully rinsed with 75% ethanol solution, and sequentially soaked in 70%, 95% and 100% concentration of ethanol solution for dehydration. After dehydration, samples were transferred to 1:1 xylene ethanol solution for 20 minutes and xylene paraffin mixture for 30 minutes. Finally, the samples were quickly embedded at 60°C. After the samples were cooled and solidified, they were sliced by a microtome (RM2016, LEICA, Germany), spread in warm water, collected by slides and dried in a constant temperature oven at 55°C for 8h. The dried sections were deparaffinized in xylene and ethanol solutions and covered with coverslips after staining with hematoxylin and eosin solutions, respectively. A forward white light microscope (Eclipse Ci-L, Nikon, Japan) was used to photograph and analyze these slices. And these slices were observed in various multiples (200×) with CaseViewer Ver 2.2 (The Digital Pathology Corp., Hungary).

Fifteen liver section samples (three replicates per group) were randomly selected for quantitative analysis of fat vacuoles. Fiji (ImageJ-win64) was used for image analysis and processing. In short, after region-of-interest (ROI) was selected on the original image, a manual threshold was further selected to mark the fat vacuoles in the samples, calculate and output the IntDen value, and use the IntDen value of the LS group samples as the control, the relative area of fat vacuoles in each group was calculated. The obtained results were processed and mapped according to Method in 2.8 (32, 33).

2.7 Hepatic transcriptome analysis and RT-qPCR

2.7.1 Total RNA extraction and detection

Total RNA was extracted by TRIzol kit, RNA purity and concentration were detected by NanoDrop 2000 spectrophotometer (manufacturer Thermerfly), and RNA integrity was detected by Agient2100 or LabChip GX.

2.7.2 Library construction

Once the samples were qualified, a sequencing library was generated using NEBNext®Ultra™ RNA library preparation using Illumina® (NEB USA) and an index code was added to the attribute sequence of each sample. In short, eukaryotic mRNA was enriched with magnetic beads with Oligo (dT), and mRNA was randomly interrupted by Fragmentation Buffer. The first cDNA strand and the second mRNA strand were synthesized using mrna as template, and cDNA purification was performed. After purification, the double-stranded cDNA was end-repaired, A-tail was added, and sequencing connectors were connected. Then AMPure XP beads (Beckman Coulter, Beverly, USA) were used for fragment size selection, and the cDNA library was enriched by PCR.

2.7.3 Library quality control

After the library was constructed, the Qubit 3.0 fluorometric quantifier was used for preliminary quantification, and the concentration of c should exceed 1 ng/ul. Then the Qsep400 high-throughput analysis system was used to detect the inserted fragments of the library. After meeting the expectation, the effective concentration of the library (effective concentration > 2 nM) was accurately quantified by q-PCR method. To ensure the quality of the library.

2.7.4 Sequencing

The Illumina NovaSeq6000 sequencing platform was used for PE150 mode sequencing.

2.7.5 Transcriptome assembly and gene functional annotation

Tanscriptome assembly was accomplished based on the left.fq and right.fq using Trinity (min_kmer_cov set to 2 by default and all other parameters set default) (34). Gene function annotation was based on the following database: NR (NCBI non-redundant protein sequences), Pfam (Protein family), KOG/COG (Clusters of Orthologous Groups of proteins), Swiss-Prot (A manually annotated and reviewed protein sequence database), KEGG (Kyoto Encyclopedia of Genes and Genomes), GO (Gene Ontology).

2.7.6 Quantification of gene expression levels

The level of gene expression in each sample was estimated by RSEM (35).

2.7.7 Differential expression analysis

Based on the Count value of genes in each sample, DESeq2 (36) software was used to screen differential gene expression, and Fold Change ≥ 2 and FDR < 0.01 were used as screening criteria. All of the above analysis was performed passing BMKCloud (www.bioloud.net).

2.7.8 RT-qPCR

RT-qPCR reaction was measured by SYBR Green I chimeric fluorescence method. Kits were purchased from Nanjing Vazyme Biotech Co., Ltd., China (Q711-02/03). Using β-actin as internal parameter, and, according to the results of transcriptomic analysis, 5 genes were randomly selected from the common differential genes of the three groups (LS, HS, HL1) for RT-qPCR reaction. Primer

information was recorded in Table 2. Specifically, 2 µl template cDNA, 10 µL of 2×ChamQ Universal SYBR qPCR Master Mix were added to the reaction system. 0.4 µL of forward and reverse primer (10 µM), 7.2 µL RNase-free ddH_2O. After preparation, the system was amplified by fluorescent quantitative PCR (LC480, Roche, Switzerland). The reaction conditions were: predenaturation at 95°C for 30 seconds, then reaction at 95°C for 10 s, 60°C for 30 s for 40 cycles; finally, the dissolution curves were collected under the reaction conditions of 95°C 15 s, 60°C 60 s and 95°C 15 s respectively. The relative gene expression between groups was calculated by 2-ΔΔCt.

2.8 Data statistics and analysis

Average values of experimental data were calculated, expressed as mean ± SD. The difference between the two control groups (HS and LS) was analyzed by independent sample T test. The LBP intake group (HL1, HL2 and HL3) was compared with the two control groups, and one-way analysis of variance was used. All statistical analysis were performed using SPSS Ver26 software. When $P < 0.05$, the difference was significant and Duncan multiple range test was performed. All figures were produced by GraphPad Prism 8 except transcriptomic analysis.

3 Results

3.1 Analysis of immune parameters

The results of immune-related indexes are shown in Figure 1. Compared with the LS group, the high soybean meal diet significantly decreased the hepatic AKP activity ($P < 0.05$). However, after adding LBP, the activities of serum LZM and IgM, hepatic AKP and ACP were significantly increased ($P < 0.05$). Among them, when the supplemental level was 1 g/kg, the serum LZM activity was significantly increased compared with the two control groups ($P < 0.05$), the serum IgM and hepatic ACP activities were significantly increased compared with the LS group ($P < 0.05$), and the hepatic AKP activity was significantly higher than the HS group ($P < 0.05$). In addition, when the supplemental level was 2 g/kg, the hepatic ACP activity was significantly higher than all groups ($P < 0.05$).

3.2 Analysis of related parameters of hepatic injury

3.2.1 Enzyme activity index

The results of liver injury-related enzyme activity indexes are shown in Figure 2. Compared with the whole fish meal diet, the intake of HSBMD caused hepatic damage, which was reflected in serum AST and ALT, and hepatic ALT activity was significantly increased ($P < 0.05$). After the addition of LBP, there was no significant difference between serum AST and the two control groups, but serum ALT and hepatic ALT were significantly decreased compared with HS group ($P < 0.05$), and even recovered to the level close to that in LS group. Among them, hepatic ALT activity of all LBP supplemental groups was significantly lower than HS group ($P < 0.05$), and had no significant difference compared with LS group. When LBP supplemental levels were 1 and 2 g/kg, the serum ALT activity was significantly lower than HS group ($P < 0.05$), but no significant difference was found between LS group and HS group.

3.2.2 Hepatic morphological analysis

The observation results of the hepatic morphology are shown in Figure 3. Few fat vacuoles and balloon deformation were observed in the LS group, and overall liver morphology was normal (Figures 3A, 4A). However, after ingestion of HSBMD, a large number of vacuoles and balloon deformation occurred in the hepatic, and the cytoplasm was subsequently loosened, showing a very unhealthy state overall (Figures 3B, 4B). LBP supplementation could improve the hepatic damage caused by HSBMD to a certain extent. Compared with the

TABLE 2 Information of primers.

Gene	Primer sequence (5′-3′)	Annealing temperature (°)
β-actin	F:AACTGGGATGACATGGAGAAG R:TTGGCTTTGGGGTTCAGG	60
TRINITY_DN1011_c0_g1	F:ACATCGCATCACTTCACTGC R:AGGACTTGGAACTGAGGTGG	60
TRINITY_DN1273_c0_g1	F:CTGACAGCCGGGACACTTT R:GCACTGTGACCCCTTTCATC	60
TRINITY_DN13763_c0_g1	F:CCAGTTCAGCGTGTATCAGC R:GGCTGGGGAGAGATCAAACT	60
TRINITY_DN14696_c0_g1	F:ATGGCTTTCTCCCTGCTTCT R:GCAAAGACAAGCACAGTGGA	60
TRINITY_DN17812_c0_g4	F: GGCGCATGGTGTTCAAGTAA R: GGGGCGAACTCAACTTTACC	60

F means forward primer, while R means reverse primer.

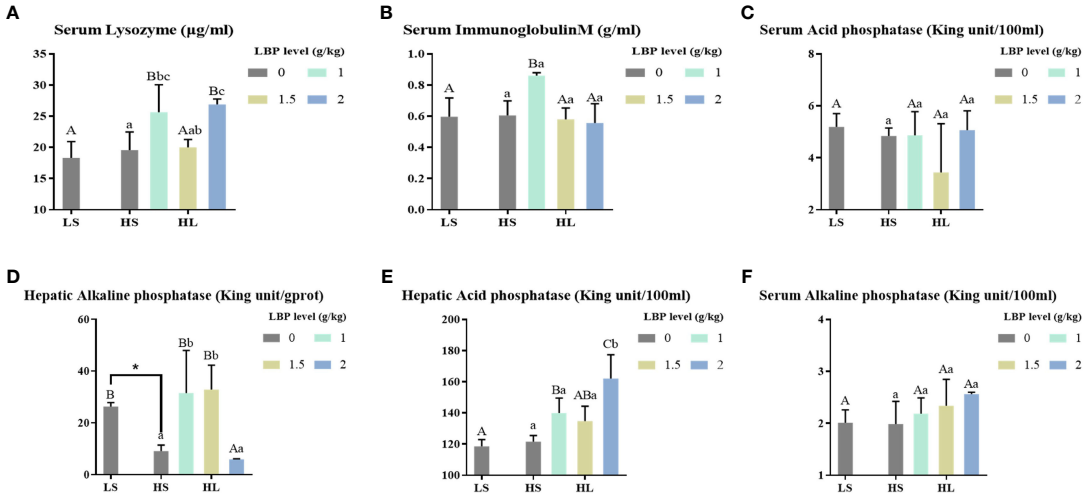

FIGURE 1
Results of immune-related enzyme activity index. Letters in corner marks **(A–F)** represent activity of serum lysozyme (serum LYZ, **A**), serum immunoglobulin M (serum IgM, **B**), serum acid phosphatase (serum ACP, **C**), hepatic alkaline phosphatase (hepatic AKP, **D**), hepatic acid phosphatase (hepatic ACP, **E**), serum alkaline phosphatase (serum AKP, **F**), respectively. The discrepancy between the LS group and HS group is indicated by * (P<0.05). Capital letters represent the discrepancy between LBP intake groups and LS group, while different letters indicate significant variation (P<0.05). Lowercase letters represent the discrepancy between LBP intake groups and HS group, while different letters indicate significant variation, too (P<0.05). Same to the following figures.

HS group, fewer lesions were observed in the LBP addition group, and fewer fat vacuoles and balloon deformation were observed. When the LBP supplemental level was 1g/kg, the hepatic health of the HL1 group was close to LS group (Figures 3C, 4C). However, when LBP adding amount of 1.5 and 2.0 g/kg, fat vacuoles and balloon deformation increased slightly (Figures 3D, E, 4D, E).

The results of the relative area of fat vacuoles between the groups showed in Figure 5. Compared with LS group, the relative area of fat vacuoles in HS group was significantly increased ($P < 0.05$). After adding LBP, the relative area of fat vacuoles was decreased significantly ($P < 0.05$). There was a tendency to decrease with the increase of LBP addition.

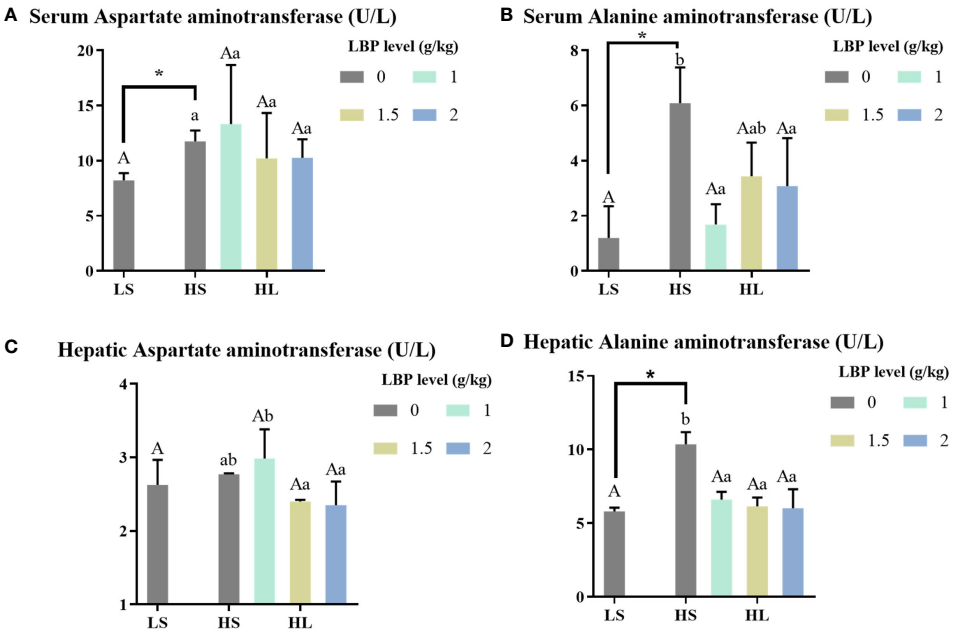

FIGURE 2
Results of hepatic injury-related enzyme activity indexes. Letters in corner marks **(A–D)** represent activity of serum aspartate aminotransferase (serum AST, **A**), serum alanine aminotransferase (serum ALT, **B**), hepatic aspartate aminotransferase (hepatic AST, **C**), hepatic alanine aminotransferase (hepatic ALT, **D**), respectively. The discrepancy between the LS group and HS group is indicated by *(P<0.05). Capital letters represent the discrepancy between LBP intake groups and LS group, while different letters indicate significant variation (P<0.05). Lowercase letters represent the discrepancy between LBP intake groups and HS group, while different letters indicate significant variation, too (P<0.05).

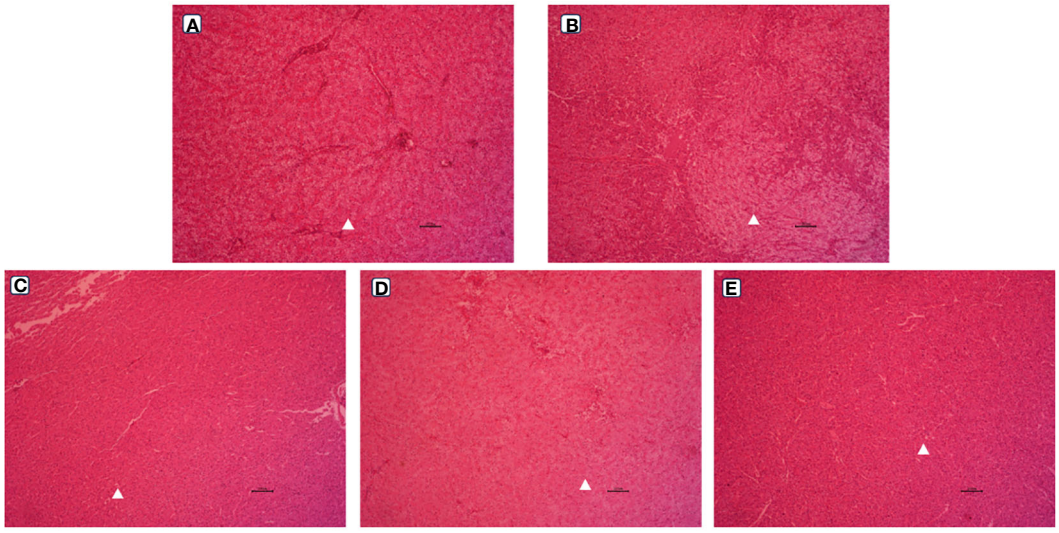

FIGURE 3
Hepatic morphological (100 ×) of spotted sea bass. Letters in corner marks A to E represent LS group **(A)**, HS group **(B)**, HL1 group **(C)**, HL2 group **(D)**, and HL3 group **(E)**, respectively. The triangular marks indicate balloon-like deformation and fat vacuoles.

3.3 Summary of results of liver transcriptome analysis

According to the above analysis results, we selected LS, HS, and HL1 groups for transcriptome sequencing, and compared the two groups. A total of three comparison groups were: LS vs HS, HS vs HL1 and LS vs HL1. A total of 57.43 Gb of Clean Data were obtained, and the Clean Data of all samples reached 5.86 Gb, and the percentage of Q30 base was 94.35% or above. A total of 44,470 Unigenes were obtained after assembly. There are 15,484 Unigenes pieces with a length of more than 1 kb. After functional annotation of Unigenes, 21,753 Unigenes annotation results were obtained.

3.3.1 Differentially expressed genes

Compared with LS group, a total of 481 DEGs were observed in HS group, including 230 up-regulated and 251 down-regulated, and 1116 DEGs were observed in HL1 group, including 540 up-regulated and 576 down-regulated. Compared with the HS group,

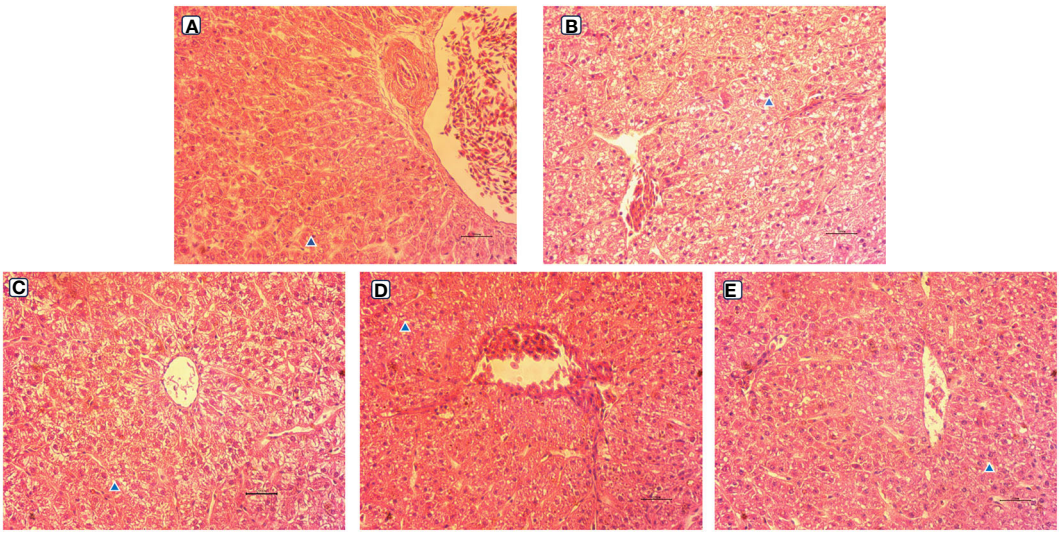

FIGURE 4
Hepatic morphological (400 ×) of spotted sea bass. Letters in corner marks A to E represent LS group **(A)**, HS group **(B)**, HL1 group **(C)**, HL2 group **(D)**, and HL3 group **(E)**, respectively. The triangular marks indicate balloon-like deformation and fat vacuoles.

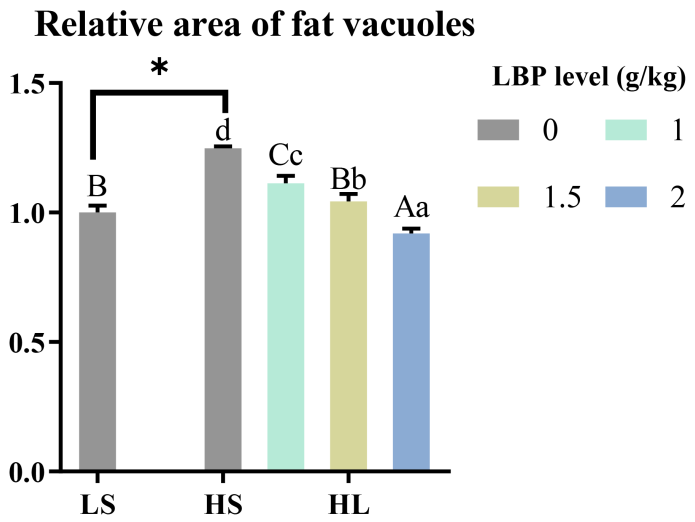

FIGURE 5
Results of the relative area of fat vacuoles. The discrepancy between the LS group and HS group is indicated by *(P<0.05). Capital letters represent the discrepancy between LBP intake groups and LS group, while different letters indicate significant variation (P<0.05). Lowercase letters represent the discrepancy between LBP intake groups and HS group, while different letters indicate significant variation, too (P<0.05).

721 DEGs were identified in the HL1 group supplemented with LBP, of which 419 were up-regulated and 302 were down-regulated (Table 3). In addition, there were a total of 18 DEGs between the three comparison groups. The specific number of total DEGs between the two comparison groups are shown in Figure 6.

3.3.2 GO classification enrichment analysis

In the three branches of biological process, cellular component and molecular function, the number of up-regulated genes in LS vs HS comparison group were more than down-regulated genes. And biological process was concentrated in terms of cellular process, metabolic process, and localization. Cellular component was focused on cellular anatomical entity and intracellular, and molecular functions was focused on binding and transporter activities. Similarly, HS vs HL1 comparison group showed similar results to LS vs HS in terms of biological process, cellular component, molecular function and their secondary classification level. However, when comparing the HL1 group with the LS group, different results emerged. In the biological process and cellular component of HL1 group, the number of up-regulated genes were greater than the number of down-regulated genes, and they were concentrated in the above levels. But, it was interesting to note that the up-regulated number of binding and transporter activities in molecular function were smaller than the down-regulated number (Figure 7).

TABLE 3 DEGs of between groups.

Group	All DEGs	Up-regulated	Down-regulated
LS vs HS	481	230	251
HS vs HL1	721	419	302
LS vs HL1	1116	540	576

ClusterProfiler was used to conduct enrichment analysis of biological process, cellular component and molecular function by hypergeometric testing method. The results showed that: in the biological process, LS vs HS comparison group differentially enriched in cellular response to unfolded protein, response to topologically incorrect protein and response to unfolded protein and other terms, and the differential genes showed up-regulation in these terms. The term difference in LS vs HL1 comparison group mainly included the Triglyceride metabolic process and response to extracellular stimulus. In the HS vs HL1 comparison group, cell redox homeostasis, endoplasmic reticulum unfolded protein response and cellular response to unfolded protein terms were down-regulated. In particular, cellular response to unfolded protein was up-regulated in the LS vs HS comparison group. The specific enrichment term of differentially expressed genes are shown in Figure 8.

3.3.3 KEGG annotation analysis

The results of KEGG enrichment analysis showed that, compared with the LS group on the whole fish meal diet, HSBMD induced changes in metabolic pathways. Insulin signaling pathway, adipocytokine signaling pathway, carbon metabolism, starch and sucrose metabolism, arginine and proline metabolism, glycolysis/gluconeogenesis and other pathways related DEGs were down-regulated. Terpenoid backbone biosynthesis, glutathione metabolism, steroid biosynthesis and protein processing in endoplasmic reticulum, PPAR signaling pathway and other pathways related DEGs were up-regulated. Including peroxisome proliferator-activated receptor alpha (PPARα), lectin, mannose-binding 2 (LMAN2) and other genes. In addition, immune-related pathways were also enriched with some DEGs, toll-like receptor signaling pathway, P53 signaling pathway, erbb signaling pathway, NOD-like receptor signaling pathway and Intestinal immune network for IgA production, and their DEGs

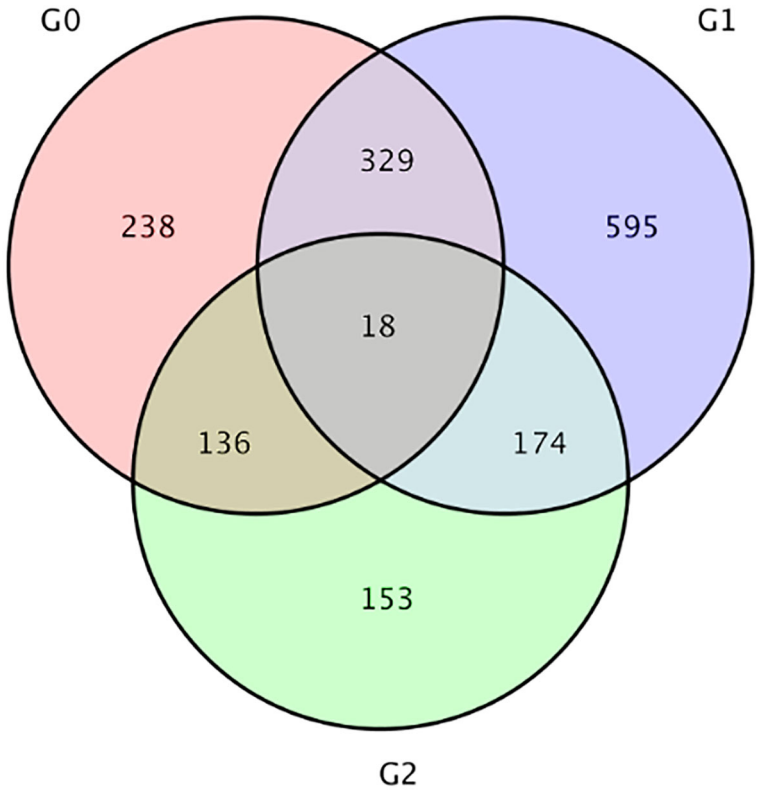

FIGURE 6
Venn diagram of differential genes. G0: HS vs HL1, G1:LS vs HL1, G2: LS vs HS. The numbers on each region represent the number of genes in the corresponding classification, where overlapping regions represent the number of differential genes shared between related combinations in the reg.

were mostly down-regulated. In particular, MAPK signaling pathway and foxo signaling pathway related DEGs downregulation, including mitogen activated protein kinase kinase 6 (MKK6) and 5'-AMP-activated protein kinase, regulatory gamma subunit (PRKAG). The same HSBMD, LBP supplementation enriched DEGs mainly in pathways related to glucose and lipid synthesis and metabolism, including insulin signaling pathway, adipocytokine signaling pathway, glycolysis/gluconeogenesis, and glycolysis/gluconeogenesis. galactose metabolism, and their associated DEGs were upregulated. DEGs were up-regulated in P53 signaling pathway, erbb signaling pathway, nod-like receptor signaling pathway and other related pathways, and showed opposite results to LS vs HS. In addition, the MAPK signaling pathway and Foxo signaling pathway also showed opposite results. DEGs were mainly upregulated, and mitogen activated protein kinase 8 (MAP3K8) and forkhead box protein O1 (FOXO1) were also upregulated. The expression of toll-like receptor 3 (TLR3) and toll-like receptor 5 (TLR5) genes were down-regulated in toll-like receptor signaling pathway. Surprisingly, PPARα did not change significantly in the PPAR signaling pathway. However, its downstream lipid metabolism-related genes fatty acid-binding protein 1 (FABP1), lipoprotein lipase (LPL), long-chain acyl-coA synthetase (ACSL), carnitine o-palmitoyltransferase 1 (CPT-1) and phosphoenolpyruvate carboxykinase (PEPCK) were upregulated. On the other hand, in the LS vs HL1 group, the above pathways related to glucose and lipid synthesis and metabolism also changed accordingly, and the related DEGs were both up-regulated and down-regulated. In addition, TLR3 and TLR5 were also down-regulated in toll-like receptor signaling pathway, and mitogen activated protein-related genes were down-regulated in MAPK signaling pathway, but the downstream genes of the PPAR signaling pathway related to lipid metabolism were significantly up-regulated (Figure 9).

3.3.4 RT-qPCR verification

After RNA-seq transcriptomic analysis of the data, in order to verify the accuracy of the transcriptomic results, RT-qPCR (biological repeat n=6) was used for verification analysis, that is, 5 common DEGs were randomly selected and pair-to-pair comparison was conducted among the three groups. The results confirmed that the five DEGs expression differences between the three groups were consistent with the RNA-Seq trend, where LS vs HS, R^2 = 0.9828; HS vs HL1, R^2 = 0.9708; LS vs HL1, R^2 = 0.9246. The results further confirmed the reliability and authenticity of the results of RNA-Seq transcriptome analysis (Figure 10).

4 Discussion

HSBMD can cause a range of uncomfortable reactions in farmed animals. Yoshinaga et al. reported that fish with a large dietary intake of soybean meal showed growth retardation and

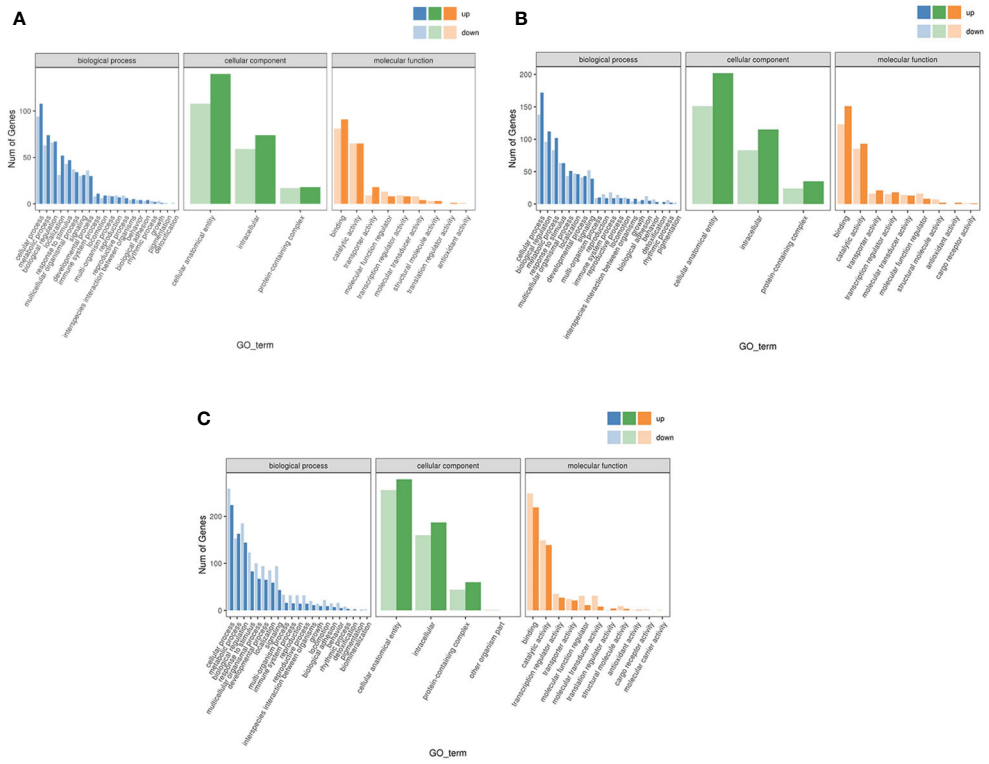

FIGURE 7
Differential expression gene GO annotation classification statistical map. Letters in corner marks **(A–C)** represent LS vs HS **(A)**, HS vs HL1 **(B)**, LS vs HL1 **(C)**, respectively. The horizontal coordinate is the GO classification, the vertical coordinate is the number of genes, and the different colors represent the different primary classification.

physiological abnormalities, and cholesterol metabolism was also affected (37). Matulić et al. reported that the replacement of fish meal with soybean meal caused hepatic tissue degeneration in brown bullhead (*Ameiurus nebulosus L*) (38). In the results of this experiment, the addition of high soybean meal decreased the immune capacity of the spotted sea bass to a certain extent. And immune-related pathways such as toll-like receptor signaling pathway, P53 signaling pathway and erbB signaling pathway are also changed. In addition, compared with LS group, the hepatic morphology of HS group showed more fat vacuoles and balloon deformation. It was accompanied by severe hepatic cell injury, and the related pathways of glucose and lipid metabolism were also disturbed. These results suggest that HSBMD can cause serious tissue damage in the liver of spotted sea bass, which may be related to the decreased immunity and the glucolipid metabolic pathway. As mentioned in the introduction, this study focused on exploring whether LBP can mitigate these adverse effects or protect liver health. Therefore, this study will be discussed and focus on the two aspects of LBP to improve immunity and regulate glucose and lipid metabolism.

LZM is a natural antibacterial enzyme, which has lytic activity against both Gram-positive and Gram-negative bacteria, and can activate the complement system and phagocytes. Its activity is an important indicator of innate immunity in fish (39). Immunoglobulins (Ig) are glycoproteins that play a fundamental role in the adaptive immune system by recognizing antigens, and there are three types in teleost, namely IgM, IgD, and IgT/IgZ (40, 41). Among them, IgM is the main systemic antibody, involved in systemic immunity and mucosal immunity (42). ACP and AKP can change the surface structure of pathogens by hydrolysis, improve the body's recognition and phagocytosis ability, and thus enhance disease resistance (43, 44). According to the results of this study, the addition of LBP significantly increased the activities of serum LYZ and IgM, hepatic ACP and AKP. Obviously, LBP improved the immunity of the spotted sea bass. Similarly, there are many studies that have reported the effect of LBP on improving immunity. Zhang et al. reported that LBP could improve the non-specific immunity of nile tilapia (*Oreochromis niloticus*) and reduce cell apoptosis (45). Zhu et al. reported that LBP induces dendritic cells to mature by stimulating the NF-κB signaling pathway mediated by Toll like receptor 2 (TLR2) and Toll like receptor 4(TLR4), so as to improve the immune capacity of the body (46). The research results of Zhang et al. show that LBP can significantly enhance the function of B cells and macrophages (47). It can be seen that LBP can enhance the body's immunity through a variety of ways. In this experiment, TLR3 and TLR5 in AMPK signaling pathway were significantly down-regulated in the LBP addition group. TLR5 can combine with bacterial flagellin and cause obvious immune responses. The authors hypothesized that flagellin stimulation of membrane TLR5 leads to the induction of soluble TLR5S in the liver, which effectively binds to flagellin and then translocates it to membrane TLR5 factors in order to amplify danger signals in a positive feedback loop (48). In addition, Tsukada et al. found that soluble TLR5S was up-regulated 8

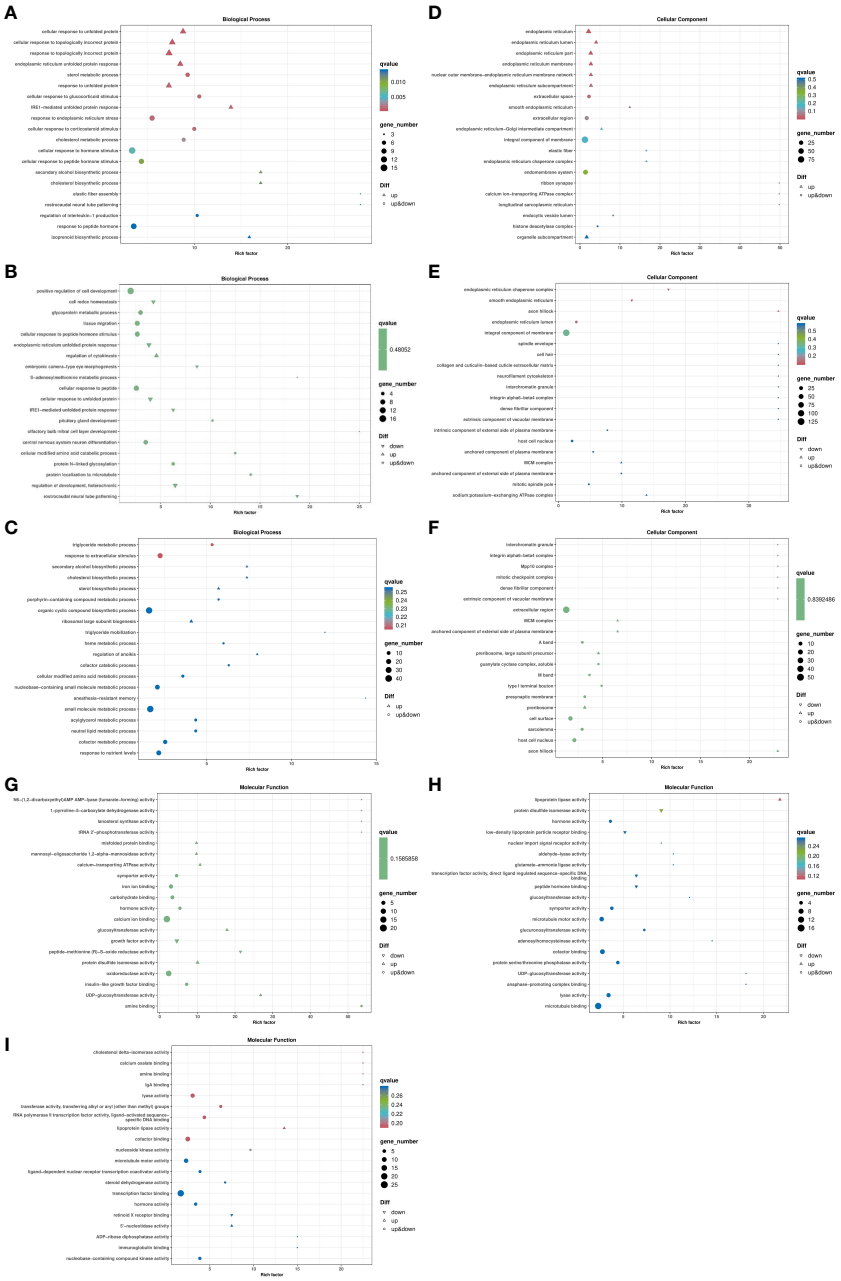

FIGURE 8
Bubble map of differentially expressed gene GO enrichment. Letters in corner marks **(A–I)** represent LS vs HS biological process **(A)**, HS vs HL1 biological process **(B)**, LS vs HL1 biological process **(C)**, LS vs HS cellular component **(D)**, HS vs HL1 cellular component **(E)**, LS vs HL1 cellular component **(F)**, LS vs HS molecular function **(G)**, HS vs HL1 molecular function **(H)**, LS vs HL1 molecular function **(I)**, respectively. The horizontal coordinate is Rich factor, which represents the ratio of the proportion of genes annotated to a pathway in differential genes to the proportion of genes annotated to that pathway in all genes, and the vertical coordinate represents the GO annotation term. The higher the enrichment factor, the more significant the enrichment level of differentially expressed genes in the GO term. Upper triangle, lower triangle and circle respectively represent the differential expression of genes enriched into the pathway, in which the upper triangle indicates that all genes enriched into the pathway are up-regulated genes, the lower triangle indicates that all genes enriched into the pathway are down-regulated genes, and the circle indicates that genes enriched into the pathway are both up-regulated and down-regulated genes. The color of the shape represents qvalue, the smaller the qvalue, the lower the qvalue. It indicates that the enrichment of differentially expressed genes in this GO term is more reliable. The size of the shape indicates the number of genes enriched in the GO term, and the larger the shape, the more genes.

hours after attack by Vibrio or its purified flagellin (49). Therefore, we speculate that the down-regulation of TLR5 in this study is the result of reduced stimulation of the organism by bacteria or their flagellin. TLR3 is responsible for virus detection. Some studies have found the TLR3 gene has been over transcribed in rainbow trout after infection hematopoietic necrosis virus (*Oncorhynchus mykiss*) (50), and in zebrafish (*Danio rerio*) after infection with Snakehead Rhabdovirus (51), as well as in the Chinese rare minnow after challenge with the infectious Grass carp reovirus (*Gobiocypris rarus*) (52). Thus, similarly to TLR5, the down-regulation of TLR3 in this study may also be the

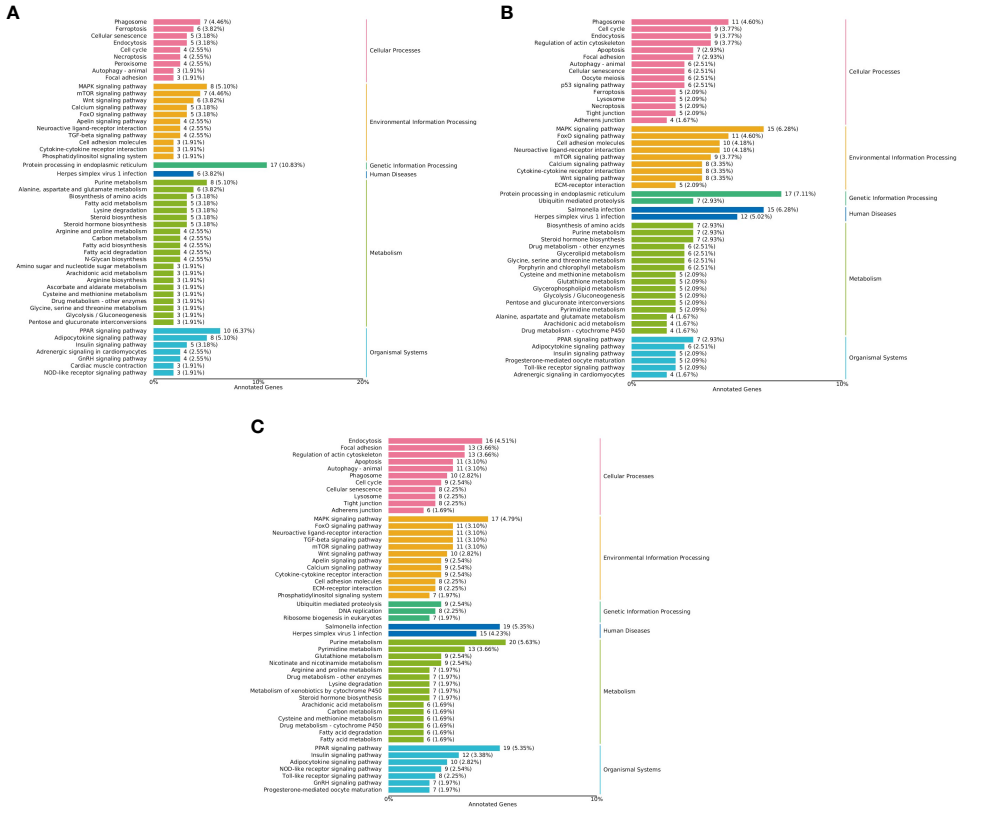

FIGURE 9
KEGG classification map of differentially expressed genes. Letters in corner marks **(A–C)** represent LS vs HS **(A)**, HS vs HL1 **(B)**, LS vs HL1 **(C)**, respectively. The left vertical coordinate is the name of the KEGG metabolic pathway, the right vertical coordinate represents the first-class classification name corresponding to the annotated pathway, and the horizontal coordinate is the number of genes annotated to the pathway and their proportion to the total number of genes annotated.

result of reduced virus attack. On the other hand, NOD-like receptor signaling pathway (NLRS) also changed accordingly, and major DEGs expressions were up-regulated. NLRS plays an important role in innate immunity, and the up-regulation of its key DEGs means that LBP can enhance the immune capacity of the body through NLRS (53). In addition, apoptosis is an important mechanism for maintaining liver development and immune stability (54). The MAPK signaling pathway, foxo signaling pathway and P53 signaling pathway are all important pathways related to apoptosis. These pathways were altered by the addition of LBP, and these changes may be due to apoptosis to balance the liver damage caused by HSBMD. Based on the above changes of these pathways in different groups and the changes of their related DEGs, we speculate that the addition of LBP may activate or promote the apoptosis process. It has been reported that low-temperature induced inflammation and apoptosis may be the adaptive mechanism of antioxidant and immunity of freshwater drum (*Aplodinotus grunniens*) in freshwater drumfish (55). This suggests that there is a certain relationship between immunity and apoptosis, and this relationship may be regulated and balanced by the body itself. There is no doubt that this connection is complex and variable, but it is also of great study value. In addition, in this experiment, only when the supplemental level of LBP was 1 g/kg, the immunity of spotted sea bass was significantly improved, and the effects were also decreased when the supplemental level was increased.

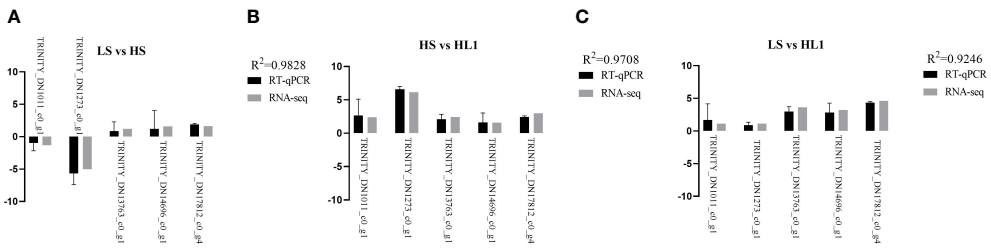

FIGURE 10
Relative expression levels (log2 fold change). Letters in corner marks **(A–C)** represent LS vs HS **(A)**, HS vs HL1 **(B)**, LS vs HL1 **(C)**, respectively.

This suggests that excessive LBP supplementation may have negative effects or there may be immune fatigue to LBP. This is also worthy of further study in the future.

AST is mostly distributed in myocardium, liver and other tissues, while ALT is mainly present in liver cells. Under normal circumstances, only a small amount of AST and ALT are released into the blood, so the activity of AST and ALT in serum are very small. However, when hepatocytes are destroyed, the activity of AST and ALT in serum increases rapidly. Therefore, AST and ALT are used as relevant indexes to evaluate hepatic injury. The significant increase of serum AST and ALT activities induced by HSBMD in this study reflects that the liver has suffered serious damage. The results of hepatic morphology observation showed that HSBMD caused the increase of fat vacuoles and balloon deformation in the liver, and the liver cells were seriously damaged, which further supported the results of enzyme activity. In addition, transcriptomic sequencing revealed significant changes in pathways associated with glycolipid metabolism, including steroid biosynthesis, glycolysis/gluconeogenesis, glutathione metabolism and insulin signaling pathway. These may be the result of HSBMD. In particular, genes related to cholesterol biosynthesis were upregulated, suggesting that HSBMD may contribute to cholesterol deficiency. Fish meal contains more cholesterol than most plant-based protein ingredients (56). Therefore, HSBMD may have a lower cholesterol content, which may lead to a deficiency of cholesterol in the fish. This study reasonably hypothesized that the up-regulation of genes related to cholesterol synthesis was the result of poor adaptation to cholesterol. The same result was also found in the study of Yoshinaga et al. (37), who reported the results of transcriptomic analysis of the red seabream (*Pagrus major*) hepatopancreas, which ingests a large amount of soybean meal. Among them, Insulin signaling pathway, Carbon metabolism related DEGs down-regulation, Steroid biosynthesis, Glutathione metabolism related DEGs up-regulation. Interestingly, upregulation of the PPARα, which regulates lipid metabolism, was observed in this study. It has been demonstrated that gluconeogenesis is a direct target of PPARα and that PPARα has a significant impact on glucose homeostasis (57–59). Therefore, the up-regulation of PPARα may be an adaptive regulation of the body to the down-regulation of gluconeogenesis, but also a mechanism of the body's self-regulation of glucose and lipid balance. This also indicates that the body may have produced a disorder in the production and metabolism of sugars and lipids, and this was also demonstrated by the changes in the glycolipid-related pathways in this experiment.

This study found that LBP can regulate the expression of downstream lipid metabolis-related genes in the PPAR signaling pathway, including FABP1, LPL, ACSL, CPT-1 and PEPCK, and they are all up-regulated. And after dietary intake of LBP, hepatic morphology was also improved to some extent, and serum ALT and AST activities were decreased. These results indicate that LBP has a positive effect on the regulation of lipid metabolism. Polysaccharides regulate lipid metabolism in many ways. One of the ways is that polysaccharides inhibit the body's absorption of exogenous lipids and further affect the lipid metabolism process by binding with lipid molecules in the gastrointestinal tract or bile salts (60, 61). In general, the higher the molecular weight of the polysaccharide, the greater the hydrophobicity or viscosity, the stronger its binding ability (60). But interestingly, the study found that the lower the molecular weight of the polysaccharide, the stronger the binding ability of the bile acid (62). This indicates that the molecular weight of polysaccharide is not the only determinant of the binding ability of polysaccharide, and the composition and structure of polysaccharide may also be an important determinant. In addition, polysaccharide regulation can also regulate animal lipid metabolism by affecting intestinal microorganisms, regulating gene expression and related enzyme activity (61). The structure of intestinal flora plays an important role in the absorption and metabolism of lipids. Martinez-Guryn et al. showed that polysaccharides can regulate lipid metabolism by regulating intestinal flora (63). Furthermore, the animal intestinal microbiota and its metabolites also influence the expression of host-related genes. Zhang et al. reported that polysaccharide can activate intestinal HIF1α gene, and increase of this gene can not only promote the expression of local antimicrobial peptides, but also affect the expression of genes related to liver lipid metabolism through the gut-liver axis (64). Therefore, the molecular weight and composition of polysaccharide and the utilization of polysaccharide by fish can affect lipid metabolism. The structure and characterization of LBP are the prerequisite to reveal its function. At present, the primary structure of LBP includes molecular weight, the position of glycosidic bond, the type and proportion of monosaccharides, etc. These factors affect their biological activity to varying degrees (65). LBP mainly consists of five main structures: arabinogalactan, pectin polysaccharide, xylan, glucan, and other heteropolysaccharides (16, 66–68). These structures are mainly degraded by intestinal microorganisms to produce small molecule metabolites. These small molecule metabolites play a crucial role in host-gut microbiota interactions that help regulate gut health, lipid metabolism, and systemic immunity. For example, short-chain fatty acids are the main end metabolites produced during LBP fermentation and can regulate host physiology through multiple pathways (69–71). In addition, the intermediate products produced after the degradation of LBP by microorganisms may also be beneficial to the host. For example, oligosaccharides produced by microbial degradation of polysaccharides may have the ability to cross the vascular barrier and enter the systemic circulation to play an effect. It has been demonstrated that some oligosaccharides including 6'-sialyllactose, lacto-N-neotetraose and human milk 2' -fucosyllactose can be absorbed into the plasma and thus reach the systemic circulation (72, 73). The monosaccharide composition, degree of polymerization and glycosidic linkage of LBP largely determine the regulatory effect of LBP on the host gut microbiota (74). Therefore, the structure and characterization of LBP, host gut microbiota, and metabolites have complex regulatory networks that need to be investigated through further *in vivo* and *in vitro* experiments.

On the other hand, this study found that GO and KEGG enrichment analysis and metabolism-related pathways were particularly active after ingestion of LBP. In particular, DEGs related to insulin signaling pathway, glycolysis/gluconeogenesis and galactose metabolism were upregulated. The monosaccharide

composition of LBP used in this study includes Galactose, so when fish digest, absorb and utilize LBP, glycolysis/gluconeogenesis and galactose metabolism pathways naturally change. But using LBP directly to have this effect is minimal. First, the addition of LBP in this trial was small enough not to directly have this effect. Secondly, the ability of fish to directly absorb polysaccharides is limited, and the way to maximize the utilization is with the help of intestinal microorganisms and their metabolites. Therefore, this change may not only be caused by the absorption and utilization of LBP itself, but also may include the multi-pathway regulation of the body by LBP. Cai et al. reported that LBP decreased glucose uptake by down-regulating SGLT1 in Caco2 cells (75). Zhu et al. reported that LBP promoted the proliferation of pancreatic B cells, accelerated glucose metabolism and insulin secretion (76). Similarly, there are many studies on the hypoglycemic effect of LBP (77, 78). However, in this study, changes in insulin signaling pathway and other pathways related to sugar synthesis and metabolism were only found in the rich concentration of KEGG pathway, and changes in blood glucose were not detected. The subsequent LBP regulation mechanism of sugar metabolism in aquatic animals is worthy of further study. There is no doubt that sugar metabolism and lipid metabolism are related, or can regulate each other. This is undoubtedly a huge regulatory network, and the genes and pathways involved are also very complex. At present, the discussion on the mechanism of their interaction is still few, which needs to be further studied.

In summary, LBP has great potential in improving the immunity of aquatic animals, regulating glucose and lipid metabolism, and thus protecting hepatic health, and it is recommended to be widely used in aquaculture. However, as mentioned before, there is still a lack of reports on the negative effects of polysaccharides on farmed animals. These potential negative effects not only determine the optimum addition of polysaccharides, but also restrict the popularization and application of polysaccharides. In addition, combining polysaccharides with some anti-diabetic chemicals may have unexpected positive effects. However, it is necessary to consider whether the chemical drug shares a common target with the polysaccharide, resulting in competitive inhibition. Nevertheless, it is still a direction worth taking further. It is worth noting that the regulation of polysaccharide corresponding to lipid metabolism also has great potential in the treatment of fatty liver. And it is also worth paying attention to trying to study whether other herbal plant polysaccharides have the same excellent effect.

5 Conclusion

In conclusion, the addition of LBP in the diet can improve the immune capacity of spotted sea bass and affect the immune and glycolipid metabolism related pathways, so as to improve the damage of liver and the imbalance of glycolipid metabolism caused by high soybean meal in the diet to a certain extent, and thus protect the liver health of spotted sea bass. This result reveals the potential of LBP to enhance immunity and improve glucose and lipid metabolism of aquatic animals, and subsequent studies can focus on the negative effects of LBP and development of related targets.

Data availability statement

The datasets presented in this study can be found in online repositories. The names of the repository/repositories and accession number(s) can be found below: NCBI SRA, PRJNA1070061.

Ethics statement

The animal study was approved by Jimei University Animal Ethics Committee. The study was conducted in accordance with the local legislation and institutional requirements.

Author contributions

LL: Writing – original draft, Writing – review & editing. YZ: Writing – review & editing. ZH: Writing – review & editing. ZYL: Writing – review & editing. HQ: Writing – review & editing. HL: Writing – review & editing. SZ: Writing – review & editing. LK: Writing – review & editing. JM: Writing – review & editing. ZBL: Data curation, Funding acquisition, Methodology, Resources, Writing – review & editing.

Funding

The author(s) declare financial support was received for the research, authorship, and/or publication of this article. This experiment was funded by Science and Technology Planning Project in Fujian, China (Grant No. 2015N0010) and Science and Technology Planning Project in Xiamen, China (Grant No. 3502Z20143017).

Conflict of interest

The authors declare that the research was conducted in the absence of any commercial or financial relationships that could be construed as a potential conflict of interest.

Publisher's note

References

1. Stankus A. State of world aquaculture 2020 and regional reviews: FAO webinar series. *FAO Aquaculture Newslett* (2021) 63:17–8.

2. Gephart JA, Golden CD, Asche F, Belton B, Brugere C, Froehlich HE, et al. Scenarios for global aquaculture and its role in human nutrition. *Rev Fish Sci Aquac* (2020) 29:122–38. doi: 10.1080/23308249.2020.1782342

3. Bene C, Barange M, Subasinghe R, Pinstrup-Andersen P, Merino G, Hemre GI, et al. Feeding 9 billion by 2050-Putting fish back on the menu. *Food Secur* (2015) 7:261–74. doi: 10.1007/s12571-015-0427-z

4. Tran HQ, Doan HV, Stejskal V. Environmental consequences of using insect meal as an ingredient in aquafeeds: A systematic view. *Rev Aquac* (2022) 14:237–51. doi: 10.1111/raq.12595

5. Olsen RL, Hasan MR. A limited supply of fishmeal: Impact on future increases in global aquaculture production. *Trends Food Sci Technol* (2012) 27:120–28. doi: 10.1016/j.tifs.2012.06.003

6. Naylor RL, Hardy RW, Buschmann AH, Bush SR, Cao L, Klinger DH, et al. A 20-year retrospective review of global aquaculture. *Nature* (2021) 591:551. doi: 10.1038/s41586-021-03308-6

7. Refstie S, Korsoen OJ, Storebakken T, Baeverfjord G, Lein I, Roem AJ. Differing nutritional responses to dietary soybean meal in rainbow trout (Oncorhynchus mykiss) and Atlantic salmon (Salmo salar). *Aquaculture* (2000) 190:49–63. doi: 10.1016/S0044-8486(00)00382-3

8. Wang L, Cui Z, Ren X, Li P, Wang Y. Growth performance, feed cost and environmental impact of largemouth bass Micropterus salmoides fed low fish meal diets. *Aquac Rep* (2021) 20:100757. doi: 10.1016/j.aqrep.2021.100757

9. Fu L, Liu H, Cai W, Han D, Zhu X, Yang Y, et al. 4-octyl itaconate supplementation relieves soybean diet-induced liver inflammation and glycolipid metabolic disorders by activating the nrf2-pparγ Pathway in juvenile gibel carp. *J Agric Food Chem* (2022) 70:520–31. doi: 10.1021/acs.jafc.1c05783

10. Gu M, Bai N, Zhang YQ, Krogdahl Å. Soybean meal induces enteritis in turbot *Scophthalmus maximus* at high supplementation levels. *Aquaculture* (2016) 464:286–95. doi: 10.1016/j.aquaculture.2016.06.035

11. Laporte J, Trushenski J. Production performance, stress tolerance and intestinal integrity of sunshine bass fed increasing levels of soybean meal. *J Anim Physiol Anim Nutr (Berl)* (2012) 96:513–26. doi: 10.1111/j.1439-0396.2011.01174.x

12. Ke LE, Qin YM, Song T, Wang K, Ye JD. Dietary sodium butyrate administration alleviates high soybean meal-induced growth retardation and enteritis of orange-spotted groupers (*Epinephelus coioides*). *Front Mar Sci* (2022) 9:1029397. doi: 10.3389/fmars.2022.1029397

13. Liu H, Cui B, Zhang Z. Mechanism of glycometabolism regulation by bioactive compounds from the fruits of *Lycium barbarum*: A review. *Food Res Int* (2022) 159:111408. doi: 10.1016/j.foodres.2022.111408

14. Amagase H, Farnsworth NR. A review of botanical characteristics, phytochemistry, clinical relevance in efficacy and safety of *Lycium barbarum* fruit (Goji). *Food Res Int* (2011) 44:1702–17. doi: 10.1016/j.foodres.2011.03.027

15. Shan XZ, Zhou JL, Ma T, Chai QX. *Lycium barbarum* polysaccharides reduce exercise-induced oxidative stress. *Int J Mol Sci* (2011) 12:1081–88. doi: 10.3390/ijms12021081

16. Jin M, Huang Q, Zhao K, Shang P. Biological activities and potential health benefit effects of polysaccharides isolated from *Lycium barbarum* L. *Int J Biol Macromol* (2013) 54:16–23. doi: 10.1016/j.ijbiomac.2012.11.023

17. Zhang XR, Zhou WX, Zhang YX, Qi CH, Yan H, Wang ZF, et al. Macrophages, rather than T and B cells are principal immunostimulatory target cells of *Lycium barbarum* L. polysaccharide LBPF4-OL. *J Ethnopharmacol* (2011) 136:465–72. doi: 10.1016/j.jep.2011.04.054

18. Zou S, Zhang X, Yao W, Niu Y, Gao X. Structure characterization and hypoglycemic activity of a polysaccharide isolated from the fruit of Lycium barbarum L. *Carbohydr Polym* (2010) 80:1161–67. doi: 10.1016/j.carbpol.2010.01.038

19. Tian XJ, Liang TS, Liu YL, Ding GT, Zhang FM, Ma ZR. Extraction, structural characterization, and biological functions of lycium barbarum polysaccharides: A review. *Biomolecules* (2019) 9:389. doi: 10.3390/biom9090389

20. Xiao J, Liong EC, Ching YP, Chang RCC, So KF, Fung ML, et al. *Lycium barbarum* polysaccharides protect mice liver from carbon tetrachloride-induced oxidative stress and necroinflammation. *J Ethnopharmacol* (2012) 139:462–70. doi: 10.1016/j.jep.2011.11.033

21. Huang ZF, Ye YL, Long ZY, Qin HH, Liu LH, Xu AL, et al. Lycium barbarum polysaccharides improve lipid metabolism disorders of spotted sea bass Lateolabrax maculatus induced by high lipid diet. *Int J Biol Macromol* (2023) 242:125122. doi: 10.1016/j.ijbiomac.2023.125122

22. Chinese Fisheries Bureau of Ministry of Agriculture. *China Fishery Statistical Yearbook*. Beijing: China Agriculture Press (2023).

23. Zhang CX, Rahimnejad S, Wang YR, Lu KL, Song K, Wang L, et al. Substituting fish meal with soybean meal in diets for Japanese seabass (Lateolabrax japonicus): Effects on growth, digestive enzymes activity, gut histology, and expression of gut inflammatory and transporter genes. *Aquaculture* (2018) 483:173–82. doi: 10.1016/j.aquaculture.2017.10.029

24. Cui WP. Active fractions of polysaccharides from pine pollen and their targeting nano drug delivery system in inhibiting ALV-J replication activity. *Doctor* (2021) 139.

25. Wu SJ. Dietary Astragalus membranaceus polysaccharide ameliorates the growth performance and innate immunity of juvenile crucian carp (Carassius auratus). *Int J Biol Macromol* (2020) 149:877–81. doi: 10.1016/j.ijbiomac.2020.02.005

26. Ai QH, Mai KS, Li HT, Zhang CX, Zhang L, Duan QY, et al. Effects of dietary protein to energy ratios on growth and body composition of juvenile Japanese seabass, Lateolabrax japonicus. *Aquaculture* (2004) 230:507–16. doi: 10.1016/j.aquaculture.2003.09.040

27. Holloway AC, Keene JL, Noakes DG, Moccia RD. Effects of clove oil and MS-222 on blood hormone profiles in rainbow trout Oncorhynchus mykiss, Walbaum. *Aquac Res* (2004) 35:1025–30. doi: 10.1111/j.1365-2109.2004.01108.x

28. Seki T. [Lysozyme]. Nihon rinsho. . *Japanese J Clin Med* (1995) 53:1209–12.

29. Powell M, Smith M. The determination of serum acid and alkaline phosphatase activity with 4-aminoantipyrine (aap). *J Clin Pathol* (1954) 7:245–48. doi: 10.1136/jcp.7.3.245

30. Haraguchi A, Yamada H, Kondo M, Okazaki K, Fukushi J, Oyamada A, et al. Serum IgG ACPA-IgM RF immune complexes were detected in rheumatoid arthritis patients positive for IgM ACPA. *Clin Exp Rheumatol* (2018) 36:612–18.

31. Huang Z, Ye Y, Xu A, Li Z. Effects of dietary crude polysaccharides from Lycium barbarum on growth performance, digestion, and serum physiology and biochemistry of spotted sea bass Lateolabrax maculatus. *Aquac Rep* (2023) 32:101710. doi: 10.1016/j.aqrep.2023.101710

32. Mehlem A, Hagberg CE, Muhl L, Eriksson U, Falkevall A. Imaging of neutral lipids by oil red O for analyzing the metabolic status in health and disease. *Nat Protoc* (2013) 8:1149–54. doi: 10.1038/nprot.2013.055

33. Yegin EG, Yegin K, Ozdogan OC. Digital image analysis in liver fibrosis: basic requirements and clinical implementation. *Biotechnol Biotechnol Equip* (2016) 30:653–60. doi: 10.1080/13102818.2016.1181989

34. Grabherr MG, Haas BJ, Yassour M, Levin JZ, Thompson DA, Amit I, et al. Full-length transcriptome assembly from RNA-Seq data without a reference genome. *Nat Biotechnol* (2011) 29:130–644. doi: 10.1038/nbt.1883

35. Li B, Dewey CN. RSEM: accurate transcript quantification from RNA-Seq data with or without a reference genome. *BMC Bioinf* (2011) 12. doi: 10.1186/1471-2105-12-323

36. Love MI, Huber W, Anders S. Moderated estimation of fold change and dispersion for RNA-seq data with DESeq2. *Genome Biol* (2014) 15. doi: 10.1186/s13059-014-0550-8

37. Yoshinaga H, Yasuike M, Mekuchi M, Soma S, Yamamoto T, Murashita K, et al. Multi-omics analysis of hepatopancreas of red seabream (Pagrus major) fed a soybean meal-based diet. *Aquaculture* (2023) 574. doi: 10.1016/j.aquaculture.2023.739631

38. Matulić D, Barišić J, Aničić I, Tomljanović T, Safner R, Treer T, et al. Author Correction: Growth, health aspects and histopathology of brown bullhead (Ameiurus nebulosus L.): replacing fishmeal with soybean meal and brewer's yeast. *Sci Rep* (2020) 10:11098. doi: 10.1038/s41598-020-67558-6

39. Saurabh S, Sahoo PK. Lysozyme: an important defence molecule of fish innate immune system. *Aquac Res* (2008) 39:223–39. doi: 10.1111/j.1365-2109.2007.01883.x

40. Uribe C, Folch H, Enriquez R, Moran G. Innate and adaptive immunity in teleost fish: a review. *Vet Med (Praha)* (2011) 56:486–503. doi: 10.17221/3294-VETMED

41. Castro R, Jouneau L, Pham H, Bouchez O, Giudicelli V, Lefranc M, et al. Teleost fish mount complex clonal IgM and IgT responses in spleen upon systemic viral infection. *PloS Pathog* (2013) 9:e1003098.

42. Mu QJ, Dong ZR, Kong WG, Wang XY, Yu JQ, Ji W, et al. Response of immunoglobulin M in gut mucosal immunity of common carp (Cyprinus carpio) infected with Aeromonas hydrophila. *Front Immunol* (2022) 13:1037517. doi: 10.3389/fimmu.2022.1037517

43. Pinoni SA, López Mañanes AA. Alkaline phosphatase activity sensitive to environmental salinity and dopamine in muscle of the euryhaline crab Cyrtograpsus angulatus. *J Exp Mar Biol Ecol* (2004) 307:35–46. doi: 10.1016/j.jembe.2004.01.018

44. Zhu X, Hao R, Zhang J, Tian C, Hong Y, Zhu C, et al. Dietary astaxanthin improves the antioxidant capacity, immunity and disease resistance of coral trout (*Plectropomus leopardus*). *Fish Shellfish Immunol* (2022) 122:38–47. doi: 10.1016/j.fsi.2022.01.037

45. Zhang X, Huang K, Zhong H, Ma Y, Guo Z, Tang Z, et al. Effects of *Lycium barbarum* polysaccharides on immunological parameters, apoptosis, and growth performance of Nile tilapia (*Oreochromis niloticus*). *Fish Shellfish Immunol* (2020) 97:509–14. doi: 10.1016/j.fsi.2019.12.068

46. Zhu J, Zhang YY, Shen YS, Zhou HQ, Yu XM. *Lycium barbarum* polysaccharides induce Toll-like receptor 2-and 4-mediated phenotypic and functional maturation of murine dendritic cells via activation of NF-κB. *Mol Med Rep* (2013) 8:1216–20. doi: 10.3892/mmr.2013.1608

47. Zhang XR, Li YJ, Cheng JP, Liu G, Qi CH, Zhou WX, et al. Immune activities comparison of polysaccharide and polysaccharide-protein complex from *Lycium barbarum* L. *Int J Biol Macromol* (2014) 65:441–45. doi: 10.1016/j.ijbiomac.2014.01.020

48. Tsujita T, Tsukada H, Nakao M, Oshiumi H, Matsumoto M, Seya T. Sensing bacterial flagellin by membrane and soluble orthologs of toll-like receptor 5 in rainbow trout (*Onchorhynchus mikiss*)*. *J Biol Chem* (2004) 279:48588–97. doi: 10.1074/jbc.M407634200

49. Tsukada H, Fukui A, Tsujita T, Matsumoto M, Iida T, Seya T. Fish soluble Toll-like receptor 5 (TLR5S) is an acute-phase protein with integral flagellin-recognition activity. *Int J Mol Med* (2005) 15:519–25. doi: 10.3892/ijmm.15.3.519

50. Rodriguez MF, Wiens GD, Purcell MK, Palti Y. Characterization of Toll-like receptor 3 gene in rainbow trout (Oncorhynchus mykiss). *Immunogenetics* (2005) 57:510–19. doi: 10.1007/s00251-005-0013-1

51. Phelan PE, Mellon MT, Kim CH. Functional characterization of full-length TLR3, IRAK-4, and TRAF6 in zebrafish (*Danio rerio*). *Mol Immunol* (2005) 42:1057–71. doi: 10.1016/j.molimm.2004.11.005

52. Su J, Zhu Z, Wang Y, Zou J, Hu W. Toll-like receptor 3 regulates Mx expression in rare minnow *Gobiocypris rarus* after viral infection. *Immunogenetics* (2008) 60:195–205. doi: 10.1007/s00251-007-0264-0

53. Chu Q, Xu TJ. MicroRNA regulation of Toll-like receptor, RIG-I-like receptor and Nod-like receptor pathways in teleost fish. *Rev Aquac* (2020) 12:2177–93. doi: 10.1111/raq.12428

54. Czabotar PE, Lessene G, Strasser A, Adams JM. Control of apoptosis by the BCL-2 protein family: implications for physiology and therapy. *Nat Rev Mol Cell Biol* (2014) 15:49–63. doi: 10.1038/nrm3722

55. Chen JX, Li HX, Xu P, Tang YK, Su SY, Liu GX, et al. Hypothermia-mediated apoptosis and inflammation contribute to antioxidant and immune adaption in freshwater drum, aplodinotus grunniens. *Antioxidants (Basel)* (2022) 11. doi: 10.3390/antiox11091657

56. Cheng ZJ, Hardy RW. Protein and lipid sources affect cholesterol concentrations of juvenile Pacific white shrimp, Litopenaeus vannamei (Boone)1. *J Anim Sci* (2004) 82:1136–45. doi: 10.2527/2004.8241136x

57. Rakhshandehroo M, Sanderson LM, Matilainen M, Stienstra R, Carlberg C, de Groot PJ, et al. Comprehensive analysis of PPARα-dependent regulation of hepatic lipid metabolism by expression profiling. *Ppar Res* (2007) 2007. doi: 10.1155/2007/26839

58. Xu J, Xiao G, Trujillo C, Chang V, Blanco L, Joseph SB, et al. Peroxisome proliferator-activated receptor α (PPARα) influences substrate utilization for hepatic glucose production*. *J Biol Chem* (2002) 277:50237–44. doi: 10.1074/jbc.M201208200

59. De Souza AT, Dai X, Spencer AG, Reppen T, Menzie A, Roesch PL, et al. Transcriptional and phenotypic comparisons of Ppara knockout and siRNA knockdown mice. *Nucleic Acids Res* (2006) 34:4486–94. doi: 10.1093/nar/gkl609

60. Yang X, Feng Y, Tong S, Yu J, Xu X. [Study on mechanism and structure-activity relationship of hypolipidemic polysaccharides: a review]. *Zhongguo Zhong Yao Za Zhi = Zhongguo Zhongyao Zazhi = China J Chin Materia Med* (2018) 43:4011–18. doi: 10.19540/j.cnki.cjcmm.20180703.010

61. Wu QQ, Wang QT, Fu JF, Ren RD. Polysaccharides derived from natural sources regulate triglyceride and cholesterol metabolism: a review of the mechanisms. *Food Funct* (2019) 10:2330–39. doi: 10.1039/c8fo02375a

62. Yan JK, Yu YB, Wang C, Cai WD, Wu LX, Yang Y, et al. Production, physicochemical characteristics, and in *vitro* biological activities of polysaccharides obtained from fresh bitter gourd (Momordica charantia L.) via room temperature extraction techniques. *Food Chem* (2021) 337. doi: 10.1016/j.foodchem.2020.127798

63. Martinez-Guryn K, Hubert N, Frazier K, Urlass S, Musch MW, Ojeda P, et al. Small intestine microbiota regulate host digestive and absorptive adaptive responses to dietary lipids. *Cell Host Microbe* (2018) 23:458. doi: 10.1016/j.chom.2018.03.011

64. Zhang Z, Ran C, Ding QW, Liu HL, Xie MX, Yang YL, et al. Ability of prebiotic polysaccharides to activate a HIF1α-antimicrobial peptide axis determines liver injury risk in zebrafish. *Commun Biol* (2019) 2. doi: 10.1038/s42003-019-0526-z

65. Cheng J, Zhou Z, Sheng H, He L, Fan X, He Z, et al. An evidence-based update on the pharmacological activities and possible molecular targets of Lycium barbarum polysaccharides. *Drug Des Dev Ther* (2015) 9:33–78. doi: 10.2147/DDDT.572892

66. Wang ZF, Liu Y, Sun YJ, Mou Q, Wang B, Zhang Y, et al. Structural characterization of LbGpl from the fruits of Lycium barbarum L. *Food Chem* (2014) 159:137–42. doi: 10.1016/j.foodchem.2014.02.171

67. Liu W, Liu YM, Zhu R, Yu JP, Lu WS, Pan C, et al. Structure characterization, chemical and enzymatic degradation, and chain conformation of an acidic polysaccharide from Lycium barbarum L. *Carbohydr Polym* (2016) 147:114–24. doi: 10.1016/j.carbpol.2016.03.087

68. Tang HL, Chen C, Wang SK, Sun GJ. Biochemical analysis and hypoglycemic activity of a polysaccharide isolated from the fruit of Lycium barbarum L. *Int J Biol Macromol* (2015) 77:235–42. doi: 10.1016/j.ijbiomac.2015.03.026

69. Gasaly N, de Vos P, Hermoso MA. Impact of bacterial metabolites on gut barrier function and host immunity: A focus on bacterial metabolism and its relevance for intestinal inflammation. *Front Immunol* (2021) 12:658354. doi: 10.3389/fimmu.2021.658354

70. McNabney SM, Henagan TM. Short chain fatty acids in the colon and peripheral tissues: A focus on butyrate, colon cancer, obesity and insulin resistance. *Nutrients* (2017) 9. doi: 10.3390/nu9121348

71. Tazoe H, Otomo Y, Kaji I, Tanaka R, Karaki SI, Kuwahara A. Roles of short-chain fatty acids receptors, gpr41 and gpr43 on colonic functions. *J Physiol Pharmacol* (2008) 59:251–62.

72. Difilippo E, Bettonvil M, Willems R, Braber S, Fink-Gremmels J, Jeurink PV, et al. Oligosaccharides in urine, blood, and feces of piglets fed milk replacer containing galacto-oligosaccharides. *J Agric Food Chem* (2015) 63:10862–72. doi: 10.1021/acs.jafc.5b04449

73. Vazquez E, Santos-Fandila A, Buck R, Rueda R, Ramirez M. Major human milk oligosaccharides are absorbed into the systemic circulation after oral administration in rats. *Br J Nutr* (2017) 117:237–47. doi: 10.1017/S0007114516004554

74. Cao C, Wang ZF, Gong GP, Huang WQ, Huang LJ, Song S, et al. Effects of lycium barbarum polysaccharides on immunity and metabolic syndrome associated with the modulation of gut microbiota: A review. *Foods* (2022) 11. doi: 10.3390/foods11203177

75. Cai HZ, Yang XH, Cai Q, Ren BB, Qiu HY, Yao ZQ. *Lycium barbarum* L. polysaccharide (LBP) reduces glucose uptake via down-regulation of SGLT-1 in Caco2 cell. *Molecules* (2017) 22. doi: 10.3390/molecules22020341

76. Zhu J, Liu W, Yu JP, Zou S, Wang JJ, Yao WB, et al. Characterization and hypoglycemic effect of a polysaccharide extracted from the fruit of *Lycium barbarum* L. *Carbohydr Polym* (2013) 98:8–16. doi: 10.1016/j.carbpol.2013.04.057

77. Masci A, Carradori S, Casadei MA, Paolicelli P, Petralito S, Ragno R, et al. *Lycium barbarum* polysaccharides: Extraction, purification, structural characterisation and evidence about hypoglycaemic and hypolipidaemic effects. A review. *Food Chem* (2018) 254:377–89. doi: 10.1016/j.foodchem.2018.01.176

78. Huang R, Wu E, Deng X. Potential of *Lycium barbarum* polysaccharide for the control of glucose and lipid metabolism disorders: a review. *Int J Food Prop* (2022) 25:673–80. doi: 10.1080/10942912.2022.2057529

frontiers | Frontiers in Immunology

TYPE Original Research
PUBLISHED 05 April 2024
DOI 10.3389/fimmu.2024.1319698

OPEN ACCESS

EDITED BY
Samad Rahimnejad,
University of Murcia, Spain

REVIEWED BY
Xiaohui Dong,
Guangdong Ocean University, China
Houguo Xu,
Chinese Academy of Fishery Sciences (CAFS), China

*CORRESPONDENCE
Qiyou Xu
02655@zjhu.edu.cn

RECEIVED 11 October 2023
ACCEPTED 21 March 2024
PUBLISHED 05 April 2024

CITATION
Du Y, Lin X, Shao X, Zhao J, Xu H, de Cruz CR and Xu Q (2024) Effects of supplementing coated methionine in a high plant-protein diet on growth, antioxidant capacity, digestive enzymes activity and expression of TOR signaling pathway associated genes in gibel carp, *Carassius auratus* gibelio. *Front. Immunol.* 15:1319698. doi: 10.3389/fimmu.2024.1319698

Effects of supplementing coated methionine in a high plant-protein diet on growth, antioxidant capacity, digestive enzymes activity and expression of TOR signaling pathway associated genes in gibel carp, *Carassius auratus* gibelio

Yingying Du[1], Xiaowen Lin[1], Xianping Shao[1,2,3], Jianhua Zhao[1,2,3], Hong Xu[1,2,3], Clement R. de Cruz[4] and Qiyou Xu[1,2,3]*

[1]College of Life Science, Huzhou University, Huzhou, China, [2]Zhejiang Provincial Key Laboratory of Aquatic Bioresource Conservation and Development Technology, Huzhou University, Huzhou, China, [3]Nation Local Joint Engineering Laboratory of Aquatic Animal Genetic Breeding and Nutrition, Huzhou Universityy, Huzhou, China, [4]Laboratory of Sustainable Aquaculture, International Institute of Aquaculture and Aquatic Sciences, Universiti Putra Malaysia, Port Dickson, Negeri Sembilan, Malaysia

This study explored the impacts of supplementation of different levels of coated methionine (Met) in a high-plant protein diet on growth, blood biochemistry, antioxidant capacity, digestive enzymes activity and expression of genes related to TOR signaling pathway in gibel carp (*Carassius auratus* gibeilo). A high-plant protein diet was formulated and used as a basal diet and supplemented with five different levels of coated Met at 0.15, 0.30, 0.45, 0.60 and 0.75%, corresponding to final analyzed Met levels of 0.34, 0.49, 0.64, 0.76, 0.92 and 1.06%. Three replicate groups of fish (initial mean weight, 11.37 ± 0.02 g) (20 fish per replicate) were fed the test diets over a 10-week feeding period. The results indicated that with the increase of coated Met level, the final weight, weight gain (WG) and specific growth rate initially boosted and then suppressed, peaking at 0.76% Met level ($P< 0.05$). Increasing dietary Met level led to significantly increased muscle crude protein content ($P< 0.05$) and reduced serum alanine aminotransferase activity ($P< 0.05$). Using appropriate dietary Met level led to reduced malondialdehyde concentration in hepatopancreas ($P< 0.05$), improved superoxide dismutase activity ($P< 0.05$), and enhanced intestinal amylase and protease activities ($P< 0.05$). The expression levels of genes associated with muscle protein synthesis such as insulin-like growth factor-1, protein kinase B, target of rapamycin and eukaryotic initiation factor 4E binding protein-1 mRNA were significantly regulated, peaking at Met level of 0.76% ($P< 0.05$). In conclusion, supplementing optimal level of coated Met improved on fish

growth, antioxidant capacity, and the expression of TOR pathway related genes in muscle. The optimal dietary Met level was determined to be 0.71% of the diet based on quadratic regression analysis of WG.

KEYWORDS

coated methionine, growth performance, digestive enzyme activity, TOR signaling pathway, gibel carp

1 Introduction

Along with the expansion of the aquaculture industry, the demand for fishmeal as a high-quality protein source for the production of aquafeeds has also increased leading to higher feed costs (1). Furthermore, the production amount of fishmeal will barely meet the aquaculture demands. Plant proteins are more widely available and cheaper than fishmeal (2), offer a cost-effective alternative (3). However, plant proteins come with challenges such as high crude fiber content, higher anti-nutritional properties, and imbalanced amino acid composition (4). Among these, unbalanced amino acid composition in plant protein mainly refers to essential amino acid deficiency (5).

High plant protein feed often results in a lack of essential amino acids (6). Methionine, an essential amino acid, is found in relatively small amounts in plant-based proteins, including soybean meal, rapeseed meal, and cottonseed meal, making it a limiting factor in these protein sources (7). Methionine plays a role in numerous metabolic processes and is critical for the growth of aquatic animals. However, a lack of dietary methionine can result in growth retardation (8), reduce feed efficiency (9), and affect body metabolism (10) and intestinal health development (11). Therefore, supplementing diets with the sufficient amount of methionine improves growth performance as demonstrated in previous studies with largemouth bass (*Micropterus salmoides*) (12), rohu (*Labeo rohita*) (13), grass carp (*Ctenopharyngodon idella*) (14), cobia (*Rachycentron canadum*) (15). Previous studies have reported that amino acids, acting as nutritional factors, can regulate the expression of protein synthesis genes through the target of rapamycin (TOR) pathway (16, 17). Moreover, supplementation of dietary methionine could activate the TORC1/S6K1 signaling pathway, promoting muscle protein content in grass carp (18). Previous study also demonstrated that dietary methionine levels protein turnover and gene expression of growth hormone (GH) and insulin-like growth factor-I (IGF-I), thereby regulating protein metabolism (19). However, the growth and metabolism of GH-IGF-modified organisms are primarily dependent on the phosphatidylinositol 3-kinase (PI3K)/protein kinase B (AKT) pathway (20). Through the PI3K/AKT signaling pathway to activate the TOR, TOR can affect protein synthesis by activating downstream S6 kinase 1 (S6K1) and 4E binding protein-1 (4E-BP1) (14).

Crystalline methionine is commonly used as a feed additive but its utilization varies across different fish species (21). Some studies have shown that crystalline amino acids have a high dissolution rate in water leading to unsynchronized protein absorption in feed (22). As a result, the addition of crystal amino acids to gastritis fish, such as crucian carp (*Carassius auratus gibelio*) (23) and mirror carp (*Cyprinus carpio*) (24), rendering them ineffective. Nevertheless, coating amino acids as opposed to crystalline methionine, has been shown to improve the utilization of amino acids by fish (25). This enhancement in amino acid utilization through coating compared to their crystalline counterparts has been substantiated by research on tilapia (*Oreochromis mossambicus*) (26) and mirror carp (27).

Carassius auratus gibelio has a strong adaptive ability and is an omnivorous aquaculture species, which is widely cultured crucian carp throughout China. Researchers have studied the effects of adding crystalline methionine to the feed on different sizes of gibel carp and the methionine requirement of gibel carp ranges from 0.69% to 0.98% (28–30). Thus, this experiment mainly explored the effects of different levels of coated methionine in high plant protein diets on the growth performance, serum biochemistry, liver antioxidant, intestinal digestive enzymes and expression of genes related to TOR pathway, and the optimum addition amount of coated methionine was determined by the growth parameter of gibel carp, which provided some reference for practical production.

2 Materials and methods

2.1 Experimental diets

The primary protein sources in the experimental diets included soybean meal, rapeseed meal, cottonseed protein, and fish meal, while the main fat sources were fish oil, soybean oil, and soy phospholipid. Six levels of coated methionine (0, 0.15, 0.30, 0.45, 0.60 and 0.75%) were supplemented in the diet, resulting in the final measured methionine content of 0.34 (control dietary treatment), 0.49, 0.64, 0.76, 0.92 and 1.06%, respectively (Table 1). The methionine levels were quantified using High-Performance Liquid Chromatography (HPLC) following a specific protocol (27).

The feed ingredients used in the experiment were pulverized and passed through a 60 mesh screen. All the ingredients were mixed thoroughly according to the formulation (Table 1) and the

10.3389/fimmu.2024.1319698

TABLE 1 Feed composition and nutrient level of experimental diets (%, dry matter basis).

Items	Dietary Met level (%)					
	0.34	0.49	0.64	0.76	0.92	1.06
Fish meal	5	5	5	5	5	5
Soybean meal	26.8	26.8	26.8	26.8	26.8	26.8
Rapeseed meal	12	12	12	12	12	12
Cottonseed protein	10	10	10	10	10	10
Wheat meal	30.1	30.1	30.1	30.1	30.1	30.1
Soybean oil	1	1	1	1	1	1
Soy lecithin	1.5	1.5	1.5	1.5	1.5	1.5
Fish oil	1	1	1	1	1	1
Extruded corn	7.5	6.0	4.5	3.0	1.5	0
10% Coated methionine	0	1.5	3.0	4.5	6.0	7.5
Vitamin premix[1]	0.5	0.5	0.5	0.5	0.5	0.5
Mineral premix[2]	0.2	0.2	0.2	0.2	0.2	0.2
Sodium carboxymethyl cellulose	2	2	2	2	2	2
Choline chloride	0.2	0.2	0.2	0.2	0.2	0.2
$Ca(H_2PO_4)_2$	2	2	2	2	2	2
$MgSO_4$	0.2	0.2	0.2	0.2	0.2	0.2
Nutrient levels (%)						
Crude protein	31.82	31.83	31.94	32.05	32.01	31.97
Crude lipid	5.12	5.23	5.36	5.32	5.12	5.10
Ash	6.54	6.52	6.50	6.47	6.45	6.43
Methionine	0.34	0.49	0.64	0.76	0.92	1.06

[1]The premix provided the following per kg of diets: VA 8000IU, VC 500mg, VD 3000IU, VE 60mg, VK 35mg, VB_1 15mg, VB_2 30mg, VB_6 15mg, VB_{12} 0.5mg .
[2]The premix provided the following per kg of diets: $FeSO_4{\cdot}7H_2O$ 754.56 mg, $CuSO_4{\cdot}5H_2O$ 23.81 mg, $MnSO_4{\cdot}H_2O$ 168.29 mg, $ZnSO_4{\cdot}7H_2O$ 440.00 mg, Na_2SeO_3 2.26 mg, KI 0.79 mg, $CoCl_2$ 2.21 mg, Zeolite meal 604.08mg.

mix blends were preconditioned with water prior to extrusion to produce pellets with a 2.5 mm diameter. Then the pellets were oven dried at 35°C overnight and stored in a refrigerator at -20°C.

2.2 Experimental fish and rearing

The 10-week feeding trial was conducted at the College of Life Sciences, Huzhou University. Prior to the feeding trial, all the fish were acclimatized for 2 weeks and after acclimatization, a total of 360 healthy gibel carp of similar sizes were selected for the study. The fish (initial, 11.37 ± 0.02 g) were randomly divided into 6 dietary treatments, each with 3 replicates and 20 fish per tank. The experimental recirculating system was housed outdoors and the fish were fed manually twice a day (8:30 am and 17:30 pm) at 2.5% to 3% of body weight. Additionally, feed residues were collected from the culture system 30 min after feeding. During the feeding trial, the water conditions were consistently within the specified ranges, with the water temperature ranging from 20°C to 32°C, dissolved oxygen levels maintained at or above 6.0 mg/L, ammonia nitrogen levels kept below 0.3 mg/L, and nitrite levels maintained below 0.05 mg/L.

The weight and number of fish in each tank were recorded weekly. At the end of the feeding trial, weights of the fish, viscera, and hepatopancreas were recorded, and the full length and body length of the fish were measured. The calculation formula is as follows:

$$\text{Survival rate}(\%) = 100 \times \text{final fish number}/\text{initial fish number};$$

$$\text{Weight gain}(\%) = 100 \times [(\text{final body weight} - \text{initial body weight})/\text{initial body weight}];$$

$$\text{Specific growth rate}(\%/\text{day}) = 100 \times [(\ln \text{final body weight} - \ln \text{initial body weight})/\text{days}];$$

Feed intake rate (% /day)
$= 100 \times$ dry feed intake/ [days $\times$ (initial body weight + final body weight)/2];

Feed conversion rate $= 100 \times$ dry feed fed/weight gain;

Viscerosomatic index (%)
$= 100 \times$ viscerosomatic weight/final body weight;

Hepatosomatic index (%)
$= 100 \times$ hepatosomatic weight/final body weight;

Condition factor (%)
$= 100 \times$ final body weight/(final body length)^3 .

2.3 Sample collection

At the end of the feeding trial, 6 gibel carp were chosen at random from each tank and anesthetized using MS-222 (at a concentration of 400 mg/L). Blood was attained via the tail vein and centrifuged (3500 r/min, 10 min) at 4°C to obtain plasma serum, which was stored in a refrigerator at -80°C. Subsequently, samples of hepatopancreas, intestine and muscle were collected. The samples were placed in centrifuge tubes, swiftly transferred into liquid nitrogen, and subsequently stored in a -80° C refrigerator.

2.4 Muscle composition analysis

A proximate composition analysis was performed following the standard protocol (31). Moisture content was measured through oven drying at 105°C using a DHG-9240A oven (Shanghai Jinghong Experimental Equipment Co., Ltd., China), while ash content was assessed with a muffle furnace set at 550°C (SX2-8-10, Shanghai Yiheng Technology Co., Ltd., China). The determination of crude protein content utilized the Dumas combustion method, employing an Elementar rapid N exceed apparatus (Elementar Trading (Shanghai) Co., Ltd., China), and the crude fat content was analyzed using the Soxhlet extraction method.

2.5 Biochemical assays

Saline was mixed with liver and intestine tissues in a 1: 9 (w: v) ratio and homogenized. The homogeneity was then centrifuged at 4°C at 3500 rpm for 10 minutes, and the supernatant was collected for subsequent assays. Serum biochemical assays were conducted for aspartate aminotransferase (AST, Cat. No. C010-1-1) and alanine aminotransferase (ALT, Cat. No. C009-1-1). Additionally, antioxidant enzyme activities, including catalase (CAT, Cat. No. A007-1-1), superoxide dismutase (SOD, Cat. No. A001-1), and lipid peroxidation marker malondialdehyde (MDA, Cat. No. A003-1), were measured in the hepatopancreas. Enzymatic activities of lipase (Cat. No. A054-1-1) and amylase (Cat. No. C016-1-1) were determined in the intestine. All assay kits were sourced from Nanjing Jiancheng Bioengineering Institute. The activity of intestinal protease was assessed using the folin-phenol reagent method (32).

2.6 Gene expression analysis

Total RNA was extracted from the muscle using a kit for the rapid extraction of RNA (RN28-EASYspin). The concentration and purity of total RNA were determined by spectrophotometry (A260: A280 nm), with reference to the ratio specified in the kit instructions (1.8-2.2). Subsequently, the extracted mRNA was synthesized into cDNA using a reverse transcription kit (MonScript^{TM}RTIII All-in-One Mix).

Primers were designed using online Primer through NCBI website. The determination of real-time PCR, the CFX-96 system was used (BioRad Laboratories, Inc., USA). Real-time PCR analysis of mRNA levels was performed according to the kit instructions (Mon Amp^{TM}SYBR$^{®}$Green qPCR Mix). The total reaction system was 20 μL, containing diluted cDNA 1 μL, reverse and forward primers 0.4 μL (10μM), nuclease-free water 8.2 μL, and monamp^{TM}SYBR$^{®}$Green qPCR Mix 10 μL. PCR conditions refer to Luo et al. (33). The mRNA relative expression of target gene was calculated by $2^{-\Delta\Delta Ct}$ method, and β-actin gene was a housekeeping gene. Table 2 is the primers for fluorescence quantitative analysis.

TABLE 2 Primer sequences for RT-PCR in the experiment.

Target genes	Primer sequence (5′-3′)	Gene ID
β-action	AGTACGATGAGTCTGGCCCT ATCCTGAGTCAATGCGCCAA	AB039726
PI3K	TTGACACAGAAAGGGGTCCG CTTCCAGGAGCGTTCGTCAT	XM_052557910.1
AKT	GCGGGAGGCTGGATACTAAC GTGGCATCCGAAGAATTCGC	XM_052562157.1
TOR	GCACAAATTGATGGCACGGT GCAGCACTGCCTCAAAGTTC	KF772613.1
4E-BP1	CAATTCCCACCACCAGACGA CCAACGGAGAGCTACGACAG	XM_052536897
S6K1	CCAGCCGGAGGAAAATGTCT GCGTGCCGTTCACTTCAAAA	EF373665.1
IGF-1	AGGGGATGTCTAGCGGTCAT AGAGACAGCGCATGGTACAC	KF813006.1

PI3K, Phosphatidylinositol 3-kinase; Akt, Protein kinase B; TOR, Target of rapamycin; 4E-BP1, Eukaryotic initiation factor 4E binding protein-1; S6K1, Ribosomal protein S6 kinase 1; IGF-1, Insulin-like growth factor-1.

2.7 Data analysis

All data were analyzed using SPSS 25.0 software and expressed as mean (n=3) ± standard error of the mean (SEM). Each variable evaluated was analyzed using analysis of variance (ANOVA), and data from each dietary treatment were compared using Duncan's method. A statistically significant difference was indicated when $P< 0.05$. Comparisons were made using orthogonal polynomials to assess the significance of linear and quadratic models for all dependent variables at the level of the coated methionine.

3 Results

3.1 Growth performance

At the conclusion of 10-week feeding trial, the SR of gibel carp was 100% (Table 3). As dietary levels of coated methionine (Met) increased, final body weight, weight gain (WG), and specific growth rate initially increased, peaking at 0.76% dietary treatment, before declining ($P< 0.05$). Conversely, feed conversion ratio (FCR) exhibited an opposite trend, recording its lowest value in the 0.76% dietary treatment, though this difference was not statistically significant ($P> 0.05$). Feed intake rate, FCR, viscerosomatic index, hepatosomatic index, and condition factor remained unaffected by the Met levels in the diets ($P> 0.05$).

Quadratic regression analysis showed that the WG was the highest at 0.71% Met level. Moreover, 0.34% was derived from the basal diet, and 0.37% was derived from the coated Met (Figure 1).

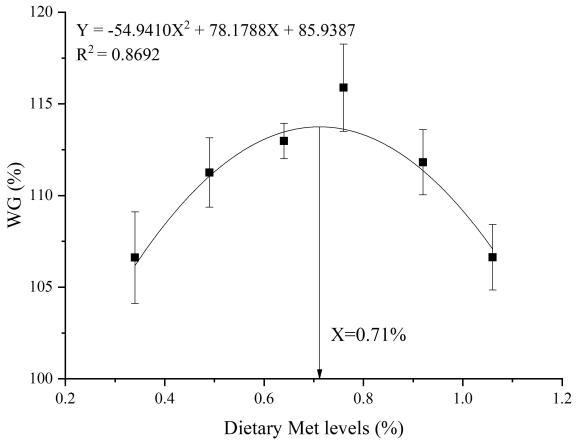

FIGURE 1
Quadratic regression analysis of WG against varying dietary coated Met levels.

3.2 Muscle composition

Dietary coated Met significantly increased muscle crude protein content, which peaked at 0.64% dietary treatment and then stabilized (Table 4). Dietary coated Met did not show significant effects on muscle moisture, crude fat and ash content ($P> 0.05$).

3.3 Serum biochemical parameters

Serum ALT activity decreased significantly with increasing levels of coated Met, reaching its lowest level in the 1.06% dietary treatment (Table 5). AST activity was not markedly influenced by the level of coated Met ($P> 0.05$). However, AST activity showed a linearly decrease by polynomial analysis ($P< 0.05$).

3.4 Hepatopancreas antioxidant capacity

Hepatopancreas MDA content (Table 6) generally decreased and then slightly increased with the level of coated Met, reaching

TABLE 3 Effects of dietary coated Met on growth performance of gibel carp.

Items	Dietary Met levels (%)						SEM	*P* values	Polynomial contrasts	
	0.34	0.49	0.64	0.76	0.92	1.06			Linear	Quadratic
IBW (g)	11.25	11.27	11.26	11.26	11.27	11.26	0.004	0.884	0.671	0.724
FBW (g)	23.25^{b}	23.80^{ab}	23.98^{ab}	24.32^{a}	23.87^{ab}	23.27^{b}	0.119	0.031	0.822	0.002
SR (%)	100	100	100	100	100	100	–	–	–	–
WG (%)	106.61^{b}	111.26^{ab}	112.98^{ab}	115.88^{a}	111.82^{ab}	106.63^{b}	1.049	0.034	0.848	0.002
SGR (%/d)	1.04^{b}	1.07^{ab}	1.08^{ab}	1.10^{a}	1.07^{ab}	1.04^{b}	0.007	0.033	0.841	0.003
FIR (%/day)	2.34	2.34	2.34	2.34	2.34	2.35	0.005	0.993	0.796	0.853
FCR	2.36	2.29	2.27	2.24	2.29	2.37	0.018	0.212	0.971	0.023
VSI (%)	9.89	9.92	10.30	10.15	10.15	10.10	0.084	0.754	0.353	0.400
HSI (%)	4.28	4.52	4.76	4.64	4.57	4.86	0.101	0.662	0.151	0.325
CF (g/cm^{3})	2.84	2.91	2.88	2.97	2.80	2.76	0.026	0.199	0.223	0.069

SEM, Standard error of the mean. There are significant differences between different letters ($P< 0.05$). IBW, Initial body weight; FBW, Final body weight; SR, Survival rate; WG, Weight gain; SGR, Specific growth rate; FIR, Feed intake rate; FCR, Feed conversion rate; VSI, Viscerosomatic index; HSI, Hepatosomatic index; CF, Condition factor.

TABLE 4 Effects of dietary coated Met on muscle composition of gibel carp.

Items	Dietary Met levels (%)						SEM	*P* values	Polynomial contrasts	
	0.34	0.49	0.64	0.76	0.92	1.06			Linear	Quadratic
Moisture	77.56	76.99	76.97	77.25	77.39	77.15	0.085	0.300	0.744	0.468
Crude protein	17.34^{b}	17.60^{ab}	17.79^{a}	17.79^{a}	17.79^{a}	17.76^{a}	0.053	0.049	0.009	0.002
Crude lipid	1.25	1.08	1.07	1.14	0.97	0.81	0.051	0.193	0.012	0.040
Ash	1.54	1.53	1.53	1.55	1.50	1.46	0.019	0.853	0.249	0.411

SEM, Standard error of the mean. There are significant differences between different letters (P< 0.05).

the lowest level in the 0.92% dietary treatment ($P< 0.05$), while the SOD activity generally showed the opposite trend, peaking in the 0.64% dietary treatment ($P< 0.05$). However, CAT activity was not significantly different among the dietary treatments ($P> 0.05$).

3.5 Intestinal digestive enzyme parameters

Intestinal amylase and protease activities (Table 7) were higher and then lower with increasing levels of coated Met, reached a high level in the 0.92% dietary treatment ($P< 0.05$). Lipase activity tended to increase, but there was no significant effect by different levels of coated Met ($P> 0.05$).

3.6 TOR pathway gene expression

The addition of coated Met to the feed significantly increased the muscle mRNA expression levels of IGF-1, AKT, TOR, and 4E-BP1 ($P< 0.05$), and all peaked at 0.76% dietary treatment (Figure 2). Moreover, the mRNA expression levels of PI3K and S6K1 tended to increase but were not significantly dietary treatment ($P> 0.05$).

4 Discussion

4.1 Effects of coated methionine on growth performance of gibel carp

Weight gain (WG) is an important indicator of normal growth of aquatic animals at a given growth stage (34). During the 70-day feeding period, the WG results for the fish ranged from 106.61% to 115.88%. The results showed normal growth, aligning with findings from other reports. For instance, after 60 days of feeding, gibel carp that started at 13.20 g showed WG rates ranging from 88.44% to 106.99% (35). Similarly, gibel carp initiated the trial with a baseline weight of 28.00 g demonstrated WG percentages ranging from 74.19% to 93.60% over the corresponding 60-day period (36).

Methionine (Met) plays an important role in fish growth and is an essential amino acid. Based on previous studies, inadequate dietary intake of Met can reduce WG in turbot (*Scophthalmus maximus*) (37) and Atlantic salmon (*Salmo salar*) (8). The excessive Met in the feed also leads to a decrease in the WG of yellow catfish (*Pelteobagrus fulvidraco*) (38). This experiment showed that as the level of coated Met in the diet increased, the WG and SGR of gibel carp initially improved, then diminished, reaching a peak at the 0.76% dietary treatment level. The results demonstrate that both an overabundance and a deficiency of Met in the feed adversely affect growth, whereas optimal supplementation of Met enhances growth. This trend has been reported in other studies for mirror carp (27) and cobia (22). In the current study, the addition of coated Met did not lead to significant differences in FCR among dietary treatments, which is consistent with findings in turbot (39). Studies on grouper (*Epinephelus coioides*) have shown that the supplementation of Met to the diet causes differences in CF among dietary treatments (40). In this study, coated Met levels did not significantly change HSI, VSI and CF. However, the HSI index of gibel carp in this experiment was higher than that reported by Jia et al. (41), but lower than the values reported by Wang et al. (29). This difference may be attributed to variations in feed composition and fish size of gibel carp.

Previous studies on this species (51.0 g), DL-Met was added to the feed (0.44% Met in basic feed), and the optimum levels of Met were 0.73% and 0.98%, respectively (29). Another study showed that adding DL-Met to the diet, resulted in an optimal Met level of 0.89% for gibel carp (with the basal diet containing 0.57% Met) (41). In this study, the optimal dietary Met content for gibel carp was determined to be 0.71% through quadratic regression analysis, with

TABLE 5 Effects of coated Met on serum biochemical indices of gibel carp.

Items	Dietary Met levels (%)						SEM	*P* values	Polynomial contrasts	
	0.34	0.49	0.64	0.76	0.92	1.06			Linear	Quadratic
AST (U/L)	45.63	43.21	44.21	43.27	40.98	36.98	0.991	0.155	0.010	0.023
ALT (U/L)	8.15^{a}	7.91^{ab}	5.24^{bcd}	6.49^{abc}	4.94^{cd}	3.55^{d}	0.437	0.006	0.000	0.001

SEM, Standard error of the mean. There are significant differences between different letters (P< 0.05). AST, Aspartate aminotransferase; ALT, Alanine aminotransferase.

TABLE 6 Effects of dietary coated Met on liver antioxidant of gibel carp.

Items	Dietary Met levels (%)						PSE	*P* values	Polynomial contrasts	
	0.34	0.49	0.64	0.76	0.92	1.06			Linear	Quadratic
CAT (U/mg prot)	40.93	46.89	43.68	48.34	46.15	49.55	1.465	0.595	0.664	0.411
MDA (nmol/mg prot)	3.47^{ab}	4.44^{a}	2.50^{bc}	2.66^{bc}	2.03^{c}	2.68^{bc}	0.188	0.001	0.188	0.231
SOD (U/mg prot)	134.05^{c}	151.25^{ab}	163.98^{a}	152.21^{ab}	151.64^{ab}	144.84^{bc}	2.634	0.009	0.413	0.003

SEM, Standard error of the mean. There are significant differences between different letters (P< 0.05). CAT, Catalase; MDA, Malondialdehyde; SOD, Superoxide dismutase.

the basal diet containing 0.34% Met and an additional 0.37% derived from coated Met. The results were consistent with the previously reported dietary Met levels of 0.71% and 0.73% (29, 30), but slightly less than 0.89% (41). This discrepancy may be attributed to variations in feed nutrient composition and types of Met used. Nevertheless, it is important to note that the present study context differs from previous studies in the natural basal diet's Met content. Specifically, previous research reported higher basal Met levels, around 0.44%, whereas our study utilized a basal diet with a lower Met content of 0.34% due to formulation with a high plant-based protein diet.

4.2 Effect of coated methionine on serum biochemical indexes of gibel carp

As an index of fish physiological state, serum biochemical index can reflect the health status of the body (42). AST and ALT are two key enzymes involved in the normal metabolism of amino acids (43). When hepatic metabolism is disturbed or impaired, it will lead to excessive increase of AST and ALT in serum (44). Previous studies on gibel carp (30) and Jian carp (*Cyprinus carpiovar.* Jian) (45) have found that the deficiency or excess of Met in feed can lead to an increase in serum transaminase activity, which negatively affects liver function in fish. The experimental results showed that AST in serum decreased with the addition of coated Met in the diet, but did not cause differences among dietary treatments, which was similar to the experimental results of golden pomfret (*Trachinotus ovatus*) (46). Similarly, ALT showed a downward trend after the addition of coated Met. AST and ALT activities were higher in the Met-deficient group, suggesting that the deficiency of Met in the diet may have disrupted the normal metabolism of the liver, leading to impaired liver function. The addition of coated Met could reduce serum ALT and AST activities, probably due to the interaction between Met and other amino acids, which maintains normal protein metabolism in the liver and is beneficial to liver health (47).

4.3 Effect of coated methionine on antioxidant capacity of liver in gibel carp

The liver of fish is the main immune organ and metabolic site, and the physiological status of the liver affects the health of the body (48). Superoxide dismutase and catalase are two enzymes that can scavenge free radicals in the body and are closely related to the antioxidant capacity of the body (49). MDA, as a lipid oxidation product, directly reflects the degree of lipid oxidation in an organism and serves as an indicator of its physiological state (50). In a report on hybrid striped bass (*Morone chrysops×M. siaxatilis*), it was found that the shortage of Met in the diet may cause changes in the body's antioxidant capacity, leading to oxidative stress (51). Previous study reported that appropriate Met level could increase the antioxidant capacity and ameliorate oxidative damage in grouper (52). Met is an important part of the cellular antioxidant system and protects cells from oxidative damage (53). In this study, gibel carp fed diets supplemented with coated Met showed lower MDA content and higher SOD activity compared to Met-deficient dietary treatments. These results indicated that Met deficiency can cause an increase in MDA content in the liver of gibel carp, which may cause oxidative damage to the body (54). However, the addition of properly coated Met decreased the MDA content in the liver and increased the activity of SOD in the body, which was similar to the results of grouper (52) and hybrid striped bass (51).

4.4 Effect of coated methionine on intestinal digestive enzymes of gibel carp

The intestinal functions of digestion and absorption are essential for the appropriate uptake of nutrients and growth in fish (55). Efficient digestion and absorption are necessary for optimal fish growth. Protease, amylase, and lipase are key enzymes involved in digestion (56). The digestive and absorptive capacity of the fish is reflected by the enzyme activity in the intestine (57). Increasing digestive enzyme

TABLE 7 Effects of dietary coated Met on intestinal digestive enzyme activities of gibel carp.

Items	Dietary Met levels (%)						SEM	*P* values	Polynomial contrasts	
	0.34	0.49	0.64	0.76	0.92	1.06			Linear	Quadratic
Amylase (U/mg prot)	62.69^{c}	64.08^{bc}	70.07^{ab}	74.56^{a}	74.75^{a}	66.70^{bc}	1.377	0.008	0.264	0.048
Lipase (U/g prot)	12.71	15.18	20.00	20.25	17.91	16.83	1.020	0.242	0.172	0.038
Proteinase(U/mg prot)	5.48^{c}	8.74^{b}	9.71^{ab}	10.56^{ab}	11.65^{a}	11.13^{ab}	0.570	0.002	0.006	0.002

SEM, Standard error of the mean. There are significant differences between different letters (P< 0.05).

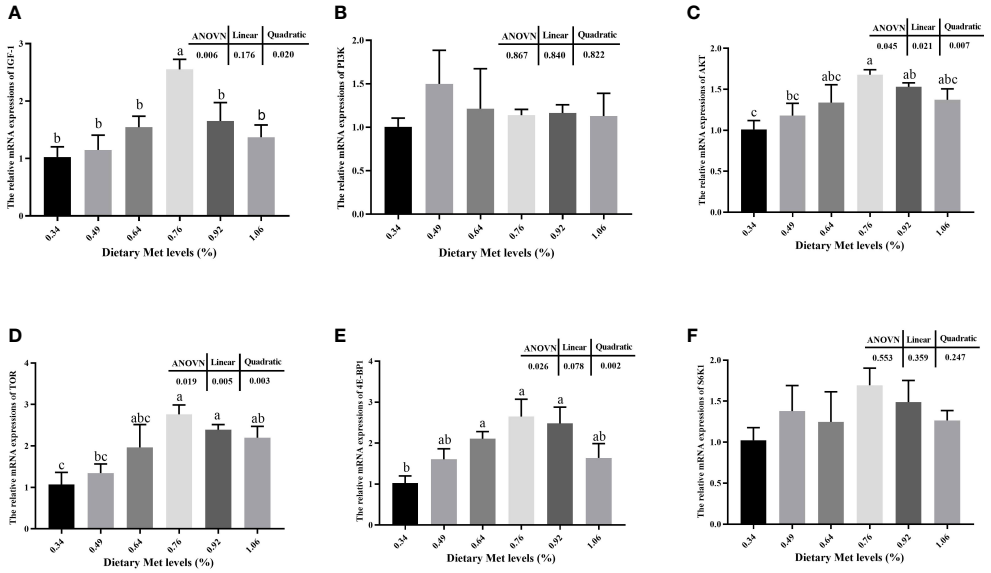

FIGURE 2
Effects of dietary coated Met on the expression of genes related to TOR signaling pathway. There are significant differences between different letters ($P< 0.05$). IGF-1, Insulin-like growth factor-1; PI3K, Phosphatidylinositol 3-kinase; Akt, Protein kinase B; TOR, Target of rapamycin; 4E-BP1, Eukaryotic initiation factor 4E binding protein-1; S6K1, Ribosomal protein S6 kinase 1. **(A)** The relative mRNA expressions of IGF-1. **(B)** The relative mRNA expressions of PI3K. **(C)** The relative mRNA expressions of AKT. **(D)** The relative mRNA expressions of TOR. **(E)** The relative mRNA expressions of 4E-BP1. **(F)** The relative mRNA expressions of S6K1.

activity promotes nutrient assimilation, leading to better growth performance (58). Previous studies on grass carp reveal that adequate dietary Met level can notably elevate the intestinal digestive enzyme activity (11). Studies have shown that Met deficiency may result in decreased activity of digestion enzymes, and that dietary supplementation with coated Met may markedly increase intestinal digestion enzyme activity. Meanwhile, the increase of intestinal digestive enzyme activity was similar to the trend of WG. We speculate that this is due to an improvement in the activity of digestive enzymes in the gut, which improves the digestion of nutrients and thus promotes the growth of gibel carp. This was confirmed in another study of mirror carp, and the addition of Met promoted intestinal villus height and muscle thickness, which had a positive effect on intestinal development (34).

4.5 Effect of coated methionine on the expression of TOR pathway related genes in gibel carp

In fish, IGF-1 plays a crucial role in growth promoting, bone formation and metabolic regulation (59). The present study elucidated that including coated Met in the diet up-regulates mRNA expression levels of IGF-1 gene. Moreover, the gene expression level trend upward was the equivalent of WG. Its hypothesized that dietary supplementation with coated Met could promote fish growth and development by up regulating IGF-1 gene expression, and similar results were found in hybrid grouper (60) and rainbow trout (*Oncorhynchus mykiss*) (61). Previous study have reported that binding of IGF-1 to receptors on the cell membrane in muscle cells activates downstream TOR via the PI3K and AKT signaling pathways, and that TOR promotes intracellular protein synthesis through activation of downstream 4E-BP1 and S6K1 (62). The present study illustrated that increased of dietary coated Met markedly influenced the expression of AKT, TOR, and 4E-BP1 gene mRNAs in the TOR pathway. Simultaneously, it was noted in the present study that there was a comparable trend in the expression of genes linked to the TOR pathway, corresponding to increased CP content in muscle (14). Therefore, a hypothesis was raised suggesting Met, as a precursor of protein synthesis, activates the expression of TOR pathway-related genes and promotes protein synthesis in muscle, thus affecting the protein deposition and growth of fish. Similar results have been observed in rainbow trout (19), cobia (7) and grass carp (18).

5 Conclusions

In conclusion, the addition of optimal level of coated Met significantly increased the WG and SGR of gible carp. Furthermore, it enhanced the antioxidant capacity of the hepatopancreas, improved the activity of intestinal digestive enzymes, and up regulated the expression of genes associated with protein synthesis in muscle. The optimal dietary methionine level, as determined through quadratic regression analysis of WG, is recommended to be 0.71%.

Data availability statement

The original contributions presented in the study are included in the article/supplementary material. Further inquiries can be directed to the corresponding author.

Ethics statement

The animal study was approved by The Animal Experimental Ethics Committee of Huzhou University (20180306). The study was conducted in accordance with the local legislation and institutional requirements.

Author contributions

YD: Formal analysis, Methodology, Writing – original draft, Writing – review & editing. XL: Formal analysis, Writing – original draft. XS: Formal analysis, Methodology, Writing – review & editing. JZ: Methodology, Writing – review & editing. HX: Methodology, Writing – review & editing. CC: Validation, Writing – review & editing. QX: Methodology, Resources, Supervision, Validation, Writing – review & editing.

Funding

The author(s) declare financial support was received for the research, authorship, and/or publication of this article. This work was financially supported by the Natural Science Foundation of China, NSFC (31972800).

Acknowledgments

Thanks to all the classmates and teachers who helped this experiment, especially to Huzhou University for providing the experimental platform.

Conflict of interest

The authors declare that the research was conducted in the absence of any commercial or financial relationships that could be construed as a potential conflict of interest.

Publisher's note

References

1. Rawles SD, Thompson KR, Brady YJ, Metts LS, Aksoy MY, Gannam AL, et al. Effects of replacing fish meal with poultry by-product meal and soybean meal and reduced protein level on the performance and immune status of pond-grown sunshine bass (Morone chrysops× M. *saxatilis). Aquac Nutr.* (2011) 17:e708–21. doi: 10.1111/j.1365-2095.2010.00831.x

2. Han YK, Xu YC, Luo Z, Zhao T, Zheng H, Tan XY. Fish meal replacement by mixed plant protein in the diets for juvenile yellow catfish *pelteobagrus fulvidraco*: effects on growth performance and health status. *Aquac Nutr.* (2022) 2022:2677885. doi: 10.1155/2022/2677885

3. Hardy RW. Utilization of plant proteins in fish diets: effects of global demand and supplies of fishmeal. *Aquac Res.* (2010) 41:770–6. doi: 10.1111/j.1365-2109.2009.02349.x

4. Anderson AD, Alam MS, Watanabe WO, Carroll PM, Wedegaertner TC, Dowd MK. Full replacement of menhaden fish meal protein by low-gossypol cottonseed flour protein in the diet of juvenile black sea bass. *Centropristis striata Aquaculture.* (2016) 464:618–28. doi: 10.1016/j.aquaculture.2016.08.006

5. Wu GY, Bazer FW, Dai ZL, Li DF, Wang JJ, Wu ZL. Amino acid nutrition in animals: protein synthesis and beyond. *Annu Rev Anim Biosci.* (2014) 2:387–417. doi: 10.1146/annurev-animal-022513-114113

6. Chi SY, Tan BP, Dong XH, Yang QH, Liu HY. Effects of supplemental coated or crystalline methionine in low-fishmeal diet on the growth performance and body composition of juvenile cobia *Rachycentron canadum* (Linnaeus). *Chin J Oceanol Limnol.* (2014) 32:1297–306. doi: 10.1007/s00343-014-3276-2

7. He YF, Chi SY, Tan BP, Dong XH, Yang QH, Liu HY, et al. dl-Methionine supplementation in a low-fishmeal diet affects the TOR/S6K pathway by stimulating ASCT2 amino acid transporter and insulin-like growth factor-I in the dorsal muscle of juvenile cobia (*Rachycentron canadum*). *Br J Nutr.* (2019) 122:734–44. doi: 10.1017/S0007114519001648

8. Espe M, Andersen SM, Holen E, Rønnestad I, Veiseth-Kent E, Zerrahn JE, et al. Methionine deficiency does not increase polyamine turnover through depletion of hepatic S-adenosylmethionine in. *juvenile Atlantic salmon Br J Nutr.* (2014) 112:1274–85. doi: 10.1017/S0007114514002062

9. Yun YH, Song DY, He ZJ, Mi JL, Wang LM, Nie GX. Effects of methionine supplementation in plant protein based diet on growth performance and fillet quality of juveniles Yellow River carp (*Cyprinus carpio haematopterus*). *Aquaculture.* (2022) 549:737810. doi: 10.1016/j.aquaculture.2021.737810

10. Espe M, Hevrøy EM, Liaset B, Lemme A, El-Mowafi A. Methionine intake affect hepatic sulphur metabolism in Atlantic salmon. *Salmo salar Aquaculture.* (2008) 274:132–41. doi: 0.1016/j.aquaculture.2007.10.051

11. Wu P, Tang L, Jiang WD, Hu K, Liu Y, Jiang J, et al. The relationship between dietary methionine and growth, digestion, absorption, and antioxidant status in intestinal and hepatopancreatic tissues of sub-adult grass carp (*ctenopharyngodon idella*). *J Anim Sci Biotechnol.* (2017) 8:1–14. doi: 10.1186/s40104-017-0194-0

12. Chen NS, Ma JZ, Zhou HY, Zhou J, Qiu XJ, Jin LN, et al. Assessment of dietary methionine requirement in largemouth bass. *Micropterus salmoides J Fish China.* (2010) 34:1244–53. doi: 10.3724/SP.J.1231.2010.06865

13. Noor Z, Noor M, Khan SA, Younas W, Ualiyeva D, Hassan Z, et al. Dietary supplementations of methionine improve growth performances, innate immunity, digestive enzymes, and antioxidant activities of rohu (*Labeo rohita*). *Fish Physiol Biochem.* (2021) 47:1–14. doi: 10.1007/S10695-021-00924-X

14. Ji K, Liang HL, Ge XP, Ren MC, Pan LK, Huang DY. Optimal methionine supplementation improved the growth, hepatic protein synthesis and lipolysis of grass carp fry (*Ctenopharyngodon idella*). *Aquaculture.* (2022) 554:738125. doi: 10.1016/j.aquaculture.2022.738125

15. Wang Z, Mai KS, Xu W, Zhang YJ, Liu YL, Ai QH. Dietary methionine level influences growth and lipid metabolism *via* GCN2 pathway in cobia (*Rachycentron canadum*). *Aquaculture.* (2016) 454:148–56. doi: 10.1016/j.aquaculture.2015.12.019

16. Rong H, Lin F, Zhang YL, Yu J, Yu CQ, Zhang HR, et al. Effects of dietary proline on growth, physiology, biochemistry and TOR pathway-related gene expression in juvenile spotted drum. *Nibea diacanthus Fish Sci.* (2020) 86:495–506. doi: 10.1007/s12562-020-01414-4

17. Ahmed I, Malla BA, Shah BA, Wani ZA, Khan YM. Dietary arginine modulates growth performance, hemato-biochemical indices, intestinal enzymes, antioxidant ability and gene expression of TOR and 4E-BP1 in rainbow trout. *Oncorhynchus mykiss Fingerlings Front Mar Sci.* (2022) 9:908581. doi: 10.3389/fmars.2022.908581

18. Fang CC, Feng L, Jiang WD, Wu P, Liu Y, Kuang SY, et al. Effects of dietary methionine on growth performance, muscle nutritive deposition, muscle fibre growth and type I collagen synthesis of on-growing grass carp (*Ctenopharyngodon idella*). *Br J Nutr.* (2021) 126:321–36. doi: 10.1017/S0007114520002998

19. Rolland M, Dalsgaard J, Holm J, Gómez-Requeni P, Skov PV. Dietary methionine level affects growth performance and hepatic gene expression of GH-IGF system and protein turnover regulators in rainbow trout (*Oncorhynchus mykiss*) fed plant protein-based diets. *Comp Biochem Physiol Part B: Biochem Mol Biol.* (2015) 181:33–41. doi: 10.1016/j.cbpb.2014.11.009

20. Engelman JA, Luo J, Cantley LC. The evolution of phosphatidylinositol 3-kinases as regulators of growth and metabolism. *Nat Rev Genet.* (2006) 7:606–19. doi: 10.1038/nrg1879

21. Chi SY, Tan BP, Lin HZ, Mai KS, Ai QH, Wang XJ, et al. Effects of supplementation of crystalline or coated methionine on growth performance and feed utilization of the pacific white shrimp. *Litopenaeus vannamei Aquac Nutr*. (2011) . 17:e1–9. doi: 10.1111/j.1365-2095.2009.00710.x

22. Chi SY, Tan BP, Dong XH, Yang QH, Liu HY, Xu YN, et al. Effect of supplementation microcapsule or crystalline methionine in diets on related enzyme activity of cobia (*Rachycentron canadum*). *J Fish Sci China*. (2011) 18:110–8. doi: 10.3724/SP.J.1118.2011.00110

23. Leng XJ, Wang G, Li XQ, Hu B, Yang ZG. Supplemental effects of crystalline or coated amino acids on growth performance and serum free amino acids of *allogynogenetic crucian carp*. *J Fish China*. (2007) 31:743–8. doi: 10.3321/j.issn:1000-0615.2007.06.007

24. Chen BG, Leng XJ, Li XQ, Hu B. Effects of crystalline or coated amino acids on carp. *Acta Hydrobiol Sin*. (2008) 5:774–8. doi: 10.3724/SP.J.0000.2008.50774

25. Mahotra M, Yu H, Xu Q, Liew WC, Kharel S, Tan LSE, et al. Solid Lipid Microparticles as leaching free, slow-release encapsulation system for Methionine in aquaculture. *Aquaculture*. (2022) 557:738342. doi: 10.1016/j.aquaculture.2022.738342

26. Gomaa A H, El-Sherbiny M A, T Eassawy M. Comparing effects of feeding crystalline or coated methionine to soybean meal based diets on the Nile tilapia (*Oreochromis niloticus*) growth performance and protein quality. *Egyptian J Aquat Biol Fisheries*. (2018) 22:221–32. doi: 10.21608/ejabf.2018.17158

27. Zhao JY, Yang X, Xu QY. Effects of coated methionine on growth performance, intestinal digestive enzymes and muscle amino acid composition of Songpu mirror carp (*Cyprinus carpio Songpu*). *Feed Industry*. (2022) 43:40–6. doi: 10.13302/j.cnki.fi.2022.20.007

28. Zhou XJ. Utilization of dietary crystalline lysine and methionine and the requirements for gibel carp. Huazhong Agricultural University, Wuhan (2005).

29. Wang X, Xue M, Figueiredo-Silva C, Wang J, Zheng Y, Wu X, et al. Dietary methionine requirement of the pre-adult gibel carp (*Carassius auratus gibeilo*) at a constant dietary cystine level. *Aquac Nutr*. (2016) 22:509–16. doi: 10.1111/anu.12271

30. Ren M, Liang H, He J, Masagounder K, Yue Y, Yang H, et al. Effects of DL-methionine supplementation on the success of fish meal replacement by plant proteins in practical diets for juvenile gibel carp (*Carassius auratus gibelio*). *Aquac Nutr*. (2017) 23:934–41. doi: 10.1111/anu.12461

31. AOAC. *Official methods of analysis of AOAC international. eighteenth ed*. Arlington, Virginia, USA: Association of Official Analytical Chemists (2005).

32. Lowry OH, Rosebrough NJ, Farr AL, Randall RJ. Protein measurement with the Folin phenol reagent. *J Biol Chem*. (1951) 193:265–75. doi: 10.1515/bchm2.1951.286.1-6.270

33. Luo QH, Qian RD, Qiu ZS, Yamamoto FY, Du YY, Lin XW, et al. Dietary α-ketoglutarate alleviates glycinin and β-conglycinin induced damage in the intestine of mirror carp (*Cyprinus carpio*). *Front Immunol*. (2023) 14:1140012. doi: 10.3389/fimmu.2023.1140012

34. Cheng L. Effects of methionine on growth performance, digestion and absorption, antioxidant capacity and gene expression of muscle synthesis pathway in Songpu mirror carp. Shanghai Ocean University, Shanghai (2020). doi: 10.27314/d.cnki.gsscu.2020.000178

35. Liu XR, Han B, Xu J, Zhu JY, Hu JT, Wan WL, et al. Replacement of fishmeal with soybean meal affects the growth performance, digestive enzymes, intestinal microbiota and immunity of. *Carassius auratus gibelio*♀× *Cyprinus carpio*♂ *Aquac Rep*. (2020) 18:100472. doi: 10.1016/j.aqrep.2020

36. Cao SP, Mo P, Xiao YB, Chen Y, Shi YX, Hu YF, et al. Dietary supplementation with fermented plant meal enhances growth, antioxidant capacity and expression of TOR signaling pathway genes in gibel carp (*Carassius auratus gibelio* var. *CAS V*). *Aquac Rep*. (2021) 19:100559. doi: 10.1016/j.aqrep.2020

37. Ma R, Hou HP, Mai KS, Bharadwaj AS, Cao H, Ji FJ, et al. Comparative study on the effects of L-methionine or 2-hydroxy-4-(methylthio) butanoic acid as dietary methionine source on growth performance and anti-oxidative responses of turbot (*Psetta maxima*). *Aquaculture*. (2013) 412:136–43. doi: 10.1016/j.aquaculture.2013.07.021

38. Elmada CZ, Huang W, Jin M, Liang X, Mai K, Zhou Q. The effect of dietary methionine on growth, antioxidant capacity, innate immune response and disease resistance of juvenile yellow catfish (*Pelteobagrus fulvidraco*). *Aquac Nutr*. (2016) 22:1163–73. doi: 10.1111/anu.12363

39. Qi GS. Effects of dietary taurine, methionine, cystine, serine and cysteamine on growth performance and taurine anabolism in turbot (*Scophthalmus maximus*). Ocean University of China, Qingdao (2012). doi: 10.7666/d.y2159733

40. Luo Z, Liu YJ, Mai KS, Tian LX, Yang HJ, Tan XY, et al. Dietary L-methionine requirement of juvenile grouper Epinephelus coioides at a constant dietary cystine level. *Aquaculture*. (2005) 249:409–18. doi: 10.1016/j.aquaculture.2005.04.030

41. Jia P, Xue M, Zhu X, Liu HY, Wu XF, Wang J, et al. Effects of dietary methionine levels on the growth performance of juvenile gibel carp (*carassius auratus gibelio*). *Acta Hydrobiol Sin*. (2013) 37:217–26. doi: 10.7541/2013.7

42. Aragao C, Corte-Real J, Costas B, Dinis MT, Conceição LEC. Stress response and changes in amino acid requirements in Senegalese sole (*Solea Senegalensis Kaup* 1858). *Amino Acids*. (2008) 34:143–8. doi: 10.1007/s00726-007-0495-2

43. Buttle LG, Uglow RF, Cowx IG. Effect of dietary protein on the nitrogen excretion and growth of the African catfish, *Clarias gariepinus*. *Aquat Living Resour*. (1995) 8:407–14. doi: 10.1051/alr:1995048

44. Jung K, Ohlrich B, Mildner D, Zubek A, Schimmelphennig W, Egger E. The apoenzyme of aspartate aminotransferase and alanine aminotransferase in the serum of healthy persons and patients suffering from liver diseases. *Clin Chim Acta*. (1978) 90:143–9. doi: 10.1016/0009-8981(78)90515-6

45. Feng L, Xiao WW, Liu Y, Jiang J, Hu K, Jiang WD, et al. Methionine hydroxy analogue prevents oxidative damage and improves antioxidant status of intestine and hepatopancreas for juvenile Jian carp (*Cyprinus carpio* var. Jian). *Aquac Nutr*. (2011) 17:595–604. doi: 10.1111/j.1365-2095.2011.00853.x

46. Niu J, Du Q, Lin HZ, Cheng YQ, Huang Z, Wang Y, et al. Quantitative dietary methionine requirement of juvenile golden pompano *Trachinotus ovatus* at a constant dietary cystine level. *Aquac Nutr*. (2013) 19:677–86. doi: 10.1111/anu.12015

47. Skiba-Cassy S, Geurden I, Panserat S, Iban S. Dietary methionine imbalance alters the transcriptional regulation of genes involved in glucose, lipid and amino acid metabolism in the liver of rainbow trout (*Oncorhynchus mykiss*). *Aquaculture*. (2016) 454:56–65. doi: 10.1016/j.aquaculture.2015.12.015

48. Xu ZH, Regenstein JM, Xie DD, Lu WJ, Ren XC, Yuan JJ, et al. The oxidative stress and antioxidant responses of *Litopenaeus vannamei* to low temperature and air exposure. *Fish Shellfish Immunol*. (2018) 72:564–71. doi: 10.1016/j.fsi.2017.11.016

49. Sies H. Oxidative stress: oxidants and antioxidants. *Exp Physiol*. (1997) 82:291–5. doi: 10.1113/expphysiol.1997.sp004024

50. Liu QD, Wen B, Li XD, Jiang YS, Liang ZP, Zuo RT. An investigation on the effects of dietary protein level in juvenile Chinese mitten crab (*Eriocheir sinensis*) reared at three salinities: Survival, growth performance, digestive enzyme activities, antioxidant capacity and body composition. *Aquac Res*. (2021) 52:2580–92. doi: 10.1111/are.15106

51. Li P, Burr GS, Wen Q, Goff JB, Murthy HS, Gatlin DM III. Dietary sufficiency of sulfur amino acid compounds influences plasma ascorbic acid concentrations and liver peroxidation of juvenile hybrid striped bass (Morone chrysops× M. *saxatilis) Aquaculture*. (2009) 287:414–8. doi: 10.1016/j.aquaculture.2008.11.004

52. Yang XY, Wang XW, Chi SY. Effects of methionine on growth performance serum biochemical indexes and liver enzyme activities of two sizes of *Epinephelus coioides*. *Chin J Anim Nutr*. (2020) 32:1305–14. doi: 10.3969/j.issn.1006-267x.2020.03.038

53. Colovic MB, Vasic VM, Djuric DM, Krstic DZ. Sulphur-containing amino acids: protective role against free radicals and heavy metals. *Curr Med Chem*. (2018) 25:324–35. doi: 10.2174/0929867324666170609075434

54. Coutinho F, Simões R, Monge-Ortiz R, Furuya WM, Pousão-Ferreira P, Kaushik S, et al. Effects of dietary methionine and taurine supplementation to low-fish meal diets on growth performance and oxidative status of European sea bass (*Dicentrarchus labrax*) juveniles. *Aquaculture*. (2017) 479:447–54. doi: 10.1016/j.aquaculture.2017.06.017

55. Zhao JY, Xu QY. Influence of soybean meal on intestinal mucosa metabolome and effects of adenosine monophosphate-activated protein kinase signaling pathway in mirror carp (*Cyprinus carpio songpu*). *Front Mar Sci*. (2022) 9:844716. doi: 10.3389/fmars.2022.844716

56. Khosravi S, Rahimnejad S, Herault M, Fournier V, Lee CR, Bui HTD, et al. Effects of protein hydrolysates supplementation in low fish meal diets on growth performance, innate immunity and disease resistance of red sea bream Pagrus major. *Fish Shellfish Immunol*. (2015) 45:858–68. doi: 10.1016/j.fsi.2015.05.039

57. Farhangi M, Carter CG. Growth, physiological and immunological responses of rainbow trout (*Oncorhynchus mykiss*) to different dietary inclusion levels of dehulled lupin (*Lupinus angustifolius*). *Aquac Res*. (2001) 32:329–40. doi: 10.0000/026999497378403

58. Bakke AM, Glover C, Krogdahl Å. Feeding, digestion and absorption of nutrients. *Fish Physiol*. (2010) 30:57–110. doi: 10.1016/S1546-5098(10)03002-5

59. Montserrat N, Sánchez-Gurmaches J, García DLSD, Navarro MI, Gutiérrez J. IGF-I binding and receptor signal transduction in primary cell culture of muscle cells of gilthead sea bream: changes throughout in *vitro* development. *Cell Tissue Res*. (2007) 330:503–13. doi: 10.1007/s00441-007-0507-2

60. Li XJ, Mu W, Wu XY, Dong Y, Zhou ZY, Wang X, et al. The optimum methionine requirement in diets of juvenile hybrid grouper (*Epinephelus fuscoguttatus*♀×*Epinephelus lanceolatus*♂): Effects on survival, growth performance, gut micromorphology and immunity. *Aquaculture*. (2020) 520:735014. doi: 10.1016/j.aquaculture.2020.735014

61. Alami-Durante H, Bazin D, Cluzeaud M, Fontagné-Dicharry S, Kaushik S, Geurden I. Effect of dietary methionine level on muscle growth mechanisms in juvenile rainbow trout (*Oncorhynchus mykiss*). *Aquaculture*. (2018) 483:273–85. doi: 10.1016/j.aquaculture.2017.10.030

62. Ma XM, Blenis J. Molecular mechanisms of mTOR-mediated translational control. *Nat Rev Mol Cell Biol*. (2009) 10:307–18. doi: 10.1107/s0108767317095794

frontiers | Frontiers in Immunology

TYPE Original Research
PUBLISHED 09 August 2024
DOI 10.3389/fimmu.2024.1368444

OPEN ACCESS

EDITED BY
Samad Rahimnejad,
University of Murcia, Spain

REVIEWED BY
Jing Xing,
Ocean University of China, China
Xianyong Bu,
Ocean University of China, China
Yun-Zhang Sun,
Jimei University, China

*CORRESPONDENCE
Houguo Xu
xuhg@ysfri.ac.cn

RECEIVED 10 January 2024
ACCEPTED 16 July 2024
PUBLISHED 09 August 2024

CITATION
Ma Q, Zhao G, Liu J, Chen I-T, Wei Y, Liang M, Dai P, Nuez-Ortin WG and Xu H (2024) Effects of a phytobiotic-based additive on the growth, hepatopancreas health, intestinal microbiota, and *Vibrio parahaemolyticus* resistance of Pacific white shrimp, *Litopenaeus vannamei*. *Front. Immunol.* 15:1368444. doi: 10.3389/fimmu.2024.1368444

Effects of a phytobiotic-based additive on the growth, hepatopancreas health, intestinal microbiota, and *Vibrio parahaemolyticus* resistance of Pacific white shrimp, *Litopenaeus vannamei*

Qiang Ma[1], Guiping Zhao[2], Jiahao Liu[1], I-Tung Chen[2], Yuliang Wei[1], Mengqing Liang[1], Ping Dai[1], Waldo G. Nuez-Ortin[2] and Houguo Xu[1]*

[1]State Key Laboratory of Mariculture Biobreeding and Sustainable Goods, Yellow Sea Fisheries Research Institute, Chinese Academy of Fishery Sciences, Qingdao, China, [2]Adisseo Life Science (Shanghai) Co., Ltd, Shanghai, China

Vibrio genus is a common pathogen in aquaculture and causes acute hepatopancreatic necrosis disease (AHPND) and massive mortality of shrimp. Many studies have suggested that a single functional ingredient such as plant extract or organic acid can reduce the dependence on antibiotics and promote the growth and immunity of aquatic animals. In this study, we evaluated the effects of a phytobiotic-based compound additive (Sanacore® GM, SNGM), which had a successful trajectory of commercial application in fish farming. However, its effects on the hepatopancreas health and intestinal microbiota of shrimp after *Vibrio* challenge have not been well evaluated. In the present study, Pacific white shrimp were fed diets with or without supplementation of SNGM, and the SNGM grades were 0-g/kg (CON), 3-g/kg (SNGM3), and 5-g/kg (SNGM5) diets. The feed trial lasted 60 days, after which a *Vibrio parahaemolyticus* challenge was performed. The results showed that compared to the CON group, both the SNGM3 and SNGM5 groups had a significantly higher weight gain and a lower feed conversion ratio as well as higher survival after *Vibrio parahaemolyticus* challenge. In the growth trial, the SNGM3 group had a significantly increased total protein, albumin concentration, and acid phosphatase activity in hemolymph compared to the CON group. In the challenge experiment, the SNGM3 and SNGM5 groups had increased albumin and glucose contents as well as the activities of phenoloxidase, lysozyme, alkaline phosphatase, and superoxide dismutase in hemolymph. Both the SNGM3 and SNGM5 groups had improved morphology of the hepatopancreas and intestine. The SNGM5 group had alleviated gut microbiota dysbiosis induced by *Vibrio* infection by increasing the potential probiotic bacterium abundance (*Shewanella*) and decreasing the potential pathogenic bacteria abundance (*Vibrio*, *Photobacteriuma*, *Pseudoalteromonas*, and *Candidatus_Bacilloplasma*). In conclusion, the dietary phytobiotic-based additive at 3-g/kg level increased

10.3389/fimmu.2024.1368444

the growth and *Vibrio parahaemolyticus* resistance of Pacific white shrimp by promoting immune-related enzyme activities and improving the morphological structure of the hepatopancreas and intestine and the intestinal microbiota composition.

KEYWORDS

shrimp, Immunity, hepatopancreas health, intestinal microbiota, *Vibrio*

1 Introduction

Pacific white shrimp (*Litopenaeus vannamei*) is the most popular aquaculture crustacean due to its high nutritional and economic value. With the development of high-density intensive farming, bacterial and viral diseases in shrimp have become a limiting factor for production. *Vibrio* genus is a common pathogen in aquaculture and can result in serious economic loss (1). Currently, acute hepatopancreatic necrosis disease (AHPND), caused by *Vibrio parahaemolyticus*, is a severe epidemic disease in white shrimp aquaculture and results in high mortality (2). Antibiotic has been a main solution for this disease threat. However, frequent and massive use of antibiotics can lead to the emergence of antibiotic-resistant bacteria. In particular, the antibiotic resistance of *Vibrio*, such as ampicillin, ceftriaxone, and imipenem, isolated from farmed shrimp has been widely reported (3). Meanwhile, antibiotics also have some negative effects on animals and threaten human health via their residue in aquatic food products (4). Therefore, searching for strategies which can reduce the dependence on antibiotics has become an urgent task in shrimp farming.

Unlike antibiotics, health additives based on natural components such as plant extracts, organic acids, and yeast extracts have less impact on the antibiotic resistance of microorganisms and are therefore being more and more frequently used in aquaculture (5, 6). The main effective components of plant extracts are polysaccharides, phenolic compounds, flavonoids, alkaloids, terpenoids, caffeic acid, saponins, and essential oils. They are effective for disease control and have also been widely used in human medicine (7–9). In Pacific white shrimp, feeding with diets supplemented with 20 g/kg Asteraceae plant (*Bidens alba*) or Indian borage (*Plectranthus amboinicus*) extract for 7 days significantly increased the total hemocyte count, phenoloxidase activity, superoxide anion production, phagocytic activity, immune gene expression, and resistance to *Vibrio alginolyticus* (10). In black tiger shrimp (*Penaeus monodon*) and freshwater crab (*Paratelphusa hydrodomous*), the injection treatment with five Indian traditional medicinal plant extracts (*Aegle marmelos*, *Cynodon dactylon*, *Lantana camara*, *Momordica charantia*, and *Phyllanthus amarus*, 100 or 150 mg/kg body weight) individually resulted in a higher antiviral activity against white spot syndrome virus (WSSV) (11). Studies have demonstrated that individually adding *Allium sativum*, *Olea europaea*, *Argemone mexicana*, *Sargassum cristaefolium*, *Nigella sativa*, *Phyllanthus amarus*, or *Eleutherine bulbosa* extract in the diet all promoted the immunity and resistance to WSSV or *Vibrio* genus in Pacific white shrimp (12). Organic acids, including formic acid, butyric acid, citric acid, malic acid, fumaric acid, etc., have been commonly used in the food industry and animal feeds. Adding formic acid (0.023%), acetic acid (0.041%), propionic acid (0.03%), and butyric acid (0.066%) could effectively inhibit the growth of *Vibrio harveyi* isolated from sick shrimp on Muller–Hinton agar medium (13). In black tiger shrimp, a novel microencapsulated organic acid blend supplementation in the diet increased the digestibility, survival after *Vibrio harveyi* challenge, and phenol oxidase activity and reduced hepatopancreatic damage, total viable bacteria, and presumptive *Vibrio* spp. counts in the hepatopancreas and intestine (14). Yeast extracts contain nucleotides, amino acids, polysaccharides, and trace elements and have been widely used in animal feeds (15). In kuruma shrimp (*Marsupenaeus japonicus*), the oral administration or injection of a nucleotide-rich baker's yeast extract increased the gene expressions of anti-microbial peptides/proteins, such as penaeidin, crustin, and lysozyme, and resistance to *Vibrio nigripulchritudo* infection (16). In Pacific white shrimp, low-fish meal diets supplemented with yeast extract (500–1,500 mg/kg) improved the growth, antioxidant enzyme activities, and intestinal morphology (17). In summary, plant extract, organic acid, and yeast extract have been widely used in aquaculture as antibiotic alternative disease control strategies.

Nonetheless, many studies have evidenced that the individual use of plant extract, organic acid, yeast extract, and other immuno-stimulants could increase the disease resistance of shrimp. Effective products, in particular, those based on the combination of functional ingredients, are less studied and applied in the aqua-feed industry. Sanacore® GM (SNGM) is a phytobiotic-based compound additive with a successful trajectory of commercial application in aqua-feeds. Studies on gilthead seabream (*Sparus aurata*) have evidenced that 0.4–0.5% SNGM supplementation increased the resistance to *Enteromyxum leei* and *Vibrio alginolyticus* by improving antioxidation and immunity (18, 19) and also reduced the amount of fishmeal in the feed (20). Meanwhile, dietary 0.2–0.3% SNGM in the Pacific white shrimp also promoted growth performance and resistance to *Fusarium solani* by improving the feed utilization, antioxidant capacity, non-specific immune response, and intestinal health (21). However, few studies have investigated the effects of SNGM on the hepatopancreas health and intestinal microbiota of

Pacific white shrimp, in particular, after *Vibrio* challenge. Therefore, the present study aimed to evaluate the efficacy of SNGM in the diets of Pacific white shrimp in terms of growth, immunity, hepatopancreas health, intestinal microbiota, and resistance to *Vibrio parahaemolyticus* challenge. The results of this study could be helpful to the green and healthy development of shrimp farming.

2 Materials and methods

2.1 Experimental diets

The basal diet (CON) used fishmeal, soybean meal, peanut cake meal, and Antarctic krill meal as main protein sources, and fish oil and soy lecithin as the main lipid sources (Table 1). The control diet contained approximately 43% protein and 8.5% lipid. A phytobiotic-based, health-promoting additive compound, Sanacore® GM [SNGM, Adisseo Life Science (Shanghai) Co., Ltd.], which is a mixture of herbal extracts, organic acids, inactivated yeast, and yeast extracts on a mineral carrier, was added into the control diet at the levels of 0.3% and 0.5%, respectively, to obtain the other two experimental diets (designated as SNGM3 and SNGM5, respectively).

TABLE 1 Formulation and proximate composition of the experimental diets (g/kg).

Ingredient	CON	SNGM3	SNGM5
Fish meal	160	160	160
Soybean meal	300	300	300
Peanut cake meal	180	180	180
Antarctic krill meal	50	50	50
Wheat gluten meal	40	40	40
High gluten flour	190	187	185
Fish oil	20	20	20
Soy lecithin	25	25	25
Monocalcium phosphate	14	14	14
Mineral premix[a]	5	5	5
Vitamin premix[a]	10	10	10
L-ascorbyl-2-polyphosphate	2	2	2
Choline chloride	2	2	2
Lysine hydrochloride	1	1	1
Methionine	1	1	1
Sanacore® GM[b]	0	3	5
Total	1,000	1,000	1,000
Proximate composition (% dry matter)			
Crude protein	43.36	43.41	43.74
Crude lipid	8.59	8.87	8.13
Ash	8.22	8.40	8.54

[a]Vitamin premix and mineral premix, designed for marine shrimp, were purchased from Qingdao Master Biotech Co., Ltd., Qingdao, China.
[b]Sanacore® GM is a broad-spectrum health-promoting additive consisting of a mixture of herbal extracts, organic acids, inactivated yeast, and yeast extracts on a mineral carrier provided by Adisseo Life Science (Shanghai) Co., Ltd.

The experimental diets were made using a customized single-screw pelleting machine in the laboratory. Before drying, the pellets (2.0 × 2.0 mm) were steamed for 10 min to enhance their stability in water. The diets were then oven-dried to a moisture content of around 5% and were stored at -20°C.

2.2 Experimental shrimp and feeding procedure

The juvenile shrimp used in the study were purchased from Rizhao Tengyun Aquaculture Co. Ltd. (Rizhao, Shandong Province, China), where the growth trial was conducted. Flow-through deep-well seawater was used in both the acclimating period and the whole growth trial period. A total of 1,200 experimental shrimp with an average initial body weight of approximately 4.5 g was distributed into 12 polyethylene tanks (300 L). Each diet was randomly assigned to for replicate tanks, and each tank was stocked with 100 shrimp. The growth trial lasted 60 days, and the experimental shrimps were hand-fed to apparent satiation four times each day (6:00, 11:30, 17:00, and 21:30). Dead shrimps were taken out when found, and the number and the weight of dead shrimp were recorded. The residual feed and feces were siphoned out 30 min after every feeding (after the shrimp stopped feeding). During the feeding trial, the water temperature ranged from 24°C to 27°C, salinity was 18 to 20, pH was 8.0 to 8.4, dissolved oxygen was 6 to 7 mg L^{-1}, and ammonia was <0.2 mg L^{-1}.

2.3 Challenge experiment

At the end of the growth trial, 30 shrimps/tank were transferred to separate tanks for the challenge experiment with *Vibrio parahaemolyticus*. A pre-experiment was conducted to determine the most suitable challenging method and corresponding semi-lethal concentration (22). The final challenge method was as follows: shrimps were immersed in 2-L bacteria solution (at a concentration of 1 × 10^8 cfu/mL) for 30 min. After that, the shrimp-and-bacteria solution was poured into 200 L of clean seawater (the final bacteria concentration was approximately 1×10^6 cfu/mL). During the challenge experiment, no more clean water was added into the tanks. The mortality was recorded daily continuously for 7 days.

2.4 Sample collection

Samplings were conducted for both the growth trial and the challenge experiment. At the end of the growth trial, the weight and the number of shrimps in each tank were recorded after having been anesthetized with eugenol (1:10,000). From each tank, six shrimps were randomly sampled to collect the hemolymph from pericardial cavity using syringes. The hemolymph was centrifuged at 4°C to

obtain the supernatant. The hemolymph of three shrimps from each tank was pooled and gently mixed with anticoagulant to count the hemocyte. After that, these nine shrimps were dissected on ice. The hepatopancreas, intestine, and muscle were collected and frozen immediately with liquid nitrogen and then stored at -80°C for further processing. The sampling process after the 7-day challenge experiment was the same as described above.

2.5 Proximate composition analysis

The proximate composition analysis of experimental diets, whole fish, and muscle was performed according to the standard methods of the Association of Official Analytical Chemists (2005). Briefly, samples were oven-dried at 105°C to a constant weight for moisture assay. Crude protein content (N × 6.25) was measured by the Kjeldahl method using the UDK142 automatic distillation unit (VELP, Usmate, MB, Italy). The crude lipid content was detected by petroleum ether extraction using the Soxhlet method (Foss Tecator, Hoganas, Sweden). The ash content was measured by incinerating the sample in a muffle furnace at 550°C to constant weight.

2.6 Biochemical indexes of the hemolymph, hepatopancreas, and intestine

The contents of total soluble protein (TP, A045–4-2), albumin (ALB, A028–2-1), glucose (GLU, F006–1-1), total cholesterol (T-CHO, A111–1-1), triglycerides (TG, A110–1-1), malonaldehyde (MDA, A003–1-1), and protein carbonyl (PC, A087–1-1) and the activities of alkaline phosphatase (AKP, A059–2-1), acid phosphatase (ACP, A060–2-1), lysozyme (LZM, A050–1-1), phenol oxidase (PO, H247–1-1), and superoxide dismutase (SOD, A001–3-2) in the hemolymph, hepatopancreas or intestine were analyzed by using commercial kits purchased from Nanjing Jiancheng Bioengineering Institute (Nanjing, China). All measurement steps were based on the manufacturer's protocols (http://www.njjcbio.com/).

2.7 Histological analysis of the hepatopancreas and intestine

The middle intestine and hepatopancreas were collected and fixed in 4% paraformaldehyde immediately. Then, the samples were conducted with a graded ethanol series and xylene solution. After paraffin embedding, the molds were sectioned for 5-μm thickness by a semiautomatic microtome. The sections were stained with the Harris hematoxylin-eosin mixture (H&E) and photographed under a light microscope (Nikon Ds-Ri2, Boston, USA).

2.8 Intestinal microbiota analysis

The whole intestines of three shrimps from the same tank were pooled as one sample (three tanks were randomly selected from each treatment) under sterile conditions. The total bacterial DNA of the intestine was isolated using marine animals DNA kit (Tiangen, China). The quantity and the quality of extracted DNA were tested by using Titertek-Berthold Colibri spectrometer (Colibri, Germany). The ratio of 260/280 nm of DNA ranged from 1.8 to 1.9 and was confirmed by agarose gel electrophoresis. 338F (5′-GTGCCAGCMGCCGCGGTAA-3′) and 806R (5′-CCGTCAATTCCTTTRAGTTT-3′) were selected as the forward and reverse primer, respectively, and the V3–V4 regions of the bacteria 16S ribosomal RNA genes were amplified by PCR using the DNA as template. The PCR (25 μL volume) was performed by mixing 20 ng DNA, 0.4 μL Fast PfuPolymerase (TransGen Biotech, China), 1 μL of each primer (5 μM), 4 μL 5 × Fast Pfu Buffer, and 2 μL dNTPs (2.5 mM). The PCR program was as follows: 95°C for 5 min, 30 cycles of 95°C for 30 s, 55°C for 30 s, and 72°C for 50 s and 72°C for 10 min. Then, Illumina high-throughput sequencing was carried out by Majorbio Bio-Pharm Technology Co., Ltd. (Shanghai, China). All sequencing data were uploaded to the NCBI database under accession number SUB14101752/PRJNA1055185 and bioinformation cloud platform of Majorbio for further analysis (http://www.i-sanger.com). Cluster analysis was carried out for non-repeating sequences (excluding single sequences) according to 97% similarity using Uparse software, and chimeras were removed in the clustering process to obtain the representative sequences of operational taxonomic units (OTUs). The taxonomic analysis of OTU representative sequences was performed by using RDP classifier. The richness and the diversity of bacteria at each taxonomic level were analyzed by using Qiime and Mothur software.

2.9 Statistical analysis

The calculations used in this study include the following:

$$\text{Weight gain (WG, \%)} = 100 \times (W1 - W0)/W0$$

$$\text{Feed conversion ratio (FCR)} = \text{feeds consumed}/(W1 - W0)$$

$$\text{Feed intake (FI, \% /day)} = 100 \times \text{feed intake}/[(W1 + W0)/2]/\text{days}$$

$$\text{Condition factor (K, g/cm}^3\text{)} = \text{final body weight}/\text{final body length}^3$$

$$\text{Survival (\%)} = 100 \times \text{final number of shrimp}/\text{initial number of shrimps}$$

where W0 = initial body weight and W1 = final body weight.

All data were subjected to one-way analysis of variance (ANOVA) using the SPSS Statistics 20.0 software for Windows. Shapiro–Wilk and Levene's tests were performed to evaluate the normality and homogeneity of data. Significant differences between the means were detected by using Tukey's multiple-range test. The results were presented as means ± standard errors of means (SEM), and the level of significance was chosen at $P < 0.05$. In the normal growth experiment, values with different lowercase superscript letters are significantly different ($P < 0.05$). In the challenge experiment, values with different capital superscript letters are significantly different ($P < 0.05$).

3 Results

3.1 Growth performance and *Vibrio parahaemolyticus* resistance

After the 60-day growth trial, shrimps fed SNGM3 and SNGM5 had significantly higher final body weight (FBW), weight gain (WG), and survival and significantly lower feed conversion ratio (FCR) compared to the CON group ($P < 0.05$) (Figures 1A, B, D, F). There were no significant differences in initial body weight, feed intake, and condition factor between the CON and SNGM groups (Figures 1A, C, E).

After the 7-day challenge experiment, the survival rates in the SNGM3 and SNGM5 groups were significantly higher than in the CON group ($P < 0.05$) (Figure 1G). As shown in Figure 1H, the color of the hepatopancreas in the CON group turned white after *Vibrio parahaemolyticus* infection, but the SNGM groups, especially the SNGM5 group, had more normal and healthier (darker color) hepatopancreas after the 7-day challenge experiment.

3.2 The body proximate compositions

As shown in Figure 2, the proximate compositions of whole shrimp and muscle were measured. There were no significant effects on moisture, crude lipid, and crude protein contents of whole shrimp and muscle between the CON and SNGM groups ($P > 0.05$).

3.3 The immune parameters of hemolymph

At the end of the growth trial, compared to the CON group, the acid phosphatase and alkaline phosphatase activities were significantly increased in the SNGM3 group (Figures 3D, E). The phenol oxidase and alkaline phosphatase activities were significantly increased in the SNGM5 group ($P < 0.05$) (Figures 3B, E). There were no significant differences in hemocyte count, protein carbonyl, and malonaldehyde contents as well as lysozyme and superoxide dismutase activities between the CON and SNGM groups ($P > 0.05$) (Figures 3A, C, F, G, H).

In the challenge experiment, the phenol oxidase, lysozyme, alkaline phosphatase, and superoxide dismutase activities in the SNGM groups were higher than in the CON group ($P < 0.05$) (Figures 3B, C, E, H), and SNGM did not affect the hemocyte count, acid phosphatase activity, protein carbonyl content, and malonaldehyde content ($P > 0.05$) (Figures 3A, D, F, G). Compared with normal-growth groups, *Vibrio* challenge reduced the hemocyte count, and activities of lysozyme, acid phosphatase, and alkaline phosphatase (Figures 3A, C-E).

3.4 The immune parameters and health status of the hepatopancreas

At the end of the growth trial, the hepatopancreas cells in all groups are star-shaped and regularly arranged, but there was an

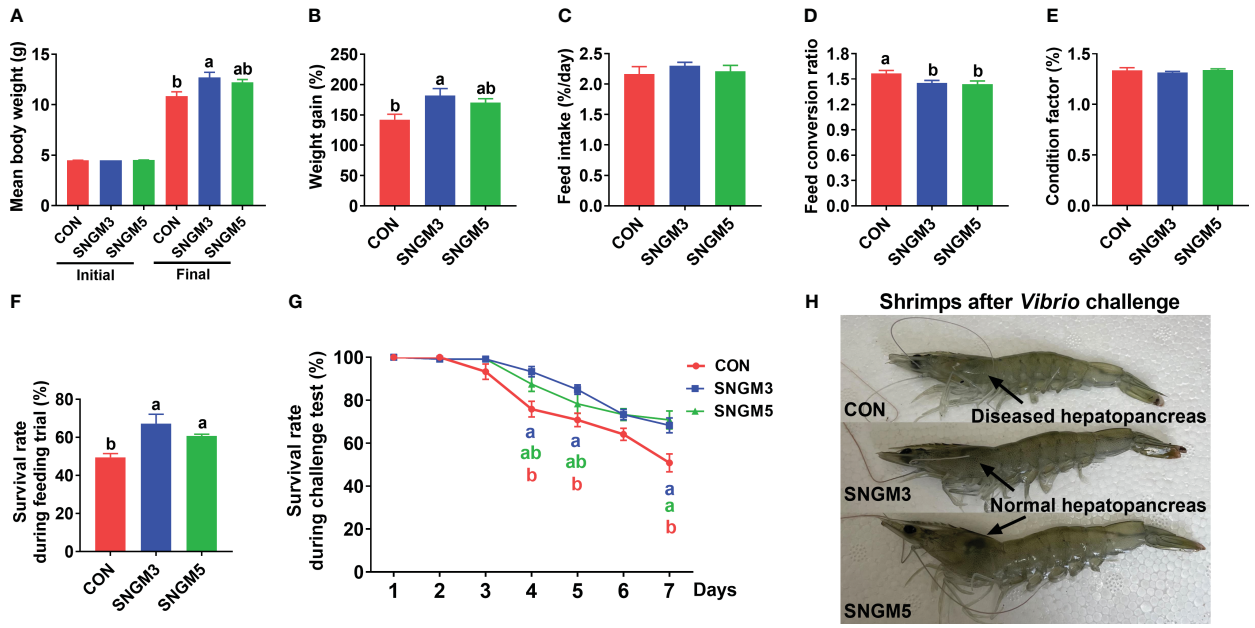

FIGURE 1
Effects of SNGM on growth performance and *Vibrio parahaemolyticus* resistance. **(A)** Initial and final body weight of the shrimp. **(B)** Weight gain. **(C)** Feed intake. **(D)** Feed conversion ratio. **(E)** Condition factor. **(F)** Survival during growth trial. **(G)** Survival during the 7-day challenge test. **(H)** Color of the hepatopancreas and the appearance of the shrimps after the 7-day challenge test. Values are means ± SEM and different lowercase letters indicate significant difference ($P < 0.05$) between groups.

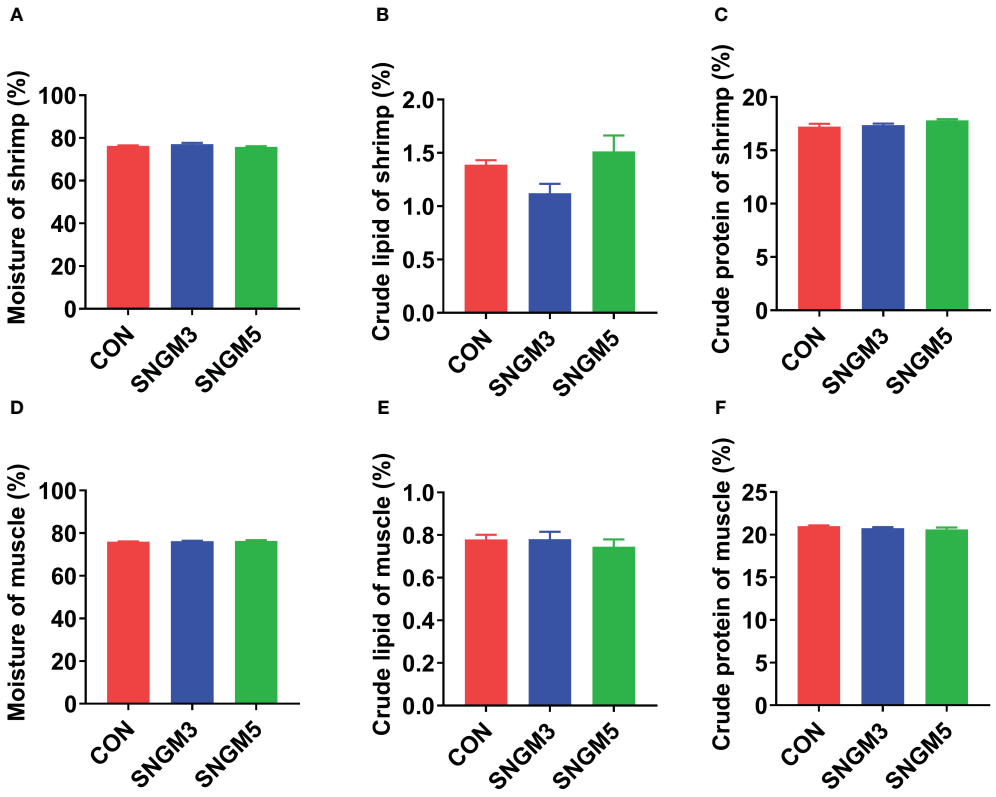

FIGURE 2
Effects of SNGM on the proximate compositions of the whole shrimp and muscle. **(A)** Moisture content of the whole shrimp. **(B)** Crude lipid content of whole shrimp. **(C)** Crude protein content of the whole shrimp. **(D)** Moisture content of the muscle. **(E)** Crude lipid content of the muscle. **(F)** Crude protein content of the muscle. Values are means ± SEM.

increase in histological status in group SNGM5 compared to the control (Figure 4A). After the challenge experiment, the hepatic corpuscles deformed to some extent, the tubule epithelial cells fell off, and the lumen was irregular and atrophied, but the SNGM3 and SNGM5 groups revealed better conditions (Figure 4A). At the growth trial, there were no significant differences in the activity of acid phosphatase, alkaline phosphatase, and superoxide dismutase, respectively, between the CON and SNGM groups ($P > 0.05$) (Figures 4B–D). In the challenge experiment, the SNGM5 group had a higher acid phosphatase activity and a lower superoxide dismutase activity than the CON group ($P < 0.05$) (Figures 4B, D).

3.5 Nutrient levels of the hemolymph and hepatopancreas

At the growth trial, compared with the CON group, the total soluble protein and albumin concentrations in the hemolymph were significantly increased in the SNGM3 group ($P < 0.05$). The SNGM5 group also resulted in an increase in numerical values, but no significant difference was observed ($P > 0.05$) (Figures 5A, B). Compared with the CON group, dietary SNGM significantly increased the hemolymph glucose content in both the growth trial and the challenge experiments ($P < 0.05$) (Figure 5D). In the challenge experiment, compared with the CON group, the SNGM supplementation increased the total soluble protein and albumin concentrations in both hemolymph and hepatopancreas (Figures 5A, E, F), and a significant difference was found in the hemolymph albumin concentration ($P < 0.05$) (Figure 5B). In addition, the SNGM supplementation did not affect the triglyceride content in the hemolymph and hepatopancreas as well as the total cholesterol content in the hepatopancreas ($P > 0.05$) (Figures 5C, G, H).

3.6 The immune parameters and morphology of the intestine

The representative slices of middle intestine histology are shown below. In the growth trial, there were no significant differences in the intestinal morphology among the CON, SNGM3, and SNGM5 groups ($P > 0.05$) (Figure 6A). However, after the challenge experiment, the intestinal folds and epithelial cells of the CON group were damaged, atrophied, and exfoliated, but the SNGM alleviated the adverse effects induced by *Vibrio parahaemolyticus*. In the growth trial, compared to the CON group, the SNGM supplementation reduced the lysozyme activity in the intestine, and significance was found between CON and SNGM3 ($P < 0.05$) (Figure 6D). In the challenge experiment, SNGM5 significantly improved the acid phosphatase and lysozyme

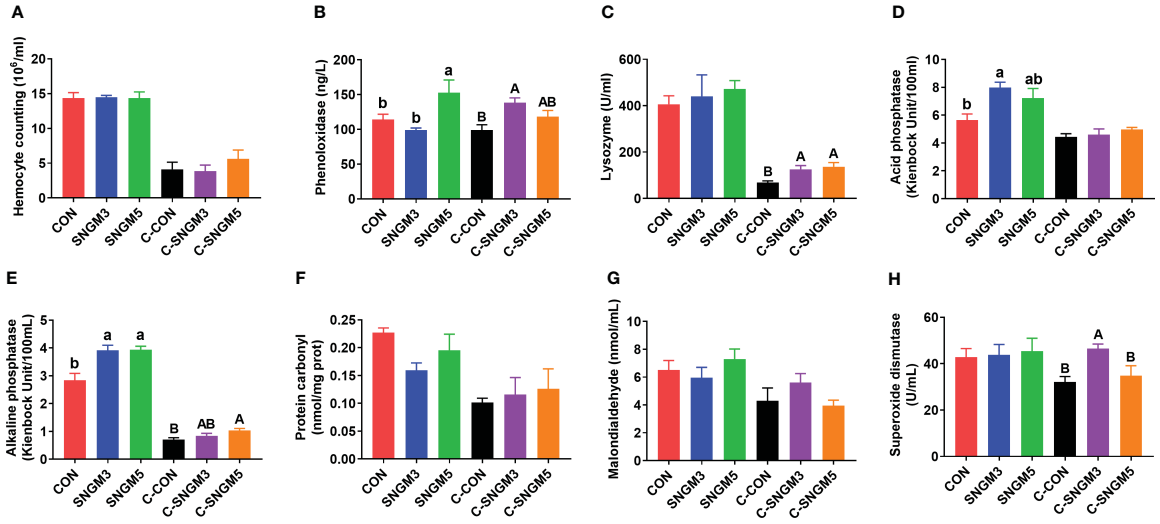

FIGURE 3
Effects of SNGM on the immune parameters of the hemolymph. **(A)** Hemocyte count. **(B)** Phenol oxidase activity. **(C)** Lysozyme activity. **(D)** Acid phosphatase activity. **(E)** Alkaline phosphatase activity. **(F)** Protein carbonyl content. **(G)** Malonaldehyde content. **(H)** Superoxide dismutase activity. Growth experiment groups: CON, SNGM3, and SNGM5. Challenge experiment groups: C-CON, C-SNGM3, and C-SNGM5. Values are means ± SEM. In the growth experiment, values with different lowercase letters are significantly different ($P < 0.05$). In the challenge experiment, values with different capital letters are significantly different ($P < 0.05$).

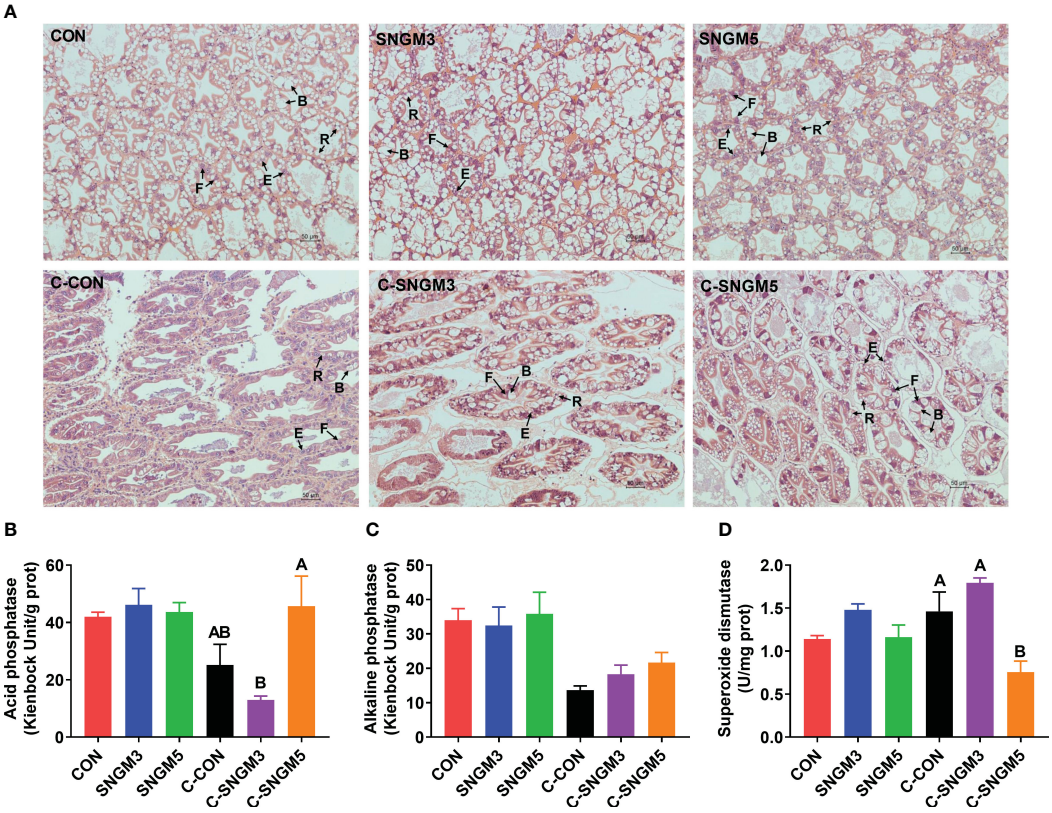

FIGURE 4
Effects of SNGM on the histology and immune parameters of the hepatopancreas. **(A)** Histological analysis (H&E staining) of the hepatopancreas. Black arrows mark the four cell types of tubules, including B ("blasenzellen") cells that typically contain a single, large secretory vesicle, R ("restzellen") cells that usually contain variable-sized lipid vacuoles, F ("fibrillenzellen" or fibrous) cells that contain a large number of ribosomes and a well-developed endoplasmic reticulum, and E ("embryonalzellen" or embryonic) cells that are the main cell types at the tip of the distal hepatopancreatic tubule. **(B)** Acid phosphatase activity. **(C)** Alkaline phosphatase activity. **(D)** Superoxide dismutase activity. Growth experiment groups: CON, SNGM3, and SNGM5. Challenge experiment groups: C-CON, C-SNGM3, and C-SNGM5. Values are means ± SEM. In the challenge experiment, values with different capital letters are significantly different ($P < 0.05$).

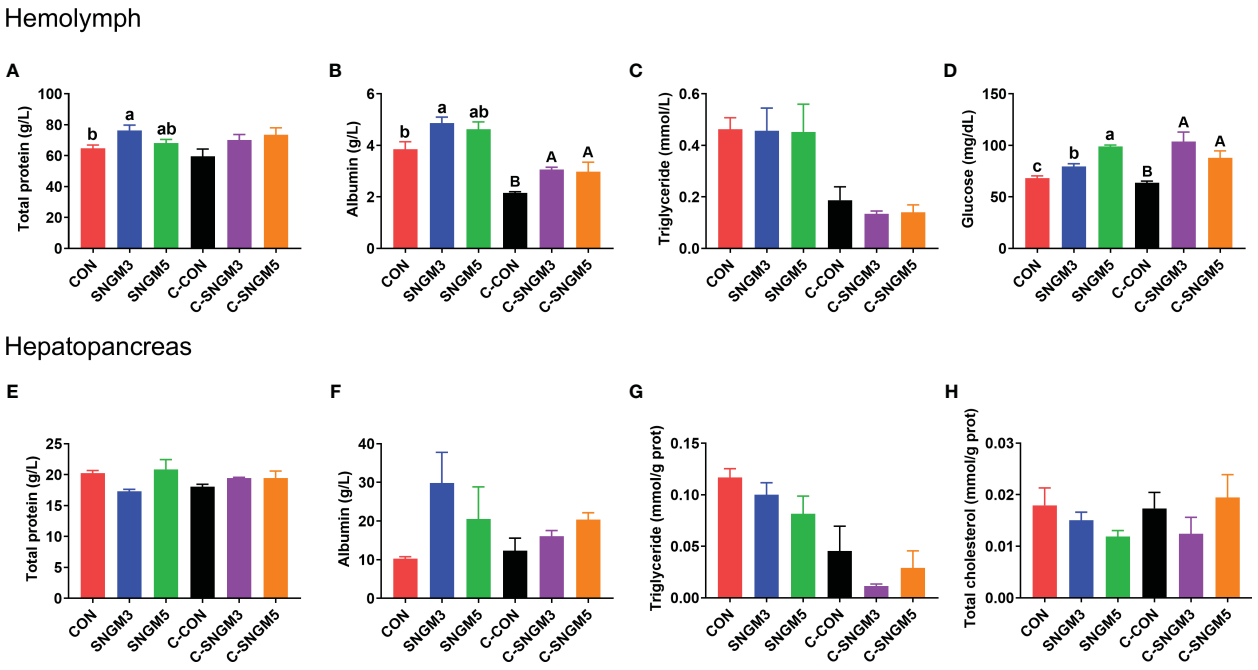

FIGURE 5
Effects of SNGM on nutrient metabolism of the hemolymph and hepatopancreas. **(A)** Total soluble protein content in the hemolymph. **(B)** Albumin content in the hemolymph. **(C)** Triglyceride content in the hemolymph. **(D)** Glucose content in the hemolymph. **(E)** Total soluble protein content in the hepatopancreas. **(F)** Albumin content in the hepatopancreas. **(G)** Triglyceride content in the hepatopancreas. **(H)** Total cholesterol content in the hepatopancreas. Growth experiment groups: CON, SNGM3, and SNGM5. Challenge experiment groups: C-CON, C-SNGM3, and C-SNGM5. Values are means ± SEM. In the growth experiment, values with different lowercase letters are significantly different ($P < 0.05$). In the challenge experiment, values with different capital letters are significantly different ($P < 0.05$).

activities in the intestine ($P < 0.05$) (Figures 6B, D). Besides, the SNGM supplementation did not affect the alkaline phosphatase activity in the intestine (Figure 6C).

3.7 The composition of intestinal microbiota

The percent of community abundance on the phylum level (Figure 7A) showed that Proteobacteria, Bacteroidota, Firmicutes, and Actinobacteria were dominant in the gut of shrimps. At the growth trial, compared with the CON group, the abundance of Proteobacteria and Actinobacteria increased while those of Bacteroidota and Firmicutes decreased in the SNGM3 and SNGM5 groups. Compared with the growth groups, after the challenge experiment, the abundance of Proteobacteria increased, but those of Bacteroidota, Firmicutes, and Actinobacteria all decreased (Figure 7A). There was no significant difference in these parameters among the control, SNGM3, and SNGM5 groups in both the growth trial and the challenge experiments ($P > 0.05$). The PCA analysis suggested that the composition of intestinal microbiota was similar among the CON, SNGM3, and SNGM5 groups in the growth trial, but it was obviously different after the challenge experiment, especially between the C-CON and C-SNGM5 groups (Figure 7B). Compared to C-CON, the C-SNGM5 group showed a shorter distance to the normal growth trial groups, which indicates generally normal intestinal microbiota.

The dominant bacteria genus abundance (top 10) is shown in Figure 7C; Table 2. At the growth trial, there was no difference in the abundance of the 10 bacteria between the CON group and SNGM groups ($P > 0.05$). Compared with the growth trial, the *Vibrio* abundance was increased in all challenge experiment groups. After the challenge experiment, the abundance of *Vibrio*, *Photobacteriuma*, *Pseudoalteromonas*, and *Candidatus_Bacilloplasma*, which belong to pathogenic bacteria, in the C-SNGM3 and C-SNGM5 groups, respectively, was lower compared to the C-CON group, while the abundance of *Shewanella*, which belongs to probiotic bacteria, was increased by SNGM. Compared with the growth trial, the community diversity (Shannon index) in the challenge experiment decreased slightly. In the challenge experiment, the community diversity of SNGM groups was slightly higher compared to the CON group (Figure 7D).

4 Discussion

In recent years, with the development of intensive aquaculture, aquatic animals are more vulnerable to environmental stresses and pathogen infection, which impaired the animal growth, metabolism, antioxidation capacity, and immunity (2, 23, 24). The AHPND outbreak took place firstly in China in 2009 and then spread to Vietnam, Malaysia, Thailand, and Mexico, which caused enormous economic losses (25). Health-promoting additives have been used in animal feeds for decades as antimicrobial and growth promoter. However, few information was available about their combination use

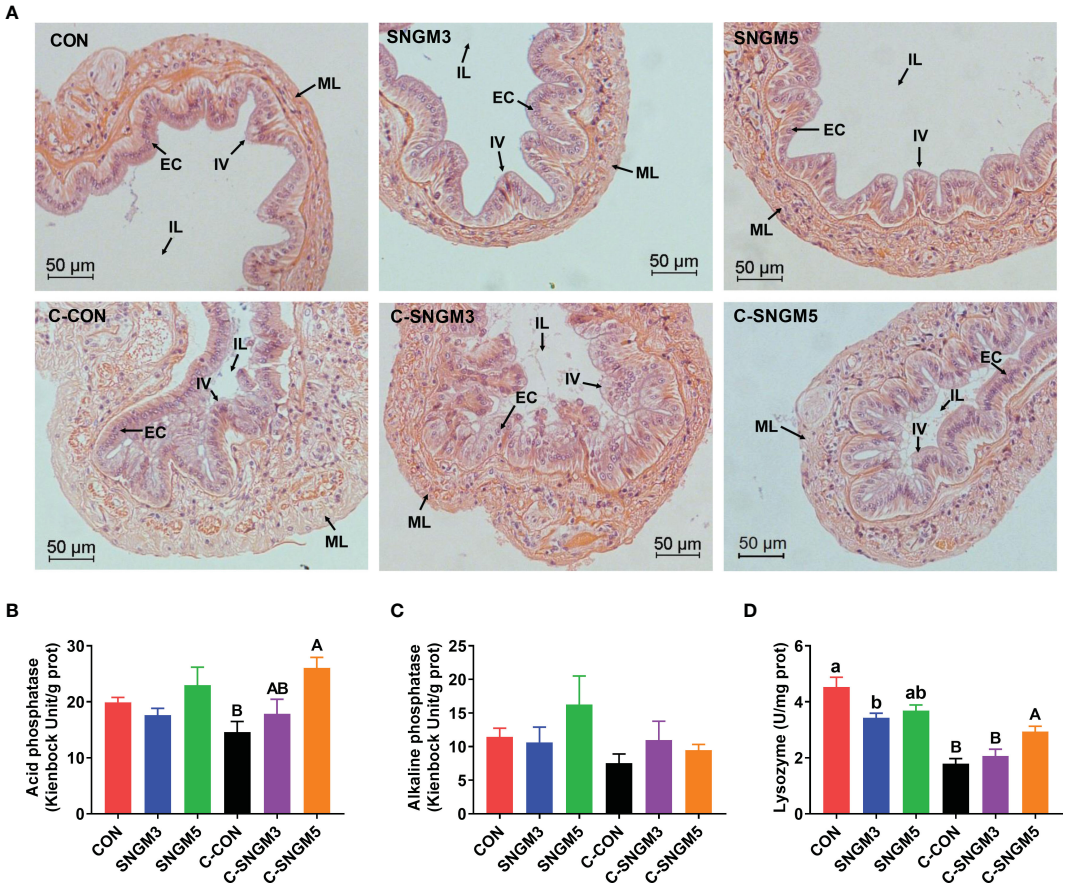

FIGURE 6
Effects of SNGM on the histology and immune parameters of the intestine. **(A)** Histological analysis (H&E staining) of the intestine. Black arrows mark the intestinal villi (IV), epithelial cell (EC), intestinal lumen (IL), and muscle layer (ML) of the intestine. **(B)** Acid phosphatase activity. **(C)** Alkaline phosphatase activity. **(D)** Lysozyme activity. Growth experiment groups: CON, SNGM3, and SNGM5. Challenge experiment groups: C-CON, C-SNGM3, and C-SNGM5. Values are means ± SEM. In the growth experiment, values with different lowercase letters are significantly different ($P < 0.05$). In the challenge experiment, values with different capital letters are significantly different ($P < 0.05$).

in the shrimp farming industry. In the present study, we evaluated the use of SNGM, a commercially available functional feed additive, in Pacific white shrimp diets. Our results showed that dietary SNGM, especially at 3 g/kg feed, promoted growth and resistance to *Vibrio*. After challenge by *Vibrio*, the SNGM also resulted in higher activities of phenol oxidase, lysozyme, alkaline phosphatase, and superoxide dismutase than the CON group. These data all clearly demonstrated that the phytobiotic-based compound additive (Sanacore® GM) could improve the growth, immunity, antioxidant capacity, and resistance to pathogenic bacteria in Pacific white shrimp. Similar results were observed in other previous studies. Plant extracts have been widely used in aquaculture to reduce the dependence on antibiotics and promote the health status of shrimp (12, 26, 27). Pacific white shrimp immersed in the seawater containing 400 or 600 mg/L plant (*Gracilaria tenuistipitata*) extract for 3 h had significantly improved levels of hemocyte count, respiratory burst, lysozyme, phenoloxidase, and superoxide dismutase as well as higher survival after WSSV challenge (28). In black tiger shrimp (*Penaeus monodon*), compared with control diet, feeding diets with methanolic extracts of nine plants at 2.5 mL/kg for 60 days resulted in higher survival during the growth process, specific growth rate, feed efficiency, and survival after *Vibrio harveyi* infection (29). In Pacific white shrimp, oral (10 g/kg feed for 14 days) or intramuscular (50 ug/g body weight for 48 h) administration of galangal extract all significantly increased the relative expression of immune-related genes in the hemocytes and survival after *Vibrio harveyi* infection (30). Organic acids also play beneficial roles by inhibiting intestinal pathogens' growth. Sodium acetate, sodium butyrate, and sodium propionate could inhibit the growth of three *Vibrio* species (*Vibrio harveyi*, *V. alginolyticus*, and *V. anguillarum*) *in vitro* (TCBS agar). Pacific white shrimp diets containing 2% sodium propionate reduced the *Vibrio* species concentration in the intestinal microbiota and increased the feed palatability and apparent digestibility of dry matter and phosphorus (31). Yeast extract is also recognized as immune-stimulant. In juvenile Pacific white shrimp, dietary yeast extract supplementation at 2.0% increased the weight gain, specific growth rate, condition factor, total antioxidant capacity, catalase and glutathione peroxidase activities, and microbiota diversity (Shannon indexes) (32). Yeast extract could replace 45% of the fish meal in Pacific white shrimp diet (containing 25% fish meal) and did not affect weight gain and muscle composition (33). In particular, our results proved that the combination of functional ingredients improved the growth and immunity in Pacific white shrimp.

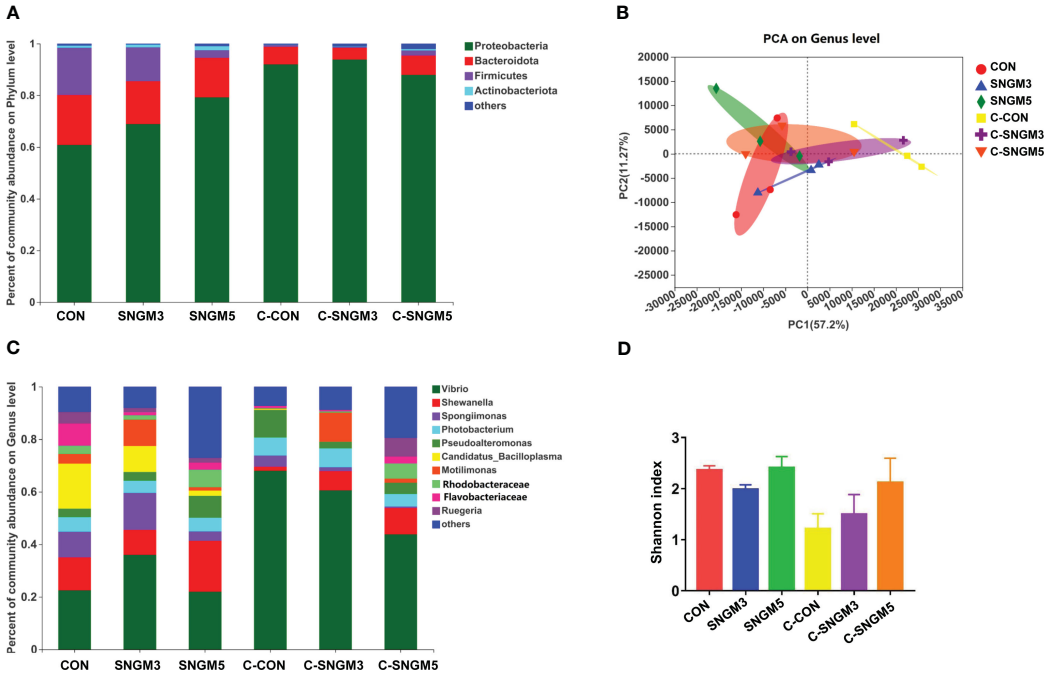

FIGURE 7
Effects of SNGM on intestinal microbiota. **(A)** Percent of community abundance on the phylum level. **(B)** Principal component analysis (PCA) on the genus level. **(C)** Percent of community abundance on genus the level. **(D)** Shannon index on the genus level. Growth experiment groups: CON, SNGM3, and SNGM5. Challenge experiment groups: C-CON, C-SNGM3, and C-SNGM5.

Disease outbreak is a major threat to the sustainable development of shrimp farming. At present, among shrimp pathogens, *Vibrio parahaemolyticus* is the most severe one, which could result in AHPND. This disease, which causes a pale and atrophied hepatopancreas with an empty gastrointestinal tract in shrimp and further causes mortality, has led to a large economic loss in white shrimp farming (2, 34). In the study, SNGM showed promising performance in resistance to *Vibrio parahaemolyticus* infection. In Pacific white shrimp, the histological analysis of AHPND showed that the tubule epithelial cells of hepatopancreas fell off into the tubule lumens (22). Similar results were also found in the challenge experiment of the present study. After challenge by *Vibrio parahaemolyticus*, the hepatic corpuscles deformed to some extent, the tubule epithelial cells fell off, and the lumen was irregular and atrophied, but the use of SNGM alleviated the adverse conditions and increased the total soluble protein and albumin concentrations in the hepatopancreas. This was similar to the previous studies demonstrating the relevant efficacy of individual use of health additives in shrimp and, more broadly, fish (35, 36). These results suggest that SNGM could improve shrimp health by maintaining the morphological structure of both hepatopancreas and intestine. In yellow drum (*Nibea albiflora*), dietary *Bacillus subtilis* B0E9 and *Enterococcus faecalis* AT5 increased the resistance to red-head disease challenged by *Vibrio harveyi* B0003 by improving the liver morphology, serum and skin immunity, and

TABLE 2 Percent of community abundance on genus level (top 10).

Genus level	CON	SNGM3	SNGM5	C-CON	C-SNGM3	C-SNGM5
Vibrio	22.56 ± 4.45	36.88 ± 8.08	26.42 ± 14.21	68.18 ± 8.56	58.42 ± 10.87	44.16 ± 18.19
Shewanella	12.31 ± 3.82	9.25 ± 2.41	17.91 ± 10.68	1.55 ± 0.89	6.86 ± 3.15	9.74 ± 6.59
Photobacterium	5.77 ± 2.30	4.35 ± 2.75	5.34 ± 0.98	6.53 ± 5.76	8.81 ± 8.62	4.66 ± 3.44
Spongiimonas	10.15 ± 4.15	12.98 ± 9.24	3.67 ± 0.73	4.37 ± 2.45	1.57 ± 0.43	0.54 ± 0.28
Pseudoalteromonas	3.02 ± 1.90	3.40 ± 0.82	8.11 ± 5.54	10.5 ± 7.65	2.71 ± 1.16	4.17 ± 2.45
Candidatus_Bacilloplasma	17.4 ± 8.87	9.84 ± 0.39	2.33 ± 0.99	0.29 ± 0.26	0.01 ± 0.01	NA
Motilimonas	3.58 ± 1.61	10.58 ± 7.89	1.14 ± 0.58	0.24 ± 0.10	10.91 ± 10.64	1.62 ± 1.1
Rhodobacteraceae	3.00 ± 0.76	1.65 ± 0.85	5.54 ± 4.17	0.19 ± 0.16	0.45 ± 0.26	5.78 ± 5.28
Flavobacteriaceae	8.02 ± 6.16	1.20 ± 0.56	2.37 ± 1.32	0.74 ± 0.42	0.52 ± 0.32	2.57 ± 1.46
Ruegeria	4.47 ± 1.51	1.69 ± 0.42	1.56 ± 0.73	0.05 ± 0.03	0.28 ± 0.18	7.27 ± 7.23

Feeding experiment groups: CON, SNGM3, and SNGM5. Challenge experiment groups: C-CON, C-SNGM3, and C-SNGM5. Data are mean ± SEM (n = 3).

intestine and skin mucosal microbiota composition (37). There have been few studies investigating the relationship between health additives and gut microbiota after *Vibrio* challenge in shrimp. We found that Proteobacteria, Bacteroidota, Firmicutes, and Actinobacteria were the dominant phyla in the intestine of Pacific white shrimp. In the growth trial, the SNGM addition increased the abundance of Proteobacteria and Actinobacteria but decreased the abundance of Bacteroidota and Firmicutes. The *Vibrio parahaemolyticus* challenge increased the Proteobacteria abundance but reduced the abundance of Bacteroidota, Firmicutes, and Actinobacteria. Meanwhile, the community diversity (Shannon index) was decreased slightly after challenge. A study on Chinese mitten crab (*Eriocheir sinensis*) showed that the hepatopancreas necrosis disease also reduced the abundance of phyla Firmicutes (38). Regulation of intestinal microbiota by plant extracts or organic acids has been reported in limited studies. The addition of bamboo leaf flavonoids (500 and 1,000 mg/kg) in crab diets decreased the Shannon (diversity) and Chao (richness) indexes as well as the phyla Bacteroidota abundance (39). A study on Pacific white shrimp showed that diets supplemented with a mixture of organic acids increased the microbiota diversity and richness in the gut and the abundance of Firmicutes and *Lactobacillus* but reduced the abundance of Proteobacteria (40). In shrimp primary cells, a mixture of organic acids increased the probiotic *Faecalibacterium prausnitzii* content, short-chain fatty acid level in the gut, and resistance to *V. parahaemolyticus* (41).

In the present study, compared with the growth trial, the *Vibrio* abundance was increased in all challenge experiment groups. After the challenge experiment, the SNGM groups had lower *Vibrio*, *Photobacteriuma*, *Pseudoalteromonas*, and *Candidatus_Bacilloplasma* abundance in the gut than the C-CON group, while these had higher *Shewanella* abundance and community diversity than the C-CON group. The PCA analysis also showed that the intestinal microbiota of the C-SNGM5 group showed a shorter distance to the normal growth trial groups than the C-CON group. Previous studies have shown that *Vibrio*, *Photobacteriuma*, *Pseudoalteromonas*, and *Candidatus_Bacilloplasma* are pathogenic bacterium and usually accumulate in the gut of diseased shrimp, but the *Shewanella*, *Chitinibacter*, and *Rhodobacter* abundance is higher in healthy shrimp (42). In shrimp with white feces syndrome (WFS), the intestinal *Paracoccus* and *Lactococcus* abundance and the bacterial diversity were reduced, whereas the abundance of *Candidatus, Bacilloplasma*, and *Phascolarctobacterium* was increased (43). Dietary sulfate-based alginate polysaccharide (2% to 3% for 56 days) improved the intestinal health and *Vibrio parahaemolyticus* resistance by decreasing the *Vibrio*, *Pseudoalteromonas*, and *Candidatus Bacilloplasma* abundance in Pacific white shrimp fed low-fishmeal diets (44). All of these results clearly indicate that the use of SNGM could promote intestinal health by increasing the probiotics level and reducing the level of harmful bacteria.

5 Conclusion

Dietary phytobiotic-based additive at 3-g/kg level significantly increased the growth and survival of Pacific white shrimp after *Vibrio parahaemolyticus* challenge. The immune-related enzyme activities, morphological structure of hepatopancreas and intestine, hepatopancreas metabolism and intestinal microbiota composition were also improved by adding 3–5 g/kg of additive. The results suggest that the suitable dosage of the phytobiotic-based additive (Sanacore® GM) is 3-g/kg feed to promote shrimp growth and disease resistance in practical applications.

Data availability statement

The data presented in the study are deposited in the NCBI repository, accession number PRJNA1055185. Further inquiries can be directed to the corresponding author.

Ethics statement

The animal study was approved by Experimental Animal Care, Ethics and Safety Inspection Committee of the Yellow Sea Fisheries Research Institute, CAFS (IACUC-20220928001). The study was conducted in accordance with the local legislation and institutional requirements.

Author contributions

QM: Conceptualization, Data curation, Formal analysis, Writing – original draft, Writing – review & editing. GZ: Investigation, Methodology, Supervision, Writing – review & editing. JL: Methodology, Software, Writing – review & editing. IC: Validation, Visualization, Writing – review & editing. YW: Data curation, Software, Writing – review & editing. ML: Formal analysis, Funding acquisition, Writing – review & editing. PD: Methodology, Software, Writing – review & editing. WN: Project administration, Supervision, Writing – review & editing. HX: Conceptualization, Methodology, Project administration, Supervision, Writing – review & editing.

Funding

The author(s) declare financial support was received for the research, authorship, and/or publication of this article. This work was supported by the National Key Research and Development Program of China (2022YFD2400205), Central Public-interest Scientific Institution Basal Research Fund, CAFS (2024CG01) and Adisseo Life Science (Shanghai) Co., Ltd. The funders had no role in the study design, data collection and analysis, decision to publish, or preparation of the manuscript.

Acknowledgments

We thank Mei Duan for technical assistance in the study.

Conflict of interest

Authors GZ, I-TC, and WN-O were employed by the company Adisseo Life Science Shanghai Co., Ltd.

The remaining authors declare that the research was conducted in the absence of any commercial or financial relationships that could be construed as a potential conflict of interest.

Publisher's note

References

1. Thillaichidambaram M, Narayanan K, Selvaraj S, Sundararaju S, Muthiah RC, Figge MJ. Isolation and characterization of *Vibrio owensii* from Palk Bay and its infection study against post larvae of *Litopenaeus vannamei*. *Microb Pathogenesis*. (2022) 172:105751. doi: 10.1016/j.micpath.2022.105751

2. Reyes G, Betancourt I, Andrade B, Panchana F, Roman R, Sorroza L, et al. Microbiome of *Penaeus vannamei* larvae and potential biomarkers associated with high and low survival in shrimp hatchery tanks affected by acute hepatopancreatic necrosis disease. *Front Microbiol*. (2022) 13:838640. doi: 10.3389/fmicb.2022.838640

3. Costa RA, Araujo RL, Souza OV, Silva dos Fernandes Vieira RH. Antibiotic-resistant *Vibrios* in farmed shrimp. *BioMed Res Int*. (2015) 2015:505914. doi: 10.1155/2015/505914

4. Li K, Liu L, Zhan J, Scippo ML, Hvidtfeldt K, Liu Y, et al. Sources and fate of antimicrobials in integrated fish-pig and non-integrated tilapia farms. *Sci Total Environ*. (2017) 595:393–9. doi: 10.1016/j.scitotenv.2017.01.124

5. Ahmadifar E, Pourmohammadi Fallah H, Yousefi M, Dawood MAO, Hoseinifar SH, Adineh H, et al. The gene regulatory roles of herbal extracts on the growth, immune system, and reproduction of fish. *Animals*. (2021) 11:2167. doi: 10.3390/ani11082167

6. Zhou S, Dong J, Liu Y, Yang Q, Xu N, Yang Y, et al. Antiparasitic efficacy of herbal extracts and active compound against gyrodactylus kobayashii in. *Carassius Auratus Front Vet Sci*. (2021) 8:665072. doi: 10.3389/fvets.2021.665072

7. Chen Z, Ye SY. Research progress on antiviral constituents in traditional Chinese medicines and their mechanisms of action. *Pharm Biol*. (2022) 60:1063–76. doi: 10.1080/13880209.2022.2074053

8. Cor D, Knez Z, Hrncic MK. Antitumour, antimicrobial, antioxidant and antiacetylcholinesterase effect of ganoderma lucidum terpenoids and polysaccharides: A review. *Molecules*. (2018) 23:649. doi: 10.3390/molecules23030649

9. Ti H. Phytochemical profiles and their anti-inflammatory responses against influenza from traditional Chinese medicine or herbs. *Mini-Rev Med Chem*. (2020) 20:2153–64. doi: 10.2174/1389557520666200807134921

10. Huang HT, Liao ZH, Wu YS, Lin YJ, Kang YS, Nan FH. Effects of Bidens alba and Plectranthus amboinicus dietary supplements on nonspecific immune responses, growth, and resistance to Vibrio alginolyticus in white leg shrimp (*Penaeus vannamei*). *Aquaculture*. (2022) 546:737306. doi: 10.1016/j.aquaculture.2021.737306

11. Balasubramanian G, Sarathi M, Kumar SR, Hameed ASS. Screening the antiviral activity of Indian medicinal plants against white spot syndrome virus in shrimp. *Aquaculture*. (2007) 263:15–9. doi: 10.1016/j.aquaculture.2006.09.037

12. Tadese DA, Song C, Sun C, Liu B, Liu B, Zhou Q, et al. The role of currently used medicinal plants in aquaculture and their action mechanisms: A review. *Rev Aquacult*. (2022) 14:816–47. doi: 10.1111/raq.12626

13. Mine S, Boopathy R. Effect of organic acids on shrimp pathogen. *Vibrio Harveyi Curr Microbiol*. (2011) 63:1–7. doi: 10.1007/s00284-011-9932-2

14. Ng WK, Koh CB, Teoh CY, Romano N. Farm-raised tiger shrimp, *Penaeus monodon*, fed commercial feeds with added organic acids showed enhanced nutrient utilization, immune response and resistance to *Vibrio harveyi* challenge. *Aquaculture*. (2015) 449:69–77. doi: 10.1016/j.aquaculture.2015.02.006

15. Tao Z, Yuan H, Liu M, Liu Q, Zhang S, Liu H, et al. Yeast extract: Characteristics, production, applications and future perspectives. *J Microbiol Biotechn*. (2023) 33:151–66. doi: 10.4014/jmb.2207.07057

16. Biswas G, Korenaga H, Nagamine R, Kono T, Shimokawa H, Itami T, et al. Immune stimulant effects of a nucleotide-rich baker's yeast extract in the kuruma shrimp. *Marsupenaeus Japonicus Aquacult*. (2012) 366:40–5. doi: 10.1016/j.aquaculture.2012.09.001

17. Ma S, Wang X, Gao W, Zhang W, Mai K. Supplementation of yeast extract to practical diet improves the growth, anti-oxidative capacity and intestinal morphology of shrimp *Litopenaeus vannamei*. *J Ocean U China*. (2019) 18:933–38. doi: 10.1007/s11802-019-3970-y

18. Abdel-Tawwab M, Selema TAMA, Abotaleb MM, Khalil RH, Sabry NM, Soliman AM, et al. Effects of a commercial feed additive (Sanacore (R) GM) on immune-antioxidant profile and resistance of gilthead seabream (*Sparus aurata*) against *Vibrio alginolyticus* infection. *Ann Anim Sci*. (2023) 23:185–93. doi: 10.2478/aoas-2022-0053

19. Palenzuela O, Del Pozo R, Piazzon MC, Isern-Subich MM, Ceulemans S, Coutteau P, et al. Effect of a functional feed additive on mitigation of experimentally induced gilthead sea bream *Sparus aurata* enteromyxosis. *Dis Aquat Organ*. (2020) 138:111–20. doi: 10.3354/dao03453

20. Piazzon MC, Naya-Catala F, Pereira GV, Estensoro I, Del Pozo R, Calduch-Giner JA, et al. A novel fish meal-free diet formulation supports proper growth and does not impair intestinal parasite susceptibility in gilthead sea bream (*Sparus aurata*) with a reshape of gut microbiota and tissue-specific gene expression patterns. *Aquaculture*. (2022) 558:738362. doi: 10.1016/j.aquaculture.2022.738362

21. Eissa EH, Elbahnaswy S, El-Baz AH, El-Haroun E, Ashour M, Mansour AT, et al. Effects of dietary commercial phytobiotic "Sanacore (R) GM" on Pacific white shrimp (*Litopenaeus vannamei*) growth, immune response, redux status, intestinal health, and disease resistance against *Fusarium solani*. *Aquacult Int*. (2023) 32:3041–60. doi: 10.1007/s10499-023-01310-5

22. Loc T, Nunan L, Redman RM, Mohney LL, Pantoja CR, Fitzsimmons K, et al. Determination of the infectious nature of the agent of acute hepatopancreatic necrosis syndrome affecting penaeid shrimp. *Dis Aquat Organ*. (2013) 105:45–55. doi: 10.3354/dao02621

23. Bu XY, Li YR, Lai WC, Yao CW, Liu YT, Wang Z, et al. Innovation and development of the aquaculture nutrition research and feed industry in China. *Rev Aquac*. (2023) 16:759–74. doi: 10.1111/raq.12865

24. Cheng W, Chen JC. Effects of pH, temperature and salinity on immune parameters of the freshwater prawn *Macrobrachium rosenbergii*. *Fish Shellfish Immun*. (2000) 10:387–91. doi: 10.1006/fsim.2000.0264

25. Nunan L, Lightner D, Pantoja C, Gomez-Jimenez S. Detection of acute hepatopancreatic necrosis disease (AHPND) in Mexico. *Dis Aquat Organ*. (2014) 111:81–6. doi: 10.3354/dao02776

26. Yin GJ, Jeney G, Racz T, Xu P, Jun M, Jeney Z. Effect of two Chinese herbs (*Astragalus radix* and *Scutellaria radix*) on non-specific immune response of tilapia, Oreochromis niloticus. *Aquaculture*. (2006) 253:39–47. doi: 10.1016/j.aquaculture.2005.06.038

27. Robertsen B. Modulation of the non-specific defence of fish by structurally conserved microbial polymers. *Fish Shellfish Immun*. (1999) 9:269–90. doi: 10.1006/fsim.1998.0186

28. Lin YC, Yeh ST, Li CC, Chen LL, Cheng AC, Chen JC. An immersion of Gracilaria tenuistipitata extract improves the immunity and survival of white shrimp Litopenaeus vannamei challenged with white spot syndrome virus. *Fish Shellfish Immun*. (2011) 31:1239–46. doi: 10.1016/j.fsi.2011.07.021

29. AftabUddin S, Siddique MAM, Romkey SS, Shelton WL. Antibacterial function of herbal extracts on growth, survival and immunoprotection in the black tiger shrimp *Penaeus monodon*. *Fish Shellfish Immun*. (2017) 65:52–8. doi: 10.1016/j.fsi.2017.03.050

30. Chaweepack T, Chaweepack S, Muenthaisong B, Ruangpan L, Nagata K, Kamei K. Effect of galangal (*Alpinia galanga Linn.*) extract on the expression of immune-related genes and *Vibrio harveyi* resistance in Pacific white shrimp (*Litopenaeus vannamei*). *Aquacult Int*. (2015) 23:385–99. doi: 10.1007/s10499-014-9822-2

31. Da Silva BC, Vieira F, Pedreira Mourino JL, Ferreira GS, Seiffert WQ. Salts of organic acids selection by multiple characteristics for marine shrimp nutrition. *Aquaculture*. (2013) 384:104–10. doi: 10.1016/j.aquaculture.2012.12.017

32. Zheng L, Xie S, Zhuang Z, Liu Y, Tian L, Niu J. Effects of yeast and yeast extract on growth performance, antioxidant ability and intestinal microbiota of juvenile Pacific white shrimp (*Litopenaeus vannamei*). *Aquaculture*. (2021) 530:735941. doi: 10.1016/j.aquaculture.2020.735941

33. Zhao L, Wang W, Huang X, Guo T, Wen W, Feng L, et al. The effect of replacement of fish meal by yeast extract on the digestibility, growth and muscle composition of the shrimp. *Litopenaeus Vannamei Aquac Res*. (2017) 48:311–20. doi: 10.1111/are.2017.48.issue-1

34. Lee CT, Chen IT, Yang YT, Ko TP, Huang YT, Huang JY, et al. The opportunistic marine pathogen Vibrio parahaemolyticus becomes virulent by acquiring a plasmid that expresses a deadly toxin. *P Natl Acad Sci USA*. (2015) 112:10798–803. doi: 10.1073/pnas.1503129112

35. Romano N, Koh CB, Ng WK. Dietary microencapsulated organic acids blend enhances growth, phosphorus utilization, immune response, hepatopancreatic integrity and resistance against *Vibrio harveyi* in white shrimp, *Litopenaeus vannamei*. *Aquaculture*. (2015) 435:228–36. doi: 10.1016/j.aquaculture.2014.09.037

36. Song C, Liu B, Xu P, Ge X, Zhang H. Emodin ameliorates metabolic and antioxidant capacity inhibited by dietary oxidized fish oil through PPARs and Nrf2-Keap1 signaling in Wuchang bream (*Megalobrama amblycephala*). *Fish Shellfish Immun*. (2019) 94:842–51. doi: 10.1016/j.fsi.2019.10.001

37. Ding XY, Wei CY, Liu ZY, Yang HL, Han F, Sun YZ. Autochthonous *Bacillus subtilis* and *Enterococcus faecalis* improved liver health, immune response, mucosal microbiota and red-head disease resistance of yellow drum (*Nibea albiflora*). *Fish Shellfish Immun*. (2023) 134:108575. doi: 10.1016/j.fsi.2023.108575

38. Zhan M, Xi C, Gong J, Zhu M, Shui Y, Xu Z, et al. 16S rRNA gene sequencing analysis reveals an imbalance in the intestinal flora of Eriocheir sinensis with hepatopancreatic necrosis disease. *Comp Biochem Phys D*. (2022) 42:100988. doi: 10.1016/j.cbd.2022.100988

39. Zhang R, Shi X, Liu J, Jiang Y, Wu Y, Xu Y, et al. The effects of bamboo leaf flavonoids on growth performance, immunity, antioxidant status, and intestinal microflora of Chinese mitten crabs (*Eriocheir sinensis*). *Anim Feed Sci Tech*. (2022) 288:115297. doi: 10.1016/j.anifeedsci.2022.115297

40. He W, Rahimnejad S, Wang L, Song K, Lu K, Zhang C. Effects of organic acids and essential oils blend on growth, gut microbiota, immune response and disease resistance of Pacific white shrimp (*Litopenaeus vannamei*) against *Vibrio parahaemolyticus*. *Fish Shellfish Immun*. (2017) 70:164–73. doi: 10.1016/j.fsi.2017.09.007

41. Butucel E, Balta I, McCleery D, Marcu A, Stef D, Pet I, et al. The prebiotic effect of an organic acid mixture on faecalibacterium prausnitzii metabolism and its anti-pathogenic role against *Vibrio parahaemolyticus* in Shrimp. *Biology-Basel*. (2023) 12:57. doi: 10.3390/biology12010057

42. Huang Z, Zeng S, Xiong J, Hou D, Zhou R, Xing C, et al. Microecological Koch's postulates reveal that intestinal microbiota dysbiosis contributes to shrimp white feces syndrome. *Microbiome*. (2020) 8:32. doi: 10.1186/s40168-020-00802-3

43. Hou D, Huang Z, Zeng S, Liu J, Wei D, Deng X, et al. Intestinal bacterial signatures of white feces syndrome in shrimp. *Appl Microbiol Biot*. (2018) 102:3701–9. doi: 10.1007/s00253-018-8855-2

44. Chen G, Liu B, Chen J, Liu H, Tan B, Dong X, et al. Supplementing sulfate-Based alginate polysaccharide improves Pacific white shrimp (*Litopenaeus vannamei*) fed fishmeal replacement with cottonseed protein concentrate: Effects on growth, intestinal health, and disease resistance. *Aquacult Nutr*. (2022) 2022:7132362. doi: 10.1155/2022/7132362

frontiers | Frontiers in Immunology

TYPE Original Research
PUBLISHED 21 November 2024
DOI 10.3389/fimmu.2024.1471261

OPEN ACCESS

EDITED BY
Samad Rahimnejad,
University of Murcia, Spain

REVIEWED BY
Byron Morales-Lange,
Norwegian University of Life Sciences, Norway
Sanjay K Gupta,
Indian Institute of Agricultural Biotechnology (ICAR), India
Yafei Duan,
South China Sea Fisheries Research Institute, China

*CORRESPONDENCE
Muhammad A. B. Siddik
m.siddik@deakin.edu.au

RECEIVED 27 July 2024
ACCEPTED 22 October 2024
PUBLISHED 21 November 2024

CITATION
Siddik MAB, Francis P, Foysal MJ and Francis DS (2024) Dietary seaweed extract mitigates oxidative stress in Nile tilapia by modulating inflammatory response and gut microbiota.
Front. Immunol. 15:1471261.
doi: 10.3389/fimmu.2024.1471261

Dietary seaweed extract mitigates oxidative stress in Nile tilapia by modulating inflammatory response and gut microbiota

Muhammad A. B. Siddik[1,2*], Prue Francis[1], Md Javed Foysal[3] and David S. Francis[1]

[1]Nutrition and Seafood Laboratory (NuSea.Lab), School of Life and Environmental Sciences, Deakin University, Queenscliff, VIC, Australia, [2]Department of Fisheries Biology and Genetics, Patuakhali Science and Technology University, Patuakhali, Bangladesh, [3]School of Environmental and Life Sciences, The University of Newcastle, Callaghan, NSW, Australia

Introduction: Extreme water temperature affects the well-being of all aquatic animals, including fish. Higher temperatures can lead to the generation of reactive oxygen species (ROS), which can induce oxidative stress and negatively impact fish health and well-being. This study investigated the protective effects of seaweed extract on growth, antioxidant status, inflammatory responses, and gut microbiota to gain a better understanding of the acclimatization ability of Nile tilapia, *Oreochromis niloticus* in response to oxidative stress caused by high water temperatures.

Methods: Red-seaweed, *Gracilaria tenuistipitata* rich in polyphenols (i.e., total phenolics and flavonoids content) was considered for the preparation of the *Gracilaria* extract (GE) for the study. Nile tilapia were fed the GE supplemented diet along with a control diet for 42 days, followed by 14 days of temperature ramping at a rate of 1°C every two days to the desired target (35°C) and 14 days of holding at 32°C for acclimatation.

Results: Nile tilapia fed the GE had a significantly higher growth performance attributed to increased muscle fiber size compared to control ($p < 0.05$) after the 70 days of feeding trial. Fish fed the GE diet also showed a significantly lower lipid peroxidation by decreased malondialdehyde level when compared to control ($p < 0.05$). Furthermore, GE diet exhibited increased red blood cell counts with the decreased number of cellular and nuclear abnormalities. The gene expression of tight junction (i.e., *occludin, claudin1, ZO-1*) and *nrf2* (antioxidant biomarker) were upregulated, while *hsp70* (related to stress response) was downregulated in fish fed the GE diet. Additionally, GE supplementation led to an increase in bacterial diversity and the abundance of phylum Firmicutes, order *Lactobacillales*, and genera *Sphingobacterium* and *Prevotella* in the distal gut of Nile tilapia, which are mostly considered as beneficial for fish.

Conclusion: The findings suggest that GE has the potential to be used as a dietary supplement to improve health, particularly as a stress-resistant supplement in the diet for Nile tilapia. This study may help make more informed decisions for tailoring the nutrient requirements of fish in the face of climate warming.

KEYWORDS

Gracilaria tenuistipitata*, phenolic and flavonoid compounds, adipocyte tissue, temperature stress, RBC abnormality, tight junction protein, *Oreochromis niloticus

1 Introduction

Climate change has emerged as a serious threat in global aquaculture production, particularly due to changes in temperature patterns around the world (1). Increased water temperatures can result in the generation of reactive oxygen species (ROS), which could increase oxidative stress and negatively impact fish by disrupting their growth, reproduction, and overall wellbeing (2). Elevated water temperature is also known to result in a reduction of dissolved oxygen leading to hypoxia, causing further negative effects in the farmed fish (3). According to Huang et al. (1), every fish species has specific temperature ranges in which they thrive, where slight deviations from these ranges can negatively impact feed intake, growth, reproduction, metabolic activity, energy requirement, and utilization, as well as the overall fitness of ectothermic fish. Furthermore, acute and chronic stress resulting from temperature alterations have been shown to manifest in several metabolic (4), immunological (5), and neuroendocrinological (6) disturbances in fish. To uphold standard physiological performance, the inclusion of functional ingredients to aquafeeds is common place, with investigations into probiotics, prebiotics, functional amino acids, fatty acids, vitamins, and organic acids featured widely in studies evaluating the increase of temperature stress (7, 8). Moreover, the ability of seaweed-supplemented diets to strengthen the fish immune system and increase resilience to stress brought on by temperature has recently attracted the attention of the aquaculture industry.

Nutrient rich red-seaweeds such as *Gracilaria* sp. and *Asparagopsis* sp. have proven health benefits in fish (9, 10). Proteins, peptides, polysaccharides, and polyphenols are among the biologically active components in red-seaweeds, and their supplementation in aquafeeds have been reported to enhance growth, boost immune response, and increase disease resistance in fish (11). Notable polyphenols present in various red-seaweeds include phenolics, flavonoids, and carotenoids (12). These compounds are reported to have antioxidative, anti-inflammatory, and immunostimulatory effects when administered in animal nutrition (13, 14). Antioxidant properties in red-seaweeds help to neutralize harmful free radicals, reducing oxidative stress (15). Lowering oxidative stress may improve fish ability to cope with environmental stressors. For instance, Silva-Brito et al. (11) discovered that incorporating a 2.5% extract of *Gracilaria gracilis* in the diets of gilthead seabream, *Sparus aurata*, enhanced the immune response and reduced cortisol levels when they were subjected to the stress of overcrowding.

Red-seaweeds also contain specific carbohydrates (e.g., agar, agarose, and carrageenans) that can function as prebiotics in promoting host health (16). Prebiotics stimulate the growth of beneficial gut bacteria, which help maintain a healthy gut microbiome, promoting better health and improving disease resistance in fish. For example, Chen et al. (17) investigated the prebiotic effect of polysaccharides (e.g., total sugar, sulfate, and monosaccharides), extracted from red-seaweeds *Grateloupia filicina* and *Eucheuma spinosum*, which enhanced the growth of *Bifidobacterium*. Additionally, Ferreira et al. (18) reported that the inclusion of *G. gracilis* in the diet of European seabass, *Dicentrarchus labrax*, increased the abundance of *Sulfitobacter* and *Methylobacterium*. These bacteria are known to produce short- and medium-chain fatty acids that help reduce intestinal pH, playing a vital role in controlling the growth of pathogenic bacteria in fish (19, 20). In addition to red-seaweed, Zhang et al. (21) reported that dietary supplementation of green-seaweed, *Ulva pertusa*, in the diet of white-spotted rabbitfish, *Siganus canaliculatus*, led to an increase in the abundance of certain Firmicutes bacteria, notably *Ruminococcus*, *Clostridium*, and *Lachnospiraceae*. These bacteria play a key role in breaking down non-starch polysaccharides in the host gut, helping to maintain gut health, strengthen the intestinal barrier, and reduce the risk of intestinal inflammation, especially during times of stress.

The results mentioned above suggest that bioactive substances found in seaweeds have positive effects on immune function, especially in enhancing resilience against different bacterial diseases. Nevertheless, the impacts of seaweed-based diets to mitigate climate-induced stress such as temperature, have not been explored in aquaculture. Nile tilapia, *Oreochromis niloticus*, is one of the most commonly farmed fish across the world (22). Given the sensitivity of aquaculture to the effects of climate change, Nile tilapia could be assessed as a model species due to its higher thermal tolerance and wide distribution (23). A study conducted by Islam et al. (24) found that Nile tilapia had normal growth at 31°C but produce lower growth and physiological imbalance (i.e., erythrocytic cellular abnormalities and nuclear abnormalities)

when cultured at high temperature (34°C). Therefore, the current study aimed to investigate the effects of dietary supplementation with red-seaweed (*Gracilaria* extract) on the potential mitigation of temperature-induced oxidative stress in Nile tilapia reared under high temperature. More precisely, it was examined how supplementing the feed of Nile tilapia with a *Gracilaria* extract containing bioactive compounds (i.e., total phenolic and flavonoid content) can regulate the immunological status and antioxidant response to cope at high temperature.

2 Materials and methods

2.1 Seaweed collection, processing, and experimental diet

Gracilaria tenuistipitata extract was prepared following the protocol described by Thépot et al. (25). The red-seaweed sample was collected in May 2022 from the Sonadia Sea Beach coast (21°29′ N 91°54′E), Moheskhali, Bangladesh [water salinity ~32 ppt, temperature ~26°C] and thoroughly washed with tap water to remove unwanted contaminants (i.e., salt, sediments, sands, invertebrates, and epiphytes). The clean seaweed samples were then kept in a freeze drier at −80°C for 72 h. Once dried, the sample was grounded and sieved (200 µm mesh size) to produce a fine powder that was then vacuum-sealed and stored at −20°C for further processing. The *Gracilaria* extract (GE) was made with 70% methanol in a 1:10 (m:v) ratio under dark conditions about 12 h in each time. The crude extract was filtered (Whatman® no. 2) and then evaporated slowly in a rotary evaporator (IKA® RV3 Eco). Once the methanol had completely evaporated, the extract was then stored at −20°C for use. The various steps involved in making the GE are depicted in Figure 1. A representative amount of GE (triplicated) was dried using a freeze dryer at −80°C. The dried GE was then assessed for its nutrient composition (%) including protein (12.47 ± 1.57), lipid (1.35 ± 0.14), and ash (27.02 ± 1.50) based on a standard protocol (AOAC, 2023). The bioactive compounds, including total phenolic content (TPC) and total flavonoid content (TFC), were determined using the procedure described by Sobuj et al. (26). The results showed a TPC of 63.46 ± 1.77 mg GAE/g (gallic acid equivalents per gram) and a TFC of 29.71 ± 1.09 mg QE/g (quercetin equivalent per gram) using methanol as the solvent. The GE was added to the feed mixture along with all the other ingredients during the water addition step to make dough. Afterward, the dough was pelletized measuring 1.0–3.0 mm using a laboratory pelletizer. The pellets were dried at 50°C for 12 h and stored in airtight polythene bags in a refrigerator at 4°C until used. The feed formulation and chemical composition of the diet are presented in Table 1.

2.2 Fish and feeding trial

Monosex Nile tilapia, *O. niloticus*, fry were purchased from a local fish hatchery (BRAC Fisheries, Khulna, Bangladesh). Nile tilapia fry were placed in eight experimental tanks, each with a 100-L water holding capacity, continuous aeration, and a water temperature of 28° C. They were then acclimatized in tanks for a period of 2 weeks where fish were fed the commercial tilapia diet (Quality Feeds Limited, Bangladesh) twice daily. After 2 weeks of acclimatization, fish were fasted for 24 h, then 200 similar-sized (1.61 ± 0.15 g) fry were randomly assigned into the same eight tanks divided into two dietary groups (four tanks per diet with 25 fish per tank). One quadruplicate group served as a control termed CON, while another group was fed the CON diet added with 1% *Gracilaria* extract (dry weight basis of feed) named GE. The concentration of GE (~1% of feed) was

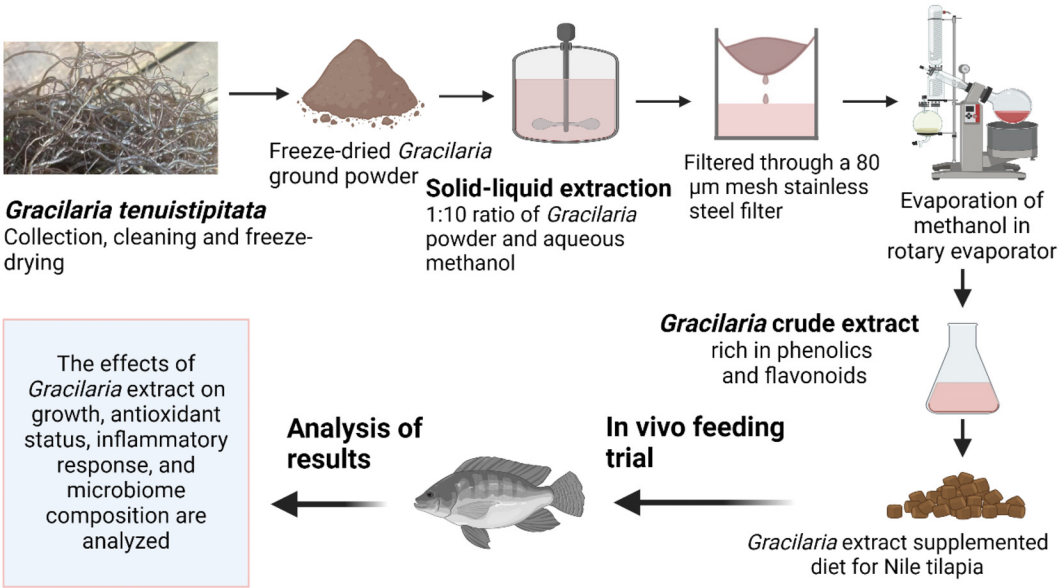

FIGURE 1
Production and utilization of *Gracilaria* extract from red-seaweed, *Gracilaria tenuistipitata*, for Nile tilapia.

10.3389/fimmu.2024.1471261

TABLE 1 Feed ingredients and proximate chemical composition of the basal Nile tilapia diet (% dry weight basis).

Feed ingredients	(%) composition
Fishmeal (anchovy) *	8.0
Soybean meal	32.0
Wheat flour	21.0
Wheat gluten	11.8
Rice bran	15.2
Vegetable oil	2.0
Fish oil	2.0
Starch	5.0
Lysine	0.5
NaCl	0.5
Mineral premix	1.0
Vitamin premix	1.0
Chemical composition (%) as fed basis	
Crude protein	33.16
Crude lipid	6.98
Crude fiber	6.22
Ash	7.75
Gross energy (kj g^{-1})	17.95

*Fishmeal: crude protein 65%, crude lipid 12%, moisture 7%, and ash 14%.

determined based on previous findings (27). The experiment duration was 10 weeks in which fish were kept under ambient temperature conditions (28°C) for the first 6 weeks. In the following 2 weeks, the water temperature was gradually increased by 1°C every 2 days from the initial temperature to 35°C to test the fish ability to withstand temperature changes. Subsequently, it was maintained at 32°C for 2 weeks to acclimatize the fish to a temperature 4°C higher than their original ambient temperature of 28°C. An overview of the experimental time chart is illustrated in Figure 2. Aerators were used in every tank to ensure enough oxygen (>5 mg/L). Fish were fed twice daily, at 08:00 and 16:00 h, until they appeared to be satisfied. The amount of feed delivered and the bulk weight of each replication tank were assessed every 2 weeks to monitor fish performance over time. To keep the water quality favorable for fish, regular siphoning was ensured to take out the unused feed and feces. Every morning, one-third of the tank water was replaced with temperature-controlled reservoir tank water to maintain the desired water temperature for fish.

2.3 Growth, survival, and feed utilization

Following the feeding trial, fish were counted and bulk weighed in each tank. Several performance parameters such as final body weight (FBW), specific growth rate (SGR), feed intake (FI), feed conversion ratio (FCR), hepatosomatic index (HSI), viscerasomatic index (VSI), and survival rate (SR) were calculated using the formula mentioned in an earlier study (28).

2.4 Histology of muscle, liver, and fat tissues

Eight randomly selected fish (two fish per each replicate) from each dietary group were sampled for liver and intraperitoneal fat histology. The collected samples were cleaned with normal saline solution to remove blood and other unwanted substances and were preserved immediately in 10% buffered formalin and stored at 4°C until further processing. The muscle and fat samples were preserved in 70% alcohol at 4°C until histological analysis. Assessment of lipid accumulation in the liver was performed using Oil Red O staining, whereas muscle and intraperitoneal fat samples were stained with hematoxylin and eosin (H&E). The histology was performed based on standard protocol. Briefly, fixed samples were dehydrated by passing through a graded series of alcohol. After dehydration, the samples were molted with wax and kept in cool storage. The samples were then sectioned (5 µm) using a microtome. The sectioned tissues were stained with H&E and observed under a light microscope (Olympus, Germany) at 400× magnification with photos captured with an onboard camera

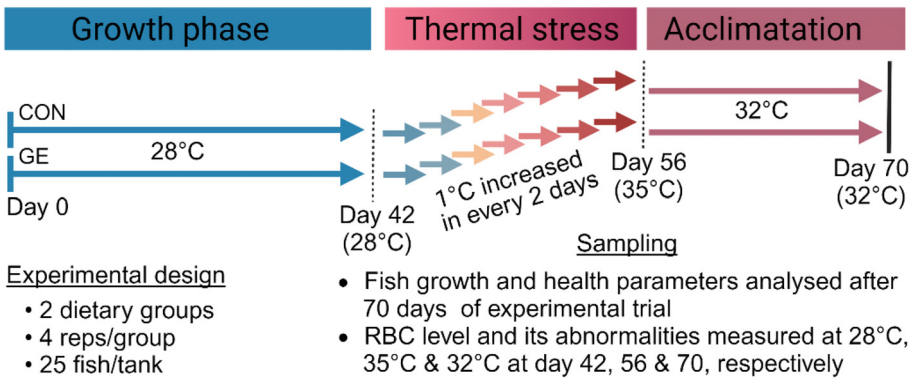

FIGURE 2
An overview of the experimental period chart.

(BX40F4, Olympus, Tokyo, Japan) connected to the microscope. Muscle microstructure such as fiber diameter and density were assessed by nonparametric statistical procedures according to Rowlerson et al. (29). The adipocyte number and diameter were determined from 30 intact cells from each dietary group according to Chaklader et al. (30). All images were captured using a light digital microscope connected to a camera and ImageJ software (version: 1.53). The protocol used to calculate lipid droplet accumulation in the liver was described in Supplementary Figure S1).

2.5 Serum biochemical responses

At the end of the feeding trial, 4 fish from each replicate tank (16 fish/dietary group) were chosen at random, and blood samples were taken by puncturing the caudal vein and kept in non-heparinized tubes, left to settle for 6 h, and then centrifuged at 4°C for 10 min to extract serum that was kept at −20°C. The lysozyme activity of serum was analyzed following Siddik et al. (31). The levels of aspartate aminotransferase (AST), alanine transaminase (ALT), cholesterol, triglycerides, and glycogen were analyzed by an automated blood analyzer (SLIM; SEAC Inc., Florence, Italy) following Blanc et al. (32).

2.6 Antioxidant response

Fish that were being considered for blood collection were dissected to obtain liver tissue for measuring the antioxidant response. The activities of antioxidant enzymes including malondialdehyde (MDA), superoxide dismutase (SOD), and catalase (CAT) were assessed using commercial kits from ZellBio GmbH, Lonsee, Germany.

2.7 Real-time quantitative PCR

Total RNA from frozen hind gut samples of GE and control-fed fish was isolated using RNeasy Mini Plus Kit (Qiagen, Hilden, Germany) following the manufacturer's instructions. The quality and quantity of the RNA were evaluated through agarose gel electrophoresis and spectrophotometry (NanoDrop® ND-2000), respectively. cDNA synthesis was performed using a PrimeScript™ RT reagent kit (Takara, Japan). The real-time quantitative PCR (RT-qPCR) primers used in this study for Nile tilapia are listed in Table 2. The melting curve of the amplicon from the primers was obtained using uMELT software. Gene expression levels were measured by RT-qPCR with PowerUp™ SYBR Green Master Mix (Thermo Scientific, USA) on the 7500 Real-Time PCR System (Applied Biosystems, USA). The following conditions were used for real-time PCR: initial denaturation for 2 min at 95°C, followed by 40 cycles of amplification stating 30 s denaturation at 95°C, annealing for 1 min at 60°C, and extension at 72°C for 30 s. The melting stage in PCR began with the 95°C heating step for 15 s and cycled to 70°C cooling for 1 minute, with the continuous increase of 0.015°C per second. The analysis of RT-qPCR data for relative gene expression levels was normalized to the β-actin content in each sample and quantified using the $2^{-\Delta\Delta Ct}$ method as outlined by Livak and Schmittgen (33).

2.8 Blood RBC level and cellular and nuclear abnormalities

Blood red blood cell (RBC) level and its cellular and nuclear abnormalities in fish were measured in Nile tilapia at three different temperatures across the feeding trial in D42 (pre-temperature stress at 28°C), D56 (post-temperature stress at 35°C), and D70 (post-temperature adaptation at 32°C). Two fish from each replicate tank were selected for blood sampling and euthanized after recording their weights for biomass calculations. RBC counts were determined using a hemocytometer. The blood smear slides were prepared immediately after collecting the blood. The blood was spread along the edge of the slide and tilted at a 45° angle to create a thin, even smear. After air-drying for 5 min, the smear was fixed in methanol for approximately 2 min. Once dry and fixed, it was stained with a 5% Giemsa solution. The slides were then air-dried overnight and mounted with dibutylphthalate polystyrene xylene (DPX). The samples were examined under an optical microscope (G-206, Italy) using a 100× objective lens to assess RBC cellular and nuclear abnormalities. RBC cellular abnormalities were categorized as elongated (significantly longer than wider), fusion (joining of more than two cells to create a larger mass), and twin (two cells connected by their surfaces). RBC nuclear abnormalities consisted of micronucleus (circular chromatin bodies resembling the central nucleus), nuclear bridge (a strip of nuclear material connecting two nuclei within separate erythrocytes or within a single erythrocyte), and nuclear degeneration (nuclear condensation and extrusion leading to the creation of a pyrenocyte structure, which is subsequently engulfed and broken down by macrophages).

2.9 Amplicon sequencing

Eight fish from each dietary treatment were randomly selected to obtain hind gut samples, following appropriate biosafety measures. The gut samples, which included mucosa and digesta, were homogenized using a TissueLyser II (Qiagen, Hilden, Germany). Genomic DNA extraction was then carried out using the DNeasy PowerSoil Pro Kit (Qiagen, Hilden, Germany) following the instructions provided by the manufacturer. The DNA was quantified using a NanoDrop 2000c (Thermo Fisher Scientific, USA), and its quality was assessed by running it on a 1% agarose gel. To prepare the final master mix, 50 µL of Hot Start 2× Master mix (New England BioLabs Inc., USA), as per the manufacturer's instructions, was combined with 2 µL of template DNA, 1 µL each of V3V4 primers (10 µM) with Illumina overhang adapter, and 21 µL of nuclease-free treated water. The mixture was then subjected to 35 cycles of amplification using a BioRad S1000 Thermal Cycler (BioRad Laboratories Inc., USA). Positive

TABLE 2 The list of primer sequences utilized for RT-qPCR analysis.

Target genes	Primer sequences (5′ −3′) (F: Forward, R: Reverse)	Target size (bp)	Annealing temp. (°C)	Efficiency (%)	Reference
il-1β	F: GACAGCCAAAAGAGGAGC R: TCTCAGCGATGGGTGTAG	95	61	99.66	KF747686.1
tnf-α	F: CCAGAAGCACTAAAGGCGAAGA R: CCTTGGCTTTGCTGCTGATC	119	59	87.63	AY428948.1
ZO-1	F: CCGCAGATCAGTCCCTCTTC R: GTACGGAGTTAGCATCGCCA	134	67	88.45	XM_013270540
occludin	F: GGAGGAAAGCCGCAGTGTTCAG R: GTCGTAGGCATCGTCATTGTAGGA	109	62	89.45	XM_025899615.1
claudin1	F: GTCTGTTTCTGGGCGTGGTGTC R: ACTCCGACTGACTCCTCATCTTCC	135	60	88.61	XM_019367708.2
nrf2	F: CTGCCGTAAACGCAAGATGG R: ATCCGTTGACTGCTGAAGGG	40	62	92.38	XM_003447296.
hsp70	F: TGGAGTCCTACGCCTTCAACA R: CAGGTAGCACCAGTGGGCAT	85	59	94.17	FJ213839.1
β-actin	F: AGCAAGCAGGAGTACGATGAG R: TGTGTGGTGTGTGGTTGTTTTG	143	60	95.31	KJ126772.1

amplicons were purified using AMPure beads and indexed according to the Illumina 16S Sequencing Library Preparation protocol (Part # 15044223 Rev. B). Finally, the equimolar amplicons were pooled and sequenced on an Illumina MiSeq platform (Illumina Inc., San Diego, California, USA) using the paired-end, v3 kit with 600 cycles.

2.10 Processing of Illumina data

Paired-end amplicon sequence data (gz format) were imported in qiime2 (v2021.11) for further processing. The denoising of reads was performed using DADA2 followed by trimming of demultiplexed reads with parameters such as -p-trim-left-f l0; -p-trunc-len-f 260; -p-trim-left-r 10; -p-trunc-len-r 220. Chimeric sequences with >0.05% error rates were removed and non-chimeric reads (82%) indicating biological features were tabulated for feature frequency amplicon sequence variants (ASVs). The lowest non-zero frequency of 10 was set to filter the feature ASV table. Phylogenetic classification of ASVs into different taxa levels was performed using the qiime2 "classify consensus- blast" plug-in against SILVA 138 release (34). The feature table collapsed with taxonomy and subsequently removed mitochondrial and chloroplast sequences (<1% of reads). There were variations in *Clostridium* classification, and as a result, these variations were classified as "*Clostridium* sensu stricto 1-9" throughout the dataset. To make a homogeneous dataset for *Clostridium*, we renamed all "*Clostridium* sensu stricto 1-9" as "*Clostridium*", and other non-classified reads into the "Unclassified" bacterial group. The final set of data was normalized (also called "rarefaction") at an even depth of 15,236 for bacterial community analysis. Metagenome prediction of functional features from 16S rRNA data was performed with the PICRUSt2 pipeline (35).

2.11 Diversity and composition analysis

The ASV table, taxonomy, and metadata files were imported into R software (v4.22) for diversity and composition analysis (36). The number of shared and unique taxa were calculated using the MicEco package (37). Species richness (observed), Chao1, Shannon, and Simpson diversity were considered for alpha-diversity measurements. Beta-diversity was performed as a UniFrac distance metric (Unweighted and Weighted) and PERMANOVA was conducted for the visualization of feeding effects on beta-dispersion with 1,000 permutations using vegan and phyloseq (38) R packages. The distance between samples for a group was calculated as the "Bray–Curtis " distance. We considered 1% taxa abundance per sample as a threshold for composition analysis at the phylum and genus level (39). Further analysis of differential abundance between groups was performed as Linear Discriminant Analysis (LDA) using the MicrobiomeMarker R package (40). An LDA cutoff value of 2.0 and a p-value of <0.05 were considered as statistically significant for compositional difference analysis.

2.12 Statistical analysis

Data were assessed for normality using the Shapiro–Wilk test and then analyzed with two-tailed Student's t-tests and two-way analysis of variance (ANOVA). Two-tailed Student's t-tests were applied to compare the effects of GE diet to control. The total RBC count, along with its cellular and nuclear abnormalities, was analyzed using two-way ANOVA. Additionally, alpha-diversity, beta-diversity, and compositional log-fold changes between the two dietary groups in microbiome composition were analyzed using two-tailed t-tests. Gut microbiome analysis was carried out using the R software. A p-value of <0.05, <0.01, and <0.001were

considered statistically significant between the two dietary groups of GE and CON.

3 Results

3.1 Growth performances, feed utilization, and muscle health

Nile tilapia fed the GE diet showed a significant improvement in growth performance and feed utilization compared to the CON (Figures 3A–E, $p < 0.05$). However, the somatic indices such as hepatosomatic index and viscerasomatic index were not influenced by the GE supplementation (Figures 3F, G, $p > 0.05$). Additionally, there was no significant difference in the survival rate between the two dietary groups (Figure 3H). The higher growth performance was supported by the enhanced dorsal muscle fiber diameter in fish fed the GE diet (Figures 3I–K).

3.2 Liver health and adipocyte distribution

Hepatic lipid droplets significantly reduced in the GE-fed fish compared to the control, while liver weight exhibited no significant difference between the dietary groups (Figures 4A–C). Likewise, the hepatic enzymes AST and ALT were lower in GE-fed fish compared

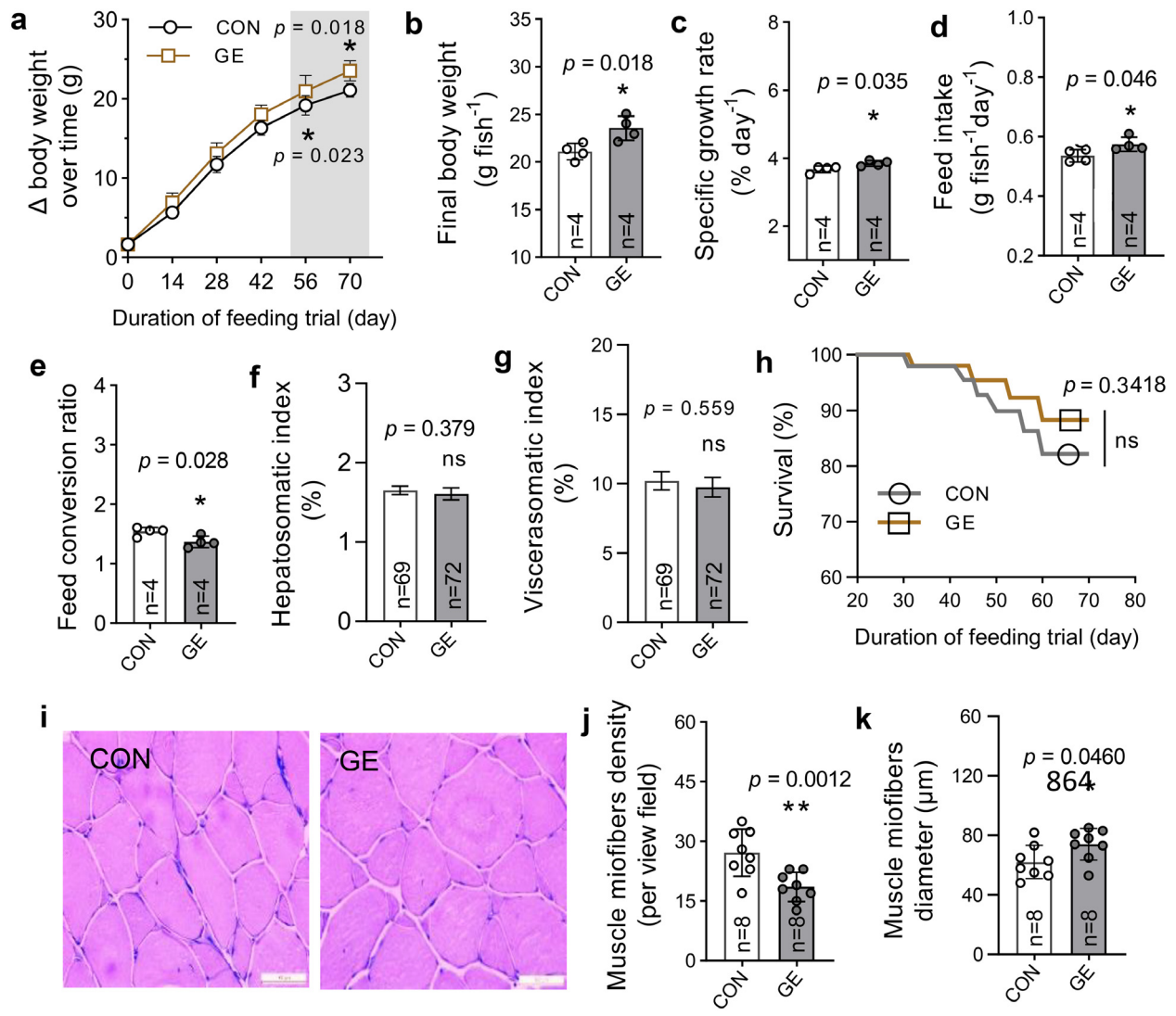

FIGURE 3
Growth and muscle health of Nile tilapia fed *Gracilaria tenuistipitata* extract for 70 days. **(A–H)** Growth performance, feed utilization, somatic indices, and survival of fish. **(I)** Transverse section of dorsal muscle microstructure (×200, H&E). **(J, K)** The myofiber development in fish in terms of fiber diameter and density. The data are presented as mean ± SD. Asterisks * and ** above the bars indicate significant differences between the two dietary groups of GE and CON, as determined by an unpaired *t*-test at $p < 0$ <.05 and $p < 0.01$, respectively. ns, non-significant; GE, *Gracilaria* extract; CON, control.

10.3389/fimmu.2024.1471261

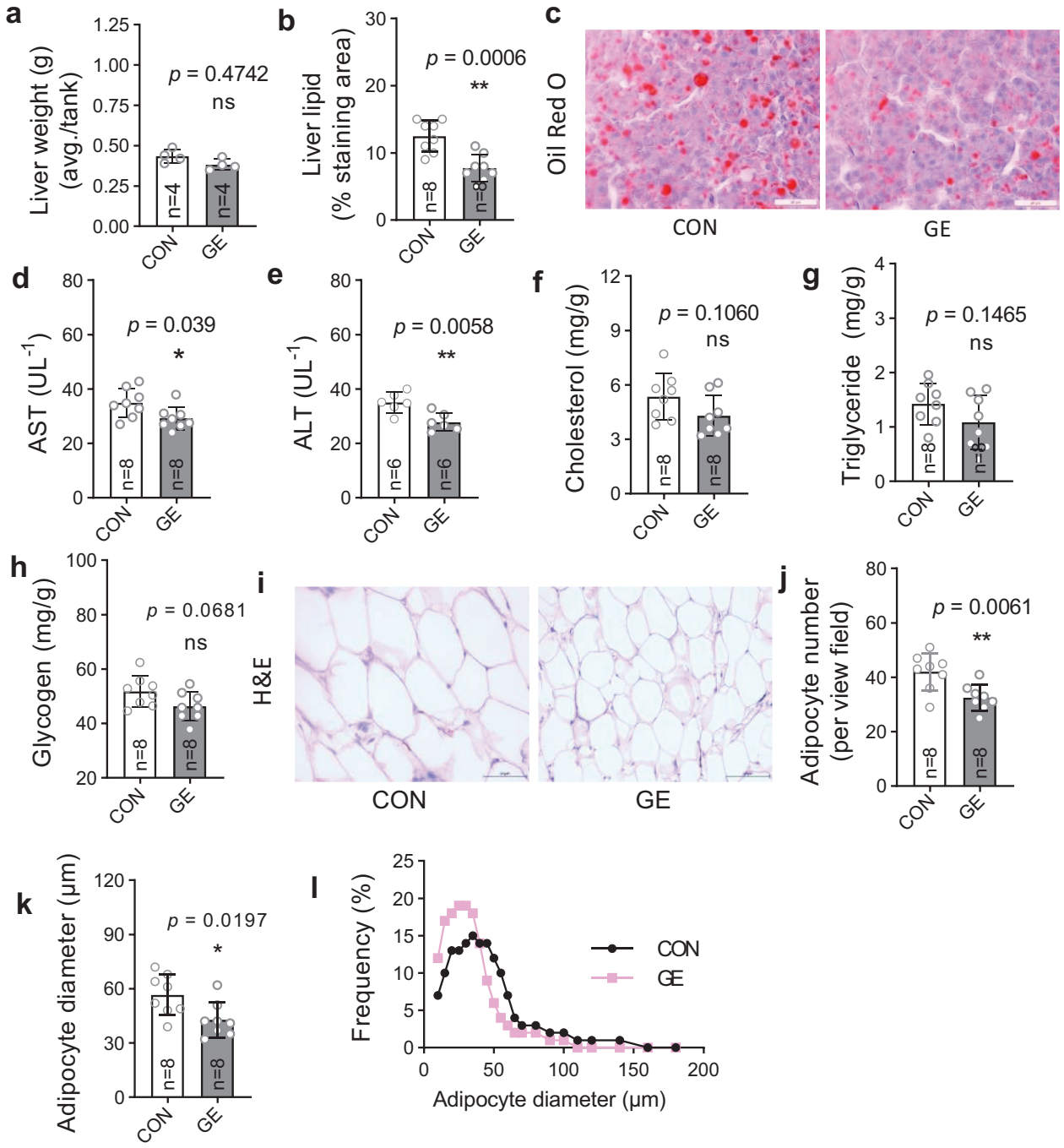

FIGURE 4
Liver health and intraperitoneal fat distribution in Nile tilapia fed *Gracilaria tenuistipitata* extract in varying water temperatures for 70 days. **(A, B)** Liver weight and quantification of lipid droplet area in liver of Nile tilapia. **(C)** Representative Oil Red O-stained liver histology showing lipid droplets (n = 8, magnification 50×). **(D-H)** Quantification of serum AST, ALT, cholesterol, triglyceride, and glycogen levels as liver health indicator. **(I)** Histomorphometry of intestinal adipocytes (n = 8, 10 fields per section, magnification 50×, H&E). **(J–L)** Quantitative image analysis for adipocyte distribution in terms of average adipocyte numbers, diameter (µm), and frequency (%). Data are the mean ± SD (standard deviation). An unpaired t-test is used to compare the results from GE-fed fish to control at $^{*}p < 0.05$ and $^{**}p < 0.01$. ns, non-significant; GE, *Gracilaria* extract; CON, control.

to control-fed fish, whereas cholesterol, triglyceride, and glycogen levels were not affected by seaweed supplementation (Figures 4D–H). Adipocyte numbers and fatty tissue diameter in fish fed the control diet were significantly decreased in comparison to fish fed the control diet (Figures 4I–K). The frequency of adipocyte diameter increased in GE-fed fish up to 50 µm, while adipocytes in fish fed the CON diet were greater in diameter (>50 to 200 µm) (Figure 4L).

3.3 Antioxidant status, immunity, and gene expression

The level of MDA significantly reduced in fish fed the GE-supplemented diet while CAT and SOD levels exhibited no difference between the two dietary groups (Figures 5A–C, $p < 0.05$). The lysozyme activity was enhanced in the GE group

10.3389/fimmu.2024.1471261

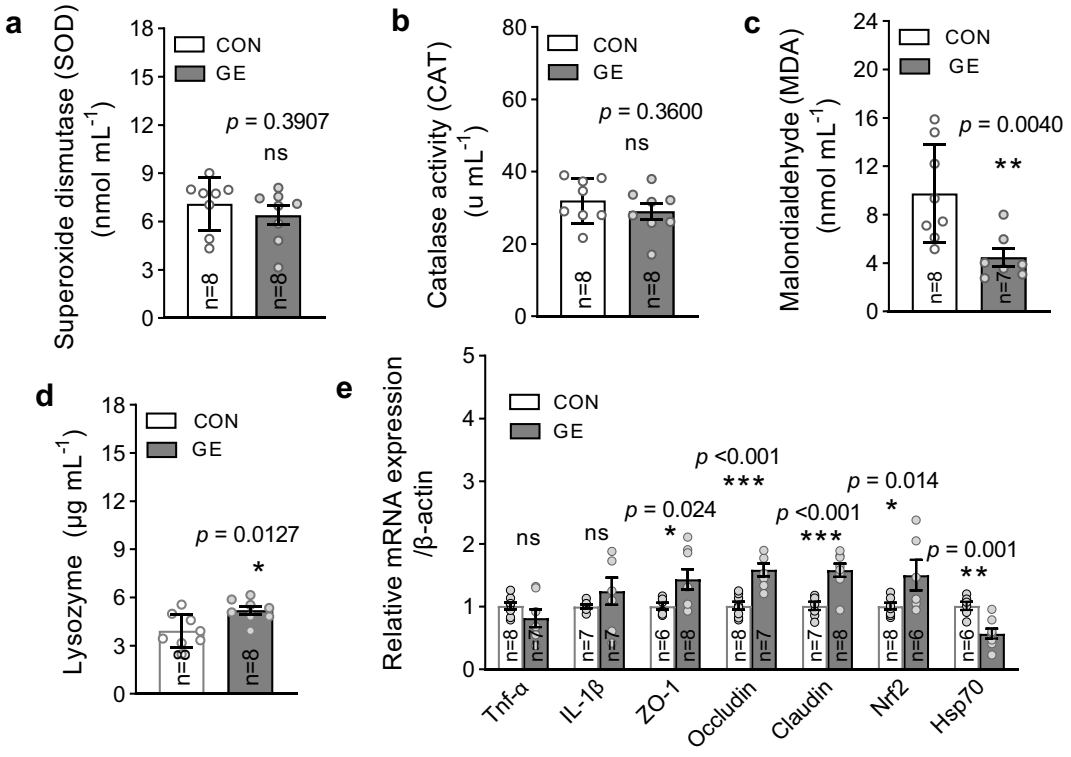

FIGURE 5
Antioxidant enzymes, lysozyme activity, and mRNA expression of Nile tilapia fed a diet supplemented with *Gracilaria tenuistipitata* extract in varying water temperatures for 70 days. **(A–C)** Quantification of oxidative stress through MDA, SOD, and CAT activities in fish liver after 10 weeks of feeding trial. **(D)** Immune response in terms of lysozyme activity in blood serum. **(E)** The relative quantification of mRNA expression of pro-inflammatory cytokines (*tnf-α* and *il-1β*), antioxidant gene (*nrf2*), tight junction genes (*ZO-1*, *occludin*, and *claudin1*), and heat shock protein 70 (*hsp70*) in the hind gut of fish. The data are presented as mean ± SD. Asterisks (*, **, and ***) indicate significant differences between the two dietary groups, control, and GE (*Gracilaria* extract), as determined by an unpaired *t*-test at $p < 0 < .05$, $p < 0 < .01$, and $p < 0 < .001$, respectively. ns, non-significant; GE, *Gracilaria* extract; CON, control.

compared to the CON group (Figure 5D). Dietary GE supplementation significantly upregulated the expression of tight junction proteins (*occludin*, *claudin1*, and *ZO-1*) and the antioxidant gene, *nrf2*, while a downregulation of *hsp70* was observed in the GE group compared to the CON group. The pro-inflammatory cytokines *tnf-α* and *il-1β* were found unaffected by seaweed supplementation (Figure 5E, $p > 0.05$).

3.4 Blood RBC level and cellular and nuclear abnormalities in response to temperature stress

RBC count and cellular and nuclear abnormalities were found significantly different by both the dietary groups and temperatures (Figure 6, $p < 0.05$). Fish fed the GE-supplemented diet significantly enhanced the RBC level when compared to the control. Likewise, the total frequencies of RBC cellular and nuclear abnormalities were found significantly lowered in the control group when compared to the control. However, fish at 35°C post-temperature stress produced more cellular and nuclear abnormalities compared to pre-temperature stress and post- temperature adaptation at 28°C and 32°C, respectively.

3.5 Sequence statistics and diversity of gut microbiota

A total of 322, 761-bp quality reads were obtained after trimming, with an average of 20,172.6 ± 941.7 and ranging from 16,860 to 30,244 bp that were classified into 1,503 ASVs, six phyla, and 455 genera. The average good's coverage index value of 0.998 and plateaued rarefaction curve were observed, indicating adequate depth and saturation level of all study sequences (Figure 7A, Supplementary Figure S2). Only 63 ASVs were shared between CON and GE diet groups while the latter generated 548 additional unique ASVs compared to 218 in CON (Figure 7B). Consistent with ASVs, species diversity (observed ASVs and Chao index) and Shannon and Simpson diversities reflecting richness and evenness of top abundant taxa were significantly higher in the GE group, compared to CON (Figure 7C). Distinct bacterial communities in terms of bacterial presence–absence and relative abundance were observed between CON and GE diet groups in the beta ordination PCoA plot. Significant *R* and *p*-values in PERMANOVA indicate the influence of dietary GE in the gut bacterial diversity in terms of shifting in relative abundance of top abundant taxa and augmenting rare bacterial communities compared to the CON group (Figures 7D, E). The Bray–Curtis distance showed more balance variation in abundance for bacterial communities in the GE diet compared to CON feed (Figure 7F).

10.3389/fimmu.2024.1471261

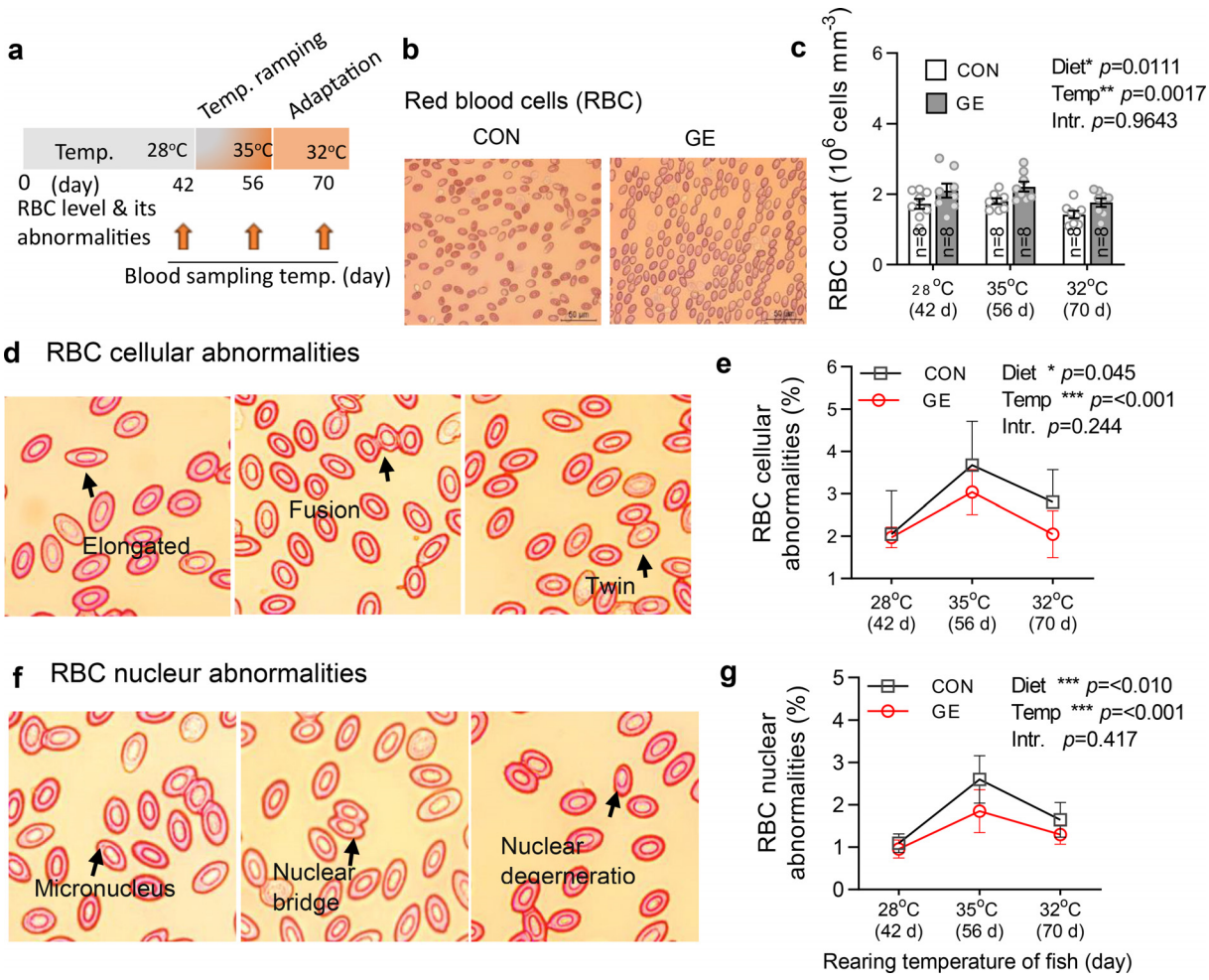

FIGURE 6
Effects of *Gracilaria* extract (GE)-supplemented diet on blood RBC level and its cellular and nuclear abnormalities in Nile tilapia in varying temperatures of 28°C, 35°C, and 32°C at days 42, 56, and 70, respectively. **(A)** Timeline of blood sampling at various temperatures during the feeding trial. **(B, C)** RBC level and its cellular and nuclear abnormalities in fish at 42 days (pre-temperature stress at 28°C), 56 days (post-temperature stress at 35°C), and 70 days (adaptation at 32°C). **(D, E)** representative H&E-stained blood histology showing RBC cellular abnormalities (elongated, fusion, and twin) and their quantification in GE and CON fed fish. **(F, G)** RBC nuclear abnormalities (micronucleus, nuclear bridge, and nuclear degeneration) and their quantification in fish fed GE and CON. Data are presented as mean ± SD. Asterisks (*, **, and ***) indicate significant differences between dietary groups and temperatures, determined by two-way ANOVA at $p < 0.05$, $p < 0.01$, and $p < 0.001$, respectively. GE, *Gracilaria* extract; CON, control; Temp, temperature; Intr, interaction.

3.6 Gut microbial composition

At the phylum level, Proteobacteria represented approximately half of the classified reads (45%) in both groups —37.8% in CON and 53.8% in GE, while Fusobacteriota (28%) and Actinobacteria (28.7%) composed 56.7% of reads in the CON diet. Firmicutes (13.8%) had a higher abundance than Fusobacteria (14.8%) and Actinobacteria (12.7%) in the fish gut-fed GE diet. Firmicutes abundance was only 2.6% in the CON diet, indicating the influential impact of GE diet on this phylum. Alongside Firmicutes and Bacteroidota, abundance also increased from <0.5% in CON to 3.8% in the GE diet (Figure 8A). At the genus level, *Aeromicrobium*, *Escherichia-Shigella*, and *Cetobacterium* comprised 84.6% of the total reads in fish fed the CON diet while *Pseudomonas* (32.3%) was the most abundant bacterial group in fish fed the GE diet, followed by *Escherichia-Shigella* (14.5%), *Cetobacterium* (13.3%), *Aeromicrobium* (4.9%), *Cutibacterium* (3.6%), and *Sphingobacterium* (2.2%) (Figure 8B). Dietary GE provision significantly promoted the abundance of Bacteroidota, Campilobactorota, Desulfobacterota, and Firmicutes at the phylum level compared to Nitrospirota in the CON diet (Figure 9A). At the order and genus level, *Sphingobacterium*, *Prevotella*, *Lactobacilliles*, *Lactobacillus*, *Roseburia*, *Bifidobacterium*, and *Ruminococcus* showed significantly higher abundance in the GE diet compared to *Rhodopirellula* and *Rhizobiales* in CON (Figure 9B, Supplementary Figure S3). The GE diet also increased abundance for some opportunistic pathogens including *Streptococcus*, *Staphylococcus*, and *Corynebacterium* (Figure 9C). A shift in bacterial abundance in the gut also modulates metabolic pathways in the dietary GE group, specifically amino acid biosynthesis and metabolism compared to glucose–sucrose metabolism in the CON group (Supplementary Figure S4). The microbial interaction based

10.3389/fimmu.2024.1471261

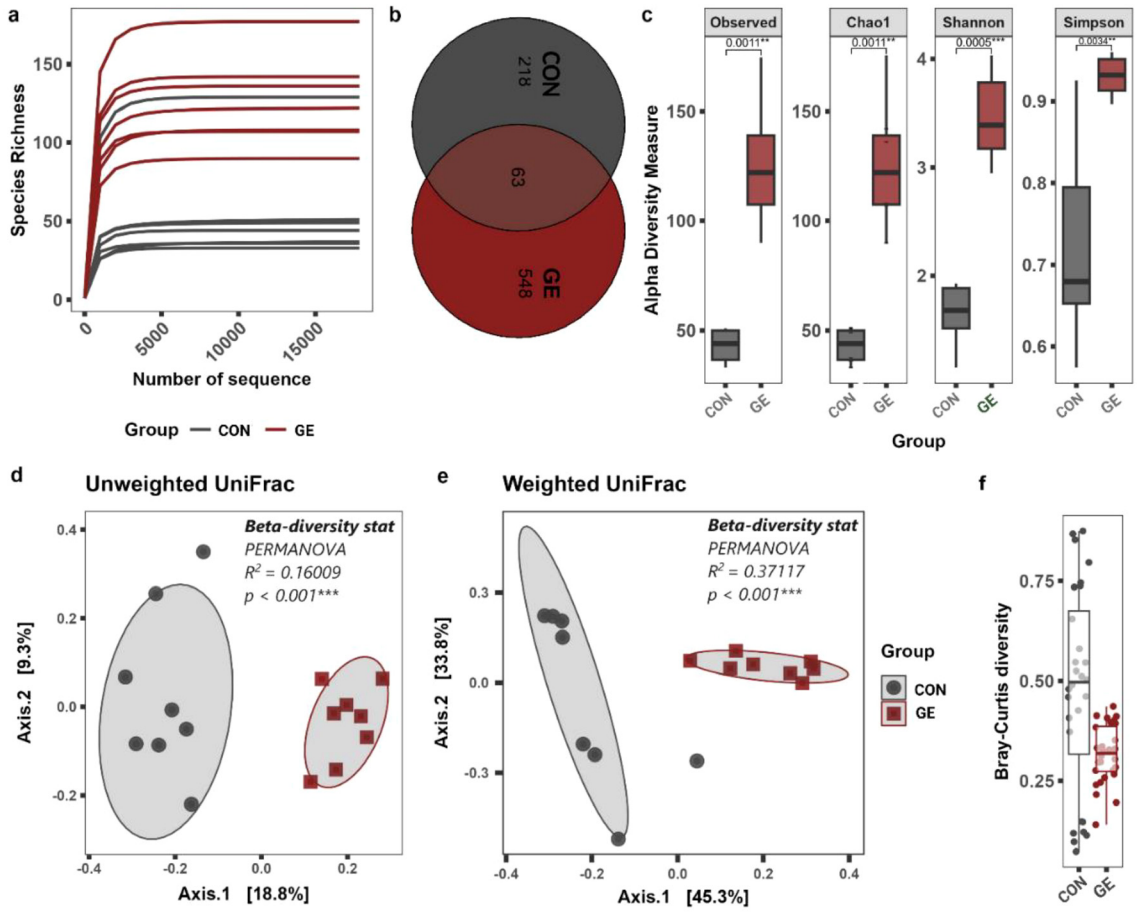

FIGURE 7
Effects of seaweed extract-supplemented diet on alpha-/beta-diversity of gut microbiota in Nile tilapia. **(A)** Rarefaction curve showing the depth and saturation level of study samples. **(B)** Number of shared and unique taxa. **(C)** Alpha-diversity measurements in terms of observed species, Chao1, Shannon, and Simpson diversity index. **(D, E)** Beta- diversity PCoA plot based on unweighted and weighted UniFrac distance matric. **(F)** The normalized pattern of Bray–Curtis distance represents the patterns of community distributions for CON and GE diets. Asterisks (** and ***) above the bars indicate significant differences between the two dietary groups of CON and GE determined by an unpaired *t*-test at $p < 0 < .01$, and $p < 0 < .001$, respectively. GE, *Gracilaria* extract; CON, control.

on ASV correlation showed the dominance of Proteobacteria and Firmicutes in the network. Some of the Proteobacteria and Firmicutes communities were found to be self-interactive (Figure 10A). Despite their high abundance, Actinobacteria and Fusobacteria were less interactive. Microbial co-occurrence network analysis revealed that Firmicutes led interactions in the community, despite the Proteobacteria-rich environment and their dominance in strong interactions. Firmicutes were associated with over 70% of medium and 50% of weak interactions, mostly with Bacteroidetes and Actinobacteria. Proteobacteria led the strong interactions and showed no involvement with Firmicutes (Figure 10B).

4 Discussion

Extreme temperature events caused by climate change have substantial impacts on aquatic ecosystems and can affect the aquaculture industry in various ways. These include changes in water temperature, reduced dissolved oxygen levels, and facilitating the spread of pathogens and parasites in farming environments (2). These challenges lead to increased stress and disease susceptibility and reduced growth rates in fish. Sustainable and responsible aquaculture practices, coupled with a broader commitment to mitigating temperature-induced stress, are essential for ensuring the resilience of fish farming in the face of global warming. Nutritional modulation and enrichment of aquafeeds can play a crucial role in mitigating the negative effects of acute temperature stress on aquaculture systems. Nowadays, the application of seaweeds and seaweed -based functional metabolites in aquafeeds has greatly attracted worldwide attention, demonstrating positive effects on stress reduction and improved disease resistance and overall health (14, 41). The findings of the present study demonstrate the potential of using GE in aquafeeds to counteract stress and improve growth performance while rearing at high temperature via the modulation of antioxidant status and gut microbiota composition in Nile tilapia.

Fish fed the GE-supplemented diet in the present study significantly improved the growth performance and feed

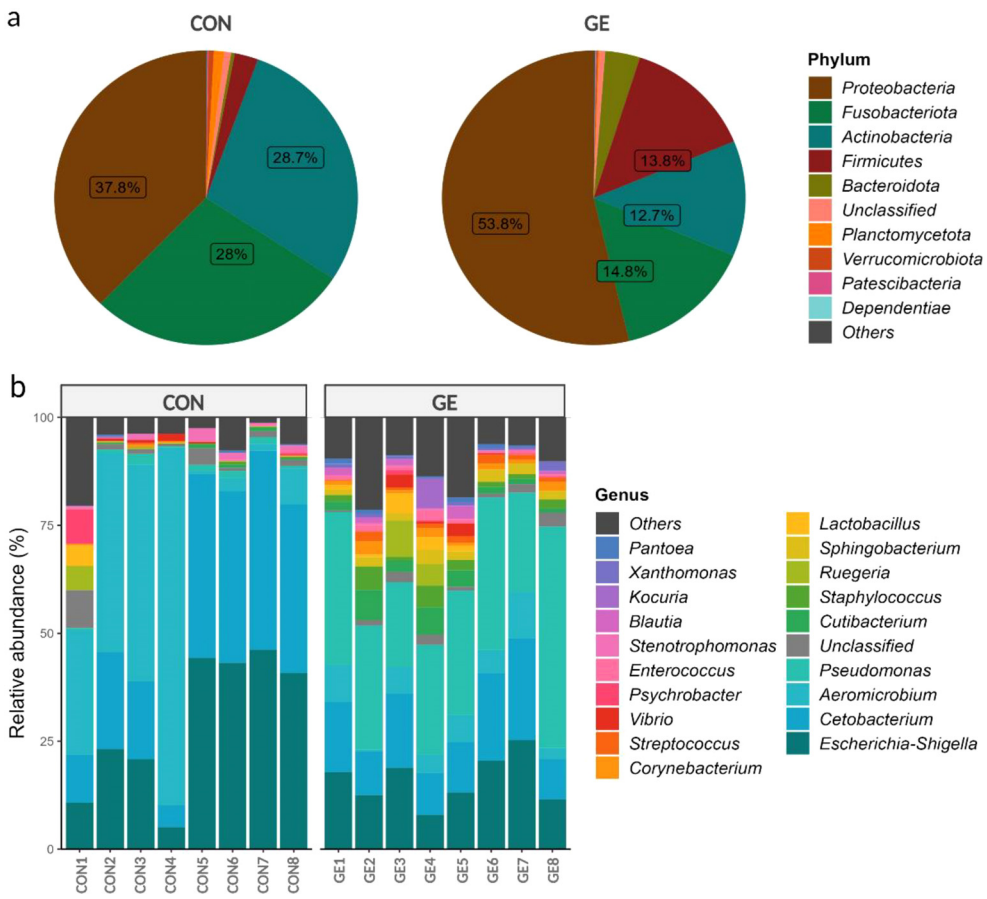

FIGURE 8
Relative abundance (≥1%) of bacteria in the hind gut of Nile tilapia. **(A)** Pie chart representing gut bacteria at the phylum level. **(B)** Bar plot representing gut bacteria at the genus level. GE, *Gracilaria* extract; CON, control.

utilization. These findings align with previous studies that have demonstrated the positive effects of incorporating seaweeds such as *Gracilaria persica* into fish diets, benefitting the growth performance of Atlantic salmon (42) and Persian sturgeon, *Acipenser persicus* (43), respectively. The improved growth realized in the present study may be due to the availability of nutrients (polyunsaturated fatty acids, favorable amino acids, minerals, and vitamins) and bioactive metabolites (phenolic, flavonoid, and β-carotene) in the seaweed extract that stimulated the digestion and absorption by fish (44, 45). Furthermore, the growth increment shown in this study may also be attributed to the presence of large amounts of polysaccharides and oligosaccharides present in seaweeds that act as prebiotics, thus positively increasing the digestion and assimilation of nutrients by enhanced activity of the beneficial bacteria (46). Moreover, the growth of fish has a close connection with the development of muscle that is attributed to its hyperplastic and hypertrophic fiber production (47, 48). Quantitative observations of muscle fiber morphology have been considered to be essential to evaluate muscle growth in nutritional research. Production of new muscle (hyperplasia) and the increment of existing muscle (hypertrophy) have been greatly stimulated by dietary composition (47). The increment of size and consequent decrease in the number of muscle fibers of Nile tilapia fed the GE diet in this study revealed the positive impacts of dietary GE, assisting in growth enhancement. In the current study, the FCR of Nile tilapia significantly improved due to the dietary supplementation of GE. This result is consistent with the study on Indian major carp, *Labeo rohita*, fed fucoidan-rich *Sargassum wightii* extract (49). The improved FCR could be attributed to the enhanced feed palatability and feed intake, which may have resulted from the activity of phenolic and flavonoid bioactive compounds in seaweed (50). Moreover, these biologically active compounds stimulate the secretion of important digestive enzymes such as amylase, lipase, and protease that significantly improve digestion and improve feed utilization (51).

The liver is an important organ that regulates the metabolism of essential nutrients and controls energy storage and utilization to maintain homeostasis (52). Aquafeeds high in fat and carbohydrates can lead to an increase in liver fat as well as larger adipocyte size (hypertrophy), causing the accumulation of body fat, while optimum feeding and proper nutrition can reduce adipocyte size (atrophy) as excess fat is utilized for energy (53). Therefore, understanding liver health and adipocyte tissue and their regulation is essential in studying dietary nutrition and related metabolic issues in fish. The significant reduction in liver fat coupled with the reduction of adipocyte size in fish fed the GE diet could be

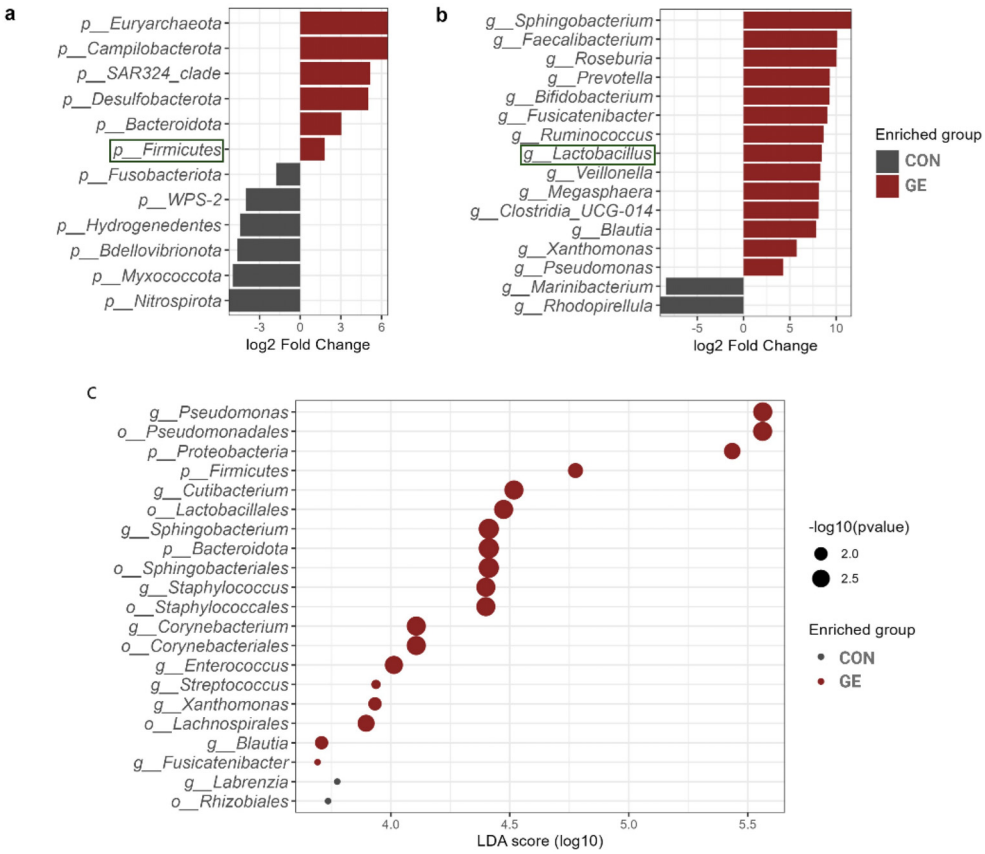

FIGURE 9
Differential abundant taxa in the hind gut of Nile tilapia. **(A)** Comparison of different phyla in the two dietary groups of GE and control. **(B)** Comparison of different genera in the two dietary groups of GE and control. The health beneficial genus is marked with green color. **(C)** Enriched phyla, order, and genera with log10 *p*-value. The *X*-axis indicates the LDA score with dots representing the significance level of *p*-values. Bigger dots indicate more significant *p*-value. GE, *Gracilaria* extract; CON, control.

related to the reduction of AST and ALT enzyme activity levels compared to the control diet. This reduction in liver fat and adipocyte size in GE-fed fish may also be related to the abundance of intestinal microbiota, which may influence fat absorption by producing metabolites such as short-chain fatty acids and secondary bile acids, as well as pro-inflammatory bacterially derived factors such as lipopolysaccharides (54, 55). However, more research is needed to gain a comprehensive understanding of how GE affects liver lipid accumulation and adipose tissue quantity and size in fish.

Lysozyme activity is a vital component of fish innate immune system to defend against infections (56). The current study revealed higher lysozyme activity in fish fed GE, suggesting a boosting immunity possibly triggered by active compounds including polyphenols and polysaccharides present in *Gracilaria* sp. (57). Moreover, this finding can be attributed to the seaweed's role in activating the immune response and scavenging excessive reactive oxygen metabolites (ROS). In accordance with the current study, the administration of *Gracilaria* sp. extract increased lysozyme activity in European seabass (58). Fish under stressful conditions often experience oxidative stress, which is caused by an imbalance between the production and elimination of ROS within cells (59). The disruption of scavenging capacity results in lipid peroxidation, ROS buildup, and rupturing the lipid membrane of body cells (60). The DNA of immune cells is likewise harmed by this interruption. In this instance, the body secretes SOD, CAT, and GPx, which are enzymatic and non-enzymatic antioxidative responses that reduce ROS and increase antioxidative capacity (61). However, failing to do so leads to elevated lipid peroxidation and the generation of MDA (62). The current study revealed that dietary GE-based diet significantly reduced the MDA level in fish confirming the stress-inhibitory role of dietary GE. These results align with other studies that have found dietary supplementation of *Sargassum horneri*, and a mixture of seaweed (i.e., *Ulva lactuca*, *Jania rubens*, and *Pterocladia capillacea*) extract induced significantly lower MDA levels in black sea bream, *Acanthopagrus schlegelii*, and striped catfish, *Pangasianodon hypophthalmus* (63, 64). The ameliorative capacity of the seaweed extract was associated with the high content of bioactive substances such as flavonoids and phenolic substances and could act as natural antioxidants and play an important role to neutralize free radicals and improve stress resilience (65, 66). In line with the present results, we also observed an increased upregulation of tight junction proteins and antioxidant gene in the hind gut of GE-fed Nile tilapia. These data suggested that GE supplementation protects gut permeability and translocation of pathogens in fish while improving nrf2 pathway and strengthening antioxidant

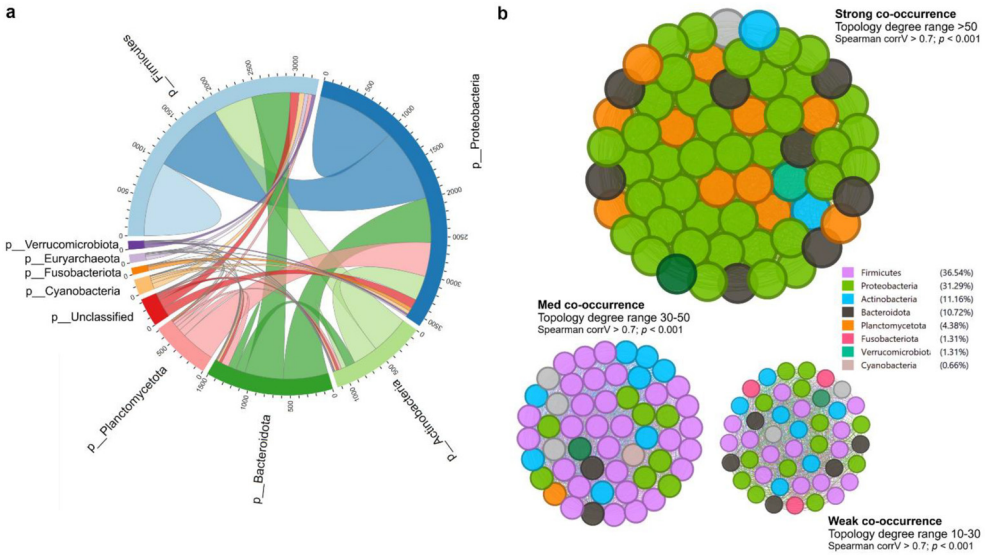

FIGURE 10
Microbial interaction and co-occurrence network. **(A)** Cladogram representing the correlation of amplicon sequence variants (ASVs) between two diets in terms of interactions. The number in the outer circular part indicates the average ASV counts per sample. **(B)** Co-occurrence network of bacterial community regarding the degree of interactions. The network was segregated based on topology wherein the size of the nodes represents the degree of interaction (10%–100%). The color code on the right side indicates the phyla and contributions to the interaction.

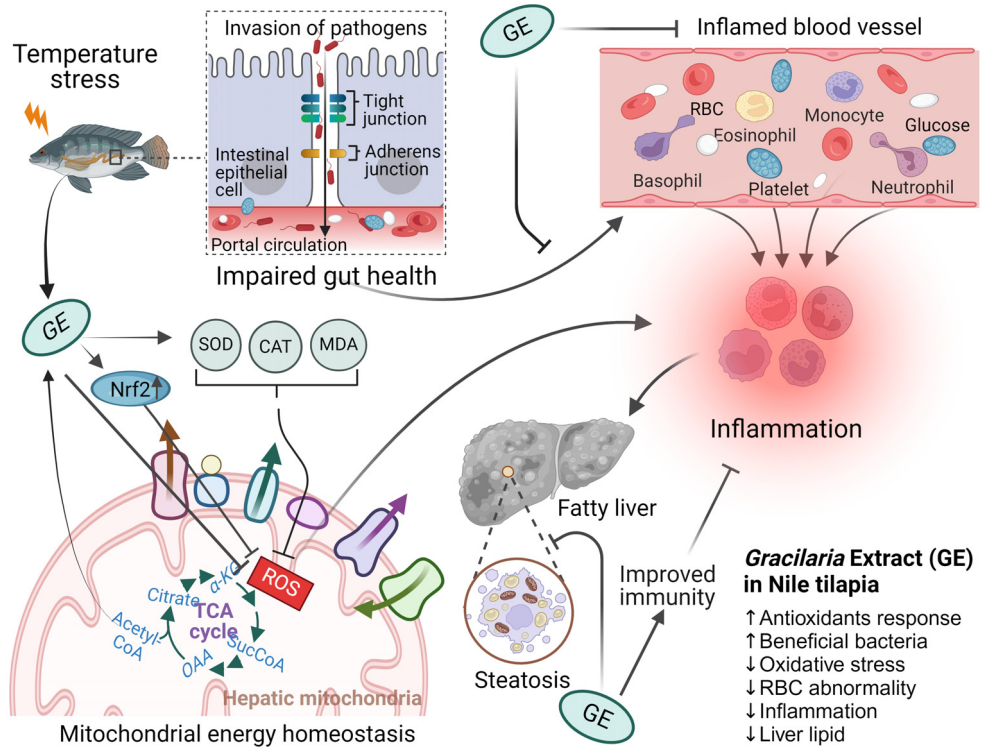

FIGURE 11
The possible roles of *Gracilaria* extract (GE) on the gut–liver axis and its underlying mechanisms in Nile tilapia. Nile tilapia under acute temperature stress is susceptible to pathogen invasion through a leaky gut caused inflammation that compromises immune function of fish. Dietary supplementation with GE increases the expression of antioxidant gene (*nrf2*) and reduces MDA level, which leads to improved mitochondrial function and energy production to help prevent inflammation and subsequent oxidative stress in fish. The GE diet has also been found to reduce liver lipid content, an indication of improved health of fish. The figure includes up and down arrows, denoting increased and decreased cellular functions and systems, respectively.

defense. Likewise, in the present study, *hsp70* protein expression was downregulated in the GE group compared to the CON group, indicating stress-mediating effects of GE in fish under adverse conditions.

RBCs play a crucial role in oxygen transport throughout the body, and an increase in their count can lead to higher levels of haemoglobin (67). This allows fish to efficiently transport oxygen from the gills to various tissues and organs. As a result, fish are likely to cope better with stressors, such as changes in water temperature, pollution, or other environmental challenges. In the present study, a significant increase in RBC levels was found in fish fed a GE diet. Similar findings have been observed in striped catfish, where a mixture of seaweeds (*U. lactuca*, *J. rubens*, and *P. capillacea*) increased the RBC count (63). Another study showed that a *Sargassum angustifolium* algae extract-supplemented diet enhanced the number of RBCs in rainbow trout (68). These results suggest that supplementing the diet with seaweed may enhance erythropoietin production and erythrocytic stability, which may increase the RBC level in fish (69). Furthermore, fish fed the GE diet in the present study demonstrated a significant decrease in RBC cellular and nuclear abnormalities, indicating the beneficial effects of seaweed in mitigating stress during extreme warm exposure. Warm stress generally results in transmembrane alterations and metabolic inhibition that trigger the DNA-damaging mitochondrial caspase-3, which leads to erythrocytic cellular and nuclear anomalies (70–73). Furthermore, elevated water temperatures can also damage DNA by causing the release of DNase enzymes from lysosomes and thermally inactivating the enzymes that repair DNA, which can change the shape of cells (74). Significantly higher RBC cellular and nuclear abnormalities observed in fish fed the control diet could be due to the excess lipid peroxidation that considerably increased the permeability and decreased the symmetry of the erythrocyte cell membrane, which is also responsible for higher abnormalities in erythrocytes (75). Nevertheless, the higher RBC abnormalities with the control diet are justified by the much higher overexpression of *hsp70* identified in these fish when compared to GE-fed fish.

The present study found that Nile tilapia fed a diet supplemented with GE exhibited a healthier gut, as indicated by the higher diversity and abundance of bacterial populations and enrichment of phylum Firmicutes, family *Lactobacillales*, and genus *Lactobacillus*. These bacteria are mostly considered beneficial for fish and other aquatic animals (76). A study by Cui et al. (77) has shown that supplementing the diet with fucoidan, a polysaccharide extracted from brown-seaweed *Undaria pinnatifida*, enhanced the activity of digestive enzymes and regulated the microbial populations and increased beneficial bacteria in fish. The increased abundance of *Lactobacillus* is of considerable interest since an enrichment in these bacteria is associated with improved health (76). The increased bacterial diversity and higher number of *Lactobacillus* in Nile tilapia fed GE may be due to the presence of bioactive compounds (e.g., short-chain peptides, polyphenols, and polysaccharides) in seaweed, which might have induced the colonization of health-promoting bacteria. Polysaccharides in seaweed are a preferential substrate for lactic acid bacteria (78), as demonstrated in the gut of zebrafish, *Danio rerio* (79), and barramundi, *Lates calcarifer* (80). Additionally, *Lactobacillus* has been linked to various protective mechanisms in the host against pathogens, such as producing bacteriocin to remove pathogens from the gut epithelium (81). In the present study, feeding fish with seaweed extract decreased the abundance of opportunistic pathogen *Escherichia-Shigella* ($p < 0.05$, LDA < 2.0) in Nile tilapia gut. This result is supported by *Sargassum dentifolium* extract that reduced the abundance of *Escherichia coli* in the gut of king prawn, *Litopenaeus vannamei* (82). Studies indicate that increasing environmental temperatures have adverse effects on fish, leading to reduced digestive efficiency, lower gut bacterial abundance, and higher pathogenic bacteria with negative implications for the host's health and physiology (83, 84). Despite the augmentation of Firmicutes and *Lactobacillus*, GE also influenced the colonization of some opportunistic clinical pathogens including *Streptococcus*, *Staphylococcus*, and *Corynebacterium* that needs further investigation. Nevertheless, the higher diversity of bacteria in the GE-fed group compared to the control group indicates the effects of seaweed even at high temperatures. Future research should focus on understanding the impact of temperature variations on the fish microbiome and the consequences of microbial changes on fish performance.

5 Conclusion

This study demonstrates that dietary *Gracilaria* extract (1% of feed) supplementation could counteract the adverse effects of temperature-induced oxidative stress in fish through (1) enhancing the antioxidant capacity indicated by the upregulation of *nrf2* expression and reduction of MDA production; (2) protecting gut permeability by improving the expression of tight junction proteins (*occludin* and *claudin1*); (3) increasing the RBC count, which could indicate a higher blood flow in the circulatory system; (4) reduction of stress levels indicated by the reduction of *hsp70* mRNA expression; and (5) increasing the number of potentially health-promoting bacteria in fish gut. A summary of the beneficial role of seaweed extract in the gut–liver axis and its underlying mechanisms is depicted in Figure 11. The present findings reinforce the prospect of seaweed extracts as an effective supplement in aquafeeds to attenuate temperature-induced stress in aquaculture production during summer in the face of global warming.

Data availability statement

The datasets presented in this study can be found in online repositories. The names of the repository/repositories and accession number(s) can be found in the article/Supplementary Material.

Ethics statement

The animal study was approved by The experimental design, husbandry protocol and fish sampling procedures were performed in

this study was approved and guided by animal ethics committee (AEC), Patuakhali Science and Technology University, Bangladesh (Approval Number: AEC-FoF/2022/002). The study was conducted in accordance with the local legislation and institutional requirements.

Author contributions

MS: Conceptualization, Data curation, Formal analysis, Funding acquisition, Investigation, Methodology, Project administration, Visualization, Writing – original draft, Writing – review & editing. PF: Conceptualization, Funding acquisition, Project administration, Software, Validation, Visualization, Writing – review & editing. MF: Formal analysis, Methodology, Resources, Software, Validation, Visualization, Writing – review & editing. DF: Conceptualization, Funding acquisition, Project administration, Resources, Software, Supervision, Validation, Writing – review & editing.

Funding

The author(s) declare that financial support was received for the research, authorship, and/or publication of this article. This work was financially supported by the Alfred Deakin Postdoctoral Research Fellowship [RM42943, 2022] to MS from the Faculty of Science, Engineering and Built Environment, Deakin University, Australia.

Conflict of interest

The authors declare that the research was conducted in the absence of any commercial or financial relationships that could be construed as a potential conflict of interest.

Publisher's note

All claims expressed in this article are solely those of the authors and do not necessarily represent those of their affiliated organizations, or those of the publisher, the editors and the reviewers. Any product that may be evaluated in this article, or claim that may be made by its manufacturer, is not guaranteed or endorsed by the publisher.

Supplementary material

The Supplementary Material for this article can be found online at: https://www.frontiersin.org/articles/10.3389/fimmu.2024.1471261/full#supplementary-material

References

1. Huang M, Ding L, Wang J, Ding C, Tao J. The impacts of climate change on fish growth: A summary of conducted studies and current knowledge. *Ecol Indic*. (2021) 121:106976. doi: 10.1016/j.ecolind.2020.106976

2. Islam MJ, Kunzmann A, Slater MJ. Responses of aquaculture fish to climate change-induced extreme temperatures: A review. *J World Aquac Soc*. (2022) 53:314–66. doi: 10.1111/jwas.12853

3. Nowicki R, Heithaus M, Thomson J, Burkholder D, Gastrich K, Wirsing A. Indirect legacy effects of an extreme climatic event on a marine megafaunal community. *Ecol Monogr*. (2019) 89:e01365. doi: 10.1002/ecm.2019.89.issue-3

4. Fan X, Qin X, Zhang C, Zhu Q, Chen J, Chen P. Metabolic and anti-oxidative stress responses to low temperatures during the waterless preservation of the hybrid grouper (Epinephelus fuscogutatus♀ × Epinephelus lanceolatus♂). *Aquaculture*. (2019) 508:10–8. doi: 10.1016/j.aquaculture.2019.04.054

5. Feidantsis K, Pörtner HO, Giantsis IA, Michaelidis B. Advances in understanding the impacts of global warming on marine fishes farmed offshore: Sparus aurata as a case study. *J Fish Biol*. (2021) 98:1509–23. doi: 10.1111/jfb.14611

6. Goikoetxea A, et al. Genetic pathways underpinning hormonal stress responses in fish exposed to short-and long-term warm ocean temperatures. *Ecol Indic*. (2021) 120:106937. doi: 10.1016/j.ecolind.2020.106937

7. Gupta A, et al. Immunomodulation by dietary supplements: A preventive health strategy for sustainable aquaculture of tropical freshwater fish, Labeo rohita (Hamilton, 1822). *Rev Aquac*. (2021) 13:2364–94. doi: 10.1111/raq.12581

8. Dawood MA, Koshio S, Abdel-Daim MM, Van Doan H. Probiotic application for sustainable aquaculture. *Rev Aquac*. (2019) 11:907–24. doi: 10.1111/raq.2019.11.issue-3

9. Thepot V, Campbell AH, Rimmer MA, Paul NA. Meta-analysis of the use of seaweeds and their extracts as immunostimulants for fish: a systematic review. *Rev Aquac*. (2021) 13:907–33. doi: 10.1111/raq.12504

10. Silva-Brito F, et al. Fish performance, intestinal bacterial community, digestive function and skin and fillet attributes during cold storage of gilthead seabream (Sparus aurata) fed diets supplemented with Gracilaria by-products. *Aquaculture*. (2021) 541:736808. doi: 10.1016/j.aquaculture.2021.736808

11. Miyashita K, Mikami N, Hosokawa M. Chemical and nutritional characteristics of brown seaweed lipids: A review. *J Funct Foods*. (2013) 5:1507–17. doi: 10.1016/j.jff.2013.09.019

12. Gupta S, Abu-Ghannam N. Bioactive potential and possible health effects of edible brown seaweeds. *Trends Food Sci Technol*. (2011) 22:315–26. doi: 10.1016/j.tifs.2011.03.011

13. Čagalj M, Skroza D, Tabanelli G, Özogul F, Šimat V. Maximizing the antioxidant capacity of Padina pavonica by choosing the right drying and extraction methods. *Processes*. (2021) 9:587. doi: 10.3390/pr9040587

14. Siddik MAB, Francis P, Rohani MF, Azam MS, Mock TS, Francis DS. Seaweed and seaweed-based functional metabolites as potential modulators of growth, immune and antioxidant responses, and gut microbiota in fish. *Antioxid (Basel)*. (2023) 12 (12):2066. doi: 10.3390/antiox12122066

15. Michalak I, et al. Antioxidant effects of seaweeds and their active compounds on animal health and production–a review. *Vet Q*. (2022) 42:48–67. doi: 10.1080/01652176.2022.2061744

16. Cherry P, et al. Prebiotics from seaweeds: an ocean of opportunity? *Mar Drugs*. (2019) 17(6):327. doi: 10.3390/md17060327

17. Chen X, et al. *In vitro* prebiotic effects of seaweed polysaccharides. *J Oceanol Limnol*. (2018) 36:926–32. doi: 10.1007/s00343-018-6330-7

18. Ferreira M, Abdelhafiz Y, Abreu H, Silva J, Valente LMP, Kiron V. Gracilaria gracilis and Nannochloropsis oceanica, singly or in combination, in diets alter the intestinal microbiota of European seabass (Dicentrarchus labrax). *Front Mar Sci*. (2022) 9:1001942. doi: 10.3389/fmars.2022.1001942

19. Dawood MA, Koshio S. Application of fermentation strategy in aquafeed for sustainable aquaculture. *Rev Aquac*. (2020) 12:987–1002. doi: 10.1111/raq.12368

20. Wilczynski W, et al. Metagenomic analysis of the gastrointestinal microbiota of Gadus morhua callarias L. originating from a chemical munition dump site. *Toxics*. (2022) 10:206. doi: 10.3390/toxics10050206

21. Zhang X, et al. Effects of dietary supplementation of Ulva pertusa and non-starch polysaccharide enzymes on gut microbiota of Siganus canaliculatus. *J Oceanol Limnol*. (2017) 36:438–49. doi: 10.1007/s00343-017-6235-x

22. Naylor RL, et al. A 20-year retrospective review of global aquaculture. *Nature*. (2021) 591:551–63. doi: 10.1038/s41586-021-03308-6

23. Shahjahan M, Islam MJ, Hossain MT, Mishu MA, Hasan J, Brown C. Blood biomarkers as diagnostic tools: An overview of climate-driven stress responses in fish. *Sci Total Environ*. (2022) 843:156910. doi: 10.1016/j.scitotenv.2022.156910

24. Islam SM, et al. Elevated temperature affects growth and hemato-biochemical parameters, inducing morphological abnormalities of erythrocytes in Nile tilapia Oreochromis niloticus. *Aquac Res*. (2020) 51:4361–71. doi: 10.1111/are.v51.10

25. Thépot V, et al. Dietary inclusion of the red seaweed Asparagopsis taxiformis boosts production, stimulates immune response and modulates gut microbiota in Atlantic salmon, Salmo salar. *Aquaculture*. (2022) 546:737286. doi: 10.1016/j.aquaculture.2021.737286

26. Sobuj MKA, Islam MA, Haque MA, Islam MM, Alam MJ, Rafiquzzaman SM. Evaluation of bioactive chemical composition, phenolic, and antioxidant profiling of different crude extracts of Sargassum coriifolium and Hypnea pannosa seaweeds. *J Food Meas Charact*. (2020) 15:1653–65. doi: 10.1007/s11694-020-00758-w

27. Peixoto MJ, et al. Role of dietary seaweed supplementation on growth performance, digestive capacity and immune and stress responsiveness in European seabass (Dicentrarchus labrax). *Aquac Rep*. (2016) 3:189–97. doi: 10.1016/j.aqrep.2016.03.005

28. Siddik MA, Foysal MJ, Fotedar R, Francis DS, Gupta SK. Probiotic yeast Saccharomyces cerevisiae coupled with Lactobacillus casei modulates physiological performance and promotes gut microbiota in juvenile barramundi, Lates calcarifer. *Aquaculture*. (2022) 546:737346. doi: 10.1016/j.aquaculture.2021.737346

29. Rowlerson A, Mascarello F, Radaelli G, Veggetti A. Differentiation and growth of muscle in the fish Sparus aurata (L): II. Hyperplastic and hypertrophic growth of lateral muscle from hatching to adult. *J Muscle Res Cell Motil*. (1995) 16:223–36. doi: 10.1007/BF00121131

30. Chaklader MR, Siddik MA, Fotedar R, Howieson J. Insect larvae, Hermetia illucens in poultry by-product meal for barramundi, Lates calcarifer modulates histomorphology, immunity and resistance to Vibrio harveyi. *Sci Rep*. (2019) 9:16703. doi: 10.1038/s41598-019-53018-3

31. Siddik MAB, Howieson J, Partridge GJ, Fotedar R, Gholipourkanani H. Dietary tuna hydrolysate modulates growth performance, immune response, intestinal morphology and resistance to Streptococcus iniae in juvenile barramundi, Lates calcarifer. *Sci Rep*. (2018) 8:15942. doi: 10.1038/s41598-018-34182-4

32. Blanc M-C, Neveux N, Laromiguière M, Bérard M-P, Cynober L. Evaluation of a newly available biochemical analyzer: the Olympus AU 600. *Clin Chem Lab Med*. (2000) 38(5):465–75. doi: 10.1515/CCLM.2000.067

33. Livak KJ, Schmittgen TD. Analysis of relative gene expression data using real-time quantitative PCR and the 2(-Delta Delta C(T)) Method. *Methods*. (2001) 25:402–8. doi: 10.1006/meth.2001.1262

34. Quast C, et al. The SILVA ribosomal RNA gene database project: improved data processing and web-based tools. *Nucleic Acids Res*. (2012) 41:D590–6. doi: 10.1093/nar/gks1219

35. Caicedo HH, Hashimoto DA, Caicedo JC, Pentland A, Pisano GP. Overcoming barriers to early disease intervention. *Nat Biotechnol*. (2020) 38:669–73. doi: 10.1038/s41587-020-0550-z

36. Team RDC. R: A language and environment for statistical computing. (2010). Available online at: http://www.R-project.org/.

37. Liu C, Cui Y, Li X, Yao M. microeco: an R package for data mining in microbial community ecology. *FEMS Microbiol Ecol*. (2021) 97:fiaa255. doi: 10.1093/femsec/fiaa255

38. McMurdie PJ, Holmes S. phyloseq: an R package for reproducible interactive analysis and graphics of microbiome census data. *PloS One*. (2013) 8:e61217. doi: 10.1371/journal.pone.0061217

39. Siddik MAB, Fotedar R, Chaklader MR, Foysal MJ, Nahar A, Howieson J. Fermented Animal Source Protein as Substitution of Fishmeal on Intestinal Microbiota, Immune-Related Cytokines and Resistance to Vibrio mimicus in Freshwater Crayfish (Cherax cainii). *Front Physiol*. (2019) 10:1635. doi: 10.3389/fphys.2019.01635

40. Cao Y, Dong Q, Wang D, Zhang P, Liu Y, Niu C. microbiomeMarker: an R/Bioconductor package for microbiome marker identification and visualization. *Bioinformatics*. (2022) 38:4027–9. doi: 10.1093/bioinformatics/btac438

41. Siddik MAB, Francis DS, Islam SMM, Salini MJ, Fotedar R. Fermentation and fortification of Sargassum linearifolium with multi-strain probiotics improves mucosal barrier status, inflammatory response and resistance to Vibrio harveyi infection in barramundi Lates calcarifer. *Aquaculture*. (2025) 595:741502. doi: 10.1016/j.aquaculture.2024.741502

42. Kamunde C, Sappal R, Melegy TM. Brown seaweed (AquaArom) supplementation increases food intake and improves growth, antioxidant status and resistance to temperature stress in Atlantic salmon, Salmo salar. *PloS One*. (2019) 14:e0219792. doi: 10.1371/journal.pone.0219792

43. Adel M, Omidi AH, Dawood MA, Karimi B, Shekarabi SPH. Dietary Gracilaria persica mediated the growth performance, fillet colouration, and immune response of Persian sturgeon (Acipenser persicus). *Aquaculture*. (2021) 530:735950. doi: 10.1016/j.aquaculture.2020.735950

44. Hashim R, Saat MAM. The utilization of seaweed meals as binding agents in pelleted feeds for snakehead (Channa striatus) fry and their effects on growth. *Aquaculture*. (1992) 108:299–308. doi: 10.1016/0044-8486(92)90114-Z

45. Lordan S, Ross RP, Stanton C. Marine bioactives as functional food ingredients: potential to reduce the incidence of chronic diseases. *Mar Drugs*. (2011) 9:1056–100. doi: 10.3390/md9061056

46. O'Sullivan L, et al. Prebiotics from marine macroalgae for human and animal health applications. *Mar Drugs*. (2010) 8:2038–64. doi: 10.3390/md8072038

47. Jiang Q, et al. Effects of dietary tryptophan on muscle growth, protein synthesis and antioxidant capacity in hybrid catfish Pelteobagrus vachelli♀× Leiocassis longirostris♂. *Br J Nutr*. (2022) 127:1761–73. doi: 10.1017/S0007114521002828

48. Zhao H, et al. Diet affects muscle quality and growth traits of grass carp (Ctenopharyngodon idellus): a comparison between grass and artificial feed. *Front Physiol*. (2018) 9:283. doi: 10.3389/fphys.2018.00283

49. Sajina KA, Sahu NP, Varghese T, Jain KK. Fucoidan-rich Sargassum wightii extract supplemented with α-amylase improve growth and immune responses of Labeo rohita (Hamilton, 1822) fingerlings. *J Appl Phycol*. (2019) 31:2469–80. doi: 10.1007/s10811-019-1742-0

50. Sattanathan G, et al. Effects of Dietary Blend of Algae Extract Supplementation on Growth, Biochemical, Haemato-Immunological Response, and Immune Gene Expression in Labeo rohita with Aeromonas hydrophila Post-Challenges. *Fishes*. (2022) 8:7. doi: 10.3390/fishes8010007

51. Abdel-Tawwab M, et al. Dietary curcumin nanoparticles promoted the performance, antioxidant activity, and humoral immunity, and modulated the hepatic and intestinal histology of Nile tilapia fingerlings. *Fish Physiol Biochem*. (2022) 48:585–601. doi: 10.1007/s10695-022-01066-4

52. Choe SS, Huh JY, Hwang IJ, Kim JI, Kim JB. Adipose tissue remodeling: its role in energy metabolism and metabolic disorders. *Front Endocrinol (Lausanne)*. (2016) 7:30. doi: 10.3389/fendo.2016.00030

53. Weil C, Lefèvre F, Bugeon J. Characteristics and metabolism of different adipose tissues in fish. *Rev Fish Biol Fish*. (2013) 23:157–73. doi: 10.1007/s11160-012-9288-0

54. Schoeler M, Caesar R. Dietary lipids, gut microbiota and lipid metabolism. *Rev Endocr Metab Disord*. (2019) 20:461–72. doi: 10.1007/s11154-019-09512-0

55. Semova I, et al. Microbiota regulate intestinal absorption and metabolism of fatty acids in the zebrafish. *Cell Host Microbe*. (2012) 12:277–88. doi: 10.1016/j.chom.2012.08.003

56. Saurabh S, Sahoo PK. Lysozyme: an important defence molecule of fish innate immune system. *Aquac Res*. (2008) 39:223–39. doi: 10.1111/j.1365-2109.2007.01883.x

57. Xie SP. Ocean warming pattern effect on global and regional climate change. *AGU Adv*. (2020) 1:e2019AV000130. doi: 10.1029/2019AV000130

58. Peixoto MJ, et al. Effects of dietary supplementation of Gracilaria sp. extracts on fillet quality, oxidative stress, and immune responses in European seabass (Dicentrarchus labrax). *J Appl Phycol*. (2019) 31:761–70. doi: 10.1007/s10811-018-1519-x

59. Pamplona R, Costantini D. Molecular and structural antioxidant defenses against oxidative stress in animals. *Am J Physiol Regul Integr Comp Physiol*. (2011) 301:R843–63. doi: 10.1152/ajpregu.00034.2011

60. Burgos-Aceves MA, et al. Modulation of mitochondrial functions by xenobiotic-induced microRNA: from environmental sentinel organisms to mammals. *Sci Total Environ*. (2018) 645:79–88. doi: 10.1016/j.scitotenv.2018.07.109

61. Goes ESdR, Goes MD, d. Castro PL, d. Lara JAF, Vital ACP. and R. P. Ribeiro, "Imbalance of the redox system and quality of tilapia fillets subjected to pre-slaughter stress. *PloS One*. (2019) 14:e0210742. doi: 10.1371/journal.pone.0210742

62. Silvestre MA, Yániz JL, Peña FJ, Santolaria P, Castelló-Ruiz M. Role of antioxidants in cooled liquid storage of mammal spermatozoa. *Antioxidants*. (2021) 10:1096. doi: 10.3390/antiox10071096

63. Abdelhamid AF, Ayoub HF, Abd El-Gawad EA, Abdelghany MF, Abdel-Tawwab M. Potential effects of dietary seaweeds mixture on the growth performance, antioxidant status, immunity response, and resistance of striped catfish (Pangasianodon hypophthalmus) against Aeromonas hydrophila infection. *Fish Shellfish Immunol*. (2021) 119:76–83. doi: 10.1016/j.fsi.2021.09.043

64. Shi Q, et al. Effects of dietary Sargassum horneri on growth performance, serum biochemical parameters, hepatic antioxidant status, and immune responses of juvenile black sea bream Acanthopagrus schlegelii. *J Appl Phycol*. (2019) 31:2103–13. doi: 10.1007/s10811-018-1719-4

65. Chew YL, Lim YY, Omar M, Khoo KS. Antioxidant activity of three edible seaweeds from two areas in South East Asia. *LWT Food Sci Technol*. (2008) 41:1067–72. doi: 10.1016/j.lwt.2007.06.013

66. Ganesan P, Kumar CS, Bhaskar N. Antioxidant properties of methanol extract and its solvent fractions obtained from selected Indian red seaweeds. *Bioresour Technol*. (2008) 99:2717–23. doi: 10.1016/j.biortech.2007.07.005

67. Wei Z, Xie L, Wang Y, Zhuang J, Niu J, Liu L. Red blood cell lysis pretreatment can significantly improve the yield of *Treponema pallidum* DNA from blood. *Microbiol Spectr*. (2024) 11:e05198-22. doi: 10.1128/spectrum.05198-22

68. Zeraatpisheh F, Firouzbakhsh F, Khalili KJ. Effects of the macroalga Sargassum angustifolium hot water extract on hematological parameters and immune responses in rainbow trout (Oncohrynchus mykiss) infected with Yersinia rukeri. *J Appl Phycol*. (2018) 30:2029–37. doi: 10.1007/s10811-018-1395-4

69. Marques A, et al. Macroalgae-enriched diet protects gilthead seabream (Sparus aurata) against erythrocyte population instability and chromosomal damage induced by aqua-medicines. *J Appl Phycol*. (2019) 32:1477–93. doi: 10.1007/s10811-019-01996-2

70. Antonopoulou E, Chatzigiannidou I, Feidantsis K, Kounna C, Chatzifotis S. Effect of water temperature on cellular stress responses in meagre (Argyrosomus regius). *Fish Physiol Biochem*. (2020) 46:1075–91. doi: 10.1007/s10695-020-00773-0

71. Gomes JM, et al. What the erythrocytic nuclear alteration frequencies could tell us about genotoxicity and macrophage iron storage? *PloS One*. (2015) 10:e0143029. doi: 10.1371/journal.pone.0143029

72. Shuey DL, Gudi R, Krsmanovic L, Gerson RJ. Evidence that oxymorphone-induced increases in micronuclei occur secondary to hyperthermia. *Toxicol Sci*. (2007) 95:369–75. doi: 10.1093/toxsci/kfl148

73. Zafalon-Silva B, et al. Erythrocyte nuclear abnormalities and leukocyte profile in the Antarctic fish Notothenia coriiceps after exposure to short-and long-term heat stress. *Polar Biol*. (2017) 40:1755–60. doi: 10.1007/s00300-017-2099-y

74. Davis A, Maney D, Maerz J. The use of leukocyte profiles to measure stress in vertebrates: a review for ecologists. *Funct Ecol*. (2008) 22:760–72. doi: 10.1111/j.1365-2435.2008.01467.x

75. Hussain R, Khan I, Jamal A, Mohamed BB, Khan A. Evaluation of hematological, oxidative stress, and antioxidant profile in cattle infected with brucellosis in Southern Punjab, Pakistan. *BioMed Res Int*. (2022) 2022:7140909. doi: 10.1155/2022/7140909

76. Jin W, Jiang L, Hu S, Zhu A. Effects of Lactobacillus plantarum and Bacillus subtilis on growth, immunity and intestinal flora of largemouth bass(Micropterus salmoides). *Aquaculture*. (2024) 583:740581. doi: 10.1016/j.aquaculture.2024.740581

77. Cui H, et al. Effects of a highly purified fucoidan fromUndaria pinnatifidaon growth performance and intestine health status of gibel carpCarassius auratus gibelio. *Aquac Nutr*. (2019) 26:47–59. doi: 10.1111/anu.12966

78. Healy LE, et al. Fermentation of brown seaweeds Alaria esculenta and Saccharina latissima for new product development using Lactiplantbacillus plantarum, Saccharomyces cerevisiae and kombucha SCOBY. *Algal Res*. (2023) 76:103322. doi: 10.1016/j.algal.2023.103322

79. Kim YS, et al. Structural characteristics of sulfated polysaccharides from Sargassum horneri and immune-enhancing activity of polysaccharides combined with lactic acid bacteria. *Food Funct*. (2022) 13:8214–27. doi: 10.1039/d1fo03946f

80. Nazarudin MF, et al. Chemical, nutrient and physicochemical properties of brown seaweed, sargassum polycystum C. Agardh (Phaeophyceae) collected from Port Dickson, Peninsular Malaysia. *Molecules*. (2021) 26:5216. doi: 10.3390/molecules26175216

81. Anjana, Tiwari SK. Bacteriocin-producing probiotic lactic acid bacteria in controlling dysbiosis of the gut microbiota. *Front Cell Infect Microbiol*. (2022) 12:851140. doi: 10.3389/fcimb.2022.851140

82. Sharawy ZZ, et al. Effects of dietary marine microalgae,Tetraselmis suecica, on production, gene expression, protein markers and bacterial count of Pacificwhite shrimp Litopenaeus vannamei. *Aquac Res*. (2020) 51:2216–28. doi: 10.1111/are.14566

83. Pelusio NF, et al. Interaction between dietary lipid level and seasonal temperature changes in gilthead sea bream sparus aurata: effects on growth, fat deposition, plasma biochemistry, digestive enzyme activity, and gut bacterial community. *Front Mar Sci*. (2021) 8:664701. doi: 10.3389/fmars.2021.664701

84. Steiner K, Laroche O, Walker SP, Symonds JE. Effects of water temperature on the gut microbiome and physiology of Chinook salmon (Oncorhynchus tshawytscha) reared in a freshwater recirculating system. *Aquaculture*. (2022) 560:738529. doi: 10.1016/j.aquaculture.2022.738529

frontiers | Frontiers in Immunology

TYPE Original Research
PUBLISHED 26 November 2024
DOI 10.3389/fimmu.2024.1480897

OPEN ACCESS

EDITED BY
Qun Zhao,
Hainan University, China

REVIEWED BY
Jianfei Lu,
Ningbo University, China
Chang Xu,
Hainan University, China
Ruixue Tong,
Chinese Academy of Fishery Sciences (CAFS), China

*CORRESPONDENCE
Xiaochuan Zheng
zhengxiaochuan@ffrc.cn
Bo Liu
liub@ffrc.cn

†PRESENT ADDRESS
Bo Liu,
Freshwater Fisheries Research Center,
Chinese Academy of Fishery Sciences,
Wuxi, China

RECEIVED 14 August 2024
ACCEPTED 04 November 2024
PUBLISHED 26 November 2024

CITATION
Liu M, Sun C, Zhou Q, Xu P, Wang A, Zheng X and Liu B (2024) Supplementation of Yupingfeng polysaccharides in low fishmeal diets enhances intestinal health through influencing the intestinal barrier, immunity, and microflora in *Macrobrachium rosenbergii*. *Front. Immunol.* 15:1480897.
doi: 10.3389/fimmu.2024.1480897

Supplementation of Yupingfeng polysaccharides in low fishmeal diets enhances intestinal health through influencing the intestinal barrier, immunity, and microflora in *Macrobrachium rosenbergii*

Mingyang Liu[1,2], Cunxin Sun[1,2], Qunlan Zhou[1,2], Pao Xu[1,2], Aimin Wang[3], Xiaochuan Zheng[1,2]* and Bo Liu[1,2*†]

[1]Key Laboratory of Freshwater Fisheries and Germplasm Resources Utilization, Ministry of Agriculture and Rural Affairs, Freshwater Fisheries Research Center, Chinese Academy of Fishery Sciences, Wuxi, China, [2]Wuxi Fisheries College, Nanjing Agricultural University, Wuxi, China, [3]College of Marine and Biology Engineering, Yancheng Institute of Technology, Yancheng, China

Introduction: This study aimed to investigate the effects of a low-fishmeal diet (LF, substituting soybean meal for 40% fish meal) and the supplementation of 500 mg/kg and 1000 mg/kg Yu Ping Feng (YPF) polysaccharides on the growth performance, antioxidant enzyme activities, intestinal ultrastructure, non-specific immunity, and microbiota of *Macrobrachium rosenbergii*.

Methods: The study involved the administration of different diets to M. rosenbergii, including a control diet, a low-fishmeal diet (LF), and LF diets supplemented with 500 mg/kg and 1000 mg/kg YPF polysaccharides. Growth performance, antioxidant enzyme activities, intestinal ultrastructure, non-specific immunity, and microbiota were assessed.

Results: The LF diet significantly reduced growth performance parameters compared to the control group. However, YPF supplementation notably improved these parameters, with the greatest improvement observed at a 1000 mg/kg dosage. Antioxidant enzyme activities (SOD, GSH-PX) were diminished in the LF group, accompanied by elevated MDA levels, whereas YPF supplementation restored these activities and reduced MDA levels. Ultrastructural analysis revealed that the LF diet caused intestinal villi detachment and peritrophic matrix (PM) shedding, which were alleviated by YPF. Gene expression related to PM formation (GS, CHS, EcPT) was downregulated in the LF group but significantly upregulated in the 1000P group. Non-specific immune gene expressions (IMD, Relish, IκBα) and enzyme activities (NO, iNOS) were suppressed in the LF group but enhanced by YPF supplementation. Microbial community analysis showed reduced diversity and altered composition in the LF group, with increased Proteobacteria and decreased Firmicutes, which were partially restored by YPF. Correlation analysis revealed that *Lactobacillus* and *Chitinibacter* play pivotal roles in regulating intestinal health. *Lactobacillus* exhibited a positive relationship with the intestinal PM and immune-related indicators, whereas *Chitinibacter* was negatively associated with these factors.

Discussion: These results highlight the adverse impacts of a low-fishmeal diet on the intestinal health of M. rosenbergii and demonstrate the beneficial effects of

YPF polysaccharides in alleviating these negative consequences through various mechanisms, including improved growth performance, enhanced antioxidant enzyme activities, restored intestinal ultrastructure, and modulated immune responses. The findings suggest that YPF supplementation could be a valuable strategy for mitigating the negative effects of low-fishmeal diets in aaquaculture.

KEYWORDS

Yupingfeng polysaccharides, alternative fish meal diet, peritrophic matrix, intestinal immunity, intestinal microbes, *Macrobrachium rosenbergii*

1 Introduction

The surge in global raw material and labor costs has intensified inflation, a trend particularly evident in the aquaculture feed industry, highlighted by the sharp increase in fishmeal prices (1). As economic globalization advances, the demand for high-protein aquaculture feeds rich in fishmeal has risen steadily across countries, pushing up the market price of premium fishmeal. This has prompted an urgent need within the industry to seek economically viable alternative protein sources to partially replace the expensive fishmeal in aquaculture feeds. Plant proteins, known for their high protein content, cost-effectiveness, balanced amino acid composition, and high digestibility, have become ideal substitutes for fishmeal (2). Prudent replacement of fishmeal with plant proteins not only lowers feed costs but also preserves wild resources and reduces environmental impact (3).

However, the extensive replacement of fishmeal with plant proteins in aquaculture feeds may lead to adverse effects, including reduced digestibility, stunted growth, intestinal mucosal damage, and diminished antioxidant activity and immune competence in aquatic animals (4, 5). Moreover, excessive use of plant proteins may disrupt the balance of intestinal microbiota in aquatic organisms, impairing intestinal barrier function, reducing nutrient digestion and absorption, and inducing intestinal inflammation (6, 7). Studies have shown that the substitution of fishmeal with plant protein sources such as soybean meal results in a decrease in the relative abundance of beneficial intestinal bacteria and an increase in pathogenic bacteria in aquatic animals (8, 9). The peritrophic matrix (PM), a critical structure in the intestines of crustaceans, composed of chitin and proteins, plays a vital role in maintaining intestinal health and immune function (10). It serves not only as a physical barrier preventing direct contact of pathogens with intestinal cells but also regulates immune responses, promotes nutrient absorption, influences the balance of intestinal microbiota, and enhances the host's defense against pathogens, collectively maintaining the intestinal health and overall immune status of crustaceans (11, 12). Previous research has indicated signs of PM dissolution in crustaceans such as *Eriocheir sinensis* under low-fishmeal diets (13). Therefore, identifying a feed additive that can protect the morphology of the PM and maintain intestinal health and microbiota balance is of paramount importance.

In recent years, to mitigate the adverse effects of plant protein substitution on aquatic animals, there has been a growing focus on using Chinese herbal polysaccharides as feed additives (14, 15). Notably, Yu Ping Feng (YPF) polysaccharide has been shown to exert a significant immunomodulatory effect, positively enhancing the immune function of aquatic animals (16). YPF is a traditional Chinese medicine compound consisting of Astragalus membranaceus, Atractylodes macrocephaia Koiz, and Saposhnikovia divaricata (17). The active components of these herbs, such as polysaccharides, flavonoids, and polyphenols, are particularly notable for their immunomodulatory effects, as demonstrated in numerous studies. For instance, flavonoids and plant polyphenols have been shown to enhance the activity of natural killer cells and improve immune response (18, 19). Polysaccharides, while known for their prebiotic properties, promote the growth of beneficial intestinal bacteria. As a mixture of these three herbs, YPF polysaccharide possesses a more diverse array of bioactive components compared to any single herb or combination of two herbs (20). In aquaculture, YPF polysaccharide not only exhibits superior growth-promoting effects but also improves intestinal function, enhances intestinal digestive enzyme activity and antioxidant capacity, and increases animal growth performance (16). In mammals, YPF polysaccharide has shown significant benefits in promoting the colonization of beneficial bacteria in the intestine and treating intestinal microbial dysbiosis caused by pathogens (21). However, research on the impact of YPF polysaccharide on PM formation and its role in maintaining intestinal health and microbiota balance remains insufficient.

Macrobrachium rosenbergii, a globally cultivated prawns species, holds significant economic value and serves as an important model for studying crustacean nutrition, metabolism, and immunology. The intestine plays a pivotal role in the nutritional absorption, immune defense, and overall health of crustaceans. This vital organ not only facilitates the efficient uptake of essential nutrients but also serves as a first line of defense against pathogenic invasions (22). Previous research has

10.3389/fimmu.2024.1480897

investigated the intestinal immune regulation and host health in *M. rosenbergii* (23), while recent studies have increasingly highlighted the role of gut microbiota in health and immune regulation among crustaceans (24). Developing feed additives for low-fishmeal diets in *M. rosenbergii* to enhance intestinal health is economically and scientifically significant. This study evaluates the potential of YPF polysaccharide to promote growth, protect intestinal morphology, and maintain health, thereby supporting sustainable aquaculture.

2 Materials and methods

2.1 Experimental animals and ethical statement

M. rosenbergii with an average body weight of 0.15 ± 0.01g were procured from the Freshwater Fisheries Research Center (FFRC) of the Chinese Academy of Fishery Science (CAFS). These prawns were temporarily housed for a period of seven days in three aerated tanks (dimensions: R × H, 1.0 m × 1.5 m) and were provided with commercial feed from Fuyuda Food Products Co. LTD, China, prior to the commencement of formal breeding experiments.

The experimental protocol adhered to the guidelines for scientific breeding and ethical use of animals, which were informed by our previously published work (1).

2.2 Experimental design and conditions

Based on our previous findings from growth and biochemical studies investigating the effects of YPF polysaccharide supplementation at concentrations ranging from 0 to 1000 mg/kg (Supplementary Tables S1, S2), we have formulated experimental diets. Formulating low fishmeal diets by replacing 40% of fishmeal with soybean meal. The experimental diets, as detailed in Table 1, comprise four distinct formulations: the normal fish meal diet (NF), the low fishmeal diet (LF), and the LF diet supplemented with 500 mg/kg (500P) and 1000 mg/kg YPF polysaccharide (1000P). Fish oil and soybean oil were included as lipid sources, and plant and animal meals were used as carbohydrate sources. Bentonite served as a feed binder, while squid paste acted as a feeding attractant. The actual concentrations of YPF polysaccharide were 500 and 1000 mg/kg, respectively. The ingredients were thoroughly mixed with an appropriate amount of water. The dough was then passed through a mincer, producing 1-mm-diameter strings. After drying in cool and shady conditions, the diets were broken up and stored in a refrigerator at -20°C until use.

In addition, a total of 480 prawns with an initial body weight of 0.15 ± 0.01 g were distributed into twelve tanks (dimensions: 1.0 m × 1.5 m), with 40 prawns per tank. Twelve tanks were randomly assigned to three experimental diet groups and one control group. Prawns were provided feed three times daily at 8:00, 13:00, and 18:00 until apparent satiation. Residual feed was collected using 80 mesh net bags one hour post-feeding.

TABLE 1 Ingredients and proximate chemical composition of the experimental diets.

Ingredients (%)	Groups			
	CT	LF	500P	1000P
Fish meal[a]	25.00	15.00	15.00	15.00
Soybean meal[b]	19.00	33.00	33.00	33.00
Rapeseed meal	15.50	15.50	15.50	15.50
Shrimp powder	4.00	4.00	4.00	4.00
Squid paste	3.00	3.00	3.00	3.00
α -starch	20.50	15.71	15.71	15.71
Fish oil:soybean oil (1:1)	2.00	2.70	2.70	2.70
Chellocken meal	3.00	3.00	3.00	3.00
Poultry by-product powder	2.00	2.00	2.00	2.00
Soybean phospholipids	1.00	1.00	1.00	1.00
Cholesterol	0.50	0.50	0.50	0.50
$Ca(H_2PO_4)_2$	2.00	2.00	2.00	2.00
Choline chloride	1.00	1.00	1.00	1.00
Remix[c]	1.00	1.00	1.00	1.00
Bentonite	0.990	0.990	0.940	0.890
Ecdysone (10%)	0.01	0.01	0.01	0.01
Yupingfeng polysaccharide	0.00	0.00	0.05	0.1
Proximate Composition				
Crude protein	38.36	38.28	38.28	38.28
Ether extract	8.24	8.23	8.23	8.23
Gross energy	17.89	17.70	17.70	17.70

[a]Crude protein of fish meal: 65.57%; [b]Crude protein of cottonseed protein concentrate: 65%; [c] Vitamins and mineral premix (IU, g or mg kg-1 of diet): vitamin A, 25000 IU; vitamin D3, 20000 IU; vitamin E, 0.2 g; vitamin K3, 0.02 g; ammonium sulfate, 0.04 g; riboflavin, 0.05g; calcium pantothenate, 0.01g; pyridoxine hydrochloride, 0.04g; vitamin B12, 0.2 mg; biotin, 6mg; folic acid, 20 mg; nicotinic acid, 200 mg; inositol, 1g; vitamin C, 2g; choline, 2g; calcium dihydrogen phosphate, 20g; sodium chloride, 2.6g; potassium chloride, 5 g; magnesium sulfate, 2000mg; ferrous sulfate, 900 mg; zinc sulfate, 60 mg; copper sulfate, 20 mg; magnesium sulfate, 30 mg; sodium selenate, 20 mg; cobalt chloride, 50mg; potassium iodide, 4mg.

2.3 Growth evaluation

Post the 8-week feeding trial, the survival rate, final body weights, and body lengths of prawns within each group were recorded. Concurrently, the tail muscle of the prawns was isolated and weighed. The weight gain rate, specific growth rate, coefficient of fatness, and flesh rate were calculated using the following methodologies:

Weight gain rate (WGR, %) = (Body weight (g) – Initial weight (g))/initial weight × 100

Specific growth rate (SGR, %/day) = (Ln Body weight – Ln initial weight) × 100/days

Feed conversion ratio (FCR) = Dry feed intake (g)/weight gain (g)

Coefficient of condition (CF) = Body weight (g)/Body length $(cm)^3$

Flesh rate (FR) = (Muscle weight (g)/Body weight) × 100

2.4 Samples collection

Following an 8-week feeding trial, 6 prawns were randomly selected from each tanks (18 per group) for further analysis. Initially, Elsevier's solution, comprising 13.2g/L trisodium citrate, 4.8g/L citric acid, and 14.7g/L glucose, was employed as an anticoagulant to facilitate the collection of hemolymph. Adhering to the methodology outlined by Rodriguez et al., a 1ml syringe was de-aired, filled with 200μl of anticoagulant, and used to extract hemolymph from the thoracic region of the prawns, maintaining a 1:1 ratio of hemolymph to anticoagulant. The resultant mixtures were then centrifuged at 4000 rpm for 10 minutes at 4°C to separate the hemolymph from blood cells, with the supernatant from three prawns in each replicate being transferred to a 1.5 ml centrifuge tube.

Subsequently, the prawns were dissected to procure midgut and chyme samples. The intestines from three prawns were randomly mixed in each replicate and placed into a 2 ml cryogenic vial, with the chyme being similarly stored. These cryogenic vials were subsequently snap-frozen in liquid nitrogen and stored at -80°C for subsequent analysis. Additionally, three intestines from each diet were randomly collected, fixed in a solution of 4% paraformaldehyde and 2.5% glutaraldehyde (supplied by Macklin Biochemical Co., Ltd, Shanghai, China) for histological and transmission electron microscopy (H&E and TEM) analysis, respectively. The remaining prawns samples were immediately stored in a freezer at -80°C to serve as a reserve for supplementing any insufficient test samples.

2.5 Enzyme activity analysis

In accordance with the methodologies delineated in our prior research (25), the activities of superoxide dismutase (SOD), catalase (CAT), and glutathione peroxidase (GSH-Px) in hemolymph were quantified using commercial bioengineering kits from the Nanjing Jiancheng Institute. These enzyme activities were assessed via a Spectra Max Plus spectrophotometer (Molecular Devices, Menlo Park, CA, USA), with measurements taken at wavelengths of 450 nm, 550 nm, 420 nm, and 530 nm, respectively. The concentration of malondialdehyde (MDA) in the hemolymph was determined through the thiobarbituric acid (TBA) method, with quantification performed at a wavelength of 532 nm (26).

For the determination of intestinal enzyme activities, including SOD, CAT, GSH-Px, inducible nitric oxide synthase (iNOS), nitric oxide (NO), and lysozyme (LZM), as well as MDA and lipopolysaccharide (LPS), a pretreatment protocol is necessary. This protocol is adapted from the previously published work by Liu et al. (27). Following the extraction of the supernatant for subsequent enzyme activity analysis, the parameters for intestinal SOD, CAT, GSH-Px, MDA, NO, iNOS, LZM, and LPS were measured analogously to those of the hemolymph. The activities of intestinal NO and iNOS were analyzed using commercial bioengineering kits from the Nanjing Jiancheng Institute, with measurements taken at wavelengths of 550 nm and 530 nm, respectively. The analyses of LZM and LPS were conducted using commercial bioengineering kits from Beijing Solarbio Co., Ltd., with measurements performed at wavelengths of 530 nm and 420 nm, respectively.

2.6 H&E, TUNEL and Oil Red O stainings

Fixed intestine samples, initially preserved in a 4% paraformaldehyde buffer, were subsequently embedded in optimum cutting temperature (OCT) compound and stored at -80°C. Following the protocol detailed in our published work (28), Hematoxylin-eosin (H&E) staining was performed on the intestine samples, and the resulting microstructures were imaged using a Leica DM1000 optical microscope (Wetzlar, Germany). Intestinal tissue, previously fixed in a 2.5% glutaraldehyde solution, was subjected to preprocessing and sectioning in accordance with the methodology described by Xie et al. (29). The cellular ultrastructure was then examined using a transmission electron microscope (Hitachi HT7700, Japan).

2.7 Quantitative real-time RT-PCR validation

According to the fragments obtained from the earliest intestine transcriptome determined initially in our laboratory and the ORF intercepted, designing the gene primer by Primer 5.0 for qRT-PCR analysis (Table 2). Choosing β-actin serves as an internal reference due to its stable expression. Jiangsu Gencefe Biotechnology Co., LTD synthesized PCR primers.

The total RNA of the intestine in the four experimental groups (three intestine mixtures per replicate) was extracted with RNAiso Plus (TaKaRa, Japan). Then, the concentration was determined with Nanodrop 2000 (Thermo Fisher Scientific, Waltham, Massachusetts, USA). The RNA concentration of each sample was diluted to 400 ng/mL. According to the manufacturer's directions, First-strand cDNA was generated from 400 ng DNase-treated RNA using an HiScript III 1st Strand cDNA Synthesis Kit (Vazyme Biotech Co., Ltd., Nanjing, China). Use the Two-Step SYBR® Prime Script® Plus RT-PCR Kit (TaKaRa, Japan) for the quantitative analysis of 2 μg of total RNA. The total system of sample loading was 20 μL. Based on Sun et al. (28), the PCR reaction conditions were as follows: 95°C for 30 s, followed by 40 cycles of 95°C for 5 s and 60°C for 30 s. The specificity of the primers was evaluated by melting curves and electrophoresis. The Bio-Rad CFX96 (Bio-Rad Laboratories, Inc., Hercules, USA) real-time PCR system was employed for real-time quantitative reverse transcription PCR (qRT-PCR). The $2^{-\Delta\Delta CT}$ method was utilized to calculate the relative gene expression (30).

TABLE 2 PCR primer sequence of gene of *M. rosenbergii*.

Gene	Primer sequences (5′-3′)	Bp	Size	E (%)	Sequence source
Toll	(F) TTCGTGACTTGTCGGCTCTC (R) GCAGTTGTTGAAGGCATCGG	20	194	103.21	KX610955.1
Dorsal	(F) TCAGTAGCGACACCATGCAG (R) CGAGCCTTCGAGGAACACTT	20	280	94.52	KX219631.1
IMD	(F) CGACCACATTCTCCTCCTCCC (R) TTCAGTGCATCCACGTCCCTC	21	235	94.59	OR602697
Relish	(F) GATGAGCCTTCAGTGCCAGA (R) CCAGGTGACGCCATGTATCA	20	140	106.32	KR827675.1
IkBα	(F)AATCATACCGGAAGGACGGCGTTA (R)TCACGGGTCTGGTTAATTGGGTCA	24	280	100.69	HQ668091.1
GS	(F) AGCCTGCCTCTACACTGGTA (R) TGACGCCGAAATCTTCAGCT	20	163	98.37	Imaizumi et al., 2023
CHS	(F) ACCCATTGGTTTGGTGTTCG (R) TATGCGAAATGGTGCCGAAG	20	109	99.12	Lu et al., 2019
EcPT	(F) TTGTGACTGGCCACAGAACG (R) GGCGAGACTGCTTGTCGAAT	20	234	97.84	Wang et al., 2013
β-actin	(F) TCCGTAAGGACCTGTATGCC (R) TCGGGAGGTGCGATGATTTT	20	126	90.08	KX610955.1

E, reaction efficiencies.

2.8 Bacterial 16S rRNA gene amplification, cDNA library construction and sequencing

To characterize the diversity and structure of microbial communities, the 16S rDNA V3-V4 region of the ribosomal RNA gene was amplified via PCR (95°C for 2 min, followed by 27 cycles at 98°C for 10 s, 62°C for 30 s, and 68°C for 30 s, with a final extension at 68°C for 10 min) using the primers 338F: ACTCC TACGGGAGGCAGCAG and 806R: GGACTACHVGGGTWTCT AAT, where the barcode is an eight-base sequence unique to each sample. PCR reactions were conducted in triplicate 50 μL mixtures, following the methodology of Xue et al. (31). All PCR products were extracted from 2% agarose gels and purified using the Merck DNA Gel Extraction Kit (Merck Sigma-Aldrich, Darmstadt, Germany) according to the manufacturer's instructions, and quantified using the Bio-Rad CFX96 Real-Time PCR System (Bio-Rad Laboratories, Inc., Hercules, USA). Purified PCR amplicons were pooled in equimolar concentrations and subjected to paired-end sequencing (2 × 250) on an Illumina platform, adhering to standard protocols provided by the manufacturer.

Following these steps, clean reads were obtained. Barcode and linker sequences were removed, and paired-end reads were combined into longer fragments. Reads with average quality scores below 20 and lengths less than 100 bp were excluded. Sequences with mismatched primer sequences or ambiguous bases (Ns) exceeding 5% were removed from downstream analyses. Unassembled reads were discarded. Spliced paired-end sequences were generated using FLASH. Chimeric sequences were eliminated using VSEARCH. Sequences were then clustered into operational taxonomic units (OTUs) at a 97% sequence similarity threshold using UPARSE (version 7.1), and taxonomic classifications were annotated in the RDP database (1).

Microbial variation was assessed through a multifaceted analytical approach. Principal coordinate analysis (PCoA) and heatmaps depicting the composition of operational taxonomic units (OTUs) were generated using R software. The Stamp tool, accessible through the Tutools platform (http://www.cloudtutu.com/), was employed to discern differences in microbial abundance at the genus level among the three dietary treatments. The Kruskal-Wallis test was utilized to evaluate differences across all samples, and KEGG histograms were produced using Prism software version 8.0. Correlation analysis between intestinal microbes and metabolites was performed with R software, resulting in the generation of network diagrams. These network diagrams were subsequently refined using the Gephi software.

2.9 Statistical analysis

All experimental results were presented as mean ± standard error of the mean (S.E.M.). The Duncan multiple range test was employed to assess the differences among the four groups. Significant differences ($p < 0.05$) among different groups are indicated by different lowercase letters on the histogram. The statistical analysis was conducted using SPSS software version 16.0 (SPSS Inc., Michigan Avenue, Chicago, IL, U.S.A.). Pearson correlation analysis was utilized to examine the relationship between two variables that met the criteria for normality, with the following significance indicators: a single asterisk (*) denoted a significant difference ($p < 0.05$), and a double asterisk (**) signified a highly significant difference ($p < 0.01$).

3 Result

3.1 Growth performance

As shown in Figure 1, BW (body weight), WGR (weight gain rate), and CF (condition factor) in the LF group were significantly lower than in the CT group ($p < 0.05$). The inclusion of YPF polysaccharides in LF diets resulted in increased levels of BW, WGR, SGR, and CF ($p < 0.05$). Particularly significant improvements were observed in the 1000P group, as the WGR in the 1000P group was significantly higher than that in the 500P group ($p < 0.05$). Conversely, the FCR in the LF group was significantly higher than in the other three groups ($p < 0.05$). Lastly, there were no statistically significant differences in FR (flesh rate) and SR (survival rate) among the four groups ($p > 0.05$).

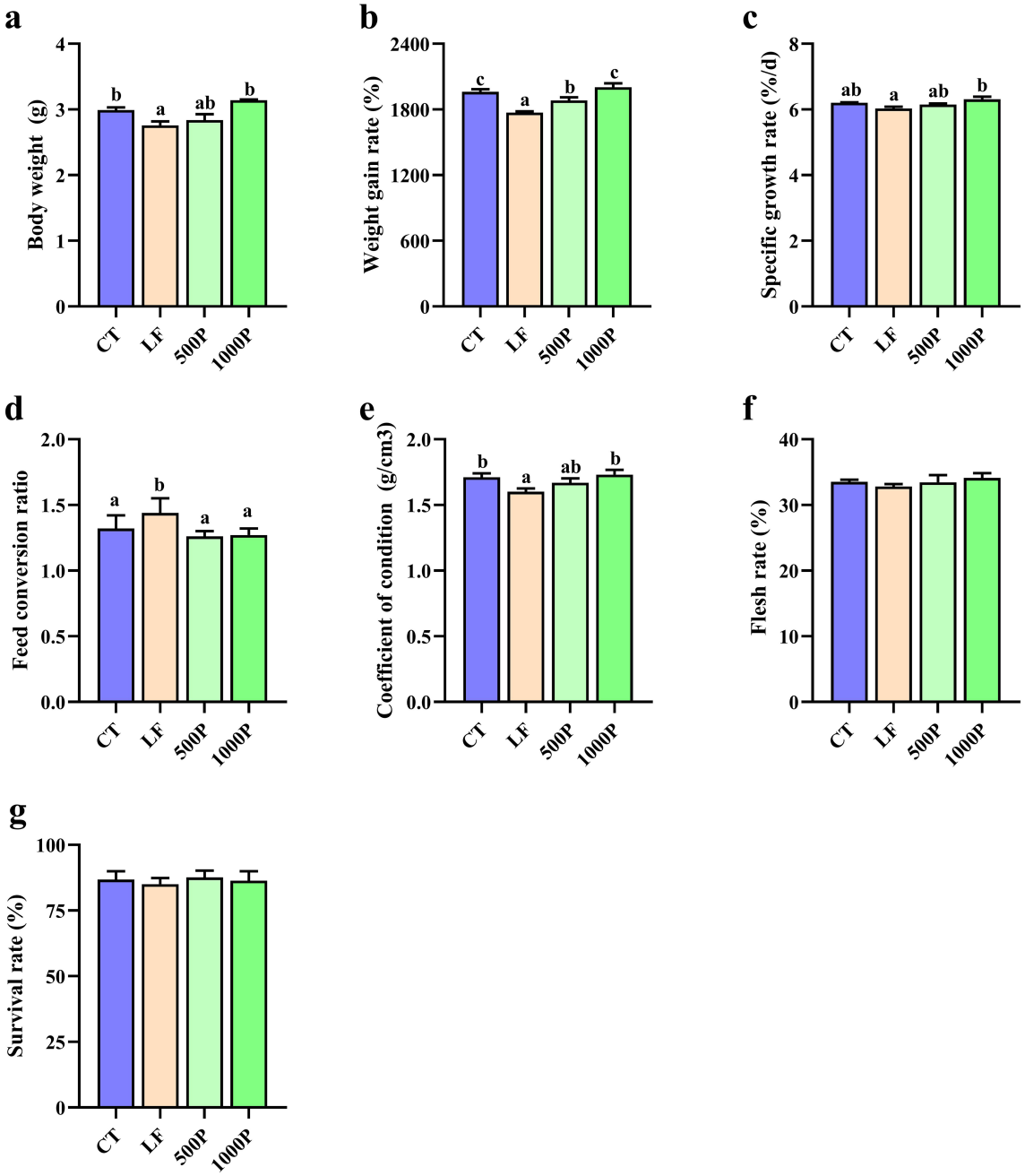

FIGURE 1
Effects of four diet on growth evaluation of *M. rosenbergii*. The six indicators body weight **(A)**, weight gain rate **(B)**, specific growth rate **(C)**, Feed conversion ratio **(D)**, coefficient of condition **(E)**, flesh rate **(F)** and survival rate **(G)** were compared in each group. Significant differences between the four groups are indicated by different lowercase letters ($p < 0.05$).

3.2 Antioxidant enzyme activity in hemolymph and intestine

Four dietary groups exhibited significantly different levels of antioxidant enzyme activity in the hemolymph and intestine (Figure 2). Both in the hemolymph and intestine, compared to the CT group, the LF group showed significantly reduced levels of SOD and GSH-PX, MDA content was significantly elevated ($p < 0.05$). In addition, the 500P and 1000P groups, which were supplemented with YPF polysaccharides, exhibited significantly elevated levels of SOD and GSH-PX and significantly reduced levels of MDA compared to the LF group ($p < 0.05$). Moreover, the 1000P group exhibited a more pronounced effect. Notably, the CAT levels in the hemolymph of the LF group did not exhibit significant differences compared to the other three groups ($p > 0.05$); however, mirroring the results observed for SOD in the gut, the addition of 1000 mg/kg YPF polysaccharides to the LF group led to CAT levels that were higher than those in the control group.

3.3 Ultrastructural observation of the intestine

As shown in Figure 3A, intestinal villi of the control group are neatly arranged and closely connected to the basement membrane (BM), with R cells evenly and densely distributed on the intestinal villi. In contrast, the LF group exhibited detachment of intestinal villi from the BM, accompanied by a visible reduction in R cells, and the shedding of the PM was also observed. However, the addition of YPF polysaccharide to the LF group alleviated the detachment of the BM and the reduction of R cells, and the shedding of the PM also seemed to be improved. Statistically, the BM thickness and the number of R cells in the LF group were significantly lower compared to the other three groups ($p < 0.05$); Furthermore, these two indicators in the YPF polysaccharide-supplemented group were significantly lower than those in the control group ($p < 0.05$, Figure 3B).

Further observation of the structure of intestinal microvilli using transmission electron microscopy revealed that the LF group exhibited extensive shedding, necrosis, and scattered distribution of microvilli, with no perisoteal membrane observed to be tightly attached to the microvilli compared to the CT group (Figure 3C). However, the addition of YPF polysaccharide improved the damaged structure of intestinal microvilli and the perisoteal membrane, especially after the addition of 1000 mg/kg of YPF polysaccharide, where the microvilli on the surface of the intestinal epithelial cells were evenly distributed and neatly arranged, and the perisoteal membrane was tightly attached to the microvilli.

3.4 Determination of intestinal peritrophic matrix related indicators

As shown in Figure 4A, significant alterations in the expression levels of several genes involved in peritrophic matrix formation were evident. The expression level of the *GS*, *CHS* and *EcPT* gene

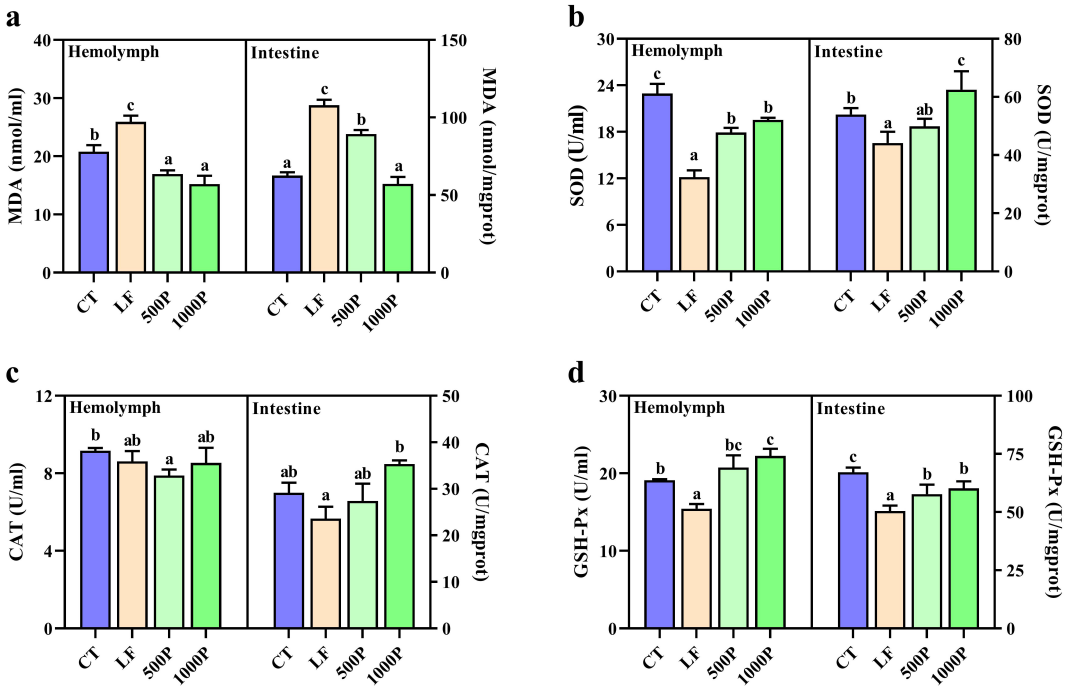

FIGURE 2
Related antioxidant enzyme activities in hemolymph and intestines of *M. rosenbergii* during the experimental period. **(A)** MDA, malondialdehyde. **(B)** SOD, superoxide dismutase. **(C)** CAT, catalase. **(D)** GSH-Px, glutathione peroxidase. Significant differences between the four groups are indicated by different lowercase letters ($p < 0.05$).

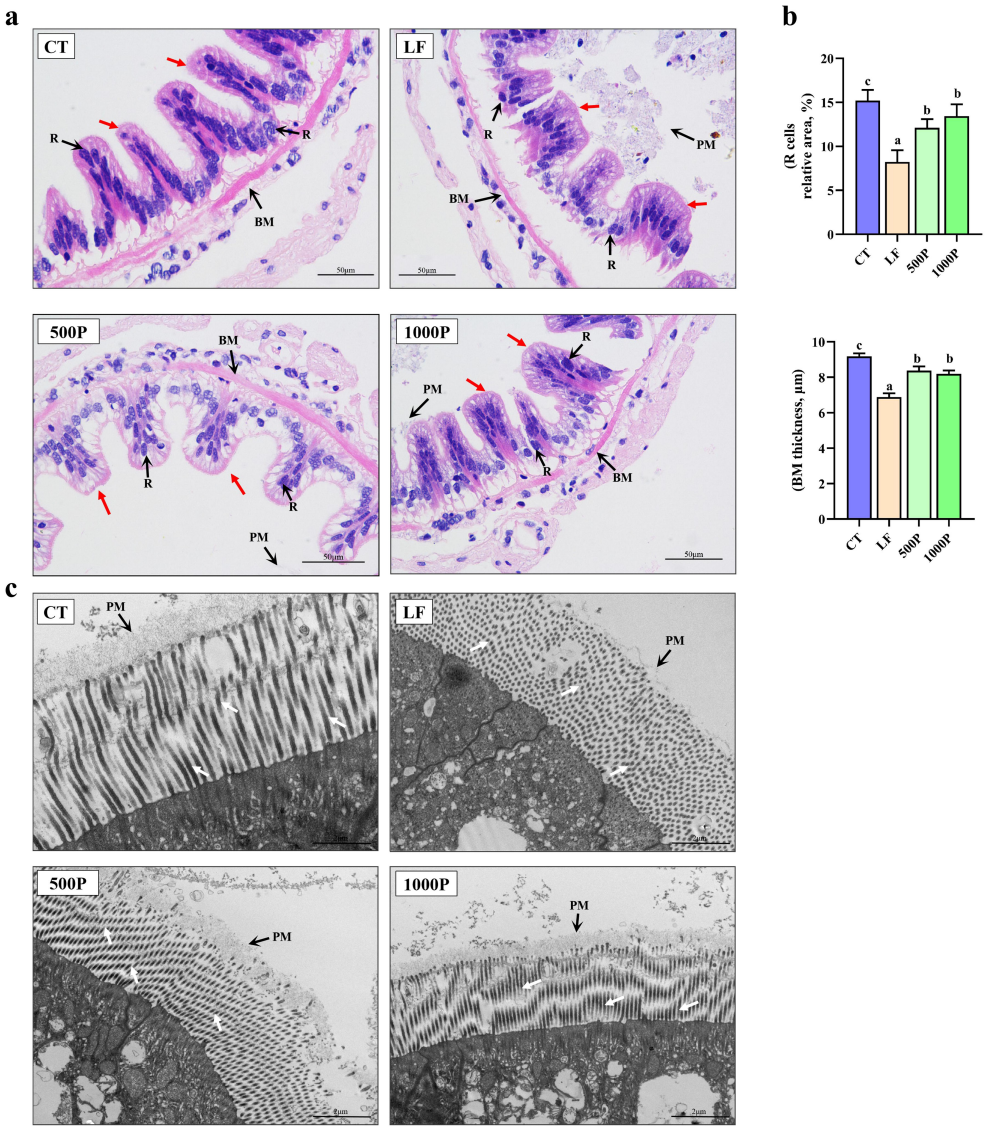

FIGURE 3
Intestinal histological structure alterations of *M. rosenbergii*. **(A)** Microscopy of H & E stained intestinal structures. PM, Peritrophic Matrix; R, Regenerative Cell; BM, Basement Membrane. **(B)** The relative R cell area and BM thickness. **(C)** Transmission electron microscopy of intestinal structure. Red arrows represent intestinal villus, white arrows represent intestinal microvilli. Significant differences between the four groups are indicated by different lowercase letters ($p < 0.05$).

in the LF group was significantly decreased compared to the control group, and it was also markedly lower when compared to the 1000P group ($p < 0.05$). Additionally, the expression levels of *EcPT* in the 1000P group exhibited a significant increase compared to those in the control. It is noteworthy that the trends in the levels of LZM and LPS also exhibited opposite patterns (Figure 4B). The LZM level in the LF group was significantly lower than in the other three groups ($p < 0.05$), whereas the LPS level was significantly elevated ($p < 0.05$).

3.5 Determination of intestinal non-specific immunity related indicators

As depicted in Figure 5A, both the LF group and the addition of YPF polysaccharide at 1000 mg/kg exerted significant effects on the relative expression levels of genes associated with non-specific immunity in *M. rosenbergii*. The expression levels of *IMD* and *Relish* mRNA in the LF group were significantly lower than those in the control group ($p < 0.05$); however, after the addition of 1000 mg/kg YPF polysaccharide, the expression levels of *IMD* and *Relish* mRNA significantly increased ($p < 0.05$). For *IκBα*, both the control group and the YPF polysaccharide-supplemented group exhibited significantly lower expression levels compared to the LF group ($p < 0.05$). Additionally, there were no significant differences in the expression levels of *Toll* and *Dorsal* mRNA among four groups ($p > 0.05$).

Figure 5B illustrates the activity levels of two enzymes associated with non-specific immune responses in prawns. It was observed that the levels of NO and iNOS in the LF group were significantly reduced compared to the control ($p < 0.05$). However, after the addition of 1000 mg/kg YPF polysaccharide, the activity

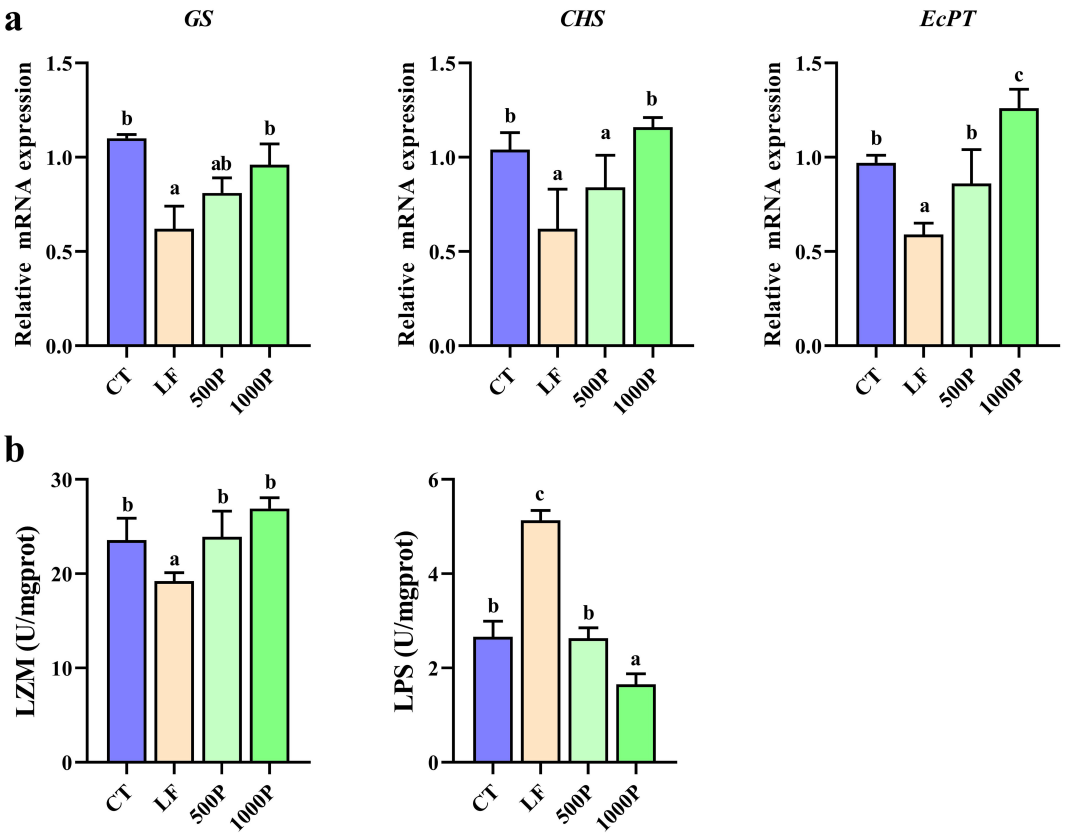

FIGURE 4
Changes in peritrophic matrix-related genes and enzymes in *M. rosenbergii*. **(A)** Gene mRNA expression of glutamine synthetase (GS), chitin synthase (CHS) and peritrophin-like protein (EcPT). **(B)** Related antioxidant enzyme activities of lysozyme (LZM) and lipopolysaccharide (LPS). Significant differences between the four groups are indicated by different lowercase letters ($p < 0.05$).

levels of these two enzymes significantly increased in comparison to the LF group ($p < 0.05$), reaching levels comparable to those of the control.

3.6 Alterations in the microecological structure in the intestine

Due to previous results indicating that the addition of 1000 mg/kg YPF polysaccharide had a more pronounced effect compared to the addition of 500 mg/kg, the structural changes in the intestinal microbiota were only compared among the 1000P group, the control group, and the LF group (Figure 6). The principal coordinate analysis (PCoA) results showed that the microbial composition in the LF group was evidently different from the control and 1000P groups (Figure 6A). Compared to the LF group, the microbial community in the CT and 1000P groups exhibited shorter dispersal distances. Meanwhile, Observed_species, Goods_coverage, Chao1, Shannon, and Simpson indices were calculated based on the OTUs to evaluate each group's microbial community diversity (Figure 6B). The Observed_species, Chao1, and Shannon in the LF group were significantly lower than in the CT and 1000P groups ($p < 0.05$). In addition, the Simpson results showed that there were no statistically significant differences among the three groups ($p > 0.05$).

The analysis of microbial composition revealed that at the phylum level (Figure 6C), Proteobacteria, Firmicutes, Bacteroidetes, and Tenericutes were the predominant bacteria in the intestinal microecology of prawns across the three groups. Specifically, when examining the microbial composition of each group (Figure 6E), it was observed that in the LF group, the levels of Proteobacteria and Tenericutes were significantly higher than those in the control group and the 1000P group, whereas the level of Firmicutes was significantly lower than in these two groups ($p < 0.05$). Additionally, compared to the control group, the level of Firmicutes in the 1000P group was significantly increased, while the level of Proteobacteria was significantly decreased ($p < 0.05$). At the genus level shown in Figure 6D, *Lactococcus*, *Aeromonas*, *Chitinibacter*, *Candidatus Hepatoplasma*, *Klebsiella*, *Pseudomonas*, and *Lactobacillus* were the dominant bacterial genera across the three groups. Comparing the levels of each genus within each group (Figure 6F), it was found that compared to the CT group and the 1000P group, the levels of *Aeromonas*, *Klebsiella*, and *Pseudomonas* were significantly increased in the LF group, while the levels of *Lactococcus* and *Lactobacillus* were significantly decreased ($p < 0.05$). Notably, the level of *Lactobacillus* in the 1000P group was significantly higher than

10.3389/fimmu.2024.1480897

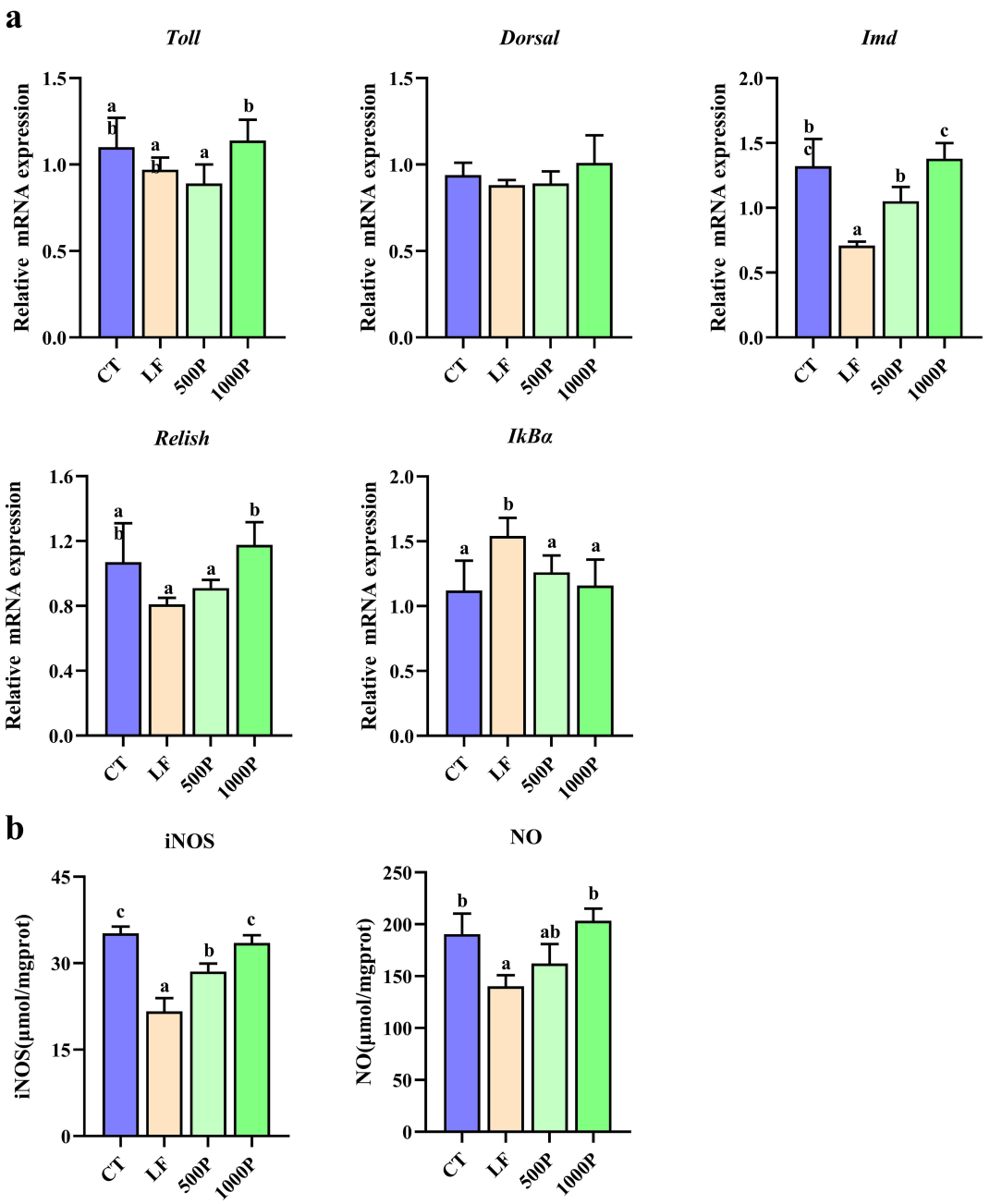

FIGURE 5
Changes in non-specific immunity related genes and enzymes in *M. rosenbergii*. **(A)** Gene mRNA expression. **(B)** Related antioxidant enzyme activities of inducible nitric oxide synthase (iNOS) and nitric oxide (NO). Significant differences between the four groups are indicated by different lowercase letters ($p < 0.05$).

in the control group, whereas the results for *Pseudomonas* and *Candidatus Hepatoplasma* were opposite ($p < 0.05$).

3.7 Enrichment function of intestinal microorganisms

The prediction of the function of intestinal microorganisms in different diets is shown in Figure 7. The secondary function prediction (Figure 7A) showed that the LF group decreased the abundance of Cancers: Specific types, Cellular community-prokaryotes, Amino acid metabolism, and Cell motility pathways compared to the other two groups, and increased the abundance of Cellular community-eukaryotes, Carbohydrate metabolism, and Endocrine and metabolic diseases pathways ($p < 0.05$).

In addition, in tertiary function prediction (Figure 7B), the abundance of Galactose metabolism, Fructose and mannose metabolism, and Pentose and glucuronate interconversions in the LF group was lower than in the CT and 1000P groups. It's worth noting that the 1000P group predicted a higher abundance of the

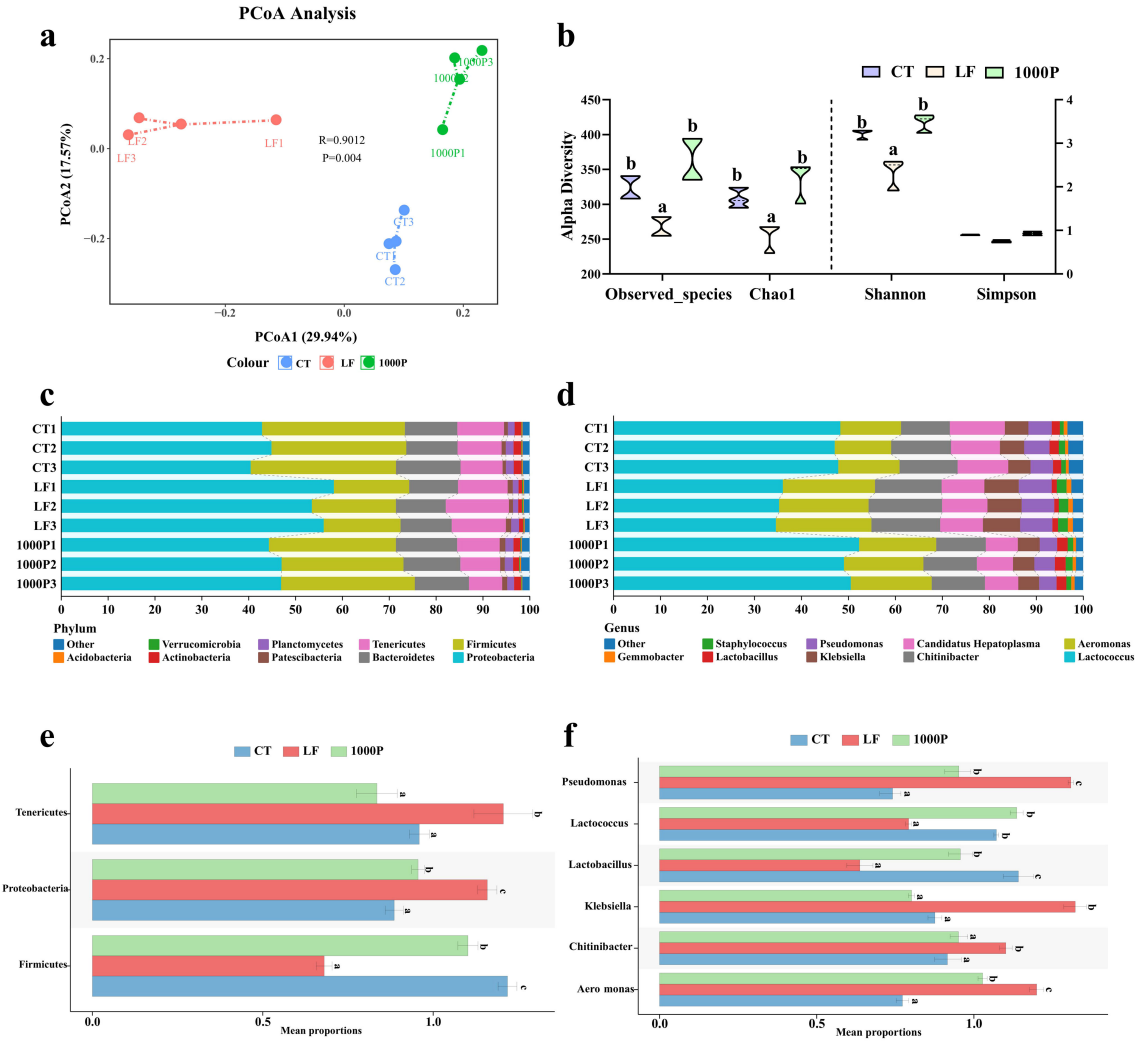

FIGURE 6
Effects of three diets on the intestinal microflora. **(A)** Principal coordinate analysis of community. **(B)** Alpha diversity indices. **(C, D)** Histogram analysis of microbial taxonomic composition at phylum and genus levels in the top ten, respectively. **(E, F)** Microbial comparation analysis on phylum and genus level. Significant differences between the four groups are indicated by different lowercase letters ($p < 0.05$).

Synthesis and degradation of ketone bodies, Oxidative phosphorylation, Glycolysis/Gluconeogenesis, Citrate cycle (TCA cycle), and Purine metabolism pathways than in the LF group, even in the CT group ($p < 0.05$).

3.8 Correlation analysis

Figures 8A, B presented the significance of correlation between seven intestinal genera with differentiated abundance and intestinal health indicators through Pearson's correlation analysis. The comparative analysis of the correlation between intestinal microbiota and PM-associated molecular indicators (*GS*, *CHS*, *EcPT*, and LZM) revealed that *Lactobacillus* exhibited a significant positive correlation with these indicators, whereas *Chitinibacter* demonstrated a significant negative correlation ($p < 0.05$). Regarding LPS, *Lactobacillus* and *Chitinibacter* demonstrated a correlation trend that was contrary to LZM observations: *Lactobacillus* exhibited a negative correlation with LPS, while *Chitinibacter* showed a positive correlation ($p < 0.05$). Additionally, *Lactococcus* and *Lactobacillus* showed a significant positive correlation with the majority of intestinal immune indicators measured in this study: iNOS, NO, *Toll*, *Dorsal*, *Imd*, and *Relish* ($p < 0.05$); however, the results for *Chitinibacter* diverged, exhibiting an opposite trend. In the interpretation of the correlation network diagram (Figure 8C), it was observed that the genera Lactobacillus, *Chitinibacter*, and *Klebsiella* occupy central positions within the network and exhibit correlations with a majority of intestinal molecular indicators.

4 Discussion

In animal nutrition, growth performance serves as the most fundamental phenotypic indicator for assessing the impact of feed components on animal health (24). This study revealed that a low-

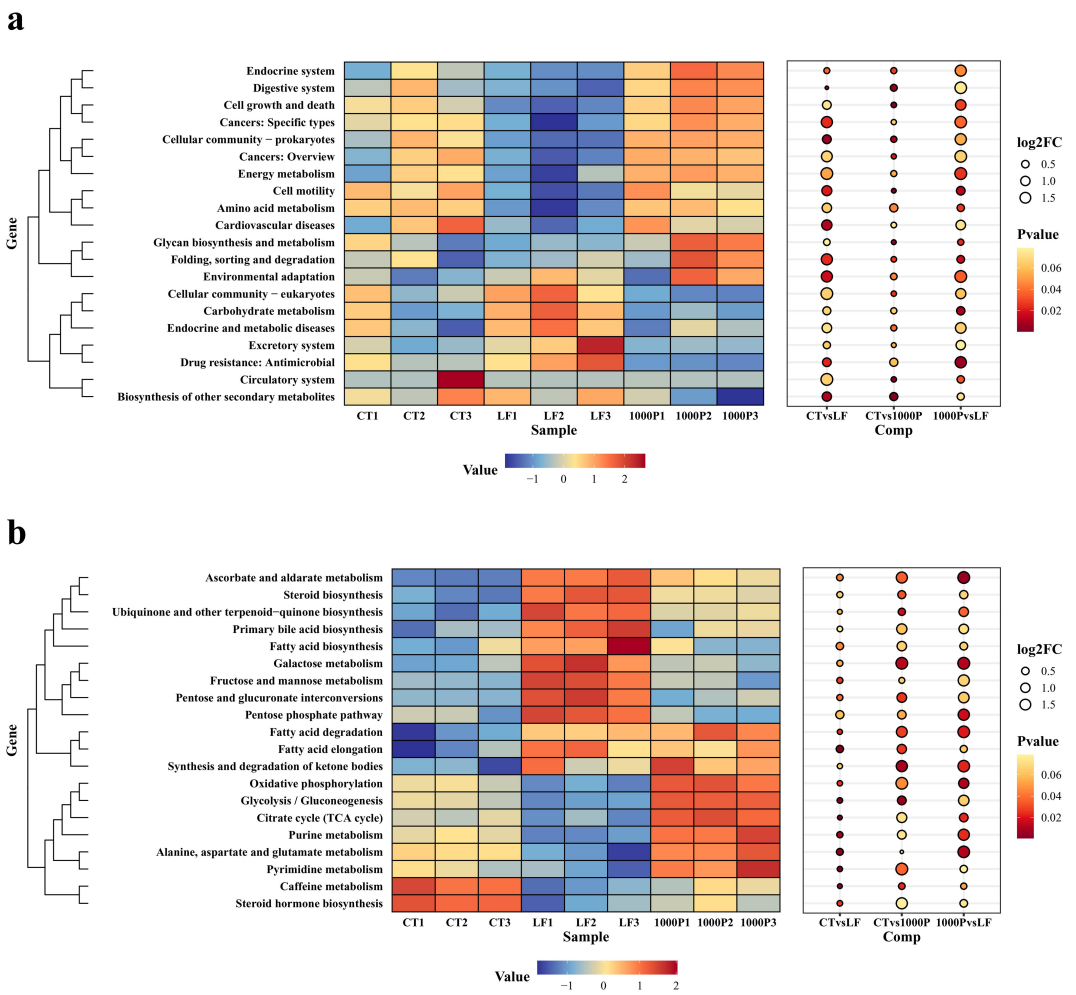

FIGURE 7
Effect of three diets on intestinal microbial functions. **(A)** Secondary functional annotation; **(B)** Tertiary functional annotation; red color represents upregulated function, and bule color represents downregulated function.

fishmeal (LF) diet negatively affected the growth performance of *M. rosenbergii*, evidenced by significant reductions in BW, WGR, and CF. Such negative growth outcomes signify compromised health and immune function (32), although survival rates remained unaffected. Previous research has shown that prolonged consumption of a LF diet can lead to reduced growth performance and concurrent oxidative stress (33). Further studies have identified oxidative stress induced by a LF diet as a critical factor in diminished growth performance (1). To substantiate this, our study measured four oxidative stress-related indicators, including MDA, a marker of lipid peroxidation reflecting cellular oxidative damage (34), and three antioxidant enzymes (SOD, CAT, and GSH-Px) known to mitigate oxidative damage in crustaceans by eliminating excess free radicals (35). The elevated MDA levels and decreased antioxidant enzyme activities in the hemolymph of the LF group confirmed the anticipated oxidative stress damage.

To mitigate the growth and antioxidant deficits induced by the LF diet, YPF Polysaccharide was incorporated into the diet, leveraging its known antioxidant properties (16). YPF, derived from a traditional Chinese medicinal herb, is believed to enhance its bioactive potential due to the higher concentration of polysaccharides compared to the raw herb (36). In aquaculture, YPF has been used as a feed additive for grass carp, enhancing antioxidant enzyme activities and antioxidant capacity (37). Our study found that YPF supplementation improved oxidative stress damage by boosting antioxidant enzyme activities, providing evidence for the enhanced growth performance observed.

The relationship between oxidative stress and intestinal health has been a focal point in animal nutrition, given the intestinal critical role in nutrient digestion, absorption, and as the first line of defense against external pathogens (38). Our analysis of intestinal tissue antioxidant enzyme activities mirrored the findings in hemolymph, indicating oxidative stress damage induced by the LF diet. Notably, YPF supplementation showed more pronounced benefits in mitigating intestinal oxidative damage compared to hemolymph results, with the 1000P group exhibiting even higher antioxidant enzyme activities than the CT group. This suggests that 1000mg/kg YPF has a significant positive impact on optimizing the LF diet by improving intestinal oxidative damage. These superior repair effects of YPF on intestinal oxidative damage may be attributed to its

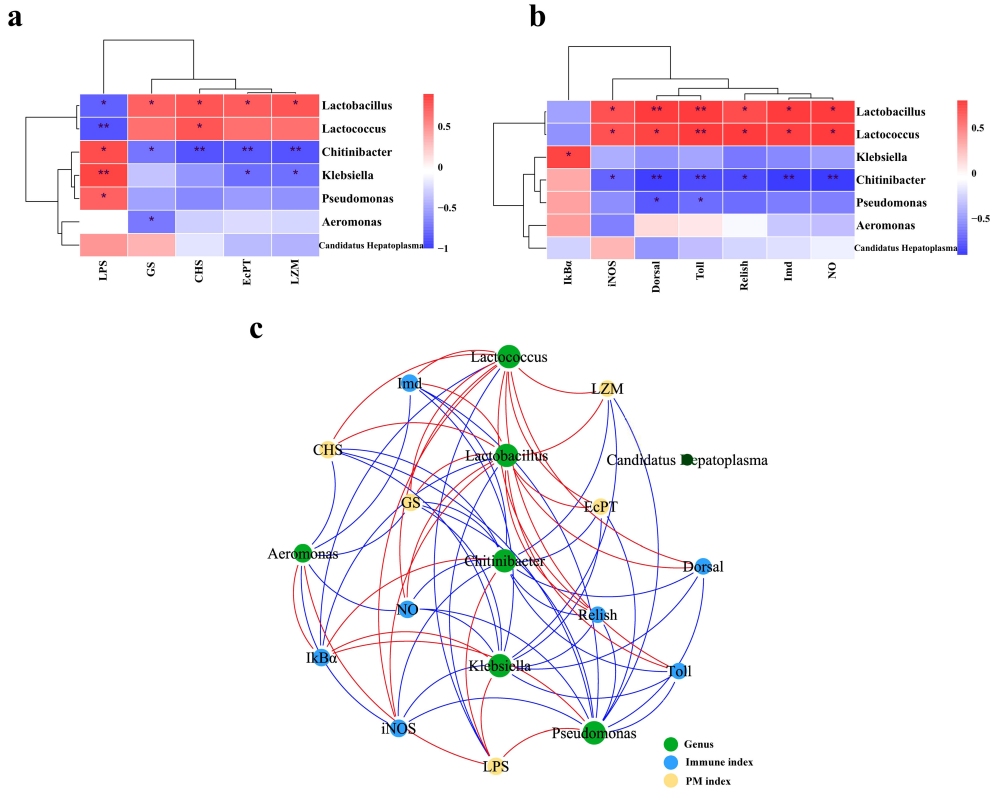

FIGURE 8
Correlation analysis. Correlation analysis between typical microbial genera and peritrophic matrix (PM) indices **(A)** and intestinal immune indices **(B)**, respectively. Red indicates positive correlation, while blue indicates negative correlation. The intensity of the color reflects the strength of the correlation. *$p < 0.05$, **$p < 0.01$. **(C)** Network diagram depicting the Spearman's correlation of microbial genera with intestinal molecular indicators. A red line signifies positive correlation, a blue line signifies negative correlation, and the width of the line corresponds to the magnitude of the correlation.

enhancement of the intestinal barrier, modulation of immune cells, and influence on gut microbiota metabolism (39–41).

Our initial focus is on exploring the function of the intestinal barrier. Ultrastructural analysis revealed that the LF diet significantly impaired intestinal morphology, including damage to the villi and basal membrane. Notably, the peritrophic matrix (PM), a semi-permeable membrane unique to invertebrate intestines, exhibited detachment and degradation under the LF diet (42). Transmission electron microscopy further confirmed this structural damage, showing a lack of tightly attached PM on the microvilli in the LF diet group. The PM, composed mainly of chitin and proteins, plays a crucial role in protecting intestinal epithelial cells from physical damage and facilitating nutrient digestion and absorption (43). Previous research has linked PM disruption with intestinal oxidative stress and functional impairment (44, 45). YPF supplementation in the LF group significantly alleviated PM damage, demonstrating a protective effect on maintaining intestinal PM structure. The synthesis of chitin, a key component of PM, relies on chitin synthase (CHS) (46) and glutamine synthetase (GS), which provides the necessary nitrogen source, glutamine, for chitin synthesis (47). Eritrophin-like protein (EcPT) has also been shown to maintain PM stability and function in prawns (48). Our study found that the LF diet significantly suppressed the expression of these three key PM-related genes, corroborating that the LF diet caused PM damage. Additionally, we assessed the levels of LZM and LPS, which are associated with PM function, finding that the LF group exhibited downregulated LZM and elevated LPS levels, a phenomenon also indicative of PM damage (13, 49). YPF supplementation notably improved this condition, especially at 1000mg/kg YPF, further validating the protective effect of YPF on PM function. The decrease in LZM and increase in LPS suggest that the LF diet may exacerbate intestinal dysfunction (50), while YPF may restore PM integrity through various mechanisms, including modulation of cellular interactions and providing antioxidant and immune protection (51). Consequently, it is warranted to investigate how YPF polysaccharide supplementation can further enhance intestinal immunity under a low-fishmeal diet.

In examining the immune responses of *M. rosenbergii* in this study, we focused on non-specific immune capacity regulation, as it is widely accepted that crustaceans do not exhibit inflammatory responses and lack a specific immune system akin to mammals. In invertebrate non-specific immunity, the NF-κB pathway plays a crucial role, with IMD-Relish and Toll-Doral being the main homologs in this signaling pathway (52). Our results showed that the LF diet primarily affected the IMD-Relish pathway, suppressing its expression levels. Studies indicate that inhibition of the IMD-Relish pathway may exacerbate oxidative stress and impact overall

host health and immune function (28). The up-regulation of IκBα in the LF group supports this, as increased IκBα indicates suppressed NF-κB pathway activity and diminished innate immune response (53). Additionally, research has shown that NO produced by iNOS can clear oxygen radicals and inhibit lipid peroxidation (54). The activation of the NF-κB signaling pathway (IMD-Relish) being a key step in increasing iNOS activity and inducing NO release (55). The LF group exhibited suppressed IMD-Relish pathway activity and decreased iNOS and NO levels, which aligns with this understanding, suggesting that inhibiting the NF-κB/NO signaling pathway may be a causative factor in oxidative stress induced by the LF diet. And supplementing with 1000mg/kg YPF activated the IMD-Relish pathway and regulated iNOS and NO levels, thereby improving non-specific immune capacity compromised by the LF diet.

Recent attention has been drawn to the significant role of gut microbiota in enhancing intestinal health and immunity in aquatic animals (56). Our study found that the intestinal microbiota composition in LF group prawns differed markedly from the other groups, with a decline in microbial diversity. A diverse gut microbiota promotes nutrient absorption, helps maintain intestinal barrier function, and establishes the intestinal immune system (57). The results from the LF group indirectly reflect deficiencies in intestinal health. To delve deeper into the impact of gut microbiota, we analyzed the composition of each group, finding that the LF diet increased Proteobacteria levels and decreased Firmicutes levels, suggesting a potential negative health state in the host (58). Further analysis of bacterial genera revealed that the LF group experienced a disruption in gut microbial balance, with pathogenic bacteria such as *Pseudomonas*, *Aeromonas*, and *Klebsiella* proliferating, while the levels of probiotic bacteria like *Lactococcus* and *Lactobacillus* significantly decreased (59). Supplementing with 1000mg/kg YPF reversed these phenomena, indicating that YPF may regulate microbiota balance by fostering the growth of beneficial bacteria and curbing the proliferation of harmful bacteria, thus restoring microbial diversity and stability. These enhancements may contribute to strengthening the intestinal barrier and immune function. Several studies corroborate our findings, showing that YPF polysaccharides possess prebiotic potential and positively impact the composition of the intestinal microbiota, increasing the abundance of beneficial bacteria in the intestine (21, 60). Moreover, these studies highlight a strong correlation between the modulation of intestinal microbiota by YPF polysaccharides and the promotion of intestine health, as well as the prevention of gut-related disorders (61). Further investigation is needed to elucidate the effects of gut microbiota alterations on the intestinal barrier (PM) and immunity, and to explore their interaction mechanisms, which are crucial for intestinal health and pathogen defense.

Analyzing the functional aspects of intestinal microbiota, we found that changes in the LF group's microbial community altered microbiota function, affecting intestinal barrier function and immunity. This analysis revealed a significant reduction in microbial taxa involved in amino acid metabolism and cell motility, suggesting decreased competition for host nutrients. This reduction likely leads to reduced immune stimulants and affects immune cell activity. Supporting evidence includes studies showing a correlation between microbial competition for nutrients and immune stimulant production, such as Puig et al. (2015), which demonstrated that intestinal microbial competition influences the host's immune response (62). In contrast, the 1000P group's microbiota exhibited enhanced oxidative phosphorylation, glycolysis/gluconeogenesis, the citric acid cycle, and purine metabolism, improving energy utilization efficiency. This enhancement may produce beneficial metabolites such as short-chain fatty acids (SCFAs) and bile acids, strengthening PM integrity and intestinal immunity, and positively impacting intestinal health (63, 64).

Subsequent correlation analysis between distinct microbial genera and intestinal health factors revealed close associations between certain intestinal microbes and PM formation and intestinal innate immunity. *Lactobacillus* showed a significant positive correlation with PM formation factors, suggesting that this microbe may contribute to maintaining PM, likely by protecting intestinal epithelial cells through SCFA production and enhancing PM barrier function (65). Conversely, *Chitinibacter*, which negatively correlated with PM factors, is prevalent in chitin-rich environments and degrades chitin (primary component of PM) (66), implying that *Chitinibacter* may negatively impact PM formation by degrading chitin. *Lactobacillus, Chitinibacter*, and *Lactococcus* significantly correlated with indicators of non-specific immunity. *Lactobacillus* and *Lactococcus* are known for supporting intestinal immunity through NF-κB pathway regulation, antimicrobial substance production, and interactions with the host immune system (67, 68). In contrast, *Chitinibacter*'s specific role remains unclear but may indirectly influence intestinal immunity by affecting PM formation. Network analysis identified *Lactobacillus* and *Chitinibacter* as key regulators of intestinal PM and non-specific immunity, suggesting that LF diet and YPF supplementation may modulate intestinal immune status through these microbes. For further studies, multi-omics and *in vivo* approaches are necessary to elucidate whether these microbes influence intestinal health through metabolic products or direct immune regulation (69).

5 Conclusions

In summary, the low-fishmeal (LF) diet may impair the peritrophic matrix (PM) and intestinal immunity by increasing *Chitinibacter* and decreasing *Lactobacillus*, leading to compromised intestinal health and oxidative stress of *M. rosenbergii*. YPF supplementation may mitigate the effects of the LF diet on these microbial populations, thereby protecting intestinal health, especially at a concentration of 1000mg/kg YPF.

Data availability statement

The raw dataset for 16SrDNA sequencing have been deposited in the National Institutes of Health's Short Read Archive database (SRA accession no. PRJNA1048554).

Ethics statement

The animal study was approved by the scientific breeding and use of animals by the Institutional Animal Care and Use Committee. The study was conducted in accordance with the local legislation and institutional requirements.

Author contributions

ML: Conceptualization, Data curation, Formal analysis, Funding acquisition, Investigation, Methodology, Project administration, Resources, Software, Supervision, Validation, Visualization, Writing – original draft, Writing – review & editing. CS: Investigation, Methodology, Project administration, Software, Supervision, Validation, Writing – review & editing. QZ: Conceptualization, Data curation, Formal analysis, Funding acquisition, Writing – review & editing. PX: Methodology, Project administration, Resources, Writing – review & editing. AW: Resources, Supervision, Writing – review & editing. XZ: Writing – review & editing. BL: Project administration, Resources, Validation, Visualization, Writing – review & editing.

Funding

The author(s) declare financial support was received for the research, authorship, and/or publication of this article. This work was supported by the Project of the Natural Science Foundation of Jiangsu Province for Youths (BK20230178), Key Laboratory of Healthy Freshwater Aquaculture, Ministry of Agriculture and Rural Affairs, Key Laboratory of Fish Health and Nutrition of Zhejiang Province, Zhejiang Institute of Freshwater Fisheries (ZJK202304), Jiangsu Province Agricultural Science and Technology Independent Innovation Fund (CX(23)2008), China Agriculture Research System of MOF and MARA (CARS-48), the Central Public-interest Scientific Institution Basal Research Fund, CAFS (2023TD63) and the "333 High Level Talent Project in Key Industry" of Jiangsu Province. The authors would like to thank the staff of these teams for their kind assistance.

Conflict of interest

The authors declare that the research was conducted in the absence of any commercial or financial relationships that could be construed as a potential conflict of interest.

Publisher's note

All claims expressed in this article are solely those of the authors and do not necessarily represent those of their affiliated organizations, or those of the publisher, the editors and the reviewers. Any product that may be evaluated in this article, or claim that may be made by its manufacturer, is not guaranteed or endorsed by the publisher.

Supplementary material

The Supplementary Material for this article can be found online at: https://www.frontiersin.org/articles/10.3389/fimmu.2024.1480897/full#supplementary-material

References

1. Liu M, Xu X, Sun C, Xu P, Gao Q, Liu B, et al. Tea Tree Oil improves energy metabolism, non-Specific immunity, and microbiota diversity via the intestine–hepatopancreas axis in macrobrachium rosenbergii under low fish meal diet administration. *Antioxidants*. (2023) 12:1879. doi: 10.3390/antiox12101879

2. Kesselring J, Gruber C, Standen B, Wein S. Effect of a phytogenic feed additive on the growth performance and immunity of Pacific white leg shrimp, *Litopenaeus vannamei*, fed a low fishmeal diet. *J World Aquaculture Soc*. (2020) 52:303–15. doi: 10.1111/jwas.12739

3. Zheng X, Liu B, Wang N, Yang J, Zhou Q, Sun C, et al. Low fish meal diet supplemented with probiotics ameliorates intestinal barrier and immunological function of *Macrobrachium rosenbergii* via the targeted modulation of gut microbes and derived secondary metabolites. *Front Immunol*. (2022) 13:3389/fimmu.2022.1074399. doi: 10.3389/fimmu.2022.1074399

4. Han D, Shan X, Zhang W, Chen Y, Wang Q, Li Z, et al. A revisit to fishmeal usage and associated consequences in Chinese aquaculture. *Rev In Aquaculture*. (2018) 10:493–507. doi: 10.1111/raq.12183

5. Lin Z, Yoshikawa S, Hamasaki M, Koyama T, Kikuchi K, Hosoya S. Effects of low fishmeal diets on growth performance, blood chemical composition, parasite resistance, and gene expression in the tiger pufferfish. *Takifugu rubripes*. *Aquaculture*. (2022) 560:738484. doi: 10.1016/j.aquaculture.2022.738484

6. Josefa SA, Hernández-Llamas A, Ortiz L, Fraga I, Villarreal H. Substitution of fishmeal with soybean meal in practical diets for juvenile white shrimp. *Litopenaeus schmitti*. *Aquaculture Res*. (2007) 38:689–95. doi: 10.1111/j.1365-2109.2007.01654.x

7. Dan Z, Zhang W, Zheng J, Gong Y, Mai K, Ai Q. Effects of fishmeal substitution by α-galactosidase hydrolytic soybean meal (EhSBM) on growth, antioxidant capacity, inflammatory responses and intestinal health of turbot juveniles (*Scophthalmus maximus* L.). *Aquaculture*. (2023) 563:738927–7. doi: 10.1016/j.aquaculture.2022.738927

8. Han F, Qian J, Qu Y, Li Z, Chen H, Xu C, et al. Partial replacement of soybean meal with fermented cottonseed meal in a low fishmeal diet improves the growth, digestion and intestinal microbiota of juvenile white shrimp *Litopenaeus vannamei*. *Aquaculture Rep*. (2022) 27:101339. doi: 10.1016/j.aqrep.2022.101339

9. Tao X, He J, Lu J, Chen Z, Jin M, Jiao L, et al. Effects of Bacillus subtilis DSM 32315 (Gutcare®) on the growth performance, antioxidant status, immune ability and intestinal function for juvenile *Litopenaeus vannamei* fed with high/low-fishmeal diets. *Aquaculture Rep*. (2022) 26:101282. doi: 10.1016/j.aqrep.2022.101282

10. Lehane MJ. Peritrophic matrix structure and function. *Annu Rev Entomology*. (1997) 42:525–50. doi: 10.1146/annurev.ento.42.1.525

11. Hegedus D, Erlandson M, Gillott C, Toprak U. New insights into peritrophic matrix synthesis, architecture, and function. *Annu Rev Entomology*. (2009) 54:285–302. doi: 10.1146/annurev.ento.54.110807.090559

12. Narasimhan S, Rajeevan N, Liu L, Zhao YO, Heisig J, Pan J, et al. Gut microbiota of the tick vector ixodes scapularis modulate colonization of the lyme disease spirochete. *Cell Host Microbe*. (2014) 15:58–71. doi: 10.1016/j.chom.2013.12.001

13. Cai C, Wu P, Ye Y, Song L, Hooft J, Yang C, et al. Assessment of the feasibility of including high levels of oilseed meals in the diets of juvenile Chinese mitten crabs (*Eriocheir sinensis*): Effects on growth, non-specific immunity, hepatopancreatic function, and intestinal morphology. *Anim Feed Sci Technol*. (2014) 196:117–27. doi: 10.1016/j.anifeedsci.2014.07.002

14. Liu Y, Tong B, Wang S, Li G, Tan Y, Yu H, et al. A mini review of Yu-Ping-Feng polysaccharides: Their biological activities and potential applications in aquaculture. *Aquaculture Rep*. (2021) 20:100697–7. doi: 10.1016/j.aqrep.2021.100697

15. Jiang W, Lin Y, Qian L, Lu S, Shen H, Ge X, et al. Mulberry leaf polysaccharides attenuate oxidative stress injury in peripheral blood leukocytes by regulating endoplasmic reticulum stress. *Antioxidants*. (2024) 13:136–6. doi: 10.3390/antiox13020136

16. Su C, Fan D, Pan L, Lu Y, Wang Y, Zhang M. Effects of Yu-Ping-Feng polysaccharides (YPS) on the immune response, intestinal microbiota, disease resistance and growth performance of Litopenaeus vannamei. *Fish Shellfish Immunol*. (2020) 105:104–16. doi: 10.1016/j.fsi.2020.07.003

17. Xin H, Hou L, Zhou X. Progress in the immunopharmacological study of yupingfeng powder. *Chin J Integrated Med*. (2020) 6:157–60. doi: 10.1007/BF02970605

18. Bungsu I, Kifli N, Ahmad SR, Ghani H, Cunningham AC. Herbal plants: the role of AhR in mediating immunomodulation. *Front Immunol*. (2021) 12:697663. doi: 10.1016/j.aquaculture.2020.735936

19. Hughes DA. Plant polyphenols: modifiers of immune function and risk of cardiovascular disease. *Nutrition*. (2005) 21:422–3. doi: 10.1016/j.nut.2004.11.003

20. Sun H, Ni X, Zeng D, Zou F, Yang M, Peng Z, et al. Bidirectional immunomodulating activity of fermented polysaccharides from Yupingfeng. *Res Veterinary Sci*. (2017) 110:22–8. doi: 10.1016/j.rvsc.2016.10.015

21. Yang H, Tan S, Chen S, Wu Y, Yang Y, Li H, et al. Effects of fermented Yupingfeng on intramuscular fatty acids and ruminal microbiota in Qingyuan black goats. *Anim Sci J*.. (2021) 92:e13554. doi: 10.1111/asj.13554

22. Duan Y, Liu Q, Wang Y, Zhang J, Xiong D. Impairment of the intestine barrier function in *Litopenaeus vannamei* exposed to ammonia and nitrite stress. *Fish Shellfish Immunol*. (2018) 78:279–88. doi: 10.1016/j.fsi.2018.04.050

23. Feng J, Huang X, Jin M, Li T, Hui K, Ren Q. A C-type lectin (MrLec) with high expression in intestine is involved in innate immune response of *Macrobrachium rosenbergii*. *Fish Shellfish Immunol*. (2016) 59:345–50. doi: 10.1016/j.fsi.2016.11.007

24. Zheng X, Xu X, Liu M, Yang J, Yuan M, Sun C, et al. Bile acid and short chain fatty acid metabolism of gut microbiota mediate high-fat diet induced intestinal barrier damage in. *Macrobrachium rosenbergii*. *Fish Shellfish Immunol*. (2024) 146:109376. doi: 10.1016/j.fsi.2024.109376

25. Liu M, Zheng X, Sun C, Zhou Q, Liu B, Xu P. Tea tree oil mediates antioxidant factors relish and Nrf2-autophagy axis regulating the lipid metabolism of. *Macrobrachium rosenbergii*. *Antioxidants*. (2022) 11:2260. doi: 10.3390/antiox11112260

26. Liu M, Gao Q, Sun C, Zheng X, Xu P, Liu B, et al. Effects of dietary tea tree oil on the growth, physiological and non-specific immunity response in the giant freshwater prawn (*Macrobrachium rosenbergii*) under high ammonia stress. *Fish Shellfish Immunol*. (2022) 120:458–69. doi: 10.1016/j.fsi.2021.12.025

27. Liu MY, Sun C, Xu P, Liu B, Zheng X, Zhou Q. Effects of dietary tea tree (*Melaleuca alternifolia*) oil and feeding patterns on the zootechnical performance and nonspecific immune response of the giant freshwater prawn (*Macrobrachium rosenbergii*). *J World Aquaculture Soc*. (2021) 53:542–57. doi: 10.1111/jwas.12831

28. Sun C, Shan F, Liu M, Liu B, Zhou Q, Zheng X. High-fat-diet-induced oxidative stress in giant freshwater prawn (*Macrobrachium rosenbergii*) via NF-κB/NO signal pathway and the amelioration of Vitamin E. *Antioxidants*. (2022) 11:228. doi: 10.3390/antiox11020228

29. Xie S, Zheng L, Wan M, Niu J, Liu Y, Tian L. Effect of deoxynivalenol on growth performance, histological morphology, anti-oxidative ability and immune response of juvenile Pacific white shrimp. *Litopenaeus vannamei*. *Fish Shellfish Immunol*. (2018) 82:442–52. doi: 10.1016/j.fsi.2018.08.053

30. Muritu RW, Gao Q, Sun C, Liu B, Song C, Zhou Q, et al. Effect of dietary *Clostridium butyricum* and different feeding patterns on growth performance, antioxidant and immune capacity in freshwater prawn (*Macrobrachium rosenbergii*). *Aquaculture Res*. (2020) 52:12–22. doi: 10.1111/are.14865

31. Xue H, Wu X, Li Z, Lu Y, Yin X, Wang W. Correlation and causation between the intestinal microbiome and male morphotypes in the giant freshwater prawn. *Macrobrachium rosenbergii*. *Aquaculture*. (2021) 531:735936–6. doi: 10.1016/j.aquaculture.2020.735936

32. Tan X, Sun Z, Ye C, Lin H. The effects of dietary *Lycium barbarum* extract on growth performance, liver health and immune related genes expression in hybrid grouper (*Epinephelus lanceolatus*♂ × E. fuscoguttatus♀) fed high lipid diets. *Fish Shellfish Immunol*. (2019) 87:847–52. doi: 10.1016/j.fsi.2019.02.016

33. Xie SW, LX T, Li YM, Zhou W, SL Z, Yang HJ. Effect of proline supplementation on anti-oxidative capacity, immune response and stress tolerance of juvenile Pacific white shrimp. *Litopenaeus vannamei*. *Aquaculture*. (2015) 448:105–11. doi: 10.1016/j.aquaculture.2015.05.040

34. Abdel-Daim MM, Dawood MAO, Elbadawy M, Aleya L, Alkahtani S. Spirulina platensis reduced oxidative damage induced by chlorpyrifos toxicity in Nile Tilapia (*Oreochromis niloticus*). *Animals*. (2020) 10:473. doi: 10.3390/ani10030473

35. Xu Z, JM R, Xie D, Lu W, Ren X, Yuan J. The oxidative stress and antioxidant responses of *Litopenaeus vannamei* to low temperature and air exposure. *Fish Shellfish Immunol*. (2018) 72:564–71. doi: 10.1016/j.fsi.2017.11.016

36. He Y, Zhang L, Wang H. The biological activities of the antitumor drug. *Grifola frondosa*. polysaccharide. *Pro Mol Biol Transl*. (2019) 163:221–61. doi: 10.1016/bs.pmbts.2019.02.010

37. Hui Y, Hua L, Hui Y, Ying Y, Duan YW. Polysaccharides syncytic element on immunity of grass carp under heat stress. *Acta Hydrobiologica Sin*. (2024) 46:439–47. doi: 10.7541/2022.2020.182

38. Silva EN, GH S, OM W, Smyser CF. Studies on the use of 9R strain of *salmonella gallinarum* as a vaccine in chickens. *Avian Dis*. (1981) 25:38–8. doi: 10.2307/1589825

39. Xie SZ, Liu B, Ye HY, Liu J, Duan J, Luo JP. Dendrobium huoshanense polysaccharide regionally regulates intestinal mucosal barrier function and intestinal microbiota in mice. *Carbohydr Polymers*. (2019) 206:149–62. doi: 10.1016/j.carbpol.2018.11.002

40. Yu KW, Kiyohara H, Matsumoto T, HC Y, Yamada H. Intestinal immune system modulating polysaccharides from rhizomes of. *Atractylodes lancea*. *Planta Med*. (1998) 64:714–9. doi: 10.1055/s-2006-957564

41. Tang C, Ding R, Sun J, Liu J, Kan J, Jin C. The impacts of natural polysaccharides on intestinal microbiota and immune responses – a review. *Food Funct*. (2019) 10:2290–312. doi: 10.1039/c8fo01946k

42. Wang P, Granados RR. An intestinal mucin is the target substrate for a baculovirus enhancin. *Proc Natl Acad Sci United States America*. (1997) 94:6977–82. doi: 10.1073/pnas.94.13.6977

43. Tellam RL, Wijffels G, Willadsen P. Peritrophic matrix proteins. *Insect Biochem Mol Biol*. (1999) 29:87–101. doi: 10.1016/s0965-1748(98)00123-4

44. Rao R, Fiandra L, Giordana B, de Eguileor M, Congiu T, Burlini N, et al. AcMNPV ChiA protein disrupts the peritrophic membrane and alters midgut physiology of Bombyx mori larvae. *Insect Biochem Mol Biol*. (2004) 34:1205–13. doi: 10.1016/j.ibmb.2004.08.002

45. Wang L, Li F, Wang B, Xiang J. Structure and partial protein profiles of the peritrophic membrane (PM) from the gut of the shrimp. *Litopenaeus vannamei*. *Fish Shellfish Immunol*. (2012) 33:1285–91. doi: 10.1016/j.fsi.2012.09.014

46. Imaizumi K, Sano M, Kondo H, Ikuo H. Insights into a chitin synthase of kuruma shrimp *penaeus japonicus* and its role in peritrophic membrane and cuticle formation. *Mar Biotechnol*. (2023) 25:837–45. doi: 10.1007/s10126-023-10244-1

47. Lu Z, Qin Z, SB V, Shen H, Pan G, Lin L, et al. Expression and functional characterization of glutamine synthetase from giant freshwater prawn (*Macrobrachium rosenbergii*) under osmotic stress. *Aquaculture Res*. (2019) 50:2635–45. doi: 10.1111/are.14221

48. Wang L, Li F, Wang B, Xiang J. A new shrimp peritrophin-like gene from Exopalaemon carinicauda involved in white spot syndrome virus (WSSV) infection. *Fish Shellfish Immunol*. (2013) 35:840–6. doi: 10.1016/j.fsi.2013.06.018

49. Pei D, Jiang J, Yu W, Phanidhar K, Uentillie A, Xu J. The waaL gene mutation compromised the inhabitation of *Enterobacter* sp. *Ag1 Mosq gut environment*. *Parasites Vectors*. (2015) 8:437. doi: 10.1186/s13071-015-1049-1

50. Zuo Z, Shang B, Shao Y, Li W, Sun J. Screening of intestinal probiotics and the effects of feeding probiotics on the growth, immune, digestive enzyme activity and intestinal flora of. *Litopenaeus vannamei*. *Fish Shellfish Immunol*. (2019) 86:160–8. doi: 10.1016/j.fsi.2018.11.003

51. Zheng W, Guan Y, Wu B. Effects of Yupingfeng polysaccharides as feed supplement on immune function and intestinal microbiome in chickens. *Microorganisms*. (2023) 11:2774–4. doi: 10.3390/microorganisms11112774

52. De Gregorio E. The Toll and Imd pathways are the major regulators of the immune response in Drosophila. *EMBO J*. (2002) 21:2568–79. doi: 10.1093/emboj/21.11.2568

53. Bowie A, O'Neill LAJ. Oxidative stress and nuclear factor-κB activation. *Biochem Pharmacol*. (2000) 59:13–23. doi: 10.1016/s0006-2952(99)00296-8

54. Sun C, Liu B, Zhou Q, Xiong Z, Shan F, Zhang H. Response of *Macrobrachium rosenbergii* to vegetable oils replacing dietary fish oil: insights from antioxidant defense. *Front Physiol*. (2020) 11:3389/fphys.2020.00218. doi: 10.3389/fphys.2020.00218

55. Pautz A, Art J, Hahn S, Nowag S, Voss C, Kleinert H. Regulation of the expression of inducible nitric oxide synthase. *Nitric Oxide*. (2010) 23:75–93. doi: 10.1016/j.niox.2010.04.007

56. Zhang Y, XF L, He S, Feng H, Li L. Dietary supplementation of exogenous probiotics affects growth performance and gut health by regulating gut microbiota in Chinese Perch (*Siniperca chuatsi*). *Aquaculture*. (2022) 547:737405. doi: 10.1016/j.aquaculture.2021.737405

57. Yu Z, Hao Q, SB L, QS Z, XY C, Li SH, et al. The positive effects of postbiotic (SWF concentration®) supplemented diet on skin mucus, liver, gut health, the structure and function of gut microbiota of common carp (*Cyprinus carpio*) fed with high-fat diet. *Fish Shellfish Immunol*. (2023) 135:108681–1. doi: 10.1016/j.fsi.2023.108681

58. Zhang D, Zheng Y, Wang X, Wang D, Luo H, Zhu W, et al. Effects of dietary fish meal replaced by fish steak meal on growth performance, antioxidant capacity, intestinal health and microflora, inflammatory response, and protein metabolism of large yellow croaker. *Larimichthys crocea*. *Aquaculture Nutr*. (2023) 2023:1–13. doi: 10.1155/2023/2733234

59. Basak S, Banerjee A, Pathak S, Duttaroy AK. Dietary Fats and the Gut Microbiota: Their impacts on lipid-induced metabolic syndrome. *J Funct Foods*. (2022) 91:105026. doi: 10.1016/j.jff.2022.105026

60. Guan Y, Zheng W, Bai Y, Wu B. Yupingfeng polysaccharide promote the growth of chickens via regulating gut microbiota. *Front Veterinary Sci*. (2024) 11:3389/fvets.2024.1337698. doi: 10.3389/fvets.2024.1337698

61. Erlandson MA, Toprak U, Hegedus DD. Role of the peritrophic matrix in insect-pathogen interactions. *J Insect Physiol*. (2019) 117:103894. doi: 10.1016/j.jinsphys.2019.103894

62. Puig KL, AJ S, Zhou X, MA S, Combs CK. Amyloid precursor protein expression modulates intestine immune phenotype. *J Neuroimmune Pharmacol*. (2011) 7:215–30. doi: 10.1007/s11481-011-9327-y

63. Lee SI, Kang KS. Function of capric acid in cyclophosphamide-induced intestinal inflammation, oxidative stress, and barrier function in pigs. *Sci Rep*. (2017) 7:16530. doi: 10.1038/s41598-017-16561-5

64. Feng W, Feng W, Ge J, Yu J, Xu P, Tang Y, et al. Alterations of amino acid metabolism and intestinal microbiota in Chinese mitten crab (*Eriocheir sinensis*) fed on formulated diet and iced trash fish. *Comp Biochem Physiol Genomics Proteomics*. (2021) 40:100924–4. doi: 10.1016/j.cbd.2021.100924

65. Bai S, Yao Z, Raza MF, Cai Z, Zhang H. Regulatory mechanisms of microbial homeostasis in insect gut. *Insect Sci*. (2020) 28:286–301. doi: 10.1111/1744-7917.12868

66. Chern LL, Erko S, SF L, FL L, JK C, Fu HM. Chitinibacter tainanensis gen. nov., sp. nov., a chitin-degrading aerobe from soil in Taiwan. *Int J Systematic Rvolutionary Microbiol*. (2004) 54:1387–91. doi: 10.1099/ijs.0.02834-0

67. Xuan B, Park J, GS L, Kim EB. Oral administration of mice with cell extracts of recombinant lactococcus lactis IL1403 expressing mouse receptor activator of NF-kB ligand (RANKL). *Food Sci Anim Resour*. (2022) 42:1061–73. doi: 10.5851/kosfa.2022.e54

68. Shadi A, Amin S, TM S, Najafi S, Rohani M, Pourshafiea MR. The effects of the probiotic cocktail on modulation of the NF-kB and JAK/STAT signaling pathways involved in the inflammatory response in bowel disease model. *BMC Immunol*. (2022) 23:8. doi: 10.1186/s12865-022-00484-6

69. Abrigo J, Olguín H, Tacchi F, OA J, VB M, Soto J, et al. Cholic and deoxycholic acids induce mitochondrial dysfunction, impaired biogenesis and autophagic flux in skeletal muscle cells. *Biol Res*. (2023) 56:30. doi: 10.1186/s40659-023-00436-3

frontiers | Frontiers in Immunology

TYPE Original Research
PUBLISHED 10 December 2024
DOI 10.3389/fimmu.2024.1501753

OPEN ACCESS

EDITED BY
Samad Rahimnejad,
University of Murcia, Spain

REVIEWED BY
Yun Wang,
Chinese Academy of Fishery Sciences (CAFS), China
Yong-Jun Chen,
Southwest University, China

*CORRESPONDENCE
Beiping Tan
bptan@126.com
Jin Niu
niuj3@mail.sysu.edu.cn

†These authors have contributed equally to this work and share first authorship

RECEIVED 25 September 2024
ACCEPTED 25 November 2024
PUBLISHED 10 December 2024

CITATION
Lin S, Chen M, Chen X, Li Y, Liu Y, Zhang P, Hou X, Tan B and Niu J (2024) Supplemental effects of *Haematococcus pluvialis* in a low-fish meal diet for *Litopenaeus vannamei* at varying temperatures: growth performance, innate immunity and gut bacterial community.
Front. Immunol. 15:1501753.
doi: 10.3389/fimmu.2024.1501753

Supplemental effects of *Haematococcus pluvialis* in a low-fish meal diet for *Litopenaeus vannamei* at varying temperatures: growth performance, innate immunity and gut bacterial community

Sihan Lin[1†], Mengdie Chen[1†], Xuanqi Chen[1], Yanmei Li[2], Yafeng Liu[2], Peinan Zhang[2], Xiangyan Hou[2], Beiping Tan[3*] and Jin Niu[1*]

[1]State Key Laboratory of Biocontrol, Guangdong Provincial Key Laboratory for Aquatic Economic Animals and Southern Marine Science and Engineering Guangdong Laboratory (Zhuhai), School of Life Sciences, Sun Yat-sen University, Guangzhou, China, [2]Algae Health Science Co., Ltd., Kunming, China, [3]Laboratory of Aquatic Animal Nutrition and Feed, Fisheries College, Guangdong Ocean University, Zhanjiang, China

This study examined the effects of *Haematococcus pluvialis* on the growth performance, innate immunity, and gut microbiota of *Litopenaeus vannamei* under different water temperature conditions. Feeding regimens included a 20% fishmeal diet (control), a low-fish meal (LFM) diet with 10% fishmeal and an LFM diet supplemented with 0.03% *H. pluvialis*. These diets were administered to six groups of *L. vannamei* at normal (30°C) (NT) and low (20°C) (LT) temperatures (NT_C, NT_LFM, NT_LFM_HP, LT_C, LT_LFM, and LT_LFM_HP) over 8 weeks. The weight gain rate of *L. vannamei* in group NT_LFM_HP was significantly higher compared to group NT_LFM. Astaxanthin levels and body pigmentation intensity in *L. vannamei* were significantly increased in the NT_LFM_HP and LT_LFM_HP groups. Moreover, hepatopancreatic antioxidant capacities, such as superoxide dismutase (SOD) activity and total antioxidant capacity (T-AOC), were lower in normal-temperature groups compared to the low-temperature groups. Nevertheless, antioxidant capacity was significantly higher in both the NT_LFM_HP and LT_LFM_HP groups compared to the control group. Meanwhile, the expression levels of antioxidants were significantly higher at lower temperatures compared to higher temperatures, with the NT_LFM_HP and LT_LFM_HP groups exhibiting the highest expression levels. Additionally, the mRNA levels of genes associated with the Toll and IMD pathways indicated immunoregulatory effects in the organism. The expression levels of immune genes were significantly higher at lower temperatures, especially in the NT_LFM_HP and LT_LFM_HP groups compared to the control groups. Notably, significant differences in gut microbial composition were observed in the NT_LFM_HP group compared to other groups, with variations influenced by temperature and fishmeal content. Specifically, Vibrionaceae abundance was significantly lower in the LT_LFM_HP group compared to the control group. The

results also revealed that the abundance of Actinomarinales was significantly higher in low-temperature groups, with the LT_LFM_HP group displaying the greatest increase. Overall, these findings suggest that *L. vannamei* may be susceptible to reduced fishmeal levels, potentially impacting growth and immune function. Furthermore, *H. pluvialis* supplementation may assist *L. vannamei* in acclimating to prolonged low-temperature conditions.

KEYWORDS

***Litopenaeus vannamei*, *Haematococcus Pluvialis*, temperature, growth performance, innate immunity**

1 Introduction

As is well documented, *Litopenaeus vannamei* (*L. vannamei*) is an economically important aquaculture species worldwide. Fishmeal is considered the optimal source of protein in shrimp feed owing to its palatability, balanced nutritional composition, and ease of digestion and absorption. However, the price of fishmeal has increased in recent years. To cope with this change, it is essential to develop suitable protein sources to replace fishmeal. In low fishmeal diets, functional additives are introduced to ensure the growth performance and health of aquatic animals. Meanwhile, aquaculture has suffered from environmental destruction over the past decades (1). The extensive administration of antibiotics to enhance disease resistance in shrimp (2) resulted in numerous adverse effects (3). Consequently, the use of pure natural functional additives has become a trend. Shrimp body pigmentation influences consumer preference. However, shrimp are unable to synthesize astaxanthin, and earlier studies have reported that shrimp can use astaxanthin from their diet to optimize body pigmentation. Thus, natural sources of astaxanthin, such as *Haematococcus pluviali* (*H. pluvialis*), have emerged as prominent functional additives. Known to be the richest natural source of astaxanthin, *H. pluvialis* contains astaxanthin levels ranging from 1.0% to 7.0% (4). Therefore, the introduction of astaxanthin to feed can improve growth performance in *L. vannamei* (5), mitigate hepatopancreatic damage in white shrimp (6), improve immune levels in crayfish (7), and improve body color in Japanese shrimp (8).

The growth, health, and immunity of aquatic organisms are considerably impacted by water temperature. For instance, *L. vannamei* is a poikilothermic species whose growth, health, and immunity are regulated by fluctuations in environmental temperature (9). Indeed, temperature stress has been documented to significantly impact shrimp growth and immunity (10, 11), thereby promoting susceptibility to bacterial, fungal, viral, and parasitic infections and economic losses (12). The nutritional metabolism and immune function of shrimp are directly affected by the gastrointestinal tract, which plays a vital role in nutrient absorption and disease resistance. Throughout the growth of shrimp, the structure of the gut flora significantly changes (13, 14). According to earlier studies, alterations in temperature can affect the gut flora of shrimp, thereby influencing their growth and immune performance (15, 16).

To the best of our knowledge, no studies have investigated the effects of *H. pluvialis* on *L. vannamei* under different water temperatures. Given that other aquatic organisms are influenced by the multiple regulatory mechanisms of *H. pluvialis*, this study aimed to investigate the effects of *H. pluvialis* on the growth performance, antioxidant capacity, immune activity, and gut microbiology of *L. vannamei* at distinct water temperatures.

2 Materials and methods

2.1 Experimental diets

Prior to diet preparation, all raw materials were crushed using a grinder and subsequently sieved using a 60-mesh sieve. After sieving, the raw materials were weighed based on the diet formula outlined in Table 1. Briefly, the weighed raw materials were thoroughly mixed in a plastic zip-lock bag and then transferred to a commercial mixer for mixing and blending, during which fish oil, soya lecithin, and water were added and mixed. After mixing, the ingredients were extruded into long strips using a twin-screw extruder and subsequently transferred to a pelletizer to produce pellets for the trials. Next, diets were steam-conditioned at 60°C, then removed and air-dried until the moisture content of the diet was reduced to approximately 10%. Following packing into plastic ziplock bags, the diets were stored in a refrigerator at -20°C. Different feeding regimes, specifically the 20% fishmeal group, the 10% fishmeal group, and the 10% fishmeal + 0.03% *H. pluvialis* group, were administered to *L. vannamei* (NT_C, NT_LFM, NT_LFM_HP, LT_C, LT_LFM, and LT_LFM_HP) at 30°C and 20° water temperature environments.

2.2 Feeding experiments

In Lingshui Li Autonomous County, *L. vannamei* was used as the test animal for an 8-week culture experiment. Shrimp larvae were temporarily raised on commercial feed for 10 weeks before being used

in the culture experiment. A total of 720 shrimp with an average weight of approximately 0.63 g were randomly selected from the temporarily reared shrimp and assigned to 24 cement tanks, each containing 30 shrimp. Sewage pipes were installed at the bottom of each cement tank for effluent discharge, and water pipes were installed in the cement tanks for seawater replenishment. The water was changed uniformly and regularly according to predetermined water quality indices, with 80% of the water replaced at each interval. All seawater used in the aquaculture tanks was sand-filtered, precipitated, sterilized, and filtered prior to use. The cement tanks were fitted with an air tube and air stone to maintain 24-hour continuous aeration.

Feeding rates were initially set at 5% of shrimp body weight and adjusted based on satiation by observing bait residues after feeding. All groups were fed three times daily, and dead shrimp, bait residues, feces, and other bottom waste were aspirated by suction, and dead shrimp were weighed and counted. During the 8-week aquaculture experiment, the temperatures of the water were maintained at 30°C for the normal-temperature groups and 20°C for the low-temperature groups. A chiller and a water recycling system were used to adjust water temperature, which was recorded every 4 hours. Throughout the experiment, natural light cycles were maintained.

2.3 Sampling

During the 8-week culture period, 5 g of feces from each cement tank were collected and stored in a refrigerator at -20°C for apparent digestibility analysis. All shrimp were fasted for 24 hours before sampling. Shrimp in each tank was counted and weighed. The body length, weight, and hepatopancreatic weight of five shrimp from each group were measured and recorded. A total of five shrimp were randomly selected from each group and stored at -20°C for whole shrimp crude nutrient analysis. Frozen hepatopancreas samples harvested from four shrimp were analyzed for enzyme activity and gene expression. Intestinal samples were collected from four shrimp and frozen for intestinal flora analysis. For H&E staining and sectioning, hepatopancreas samples collected from two shrimp were used. For comparison, five live shrimp from each group were boiled under identical conditions.

TABLE 1 Ingredients and proximate composition of six experimental diets (g/kg).

Ingredients	C (NT/LT)	LFM (NT/LT)	LFM_HP (NT/LT)
Fish meal [1]	20	10	10
Decorticated soybean meal [2]	18	21	21
Peanut meal [3]	12	12	12
Chicken meal [5]	7	7	7
Soy protein concentrate [6]	4	11	11
Wheat flour [6]	24.86	23.94	24.21
Hermetia illucens meal [7]	6	6	6
Beer yeast [8]	2	2	2
Fish oil [9]	0.5	1.5	1.5
Soybean lecithin [10]	1	0.8	0.5
Vitamin premix [11]	0.5	0.5	0.5
Mineral premix [12]	0.5	0.5	0.5
Choline [13]	0.2	0.2	0.2
Cholesterol [14]	0.1	0.1	0.1
Ca(H2PO4)2 [15]	1.7	1.7	1.7
Lysine [16]	0.1	0.17	0.17
Vitamin C [17]	0.1	0.1	0.1
Methionine [18]	0.2	0.25	0.25
Threonine [19]	0.23	0.23	0.23
Y2O3 [20]	0.01	0.01	0.01
Sodium alginate [21]	1	1	1
Haematococcus Pluvialis [22]	0	0	0.03
Total	100	100	100
Moisture	8.42	8.45	8.37
Crude lipid	7.62	7.66	7.38
Crude protein	40.21	40.22	40.26
Ash	11.26	11.21	11.23

[1] Fish meal: Guangzhou Chengyi Industrial Group Co., Ltd., China.
[2] Decorticated soybean meal: Yihai Kerry Jinlongyu Grain and Oil Food Co., Ltd., China.
[3] Peanut meal: Zhuhai Dehai Biotechnology Co., Ltd., China.
[4] Chicken meal: Zhuhai Dehai Biotechnology Co., Ltd., China.
[5] Soy protein concentrate: Kyorin Industry (Shenzhen) Co., Ltd., China.
[6] Wheat flour: Hebei Jinshahe Noodle Industry Group Co., Ltd., China.
[7] Hermetia illucens meal: Qinghai Kunjie environmental protection technology Co., Ltd., China.
[8] Beer yeast: Guangzhou Chengyi Industrial Group Co., Ltd., China.
[9] Fish oil: Guangzhou Chengyi Industrial Group Co., Ltd., China.
[10] Soybean lecithin: Guangzhou Chengyi Industrial Group Co., Ltd., China.
[11] Vitamin premix (kg^{-1} of mixture): vitamin A, 250,000 IU; riboflavin, 750 mg; pyridoxine HCL, 500 mg; cyanocobalamin, 1 mg; thiamin, 500 mg; menadione, 250 mg; folic acid, 125 mg; biotin, 10 mg; a-tocopherol, 3750 mg; myo-inositol, 2500 mg; calcium pantothenate, 1250 mg; nicotinic acid, 2000 mg; vitamin D3, 45,000 IU; vitamin C, 7000 mg. Guangzhou Chengyi Company Ltd., China.
[12] Mineral premix (kg^{-1} of mixture): Zn, 4000 mg; K, 22,500 mg; I, 200 mg; NaCl, 2.6 g; Cu, 500 mg; Co, 50 mg; FeSO4, 200 mg; Mg, 3000 mg; Se, 10 mg. Guangzhou Chengyi Company Ltd., China.
[13] Choline: Guangzhou Chengyi Industrial Group Co., Ltd., China.
[14] Cholesterol: Guangzhou Chengyi Industrial Group Co., Ltd., China.
[15] $Ca(H_2PO_4)_2$: Guangzhou Chengyi Industrial Group Co., Ltd., China.
[16] Lysine: Shanghai Feeel Technology Development Co., Ltd., China.
[17] Vitamin C: Guangzhou Chengyi Industrial Group Co., Ltd., China.
[18] Methionine: Shanghai Feeel Technology Development Co., Ltd., China.
[19] Threonine: Shanghai Feeel Technology Development Co., Ltd., China.
[20] Y_2O_3: Shanghai Haohong scientific Co., Ltd., China.
[21] Sodium alginate: Nanjing Duly Biotechnology Co., Ltd., China.
[22] *Haematococcus Pluvialis*: The effective content of astaxanthin is 3%. Algae health Science Co., Ltd., China.

2.4 Determination of proximate composition

According to the guidelines of the Association of Official Analytical Chemists (AOAC), moisture, crude protein, and crude lipid content were determined from dried samples. After drying at 105°C, moisture content was determined, following which the samples were crushed. Next, a fully automated Dumas nitrogen tester (N Pro (DT Ar/He Basic), Gerhardt GMBH & CO.KG, Germany) was employed to determine crude protein content from 0.08 g of sample. The crude lipid content was determined using the Soxhlet extraction method on an automatic lipid analyzer (Soxtec System HT6, Tecator, Sweden) with light petroleum reflux extraction on approximately 0.5 g of the sample. Shrimp shell samples were freeze-dried and ground to extract astaxanthin and measure astaxanthin levels. Ionophore atomic emission spectrometry (ICP-AES) was utilized to quantify metal Y-ions in feces, and apparent digestibility was calculated. The methods for extracting astaxanthin in shrimp shells were performed as described in a previous study (50).

2.5 Determination of hepatopancreatic enzyme activities

After thawing hepatopancreatic tissues, samples were collected and added to PBS solution for grinding. The levels of hepatopancreatic enzyme activity indices were determined by centrifuging at 4000 rpm for 20 min at 4°C and collecting the supernatant. Superoxide dismutase (SOD), total antioxidant capacity (T-AOC), and lipid oxidation (MDA) levels were measured using kits (Nanjing Jiancheng Bioengineering Institute, Nanjing, China).

2.6 Total RNA extraction and real-time quantitative PCR

Real-time quantitative PCR (qRT-PCR) was performed for all gene expression assays in the present study. With the *Evo MMLV* Reverse transcription reagent kit (Accurate Biology, Hunan, China), total hepatopancreatic RNA was extracted using the TRIzol method, and cDNA was synthesized via reverse transcription. Moreover, qRT-PCR was performed on a Roche real-time quantitative PCR system (LightCycler 480 II, Roche Diagnostics, Basel, Switzerland). Conditions for the reaction were as follows: pre-denaturation at 95°C for 40 amplification cycles (denaturation at 95°C for 5 s, annealing at 60°C for 30 s, and extension at 72°C for 30 s). A melting curve was plotted (95°C for 20 s, 60°C for 20 s, followed by continuous maintenance at 95°C), and the samples were cooled to 4°C. Shrimp primers used in this study are presented in Table 2. The *β-actin* gene served as an internal reference gene for gene expression analysis, and relative expression levels were calculated using the $2^{-\Delta\Delta ct}$ method.

TABLE 2 Real-time quantitative PCR primers for genes of *L. vannamei*.

Gene	Primer sequence (5′ to 3′)	GenBank No.	Product size (bp)
β-actin F	CGAGGTATCCTCACCCTGA	AF300705.2	101
β-actin R	CGGAGCTCGTTGTAGAAGG	AF300705.2	
toll F	ATACCTCAGCTTCACG GCAG	XM_027356519.1	140
toll R	TATTCGTCAGCAGAGC AGGC	XM_027356519.1	
dorsal F	AGATGGAATGATAGAATG GGAAGC	XM_027382195.1	127
dorsal R	GTACACCTTTATGGGGTT CTCTATCTC	XM_027382195.1	
crustin F	GAGGGTCAAGCCTAC TGCTG	AY486426.1	157
crustin R	ACTTATCGAGGCCAG CACAC	AY486426.1	
sod F	GCCACTTGAACCACA CCATC	DQ005531.1	158
sod R	GCCAGAGCCTTTCAC TCCAA	DQ005531.1	
cat F	GGGTATTGAGGCTTCC CCTG	AY518322.1	151
cat R	GGGGCCATCTCTCTG GTAGT	AY518322.1	
gpx F	AGAAGAGTTCGGCGAC AAGC	AY973252.2	126
gpx R	TCGAAGTTGTTCCCA GGACG	AY973252.2	
imd F	TATACATCCTGCCGT TGCCG	FJ592176.1	174
imd R	GTTGTGGATAACGGGGC CAA	FJ592176.1	
relish F	ATTCTTCTGCGTTTCAAG GTGT	KM204120.1	203
relish R	GAGGTATGGTCAGGGTAT GGTG	KM204120.1	
lysc F	TACTGGTGCGGAAGC GACTA	XM_027352840.1	165
lysc R	GTAAGCCACCCAGGC AGAATA	XM_027352840.1	

β-actin, beta-actin; sod, superoxide dismutase; cat, catalase; gpx, glutathione peroxidase; imd, immune deficiency; lysc, lysozyme C-like.

2.7 Morphological microscopy of hepatopancreatic tissues

Hepatopancreatic samples were initially fixed in a 4% paraformaldehyde solution for 24 hours and subsequently transferred to a 70% ethanol solution. Prior to sectioning, the samples were subjected to graded dehydration, paraffin

embedding, and fixation, following which the sections were sliced into approximately 3.0 μm thick sections using a slicer. Afterward, the sections were subjected to hematoxylin and eosin staining and examined and imaged under a Nikon orthostatic microscope (Eclipse Ni-E, Nikon, Japan). Finally, the resulting images were analyzed utilizing NIS-Elements viewer software (National Institutes of Health, Bethesda, USA).

2.8 16S rRNA gene sequencing and microbiota analysis

The genomic DNA of intestinal microorganisms in the sample was extracted and analyzed for purity and concentration using 1% agarose gel electrophoresis. The purified genomic DNA was subsequently dispatched to Shanghai Majorbio Bio-pharm Technology Co., Ltd (51) for further processing.

Paired-end (PE) reads generated from Illumina sequencing were initially aligned based on their overlapping regions. Subsequently, sequence quality was assessed and filtered, followed by sample differentiation for operational taxonomic unit (OTU) clustering and species taxonomy analysis to facilitate the calculation of various diversity indices. OTU-based diversity index analyses and sequencing depth detection were conducted, while taxonomic information enabled statistical analyses of community structure at different taxonomic levels. Data analyses were conducted utilizing the Meggie BioCloud platform (https://cloud.majorbio.com). Specifically, mothur software was employed to compute alpha diversity metrics such as Chao 1 and Shannon index, while the Wilcoxon rank sum test was utilized to assess variations in alpha diversity among groups (52). Intergroup differences in alpha diversity were evaluated using an algorithm based on the Bray-Curtis distance, coupled with PCoA (Principal Coordinate Analysis) analysis to examine the similarities in microbial community structures across samples. Additionally, the PERMANOVA non-parametric test was utilized in conjunction with LEfSe (Linear Discriminant Analysis Effect Size) analysis (LDA>2, $P<0.05$) to assess significant variations in microbial community structure among groups, identifying bacterial taxa with differing abundances from phylum to genus level (53).

2.9 Statistical analysis

Parameters were calculated using the following formulae: Initial body weight (IBW, g)=initial total wet weight/initial number of tails; Final body weight (FBW, g)=final total wet weight/final number of tails; Weight gain (WG, %)=100×(final body weight-initial body weight)/initial body weight; Specific growth rate (SGR, %/day)=100×(Ln final mean weight-Ln initial mean weight)/number of days; Food intake (FI, g/shrimp)=total food intake/total number of shrimp; Feed conversion ratio (FCR)=dry diet fed/wet weight gain; Conversion factor (CF, g/cm^3)=100×wet weight/(body length)^3; Hepatosomatic intake (HSI, %) =100×hepatopancreas weight/wet weight; Survival rate (SR, %) =100×number of terminal surviving tails/number of initial tails; Apparent Digestibility (AD, %)=100× (Y_2O_3 intake-Y_2O_3 output)/Y_2O_3 intake.

Experimental data were expressed as "mean ± standard error". Two-way ANOVA with Bonferroni multiple comparisons were used to analyze data across treatment groups at the same temperature. Student's *t*-test was conducted to analyze data in the same treatment groups at different temperatures. $P < 0.05$ was considered statistically significant.

3 Results

3.1 Growth performance, feed utilization, and morphometric parameters

Following the conclusion of the 8-week period, the growth performance, feed utilization, and morphometric parameters for the six groups of *L. vannamei* were individually recorded, as detailed in Table 3. The weight gain rate and specific growth rate of *L. vannamei* in the NT_C, NT_LFM, and NT_LFM_HP groups were significantly higher compared to the LT_C LT_LFM and LT_LFM_HP groups ($P<0.05$). Likewise, the weight gain rate of *L. vannamei* in group NT_LFM_HP was significantly higher compared to group NT_LFM ($P<0.05$). In contrast, the weight gain rate of *L. vannamei* in group NT_LFM_HP was comparable to that in group NT_C. Interestingly, no significant differences were noted in the survival rates of *L. vannamei* across treatment groups ($P>0.05$). Conversely, variations in feed efficiency and apparent digestibility were observed between the normal and low-temperature groups ($P<0.05$).

3.2 Muscle proximate composition

The moisture, crude protein, and crude lipid content of *L. vannamei* muscle within each experimental group are outlined in Table 4. The findings revealed no significant differences in these parameters across the groups ($P>0.05$).

3.3 Astaxanthin content

As displayed in Figure 1, significant differences were observed in coloration between live and cooked shrimp, with the NT_LFM_HP and LT_LFM_HP groups exhibiting darker pigmentation compared to the NT_LFM and LT_LFM groups. Furthermore, as depicted in Figure 2, the astaxanthin content in shrimp shells was highest in the NT_LFM_HP and LT_LFM_HP groups.

3.4 Hepatopancreas morphology

Figure 3 illustrates the comparison of hepatopancreatic tissue sections across groups. The hepatic tubules within the hepatopancreas of groups NT_C, NT_LFM, NT_LFM_HP, LT_C, LT_LFM, and LT_LFM_HP displayed normal morphology, with normal B cells, R cells, and E cells and the absence of lesions.

10.3389/fimmu.2024.1501753

TABLE 3 Effect of the addition of *H. pluvialis* at varying water temperatures on growth performance and feed utilisation of *L. vannamei*.

Items	NT_C	NT-LFM	NT_LFM_HP	LT_C	LT_LFM	LT_LFM_HP	NT&LT_C	NT&LT_LFM	NT&LT_LFM_HP
IBW (g)	0.62 ± 0.00	0.62 ± 0.00	0.61 ± 0.00	0.62 ± 0.00	0.62 ± 0.00	0.63 ± 0.00	ns	ns	ns
FBW (g)	17.76 ± 0.47b	15.51 ± 0.66a	17.70 ± 0.77b	11.99 ± 0.37	10.61 ± 0.82	10.56 ± 0.35	***	**	***
FI (g/shrimp)	21.89 ± 0.35	22.60 ± 1.15	21.93 ± 0.56	11.66 ± 0.36	11.74 ± 0.72	11.21 ± 0.36	***	***	***
SR (%)	96.66 ± 2.35	95.83 ± 2.16	98.33 ± 1.66	97.50 ± 1.59	96.66 ± 3.33	99.16 ± 0.83	ns	ns	ns
WG (%)	2751.54 ± 10.41^{b}	2369.48 ± 24.86^{a}	2762.00 ± 24.13^{b}	1811.36 ± 64.39	1590.46 ± 46.27	1582.49 ± 63.92	***	**	***
SGR (%/d)	3.98 ± 0.03	3.81 ± 0.06	3.98 ± 0.05	3.51 ± 0.03	3.35 ± 0.10	3.35 ± 0.04	***	**	***
FCR	1.28 ± 0.02	1.52 ± 0.05	1.28 ± 0.04	1.03 ± 0.04	1.20 ± 0.12	1.13 ± 0.03	**	ns	*
CF (g/cm^3)	1.04 ± 0.00	0.99 ± 0.00	1.00 ± 0.01	0.99 ± 0.00	0.98 ± 0.01	0.99 ± 0.00	***	ns	ns
HSI (%)	4.21 ± 0.18	4.36 ± 0.13	4.01 ± 0.13	4.95 ± 0.17	4.64 ± 0.10	4.56 ± 0.11	*	ns	*
AD (%)	0.83 ± 0.02	0.67 ± 0.04	0.81 ± 0.02	0.46 ± 0.05	0.43 ± 0.09	0.44 ± 0.04	**	ns	***

Values are expressed as the means ± SEM with 4 replicates (n=4). Different letters indicate significant differences in the different treatment group at same temperatures ($P<0.05$). * indicates significant differences in the same treatment group at different temperatures (* $0.01<P<0.05$; ** $0.001<P<0.01$; *** $P<0.001$). ns indicates no significant difference ($P>0.05$).

3.5 Hepatopancreas biochemical parameters

3.5.1 Antioxidant enzyme activities

Figure 4 illustrates the impact of *H. pluvialis* supplementation on the hepatopancreatic antioxidant enzyme activities in *L. vannamei* shrimp under varying water temperatures. The findings demonstrated that, following exposure to elevated temperatures, total antioxidant capacity (T-AOC) was significantly higher in the NT_LFM_HP group compared to the NT_C and NT_LFM groups ($P<0.05$). Similarly, SOD activity was significantly higher in the NT_LFM_HP group compared to the NT_C and NT_LFM groups ($P<0.05$). After the inclusion of *H. pluvialis*, MDA levels were significantly lower in the NT_LFM_HP group compared to the NT_C and NT-LF groups ($P<0.05$). Following a decrease in temperature, SOD activity was significantly higher in the LT_C group compared to the LT_LFM_HP group ($P<0.05$). Besides, MDA levels were significantly lower in the LT_LFM_HP groups compared to the LT_C group ($P<0.05$).

3.5.2 Expression of antioxidant-related genes

The gene expression levels of antioxidant-related genes in the hepatopancreas of *L. vannamei* are depicted in Figure 5. Significantly lower expression levels of *cat* and *sod* were observed in the NT_LFM and LT_LFM groups compared to the NT_LFM_HP and LT_LFM_HP groups ($P<0.05$). Additionally, the relative expression of *gpx* was higher in the NT_LFM_HP and LT_LFM_HP groups compared to the NT_LFM and LT_LFM groups.

3.6 Immune response

The Toll and IMD signaling pathways were identified as pivotal elements of the innate immune response in shrimp, as evidenced by the expression of relevant genes depicted in Figures 6, 7.

In the Toll pathway, the relative expression level of *toll* mRNA was significantly higher in the NT_C and LT_C groups compared to the NT_LFM, NT_LFM_HP, LT_LFM, and LT_LFM_HP groups ($P<0.05$). The highest relative expression of *toll* was observed in the NT_C group. At the same time, *dorsal* mRNA expression levels were significantly higher in the LT_LFM_HP group compared to the other groups ($P<0.05$), while *crustin* mRNA expression levels were highest in the LT_C group, and the differences between the groups under different temperature conditions were significant ($P<0.05$).

In the IMD pathway, the relative expression level of *imd* mRNA was significantly higher in the NT_LFM_HP and LT_LFM_HP groups compared to the NT_C, NT_LFM, LT_C, and LT_LFM groups ($P<0.05$). Additionally, the relative expression level of *relish* was higher in the LT_LFM_HP group compared to the NT_LFM_HP group. The mRNA expression levels of *lysc* in the LT_LFM_HP group were significantly higher compared to the other five groups ($P<0.05$), with the lowest expression observed in the NT_LFM group. Specifically, the relative expression of *L. vannamei*

TABLE 4 Effect of the addition of *H. pluvialis* at varying water temperatures on the muscle composition of *L. vannamei* (% dry weigNT).

Parameters (% dry matter)	NT_C	NT_LFM	NT_LFM_HP	LT_C	LT_LFM	LT_LFM_HP
Moisture	76.59 ± 0.01	74.94 ± 0.01	77.95 ± 0.01	75.17 ± 0.01	75.48 ± 0.01	75.17 ± 0.01
Crude protein	77.03 ± 0.80	76.82 ± 0.45	76.87 ± 0.42	76.20 ± 0.65	75.43 ± 0.59	75.92 ± 0.92
Crude lipid	6.18 ± 0.41	5.14 ± 0.25	5.68 ± 0.44	4.88 ± 0.17	4.62 ± 0.31	4.89 ± 0.21

Values are expressed as the means ± SEM with 4 replicates (n=4).

lysc mRNA in the LT_LFM_HP group was markedly higher compared to the remaining groups ($P<0.05$), with the lowest expression detected in the NT_LFM group.

3.7 Gut microbiota analysis

Sequences were grouped into operational taxonomic units (OTUs) at a 97% similarity threshold. The constructed Venn diagram delineated that the NT_C, NT_LFM, NT_LFM_HP, LT_C, LT_LFM, and LT_LFM_HP groups contained 8, 52, 81, 8, 5, and 10 unique Operational Taxonomic Units (OTUs), respectively. As shown in Figure 8, significant differences were noted in the microbial community structure due to differences in water temperature and the presence of *H. pluvialis*. Figure 9 illustrates the analysis of alpha diversity within the shrimp gut microbiome, as determined by sequencing results of the Ace, Chao1, Shannon, and Simpson diversity indices. The findings signaled that the coverage index for each treatment group exceeded 0.998. The beta diversity analysis visualized through PCoA plots (Figure 10) demonstrated the impact of varying water temperatures (normal and low) on variations in the intestinal microbiota of *L. vannamei* following exposure to *H. pluvialis*. As anticipated, the composition of the NT_LFM_HP group was significantly different compared to the other groups ($P<0.05$).

Figure 11 illustrates the distribution of gut bacteria across treatment groups, categorized at the phylum, class, family, and genus levels. Additionally, the relative abundance of species was depicted at each taxonomic level. Figure 11A displays the relative abundance of gut bacterial phyla, primarily composed of Bacteroidota, Proteobacteria, Actinobacteriota, and Verrucomicrobia. Figure 11B displays the relative abundance of gut bacterial classes in *L. vannamei*, with major bacteria identified as Bacteroidia, Alphaproteobacteria, Gammaproteobacteria, Acidimicrobiia, Verrucomicrobia, and Actinobacteria. Figure 11C displays the relative abundance of gut bacterial families, predominantly composed of Flavobacteraceae, Rhodobacteraceae, Vibrionaceae, and Actinomarinales. Figure 11D displays the relative abundance of gut bacterial genera, including Flavobacteriales, Rhodobacteraceae, Ruegeria, Spongiimonas, Vibrio, Actinomarinales, and Haloferula.

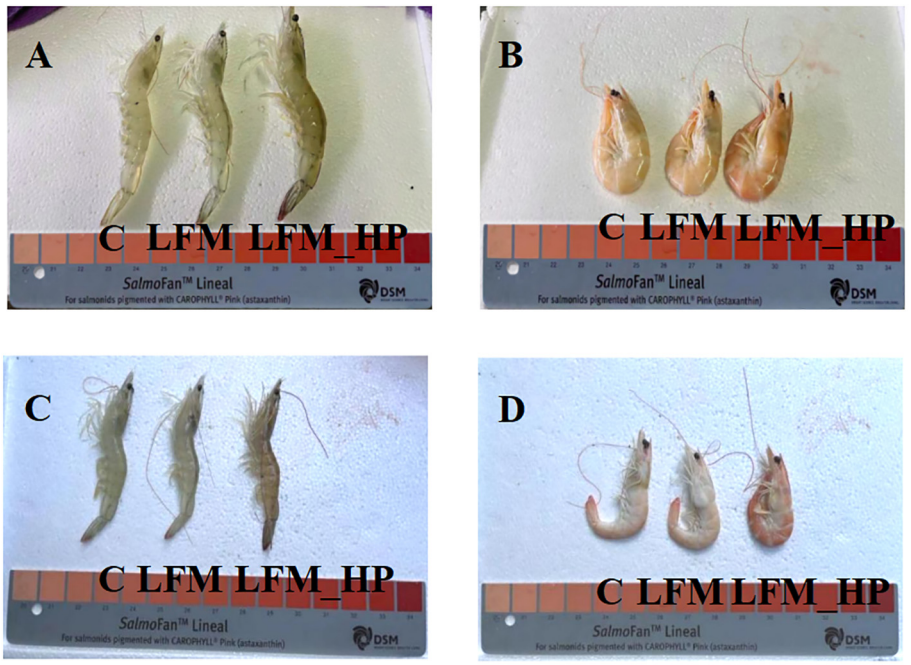

FIGURE 1
Effect of the addition of *H. pluvialis* at varying water temperatures on the body colour of *L. vannamei*. **(A)** Normal water temperature group of live shrimp; **(B)** Normal water temperature group after cooking shrimp; **(C)** Low water temperature group of live shrimp; **(D)** Low water temperature group after cooking shrimp.

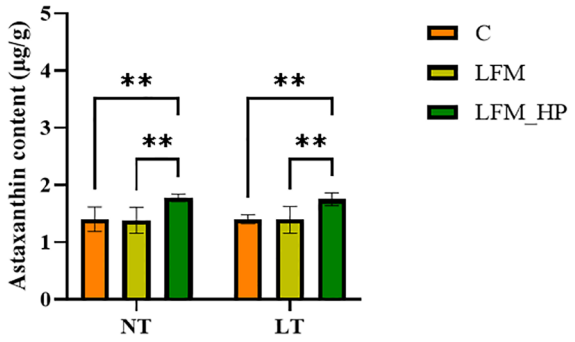

FIGURE 2
Effect of the addition of *H. pluvialis* at varying water temperatures on the astaxanthin content of shrimp shells of *L. vannamei*. Data represent the means ± SEM (n = 4). * indicates significant differences in the same treatment group at different temperatures (** 0.001<*P*<0.01).

4 Discussion

L. vannamei is considered a significant economically cultivated species (17). The growth, development, and metabolic performance of aquatic organisms are influenced by various environmental factors, with water temperature playing a critical role (18). Shrimp, as poikilothermic organisms, exhibit variations in body temperature in response to environmental conditions, which in turn impacts their metabolism and physiological regulatory mechanisms (19). Of note, nutrition, feeding, and feed utilization play crucial roles in commercial aquaculture due to the significant cost associated with feed (20). Consequently, microalgae have garnered considerable attention as a highly nutritious functional green additive in aquafeeds (21). Indeed, incorporating microalgae into aquafeeds has the potential to partially substitute fishmeal and enhance growth, performance, and immunity (22–25).

In the present study, the weight gain rate and specific growth rate of shrimp in the NT_C, NT_LFM, and NT_LFM_HP groups were significantly higher compared to the LT_C, LT_LFM, and LT_LFM_HP groups. Moreover, the weight gain rate of shrimp in the NT_LFM_HP group was higher than that of the NT_LFM group, with no significant difference observed between NT_LFM_HP and NT_C groups, suggesting that both temperature and *H. pluvialis* supplementation influenced shrimp feed intake and subsequently impacted their weight gain and specific growth rates, consistent with the findings of prior investigations indicating that *L. vannamei* exhibited enhanced growth rates within a specific temperature range (26). Noteworthily, no significant differences were noted in the survival rates of *L. vannamei* across treatment groups, whereas variations in feed conversion ratios were observed between the normal- and low-temperature treatment cohorts. In line with the findings of previous studies, at a temperature of 20°C, both the feeding and growth levels of *L. vannamei* were diminished (27). The inclusion of *H. pluvialis* did not yield statistically significant changes in the body composition and hepatopancreas of *L. vannamei* across the experimental groups. Additionally, the morphology of the hepatopancreas and hepatic ducts remained normal in all treatment groups, with B, R, and E cells displaying typical morphology and the absence of evident lesions. Overall, *L.*

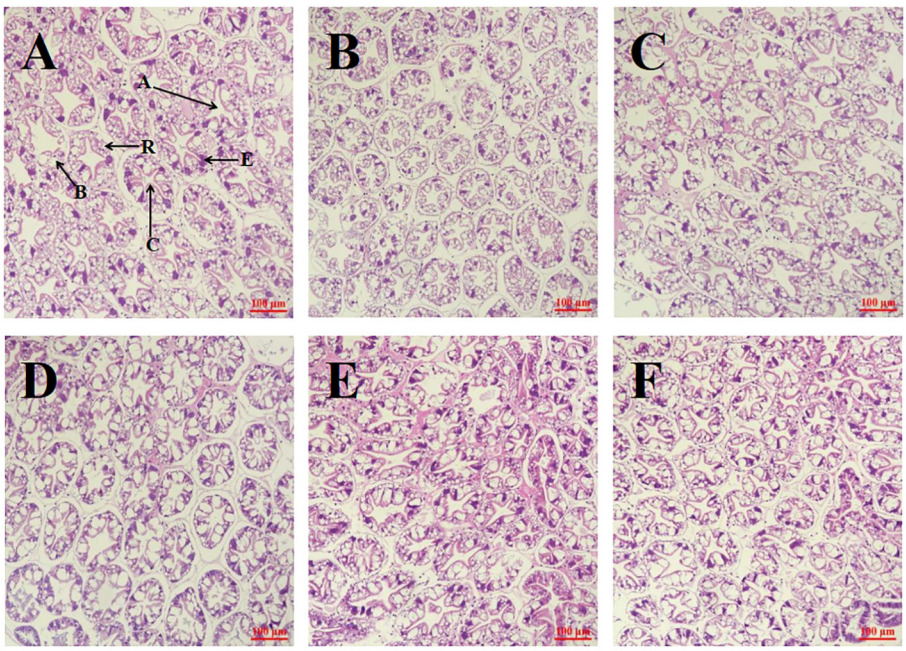

FIGURE 3
Effect of the addition of *H. pluvialis* at varying water temperatures on the hepatopancreas morphology of *L. vannamei*. Scale bar: 100 μm. Magnification: 20×. **(A)** NT_C group; **(B)** NT_LFM group; **(C)** NT_LFM_HP group; **(D)** LT_C group; **(E)** LT_LFM group; **(F)** LT_LFM_HP group. (A: stellate lumen, C: basement membrane, B: B cell, R: R cell, E: E cell).

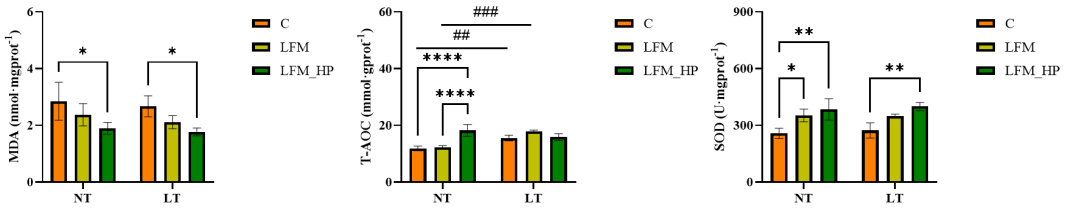

FIGURE 4
Effect of incorporating *H. pluvialis* at varying water temperatures on the hepatopancreatic antioxidant enzyme activities of *L. vannamei*. MDA, malondialdehyde; T-AOC, total antioxidant capacity; SOD, superoxide dismutase. Data represent the means ± SEM (n = 4).* indicates significant differences in the same treatment group at different temperatures (* 0.01<*P*<0.05; ** 0.001<*P*<0.01; **** *P*<0.0001). # indicates significant differences in the same treatment group at different temperatures (## 0.001<*P*<0.01; ### P<0.001).

vannamei in the normal-temperature environment with *H. pluvialis* supplemtation exhibited favorable growth and physiological outcomes. Comparable findings have been documented in studies involving *Pseudosciaena crocea* (*P. crocea*) (28) and *Trachinotus ovatus* (*T. ovatus*) (29).

Body color is a significant factor in evaluating the quality of crustaceans. *H. pluvialis*, a microalgae known for its high astaxanthin content, has garnered interest in meeting the demand for natural pigments in aquaculture (30). Astaxanthin concentrations and body pigmentation intensity in L. vannamei were significantly higher in the NT_LFM_HP and LT_LFM_HP groups, consistent with similar observations in *L. vannamei* and *Marsupenaeus japonicus* (*M. japonicus*) (31, 32).

This study also aimed to examine the antioxidant properties of *H. pluvialis* at varying water temperatures in *L. vannamei*. Carotenoids, non-enzymatic compounds within the antioxidant system, interact with reactive oxygen species (ROS) to mitigate oxidative damage in tissues (33). Superoxide dismutase (SOD) and catalase (CAT) are integral components of an organism's antioxidant system. Collectively, they play essential roles in scavenging reactive oxygen species, alleviating oxidative stress, modulating the levels of reactive oxygen species, and preserving

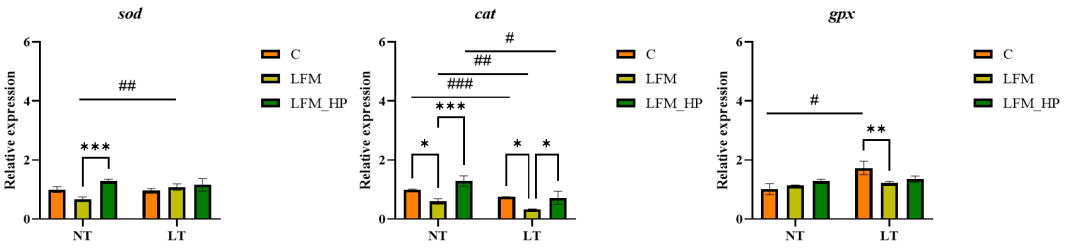

FIGURE 5
Effect of the addition of *H. pluvialis* at varying water temperatures on the expression of antioxidant genes in the hepatopancreas of *L. vannamei*. Data represent the means ± SEM (n = 4). * indicates significant differences in the same treatment group at different temperatures (* 0.01<*P*<0.05; ** 0.001<*P*<0.01; *** *P*<0.001). # indicates significant differences in the same treatment group at different temperatures (# 0.01<*P*<0.05; ## 0.001<*P*<0.01; ### *P*<0.001).

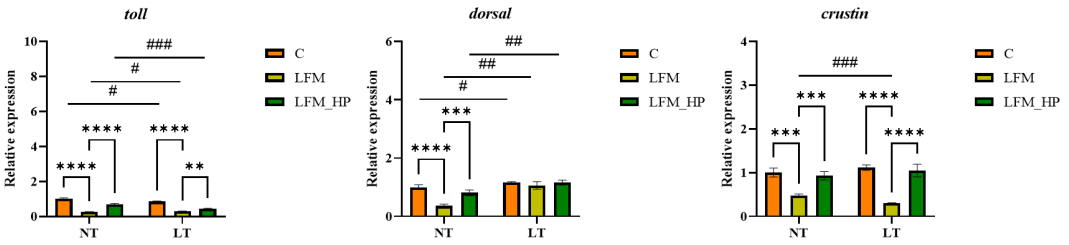

FIGURE 6
Effect of the addition of *H. pluvialis* at varying water temperatures on the expression of immune genes related to the Toll pathway of *L. vannamei*. Data represent the means ± SEM (n = 4). * indicates significant differences in the same treatment group at different temperatures (** 0.001<*P*<0.01; *** *P*<0.001; **** *P*<0.0001). # indicates significant differences in the same treatment group at different temperatures (# 0.01<*P*<0.05; ## 0.001<*P*<0.01; ### *P*<0.001).

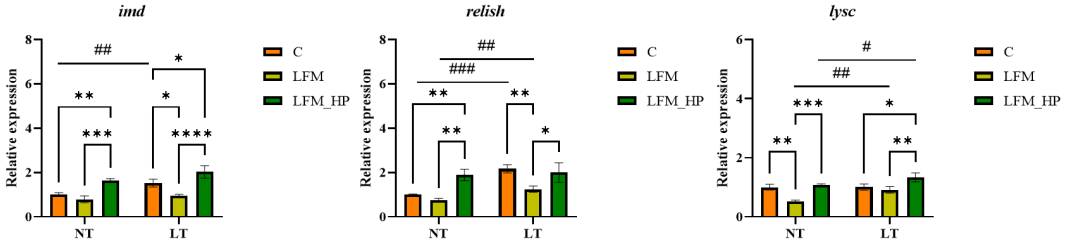

FIGURE 7
Effect of the addition of *H. pluvialis* at varying water temperatures on the expression of immune genes related to the IMD pathway of *L. vannamei*. Data represent the means ± SEM (n = 4). * indicates significant differences in the same treatment group at different temperatures (* 0.01<*P*<0.05; ** 0.001<*P*<0.01; *** *P*<0.001; **** P<0.0001). # indicates significant differences in the same treatment group at different temperatures (# 0.01<*P*<0.05; ## 0.001<*P*<0.01; ### *P*<0.001).

redox homeostasis (34, 35). In the current investigation, the incorporation of *H. pluvialis* in feeding groups (NT_LFM_HP, LT_LFM_HP) reduced MDA levels, indicative of diminished lipid peroxidation and heightened antioxidant potential, thereby enhancing the capacity to eliminate lipid hydroperoxides in shrimp. Additionally, T-AOC and SOD levels were increased, indicating that the inclusion of *H. pluvialis* may significantly enhance the ability of shrimp to counteract oxygen-free radicals and promote antioxidant defenses. A study investigating *Penaeus monodon* (*P. monodon*) concluded that the inclusion of astaxanthin could enhance antioxidant enzyme activity (36). Analysis of mRNA expression levels of antioxidant-related genes in *L. vannamei* revealed up-regulation of the *cat*, *sod*, and *gpx* genes in groups fed *H. pluvialis* (NT_LFM_HP, LT_LFM_HP), indicating that *H. pluvialis* supplementation may mitigate the decrease in antioxidant capacity caused by low fishmeal diets. Several studies have established that incorporating *H. pluvialis* into the diet could up-regulate the expression levels of antioxidant genes (5, 37, 38), leading to increased SOD enzyme activity in *L. vannamei* cultured at low temperatures compared to those raised at normal temperatures, indicating that prolonged exposure to low temperatures in aquaculture may mitigate oxidative stress and improve antioxidant capacity. The majority of recent studies explored changes in temperature in aquaculture experiments and temperature stress and did not focus on long-term low-temperature aquaculture. Therefore, we theorize that long-term low-temperature aquaculture may enhance the organism's antioxidant capacity.

In the context of innate immunity in invertebrates, various signaling pathways are activated to regulate immunity through *in vivo* signaling. The Toll and IMD signaling pathways have been extensively investigated in relation to the development of the innate immune system in crustaceans (39). This study further investigated the mRNA levels of genes involved in the immune pathway, specifically focusing on the Toll pathway. The relative expression levels of the *toll*, *dorsal*, and *crustin* genes were significantly higher in the *H. pluvialis* supplementation group compared to the control group. In the IMD signaling pathway, the expression levels of *imd*, *relish*, and *lysc* were elevated in the *H. pluvialis* supplementation group. Similarly, in the IMD immune pathway, the relative mRNA expression levels of *imd*, *relish*, and *lysc* were up-regulated, indicating that exposure to *H. pluvialis* at varying temperatures may attenuate the impact of low fishmeal diets on shrimp immunocompetence. Additionally, in crayfish, the administration of astaxanthin modulated non-specific immunity levels following exogenous

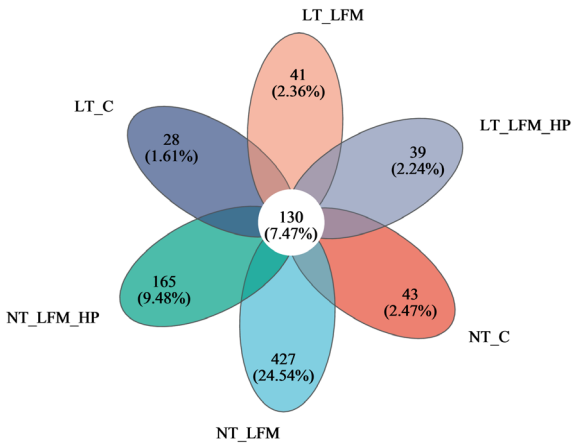

FIGURE 8
Venn diagram of OTUs Comparison of gut microbiota of the addition of *H. pluvialis* at varying water temperatures in *L. vannamei*.

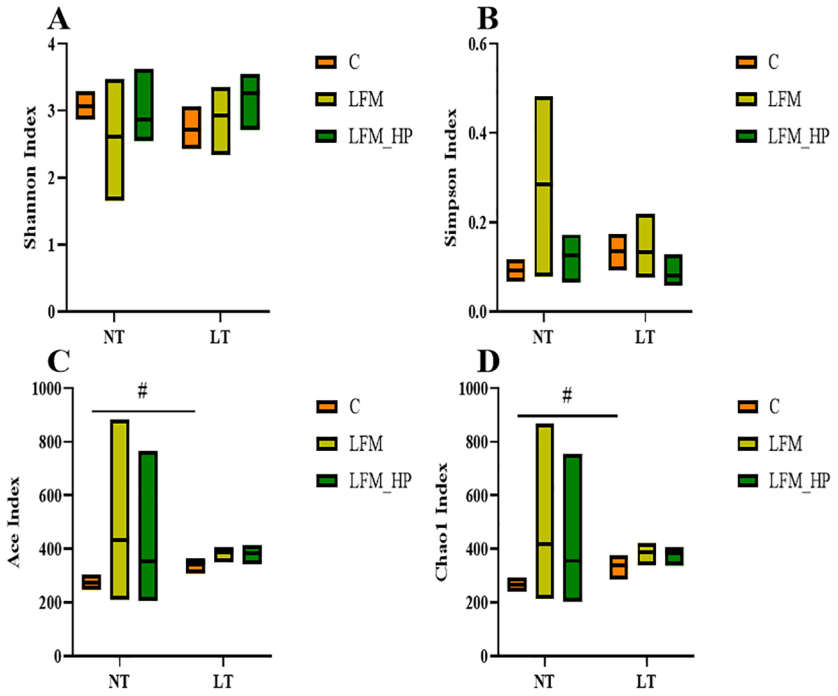

FIGURE 9
Alpha diversity index statistics of gut microbiota of the addition of (*H*) *pluvialis* at varying water temperatures in *L. vannamei*. Data represent the means ± SEM (n = 4). # indicates significant differences in the same treatment group at different temperatures ($P<0.05$). **(A)** Shannon index; **(B)** Simpson index; **(C)** Ace index; **(D)** Chao1 index.

challenges (40). Studies have demonstrated that the inclusion of astaxanthin in the diet of *M. japonicus* boosted the immune response (41). Additionally, research indicated that *H. pluvialis* may contribute to the activation of the phenoloxidase cascade, eventually leading to enhanced immunity (42, 43). In this study, the impact of varying water temperatures on the immune system was examined. Our findings indicated that in the Toll signaling immune pathway, the normal water temperature group exhibited lower immune function compared to the low water temperature group. Additionally, in the IMD signaling immune pathway, the low water temperature group displayed significantly higher relative mRNA expression levels of the *imd*, *relish*, and *lysc* genes compared to the normal water temperature group. We postulate that shrimp cultured in a prolonged low-temperature environment may regulate their own immune system, thereby sustaining stable life and health. Moreover, we theorize that under extended low-temperature conditions, shrimp may autonomously modulate its immune response to maintain consistent vital functions.

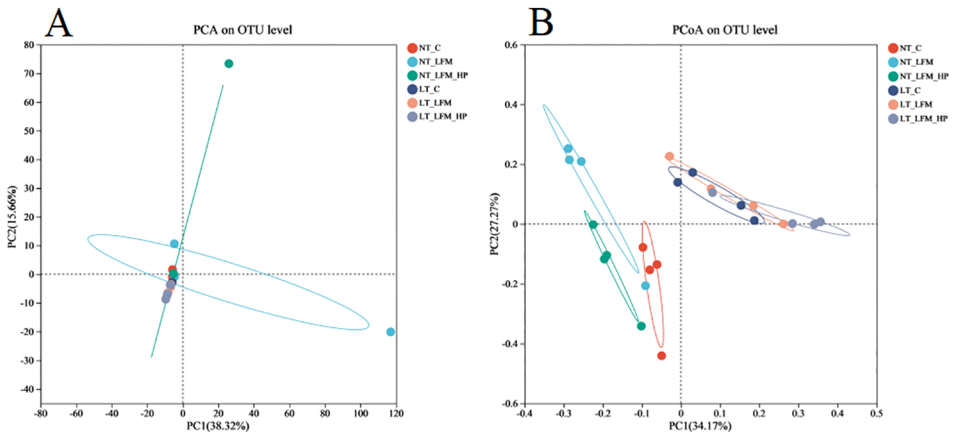

FIGURE 10
Beta diversity analysis of gut microbiota of the addition of *H. pluvialis* at varying water temperatures in *L. vannamei*. **(A)** PCA on OTU level; **(B)** PCoA on OTU level.

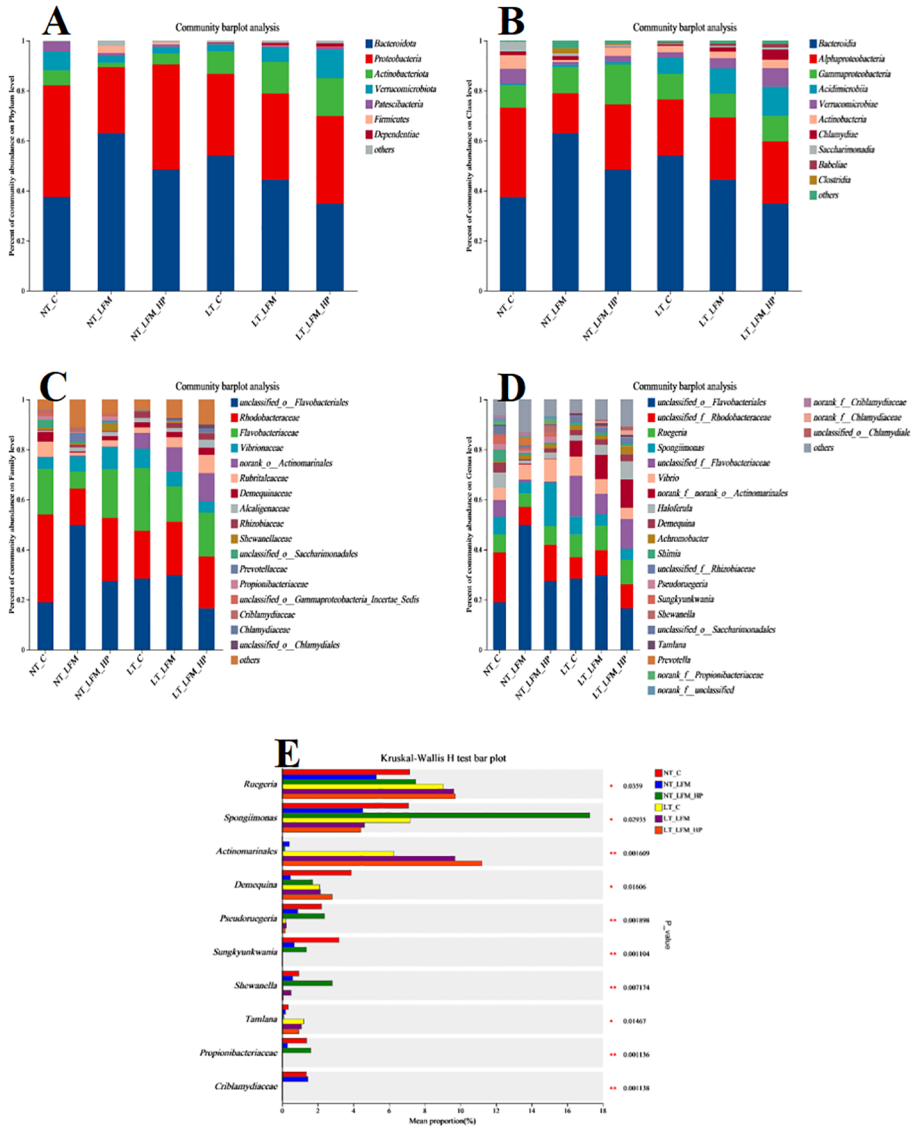

FIGURE 11
Relative abundance of bacterial community at **(A)** phylum, **(B)** class, **(C)** family, and **(D)** genus levels of gut microbiota of the addition of *H. pluvialis* at varying water temperatures in *L. vannamei*. **(E)** The significant difference among different treatments at the genus level.

The growth and health of organisms are influenced by gut microbial communities (44), while water temperature, a critical environmental factor in aquaculture, impacts the compositional structure and dynamic balance of these communities. This study investigated the gut microbiota of *L. vannamei* and identified significant differences between the NT_LFM_HP group and the remaining groups. The analysis of sample complexity revealed a significant difference in the number of operational taxonomic units (OTUs) between the NT_LFM, NT_LFM_HP, and other groups, suggesting that variations in temperature and the presence of *H. pluvialis* may impact the composition of gut microbiota, leading to distinct microbial communities. Beta diversity analysis unveiled that the gut sample points of the NT_LFM_HP group exhibited greater dissimilarity from the sample points of the other groups, with the microbial communities in the NT_LFM_HP group significantly differing from those in the other groups. This observation suggested that *H. pluvialis* influenced the relative abundance of dominant operational taxonomic units (OTUs). The relative abundance plot of the gut flora composition of *L. vannamei* indicated that Proteobacteria, Actinobacteria, and Bacteroidetes were the predominant gut microbial species, consistent with the findings of previous studies (45–47). The findings also indicated that reducing fishmeal content (NT_LFM, LT_LFM) resulted in a higher abundance of Flavobacteraceae. Importantly, *H. pluvialis* supplementation (NT_LFM_HP, LT_LFM_HP) promoted this increase, suggesting that the presence of *H. pluvialis* alleviated the detrimental impact of harmful microorganisms such as Flavobacterium. It is worthwhile

emphasizing that the results uncovered significant differences in the abundance of Vibrionaceae and Actinomarinales between low- and normal-temperature environments, with Vibrionaceae being more abundant in normal-temperature environments and Actinomarinales being more abundant in low-temperature environments. This suggested that Actinomarinales may play a decisive role in enhancing shrimp immunity by resisting bacterial invasion and improving immune parameters (48, 49). Furthermore, the findings of this study suggested that exposure to low temperatures may decrease the abundance of detrimental intestinal flora, potentially enhancing shrimp resistance to pathogens through the modulation of intestinal flora composition. Furthermore, the research indicated that cultivating shrimp in low water temperatures could promote immune responses in non-specific immune assays, thereby supporting their overall health and survival.

5 Conclusion

The study incorporated varying water temperatures and fishmeal levels, including a group with 20% fishmeal and another with 10% fishmeal supplemented with *H. pluvialis*. The findings exposed that *L. vannamei* growth and immune response were negatively affected by reducing fishmeal levels, whereas *H. pluvialis* supplementation improved growth, antioxidant capacity, and immune function. Additionally, under long-term low-temperature conditions, *L. vannamei* demonstrated enhanced resistance to external pathogens through immune system modulation. Overall, *H. pluvialis*, as a natural additive, exerted positive effects on aquatic animal nutrition, including promoting growth, improving immunity, and improving biochemical indicators. Taken together, these results collectively highlighted the extensive application potential of *H. pluvialis* in the aquatic feed industry owing to its unique characteristics.

Data availability statement

The original contributions presented in the study are included in the article/supplementary material. Further inquiries can be directed to the corresponding authors.

Ethics statement

The manuscript presents research on animals that do not require ethical approval for their study.

Author contributions

SL: Conceptualization, Data curation, Writing – original draft. MC: Data curation, Writing – review & editing. XC: Investigation, Writing – review & editing. YML: Investigation, Writing – review & editing. YFL: Investigation, Writing – review & editing. PZ: Investigation, Writing – review & editing. XH: Investigation, Writing – review & editing. BT: Supervision, Writing – review & editing. JN: Funding acquisition, Supervision, Writing – review & editing.

Funding

The author(s) declare financial support was received for the research, authorship, and/or publication of this article. The research received funding from multiple sources, including the National Key Research and Development Program of China (2023YFD2401705), Project of Algae health Science Co., Ltd. (HT99982023-0347), Project of Science and Technology of Guangxi Province (AA23062047), Project of National Natural Science Foundation of China (32172982), and Project of China Agriculture Research System of MOF and MARA 48 (CARS 48). The funders had no role in the study design, data collection and analysis, decision to publish, and preparation of the manuscript.

Conflict of interest

Authors YML, YFL, PNZ and XYH were employed by Algae Health Science Co., Ltd.

The remaining authors declare that the research was conducted in the absence of any commercial or financial relationships that could be construed as a potential conflict of interest.

Generative AI statement

The author(s) declare that no Generative AI was used in the creation of this manuscript.

Publisher's note

References

1. Zhang Y, Yu J, Su Y, Du Y, Liu Z. Long-term changes of water quality in aquaculture-dominated lakes as revealed by sediment geochemical records in Lake Taibai (Eastern China). *Chemosphere.* (2019) 235:297–307. doi: 10.1016/j.chemosphere.2019.06.179

2. Chen J, Sun R, Pan C, Sun Y, Mai B, Li QX. Antibiotics and food safety in aquaculture. *J Agric Food Chem.* (2020) 68:11908–19. doi: 10.1021/acs.jafc.0c03996

3. Santos L, Ramos F. Analytical strategies for the detection and quantification of antibiotic residues in aquaculture fishes: A review. *Trends Food Sci Technol*. (2016) 52:16–30. doi: 10.1016/j.tifs.2016.03.015

4. Bauer A, Minceva M. Direct extraction of astaxanthin from the microalgae *Haematococcus pluvialis* using liquid–liquid chromatography. *RSC Adv*. (2019) 9:22779–89. doi: 10.1039/C9RA03263K

5. Liu XH, Wang BJ, Li YF, Wang L, Liu JG. Effects of dietary botanical and synthetic astaxanthin on E/Z and R/S isomer composition, growth performance, and antioxidant capacity of white shrimp, *Litopenaeus vannamei*, in the nursery phase [For this article an Erratum has been published. *Invertebrate Survival J*. (2018) 15:131–40. doi: 10.25431/1824-307X/isj.v15i1.131-140

6. Yu Y, Liu Y, Yin P, Zhou W, Tian L, Liu Y, et al. Astaxanthin attenuates fish oil-related hepatotoxicity and oxidative insult in juvenile pacific white shrimp (*Litopenaeus vannamei*). *Mar Drugs*. (2020) 18:218. doi: 10.3390/md18040218

7. Cheng Y, Wu S. Effect of dietary astaxanthin on the growth performance and nonspecific immunity of red swamp crayfish *Procambarus clarkii*. *Aquaculture*. (2019) 512:734341. doi: 10.1016/j.aquaculture.2019.734341

8. Angell A, de Nys R, Mangott A, Vucko MJ. The effects of concentration and supplementation time of natural and synthetic sources of astaxanthin on the colouration of the prawn *Penaeus monodon*. *Algal Res*. (2018) 35:577–85. doi: 10.1016/j.algal.2018.09.031

9. Wang Z, Qu Y, Zhuo X, Li J, Zou J, Fan L. Investigating the physiological responses of Pacific white shrimp *Litopenaeus vannamei* to acute cold-stress. *PeerJ*. (2019) 7:e7381. doi: 10.7717/peerj.7381

10. Tang Y, Tao P, Tan J, Mu H, Peng L, Yang D, et al. Identification of bacterial community composition in freshwater aquaculture system farming of *Litopenaeus vannamei* reveals distinct temperature-driven patterns. *Int J Mol Sci*. (2014) 15:13663–80. doi: 10.3390/ijms150813663

11. Topuz M, Kır M. Critical temperatures and aerobic metabolism in post-larvae of Pacific white shrimp *Litopenaeus vannamei* (Boone, 1931). (2023) 193:607–14. doi: 10.1007/s00360-023-01522-4

12. Millard RS, Ellis RP, Bateman KS, Bickley LK, Tyler CR, van Aerle R, et al. How do abiotic environmental conditions influence shrimp susceptibility to disease? A critical analysis focussed on White Spot Disease. *J Invertebrate Pathol*. (2021) 186:107369. doi: 10.1016/j.jip.2020.107369

13. Xie J-J, Liu Q, Liao S, Fang H-H, Yin P, Xie S-W, et al. Effects of dietary mixed probiotics on growth, non-specific immunity, intestinal morphology and microbiota of juvenile pacific white shrimp, *Litopenaeus vannamei*. *Fish Shellfish Immunol*. (2019) 90:456–65. doi: 10.1016/j.fsi.2019.04.301

14. Xiong J, Yu W, Dai W, Zhang J, Qiu Q, Ou C. Quantitative prediction of shrimp disease incidence via the profiles of gut eukaryotic microbiota. *Appl Microbiol Biotechnol*. (2018) 102:3315–26. doi: 10.1007/s00253-018-8874-z

15. Al-Masqari ZA, Guo H, Wang R, Yan H, Dong P, Wang G, et al. Effects of high temperature on water quality, growth performance, enzyme activity and the gut bacterial community of shrimp (*Litopenaeus vannamei*). *Aquaculture Res*. (2022) 53:3283–96. doi: 10.1111/are.15836

16. Liu J, Wang K, Wang Y, Chen W, Jin Z, Yao Z, et al. Strain-specific changes in the gut microbiota profiles of the white shrimp *Litopenaeus vannamei* in response to cold stress. *Aquaculture*. (2019) 503:357–66. doi: 10.1016/j.aquaculture.2019.01.026

17. Zhang C, Guo C-Y, Shu K-H, Xu S-L, Wang D-L. Comparative analysis of the growth performance, vitality, body chemical composition and economic efficiency of the main cultivated strains of Pacific white shrimp (*Litopenaeus vannamei*) in coastal areas of China. *Aquaculture*. (2024) 587:740856. doi: 10.1016/j.aquaculture.2024.740856

18. Lutterschmidt WI, Hutchison VH. The critical thermal maximum: data to support the onset of spasms as the definitive end point. *Can J Zoology*. (1997) 75. doi: 10.1139/z97-782

19. Zhang L, Sha Z, Cheng J. Time-course and tissue-specific molecular responses to acute thermal stress in Japanese mantis shrimp oratosquilla oratoria. *Int J Mol Sci*. (2023) 24:11936. doi: 10.3390/ijms241511936

20. Hoseinifar SH, Dadar M, Ringø E. Modulation of nutrient digestibility and digestive enzyme activities in aquatic animals: The functional feed additives scenario. *Aquaculture Res*. (2017) 48:3987–4000. doi: 10.1111/are.13368

21. Roy SS, Pal R. Microalgae in aquaculture: A review with special references to nutritional value and fish dietetics. *Proc Zool Soc*. (2015) 68:1–8. doi: 10.1007/s12595-013-0089-9

22. Cerezuela R, Guardiola FA, Meseguer J, Esteban MÁ. Enrichment of gilthead seabream (Sparus aurata L.) diet with microalgae: effects on the immune system. *Fish Physiol Biochem*. (2012) 38:1729–39. doi: 10.1007/s10695-012-9670-9

23. Reyes-Becerril M, Angulo C, Estrada N, Murillo Y, Ascencio-Valle F. Dietary administration of microalgae alone or supplemented with Lactobacillus sakei affects immune response and intestinal morphology of Pacific red snapper (Lutjanus Peru). *Fish Shellfish Immunol*. (2014) 40:208–16. doi: 10.1016/j.fsi.2014.06.032

24. Reyes-Becerril M, Guardiola F, Rojas M, Ascencio-Valle F, Esteban MÁ. Dietary administration of microalgae Navicula sp. affects immune status and gene expression of gilthead seabream (Sparus aurata). *Fish Shellfish Immunol*. (2013) 35:883–9. doi: 10.1016/j.fsi.2013.06.026

25. Shah MR, Lutzu GA, Alam A, Sarker P, Kabir Chowdhury MA, Parsaeimehr A, et al. Microalgae in aquafeeds for a sustainable aquaculture industry. *J Appl Phycol*. (2018) 30:197–213. doi: 10.1007/s10811-017-1234-z

26. Ponce-Palafox J, Martinez-Palacios CA, Ross LG. The effects of salinity and temperature on the growth and survival rates of juvenile white shrimp, *Penaeus vannamei*, Boone, 1931. *Aquaculture*. (1997) 157:107–15. doi: 10.1016/S0044-8486(97)00148-8

27. Bórquez-Lopez RA, Casillas-Hernandez R, Lopez-Elias JA, Barraza-Guardado RH, Martinez-Cordova LR. Improving feeding strategies for shrimp farming using fuzzy logic, based on water quality parameters. *Aquacultural Eng*. (2018) 81:38–45. doi: 10.1016/j.aquaeng.2018.01.002

28. Li M, Wu W, Zhou P, Xie F, Zhou Q, Mai K. Comparison effect of dietary astaxanthin and *Haematococcus pluvialis* on growth performance, antioxidant status and immune response of large yellow croaker *Pseudosciaena crocea*. *Aquaculture*. (2014) 434:227–32. doi: 10.1016/j.aquaculture.2014.08.022

29. Zhao W, Fang H-H, Liu Z-Z, Huang M-Q, Su M, Zhang C-W, et al. A newly isolated strain of *Haematococcus pluvialis* JNU35 improves the growth, antioxidation, immunity and liver function of golden pompano (Trachinotus ovatus). *Aquaculture Nutr*. (2021) 27:342–54. doi: 10.1111/anu.13188

30. Guerin M, Huntley ME, Olaizola M. *Haematococcus* astaxanthin: applications for human health and nutrition. *Trends Biotechnol*. (2003) 21:210–6. doi: 10.1016/S0167-7799(03)00078-7

31. Chien Y-H, Shiau W-C. The effects of dietary supplementation of algae and synthetic astaxanthin on body astaxanthin, survival, growth, and low dissolved oxygen stress resistance of kuruma prawn, *Marsupenaeus japonicus* Bate. *J Exp Mar Biol Ecol*. (2005) 318:201–11. doi: 10.1016/j.jembe.2004.12.016

32. Ju ZY, Deng D-F, Dominy WG, Forster IP. Pigmentation of Pacific White Shrimp, *Litopenaeus vannamei*, by Dietary Astaxanthin Extracted from *Haematococcus pluvialis*. *J World Aquaculture Soc*. (2011) 42:633–44. doi: 10.1111/j.1749-7345.2011.00511.x

33. He H, Huang N, Cao R, Meng L. *Structures, Antioxidation Mechanism, and Antioxidation Test of the Common Natural Antioxidants in Plants* (2015). Available online at: https://www.semanticscholar.org/paper/Structures%2C-Antioxidation-Mechanism%2C-and-Test-of-in-He-Huang/6513dfd3177302211dea2a83811791e71b5696ea (Accessed August 28, 2024).

34. Duan Y, Zhang Y, Dong H, Zhang J. Effect of desiccation on oxidative stress and antioxidant response of the black tiger shrimp *Penaeus monodon*. *Fish Shellfish Immunol*. (2016) 58:10–7. doi: 10.1016/j.fsi.2016.09.004

35. Long X, Wu X, Zhao L, Liu J, Cheng Y. Effects of dietary supplementation with *Haematococcus pluvialis* cell powder on coloration, ovarian development and antioxidation capacity of adult female Chinese mitten crab. *Eriocheir sinensis*. *Aquaculture*. (2017) 473:545–53. doi: 10.1016/j.aquaculture.2017.03.010

36. Pan C-H, Chien Y-H, Hunter B. The resistance to ammonia stress of *Penaeus monodon* Fabricius juvenile fed diets supplemented with astaxanthin. *J Exp Mar Biol Ecol*. (2003) 297:107–18. doi: 10.1016/j.jembe.2003.07.002

37. Chuchird N, Rorkwiree P, Rairat T. Effect of dietary formic acid and astaxanthin on the survival and growth of Pacific white shrimp (*Litopenaeus vannamei*) and their resistance to Vibrio parahaemolyticus. *SpringerPlus*. (2015) 4:440. doi: 10.1186/s40064-015-1234-x

38. Wang H, Dai A, Liu F, Guan Y. Effects of dietary astaxanthin on the immune response, resistance to white spot syndrome virus and transcription of antioxidant enzyme genes in Pacific white shrimp *Litopenaeus vannamei*. *Iranian J Fisheries Sci*. (2015) 14:699–718. doi: 10.22092/ijfs.2018.114476

39. Li C, Wang S, He J. The two NF-κB pathways regulating bacterial and WSSV infection of shrimp. *Front Immunol*. (2019) 10:1785. doi: 10.3389/fimmu.2019.01785

40. Li F, Huang S, Lu X, Wang J, Lin M, An Y, et al. Effects of dietary supplementation with algal astaxanthin on growth, pigmentation, and antioxidant capacity of the blood parrot (Cichlasoma citrinellum × Cichlasoma synspilum). *J Ocean Limnol*. (2018) 36:1851–9. doi: 10.1007/s00343-019-7172-7

41. Wang W, Ishikawa M, Koshio S, Yokoyama S, Dawood MAO, Hossain Md S, et al. Interactive effects of dietary astaxanthin and cholesterol on the growth, pigmentation, fatty acid analysis, immune response and stress resistance of kuruma shrimp (Marsupenaeus japonicus). *Aquaculture Nutr*. (2019) 25:946–58. doi: 10.1111/anu.12913

42. Ngo HT, Nguyen TT, Nguyen QM, Tran AV, Do HT, Nguyen AH, et al. Screening of pigmented Bacillus aquimaris SH6 from the intestinal tracts of shrimp to develop a novel feed supplement for shrimp. *J Appl Microbiol*. (2016) 121:1357–72. doi: 10.1111/jam.13274

43. Yeh S-T, Lee C-S, Chen J-C. Administration of hot-water extract of brown seaweed *Sargassum duplicatum* via immersion and injection enhances the immune resistance of white shrimp Litopenaeus vannamei. *Fish Shellfish Immunol*. (2006) 20:332–45. doi: 10.1016/j.fsi.2005.05.008

44. Hou D, Huang Z, Zeng S, Liu J, Wei D, Deng X, et al. Intestinal bacterial signatures of white feces syndrome in shrimp. *Appl Microbiol Biotechnol*. (2018) 102:3701–9. doi: 10.1007/s00253-018-8855-2

45. Qiao F, Liu YK, Sun YH, Wang XD, Chen K, Li TY, et al. Influence of different dietary carbohydrate sources on the growth and intestinal microbiota of *Litopenaeus vannamei* at low salinity. . *Aquaculture Nutr*. (2017) 23:444–52. doi: 10.1111/anu.12412

46. Rungrassamee W, Klanchui A, Maibunkaew S, Chaiyapechara S, Jiravanichpaisal P, Karoonuthaisiri N. Characterization of intestinal bacteria in wild and domesticated adult black tiger shrimp (*Penaeus monodon*). *PloS One*. (2014) 9:e91853. doi: 10.1371/journal.pone.0091853

47. Suo Y, Li E, Li T, Jia Y, Qin JG, Gu Z, et al. Response of gut health and microbiota to sulfide exposure in Pacific white shrimp *Litopenaeus vannamei*. *Fish Shellfish Immunol*. (2017) 63:87–96. doi: 10.1016/j.fsi.2017.02.008

48. Kesarcodi-Watson A, Kaspar H, Lategan MJ, Gibson L. Probiotics in aquaculture: The need, principles and mechanisms of action and screening processes. *Aquaculture*. (2008) 274:1–14. doi: 10.1016/j.aquaculture.2007.11.019

49. Zhang M, Sun Y, Chen K, Yu N, Zhou Z, Chen L, et al. Characterization of the intestinal microbiota in Pacific white shrimp, *Litopenaeus vannamei*, fed diets with different lipid sources. *Aquaculture*. (2014) 434:449–55. doi: 10.1016/j.aquaculture.2014.09.008

50. McBeth JW. Carotenoids from nudibranchs. *Comp Biochem Physiol Part B: Comp Biochem*. (1972) 41:55–68. doi: 10.1016/0305-0491(72)90007-7

51. Xu K, Ren Y, Zhao S, Feng J, Wu Q, Gong X, et al. Oral d-ribose causes depressive-like behavior by altering glycerophospholipid metabolism via the gut-brain axis. *Commun Biol*. (2024) 7:1–14. doi: 10.1038/s42003-023-05759-1

52. Schloss PD, Westcott SL, Ryabin T, Hall JR, Hartmann M, Hollister EB, et al. Introducing mothur: open-source, platform-independent, community-supported software for describing and comparing microbial communities. *Appl Environ Microbiol*. (2009) 75:7537–41. doi: 10.1128/AEM.01541-09

53. Segata N, Izard J, Waldron L, Gevers D, Miropolsky L, Garrett WS, et al. Metagenomic biomarker discovery and explanation. *Genome Biol*. (2011) 12:R60. doi: 10.1186/gb-2011-12-6-r60

frontiers | Frontiers in Immunology

TYPE Original Research
PUBLISHED 28 January 2025
DOI 10.3389/fimmu.2025.1525992

OPEN ACCESS

EDITED BY
Samad Rahimnejad,
University of Murcia, Spain

REVIEWED BY
Omid Safari,
Ferdowsi University of Mashhad, Iran
Hamed Ghafarifarsani,
Urmia University, Iran

*CORRESPONDENCE
Sentai Liao
liaost@163.com
Dongxu Xing
dongxuxing@126.com

†These authors have contributed equally to this work

RECEIVED 11 November 2024
ACCEPTED 09 January 2025
PUBLISHED 28 January 2025

CITATION
Zhou D, Zhong W, Fu B, Li E, Hao L, Li Q, Yang Q, Zou Y, Liu Z, Wang F, Liao S and Xing D (2025) Dietary supplementation of mulberry leaf oligosaccharides improves the growth, glucose and lipid metabolism, immunity, and virus resistance in largemouth bass (*Micropterus salmoides*). *Front. Immunol.* 16:1525992. doi: 10.3389/fimmu.2025.1525992

Dietary supplementation of mulberry leaf oligosaccharides improves the growth, glucose and lipid metabolism, immunity, and virus resistance in largemouth bass (*Micropterus salmoides*)

Donglai Zhou[1,2†], Wenhao Zhong[1,3†], Bing Fu[1], Erna Li[1,2], Le Hao[4], Qingrong Li[1], Qiong Yang[1], Yuxiao Zou[1], Zhenxing Liu[4], Fubao Wang[2], Sentai Liao[1*] and Dongxu Xing[1*]

[1]Sericultural & Agri-Food Research Institute, Guangdong Academy of Agricultural Sciences, Guangdong Key Laboratory of Agricultural Products Processing, Guangzhou, China, [2]Guangdong Provincial Engineering Technology Research Center of Special Aquatic Functional Feed, Foshan, China, [3]College of Food Science and Technology, Guangdong Ocean University, Zhanjiang, China, [4]Institute of Animal Health, Guangdong Academy of Agricultural Sciences, Guangzhou, China

This study investigated the effects of dietary supplementation of mulberry leaf oligosaccharides (MLO) on the growth performance, serum biochemistry, glucose and lipid metabolism, antioxidant activity, liver health, and virus resistance in largemouth bass (*Micropterus salmoides*). The fish were fed with CK (basal diet), MLOL (basal diet supplemented with 0.5%MLO), and MLOH (basal diet supplemented with 1.0% MLO) for 80 days, and then subjected to a 21-day viral challenge experiment. The results showed that MLO supplementation had no adverse effect on the weight gain rate, specific growth rate, feed intake, and condition factor ($P > 0.05$), but significantly decreased the feed conversion rate and viscerosomatic index ($P< 0.05$). Moreover, the MLOL and MLOH group had significantly lower contents of triglyceride, blood glucose, and malondialdehyde and activities of serum alanine aminotransferase and aspartate aminotransferase, while significantly higher levels of serum and liver total superoxide dismutase and lower levels of glutathione than the CK group ($P< 0.05$). MLO supplementation significantly up-regulated the relative expression of glycolytic genes *gk* and *pfk* and lipid catabolism genes *ppar-α* and *cpt-1*, while obviously down-regulated that of *acc*, *fas*, and *dgat* related to fatty acid synthesis in the liver tissue ($P< 0.05$). In terms of liver health, MLO supplementation significantly up-regulated the relative expression of anti-inflammatory cytokines *il-10* and *tgf-β*, while decreased that of pro-inflammatory cytokines *nf-κb*, *il-8*, and *tnf-α* in the liver tissue ($P< 0.05$). The viral challenge test showed that MLO supplementation significantly improved the survival rate of *M. salmoides* after largemouth bass ranavirus (LMBV) infection. Dietary MLO supplementation promoted liver glucose

and lipid metabolism, and improved the immunity and resistance of *M. salmoides* to LMBV by regulating the PPAR signaling way and inhibiting the NF-kB signaling pathway. The appropriate addition amount of MLO to the diet was determined to be 1.0%.

KEYWORDS

largemouth bass, growth, serum biochemistry, liver metabolism, inflammation

1 Introduction

Largemouth bass (*Micropterus salmoides*) is an important economic fish species in the world as well as one of the most important freshwater economic fish in China. According to statistics, the production of *M. salmoides* in China exceeded 700,000 tons in 2021 (1). Breeding of *M. salmoides* provides a large amount of high-quality animal protein and brings great economic benefits in China. However, with the expansion of breeding scale and continuous increase in breeding density, the breeding environment has been gradually deteriorated, and the problem of diseases has become increasingly prominent, causing huge economic losses and seriously restricting the sustainable development of the industry (2). In order to treat and control diseases, antibiotics and chemicals are frequently used as therapeutic agents in aquaculture, which can lead to drug residues and have adverse effects on the safety of the environment, humans, and animals (3–5). At present, China has banned the addition of antibiotics in feed, and "reducing resistance to replace resistance" has become a new trend. Therefore, development of environment-friendly and safe alternatives to antibiotics has become a hot research topic. Among them, functional additives with preventive effects such as prebiotics and plant extracts have attracted great research attention (6).

Prebiotics are organic substances that are not directly digested and absorbed by the host, but can selectively promote the growth or activity of a few beneficial bacteria in the colon, thereby improving the health of the host (7, 8). With continuous progress in research on the functions and mechanisms of prebiotics, the application of oligosaccharides in aquaculture animals is becoming increasingly popular (9, 10). Previous research has demonstrated that dietary oligosaccharides can trap pathogenic bacteria and prevent their access to gut mucosa, and improve the activities of digestive enzymes and modulation of gut microbiota, so as to improve the growth and gut health of the reared fish (11, 12). Besides, oligosaccharides can act as immunostimulants in various fish species and significantly change the disease resistance (13, 14).

Mulberry leaf, a component of traditional Chinese medicine rich in polysaccharides, is widely grown in China (15, 16). Mulberry leaf oligosaccharides (MLO) can be obtained through enzymatic hydrolysis of mulberry leaf polysaccharides (MLP) (17). *In vitro* experiments have shown that MLO can better promote the proliferation of *Bifidobacterium* and *Lactobacillus* than glucose or galacto-oligosaccharides. In addition, bacterial cultures inoculated with MLO have higher acetic acid and lactic acid concentrations (18). A recent study has revealed that dietary supplementation of MLO can effectively reduce blood glucose level in type 2 diabetic mice (19). However, there has been limited relevant information on aquatic species. For example, *Ramulus mori* oligosaccharides could increase the abundance of Fusobacterium and *Cetobacterium* in the intestine and improve liver morphology, thereby improving the antiviral ability of *M. salmoides* (20). However, it remains unclear whether MLO can improve the immune and antioxidant capacity and glucose/lipid utilization and metabolism of *M. salmoides*. Therefore, this study aims to explore the effects of MLO supplementation on the growth performance, antioxidant capacity, glucose and lipid metabolism, liver health, and antiviral ability of *M. salmoides*, which may help improve the health outcomes in aquaculture.

2 Materials and methods

2.1 Preparation of MLO

MLP was isolated and extracted using the method as described previously (17). Briefly, defatted mulberry leaf powder was extracted with water at 80°C for 4 h at a ratio of 1: 30 (w/v), evaporated and concentrated at 50°C using a rotary evaporator (EYELA N-1100, Tokyo Rikakikai Co. Ltd, Tokyo, Japan), precipitated with 4 volumes of absolute ethanol for 12 h, and then centrifuged at 10,000× g for 10 min. The precipitate was collected and dissolved. The polysaccharide solution (50 mg/mL) was then mixed with Sevage reagent (1-butanol/chloroform, v/v = 1:4) at a ratio of 4: 1 (v/v). The mixture was shaken thoroughly for 30 min and then centrifuged at 10,000× g for 5 min. The aqueous phase separated from the supernatant was added to a quarter of its volume of the Sevage reagent. This process was repeated until the solution presented no absorption peak at 250–280 nm on a UV spectrophotometer (UV-1800, Shimadzu, Kyoto, Japan). The deproteinized liquid was further freeze-dried to obtain MLP and the phenol-sulfuric acid method was used to determine the purity.

10.3389/fimmu.2025.1525992

For production of the enzymatic hydrolysate containing MLO, the MLP was incubated with 1500 U/mL β-dextranase (Shanghai Ryon Biologcial Technology Co., Ltd., Shanghai, China) at 51°C for 4 h. Then, the hydrolysate was placed in a boiling water bath for 10 min to terminate the reaction and then centrifuged at 4000 r/min for 10 min to remove β-dextranase (the enzymatic optimization is not shown here). The supernatant was collected and freeze-dried to obtain MLO.

2.2 Molecular weight determination

The molecular weight (Mw) of MLO was determined by gel permeation chromatography (GPC) in a highperformance liquid chromatography system (LC-2050, Shimadzu, Japan) coupled with RID-20A differential refractive index detector, using a PL aquagel-OH MIXED-M column (7.5 × 300 mm, 8 µm, Agilent, USA). The MLO powder was prepared as a 10 mg/mL aqueous solution and filtered through a 0.22 µm Millipore filter. An aliquot of 20 µL sample solution was injected and eluted at a flow rate of 1.0 mL/min and a column temperature of 35°C with 0.2 mol/L $NaNO_3$ as the mobile phase. PEG of 1892 Da, 5121 Da, 10057 Da, 20552 Da, and 41531 Da were used as reference substances to calculate the Mw of MLO.

2.3 Diet preparation

All ingredients and proximate composition of the experimental diets are shown in Table 1. Fish meal, soybean meal, and peanut bran were the main protein sources; fish oil, soybean oil, and soybean phospholipid were the main fat sources; and wheat flour was the main carbohydrate source. Then, 0% (CK), 0.5% MLO (MLOL), and 1% MLO (MLOH) were supplemented to the basal feed to prepare three isonitrogenous and isolipidic diets. All ingredients were ground through a 250 µm mesh, mixed thoroughly, modulated by 102°C water vapor for 8 min, and then expanded at 95°C by a twin-screw extruder (TDSP120*2-120KW, China), cut into 3 mm (diameter), dried at 75°C and stored at −20°C until use.

TABLE 1 Ingredients and proximate composition (g/kg DM) of the experimental diets.

Item	Diets[1]		
	CK	MLOL	MLOH
Ingredients			
Fish meal	350.0	350.0	350.0
Soybean meal	151.0	151.0	151.0
Peanut bran	126.0	126.0	126.0
Corn gluten meal	80.0	80.0	80.0
Spray-dried blood cells	20.0	20.0	20.0
Wheat flour	130.0	130.0	130.0
Squid paste	20.0	20.0	20.0
Yeast extract	20.0	20.0	20.0
Monocalcium phosphate	15.0	15.0	15.0
Cellulose	20.0	15.0	10.0
MLO	0.0	5.0	10.0
Fish oil	20.0	20.0	20.0
Soybean oil	20.0	20.0	20.0
Soybean phospholipid	20.0	20.0	20.0
Vitamin premix[2]	1.0	1.0	1.0
Mineral Premix[3]	3.0	3.0	3.0
Choline chloride	4.0	4.0	4.0
Nutrient levels[4] (air-dry basis)			
Dry matter	908.4	901.8	898.6
Crude protein	485.5	485.0	486.0
Crude lipid	105.0	104.6	105.5
Ash	168.0	169.0	166.0
Crude fiber	7.5	7.3	7.2
Gross energy(MJ kg^{-1})	19.8	19.8	19.9
Nitrogen-free extract	234.0	234.1	235.3
Lysine	33.5	33.8	33.4
Methionine	11.5	11.3	11.5

[1]CK, basal diet; MLOL, supplemented with 0.5%MLO; MLOH, supplemented with 1.0%MLO.
[2]Each kilogram of vitamin premix contains vitamin A 66,666,666.7 IU, vitamin D 400,000,000 IU, vitamin E 1 g, vitamin K 2 g, vitamin B_1 5 g, vitamin B_2 5 g, vitamin B_6 5 g, vitamin B_{12} 1 g, calcium pantothenate 20 g, folic acid 10 g, biotin 1 g, niacin 20 g, choline chloride 200 g, defatted rice bran 700 g.
[3]Each kilogram of mineral premix contains $CuCO_3$ 4 g, $FeC_6H_5O_7$ 15 g, MgO 26 g, $MnSO_4$ 5 g, KCl 250 g, $ZnSO_4$ 50 g, NaCl 50 g, Zeolite powder 600 g.
[4]Nutrient levels were measured values.

2.4 Experimental design and feeding trial

Prior to the feeding trial, fish were fed with the basal diet for two weeks to allow acclimation to diet and conditions in an indoor circulating aquaculture system of the Research Institute of Sericulture and Agricultural Product Processing, Guangdong Academy of Agricultural Sciences (Guangzhou, China). After 24 h of fasting, a total of 450 *M. salmoides* (initial body weight 26.89 ± 1.16 g) were randomly distributed into nine tanks (350 L) with 50 fish in each tank and three tanks in each group. The experiment involved a completely randomized design. Fish were fed twice a day (09: 00 and 16: 30) to achieve an apparent state of satiety, over the 80 days of experiment. The water temperature was kept at 23.0–29.0°C, pH = 7.0–8.2, dissolved oxygen > 6.0 mg/L, ammonia ≤ 0.02 mg/L and nitrite ≤ 0.1 mg/L. Mortality was observed daily and the dead fish were weighed and recorded. The animal husbandry and handling protocols used in this study have been approved by the Animal Care and Use Committee, Guangdong Academy of Agricultural Sciences (GDAAS 258/2019).

2.5 Sampling

At the end of feeding trial, the fish were starved for 24 h before weighing. All fish were anesthetized with 40 mg/L tricaine methanesulfonate (MS-222, Sigma, USA) before sampling. Fish in each tank were counted and weighted to measure the final body weight, weight gain rate, specific growth rate, feed intake, feed conversion ratio, and condition factor. The blood of nine fish per tank was drawn from the caudal vein, kept at 25°C, centrifuged at 3,000 rpm for 15 min, and the supernatant was stored at –80°C for the analysis of serum biochemistry and antioxidant index. Afterwards, the fish were slaughtered and dissected using a sterile scalpel by cutting the belly on ice for determination of the viscerosomatic index and hepatosomatic index.

The livers of three fish per tank were collected and stored at –20°C for the analysis of antioxidant and immunity parameters. The livers of another three fish per tank were collected and immediately stored at –80°C for glucose and lipid metabolism, RNA extraction, and qPCR analysis.

2.6 Laboratory analyses

The nutrient composition and amino acids of the diets were analyzed using AOAC method (21) and determined by high-performance liquid chromatography (22), respectively.

The contents of blood glucose (GLU), low-density lipoprotein cholesterol (LDL-C), high-density lipoprotein cholesterol (HDL-C), total cholesterol (TC), triglycerides (TG), aspartate aminotransferase (AST), alanine aminotransferase (ALT), reduced glutathione (GSH), malondialdehyde (MDA), total antioxidant capacity (T-AOC), and total superoxide dismutase (T-SOD) in the serum or liver were determined with commercial kits (Nanjing Jiancheng Bioengineering Institute Nanjing, China).

The livers (0.5 cm × 0.5 cm × 0.5 cm) of three fish per tank were sampled, rinsed by 0.65% saline (4°C), fixed immediately in the 10% buffered formalin solution for 24 h. The fixed liver tissue was embedded in paraffin, and paraffin sections were made and stained with hematoxylin eosin (HE) using the standard histological techniques. The slices were scanned using a panoramic slicing digital scanner (PANNORAMIC-1000, 3DHISTECH), and the CaseViewer 2.2 (3DHISTECH) software was used to capture tissue photos of the slices (23).

Total RNA was extracted from each liver sample using Trizol reagent (TIANGEN, China) and the RNA quality was tested using Genios plus (Synergy LX, BioTek, USA). An aliquot of 1 mg total RNA was used for reverse transcription. The cDNA was synthesized by RevertAid Reverse Transcriptase (TIANGEN, China) using random primers. The RT-qPCR was performed according to standard protocols in a quantitative thermocycler (MiniOption TM, Bio-Rad, USA). The amplification volume was 10 μL, containing 0.3 μL of the respective primers, 1 μL of cDNA product, 5 μL of SYBR green color qPCR Master Mix (TIANGEN, China), and 3.4 μLof ddH_2O. The specific primers used for *il-8*, *il-10*, *nf-kb*, *tnf-α*, *tgf-β*, *gk*, *pfk*, *acc*, *cpt1*, *fas*, *dgat*, and *ppar-α* genes have been reported previously (24–27). The details of the primers and the PCR amplification conditions used for RT-qPCR are shown in Table 2. After the reaction, melting curve analysis was conducted to confirm the presence of a single PCR product in the reaction. The gene expression levels were calculated by the $2^{-\Delta\Delta Ct}$ method (28) with *β-actin* as the reference gene, and the experiment was performed in triplicate.

TABLE 2 Primer sequences for RT-qPCR in the experiment.

Gene	Forward primer (5′–3′)	Reverse primer (5′–3′)	Length (bp)	Sources	Amplification efficiency (%)
il-8	ACTTCTCCTGGCTGCTCTG	ACTTCTCATTTGGTTTGACACA	170	XM_038704089.1	96.4
il-10	CGGCACAGAAATCCCAGAGC	CAGCAGGCTCACAAAATAAACATCT	113	XM_038696252.1	102.5
nf-kb	AGAAGACGACTCGGGGATGA	GCTTCTGCAGGTTCTGGTCT	119	XM_038699793.1	96.4
tnf-α	AAATAGTGATTCCTCAAGACGG	TGAACAGTATGGCTCAGATGG	126	XM_038723994.1	106.3
tgf-β	GCTTCAGTTTCGGCATTT	TCTCCGTGGAGCGTTTT	186	XM_038693206.1	94.5
gk	CTCGCTCTGCTCGTATGT	CTCCCTTCCTCCGACTG	208	XM_038703172.1	101.3
pfk	TGGGCTATGATACAAGAGTGA	CCATTAGAGGCAGACGAAC	189	XM_038720351.1	98.6
acc	AAGTCCAAGAGGGCACG	ACTGGGAGTCCGCAAAT	173	XM_038704615.1	102.4
cpt-1	GATGTTTTATGACGGGCGG	TAGGTTTCACGAGCATTGGC	156	XM_038705335.1	103.1
ppar-α	CCACCGCAATGGTCGATATG	TGCTGTTGATGGACTGGGAAA	144	XM_038705497.1	103.6
β-actin	TTCACCACCACAGCCGAAAG	TCTGGGCAACGGAACCTCT	179	KJ669298.1	102.2
fas	GCCCTTGACTCATTCCG	GCCCTTGACTCATTCCG	234	XM_038735140.1	102.1
dgat	GCAACATCAAGCCGTCCGACTC	AGCACAGCGAGCCAGAGGTAAT	176	XM_038705876.1	105.3

il-8, interleukin-8; *il-10*, interleukin-10; *nf-kb*, nuclear factor-kB; *tnf-α*, tumor necrosis factor-α; *tgf-β*, transforming growth factor-β; *gk*, glucokinase; *pfk*, phosphofructokinase; *acc*, acetyl-CoA carboxylase; *cpt-1*, carnitine palmitoyl transferase 1; *ppar-α*, peroxisome proliferators-activated receptors α; *fas, fatty acid synthetase; dgat*, diacylglycerol acyltransferase.

2.7 Challenge test

The largemouth bass ranavirus (LMBV) was isolated from diseased largemouth bass and stored in our laboratory (Guangdong Provincial Key Laboratory of Livestock Disease Prevention, Institute of Animal Health, Guangdong Academy of Agricultural Sciences). After 80 days of feeding, 20 fish were randomly selected from each group for challenge experiment. Each fish was injected with 100 μL 4×10^5 $TCID_{50}$/mL of LMBV infected cell suspernatant through the intraperitoneal cavity. The virus dose was based on the results of our previous experiments (20). The mortality rate was recorded daily for 21 days. The relative percent survival (RPS) was calculated according to the following method.

2.8 Data calculation and statistical analysis

Weight gain rate (WGR, %) = (final body weight (FBW, g) – initial body weight (IBW, g))/IBW(g) × 100

Specific gain rate (SGR, %/d) = (ln FBW (g) – ln IBW (g))/days × 100

Feed intake (FI, g/fish) = feed consumed (g)/(final fish number + initial fish number)/2

Feed conversion rate (FCR) = feed intake (g)/(FBW (g) – IBW (g))

Condition factor (CF, %) = FBW (g)/final body length (cm)) × 100

Hepatosomatic index (HSI, %) = Hepatosoma weight (g)/body weight (g) × 100

Viscerosomatic index (HVI, %) = visceral weight (g)/body weight (g) × 100

Relative percent survival (RPS, %) = (percent mortality in control group – percent mortality in the treatment group)/percent mortality in control group × 100

The data were analyzed using one-way ANOVA with Duncan's method for multiple comparisons between groups. Orthogonal polynomial contrast was used to estimate the linear and quadratic effects of various amounts of MLO added. All data were analyzed using SPSS. The significance level of differences was set at $P< 0.05$ and the results were expressed as Mean ± SE. GraphPad Prism8.0 software was used to analyze the survival curves, and Log-rank (Mantel-Cox) was used for statistical difference analysis.

3 Results

3.1 Molecular weight of MLO

GPC analysis was conducted to determine the average molecular weight (Mw), number-average molecular weight (Mn), and polydispersity index (Mw/Mn) for the MLO. As shown in Figure 1, the GPC profile of MLO displayed a single symmetrical and sharp peak. The values of Mw, Mw/Mn, and intrinsic viscosity [η] were determined to be 2174 Da, 1.20, and 1.00 mL/g, respectively.

3.2 MLO supplementation has no adverse effect on the growth performance of largemouth bass

After the feeding experiments, no pathology or abnormal phenomenon was observed in all groups. The effects of dietary MLO level on FBW, WGR, SGR, FI, FCR, CF, HVI, and HSI are shown in Table 3. There was no significant difference in FBW, WGR, SGR, FI, and CF among all groups ($P > 0.05$). However, compared with the CK group, the MLOL and MLOH group showed significant decreases in FCR and HVI ($P< 0.05$). Moreover, the MLOH group had significantly lower HSI than the CK group ($P< 0.05$). With increasing level of MLO added to the diet, there were significant decreases in FCR (linear or quadratic, $P< 0.05$) and VSI and HSI (linear, $P< 0.05$).

3.3 MLO improves the serum biochemical parameters of largemouth bass

The biochemical parameters in the serum of *M. salmoides* after feeding with MLO diets for 80 days are presented in Table 4. The

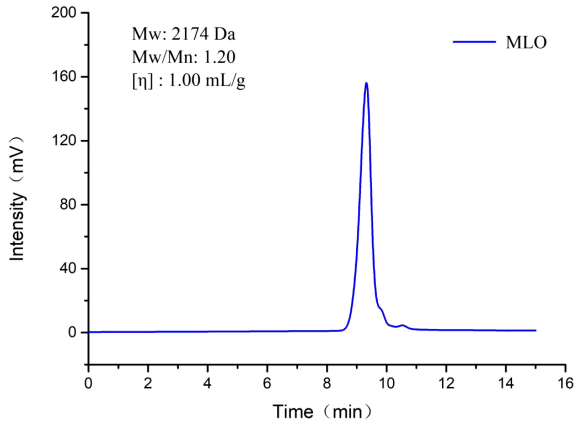

FIGURE 1
Molecular weight distribution diagram of MLO. Mw, average molecular weight; Mn, number-average molecular weight; Mw/Mn, polydispersity index; [η], intrinsic viscosity.

MLOL and MLOH group had significantly lower TG and GLU contents as well AST and ALT activities than the CK group ($P< 0.05$), but showed no significant change in the contents of TC, LDL-C, and HDL-C in the serum ($P > 0.05$). With increasing level of MLO added to the diet, there were significant decreases in the serum TG content and ALT activity (linear or quadratic, $P< 0.05$), GLU content (quadratic, $P< 0.05$), and ALT activity (linear, $P< 0.05$).

3.4 MLO modulates glucose and lipid metabolism in the liver

The liver plays an important role in regulating blood glucose homeostasis (29). The MLOL and MLOH groups showed significant increases in the expression of genes related to glycolysis (*pfk* and *gk*) and lipid catabolism (*ppar-α* and *cpt1*), while significant decreases in that of genes associated with fatty acid synthesis (*acc*, *fas*, and *dgat*) relative to the CK group ($P< 0.05$) (Figure 2).

3.5 Feeding of MLO enhances the antioxidant capacity of largemouth bass

In the serum, the MLOL and MLOH group had significantly higher activities of T-SOD and GSH ($P< 0.05$), while no significant difference in the activity of T-AOC ($P > 0.05$) compared with the CK group. MLO feeding significantly increased the activities of T-SOD, GSH, and T-AOC in the liver, but obviously reduced the MDA content in the serum and liver compared with the CK ($P< 0.05$) (Table 5). With increasing level of MLO added to the diet, there were significant increases in serum and liver T-SOD and GSH activities (linear or quadratic, $P< 0.05$), a significant decrease in serum MDA content (linear, $P< 0.05$), a significant reduction of liver MDA content (linear or quadratic, $P< 0.05$), and a significant increase in liver T-AOC capacity (linear, $P< 0.05$).

3.6 MLO supplementation inhibits inflammation in the liver

The expression levels of immune-related genes are shown in Figure 3. Compared with the CK, MLO supplementation significantly up-regulated the relative expression of anti-inflammatory cytokines *il-10* and *tgf-β*, while down-regulated that of pro-inflammatory cytokines *nf-κb*, *il-8*, and *tnf-α* in the liver ($P< 0.05$) (Figure 3).

3.7 MLO supplementation maintains the structural integrity of the liver

The liver histomorphology is shown in Figure 4. The liver cells of the CK group showed obvious vacuolation and nuclear displacement, while those of MLOL and MLOH group exhibited much less obvious cell vacuolization and nuclear displacement.

3.8 MLO supplementation improves the resistance of largemouth bass to LMBV infection

As shown in Figure 5, the cumulative survival rate was calculated after 21 days of LMBV infection. Compared with the CK group, the MLO groups showed significantly delayed death time of largemouth bass. There was no significant difference in the number of deaths in each group after 14 days of infection. Among different groups, the final survival rates of the CK, MLOL, and MLOH group were 25%, 60%, and 65%, respectively, indicating that MLO supplementation can significantly improve the resistance of largemouth bass to LMBV infection and enhance the survival rate ($P< 0.05$). Compared with that of the CK, the relative protection rate of MLOL and MLOH was 46.67% and 53.33%, respectively (Figure 5).

4 Discussion

4.1 Growth performance

To date, there have been numerous studies of the application of oligosaccharides (prebiotics) such as fructooligosaccharides, galactooligosaccharides, and isomaltooligosaccharides in aquaculture, but there has been no report about the application of MLO in aquatic animals. In the present study, diets supplemented with 0.5% and 1% MLO were found to significantly decrease the FCR and HIS, but showed no significant effect on WGR, which may be directly related to the lower feed intake of the treatment groups. Some prebiotics have also been found to have no significant effect on the growth of aquatic animals, such as short-chain fuctooligosaccharides for hybrid tilapia (*Oreochromis niloticus*×*O. aureus*) (14) and chito-oligosaccharide (COS) for the same species (30). Previous studies have demonstrated that oligosaccharides can significantly increase the WGR and SGR while decrease the FCR of *Oreochromis niloticus* (31), hybrid catfish (*Pangasianodon gigas* × *Pangasianodon hypophthalmus*) (32) and Caspian trout (*Salmo trutta caspius*) (33). Besides, another study has revealed that Grobiotic-A has an adverse effect on the growth of *M. salmoides* (34). These results indicate that prebiotics have different effects on the growth performance of different aquatic animals, which may be related to the type and dosage of the prebiotics used.

4.2 Glucose and lipid metabolism in the liver

Compared with herbivorous and omnivorous species, carnivorous fish have a poor ability to utilize starch as an energy source. Generally, digestible carbohydrate at levels of ≤15–25% is appropriate for marine and carnivorous fish, but the suitable carbohydrate level appears to be lower for *M. salmoides* (35, 36). Mulberry leaf is a Chinese medicinal component widely used to regulate blood GLU (37). Flavonoids are one of the main classes of

TABLE 3 Growth performance of *M. salmoides* fed with the experimental diets.

Items[2]	Diets[1]			SEM[2]	*P*-value		
	CK	MLOL	MLOH		ANOVA	Linear	Quadratic
Initial body weight, g	28.53	26.00	26.13	1.97	0.407	0.269	0.464
Final body weight, g	173.54	166.98	163.15	5.50	0.241	0.108	0.785
Weight gain rate, %	515.78	543.12	524.61	25.77	0.585	0.743	0.344
Specific growth rate, %/d	3.98	4.12	4.06	0.11	0.491	0.498	0.338
Feed intake, g/fish	203.02	192.99	189.28	6.59	0.179	0.082	0.600
Feed conversion rate	0.89[a]	0.71[c]	0.78[b]	0.01	<0.001	<0.001	<0.001
Condition factor, g/cm^3	2.28	2.27	2.20	0.06	0.504	0.296	0.648
Viscerosomatic index, %	9.14[a]	8.68[b]	8.41[b]	0.12	0.002	0.001	0.381
Hepatosomatic index, %	2.24[a]	2.14[a]	1.87[b]	0.05	0.001	<0.001	0.075

[1]CK, basal diet; MLOL, supplemented with 0.5% MLO; MLOH, supplemented with 1.0% MLO.
[a,b,c]Different letters with a row indicate significant differences ($P< 0.05$).
[2]SEM, Standard error of the mean.

active ingredients in mulberry leaves, which contribute to the potential to treat type II diabetes and maintain the glucose metabolism balance of *Monopterus albus* under high glucose stress (38, 39). It has been demonstrated that *M. salmoides* can strengthen the glycolysis pathway to cope with the rising of blood GLU level so as to maintain GLU metabolism homeostasis (35, 40). Another study has also revealed that mannan oligosaccharides (MOS) can decrease serum glucose and liver glycogen by increasing the activities of enzymes related to glycolysis in *O. niloticus* (41). In this study, feeding of MLO diets significantly decreased the serum GLU content in *M. salmoides*. The liver plays an important role in regulating blood GLU homeostasis (29), and this regulation involves several important pathways, such as gluconeogenesis and glycolysis, where PFK, PK, and GK are limiting enzymes in the glycolysis pathway (40). This study showed that *M. salmoides* fed with MLO diets had significantly higher mRNA expression of *pfk* and *gk*, which is similar to the result reported for *M. salmoides* (42), indicating that MLO has great potential to lower GLU.

CPT1 and ACC are key enzymes involved in lipid catabolism and fatty acid synthesis, respectively (43). PPAR-α is a transcription factor that mediates the oxidative breakdown of liver fatty acids, upregulates the expression of fatty acid transport- and oxidation-related gene *cpt-1*, and promotes the transport of long-chain fatty acids in mitochondrial *β*-oxidation, thereby improving fatty acid oxidation in mitochondria and peroxisomes (44). It has been reported that MOS can significantly reduce the TG level of *O. niloticus* and *M. salmoides* fed with high carbohydrate diets (41, 45). In this study, MLO diet up-regulated the expression of *cpt-1* and *ppar-α*, down-regulated that of fatty acid synthesis-related gene *acc*, and significantly reduced the content of TG in the serum, indicating that MLO may accelerate lipid metabolism by regulating the expression of liver metabolism-related genes, thereby reducing lipid deposition in the liver.

TABLE 4 Serum biochemical parameters of *M. salmoides*.

Items[3]	Diets[1]			SEM[2]	*P*-value		
	CK	MLOL	MLOH		ANOVA	Linear	Quadratic
TG (mmol/L)	23.68[a]	17.03[b]	19.05[b]	1.16	0.003	0.007	0.005
TC (mmol/L)	14.19	11.07	12.23	1.28	0.123	0.176	0.102
GLU (mmol/L)	3.37[a]	2.59[b]	2.82[b]	0.23	0.005	0.093	0.002
LDL-C (mmol/L)	6.39	5.87	6.41	0.39	0.362	0.951	0.171
HDL-C (mmol/L)	9.43	5.76	8.87	1.85	0.184	0.774	0.079
ALT (U/mL)	45.36[a]	41.27[b]	40.19[b]	0.80	<0.001	<0.001	0.004
AST (U/mL)	32.33[a]	26.10[b]	26.11[b]	1.00	0.005	0.002	0.135

[1]CK, basal diet; MLOL, supplemented with 0.5%MLO; MLOH, supplemented with 1.0%MLO.
[a,b]Different letters with a row indicate significant differences ($P< 0.05$).
[2]SEM, Standard error of the mean.
[3]TG, triglycerides; TC, total cholesterol; GLU, blood glucose; LDL-C, low-density lipoprotein cholesterol; HDL-C, high-density lipoprotein cholesterol; ALT, alanine aminotransferase; AST, aspartate aminotransferase.

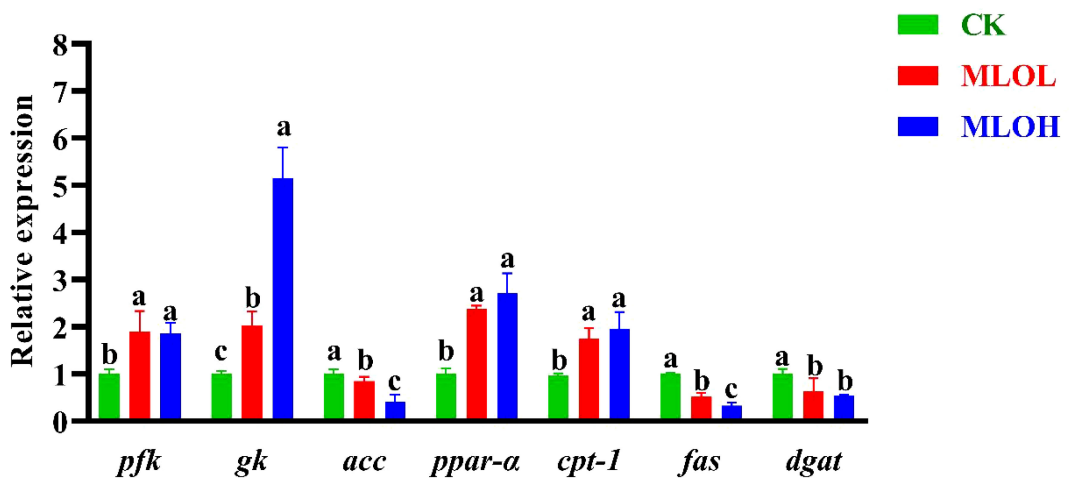

FIGURE 2
mRNA expression of *pfk*, *gk*, *acc*, *ppar-α*, *cpt-1*, *fas* and *dgat* in the liver of *M. salmoides*. CK, basal diet; MLOL, supplemented with 0.5% MLO; MLOH, supplemented with 1.0% MLO. Different letters above the bars denote significant differences among diets ($P< 0.05$).

4.3 Antioxidant and immune responses

Oxidative stress and inflammatory response are interrelated processes with significant contribution to the body's response to various stresses. There were decreases in serum GLU, AST, and ALT after dietary MLO supplementation in this study, suggesting that dietary MLO has obvious positive effects on the immune function and liver health of *M. salmoides*, since high concentrations of serum GLU, AST, and ALT are generally related to liver damage or necrosis (46, 47). It is generally believed that hepatocyte is highly sensitive to the nutritional status of fish and the quality of diet. In this study, dietary MLO significantly alleviated liver vacuolization and nuclear displacement, suggesting that it can improve the liver health of *M. salmoides*. The concentration of MDA can directly reflect the level of lipid peroxidation and the degree of endogenous oxidative damage. GSH and T-SOD are both antioxidant enzymes that assist the maintenance of a healthy cellular antioxidant state. In particular, GSH, as a substrate for glutathione peroxidase and glutathione transferase, reacts with intracellular free radicals and peroxides under the catalysis of both enzymes to maintain the normal physiological functions of cells, making it a critical enzyme for protecting cells from oxidative damage (48). T-SOD is a necessary antioxidant enzyme in all oxygen-breathing organisms, playing important roles in converting superoxide into hydrogen peroxide and removing excess active oxygen (49). Oligosaccharides have been demonstrated to have antioxidant activities in *O. niloticus* (50). Similarly, in the present study, the increase in MLO supplementation enhanced the GSH and T-SOD activities in the

TABLE 5 Serum and liver antioxidant parameters of *M. salmoides*.

Items[3]	Diets[1]			SEM[2]	*P*-value		
	CK	MLOL	MLOH		ANOVA	Linear	Quadratic
Serum							
T-SOD (U/mL)	49.39^{c}	53.85^{b}	64.08^{a}	0.84	<0.001	<0.001	0.008
GSH (U/mL)	11.93^{b}	19.88^{a}	18.18^{a}	1.91	0.014	0.017	0.027
T-AOC (U/mL)	0.45	0.49	0.52	0.03	0.157	0.064	0.909
MDA (nmol/mL)	22.43^{a}	16.61 ^{b}	12.41^{b}	1.75	0.004	0.001	0.609
Liver							
T-SOD (U/mgprot)	11.60^{c}	11.93^{b}	14.02^{a}	0.10	<0.001	<0.001	<0.001
GSH (U/mgprot)	9.59^{b}	10.86^{a}	11.04^{a}	0.20	0.001	<0.001	0.019
T-AOC (U/mgprot)	0.04 ^{c}	0.05 ^{b}	0.06^{a}	0.002	<0.001	<0.001	0.642
MDA (nmol/mgprot)	0.85^{a}	0.50^{b}	0.54^{b}	0.02	<0.001	<0.001	<0.001

[1]CK, basal diet; MLOL, supplemented with 0.5%MLO; MLOH, supplemented with 1.0%MLO.
[a,b,c]Different letters with a row indicate significant differences ($P<0.05$).
[2]SEM, Standard error of the mean.
[3]T-SOD, total superoxide dismutase; GSH, reduced glutathione; T-AOC, total antioxidant capacity; MDA, malondialdehyde.

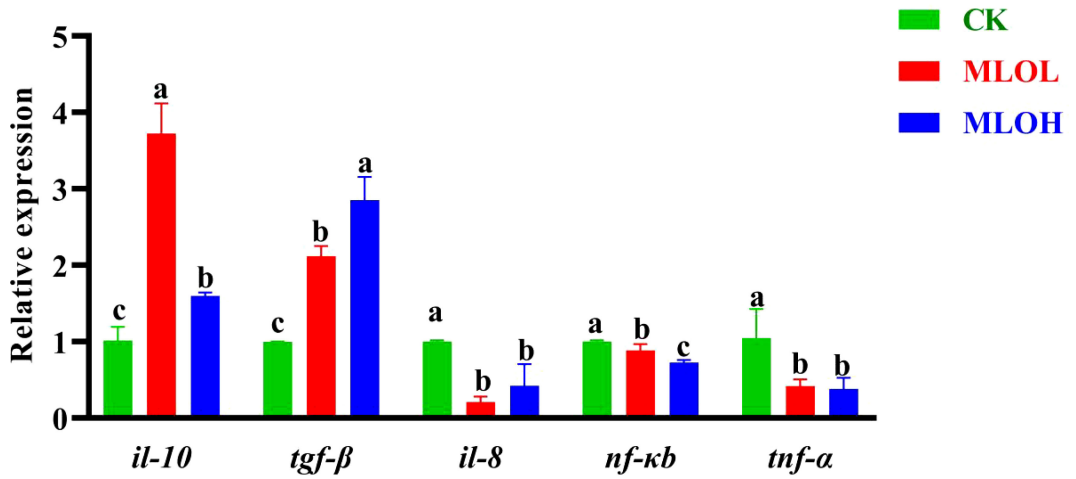

FIGURE 3
mRNA expression of *il-10*, *tgf-β*, *il-8*, *nf-kb*, and *tnf-α* in the liver of *M. salmoides*. CK, basal diet; MLOL, supplemented with 0.5%MLO; MLOH, supplemented with 1.0% MLO. Different letters above the bars denote significant differences among diets ($P < 0.05$).

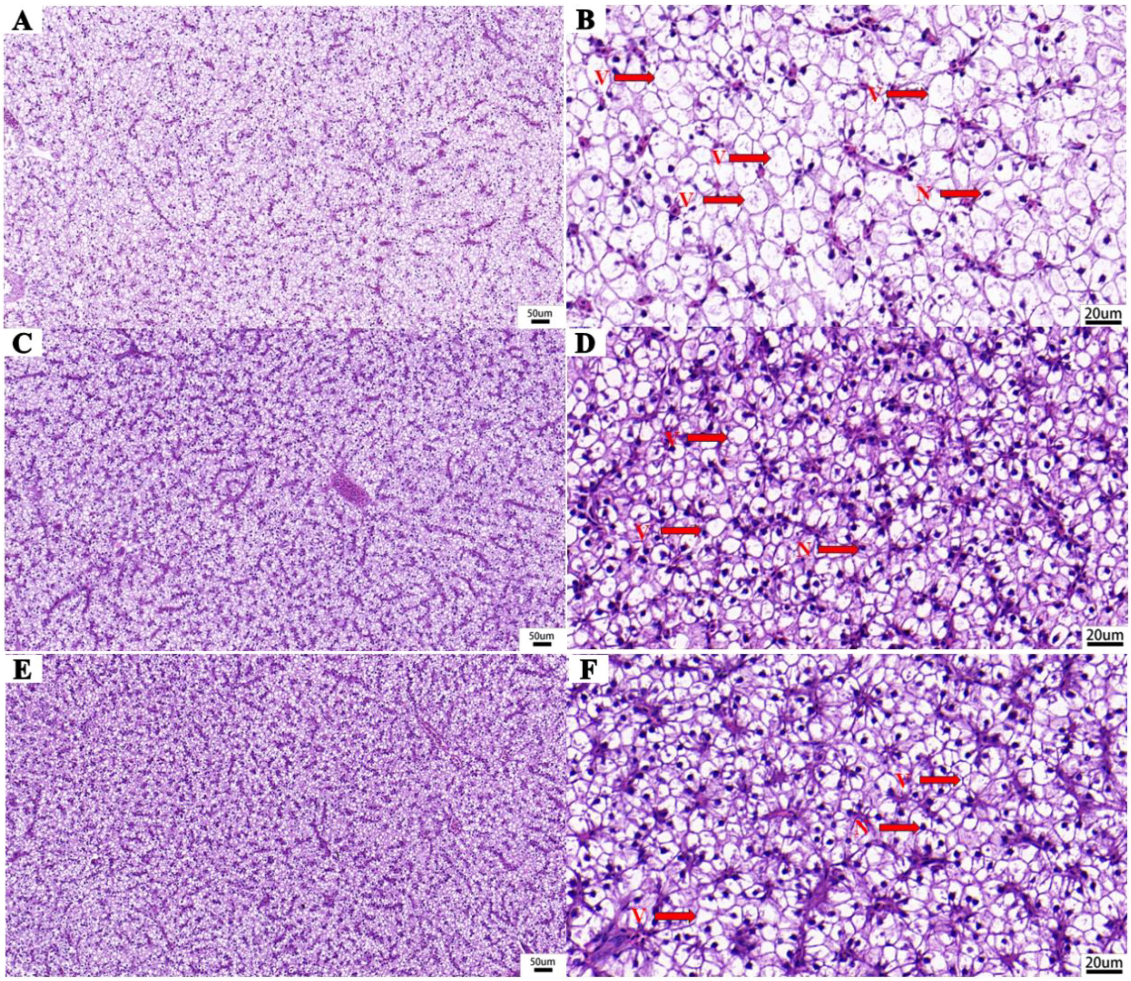

FIGURE 4
Liver histomorphology (H&E staining) of *M. salmoides*. **(A, B)** basal diet; **(C, D)** supplemented with 0.5% MLO; **(E, F)** supplemented with 1.0% MLO. V, cytoplasmic vacuolation; N, nucleus.

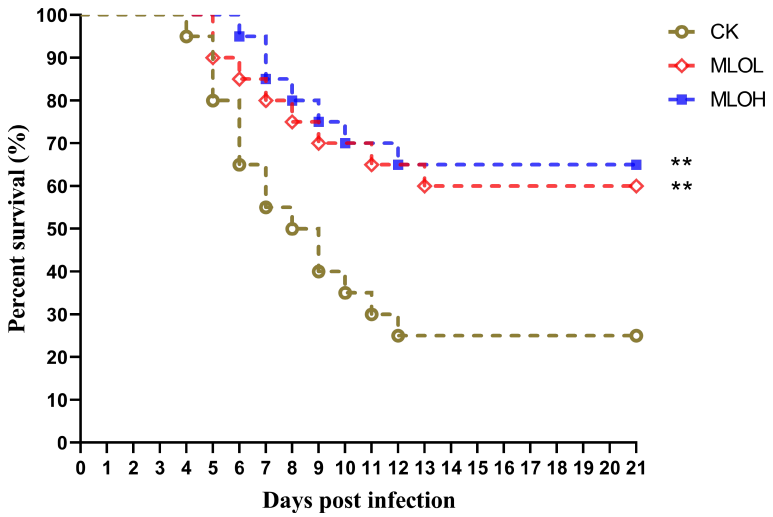

FIGURE 5
Survival rate curve analysis of *M. salmoides* after infection with LMBV. CK, basal diet; MLOL, supplemented with 0.5% MLO; MLOH, supplemented with 1.0% MLO (n = 25).

serum and liver while reduced the MDA content in *M. salmoides*. Therefore, MLO can enhance the antioxidant capacity of *M. salmoides*.

The inflammatory responses in animals are regulated by the NF-κB/TLRs signaling pathway (49). After activation by pro-inflammatory cytokines (such as *il-8*, *tnf-α*, and *nf-κb*), this signaling pathway can promote cellular immune response and up-regulate the expression of anti-inflammatory cytokines (such as *il-10* and *tgf-β*). This study showed that MLO supplementation remarkably up-regulated the transcription of *il-10* and *tgf-β* in the liver, whereas down-regulated that of *il-8*, *tnf-α*, and *nf-κb*. These results indicate that MLO supplementation can reduce inflammatory response by inhibiting the NF-κB signaling pathway.

4.4 Disease resistance

With the expansion of breeding scale, increase in breeding density, and deterioration of water environment, the problem of diseases is becoming increasingly prominent for *M. salmoides*. *M. salmoides* suffers from high mortality rates caused by viral diseases, particularly iridescent virus diseases, which poses serious threats to the aquaculture industry worldwide. *M. salmoides* infected with iridovirus generally exhibits liver and intestinal necrosis and inflammatory lesions, increased cell apoptosis, and decreased immunity (51, 52).

In the present study, MLO supplementation significantly delayed the death time of *M. salmoides* infected with LMBV compared with the CK. In addition, the cumulative mortality rate significantly decreased with increasing dietary MLO, indicating that MLO can reduce the LMBV-induced mortality rate. This may be due to the combined effect of MLO induced up-regulation of anti-inflammatory cytokines and down-regulation of pro-inflammatory cytokines, inhibition of NF-κB signaling pathway, and enhancement of the antioxidant capacity (T-SOD and GSH) in the serum and liver. Some studies have also shown that oligosaccharides can stimulate fish tissue, induce the expression of *iNOS* and produce NO, thereby killing pathogens and enhancing the innate immune response of the body (53). However, further research is still needed to clarify the mechanisms through which these oligosaccharides improve the health and immunity of *M. salmoides*.

5 Conclusion

In summary, MLO supplementation can significantly reduce the feed conversion rate, enhance the antioxidant capacity and liver glucose and lipid metabolism, improve the immunity by inhibiting the NF-kB signaling pathway, and increase the survival rate of *M. salmoides* infected with LMBV. This study provides a practical strategy to apply MLO in the diet for improving the immune and antioxidant abilities of *M. salmoides*.

Data availability statement

The original contributions presented in the study are included in the article, further inquiries can be directed to the corresponding authors.

Ethics statement

The animal study was approved by Collaborative Innovation Center of Aquatic Sciences, Guangdong Academy of Agricultural Sciences. The study was conducted in accordance with the local legislation and institutional requirements.

Author contributions

DZ: Conceptualization, Funding acquisition, Investigation, Methodology, Project administration, Writing – original draft, Writing – review & editing. WZ: Writing – original draft, Data curation, Formal analysis, Investigation, Methodology. BF: Methodology, Writing – original draft, Formal analysis. EL: Methodology, Writing – original draft. LH: Formal analysis, Investigation, Methodology, Writing – original draft. QL: Methodology, Writing – original draft. QY: Writing – review & editing, Methodology, Supervision. YZ: Writing – review & editing, Supervision, Validation. ZL: Methodology, Writing – original draft. FW: Investigation, Writing – review & editing, Methodology. SL: Conceptualization, Writing – review & editing, Supervision, Validation. DX: Conceptualization, Writing – review & editing, Project administration, Supervision, Validation.

Funding

The author(s) declare financial support was received for the research, authorship, and/or publication of this article. This research was funded by the Collaborative Innovation Center of Guangdong Academy of Agricultural Sciences (XT202304); the Basic and Applied Basic Research Foundation of Guangzhou City (202201010474); the Key Science and Technology Research Projects in Foshan City (2220001018588), and the High-level Guangdong Province Agricultural Science and Technology Demonstration City Construction Fund Project in 2023 (2320060002429); the Innovation Foundation of Guangdong Academy of Agricultural Sciences (202113); the Special Funds for 2021 Rural Revitalization Strategy (Jiangke [2021] No. 183).

Conflict of interest

The authors declare that the research was conducted in the absence of any commercial or financial relationships that could be construed as a potential conflict of interest.

Generative AI statement

The author(s) declare that no Generative AI was used in the creation of this manuscript.

Publisher's note

References

1. Zou J, Hu P, Wang M, Chen Z, Wang H, Guo X, et al. Liver injury and metabolic dysregulation in Largemouth bass (*Micropterus salmoides*) after ammonia exposure. *Metabolites*. (2023) 13:274. doi: 10.3390/metabo13020274

2. Parsaian M, Shokri M, Pazooki J. The response of benthic foraminifera to aquaculture and industrial pollution: a case study from the Northern Persian Gulf. *Mar pollut Bull*. (2018) 35:682–93. doi: 10.1016/j.marpolbul.2018.07.073

3. Rico R, Van den Brink P. Probabilistic risk assessment of veterinary medicines applied to four major aquaculture species produced in Asia. *Sci Total Environ*. (2014) 468:630–41. doi: 10.1016/j.scitotenv.2013.08.063

4. Mehdi Y, Létourneau-Montminy M, Gaucher M, Chorfi Y, Suresh G, Rouissi T, et al. Use of antibiotics in broiler production: global impacts and alternatives. *Anim Nutr*. (2018) 4:170–78. doi: 10.1016/j.aninu.2018.03.002

5. Chu L, Su D, Wang H, Aili D, Yimingniyazi B, Jiang Q, et al. Association between antibiotic exposure and type 2 diabetes mellitus in middle-aged and older adults. *Nutrients*. (2023) 15:1290. doi: 10.3390/nu15051290

6. Patel S, Goyal A. The current trends and future perspectives of prebiotics research: a review. *3 Biotech*. (2012) 2:115–25. doi: 10.1007/s13205-012-0044-x

7. Gibson G, Probert H, Loo J, Rastall R, Roberfroid M. Dietary modulation of the human colonic microbiota: updating the concept of prebiotics. *Nutr Res Rev*. (2004) 17:259–75. doi: 10.1079/NRR200479

8. Ringo E, Olsen R, Gifstad T, Dalmo R, Amlund H, Hemre G, et al. Prebiotics in aquaculture: a review. *Aquacult Nutr*. (2010) 16:117–36. doi: 10.1111/j.1365-2095.2009.00731.x

9. El-Saadony M, Alagawany M, Patra A, Kar I, Tiwari R, Dawood M, et al. The functionality of probiotics in aquaculture: an overview. *Fish Shellfish Immun*. (2021) 117:36–52. doi: 10.1016/j.fsi.2021.07.007

10. Wee W, Hamid N, Mat K, Khalif R, Rusli N, Rahman M, et al. The effects of mixed prebiotics in aquaculture: a review. *Aquacult Fish*. (2024) 9:28–34. doi: 10.1016/j.aaf.2022.02.005

11. Akrami R, Nasri-Tajan M, Jahedi A, Jahedi M, Razeghi Mansour M, Jafarpour S. Effects of dietary synbiotic on growth, survival, lactobacillus bacterial count, blood indices and immunity of beluga (*Huso huso* Linnaeus, 1754) juvenile. *Aquacult Nutr*. (2015) 21:952–59. doi: 10.1111/anu.12219

12. Akter M, Sutriana A. Dietary supplementation with mannan oligosaccharide influences growth, digestive enzymes, gut morphology, and microbiota in juvenile striped catfish, *Pangasianodon hypophthalmus*. *Aquacult Int*. (2016) 24:127–44. doi: 10.1007/s10499-015-9913-8

13. Hoseinifar S, Soleimani N, Ringø E. Effects of dietary fructo-oligosaccharide supplementation on the growth performance, haemato-immunological parameters, gut microbiota and stress resistance of common carp (*Cyprinus carpio*) fry. *Brit J Nutr*. (2014) 112:1296–2. doi: 10.1017/S0007114514002037

14. Liu W, Wang W, Ran C, He S, Yang Y, Zhou Z. Effects of dietary scFOS and lactobacilli on survival, growth, and disease resistance of hybrid tilapia. *Aquaculture*. (2017) 470:50–5. doi: 10.1016/j.aquaculture.2016.12.013

15. Wang L, Gao H, Sun C, Huang L. Protective application of *Morus* and its extracts in animal production. *Animals*. (2022) 12:3541. doi: 10.3390/ani12243541

16. Sánchez MD. World distribution and utilization of mulberry, potential for animal feeding. *FAO Anim Prod Health Pap*. (2000) 111:1–11.

17. Hu T, Zou Y, Li E, Liao S, Wu H, Wen P. Effects of enzymatic hydrolysis on the structural, rheological, and functional properties of mulberry leaf polysaccharide. *Food Chem*. (2021) 355:129608. doi: 10.1016/j.foodchem.2021.129608

18. Hu T, Wu H, Yu Y, Xu Y, Li E, Liao S, et al. Preparation, structural characterization and prebiotic potential of mulberry leaf oligosaccharides. *Food Funct*. (2022) 13:5287–98. doi: 10.1039/D1FO04048K

19. Hu T, Yu Y, Wu J, Xu Y, Xiao G, An K, et al. Structural elucidation of mulberry leaf oligosaccharide and its selective promotion of gut microbiota to alleviate type 2 diabetes mellitus. *Food Sci Hum Well*. (2024) 13:2161–73. doi: 10.26599/FSHW.2022.9250180

20. Li S, Zhou D, Pang D, Li Q, Li Q, Wang H, et al. Effects of *Ramulus mori* oligosaccharides on growth performance, serum physiological and biochemical parameters, and immunomodulation in largemouth bass (*Micropterus salmoides*). *Aquaculture*. (2024) 589:741008. doi: 10.1016/j.aquaculture.2024.741008

21. AOAC. *Official methods of analysis of the association of official agricultural chemists. 16th ed*. Gaithersburg: AOAC international (1999). 5th rev.

22. Araújo F, Michelato M, Schemberger M, Salaro A, Vidal L, Da Cruz T, et al. Assessment of isoleucine requirement of fast-growing Nile tilapia fingerlings based on growth performance, amino acid retention, and expression of muscle growth-related and mTOR genes. *Aquaculture*. (2021) 539:736645. doi: 10.1016/j.aquaculture.2021.736645

23. Su C, Chang C, Chou C, Wu Y, Yang K, Tseng J, et al. L-carnitine ameliorates dyslipidemic and hepatic disorders induced by a high-fat diet via regulating lipid metabolism, self-antioxidant capacity, and inflammatory response. *J Funct Foods*. (2015) 15:497–8. doi: 10.1016/j.jff.2015.04.007

24. Wei Y, Huang J, Sun H, Feng Z, He Y, Chen Y, et al. Impact of different processing mulberry leaf on growth, metabolism and liver immune function of largemouth bass (*Micropterus salmoides*). *Aquacult Rep*. (2023) 29:101508. doi: 10.1016/j.aqrep.2023.101508

25. Xv Z, He G, Wang X, Shun H, Chen Y, Lin S. Mulberry leaf powder ameliorate high starch-induced hepatic oxidative stress and inflammation in fish model. *Anim Feed Sci Tech*. (2021) 278:115012. doi: 10.1016/j.anifeedsci.2021.115012

26. Che M, Lu Z, Liu L, Li N, Ren L, Chi S. Dietary lysophospholipids improves growth performance and hepatic lipid metabolism of largemouth bass (*Micropterus salmoides*). *Anim Nutr*. (2023) 13:426–34. doi: 10.1016/j.aninu.2023.04.007

27. Chen W, Gao S, Chang K, Zhao X, Niu B. Dietary sodium butyrate supplementation improves fish growth, intestinal microbiota composition, and liver health in largemouth bass (*Micropterus salmoides*) fed high-fat diets. *Aquaculture*. (2023) 564:739040. doi: 10.1016/j.aquaculture.2022.739040

28. Livak K, Schmittgen T. Analysis of relative gene expression data using real-time quantitative PCR and the $2^{-\Delta\Delta Ct}$ method. *Methods*. (2001) 25:402–8. doi: 10.1006/meth.2001.1262

29. Rito J, Viegas I, Pardal M, Jones J. Evidence of extensive plasma glucose recycling following a glucose load in seabass. *Comp Biochem Phys A*. (2017) 211:41–8. doi: 10.1016/j.cbpa.2017.05.009

30. Qin C, Zhang Y, Liu W, Xu L, Yang Y, Zhou Z. Effects of chito-oligosaccharides supplementation on growth performance, intestinal cytokine expression, autochthonous gut bacteria and disease resistance in hybrid tilapia *Oreochromis niloticus* ♀ × *Oreochromis aureus* ♂. *Fish Shellfish Immun*. (2014) 40:267–74. doi: 10.1016/j.fsi.2014.07.010

31. Selim K, Reda R. Beta-glucans and mannan oligosaccharides enhance growth and immunity in Nile tilapia. *N Am J Aquacult*. (2015) 77:22–30. doi: 10.1080/15222055.2014.951812

32. Hahor W, Thongprajukaew K, Suanyuk N. Effects of dietary supplementation of oligosaccharides on growth performance, gut health and immune response of hybrid catfish (*Pangasianodon gigas* × *Pangasianodon hypophthalmus*). *Aquaculture*. (2019) 507:97–7. doi: 10.1016/j.aquaculture.2019.04.010

33. Jami M, Kenari A, Paknejad H, Mohseni M. Effects of dietary b-glucan, mannan oligosaccharide, Lactobacillus plantarum and their combinations on growth performance, immunity and immune related gene expression of Caspian trout, *Salmo trutta caspius* (Kessler, 1877). *Fish Shellfish Immun*. (2019) 91:202–8. doi: 10.1016/j.fsi.2019.05.024

34. Rossi W, Allen K, Habte-Tsion H, Meesala K. Supplementation of glycine, prebiotic, and nucleotides in soybean meal-based diets for largemouth bass (*Micropterus salmoides*): effects on production performance, whole-body nutrient composition and retention, and intestinal histopathology. *Aquaculture*. (2021) 532:736031. doi: 10.1016/j.aquaculture.2020.736031

35. Ma H, Mou M, Pu D, Lin S, Chen Y, Luo L. Effect of dietary starch level on growth, metabolism enzyme and oxidative status of juvenile largemouth bass, *Micropterus salmoides*. *Aquaculture*. (2019) 498:482–87. doi: 10.1016/j.aquaculture.2018.07.039

36. Li S, Wang A, Wei Z, Liu R, Wang D, Chen N. Insulin receptors in largemouth bass (*Micropterus salmoides*): Cloning, characterization, tissue expression profile and transcriptional response to glucose tolerance test. *Aquac Res*. (2021) 52:625–34. doi: 10.1111/are.14919

37. Hassan F, Arshad M, Li M, Rehman M, Loor J, Huang J. Potential of mulberry leaf biomass and its flavonoids to improve production and health inruminants: mechanistic insights and prospects. *Animals*. (2020) 10:2076. doi: 10.3390/ani10112076

38. Duan Y, Dai H, An Y, Cheng L, Shi L, Lv Y, et al. Mulberry leaf flavonoids inhibit liver inflammation in type 2 diabetes rats by regulating TLR4/MyD88/NF-κB signaling pathway. *Evidence-Based Complementary Altern Med*. (2022) 2022:3354062. doi: 10.1155/2022/3354062

39. Shi Y, Zhong L, Fan Y, Zhang J, Zhong H, Liu X, et al. The protective effect of mulberry leaf flavonoids on high-carbohydrate-induced liver oxidative stress, inflammatory response and intestinal microbiota disturbance in *Monopterus albus*. *Antioxidants*. (2022) 11:976. doi: 10.3390/antiox11050976

40. Chen S, Jiang X, Liu N, Ren M, Wang Z, Li M, et al. Effects of dietary berberine hydrochloride inclusion on growth, antioxidant capacity, glucose metabolism and intestinal microbiome of largemouth bass (*Micropterus salmoides*). *Aquaculture*. (2022) 552:738023. doi: 10.1016/j.aquaculture.2022.738023

41. Wang T, Wu H, Li W, Xu R, Qiao F, Du Z, et al. Effects of dietary mannan oligosaccharides (MOS) supplementation on metabolism, inflammatory response and gut microbiota of juvenile Nile tilapia (*Oreochromis niloticus*) fed with high carbohydrate diet. *Fish Shellfish Immun*. (2022) 130:550–59. doi: 10.1016/j.fsi.2022.09.052

42. Li S, Sang C, Turchini G, Wang A, Zhang J, Chen N. Starch in aquafeeds: the benefits of a high amylose to amylopectin ratio and resistant starch content in diets for the carnivorous fish, largemouth bass (*Micropterus salmoides*). *Brit J Nutr*. (2020) 124:1145–55. doi: 10.1017/S0007114520002214

43. Wu X, Huang T. Recent development in acetyl-CoA carboxylase inhibitors and their potential as novel drugs. *Future Med Chem*. (2020) 12:533–61. doi: 10.4155/fmc-2019-0312

44. Schlaepfer I, Joshi M. CPT1A-mediated fat oxidation, mechanisms, and therapeutic potential. *Endocrinology*. (2020) 161:bqz046. doi: 10.1210/endocr/bqz046

45. Wang T, Xu R, Qiao F, Du Z, Zhang M. Effects of mannan oligosaccharides (MOS) on glucose and lipid metabolism of largemouth bass (*Micropterus salmoides*) fed with high carbohydrate diet. *Anim Feed Sci Tech*. (2022) 292:115449. doi: 10.1016/j.anifeedsci.2022.115449

46. Wang L, Liu W, Lu K, Xu W, Cai D, Zhang C, et al. Effects of dietary carbohydrate/lipid ratios on non-specific immune responses, oxidative status and liver histology of juvenile yellow catfish pelteobagrus fulvidraco. *Aquaculture*. (2014) 426:41–8. doi: 10.1016/j.aquaculture.2014.01.022

47. Peng K, Zhou Y, Wang Y, Wang G, Huang Y, Cao J. Inclusion of condensed tannins in Lateolabrax japonicus diets: effects on growth, nutrient digestibility, antioxidant and immune capacity and copper sulphate stress resistance. *Aquacult Rep*. (2020) 18:100525. doi: 10.1016/j.aqrep.2020.100525

48. Liu Y, Li Y, Xiao Y, Peng Y, He J, Chen C, et al. Mulberry leaf powder regulates antioxidative capacity and lipid metabolism in finishing pigs. *Anim Nutr*. (2021) 7:421–29. doi: 10.1016/j.aninu.2020.08.005

49. Meng Q, Chen J, Xu C, Huang Y, Wang Y, Wang T, et al. The characterization, expression and activity analysis of superoxide dismutases (SODs) from Procambarus clarkii. *Aquaculture*. (2013) 406:131–40. doi: 10.1016/j.aquaculture.2013.05.008

50. El-Nobi G, Hassanin M, Khalil A, Mohammed A, Amer S, Montaser M, et al. Synbiotic effects of saccharomycescerevisiae, mannan oligosaccharides, and β-glucan on innate immunity, antioxidant status, and disease resistance of Nile tilapia, Oreochromis niloticus. *Antibiotics*. (2021) 10:567. doi: 10.3390/antibiotics10050567

51. Zhao L, Zhong Y, Luo M, Zheng G, Huang J, Wang G, et al. Largemouth bass ranavirus: current status and research progression. *Aquacult Rep*. (2023) 32:101706. doi: 10.1016/j.aqrep.2023.101706

52. Xu W, Zhang Z, Lai F, Yang J, Qin Q, Huang Y, et al. Transcriptome analysis reveals the host immune response upon LMBV infection in largemouth bass (*Micropterus salmoides*). *Fish Shellfish Immun*. (2023) 137:108753. doi: 10.1016/j.fsi.2023.108753

53. Lin S, Jiang Y, Chen Y, Luo L, Doolgindachbaporn S, Yuangsoi B. Effects of astragalus polysaccharides (APS) and chitooligosaccharides (COS) on growth, immune response and disease resistance of juvenile largemouth bass, *Micropterus salmoides*. *Fish Shellfish Immun*. (2017) 70:40–7. doi: 10.1016/j.fsi.2017.08.035

frontiers | Frontiers in Nutrition

TYPE Original Research
PUBLISHED 13 February 2025
DOI 10.3389/fnut.2025.1519140

OPEN ACCESS

EDITED BY
Samad Rahimnejad,
University of Murcia, Spain

REVIEWED BY
Ishtiyaq Ahmad,
Sher-e-Kashmir University of Agricultural Sciences and Technology, India
Sérgio D. C. Rocha,
Norwegian University of Life Sciences, Norway

*CORRESPONDENCE
Taesun Min
tsmin@jejunu.ac.kr
Seunghyung Lee
shlee@pknu.ac.kr

†These authors have contributed equally to this work

‡PRESENT ADDRESS
Wonsuk Choi,
CJ Feed and Care, AN R&D Center, Seoul, Republic of Korea

RECEIVED 29 October 2024
ACCEPTED 29 January 2025
PUBLISHED 13 February 2025

CITATION
Choi W, Moniruzzaman M, Lee S, Bae J, Bai SC, Min T and Lee S (2025) Evaluation of three fish-derived probiotic bacteria replacing antibiotics on growth, immunity, gut morphology and disease resistance in juvenile olive flounder *Paralichthys olivaceus* fed reduced fish meal diets.
Front. Nutr. 12:1519140.
doi: 10.3389/fnut.2025.1519140

Evaluation of three fish-derived probiotic bacteria replacing antibiotics on growth, immunity, gut morphology and disease resistance in juvenile olive flounder *Paralichthys olivaceus* fed reduced fish meal diets

Wonsuk Choi[1†‡], Mohammad Moniruzzaman[2†], Seunghan Lee[3], Jinho Bae[4], Sungchul C. Bai[1,5], Taesun Min[6*] and Seunghyung Lee[1,7*]

[1]Feeds and Foods Nutrition Research Center, Pukyong National University, Busan, Republic of Korea, [2]Department of Animal Biotechnology, Jeju International Animal Research Center, Sustainable Agriculture Research Institute (SARI), Jeju National University, Jeju, Republic of Korea, [3]Department of Aquaculture and Aquatic Science, Kunsan National University, Gunsan, Republic of Korea, [4]Aquafeed Research Center, National Institute of Fisheries Science, Pohang, Republic of Korea, [5]FAO World Fisheries University Pilot Program, Busan, Republic of Korea, [6]Department of Animal Biotechnology, Bio-Resources Computing Research Center, Sustainable Agriculture Research Institute (SARI), Jeju National University, Jeju, Republic of Korea, [7]Major of Aquaculture and Applied Life Sciences, Division of Fisheries Life Sciences, Pukyong National University, Busan, Republic of Korea

A basal diet without feed additives was used as a control (CON) and three diets were formulated by supplementing with *Bacillus subtilis* WB60 at 1×10^8 CFU/g (Pro-A), *B. subtilis* SJ10 at 1×10^8 CFU/g (Pro-B), *Enterococcus faecium* SH30 at 1×10^7 CFU/g (Pro-C), and two other diets supplementing with antibiotics such as amoxicillin (AMO) at 4 g/kg and oxytetracycline (OTC) at 4 g/kg of the basal diet. A total of 450 fish averaging 12.1 ± 0.09 g (mean ± SD) were fed one of the six experimental diet groups in triplicates for 8 weeks. In disease resistance test, 45 fish from each group were intraperitoneally injected with the pathogenic bacteria, *Edwardsiella tarda*, and mortality was recorded for 15 days. At the end of 8-week feeding trial, weight gain, specific growth rate and feed efficiency of fish fed the Pro-A diet were significantly greater than those of fish fed the CON, OTC and AMO diets ($p < 0.05$). Furthermore, feeding efficiency and protein efficiency ratio of fish fed the Pro-A diet were significantly greater than those of fish fed the CON, OTC and AMO diets. Serum aspartate aminotransferase levels were significantly greater in fish fed the Pro-B diet than in those fed the Pro-A diet. The lysozyme activity of fish fed the Pro-A, Pro-B and Pro-C diets was significantly greater than that of the CON, OTC and AMO diets. The myeloperoxidase activity of fish fed the Pro-A diet was significantly greater than that of the fish fed the CON and AMO diets. The flounder growth hormone levels of fish fed the Pro-A, Pro-B, Pro-C and AMO diets were significantly greater than that of the fish fed the CON diet. The interleukin 1β gene expression levels in fish fed the Pro-B and Pro-C diets were significantly greater than those in fish fed the CON, OTC and AMO diets. The interleukin 10 gene expression levels in fish fed the Pro-A, Pro-B, Pro-C and OTC diets were significantly greater than those of fish fed the CON and AMO diets. Intestinal histology revealed that the average villi length of fish fed the Pro-A, Pro-B, and Pro-C diets were significantly greater than that of fish fed

the CON, OTC and AMO diets. The cumulative survival rates of fish fed the Pro-A, Pro-B and Pro-C diets were significantly greater than those of fish fed the CON diet after the 15th day of the challenge test. Overall, the results demonstrated that the supplementation of fish-derived bacteria, *B. subtilis* (1×10^8 CFU/g diet) or *E. faecium* (1×10^7 CFU/g diet) in the diet could be the ideal probiotics to replace antibiotics in olive flounder fed FM reduced diet.

KEYWORDS

beneficial bacteria, growth performance, innate immunity, gastrointestinal tract, challenge test, olive flounder

Introduction

Olive flounder (*Paralichthys olivaceus* Temminck and Schlegel, 1846) is a flat fish native to the temperate coastal waters of East Asia that represents both an important capture as well as aquaculture industry. Olive flounder is most popular in Northeast Asian nations such as Korea, China, and Japan (1, 2). In South Korea, it is the most cultured species at more than 46,000 MT and accounts for more than 50% of the country's overall production, which was 91,000 MT in 2022 (3). As olive flounder culture exceeds the capture fishery, there is an ever increasing pressure to reduce its reliance on fish meal (FM). FM accounts for up to 50% of the cost of olive flounder aqua feed. Although FM is an ideal source of essential amino acids (EAAs) and fatty acids (FAs), it comes at the expense of increased production for producers and great pressure on wild fisheries. Since the world's production of FM is in decline and will unlikely increase in the future (4), the sustainability of the aquaculture industry is dependent on reducing reliance on this commodity moving forward. In olive flounder aquaculture, pathogenic bacteria *Edwardsiellatarda* infection (Edwardsiellosis) have become a major problem which cause severe economic losses. For this, farmers are mostly depend on the uses of antibiotics or vaccines for disease outbreak.

Fish meal replacement has been a major objective for aquaculture nutritionists for several decades. There are many candidates for FM replacement, such as meat and bone meal (5), poultry by-product meal (6), blood meal (7) and plant-based protein sources such as soybean meal (8). Proteins obtained from animal sources have great potential with some of the most popular sources being poultry byproduct meals, blood meals, and meat and bone meal (9). However, fish fed diets with low FM often suffer from issues related to growth, digestibility, palatability, and disease resistance. To overcome these problems, fish farmers have started to rely on various feed additives and antibiotics. The excessive application of the antibiotics is becoming a major health and environmental hazard since antibiotic-resistant strains are becoming increasingly prevalent (10, 11). Thus, the development of safe and sustainable alternatives to these pharmaceuticals has become an ever expanding field of research.

One of the most promising tools for reducing antibiotic reliance in the aquaculture industry is probiotics. Probiotics are microbes that help to correct imbalances in the microbiota of the intestines and confer benefits to the host organism's health status when consumed in sufficient amounts (12). Some of the specific benefits of probiotics include their ability to retard and outcompete the growth of pathogens (13), aid in digestion by contributing to enzymatic activities (14), antiviral properties, enhancing immune responses (15, 16), reproductive performance (17), gut health and disease resistance (18) in fish. Recently, there have been tremendous interests in dietary intervention of host-associated or fish-derived probiotics research within the aquaculture industries (19–26). This kind of probiotic bacteria are generally isolated from fish intestine which would be more suitable in terms of enhanced growth and immune system in target animals than the so called probiotics using in aquaculture (13–18). In previous studies reported the positive single effect of the probiotics *Bacillus subtilis* WB60, *Bacillus subtilis* SJ10 and *Enterococcus faecium* in olive flounder. However, very few studies reported the efficacy of fish-derived multiple strains of probiotic bacteria in aquaculture. Therefore, in this study, we aimed to evaluate the comparison of dietary supplementation of the three fish-derivedprobiotics, *Bacillus subtilis* WB60, *Bacillus subtilis* SJ10 and *Enterococcus faecium* as well as two most widely used antibiotics in flounder aquaculture such as oxytetracycline and amoxicillin (27) based on the growth, immunity and disease resistance against *E. tarda* infection in juvenile olive flounder.

Materials and methods

Bacterial isolation and culture condition

The candidate probiotics, *B. subtilis* WB60 was isolated from the intestines of healthy Japanese eel (*Anguilla japonica*) and was identified by cluster analysis via 16S rDNA sequencing. The *B. subtilis* WB60 was isolated according to Lee et al. (28) and incubated at 30°C for 72 h in Luria-Bertani broth (LB broth; Sigma-Aldrich, St. Louis, USA), after which the optical density (OD600) was measured at 600 nm using spectrophotometry. The *B. subtilis* SJ10 was isolated from *jeotgal*, a traditional Korean fermented dish made from salt-preserved seafood such as squid, pollock roe, and shrimp, according to Hasan et al. (29) and it was incubated from a single colony on lysogeny broth (LB, USB Corporation, USA) agar, and was subsequently cultured in 10 mL of LB broth for 16 h at 37°C in a shaking incubator. Furthermore, *E. faecium* SH30 was isolated from the intestine of healthy Nile tilapia (*Oreochromis niloticus*), and the bacteria were grown in MRS (deMan, Rogosa, and Sharpe) broth at 36°C for 48 h according to Wang et al. (30). All probiotics were washed in sterile saline and the concentration of the final suspension was calculated to be 1×10^8 CFU/g for WB60 and SJ10, and 1×10^7 CFU/g for SH30 in the diets (28–30).

Experimental fish and feeding trial

Juvenile olive flounder were obtained from a private farm (JUNGANG Fisheries, Chungcheongnam-do, Taean-gun, Republic of

Korea). Prior to the start of the feeding trial, the apparent health status of the fish was checked visually, and the fish were starved for 24 h. All the fish were then fed a commercial diet for two weeks prior to the start of the feeding trial to acclimatize to the laboratory conditions. On average, 12.1 ± 0.09 g (mean ± SD) of fish were weighed, divided into triplicate groups of 25 fish corresponding to the dietary treatment, and randomly distributed into 18 indoor fiberglass tanks (40 L each) receiving a constant flow (1.2 L/min) of filtered seawater. During the experiment, supplemental aeration was provided in each tank to maintain adequate dissolved oxygen. The temperature was maintained at 19.0 ± 1.0°C throughout the experiment by electric heaters in a concrete reservoir. Fish were fed twice a day (09:00 and 19:00) for 8 weeks at a rate of 2.5 ~ 5% body weight per day. Dead fish were immediately removed and weighed, after which the amount of feed provided to the remaining fish was adjusted. The uneaten feed was siphoned 1 h after feeding. The inside of the tanks was scrubbed once per week to minimize algal and fungal growth.

Experimental diets

The basal or control diet (**CON**) formulation is shown in Table 1. Anchovy fish meal (68.75% CP, crude protein) and soybean meal (47.04% CP) were used as the main protein sources, while fish oil was used as the main lipid source. The feed additives (probiotics) used in this experiment were **Pro-A**: *B. subtills* WB60 (1×10^8 CFU/g) based on Lee et al. (28), **Pro-B**: *B. subtills* SJ10 (1×10^8 CFU/g) based on Hasan et al. (29), **Pro-C**: *E. faecium* SH30 (1×10^7 CFU/g) based on Wang et al. (30), as well as **OTC**: oxytetracycline, 4 g/kg diet and **AMO**: amoxicillin, 4 g/kg diet which were based on Won et al. (31). The procedures for feed manufacturing and preparation were performed as previously described by Lee et al. (28). According to the feed formulation table, all fine powdered ingredients were mixed thoroughly with an electric mixer (HYVM-1214, Hanyoung Food Machinery, Republic of Korea). Then, a stiff dough was formed by adding fish oil and the desired amount of water (~10%). The dough was passed through a pellet machine (SFD-GT, Shinsung, Republic of Korea) with a 0.2 cm die. The prepared diets were air-dried in a drying room for 48 h, broken into smaller pieces and stored at -20°C. According to the proximate composition analysis, shown in Table 2, all the diets were iso-nitrogenous and iso-lipidic.

TABLE 1 Composition of the basal diet (% of dry matter basis).

Ingredients	%
Anchovy fish meal[1]	45
Soybean meal	12
Starch[2]	3.8
Wheat flour	7.0
Blood meal	4.5
Squid liver powder	5.6
Meat and bone meal	8.0
Poultry by product meal	4.5
Fish oil[3]	4.3
Vitamin premix[4]	1.2
Mineral premix[5]	1.2
etc.[6]	3.0
Proximate analysis (% of DM basis)	
Moisture	8.56
Crude protein	56.2
Crude lipid	8.35
Crude ash	11.4

[1]Suhyup Feed Co. Uiryeong, Korea.
[2]The Feed Co. Goyang, Korea.
[3]Jeil Feed Co. Hamman, Korea.
[4]Contains (as mg/kg in diets): Ascorbic acid, 300; dl-Calcium pantothenate, 150; Choline bitate, 3,000; Inositol, 150; Menadion, 6; Niacin, 150; Pyridoxine HCl, 15; Rivoflavin, 30; Thiamine mononitrate, 15; dl-α-Tocopherol acetate, 201; Retinyl acetate, 6; Biotin, 1.5; Folic acid, 5.4; Cobalamin, 0.06.
[5]Contains (as mg/kg in diets): NaCl, 437.4; $MgSO_4 \cdot 7H_2O$, 1379.8; $ZnSO_4 \cdot 7H_2O$, 226.4; Fe-Citrate, 299; $MnSO_4$, 0.016; $FeSO_4$, 0.0378; $CuSO_4$, 0.00033; $Ca(IO)_3$, 0.0006; MgO, 0.00135; $NaSeO_3$, 0.00025.
[6]etc.: Calcium phosphate; Lecithin, Batain; Taurine; Choline; Vitamin C; Lysine; Methionine.

Sample collection and analysis

At the end of the feeding trial, fish were starved for 24 h prior to sample and data collection. The fish were subsequently counted and weighed to calculate the final weight (FW), weight gain (WG), specific growth rate (SGR), feed efficiency (FE) protein efficiency ratio (PER) and survival (SR). Four fish from each tank were selected at random, weighed individually, and dissected to obtain liver and visceral metrics for calculation of hepatosomatic index (HSI) and visceral somatic index (VSI); thereafter, the same intestinal samples were used for histological observation and enzyme activity. Three additional fish per tank were captured at random and anesthetized with ethylene glycol phenyl ether (200 mg/L for 5–10 min). After this, blood was drawn from the caudal vein, which was subsequently centrifuged at 5000 × g for 10 min to obtain the serum. Serum samples were then stored at −70°C for the analysis of non-specific immune responses, such as lysozyme, and myeloperoxidase (MPO) activities, in addition to biochemical parameters, including aspartate aminotransferase (AST), alanine aminotransferase (ALT), glucose and total protein (TP) levels. The serum levels of AST, ALT, glucose, and total protein were determined by a chemical analyzer (Fuji DRI-CHEM 3500i, Fuji Photo Film Ltd., Tokyo, Japan) following the manufacturer's instructions.

Three additional fish from each tank were collected for whole-body proximate composition analysis. Proximate composition analyses of both whole fish and experimental diets were performed by the standard methods of AOAC (32). Whole fish and diet samples were dried at 105°C to a constant weight to determine their moisture content. The ash content was determined by incinerating the samples at 550°C. The protein concentration was determined by using the Kjeldahl method (N × 6.25) after acid digestion. Crude lipids were measured by Soxhlet extraction using Soxhlet system 1,046 (Tacator AB, Hoganas, Sweden) after the samples were freeze-dried for 20 h.

Antioxidant capacity and non-specific immune response analyses

Olive flounder serum lysozyme activity was analyzed as follows: 0.1 mL of test serum was added to 2 mL of a suspension of

TABLE 2 Proximate composition of the eight experimental diets (% of DM basis).[1]

Parameters	Diets					
	CON	Pro-A	Pro-B	Pro-C	OTC	AMO
Moisture	8.56	9.01	8.91	8.56	8.91	8.71
Crude protein	56.2	55.9	54.8	57.1	55.9	56.1
Crude lipid	8.35	8.29	8.34	8.23	8.11	8.32
Crude ash	11.4	10.9	11.2	10.9	11.2	11.8

[1]Values are means of triplicate samples. Values in each row without superscripts are non-significantly different ($P > 0.05$).

Micrococcus lysodeikticus (0.2 mg/mL) in 0.05 M sodium phosphate buffer (pH 6.2). The reactions were carried out at 20°C, and the absorbance was measured at 530 nm. Measurements were taken between 0.5 min and 4.5 min on a spectrophotometer. One lysozyme activity unit was defined as the amount of enzyme that produced a decrease in absorbance corresponding to 0.001/min. Myeloperoxidase activity was measured according to the method described by Quade and Roth (33). Briefly, 20 µL of serum was diluted with Hank's balanced salt solution (HBSS) without Ca^{2+} or Mg^{2+} (Sigma- Aldrich) in 96-well plates. Then, 35 µL of 3, 3′, 5, 5′ tetramethylbenzidine hydrochloride (TMB, 20 mM) (Sigma-Aldrich) and H_2O_2 (5 mM) were added. The color change reaction was stopped after 2 min by adding 35 µL of 4 M sulfuric acid. Finally, the optical density was read at 450 nm in a microplate reader.

Real-time PCR

Tissue fragments from intestine of fish were obtained and immediately stored at −80°C in TRIzol reagent (Thermo Fisher Scientific) for RNA extraction. Total RNA was extracted from 0.5 g of olive flounder tissue using TRIzol Reagent (Thermo Fisher Scientific, San Jose, CA, USA). Afterwards, the RNA was quantified and the purity was assessed spectrophotometrically. The RNA was then treated with DNase I (Cosmogenetech, Seoul, Republic of Korea) to remove genomic DNA contamination. Complementary DNA (cDNA) was synthesized using M-MuLV reverse transcriptase (Cosmogenetech). The expressions of three selected immune-related genes were analyzed by real-time quantitative polymerase chain reaction (RT-qPCR), which was performed with a Bio-Rad CFX96 (Bio-Rad, Hercules, CA, USA) using SYBR Green PCR Core Reagents (Cosmogenetech). The relative expression levels of the target gene transcripts such as flounder growth hormone (FGH), interleukin-1beta (IL-1β) and interleukin-10 (IL-10) were measured with β-actin as an internal control were using CFX Manager software version 2.0 (Bio-Rad) (Table 3). In all the cases, each PCR was performed with triplicate samples.

Histology

The anterior intestinal tissues from the fish (n = 3) were dissected and fixed in 10% neutral buffered formalin, dehydrated in a graded ethanol series and embedded in paraffin. The tissue blocks were sectioned by a microtome machine (HistoCore AUTOCUT, Leica Biosystems, Germany) each of 4 µm thick and stained with hematoxylin and eosin (H&E). At least 6 tissue sections from each sample were examined for intestinal villi length (small fingerlike projections protruded from the intestinal wall) under a light microscope (AX70 Olympus, Tokyo, Japan) equipped with a digital camera (DIXI Optics, Daejeon, Republic of Korea), and an image analysis software (Image J 1.32j, National Institute of Health, USA). Data are presented as means ± SE.

Challenge test

After sampling, seven fish from each tank were redistributed into 18 tanks in a non-recirculating system without water renewal to perform the 15 days of challenge test. The pathogenic bacterium, *Edwardsiella tarda* (*E. tarda*) FSW910410 was obtained from the Department of Biotechnology, Pukyong National University, Busan, Rep. Korea. The bacteria were originally sourced from diseased olive flounder and cultured on tryptic soy agar (TSA, Sigma) plates (24 h at 27°C). All the fish were subjected to intraperitoneal injection of 50 µL of active *E. tarda* (3×10^8 CFU/mL) solution. The water temperature was maintained at 19 ± 1.0°C (mean ± SD) during 15 days of challenge test and fish mortalities were recorded daily from each tank. Dead fish were necropsied and kidney samples were taken and streaked on Salmonella-Shigella agar (SS agar, Difco). The presence of black pigments confirmed *E. tarda* infection.

Statistical analysis

The results are presented as means ± SE (number of replicates as indicated). All the data were analyzed by one-way ANOVA (Statistix 3.1; Analytical Software, St. Paul, MN, USA) to test the effects of the dietary treatments. Prior to the one-way ANOVA, normality and homogeneity of variances were checked. When a significant treatment effect was observed, an LSD *post hoc* test was used to compare the means. Treatment effects were considered significant at the $p < 0.05$ level.

Results

Growth performance and feed utilization in fish

Table 4 shows the growth performance and feed utilization of juvenile olive flounder fed different experimental diets for 8 weeks. At the end of the feeding trial, WG and SGR of fish fed the Pro-A diet were significantly higher greater those of fish fed the CON diet

TABLE 3 Gene specific primers, amplicon lengths and gene bank accession numbers of immune and growth-related genes used in this study.

Name of gene	Sense	Oligonucleotide sequence (5′ to 3′)	Base pair (bp)	Gene bank accession number
β-actin	F	CAGCATCATGAAGTGTGACGTG	107	HQ386788.1
	R	CTTCTGCATACGGTCAGCAATG		
FGH	F	CGCCGTATGGAAACTCTGAACT	160	M23439.1
	R	GGGTGCAGTTAGCTTCTGGAAA		
IL-1β	F	ATGGAATCCAAGATGGAATGC	250	AB720983.1
	R	GAGACGAGCTTCTCTCACAC		
IL-10	F	AGCGAACGATGACCTAGACACG	114	KF025662.1
	R	ACCGTGCTCAGGTAGAAGTCCA		

[1]FGH, flounder growth hormone.
[2]IL-1β, interleukin-1beta.
[3]IL-10, interleukin-10.

TABLE 4 Growth performance and feed utilization of olive flounder fed the six experimental diets for 8 weeks.[1]

Parameters	Diets						
	CON	Pro-A	Pro-B	Pro-C	OTC	AMO	*p*-value
IBW[2]	12.5 ± 0.4	12.4 ± 0.3	12.2 ± 0.2	12.4 ± 0.3	12.4 ± 0.3	12.4 ± 0.3	0.36
FBW[3]	36.7 ± 4.2^{b}	42.0 ± 3.2^{a}	40.8 ± 4.5^{ab}	40.7 ± 3.4^{ab}	36.9 ± 4.5^{b}	37.0 ± 1.4^{b}	0.04
WG (%)[4]	194 ± 2.3^{b}	230 ± 10.1^{a}	224 ± 8.3^{ab}	229 ± 8.3^{ab}	202 ± 4.0^{b}	199 ± 2.3^{b}	0.03
SGR (%/day)[5]	1.95 ± 0.2^{b}	2.24 ± 0.2^{a}	2.16 ± 0.2^{ab}	2.16 ± 0.2^{ab}	2.01 ± 0.1^{b}	1.99 ± 0.1^{b}	0.03
FE (%)[6]	106 ± 7.8^{b}	118 ± 4.5^{ab}	125 ± 5.5^{a}	115 ± 7.2^{ab}	111 ± 7.8^{b}	110 ± 2.3^{b}	0.03
PER[7]	0.65 ± 0.1^{b}	0.84 ± 0.1^{a}	0.76 ± 0.1^{ab}	0.76 ± 0.1^{ab}	0.70 ± 0.1^{ab}	0.66 ± 0.1^{b}	0.04
Survival (%)[8]	93.3 ± 0.2	90.7 ± 0.2	89.3 ± 0.2	89.3 ± 0.2	96.0 ± 0.1	98.7 ± 0.1	0.12
HSI (%)[9]	1.24 ± 0.1	1.66 ± 0.3	1.29 ± 0.4	1.31 ± 0.3	1.13 ± 0.2	1.12 ± 0.4	0.22
VSI (%)[10]	2.05 ± 0.5	1.94 ± 0.2	1.74 ± 0.7	1.94 ± 0.1	1.88 ± 0.6	1.74 ± 0.2	0.12
CF (%)[11]	0.92 ± 0.1	0.97 ± 0.2	0.93 ± 0.1	0.93 ± 0.2	0.92 ± 0.1	0.91 ± 0.1	0.32

[1]Values are means from triplicate groups of fish where the values in each row with different superscripts (a,b) are significantly different ($p < 0.05$). Data are presented as means ± SE.
[2]IBW, initial body weight.
[3]FBW, final body weight.
[4]WG, Weight gain (%) = (final weight - initial weight) / initial weight × 100.
[5]SGR, specific growth rates (%/day) = ($\log_e$ final weight - $\log_e$ initial weight) / days × 100.
[6]FE, feed efficiency (%) = (body weight gain / dry feed intake) × 100.
[7]PER, protein efficiency ratio = (final weight - initial weight) / protein intake.
[8]SR (%) = (total fish – dead fish) / total fish × 100.
[9]HSI, hepatosomatic index (%) = liver weight / body weight × 100.
[10]VSI, viscerosomatic index (%) = viscerai weight / body weight × 100.
[11]CF, condition factor (%) = body weight / body length^3 × 100.

($p > 0.05$). The FE of fish fed the Pro-B diet was significantly greater than that of fish fed the CON, OTC, or AMO diets ($p > 0.05$). The PER of fish fed the Pro-A diet was significantly greater than that of fish fed the CON and AMO diets ($p > 0.05$). Moreover, probiotics supplemented diets were not significantly different from fish fed the Pro-A, Pro-B and Pro-C diets ($p > 0.05$) in terms of growth performance. Furthermore, there were no significant differences ($p > 0.05$) in terms of SR, CF, HSI or VSI among fish fed the experimental diets.

Whole-body proximate composition

There were no significant differences ($p > 0.05$) in terms of crude protein, lipid, moisture or ash content among any of the group of fish fed the experimental diets for 8 weeks (Table 5).

Hematological parameters

The blood parameters of the juvenile olive flounder fed the experimental diets are shown in Figure 1. The serum ALT level in the fish fed the Pro-A diet was significantly lower than those of fish fed the Pro-A, Pro-C and AMO diets ($p < 0.05$). There were no significant differences in AST, glucose, or total protein content among any of the group of fish fed the experimental diets for 8 weeks ($p > 0.05$).

Non-specific immune responses

Figure 2 shows the non-specific immune responses of juvenile olive flounder fed different experimental diets for 8 weeks. The serum lysozyme activities of fish fed the Pro-A, Pro-B and Pro-C diets were significantly greater than that of fish fed CON,OTC and AMO diets

($p > 0.05$). Myeloperoxidase activity of fish fed Pro-A diet was significantly higher than those from the CON and AMO diets ($p > 0.05$). However, there were no significant differences in MPO activities among fish fed the CON, Pro-B, Pro-C, OTC and AMO diets.

Growth and immune related gene expressions

The gene expression profiles of the immunological parameters in the intestine of olive flounder fed diets supplemented with probiotics are presented in Figure 3. The mRNA expression levels of the FGH in fish fed the Pro-A and Pro-B diets were significantly greater than those in fish fed the CON, Pro-C, OTC and AMO diets ($P < 0.05$). However, there were no significant differences in FGH concentrations in fish fed the CON and OTC diets ($p > 0.05$). The IL-1β expressions in fish fed the Pro-A, Pro-B and Pro-C diets were significantly greater than those in fish fed the CON and AMO diets ($P < 0.05$). The IL-10 expressions in fish fed the Pro-A and Pro-C diets were significantly greater than those in fish fed the CON, OTC and AMO diets ($P < 0.05$). However, there were no significant differences in IL-10 mRNA expressions in fish fed the CON and AMO diets ($p > 0.05$).

Histology

Histological analysis of the anterior intestine of olive flounder fed different experimental diets for 8 weeks is shown in Figure 4. The intestinal villi length in fish fed the Pro-A, Pro-B and Pro-C diets had significantly greater villi lengths than the fish fed the CON, OTC and AMO diets (Figure 4A). The fish fed the Pro-A, Pro-B, Pro-C, OTC and AMO diets clearly exhibited better intestinal histomorphology with more massive villi in comparison to the CON diet (Figure 4B). In addition, the images which corresponds to the CON group, shows certain irregular shape and improper arrangement of villi in fish fed the CON, OTC and AMO diets compared to those of the Pro-A, Pro-B and Pro-C groups.

Challenge test

The percent cumulative survival of juvenile olive flounder challenged with *E. tarda* for 15 days is shown in Figure 5. During the challenge test, the first mortalities occurred on the second day. At the end of the 15 day challenge, the percent cumulative survivals of fish fed the Pro-A, Pro-B, and Pro-C diets were significantly greater than that of fish fed the CON diet ($p < 0.05$). However, there were no significant differences in cumulative survival rates in fish fed the Pro-A, Pro-B, Pro-C, OTC, and AMO diets ($p > 0.05$).

TABLE 5 Whole-body proximate composition of olive flounder fed the experimental diets.[1]

Parameters	Diets						
	CON	Pro-A	Pro-B	Pro-C	OTC	AMO	*P*-value
Moisture	76.3 ± 1.2	75.5 ± 2.6	75.1 ± 0.7	75.8 ± 1.6	76.8 ± 0.5	76.2 ± 1.2	0.22
Protein	20.3 ± 0.1	21.0 ± 0.2	20.8 ± 0.2	21.5 ± 0.3	22.3 ± 0.1	20.7 ± 0.3	0.32
Lipid	2.42 ± 0.1	2.39 ± 0.1	2.30 ± 0.1	2.34 ± 0.1	2.41 ± 0.1	2.41 ± 0.1	0.42
Ash	4.09 ± 0.2	4.25 ± 0.3	4.21 ± 0.3	4.16 ± 0.4	4.14 ± 0.1	4.19 ± 0.3	0.31

[1]Values are means from triplicate groups of fish ($n = 3$) where the values in each row without superscripts are non-significantly different ($p > 0.05$). Data are presented as means ± SE.

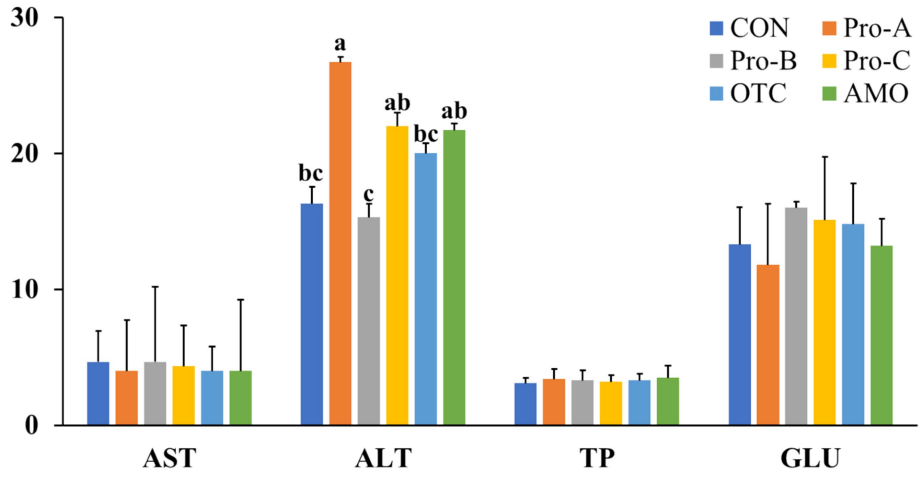

FIGURE 1
Hematological parameters of olive flounder fed the six experimental diets. Values are means from triplicate groups of fish ($n = 3$) where the values in each row with different superscripts (a,b,c) are significantly different ($p < 0.05$). AST: Aspartate aminotransferase (U/l), ALT, alanine aminotransferase (U/l), GLU, glucose (mg/dl), TP: Total protein (g/dl). Data are presented as means ± SE.

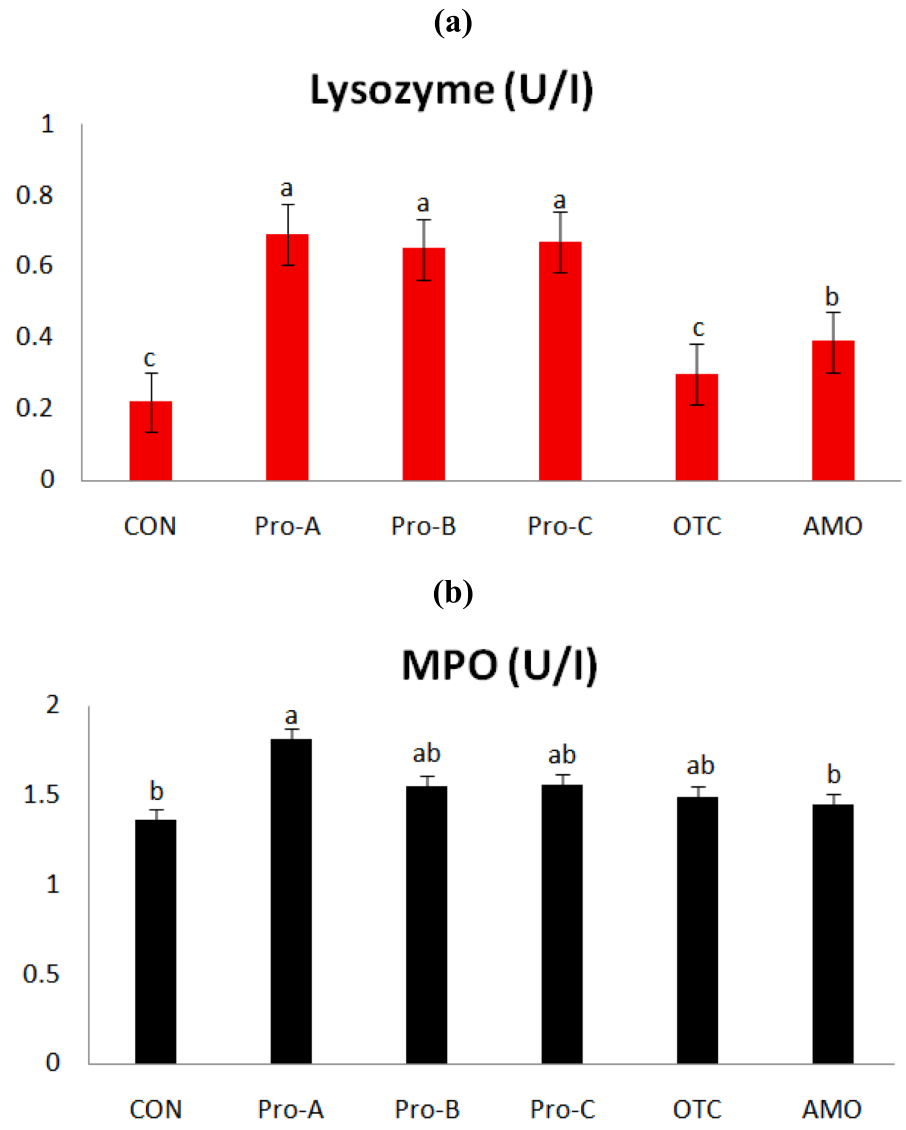

FIGURE 2
Non-specific immune responses of olive flounder fed the six experimental diets. Values are means from triplicate groups of fish (n = 3) where the values in each row with different superscripts (a,b,c) are significantly different ($p < 0.05$); **(A)** Lysozyme (U/ml): lysozyme activity and **(B)** MPO (absorbance): myeloperoxidase (OD at 450 nm). Data are presented as means ± SE.

Discussion

Research into the use of probiotics in aquaculture nutrition has attracted much interest due to their health benefits and because they are considered environmentally friendly (34). In recent years, probiotic effects have been studied in different fish species (35). Additionally, many trials have investigated the extraction of probiotic strains from the intestines of various fish, which are subsequently added to aquafeeds. This strategy of sourcing and using probiotics from these species has improved growth performance, feed efficiency and immune response (36, 37). Therefore, to build on this growing body of knowledge, the present study utilized three different probiotics according to the results of previous experiments.

The two probiotics used were *Bacillus subtilis* extracted from the intestines of Japanese eel and *jeotgal* (28, 29), because most other probiotic studies have focused on the use of *Bacillus* spp. (34–41). The other probiotics used was *E. faecium* isolated from the intestine of healthy Nile tilapia (18). In this study, we used dietary live or active probiotics during feeding of fish to ensure direct interaction with fish physiology in terms of gut microbiome and mucosal immunity. Moreover, a previous experiment in which Pirarucu, *Arapaima gigas* was fed diets containing live probiotics, *E. faecium* 1×10^8 CFU/g showed increased weight gain compared to that in the control treatment group (42). The results of the present study showed that all the experimental diets containing the probiotics were equally effective and resulted in increased weight gain and feed efficiency compared with the control diet. These results are likely due to the increased secretion of proteolytic enzymes, which increase feed efficiency, similar to the findings of probiotic experiments in olive flounder (35). Likewise, beneficial effects of probiotics have also been reported on

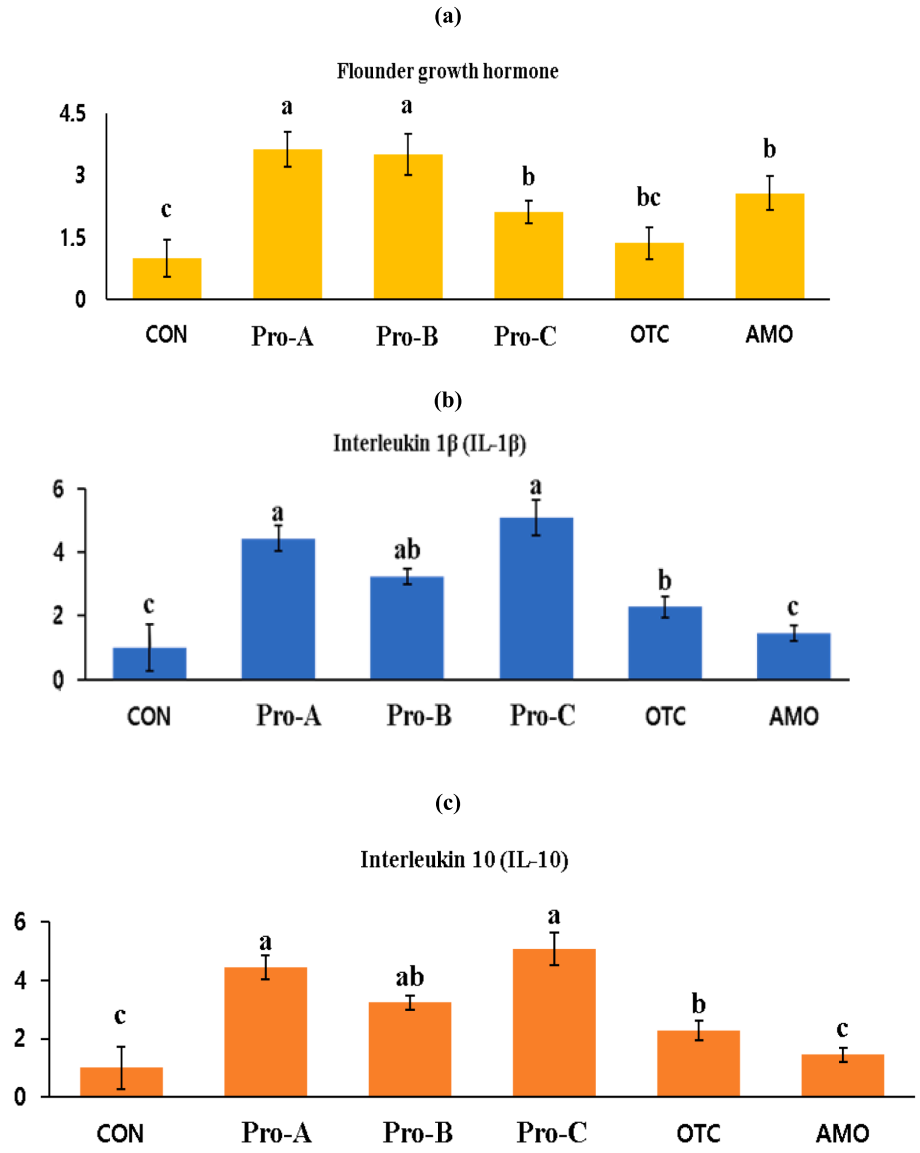

FIGURE 3
Relative mRNA gene expression levels of **(A)** flounder growth hormone (FGH), **(B)** interleukin-1 beta (IL-1β) and **(C)** interleukin-10 (IL-10) of intestine from olive flounder fed the experimental diets for 8 weeks. Data are presented as means ± SE.

growth performance in terms of improving weight gain, specific growth rate, and feed efficiency in tilapia (18, 30, 43, 44), whiteleg shrimp (31), Japanese eel (28, 36), starry flounder (39), red sea bream (26), rainbow trout (16, 37, 40), Pirarucu (42) and olive flounder (29, 35). In agreement of the present study, Won et al. (31, 41) reported that *B. subtilis* WB60 at 1×10^8 CFU/g can enhance growth and feed utilization in whiteleg shrimp and Nile tilapia. Furthermore, probiotic bacteria, *E. faecium* at 1×10^7 CFU/mL in water showed significantly better final weight and daily weight gain in tilapia which endorsed the results of the present study (30).

Modulation of the immune system is one of the most common benefits of probiotics (44). Lysozyme activity is frequently used as an indicator of non-specific immune functions and is the principle means of responding infections in fish (28). This enzyme not only has bacteriolytic activity against gram-positive and gram-negative bacteria (45), but also has anti-inflammatory and antiviral properties. The MPO is another important enzyme that utilizes oxidative radicals to produce hypochlorous acid, which kills pathogens (29). In the present study, the immune parameters, lysozyme including MPO activities were measured and the beneficial effects of both probiotic bacteria on nonspecific immune related enzyme responses, were clearly shown to be greatest for the olive flounder fed *B. subtilis*, at the 1×10^8 CFU/g (Pro-A and Pro-B) and *E. faecium*, at the 1×10^7 CFU/g (Pro-C). In agreement of the present study, previous research findings reported that dietary supplementation of BSWB60, BSSJ10 and EFSH30 in the diets can improve the lysozyme and MPO activities in olive flounder (28–30).

Growth hormone is a hormone that stimulates the secretion of IGF-1 in the liver, increases the concentration of glucose and vitreous acid (46), produces IGF-1 induced protein synthesis (47), and is

10.3389/fnut.2025.1519140

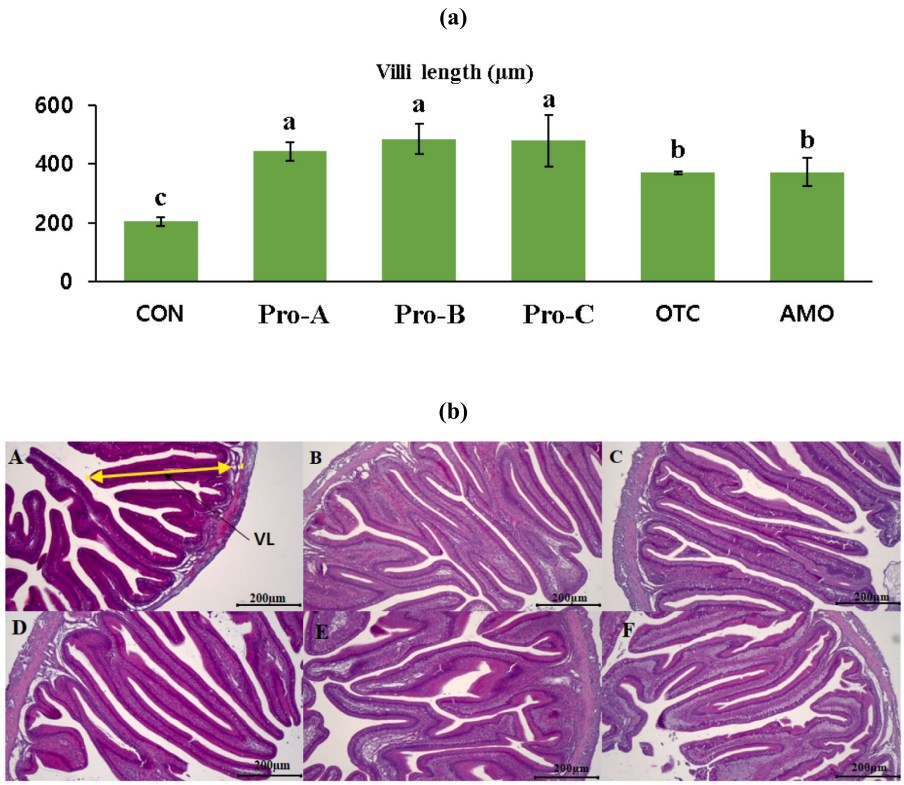

FIGURE 4
Intestinal histology of juvenile olive flounder fed the experimental diets for 8 weeks; **(a)** villi lengths in fish fed the different diets; **(b)** histological photomicrographs of **(A)** CON **(B)** Pro-A **(C)** Pro-B **(D)** Pro-C **(E)** OTC **(F)** AMO diet groups; (scale bar = 200 μm; original magnification×40).

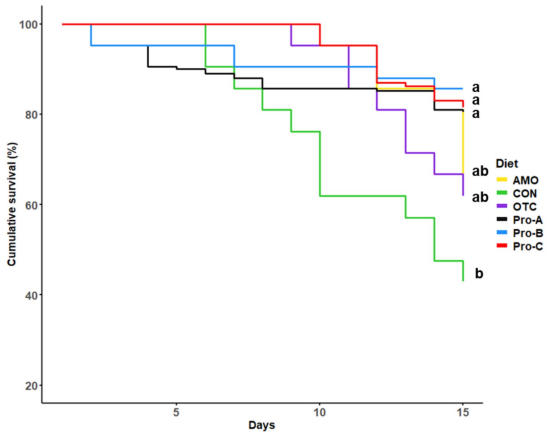

FIGURE 5
Cumulative survival (%) of olive flounder during 15 days challenge test. For the survival analysis, we used R 4.4.1 (R Development Core Team, 2023) with the survival and survminer packages to perform Kaplan–Meier survival analysis. This approach allowed us to estimate survival curves and compare survival rates among groups using the log-rank test. Specifically, the Kaplan–Meier method (via the survfit function) was employed to analyze survival data across different dietary treatments.

reported to be an indicator of growth factors in fish such as promoting cell division (48). In the present study, olive flounder fed probiotics supplemented diets exhibited significantly greater FGH expression than did those fed the control diet (Figure 3A). Similarly, previous studies in which probiotics were added showed high FGH value (49, 50). These studies have reported that probiotic supplementation can affect growth hormone-related gene expression in fish (28, 29). In consistent of the present study, Jang et al. (26) found that dietary supplementation of *Bacillus* sp. as a host-associated probiotic in red sea bream can enhance the growth hormone in fish which is also reflected in the growth performance of fish.

The IL-1β is one of the earliest expressed pro-inflammatory cytokines and enables organisms to respond promptly to infection by inducing a cascade of reactions leading to inflammation (51). Many of the effector roles of IL-1β are mediated through the up- or down-regulation of the expressions of other cytokines and chemokines (52). The IL-1β was the first interleukin to be characterized in fish and has since been identified in a number of fish species, such as rainbow trout (53), carp (54), seabass (55), gilt head seabream (56), haddock (57), tilapia (58). The IL-10 on the other hand, is an anti-inflammatory cytokine that down-regulates the expression of pro-inflammatory cytokines (59). Additionally, IL-10 was initially discovered to be an inhibitory factor for the production of Th1 cytokines. Subsequently, pleiotropic inhibitory and stimulatory effects of IL-10 on various types of blood cells were described, including its role as a survival and differentiation factor for B cells. The IL-10, which is produced by activated monocytes, T cells and other cell types, such as keratinocytes, appears to be a crucial factor for at least some forms of peripheral tolerance and a major suppressor of the immune response and inflammation. The inhibitory function of IL-10 is mediated by the

induction of regulatory T cells (60). In the present study, the activities of IL-1β and IL-10 in the intestine of the fish that were administered probiotics were significantly greater than those in the control with low FM diet. Therefore, dietary probiotics appears to increase the immune function of fish even though fish were offered with low FM diets. The results suggest that dietary supplementation of probiotics might be attenuated the inflammation in fish through up-regulating the cytokine gene (IL-1β and IL-10) expressions in fish. In agreement of the present study, Lara-Flores et al. (43) and Back et al. (50) reported that probiotics supplemented in low protein or low FM diets can enhance the immunity in tilapia and olive flounder, respectively without compromising the health status of fishes.

Intestinal morphological parameters (villus length and muscular layer thickness) are indicative of a healthy gut in fish. The intestine is very important for the digestion and absorption of nutrients. The length of the intestinal villi determines the absorption of nutrients in the GI tract (gastrointestinal tract) (61, 62). Thus, digestive function is associated with intestinal development (62). In this study, the beneficial effects of probiotics on intestinal morphology were clearly observed. The length of the villi increased in a dose dependent manner and villi length was significantly highest for the olive flounder fed the Pro-A, Pro-B, and Pro-C diets (Figure 4A). In the same manner, Lee et al. (28) reported that probiotics are capable of increasing the villus length in the proximal intestine of Japanese eel. Furthermore, Won et al. (31, 41) postulated that dietary *Bacillus subtilis* WB60 can increase the villus length and muscular thickness in the intestine of whiteleg shrimp and Nile tilapia which supported the results of the present study.

With regard to disease resistance, olive flounder fed with probiotics, Pro-A and Pro-B at 1×10^8 CFU/g as well as Pro-C at 1×10^7 CFU/g supplemented in the diet exhibited the highest disease resistance compared to the control group. However, there were no significant differences in cumulative survival rates in fish fed the Pro-A, Pro-B, Pro-C, OTC and AMO diets suggesting that the three fish-derived probiotics were equally effective to the antibiotics. In this study, the mode of probiotic action is attributed to follow the host-specific (63) and strain-specific (64) properties. The major factors that affecting the disease resistance in fish perhaps the origin, source, viability and dose of the probiotics and their duration of administration (65–68). Likewise, in recent studies, it is reported that dietary supplementation of host-associated probiotic bacteria *B. subtilis* and *E. faecium* could enhance the disease or stress resistance in Japanese eel, shrimp, hybrid yellow catfish, Chinese perch, hybrid grouper, olive flounder, rainbow trout, red sea bream and tilapia (20–31, 41). In consistent with the present study, it has been reported that the higher levels of lysozyme improved disease resistance in infected fish such as Atlantic salmon challenged with *Aeromonas salmonicida* (69) and sheatfish challenged with *Edwardsiella tarda* (70).

Conclusion

In conclusion, the present study revealed the potential benefits of supplementation with the bacteria species, *B. subtilis* and *E. faecium* as probiotics in the diet of olive flounder. Therefore, *B. subtilis* at 1×10^8 CFU/g and *E. faecium* at 1×10^7 CFU/g could be ideal probiotics for improving growth performance, immune responses, enzyme activity and disease resistance, while replacing the dietary supplementation of antibiotics in juvenile olive flounder fed a reduced FM diet. The utilization of these probiotics could help to further enhance the olive flounder production in the farm level and to replace indiscriminate use of antibiotics without compromising health status in fish as well as to reduce environmental pollution in terms of antimicrobial resistance with higher consumer acceptance. However, further research is warranted to evaluate the effects of the current probiotics on the diversity of intestinal microbiota and immunity on gut-brain axis in fish.

Data availability statement

The datasets presented in this study can be found in online repositories. The names of the repository/repositories and accession number(s) can be found at: https://www.ncbi.nlm.nih.gov/genbank/, HQ386788.1, https://www.ncbi.nlm.nih.gov/genbank/, M23439.1, https://www.ncbi.nlm.nih.gov/genbank/, AB720983.1, https://www.ncbi.nlm.nih.gov/genbank/, KF025662.1.

Ethics statement

The animal study was approved by the Institutional Animal Care and Use Committee, Pukyong National University, Busan, Republic of Korea. The study was conducted in accordance with the local legislation and institutional requirements.

Author contributions

WC: Conceptualization, Data curation, Formal analysis, Investigation, Methodology, Software, Writing – original draft, Writing – review & editing. MM: Data curation, Formal analysis, Investigation, Methodology, Writing – original draft, Writing – review & editing. SAL: Formal Analysis, Software, Writing – review & editing. JB: Formal Analysis, Software, Writing – review & editing. SB: Conceptualization, Methodology, Project administration, Writing – review & editing. TM: Funding acquisition, Resources, Supervision, Validation, Visualization, Writing – review & editing. SYL: Conceptualization, Data curation, Funding acquisition, Methodology, Project administration, Resources, Software, Supervision, Validation, Visualization, Writing – review & editing.

Funding

The author(s) declare that financial support was received for the research, authorship, and/or publication of this article. This research was funded by the Pukyong National University Research Fund in 2021 (CD20210975). This work was also supported by the Basic Science Research Program (Grant No. 2019R1A6A1A11052070) funded by the Ministry of Education and the Basic Science Research Program (Grant No. 2022R1A2B5B02001711) funded by the Ministry of Science and ICT through the National Research Foundation of Korea (NRF) to Taesun Min. This work was supported by the Brain Pool Program (Grant No.

RS-2024-00445420) through the National Research Foundation of Korea (NRF) funded by the Ministry of Science and ICT to Mohammad Moniruzzaman.

Conflict of interest

The authors declare that the research was conducted in the absence of any commercial or financial relationships that could be construed as a potential conflict of interest.

The author(s) declared that they were an editorial board member of Frontiers, at the time of submission. This had no impact on the peer review process and the final decision.

Generative AI statement

The authors declare that no Generative AI was used in the creation of this manuscript.

Publisher's note

References

1. Fuji K, Kobayashi K, Hasegawa O, Coimbra MRM, Sakamoto T, Okamoto N. Identification of a single major genetic locus controlling the resistance to lymphocystis disease in Japanese flounder (*Paralichthys olivaceus*). *Aquaculture*. (2006) 254:203–10. doi: 10.1016/j.aquaculture.2005.11.024

2. Hamidoghli A, Won S, Lee S, Lee S, Farris NW, Bai SC. Nutrition and feeding of olive flounder *Paralichthys olivaceus*: a review. *Rev Fish Sci Aquac*. (2020) 28:340–57. doi: 10.1080/23308249.2020.1740166

3. Statistics Korea. Results of the year 2022 fish farming trend survey. Text by Department of Agriculture and Fisheries Trends Department, Fish Farming Trend Survey. Daejeon. (2023). Available at: https://kostat.go.kr/board.es?mid=a10301080400&bid=225&act=view&list_no=424510 (Accessed February 20, 2024).

4. Boyd CE. Overview of aquaculture feeds: Global impacts of ingredient use In: Feed and feeding practices in aquaculture: Elsevier (2015). 3–25. doi: 10.1016/B978-0-08-100506-4.00001-5

5. Bharadwaj AS, Brignon WR, Gould NL, Brown PB, Wu YV. Evaluation of meat and bone a.S. Meal in practical diets fed to juvenile hybrid striped bass *Morone chrysops* × *M. saxatilis*. *J World Aquac Soc*. (2002) 33:448–57. doi: 10.1111/j.1749-7345.2002.tb00024.x

6. Markey JC, Amaya EA, Davis DA. Replacement of poultry by-product meal in production diets for the Pacific white shrimp, *Litopenaeus vannamei*. *J World Aquac Soc*. (2010) 41:893–902. doi: 10.1111/j.1749-7345.2010.00432.x

7. Kang YJ, Lee SM, Yang SG, Bai SC. Effects of meat meal, blood meal or soybean meal as a dietary protein source replacing fish meal in parrot fish, *Oplegnathus fasciatus*. *J Aquacult*. (1999) 12:205–12.

8. McGoogan BB, Gatlin DM III. Effects of replacing fish meal with soybean meal in diets for red drum Sciaenops ocellatus and potential for palatability enhancement. *J World Aquac Soc*. (1997) 28:374–85. doi: 10.1111/j.1749-7345.1997.tb00284.x

9. Tacon AGJ. Feed ingredients for warmwater fish: fish meal and other processed feedstuffs. Food and Agriculture Organization of the United Nations, 1993 FAO Fish. Circ (FAO). No. 856.

10. Cabello FC, Godfrey HP, Tomova A, Ivanova L, Dölz H, Millanao A, et al. Antimicrobial use in aquaculture re-examined: its relevance to antimicrobial resistance and to animal and human health. *Environ Microbiol*. (2013) 15:1917–42. doi: 10.1111/1462-2920.12134

11. Done HY, Venkatesan AK, Halden RU. Does the recent growth of aquaculture create antibiotic resistance threats different from those associated with land animal production in agriculture? *AAPSJ*. (2015) 17:513–24. doi: 10.1208/s12248-015-9722-z

12. Balcázar JL, De Blas I, Ruiz-Zarzuela I, Cunningham D, Vendrell D, Múzquiz JL. The role of probiotics in aquaculture. *Vet Microbiol*. (2006) 114:173–86. doi: 10.1016/j.vetmic.2006.01.009

13. Balcázar JL, Vendrell D, De Blas I, Ruiz-Zarzuela I, Muzquiz JL. Probiotics: a tool for the future of fish and shellfish health management. *J Aquac Trop*. (2004) 19:239–42.

14. Garriques D. An evaluation of the production and use of a live bacterial isolate to manipulate the microbial flora in the commercial production of *Penaeus vennamei* postlarvae in Ecuador., swim. Through Troubl Water Proc Spec Sess Shrimp Farming, Aquac World Aquac Soc (1995). pp. 53–59.

15. Direkbusarakom S, Yoshimizu M, Ezura Y, Ruangpan L, Danayadol Y. Vibrio spp., the dominant flora in shrimp hatchery against some fish pathogenic viruses. *J Mar Biotechnol*. (1998) 6:266–7.

16. Habibnia M, Bahrekazemi M, Bahram S, Javadian SR, Hedayatifard M, Abdel-Tawwab M. Growth performance, hematological and immune parameters, and mRNA levels of cytokines and antioxidant-related genes in rainbow trout (*Oncorhynchus mykiss*) fed on *Pediocuccus pentosaceus* and/or ferulic acid. *Anim Feed Sci Technol*. (2024) 308:115872. doi: 10.1016/j.anifeedsci.2023.115872

17. Eissa EH, El-Sayed AFM, Hendam BM, Ghanem SF, Elnabi HEA, El-Aziz YMA, et al. The regulatory effects of water probiotic supplementation on the blood physiology, reproductive performance, and its related genes in red Tilapia (*Oreochromis niloticus* X *O. mossambicus*). *BMC Vet Res*. (2024) 20:351. doi: 10.1186/s12917-024-04190-w

18. Xia Y, Wang M, Gao F, Lu M, Chen G. Effects of dietary probiotic supplementation on the growth, gut health and disease resistance of juvenile Nile tilapia (*Oreochromis niloticus*). *Anim Nutri*. (2020) 6:69–79. doi: 10.1016/j.aninu.2019.07.002

19. Lazado CC, Caipang CMA, Estante EG. Prospects of host-associated microorganisms in fish and penaeids as probiotics with immunomodulatory functions. *Fish Shell Immunol*. (2015) 45:2–12. doi: 10.1016/j.fsi.2015.02.023

20. Ji Z, Lu X, Xue M, Fan Y, Tian J, Dong L, et al. The probiotic effects of host-associated *Bacillus velezensis* in diets for hybrid yellow catfish (*Pelteobagrusfulvidraco* × *Pelteobagrusvachelli*). *Anim Nutri*. (2023) 15:114–25. doi: 10.1016/j.aninu.2023.08.004

21. Liao Z, Liu Y, Wei H, He X, Wang Z, Zhuang Z, et al. Effects of dietary supplementation of *Bacillus subtilis* DSM 32315 on growth, immune response and acute ammonia stress tolerance of Nile tilapia (*Oreochromis niloticus*) fed with high or low protein diets. *Anim Nutri*. (2023) 15:375–85. doi: 10.1016/j.aninu.2023.05.016

22. Büyükdeveci ME, Cengizler I, Balcazar JL, Demirkale I. Effects of two host-associated probiotics *Bacillus mojavensis* B191 and *Bacillus subtilis* MRS11 on growth performance, intestinal morphology, expression of immune-related genes and disease resistance of Nile tilapia (*Oreochromis niloticus*) against *Streptococcus iniae*. *Dev Comp Immunol*. (2023) 138:104553. doi: 10.1016/j.dci.2022.104553

23. Lee SJ, Da-In Noh DI, Lee YS, Hasan MT, Hur SW, Lee S, et al. Effects of host-associated low-temperature probiotics in olive founder (*Paralichthysolivaceus*) aquaculture. *Sci Rep*. (2024) 14:2134. doi: 10.1038/s41598-024-52491-9

24. Ji Z, Zhu C, Zhu X, Ban S, Yu L, Tian J, et al. Dietary host-associated *Bacillus subtilis* supplementation improves intestinal microbiota, health and disease resistance in Chinese perch (*Siniperca chuatsi*). *Anim Nutri*. (2023) 13:197–205. doi: 10.1016/j.aninu.2023.01.001

25. Amoah K, Tan B, Zhang S, Chi S, Yang Q, Liu H, et al. Host gut-derived Bacillus probiotics supplementation improves growth performance, serum and liver immunity, gut health, and resistive capacity against *Vibrio harveyi* infection in hybrid grouper (*Epinephelus fuscoguttatus* × *Epinephelus lanceolatus*). *Anim Nutri*. (2023) 14:163–84. doi: 10.1016/j.aninu.2023.05.005

26. Jang WJ, Lee KB, Jeon MH, Lee SJ, Hur SW, Lee S, et al. Characteristics and biological control functions of Bacillus sp. PM8313 as a host-associated probiotic in red sea bream (*Pagrus major*) aquaculture. *Anim Nutri*. (2023) 12:20–31. doi: 10.1016/j.aninu.2022.08.011

27. Choi S, Sim W, Jang D, Yoon Y, Ryu J, Oh J, et al. Antibiotics in coastal aquaculture waters: occurrence and elimination efficiency in oxidative water treatment processes. *J Hazard Mat*. (2020) 396:122585. doi: 10.1016/j.jhazmat.2020.122585

28. Lee S, Katya K, Hamidoghli A, Hong J, Kim DJ, Bai SC. Synergistic effects of dietary supplementation of *Bacillus subtilis* WB60 and mannanoligosaccharide (MOS) on growth performance, immunity and disease resistance in Japanese EEL, *Anguilla japonica*. *Fish Shell Immunol*. (2018) 83:283–91. doi: 10.1016/j.fsi.2018.09.031

29. Hasan MT, Jang WJ, Kim H, Lee BJ, Kim KW, Hur SW, et al. Synergistic effects of dietary Bacillus sp. SJ-10 plus β-glucooligosaccharides as a synbiotic on growth performance, innate immunity and streptococcosis resistance in olive flounder (*Paralichthys olivaceus*). *Fish Shell Immunol*. (2018) 82:544–53. doi: 10.1016/j.fsi.2018.09.002

30. Wang YB, Tian ZQ, Yao JT, Li WF. Effect of probiotics, *Enteroccus faecium*, on tilapia (*Oreochromis niloticus*) growth performance and immune response. *Aquaculture*. (2008) 277:203–7. doi: 10.1016/j.aquaculture.2008.03.007

31. Won S, Hamidoghli A, Choi W, Park Y, Jang WJ, Kong IS, et al. Effects of *Bacillus subtilis* WB60 and *Lactococcus lactis* on growth, immune responses, histology and gene expression in Nile Tilapia, *Oreochromis niloticus*. *Microorganisms*. (2020) 8:67. doi: 10.3390/microorganisms8010067

32. AOAC. Association of Official Analytical Chemists Official Methods of Analysis, Aquac. Res. Sixteenth (1995).

33. Quade MJ, Roth JA. A rapid, direct assay to measure degranulation of bovine neutrophil primary granules. *Vet Immunol Immunopathol*. (1997) 58:239–48. doi: 10.1016/S0165-2427(97)00048-2

34. Kuebutornye FKA, Abarike ED, Lu Y. A review on the application of Bacillus as probiotics in aquaculture. *Fish Shell Immunol*. (2019) 87:820–8. doi: 10.1016/j.fsi.2019.02.010

35. Cha JH, Yang SY, Woo SH, Song JW, Oh DH, Lee KJ. Effects of dietary supplementation with *Bacillus* sp. on growth performance, feed utilization, innate immunity and disease resistance against *Streptococcus iniae* in olive flounder *Paralichthys olivaceus*. *Korean J Fish Aquat Sci*. (2012) 45:35–42. doi: 10.5657/KFAS.2012.0035

36. Park Y, Kim H, Won S, Hamidoghli A, Hasan MT, Kong IS, et al. Effects of two dietary probiotics (*Bacillus subtilis* or *licheniformis*) with two prebiotics (mannan or fructo oligosaccharide) in Japanese EEL, *Anguilla japonica*. *Aquac Nutr*. (2020) 26:316–27. doi: 10.1111/anu.12993

37. Vazirzadeh A, Roosta H, Masoumi H, Farhadi A, Jeffs A. Long-term effects of three probiotics, singular or combined, on serum innate immune parameters and expressions of cytokine genes in rainbow trout during grow-out. *Fish Shell Immunol*. (2020) 98:748–57. doi: 10.1016/j.fsi.2019.11.023

38. Kim YR, Kim EY, Lee JM, Kim JK, Kong IS. Characterisation of a novel Bacillus sp. SJ-10 β-1,3–1,4-glucanase isolated from jeotgal, a traditional Korean fermented fish. *Bioprocess Biosyst Eng*. (2013) 36:721–7. doi: 10.1007/s00449-013-0896-4

39. Park Y, Moniruzzaman M, Lee S, Hong J, Won S, Lee JM, et al. Comparison of the effects of dietary single and multi-probiotics on growth, non-specific immune responses and disease resistance in starry flounder. *Platichthysstellatus Fish Shell Immunol*. (2016) 59:351–7. doi: 10.1016/j.fsi.2016.11.006

40. Park Y, Lee S, Hong J, Kim D, Moniruzzaman M, Bai SC. Use of probiotics to enhance growth, stimulate immunity and confer disease resistance to *Aeromonas salmonicida* in rainbow trout (*Oncorhynchus mykiss*). *Aquac Res*. (2017) 48:2672–82. doi: 10.1111/are.13099

41. Won S, Hamidoghli A, Choi W, Bae J, Jang WJ, Lee S, et al. Evaluation of potential probiotics *Bacillus subtilis* WB60, *Pediococcus pentosaceus*, and *Lactococcus lactis* on growth performance, immune response, gut histology and immune-related genes in Whiteleg shrimp, *Litopenaeus vannamei*. *Microorganisms*. (2020) 8:281. doi: 10.3390/microorganisms8020281

42. da Costa SN, do Couto MVS, Abe HA, Paixao PEG, Cordeiro CAM, Lopes EM, et al. Effects of an *Enterococcus faecium*-based probiotic on growth performance and health of Pirarucu, *Arapaima gigas*. *Aquac Res*. (2019) 50:3720–8. doi: 10.1111/are.14332

43. Lara-Flores MM, Olvera-Novoa A. The use of lactic acid bacteria isolated from intestinal tract of Nile tilapia (*Oreochromis niloticus*), as growth promoters in fish fed low protein diets. *Lat Am J Aquat Res*. (2013) 41:490–7. doi: 10.3856/vol41-issue3-fulltext-12

44. Aly SM, Mohamed MF, John G. Effect of probiotics on the survival, growth and challenge infection in *Tilapia nilotica* (*Oreochromis niloticus*). *Aquac Res*. (2008) 39:647–56. doi: 10.1111/j.1365-2109.2008.01932.x

45. Helal R, Melzig MF. In vitro effects of selected saponins on the production and release of lysozyme activity of human monocytic and epithelial cell lines. *Sci Pharm*. (2011) 79:337–49. doi: 10.3797/scipharm.1012-15

46. Greenwood FC, Landon J. Growth hormone secretion in response to stress in man. *Nature*. (1966) 210:540–1. doi: 10.1038/210540a0

47. Bornfeldt KE, Arnqvist HJ, Dahlkvist HH, Skottner A, Wikberg JES. Receptors for insulin-like growth factor-I in plasma membranes isolated from bovine mesenteric arteries. *Eur J Endocrinol*. (1988) 117:428–34. doi: 10.1530/acta.0.1170428

48. Clemmons DR, Busby W, Clarks JB, Parker A, Duan C, Nam TJ. Modifications of insulin-like growth factor binding proteins and their role in controlling IGF actions. *Endocr J*. (1998) 45:S1–8. doi: 10.1507/endocrj.45.Suppl_S1

49. Kuebutornye FKA, Tang J, Cai J, Yu H, Wang Z, Abarike ED, et al. In vivo assessment of the probiotic potentials of three host-associated Bacillus species on growth performance, health status and disease resistance of *Oreochromis niloticus* against *Streptococcus agalactiae*. *Aquaculture*. (2020) 527:735440. doi: 10.1016/j.aquaculture.2020.735440

50. Back SJ, Park SJ, Moon JS, Lee SB, Jo SJ, Nam TJ, et al. The effects of dietary heat-killed probiotics bacteria additives in low-fishmeal feed on growth performance, immune responses, and intestinal morphology in juvenile olive flounder *Paralichthys olivaceus*. *Aquac Rep*. (2020) 18:100415. doi: 10.1016/j.aqrep.2020.100415

51. Reyes-Cerpa S, Maisey K, Reyes-López F, Toro-Ascuy D, Sandino AM, Imarai M. Fish cytokines: current research and application. *Fish Sci*. (2021) 87:1–9. doi: 10.1007/s12562-020-01476-4

52. Dinarello CA. Interleukin-1 and its biologically related cytokines. *Adv Immunol*. (1989) 44:153–205. doi: 10.1016/S0065-2776(08)60642-2

53. Pleguezuelos O, Zou J, Cunningham C, Secombes CJ. Cloning, sequencing, and analysis of expression of a second IL-1 β gene in rainbow trout (*Oncorhynchus mykiss*). *Immunogenetics*. (2000) 51:1002–11. doi: 10.1007/s002510000240

54. Fujiki K, Shin DH, Nakao M, Yano T. Molecular cloning and expression analysis of carp (*Cyprinus carpio*) interleukin-1β, high affinity immunoglobulin E fc receptor γ subunit and serum amyloid a. *Fish Shell Immunol*. (2000) 10:229–42. doi: 10.1006/fsim.1999.0253

55. Scapigliati G, Buonocore F, Bird S, Zou J, Pelegrin P, Falasca C, et al. Phylogeny of cytokines: molecular cloning and expression analysis of sea bass *Dicentrarchus labrax* interleukin-1β. *Fish Shell Immunol*. (2001) 11:711–26. doi: 10.1006/fsim.2001.0347

56. Pelegrín P, García-Castillo J, Mulero V, Meseguer J. Interleukin-1β isolated from a marine fish reveals up-regulated expression in macrophages following activation with lipopolysaccharide and lymphokines. *Cytokine*. (2001) 16:67–72. doi: 10.1006/cyto.2001.0949

57. Corripio-Miyar Y, Bird S, Tsamopoulos K, Secombes CJ. Cloning and expression analysis of two pro-inflammatory cytokines, IL-1β and IL-8, in haddock (*Melanogrammus aeglefinus*). *Mol Immunol*. (2007) 44:1361–73. doi: 10.1016/j.molimm.2006.05.010

58. Lee DS, Hong SH, Lee HJ, Jun LJ, Chung JK, Kim KH, et al. Molecular cDNA cloning and analysis of the organization and expression of the IL-1β gene in the Nile tilapia, *Oreochromis niloticus*. *Comp Biochem Physiol Part A Mol Integr Physiol*. (2006) 143:307–14. doi: 10.1016/j.cbpa.2005.12.014

59. Huo HJ, Chen SN, Li L, Nie P. Functional characterization of IL-10 and its receptor subunits in a perciform fish, the mandarin fish, *Siniperca chuatsi*. *Dev Comp Immunol*. (2019) 97:64–75. doi: 10.1016/j.dci.2019.03.017

60. Moore KW, de Waal MR, Coffman RL, O'Garra A. Interleukin-10 and the interleukin-10 receptor. *Annu Rev Immunol*. (2001) 19:683–765. doi: 10.1146/annurev.immunol.19.1.683

61. Gao YJ, Yang HJ, Liu Y, Chen SJ, Guo DQ, Yu Y, et al. Effects of graded levels of threonine on growth performance, biochemical parameters and intestine morphology of juvenile grass carp *Ctenopharyngodon idella*. *Aquaculture*. (2014) 424-425:113–9. doi: 10.1016/j.aquaculture.2013.12.043

62. Klurfeld DM. Nutritional regulation of gastrointestinal growth. *Front Biosci*. (1999) 4:D299–302. doi: 10.2741/klurfeld

63. Madsen K. Probiotics and the immune response. *J Clin Gastroenterol*. (2006) 40:232–4. doi: 10.1097/00004836-200603000-00014

64. Ibnou-Zekri N, Blum S, Schiffrin E, von der Weid T. Divergent patterns of colonization and immune response elicited from two intestinal lactobacillus strains that display similar properties in vitro. *Infec Immun*. (2003) 71:428–36. doi: 10.1128/IAI.71.1.428-436.2003

65. Donnet-Hughes A, Rochat F, Serrant P, Aeschlimann JM, Schiffrin EJ. Modulation of nonspecific mechanisms of defense by lactic acid bacteria: effective dose. *J Dairy Sci*. (1999) 82:863–9. doi: 10.3168/jds.S0022-0302(99)75304-X

66. Gill HS, Rutherfurd KJ, Cross ML, Gopal PK. Enhancement of immunity in the elderly by dietary supplementation with the probiotic *Bifidobacterium lactis* HN019. *Am J Clin Nutr*. (2001) 74:833–9. doi: 10.1093/ajcn/74.6.833

67. Sharifuzzaman SM, Austin B. Kocuria SM1 controls vibriosis in rainbow trout (*Oncorhynchus mykiss*, Walbaum). *J Appl Microbiol*. (2010) 108:2162–70. doi: 10.1111/j.1365-2672.2009.04618.x

68. Vollstad D, Bogwald J, Gaserod O, Dalmo RA. Influence of high-M alginate on the growth and survival of Atlantic cod (*Gadus morhua* L.) and spotted wolf fish (*Anarhichas minor* Olafsen) fry. *Fish Shell Immunol*. (2006) 20:548–61. doi: 10.1016/j.fsi.2005.07.004

69. Moyner K, Roed KH, Sevatdal S, Heum M. Changes in non-specific immune parameters in Atlantic salmon, *Salmo salar* (L.), induced by *Aeromonas salmonicida* infection. *Fish Shell Immunol*. (1993) 3:253–65. doi: 10.1006/fsim.1993.1025

70. Caruso D, Schlumberger O, Dahm C, Proteau JP. Plasma lysozyme levels in sheatfish *Silurus glanis* (L.) subjected to stress and experimental infection with *Edwardsiella tarda*. *Aquac Res*. (2002) 33:999–1008. doi: 10.1046/j.1365-2109.2002.00716.x

frontiers | Frontiers in Immunology

TYPE Original Research
PUBLISHED 22 April 2025
DOI 10.3389/fimmu.2025.1551816

OPEN ACCESS

EDITED BY
Hongyu Liu,
Guangdong Ocean University, China

REVIEWED BY
Yueling Zhang,
Shantou University, China
Peng Xie,
Huaiyin Normal University, China

*CORRESPONDENCE
Qi Wang
18409496835@163.com
Ziming Chen
chenzm818@163.com

RECEIVED 26 December 2024
ACCEPTED 07 March 2025
PUBLISHED 22 April 2025

CITATION
Zeng L, Sun Y, Zhang H, Yi X, Du R, Chen Z and Wang Q (2025) Scorpion venom peptides enhance immunity and survival in *Litopenaeus vannamei* through antibacterial action against *Vibrio parahaemolyticus*. *Front. Immunol.* 16:1551816. doi: 10.3389/fimmu.2025.1551816

Scorpion venom peptides enhance immunity and survival in *Litopenaeus vannamei* through antibacterial action against *Vibrio parahaemolyticus*

Ling Zeng[1], Yulin Sun[2], Hualin Zhang[1], Xiangxi Yi[3], Ran Du[3], Ziming Chen[1*] and Qi Wang[4*]

[1]School of Chemistry and Chemical Engineering, Lingnan Normal University, Zhanjiang, Guangdong, China, [2]Life Science & Technology School, Lingnan Normal University, Zhanjiang, Guangdong, China, [3]Guangxi Key Laboratory of Marine Drugs, Guangxi University of Chinese Medicine, Nanning, Guangxi, China, [4]Shenzhen Institute of Guangdong Ocean University, Guangdong Ocean University, Shenzhen, Guangdong, China

Introduction: Scorpion venom-derived antimicrobial peptides (AMPs) have emerged as promising candidates for combating bacterial infections owing to their potent activity and unique mechanisms of action. This study focuses on three 13-amino-acid peptides—BmKn1, BmKn2, and BmKn2-7—derived from the venom of *Mesobuthus martensii*. The aim is to elucidate their structural features, antibacterial efficacy, and immunomodulatory effects in *Litopenaeus vannamei* infected with *Vibrio parahaemolyticus* (VP).

Methods: The peptides were synthesized and comprehensively characterized for their amphipathic α-helical structures, net charges, and hydrophobicity. Their antibacterial mechanisms were investigated using a series of assays, including membrane permeability (inner/outer membrane disruption), membrane depolarization, reactive oxygen species (ROS) quantification, and ATPase activity measurement. In vivo challenge experiments were conducted to evaluate survival rates in L. vannamei infected with VP. Additionally, immune enzyme activities (phenoloxidase [PO], complement component 3 [C3]) and inflammatory/antimicrobial gene expression levels (TNF-α, IL-1β, TGF-β, ALF, Crus) were analyzed. Furthermore, intestinal transcriptome profiling was performed to identify the activated immune pathways.

Results: All peptides exhibited membrane-targeting activity: BmKn2-7 showed superior outer membrane penetration and depolarization, while BmKn1 was more effective in inner membrane disruption and ROS induction. In vivo, all peptides significantly improved survival rates in VP-infected shrimp ($P < 0.01$), with BmKn2-7 ≈ BmKn1 > BmKn2 in efficacy. Immune modulation was evident through increased PO and C3 activity ($P < 0.05$) and reduced expression of inflammatory cytokines and antimicrobial genes ($P < 0.05$). Transcriptome analysis revealed BmKn2-7 activated PPAR, AMPK, and FoxO signaling pathways.

Discussion: The amphipathic α-helical structure of these peptides is fundamental to their membrane-disruptive activity. The enhanced outer membrane targeting of BmKn2-7 likely correlates with structural modifications that optimize hydrophobicity and charge distribution. The differential efficacy in immune regulation, such as BmKn2-7's broad pathway activation versus BmKn1's selective ROS induction, indicates structure-dependent functional divergence. These findings highlight the potential of tailored scorpion venom peptides as dual-action agents against bacterial infections and immune dysregulation

KEYWORDS

scorpion venom peptide, BmKn1, *Litopenaeus vannamei*, immunity, *Vibrio parahaemolyticus*, antibacterial mechanism

1 Introduction

Litopenaeus vannamei is recognized as one of the most nutritionally and economically significant shrimp species in aquaculture (1). However, the intensification and industrialization of aquaculture practices have resulted in environmental degradation and an increased incidence of diseases among farmed animals, significantly impeding the growth of the shrimp aquaculture industry (2). Vibrio species are recognized as principal pathogens responsible for infectious disease outbreaks in shrimp aquaculture, leading to significant economic losses for farmers due to the elevated mortality rates in intensive culture systems (3–6). In response to these diseases, large amounts of antibiotics are frequently employed. This excessive reliance on antibiotics has not only facilitated the emergence of antibiotic-resistant pathogens but has also caused environmental damage and raised concerns about food safety. As a result, there is a growing interest in exploring natural and environmentally friendly treatment options to protect aquaculture (7).

Antimicrobial peptides (AMPs) demonstrate a wide range of bactericidal activities, effectively suppressing the growth of diverse microbial organisms, encompassing both gram-positive and gram-negative bacteria, protozoa, fungi, and enveloped viruses (8, 9). The positive charge characteristic of AMPs facilitates their binding to the negatively charged microbial membranes. AMPs disrupt the structural integrity of microbial organisms cell membranes, thereby hindering the development of drug resistance (10). Consequently, these peptides are regarded as a promising alternative to traditional antibiotics. AMPs not only exhibit significant antibacterial activity but also potentiate the host's immune response. The immunomodulatory properties of certain peptides have been effectively utilized in agricultural trials (11, 12), especially in aquaculture (13–15), yielding results that stimulate innate immune responses and significantly improve overall health. AMPs are anticipated to offer a sustainable, safe, and effective approach for preventing and controlling diseases in aquaculture. One such AMP derived from scorpion venom is BmKn2, which exhibits potent antimicrobial activity against both Gram-positive and Gram-negative bacteria due to its alpha-helical structure and C-terminal amidation. A chemically modified variant of BmKn2, BmKn2-7, has been shown to exhibit superior antibacterial activity compared to its precursor.

In our preliminary studies, we identified another peptide, BmKn1, from the venom of the scorpion *Buthus martensii*, which shares an 85% amino acid sequence similarity with BmKn2. However, the functional characterization of BmKn1 has yet to be elucidated. Previous studies indicate that BmKn2 exhibits more potent antimicrobial activity compared to IsCT, a peptide utilized in aquaculture to enhance the growth performance and intestinal immune function of juvenile grass carp (*Ctenopharyngodon idella*). However, the functions of BmKn2 in aquaculture species have not been thoroughly investigated. It remains to be determined whether BmKn2, BmKn2-7, and BmKn1 can similarly enhance the growth performance and intestinal immune function of aquaculture species, warranting further in-depth investigation. This study aims to investigate the effects of peptides BmKn1, BmKn2, and BmKn2-7 on antivibriosis mechanisms, as well as their impact on the growth performance and immune response of *L. vannamei*. The results are expected to provide valuable insights for enhancing the production of *L. vannamei* and improving disease resistance.

2 Materials and methods

2.1 Materials

Vibrio parahaemolyticus was purchased from Guangdong Microbial Culture Collection Centre (GDMCC). 2216E liquid medium was purchased from Qingdao Hope Bio-Technology Co., Ltd. Reactive Oxygen Species Assay Kit, N-phenylnaphthalen-1-amine (NPN), Propidium iodide (PI) and 3,3'-Dipropylthiadicarbocyanine iodide (DiSC3 (5)) were purchased from Shanghai Aladdin Biochemical Technology Co., Ltd. Alkaline phosphatase and adenosine triphosphatase were assayed using commercial kits (Nanjing Jiancheng Biological Engineering Institute, China).

2.2 Synthesis and characterization of peptides

The three peptides BmKn1, BmKn2 and BmK2-7 were synthesized with amidated C-termini by Sangon Biotech (Shanghai) Ltd., China. The purity (>98%) of three peptides utilized in the biological experiments was assessed using RP-HPLC at 220 nm. The analysis was conducted on a C18 column measuring 4.6 × 250 mm, with a flow rate of 1.0 mL min^{-1}. A water/acetonitrile gradient containing 0.1% trifluoroacetic acid was employed to ensure precise determination of peptide purity. The synthesized peptides were stored at a temperature of -80°C until further evaluations were conducted.

The hydrophobicity of the peptides and their hydrophobic moment (μH) values were determined using the HeliQuest analysis website, available at http://heliquest.ipmc.cnrs.fr/cgi-bin/ComputParams.py. Helical wheel projections were performed using the online tool Helical Wheel Projections, accessible at http://rzlab.ucr.edu/scripts/wheel/wheel.cgi. To predict the three-dimensional structure of the peptides, I-TASSER was employed from http://zhanglab.ccmb.med.umich.edu/I-TASSER/.

2.3 Antimicrobial mechanism

2.3.1 External membrane permeation test

The effects of BmKn1, BmKn2, and BmK2-7 on bacterial outer membrane permeability were assessed using a hydrophobic fluorescent probe. The VP strain was cultured in 2216E medium for 24 hours and subsequently centrifuged. The bacteria were washed with PBS and resuspended to an OD600 of 0.5. A final concentration of 40 μM NPN and 125 μg/mL of each of the three peptides were added to the bacterial suspension. Sterile PBS served as the control (CG). Following a 6-hour incubation at 37°C, the fluorescence intensity at 420 nm (excitation wavelength 350 nm) was measured using an MD SpectraMax i3x multifunctional enzyme labeller.

2.3.2 Inner membrane permeability test

The effect of BmKn1, BmKn2, and BmK2-7 on the permeability of the VP inner membrane were assessed by PI determination. Bacteria cultured for 24 hours were harvested by centrifugation, washed with PBS, and resuspended to an OD600 of 0.5. PI was added to achieve a final concentration of 40 μM, in conjunction with 125 μg/mL of each of the three peptides. PBS was used as the control group. Following a 6-hour incubation at 37°C, the fluorescence intensity at 617 nm (excitation wavelength of 535 nm) was quantified using an MD SpectraMax i3x multifunctional enzyme labeller.

2.3.3 Cytoplasmic membrane depolarization test

The depolarizing effects of BmKn1, BmKn2, and BmK2-7 on bacterial cytoplasmic membranes were assessed using the membrane potential-sensitive fluorescent dye DISC3 (5). Bacterial cultures, grown for 24 hours, were harvested via centrifugation, washed with PBS, and resuspended to an optical density (OD600) of 0.5. Subsequently, the bacterial suspension was incubated with a final concentration of 20 μM DISC3 (5) dye for 10 hours at 37°C in the dark. The three peptides (125 μg/mL) were subsequently added to the mixture, with sterile PBS used as the control. Following a 6-hour incubation period at 37°C, the fluorescence intensity at 670 nm (excitation wavelength 622 nm) was quantified using an MD SpectraMax i3x multifunctional enzyme labeller.

2.3.4 Measurement of reactive oxygen species

Bacterial intracellular ROS levels were quantified using a ROS assay kit. The VP culture was incubated for 24 hours, after which the cells were harvested by centrifugation, washed with PBS, and resuspended to an optical density (OD600) of 0.5. Equal volumes of the bacterial suspension and the three peptide solutions (125 μg/mL each) were combined and incubated at 37°C for 10 hours. A final concentration of 10 μM DCFH-DA solution was then added. Sterile PBS served as the control group. Following a 6-hour incubation at 37°C, the fluorescence intensity at 525 nm (excitation wavelength 488 nm) was measured using an MD SpectraMax i3x multifunctional enzyme labeller.

2.3.5 Alkaline phosphatase test

The VP was incubated for 24 hours, followed by centrifugation to collect the organisms, which were then washed with PBS and resuspended to an OD600 of 0.5. Subsequently, the three peptides were added sequentially, each at a final concentration of 62.5 μg/mL. A sterile PBS solution served as the control group. The samples were then incubated at 37°C for 10 hours, after which alkaline phosphatase activity was measured according to the kit instructions.

2.3.6 Adenosine triphosphatase activity test

The VP was incubated for 24 hours, followed by centrifugation to collect the organisms. The collected organisms were washed with PBS and resuspended to an OD600 of 0.5. The three peptides were then added sequentially, each achieving a final concentration of 62.5 μg/mL. A sterile PBS solution served as the control group. The samples were then incubated at 37°C for 6 hours, after which adenosine triphosphatase activity was measured according to the kit instructions.

2.4 Challenge test

The challenge test for *L. vannamei* was conducted at the Marine Biology Research Base of Guangdong Ocean University in Zhanjiang, China. The *L. vannamei* specimens were sourced from Zhanjiang Hisenor Marine Biotechnology Co., Ltd., also located in Zhanjiang, China. VP for the challenge test was obtained from the Guangdong Microbial Culture Collection Centre (GDMCC 1.306). The strain was cultured in 2216E liquid medium at 37°C for 24 hours, followed by centrifugation. According to the preliminary experiment results, the centrifuged bacterial suspension was adjusted to a concentration of 5 × 106 CFU/ml using PBS. Additionally, the three peptides were prepared in PBS at a concentration of 125 μg/mL (use it right after it was ready). The challenge test was divided into five groups, each with three replicates, and each replicate comprised 30 shrimp (7.00 ± 0.50g). In the control group (CG), each shrimp received an injection of 100

μL of sterile physiological saline. In the negative control group (VA), each shrimp was first injected with 50 μL of VP, followed by an injection of 50 μL of sterile physiological saline 2 hours later. The experimental groups (Bmkn1, Bmkn2, and Bmkn2-7) were injected with three different types of scorpion venom peptides, respectively. Specifically, each shrimp was first injected with 50uL of VP, and then 2h later an equal volume of scorpion venom peptide was injected separately. The mortality rate was recorded every 24 hours post-injection, and the challenge test continued for 7 days.

2.4.1 Immune response of *L. vannamei*

At the end of the challenge test, three shrimp hepatopancreases were randomly selected from each replicate and stored at -80°C for enzyme activity analysis. Additionally, three shrimp hepatopancreases were collected from each replicate and preserved in 1.5 mL RNA Later solution in enzyme-free centrifuge tubes for gene expression analysis. The levels of hepatopancreatic phenoloxidase (PO, H247-1-2), malondialdehyde (MDA, A003-1-2), lysozyme (LZM, A050-1-1), complement 3 (C3, H186-1-2), and complement 4 (C4, H186-2-2) were measured following the protocols provided by commercial kits (Nanjing Jiancheng Biological Engineering Institute, China).

The total RNA from the samples was extracted using an RNA extraction kit (Hunan Aikeri Biological Engineering Co., Ltd., Hunan, China). The RNA concentration was quantified using a Nanodrop2000 nucleic acid protein analyzer (Thermo Scientific), and the quality was evaluated by 1% agarose gel electrophoresis. RNA was reverse transcribed into cDNA using the Evo M-MLV RT Kit with gDNA Clean for qPCR II (Hunan Aikeri Biological Engineering Co., Ltd., Hunan, China). The primers listed in Table 1 were synthesized by Shanghai Sangon Biotech Co., Ltd. Qualitative analysis of the cDNA was conducted using a SYBR reagent kit (Hunan Aikeri Biological Engineering Co., Ltd.). A 10 μL reaction mixture was prepared, consisting of 5 μL SYBR® Green Pro Taq HS, 1 μL cDNA, 0.5 μL of each primer (forward and reverse), and 3 μL nuclease-free water. The reaction was performed on a quantitative thermal cycler under the following conditions: initial denaturation at

TABLE 1 Primers used in this experiment for quantitative RT-PCR.

Genes	Forward (5′-3′)	Reverse (5′-3′)	GenBank no.
β-actin	TGGACTTCGAGCAGGAGATG	GGAATGAGGGCTGGAACAGG	XM_027364954.1
TNF-α	CTCAGCCATCTCCTTCTTG	TGTTCTCCTCGTTCTTCAC	XM_027368774.1
IL-1β	TGTGACCACCATCCACCAGAAC	GATCCCGCAGTAACCGAATAAG	Designed by author
TGF-β	GAAGCAATAAACCAAAGCGA	CAAAAGCCAACAGGGAAAA	XM_027378574.1
ALF	CGCTTCACCGTCAAACCTTAC	GCCACCGCTTAGCATCTTGTT	KJ000049
Pen-3	ATACCCAGGCCACCACCCTT	TGACAGCAACGCCCTAACC	Y14926
Crus	GGTGTTGGTGGTGGTTTCCC	CGAGGCCAGCACACTTGTAG	AY486426
Cyt-c	AGGGAAAGAAGCTGTTCGTG	CAGTCGCTTGTGCCAGTTCC	KF601549.1
Bax	GGTGGAATCACAAGAGAGCGA	TGTTCTCCACGGTGTCTCAC	XM_027383277.1
Bcl-2	CCTTGCTTGACACAGTCGGA	CAGACAAGGTCGTGAGGTGG	XM_070143368.1
Caspase3	ACATTTCTGGGCGGAACACC	GTGACACCCGTGCTTGTACA	KC660103.1
Caspase8	CACGGAAGCTCTCCCTACAG	GAAGACCTTGGGTTTCCCCC	Designed by author
P53	CGAATCCCCACATCCACG	GGCGGCTGATACACCACC	KX179650.1
Apod	TCTTAACTGCTGCCCTCGTG	AAAGCTGTTGGAGAGAAGGGG	Primer design based on RNA-seq gene fragments.
4CL1	TGCATGTGGTGCTGTATATTGT	CGCTCGTGCTGATGTCCTAT	
tpi1b	CAAGGTCAGCCTCTTCCTCA	ACTTCATCTGGCCGAACAGG	
GNBP1	CAGCTCAGCTAACCAAGGCT	GGCTCGTCAGGAATTGGGAA	
RBBP6	GTGCGACCTCTGTTGTCTGA	ACTATTCCCCCTGAGTGGTCA	
Hirip3	TCAACGTCCCTCTGCTTTCA	CTCATCATGCGCCTTCTTGC	
PLAT	GTGGAGAAGAACGGCGACAT	CCTGTAACGAGTTGCCAGGT	
SPE	GCTGGTTAACGGACAGGTGA	CGGAGGTTGACGTCGTGATA	
lbp-6	AGAGAGGGAATGACAGTGCG	ATGGCGGCTATGCTCTTACG	
PCK2	GCTTCACCACAGACGCAAAG	CCTCCACATCACTTACCTTCAGA	
nas-4	TGACATCGGCCTCAGAATCG	TGTCAATGACTGCCCACGAA	
SLC5A6	CTATGACGGCGCTACTCTGG	CCCTCCACATCACTTACCTTC	

95°C for 30 seconds; 40 cycles of denaturation at 95°C for 5 seconds, annealing at 60°C for 30 seconds; and a final melt curve analysis at 95°C, followed by cooling to 4°C. The relative gene expression levels were determined using the $2^{-\Delta\Delta CT}$ method.

2.4.2 Transcriptome sequencing

The transcriptomes of the intestines of *Litopenaeus vannamei* were sequenced in this study for the CG, VP, and BmK2-7 groups. At the end of the challenge test, intestines from three randomly selected shrimp from each replicate were collected and placed in 1.5 mL enzyme-free centrifuge tubes containing RNA Later for transcriptome sequencing. The experimental procedure is as follows: mRNA was enriched using mRNA Capture Beads, and after bead-based purification, the mRNA was fragmented at high temperatures. The fragmented mRNA served as the template for synthesizing the first-strand cDNA in a reverse transcriptase reaction system. During the synthesis of the second-strand cDNA, end repair and A-tailing were simultaneously performed. Subsequently, adapters were ligated, and target fragments were purified and selected using Hieff NGS® DNA Selection Beads. Finally, PCR amplification was carried out to construct the sequencing library, which was analyzed using the Illumina NovaSeq X Plus platform. The sequenced data underwent quality control, sequence alignment analysis, and gene analysis. Principal Component Analysis (PCA) was performed using R (http://www.r-project.org/) to investigate the distance relationships between samples through dimensionality reduction. The input data for differential gene expression analysis were the read count data obtained from gene expression level analysis. EdgeR software was used for analysis, including GO and KEGG enrichment analysis. In this study, 12 DEGs were randomly selected for RT-qPCR to validate the results of RNA sequencing. The validation procedure was performed as described in section 2.4.1. For detailed procedures of transcriptome sequencing, refer to Supplementary Material 1.

2.5 Statistical analysis

The experimental data were presented as the mean ± standard error of the mean (Mean ± SEM) and were statistically analyzed using SPSS 23.0 software. One-way analysis of variance (ANOVA) was conducted, followed by Duncan's multiple range test for *post-hoc* comparisons.

3 Results

3.1 Peptide characterization

BmKn1, BmKn2, and BmKn2-7, each comprising 13 amino acids and derived from scorpion venom, display similar sequences. The 3D structure of BmKn1, BmKn2 and BmKn2-7 were predicted by software I-TASSER, as illustrated in Figure 1A. Structural

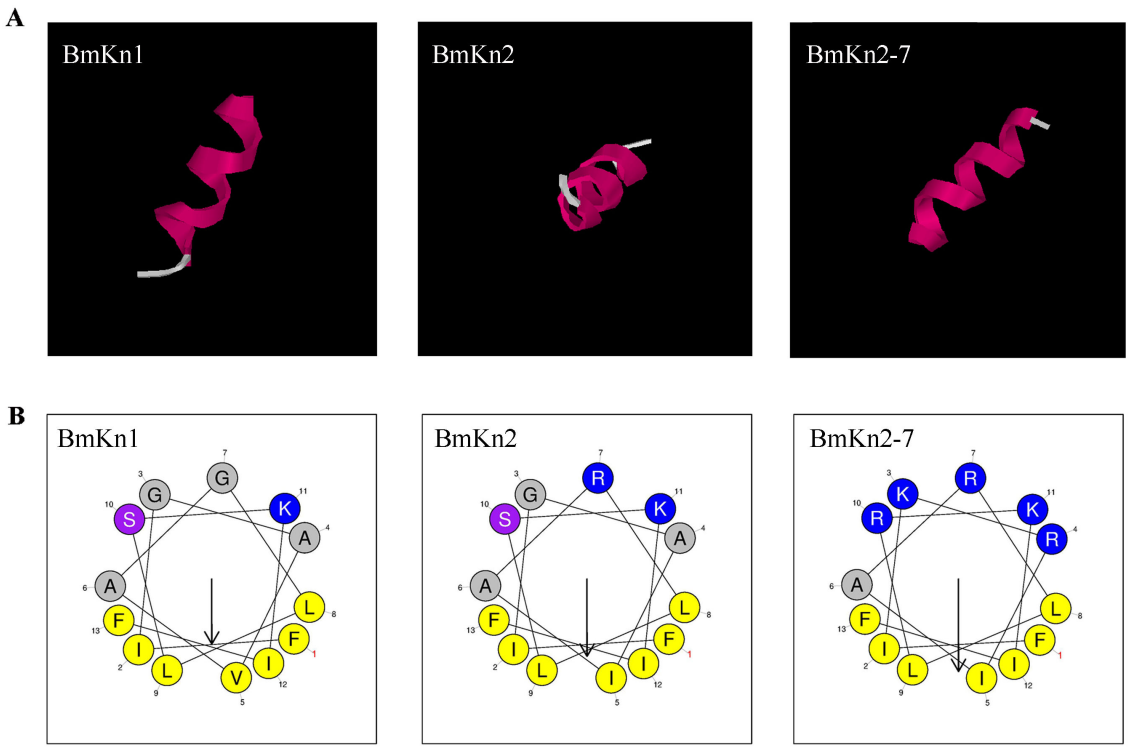

FIGURE 1
The structure of BmKn1, BmKn2 and BmKn2-7. **(A)** The prediction of three-dimensional structures of peptides utilizing I-TASSER. **(B)** Helical wheel projections of the three peptides. Alkaline amino acids, characterized by their positively charged residues, are highlighted in blue, whereas hydrophobic residues are illustrated in yellow.

predictions suggest that all the three peptides exhibit amphipathic alpha-helical conformations. Their net charges are +2, +3, and +6, respectively. In terms of hydrophobic moments, BmKn1 has the lowest value, BmKn2 has an intermediate value, and BmKn2-7 has the highest value (Table 2). The composition of amino acids is illustrated in Figure 1B. Helical wheel analysis has demonstrated that the arrangement of amino acids within the sequences constitutes an amphipathic structure, distinguished by two distinct regions: one side of the helix is primarily hydrophobic, comprising hydrophobic residues, whereas the opposing side is hydrophilic, featuring a concentration of charged amino acids. By comparing BmKn1 with BmKn2 and BmKn2-7, it was observed that BmKn1 exhibits identical hydrophilic regions on one side of its helical structure, similar to those of BmKn2 and BmKn2-7. However, on the opposite side, BmKn1 displays a decreased charge density relative to BmKn2 and BmKn2-7, indicating a lesser degree of amphipathicity.

3.2 Antimicrobial mechanisms

3.2.1 External membrane permeation test

The permeabilization of the outer membrane in VP after treatment with the three peptides was evaluated by monitoring the uptake of the fluorescent dye NPN, using an excitation wavelength of 350 nm and an emission wavelength of 420 nm. A significant increase in NPN fluorescence intensity was observed following the addition of the peptides (Figure 2A), suggesting that the peptides had compromised the integrity of the outer membranes. Upon comparing the fluorescence intensity of the three peptides, it was found that BmKn2-7 exhibits a higher value than both BmKn1 and BmKn2, with BmKn1 surpassing BmKn2. These results indicate that among the three peptides, BmKn2-7 possesses the strongest penetration capability, followed by BmKn1, while BmKn2 demonstrates the weakest penetration capability.

3.2.2 Inner membrane permeability test

An extended analysis was conducted utilizing PI staining to assess the integrity of bacterial inner membranes. The fluorescence intensity observed in the experimental groups treated with the three peptides showed a significant increase, indicating compromised bacterial inner membranes post-peptide treatment (Figure 2B). Notably, among these groups, BmKn1 exhibited the most pronounced effect, with its fluorescence level being twice that of the control group. BmKn2-7 demonstrated a less pronounced yet still significant impact, whereas BmKn2 had the least effect, thus establishing the relative efficacy in disrupting the inner membrane as follows: BmKn1 > BmKn2-7 > BmKn2.

3.2.3 Cytoplasmic membrane depolarisation test

To assess the effects of BmKn1, BmKn2, and BmKn2-7 on the cytoplasmic membrane of VP, the membrane potential-sensitive fluorescent dye diSC3 (5) was employed. Compared to the control group, the introduction of these peptides resulted in a significant increase in fluorescence intensity (Figure 2C), with the intensity surpassing that of the control by more than 100%. In the DiSC3 (5) assay, BmKn2 exhibited relatively diminished depolarizing activity on the bacterial cytoplasmic membrane compared to BmKn1 and BmKn2-7. Notably, BmKn2-7 achieved the highest fluorescence intensity, approximately tripling that of the control. Therefore, the depolarizing capabilities of the three peptides can be ranked as follows: BmKn2-7 > BmKn1 > BmKn2.

TABLE 2 The sequences, charges, hydrophobicity and hydrophobic moments of the three peptides.

peptides	sequences	Net Charge	H	μH	Similarty
BmKn1	FIGAVAGLLSKIF-NH_2	+2	0.876	0.639	100%
BmKn2	FIGAIARLLSKIF-NH_2	+3	0.843	0.760	85%
BmKn2-7	FIKRIARLLRKIF-NH_2	+6	0.591	0.908	62%

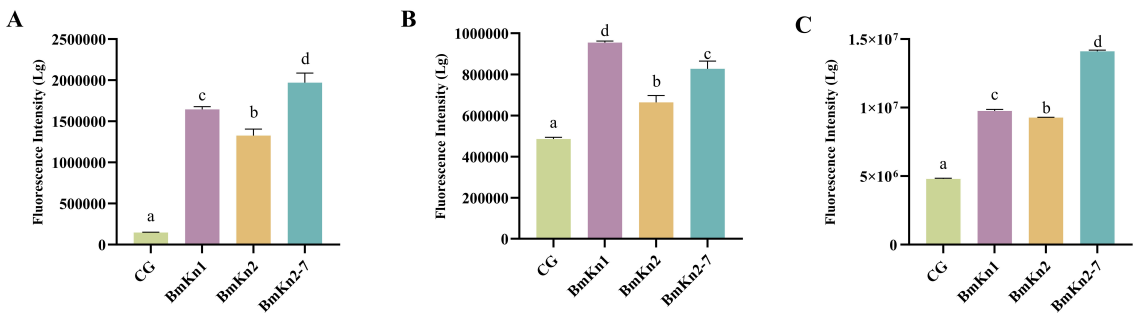

FIGURE 2
(A) Analysis of the external membrane permeability of VP in BmKn1, BmKn2, and BmKn2-7. **(B)** Analysis of inner membrane permeability of VP in BmKn1, BmKn2, and BmKn2-7. **(C)** Analysis of cytoplasmic membrane depolarization of VP in BmKn1, BmKn2, and BmKn2-7. Data was presented as mean ± SEM (n = 3). There were significant differences in the representation of different letters on the histogram (P <0.05).

3.2.4 Determination of ROS

ROS are increasingly recognized for their critical role in bacterial responses to lethal stress. To assess the impact of BmKn1, BmKn2, and BmKn2-7 on intracellular ROS levels, the fluorescence intensity of DCFH-DA within the VP was utilized as an analytical indicator. Following the treatment of the three peptides, a significant elevation in ROS levels in the bacterial was observed, with levels increasing by at least 2.5-fold compared to the control group (Figure 3A). Notably, there were marked differences among the three experimental groups. Specifically, the ROS level induced by BmKn1 was more than three times higher than that of BmKn2, while the ROS level elicited by BmKn2-7 was over two times greater than that of BmKn2. These results suggest that all three peptides effectively induce a substantial increase in ROS levels in VP, with the order of efficacy being BmKn1 > BmKn2-7 > BmKn2.

3.2.5 Alkaline phosphatase test

The impact of BmKn1, BmKn2, and BmKn2-7 on the enzymatic activity of VP alkaline phosphatase was evaluated. The findings indicated that the alkaline phosphatase activity in the experimental groups treated with BmKn1 and BmKn2 was marginally elevated compared to the control group; however, this increase was not statistically significant. Conversely, the alkaline phosphatase activity in the bacterial samples treated with BmKn2-7 demonstrated a substantial enhancement (Figure 3B). Following treatment with these three peptides, the relative alkaline phosphatase activities of VP were ranked in the following order: BmKn2-7 > BmKn1 > BmKn2.

3.2.6 Adenosine triphosphatase activity test

To evaluate the impact of BmKn1, BmKn2, and BmKn2-7 on bacterial energy metabolism, the cellular ATPase activity activity of VP was assessed. The results indicated that there were no significant differences among the three peptides; however, they markedly reduced the cellular ATPase activity in VP by approximately 25% compared to the control (Figure 3C). These findings indicate that BmKn1, BmKn2, and BmKn2-7 can influence the energy metabolism of VP by decreasing ATPase activity.

3.3 Challenge test

The challenge test results for *L. vannamei* are presented in Figure 4. No mortality was observed in the control group (CG). The cumulative survival rate of the VP group was significantly lower than that of all other groups ($P < 0.05$). Among the three peptide injection groups, no significant differences in cumulative survival rates were observed ($P > 0.05$); however, their survival rates were significantly lower than that of the CG ($P < 0.05$). Specifically, the survival rates among the peptide groups followed this order: BmKn2-7 > BmKn1 > BmKn2.

3.3.1 Hepatopancreatic immune enzyme analysis

Hepatopancreatic immune enzyme activities in different treatment groups following challenge testing are summarized in Table 3. The VP group demonstrated significantly lower PO activity compared to the other groups ($P < 0.05$). LZM activity was lowest in the BmKn1 group and highest in the CG group ($P < 0.05$). C3 content was lowest in the VP group, while C4 content in the peptide supplementation groups was significantly lower than that in both the CG and VP groups ($P < 0.05$).

3.3.2 Hepatopancreatic immunity-related gene expression

The relative expression levels of *TNF-α* and *ALF* genes in the VP group were significantly higher than those in the other groups ($P < 0.05$; Table 4). Conversely, the relative expression of *IL-1*β gene was significantly lower in the BmKn1 and BmKn2-7 groups than in the other groups ($P < 0.05$). Additionally, the relative expression level of the *TGF-β* and *Bal-2* genes of CG was significantly higher than that in the VP and the three peptides injection groups ($P < 0.05$). There was no significant difference in the relative expression of *Cyt-c* gene between the groups ($P > 0.05$). Notably, the VP group

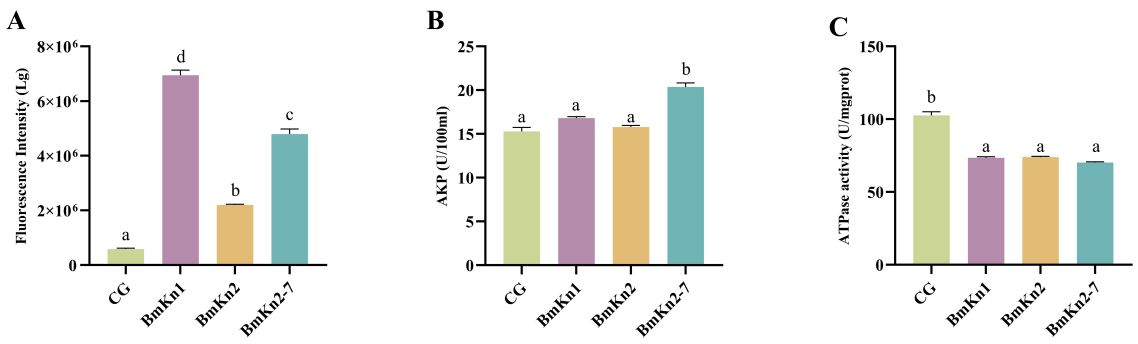

FIGURE 3
(A) Analysis of ROS of VP in BmKn1, BmKn2, and BmKn2-7. **(B)** Analysis of alkaline phosphatase activity of VP in BmKn1, BmKn2, and BmKn2-7 Variants. **(C)** Analysis of the ATPase activity of VP in BmKn1, BmKn2, and BmKn2-7. Data was presented as mean ± SEM (n = 3). There were significant differences in the representation of different letters on the histogram ($P < 0.05$).

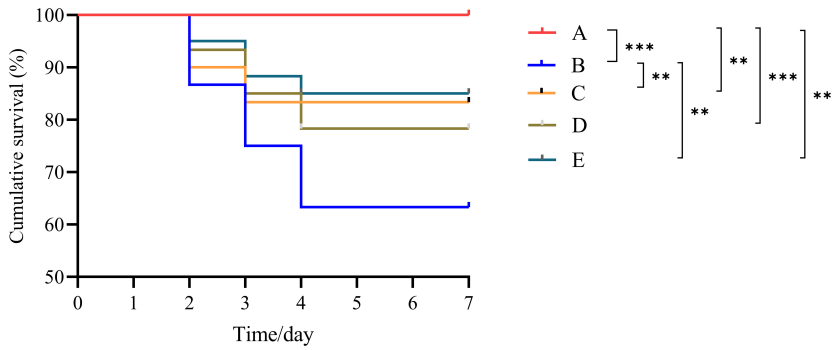

FIGURE 4
Cumulative survival of *L. vannamei* after challenge testing. ** indicates $P < 0.01$; *** indicates $P < 0.001$. A: CG; B: VP; C: BmKn1; D: BmKn2; E: BmKn2-7.

exhibited the highest relative expression level of the Crus gene ($P < 0.05$). In contrast, the Pen-3 gene showed the lowest relative expression in the VP group, which significantly increased following peptide injection ($P < 0.05$). Furthermore, the relative expression of *Bax* gene in the peptide injection groups was significantly lower than that in the CG and VP groups ($P < 0.05$). Lastly, the relative expression levels of *Caspase3*, *Caspase8*, and *P53* genes were higher in the VP group compared to the peptide injection groups ($P < 0.05$).

3.3.3 Transcriptome sequencing

The PCA analysis revealed that the CG, VP, and BmKn2-7 sample groups exhibit high levels of dispersion, indicating significant differences among the three groups (Figure 5A). The visualization of gene abundances across the three groups is shown in Figure 5B. The gene expression abundance in the VP and BmKn1 groups was slightly lower than that in the CG group. Further analysis was conducted to investigate the differences among various comparison groups. The scatter plot of multiple group differences is shown in Figure 6A. In the CG-vs-VP comparison group, 320 differentially expressed genes (DEGs) were upregulated, while 804 DEGs were downregulated. In the CG-vs-BmKn2-7 comparison group, 239 DEGs were upregulated, and 1711 DEGs were downregulated. In the VP-vs-BmKn2-7 comparison group, 310 DEGs were upregulated, and 382 DEGs were downregulated. The differences between comparison groups are visualized using upset plots, as shown in Figure 6B. The numbers of uniquely DEGs in the three comparison groups were 1324 (CG-vs-BmKn2-7), 550 (CG-vs-VP), and 205 (VP-vs-BmKn2-7), respectively.

The GO enrichment analysis (top 20) of DEGs across different comparison groups is shown in Figure 7. In the CG-vs-VP comparison group (Figure 7A), the significantly enriched GO terms are predominantly related to immune responses, such as evasion or tolerance of host defense response, evasion or tolerance of defense response of other organism involved in symbiotic interaction, avoidance of host defenses, and avoidance of defenses of other organism involved in symbiotic interaction. Moreover, the DEGs annotated under these terms were all significantly downregulated. Similarly, the DEGs annotated under other GO terms were mostly significantly downregulated. And these DEGs are mainly *Apod* and *tpi1b*. Furthermore, it was found that most DEGs annotated to the term oxidoreductase activity were downregulated. In the CG-vs-BmKn2-7 comparison group, 16 of the top 20 GO terms were categorized under molecular function. GO terms with a higher number of annotated DEGs included binding, protein binding, organic cyclic compound binding, and heterocyclic compound binding (Figure 7B). In the VP-vs-BmKn2-7 comparison group, differential expression genes annotated with all terms, except for chitin binding, were significantly upregulated. The two most significantly enriched GO terms were galactosylceramide sulfotransferase activity and galactose 3-O-sulfotransferase activity. In addition, it was observed that the GO terms related to the PPAR signaling pathway, namely Positive regulation of peroxisome proliferator-activated receptor (PPAR)

TABLE 3 Hepatopancreatic immune enzyme activity in different treatment groups after challenge testing.

Items	Treatment				
	CG	VP	BmKn1	BmKn2	BmKn2-7
PO (U/ml)	25.47+1.83^{b}	21.34+1.15^{a}	27.25+1.51^{b}	26.15+0.69^{b}	28.32+1.07^{b}
LZM (U/L)	7.41+0.24^{c}	5.23+0.09^{b}	4.41+0.24^{a}	5.32+0.27^{b}	5.25+0.19^{b}
C3 (μg/mL)	159.26+6.27^{c}	79.08+2.35^{a}	103.49+6.65^{b}	103.40+4.67^{b}	109.27+3.04^{b}
C4 (μg/mL)	176.13+4.23^{b}	208.88+2.45^{c}	144.21+6.55^{a}	141.29+5.62^{a}	154.29+3.24^{a}

Data was presented as mean ± SEM (n = 3). Different superscript letters represent significant differences ($P<0.05$).

10.3389/fimmu.2025.1551816

TABLE 4 Relative expression of hepatopancreatic immunity genes in different treatment groups after challenge testing.

Items	Treatment				
	CG	VP	BmKn1	BmKn2	BmKn2-7
TNF-α	1.01+0.08^{a}	1.54+0.06^{b}	0.91+0.08^{a}	0.92+0.11^{a}	0.85+0.15^{a}
IL-1β	1.00+0.03^{c}	1.03+0.02^{c}	0.64+0.01^{a}	0.80+0.03^{b}	0.63+0.04^{a}
TGF-β	1.00+0.04^{d}	0.65+0.05^{bc}	0.46+0.04^{a}	0.72+0.06^{c}	0.51+0.08^{ab}
ALF	1.01+0.02^{a}	2.95+0.09^{b}	0.95+0.07^{a}	0.98+0.05^{a}	0.99+0.03^{a}
Cyt-c	1.00+0.03^{a}	1.38+0.12^{a}	1.21+0.20^{a}	1.19+0.14^{a}	1.07+0.06^{a}
Crus	1.01+0.08^{a}	1.89+0.08^{c}	1.26+0.06^{b}	1.44+0.03^{b}	1.25+0.10^{b}
Pen-3	1.00+0.03^{d}	0.29+0.00^{a}	0.54+0.02^{b}	0.62+0.03^{b}	0.82+0.04^{c}
Bax	1.00+0.05^{c}	1.01+0.04^{c}	0.54+0.03^{ab}	0.73+0.12^{b}	0.41+0.05^{a}
Bcl-2	1.01+0.10^{b}	0.57+0.02^{a}	0.72+0.03^{a}	0.62+0.08^{a}	0.63+0.02^{a}
Caspase3	1.00+0.00^{b}	1.84+0.09^{c}	0.72+0.03^{a}	0.73+0.07^{a}	0.64+0.03^{a}
Caspase8	1.00+0.04^{b}	0.85+0.06^{ab}	0.70+0.07^{a}	0.74+0.06^{a}	0.67+0.02^{a}
P53	1.03+0.05^{b}	1.29+0.02^{c}	0.79+0.09^{a}	0.72+0.05^{a}	0.75+0.05^{a}

Data was presented as mean ± SEM (n = 3). Different superscript letters represent significant differences (P<0.05).

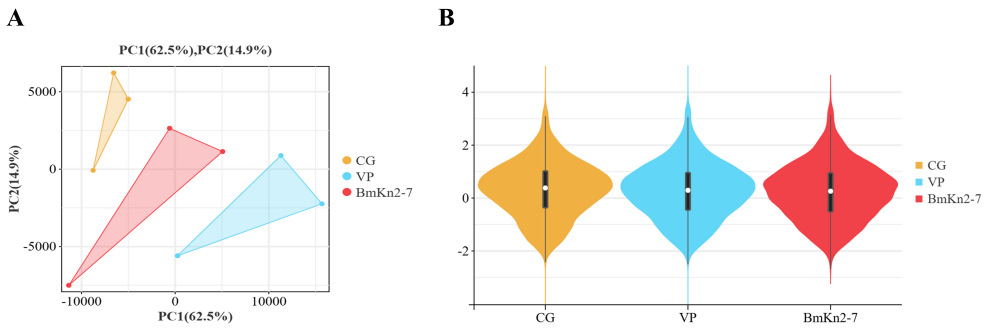

FIGURE 5
The relationship among transcriptome samples from the intestines of *Litopenaeus vannamei*. **(A)** PCA analysis of samples. **(B)** Violin plots of different groups.

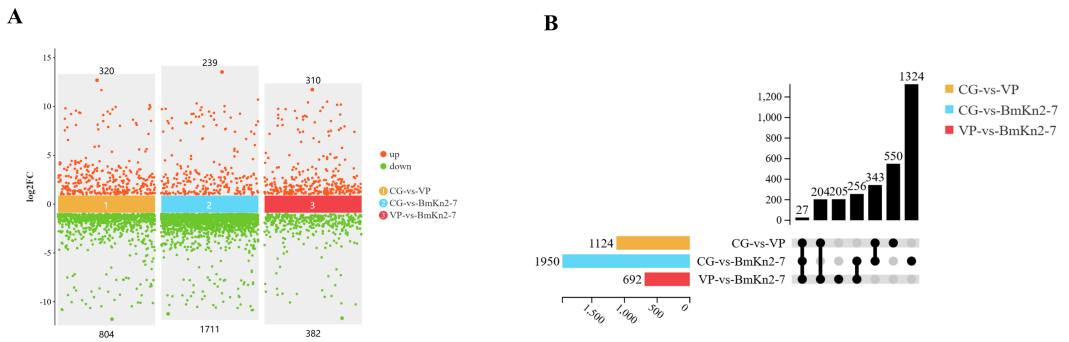

FIGURE 6
Differential analysis of the intestinal transcriptome of *Litopenaeus vannamei*. **(A)** Scatter plot of multiple group differences (P < 0.05, Fold change > 2). **(B)** Upset plot (P < 0.05, Fold change > 2).

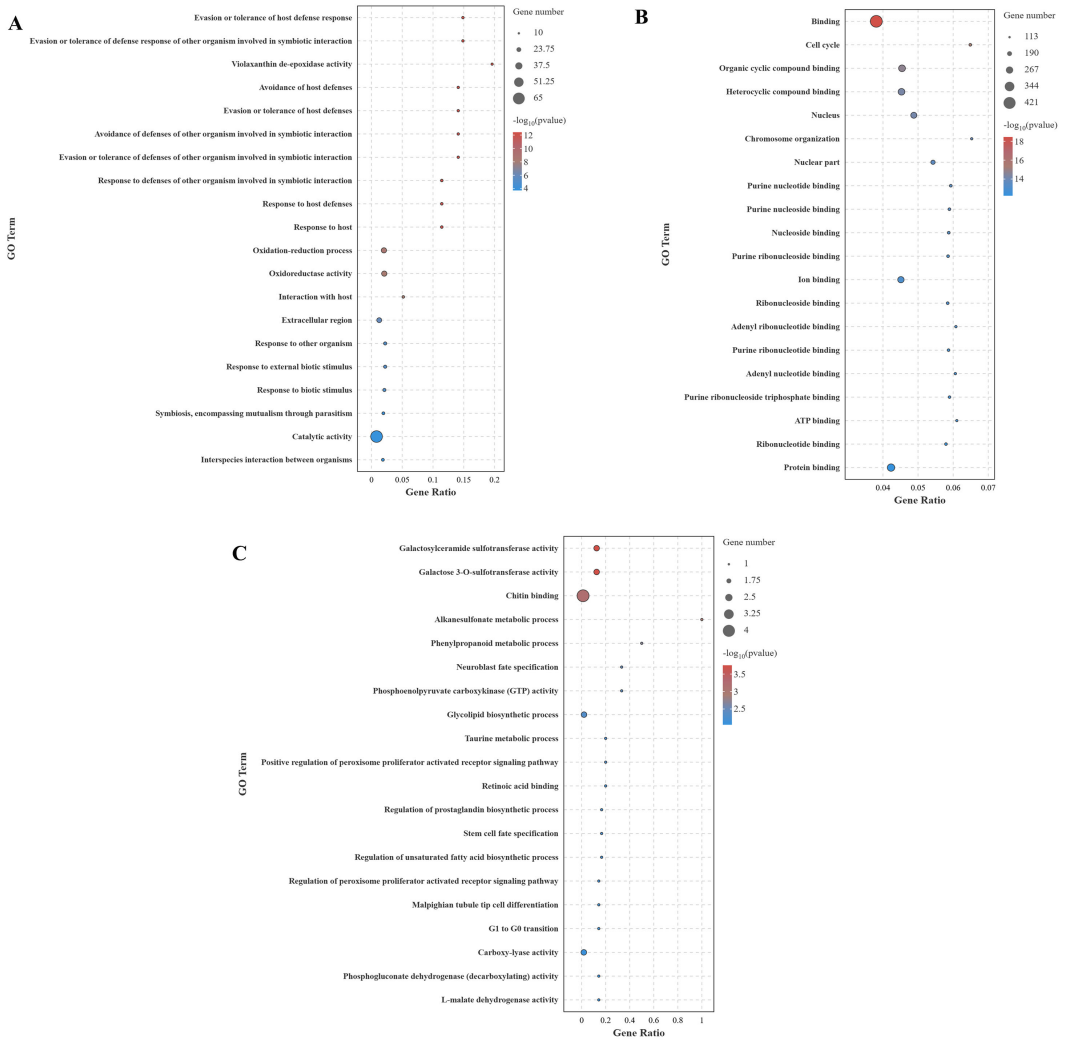

FIGURE 7
GO enrichment analysis of DEGs across different comparison groups (Top 20). **(A)** CG-vs-VP; **(B)** CG-vs-BmKn2-7; **(C)** VP-vs-BmKn2-7.

signaling pathway and Regulation of peroxisome proliferator-activated receptor signaling pathway, were significantly upregulated. The detailed information on the GO enrichment analysis of the three comparison groups is provided in Supplementary Materials 2.

The KEGG enrichment analysis (top 20) of DEGs across different comparison groups is shown in Figure 8. In the CG-vs-VP comparison group, the largest number of DEGs were annotated to the Metabolic pathway, followed by Amino sugar and nucleotide sugar metabolism and Glutathione metabolism (Figure 8A). In addition, immune-related pathways were found to be significantly enriched, such as Influenza A, Antigen processing and presentation, and Hematopoietic cell lineage. In the CG-vs-BmKn2-7 comparison group, the largest number of DEGs was annotated to the Endocytosis pathway, followed by the MAPK signaling pathway, and Regulation of actin cytoskeleton (Figure 8B). In the VP-vs-BmKn2-7 comparison group (Figure 8C), Proximal tubule bicarbonate reclamation was the most significantly enriched, followed by the Adipocytokine signaling pathway and the Citrate cycle (TCA cycle). In addition, immune-related pathways were also significantly enriched, such as the PPAR signaling pathway, FoxO signaling pathway, and AMPK signaling pathway. Interestingly, the number of genes annotated to these pathways was limited to just one, with the key genes being *PCK2*. The detailed information on the KEGG enrichment analysis of the three comparison groups is provided in Supplementary Materials 3.

The RT-qPCR results for the 12 randomly selected DEGs are shown in Figure 9. The expression levels of all 12 DEGs were consistent with the RNA-seq results, demonstrating the reliability of the RNA-seq data.

4 Discussion

The peptide BmKn1 was identified in the venom in our previous research (16), and its structure and function remains to be elucidated. BmKn1 shares a remarkably high homology (85%) with BmKn2. Both peptides originate from the venom of

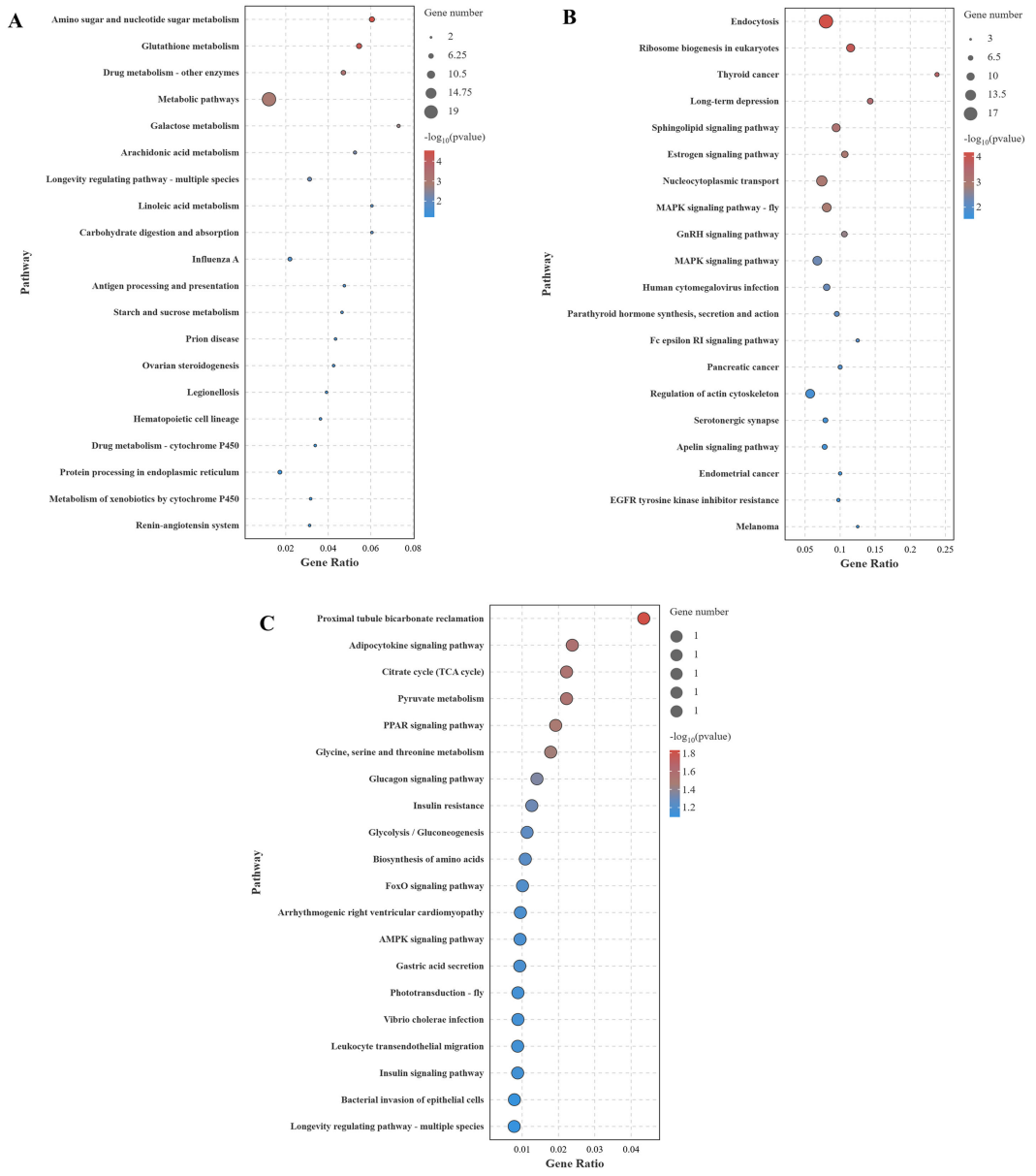

FIGURE 8
KEGG enrichment analysis of DEGs across different comparison groups (Top 20). **(A)** CG-vs-VP; **(B)** CG-vs-BmKn2-7; **(C)** VP-vs-BmKn2-7.

Mesobuthus martensii, have an identical length of 13 amino acids, and exhibit a high degree of sequence similarity, differing only at the fifth and seventh positions. The BmKn2-7 variant was developed from BmKn2 by enhancing the overall positive charge (17). The C-termini of all the three peptides have been amidated. Amidation of peptides is crucial for both their biological functions and resistance to exopeptidase degradation (18). Generally, C-terminally amidated peptides demonstrate enhanced structural stability and increased activity compared to their non-amidated counterparts (19). Secondary structure prediction by previoused research showed that BmKn2 contains one alpha-helix domain, and two flexible random coiled regions at both terminus (20). Our predicted results align with the aforementioned findings. Previous research on secondary structure prediction has demonstrated that BmKn-2 comprises one alpha-helix domain and two flexible random coil regions at its termini (20). Our predicted results align with this earlier finding. The secondary structures of the peptides BmKn1, BmKn2, and BmKn-7 display a high degree of similarity, characterized by the presence of a singular alpha-helical domain. Each peptide exhibits distinct hydrophobic and hydrophilic regions, which confer a pronounced amphipathic nature to their molecular structure.

The antimicrobial experiments demonstrated that BmKn1, BmKn2, and BmKn2-7 can eliminate bacteria through multiple mechanisms, including increasing the permeability of both inner and outer membranes, inducing cell membrane depolarization, elevating ROS levels, and reducing ATPase activity. These mechanisms collectively disrupt bacterial physiological functions.

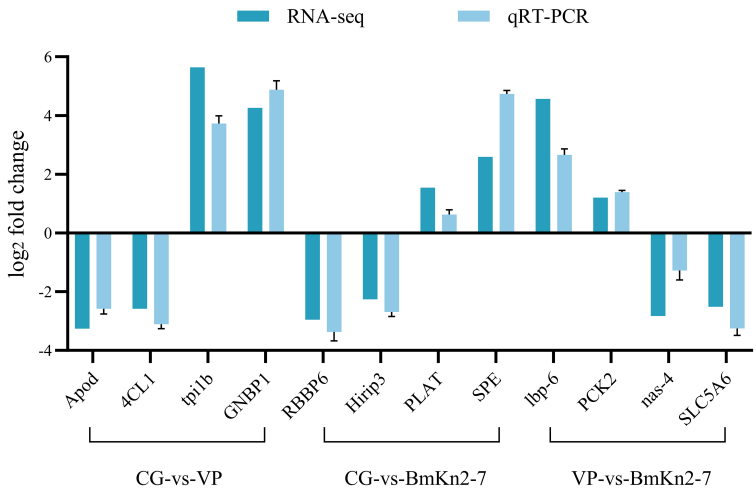

FIGURE 9
Validation of selected DEGs by qPCR.

Notably, the antibacterial activities of these peptides exhibit significant variation, which can be attributed to their structural differences.

Charge and hydrophobicity are regarded as the primary physicochemical attributes that influence the biological activity of membrane-active peptides (21–23). Hydrophobicity governs the capacity of AMPs to partition into the lipid bilayer of microbial membranes. Positively charged AMPs will generate electrostatic attraction with the negatively charged components of the bacterial membranes. Enhancing the overall positive charge of AMPs can further strengthen this interaction (24). Research by Ringstad et al. (25) demonstrated that the capacity of peptides to compromise microbial membranes enhances as their net charge or hydrophobicity increase. This finding explains why BmKn1 exhibits superior external membrane penetration ability compared to BmKn2 in this study, as BmKn1 has a higher hydrophobicity (0.876 vs. 0.843). Additionally, BmKn2-7, which carries six positive charges, demonstrates the strongest external membrane penetration among the three peptides due to its higher number of positive charges compared to BmKn1 (two positive charges) and BmKn2 (three positive charges). However, our findings indicate that characterizing peptides solely by their hydrophobicity or charge is inadequate to fully elucidate their capacity to penetrate biological membranes. For instance, in this study, the hydrophobicity of the three peptides was ranked as BmKn1 > BmKn2 > BmKn2-7. Based on this criterion alone, one might expect a corresponding order of membrane penetration ability. Similarly, the charge distribution was observed as BmKn1 < BmKn2 < BmKn2-7, which would suggest a similar ranking for their penetration ability. However, contrary to these expectations, the experimental results demonstrated that the external membrane penetration ability of the three peptides was BmKn2-7 > BmKn1 > BmKn2 (Figure 2). Therefore, when comparing the activity of peptides with varying hydrophobic and charge properties, their cumulative effects on activity should be evaluated in a systematic and comprehensive manner.

For the external membrane, the peptide's charge is crucial for its penetration capability because of the abundance of negatively charged components like lipopolysaccharide (LPS), which can be specifically recognized and bound by the peptide (26, 27). Peptides with higher positive charges are more likely to penetrate through electrostatic interactions, thereby enhancing their penetration efficiency. Specifically, BmKn2-7, which carries six positive charges, exhibits stronger electrostatic interactions compared to BmKn1 (two positive charges) and BmKn2 (three positive charges), making it more effective in penetrating the external membrane. However, when structural differences among peptides are minimal, their antibacterial activity tends to increase with greater hydrophobicity (21). Given that BmKn1 and BmKn2 share a highly similar structure (85%), and BmKn1 exhibits a higher degree of hydrophobicity than BmKn2, BmKn1 demonstrates superior membrane penetration capability. For the bacterial inner membrane, hydrophobicity is a critical determinant of peptide penetration. Among the three peptides, BmKn1 exhibits the highest hydrophobicity, consequently demonstrating superior membrane permeability. This observation provides substantial evidence to support the conclusion.

Depolarization is often correlated with an increase in cell membrane permeability and the efflux of intracellular components, serving as a critical mechanism for peptide antibacterial activity (28, 29). This study reveals that BmKn2-7, owing to its higher charge density, exhibits the most significant depolarizing effect. This indicates a greater propensity for BmKn2-7 to form ion channels or compromise the integrity of the cell membrane, thereby leading to a more potent depolarizing action. The levels of ROS in VP treated with BmKn1, BmKn2, and BmKn2-7 were significantly elevated. Notably, the order of ROS induction paralleled the order of inner membrane penetration efficacy: BmKn1 > BmKn2-7 > BmKn2. This suggests a strong correlation between ROS production and the peptides' ability to penetrate the bacterial inner membrane. Elevated ROS levels can induce oxidative

damage to bacterial DNA, proteins, and lipids (30, 31), leading to cell death. These findings further substantiate the antibacterial activity of these peptides.

Through a comparative analysis of three peptides, it was found that the charge of the peptide played a dominant role in external membrane permeability and cell membrane depolarization, whereas hydrophobicity had a more significant impact on inner membrane permeability and ROS generation. Among the results mentioned above, BmKn1 and BmKn2-7 demonstrated superior performance compared to BmKn2. Previous studies have shown that BmKn2 exhibits notable antibacterial activity (32, 33), indicating that BmKn1 and BmKn2-7 may serve as even more effective antibacterial agents.

AMPs not only exhibit broad-spectrum antibacterial activity and high efficacy against resistant strains but also modulate the host immune system, thereby attracting significant attention for their multifaceted roles (34). In addition to directly reducing bacterial loads through their antimicrobial properties, AMPs can indirectly combat microbial invasion and infection by regulating host cellular functions (35). Specifically, they activate immune cells, enhance the production of pro-inflammatory cytokines, mitigate inflammation caused by microbes, and promote the formation of neutrophil extracellular traps (36). Wang et al. demonstrated that co-injection of antimicrobial peptides with neurotropic virus (NNV) significantly increased the survival rate of medaka compared to injection of NNV alone (37). Additionally, previous studies have shown that an antimicrobial peptide from crabs can markedly enhance the survival rate of *L. vannamei* infected with acute hepatopancreatic necrosis disease virus (38). Similarly, research on *Oncorhynchus mykiss* has found that antimicrobial peptides can effectively reduce mortality rates (39). The findings of this study demonstrate that treatment with the peptides BmKn1, BmKn2, and BmKn2-7 significantly enhanced the cumulative survival rate of *L. vannamei*, indicating that these peptides play a critical role in strengthening its immune response.

The activity of immune-related enzymes in the hepatopancreas of *L. vannamei* was investigated to elucidate their roles in the immune response. The enzyme PO is vital for immune function, catalyzing the oxidation of phenols to quinones, which polymerize into melanin, facilitating pathogen encapsulation and wound healing (5). We observed that PO activity was significantly lower in the group exposed solely to VP compared to the group co-injected with peptides and the pathogen, which exhibited markedly elevated PO activity. These results suggest that the peptides may stimulate the immune response in the hepatopancreas of shrimp, leading to increased synthesis and secretion of PO. LZM, another critical immune component, exhibits bacteriolytic activity that disrupts bacterial cell walls, thus playing a significant role in innate defense against infections (14, 40). Our findings indicate that LZM activity was significantly higher in the control group than in the other treatment groups. Therefore, it is plausible that the peptides exert an inhibitory effect on LZM activity. Additionally, the complement components C3 and C4 are essential in enhancing phagocytosis, mediating inflammation, and facilitating pathogen lysis (6). The VP group displayed the lowest levels of C3, indicating potential consumption of this component during the immune response to bacterial infection. In contrast, this group showed the highest C4 levels. The peptide injection groups exhibited opposite trends in C3 and C4 concentrations. The decline in hepatopancreatic C3 after VP injection suggests activation and subsequent consumption of C3 as part of the immune response. Conversely, the increased C4 levels may represent a compensatory mechanism, whereby the immune system enhances C4 production to strengthen the complement cascade and improve defense against the bacterial threat.

The activities of the expression of immune-related genes in the hepatopancreas of *Litopenaeus vannamei* were investigated to elucidate their roles in the immune response. *TNF-α*, *IL-1β*, and *TGF-β* genes are essential for orchestrating a balanced immune response, contributing to both the defense against pathogens and the maintenance of immune homeostasis in *L.vannamei* (41–43). In this experiment, following infection with VP, a significant upregulation of the pro-inflammatory cytokine TNF-α and a concurrent downregulation of the anti-inflammatory cytokine TGF-β in the *L. vannamei* were observed. These alterations suggest that an inflammatory response has been activated in the hepatopancreas at this stage. The mRNA expression levels of *TNF-α* and *IL-1β* were significantly decreased following peptide supplementation, indicating that these peptides can effectively attenuate the inflammatory response elicited by *Vibrio parahaemolyticus* infection. Administration of antibacterial peptides to shrimp infected with VP rapidly inhibited bacterial proliferation and reproduction, effectively reducing pathogen load and thereby alleviating the burden on the immune system.

ALF, *Crus*, and *Pen-3* genes encode peptides that are critical components of the shrimp's immune system, forming a multi-layered defense mechanism against diverse pathogens. The upregulation of their expression in response to infection underscores their vital role in sustaining health and survival in the pathogen-rich environments typical of shrimp habitats (44, 45). In the research, the relative expression levels of the ALF and Crus genes were markedly increased in the VP group in comparison to the groups receiving peptide injections. This elevation is likely attributable to the activation of the innate immune response as a direct defense mechanism against bacterial infection. Conversely, the diminished expression of these genes in the co-injection group (peptides and VP) may be attributed to the antimicrobial properties of the peptides. The introduction of these antimicrobial peptides likely provides external support to the shrimp's immune system, thereby reducing the reliance on endogenous production of *ALF* and *Crus* as primary defense mechanisms. This supplementation may modulate the shrimp's immune response by partially alleviating the burden on the internal immune machinery for producing these peptides, leading to the observed reduction in their gene expression.

Environmental or physiological stressors trigger the cellular apoptosis pathway, which is a critical response mechanism that enables shrimp to mitigate cellular damage and preserve overall

health under adverse conditions (46). In *L. vannamei*, genes such as *Cyt-c*, *Bax*, *Bcl-2*, *Caspase-3*, *Caspase-8*, and *P53* play pivotal roles in regulating cellular apoptosis (47–49). Previous research has demonstrated that six hours post-infection with *Vibrio alginolyticus*, there is a significant upregulation of apoptosis-related genes in both the hemocytes and hepatopancreas of *L. vannamei* (50). In this study, we observed that the relative expression levels of apoptosis-related genes were significantly higher in the VP group compared to the peptide injection groups. This difference is likely attributable to the host's cellular response to bacterial infection. The pathogenic bacteria induce intracellular stress and damage, thereby activating apoptosis pathways as a defensive mechanism to contain and limit the spread of infection through the elimination of infected cells. In contrast, the downregulation of apoptosis-related genes observed in the group co-injected with peptides and VP indicates a protective role of the peptides. These peptides may alleviate cellular stress and damage caused by bacterial infection, potentially through direct inhibition of bacterial activity or by enhancing the shrimp's overall immune response.

Furthermore, this study investigated the effects of *Vibrio parahaemolyticus* and BmKn2-7 on *L. vannamei vannamei* through intestinal transcriptome analysis. The results showed that in the CG-vs-VP comparison group, 320 genes were upregulated and 804 genes were downregulated; in the CG-vs-BmKn2-7 comparison group, 239 genes were upregulated and 1,711 genes were downregulated; and in the VP-vs-BmKn2-7 comparison group, 310 genes were upregulated and 382 genes were downregulated. GO enrichment analysis revealed that numerous GO terms related to immunity were identified in the CG-vs-VP comparison group. In the CG-vs-VP comparison group, evasion or tolerance of host defense response was found to be the most significantly enriched. This may be related to the interference of *Vibrio parahaemolyticus* with the host's immune signaling pathways. *V. parahaemolyticus* can secrete certain toxic factors or signaling molecules that disrupt the immune signaling pathways of shrimp (51). For example, specific proteases produced by *V. parahaemolyticus* can degrade key proteins involved in the immune signal transduction process in shrimp, preventing proper transmission of immune signals (52). Consequently, immune cells fail to be effectively activated, resulting in the inability to initiate a robust immune response to eliminate the pathogen. The previous study revealed that *V. parahaemolyticus* disrupts the antioxidative system in *Penaeus monodon*, inducing oxidative stress and tissue damage through altered activities of antioxidant enzymes (53). This study also found that oxidoreductase activity was significantly enriched, indicating that *Vibrio parahaemolyticus* infection induces oxidative stress in host tissues, resulting in dysregulation of redox-related gene expression and further impairing the host's immune response. The immune system of *Litopenaeus vannamei* relies on innate immunity and lacks specific adaptive immune responses (54). Chitin-binding proteins play a critical role in the shrimp's immune defense. In the immune systems of crustaceans such as shrimp, as well as in insects, chitin-binding proteins function as opsonins by binding to pathogens, thereby promoting the phagocytosis of pathogens by phagocytic cells (55). Moreover, chitin-binding proteins can activate the complement system or other immune signaling pathways, triggering a series of immune responses that further enhance the organism's ability to eliminate pathogens (56). These findings underscore their important role in pathogen recognition and immune defense. In this study, the VP-vs-BmKn2-7 comparison group showed significant enrichment of chitin binding, which may be attributed to IsCT's ability to suppress overactivated immune responses, allowing immune cells and effector molecules to return to homeostasis. This, in turn, reduces the expression levels of genes associated with oxidative stress and pathogen recognition. The Peroxisome Proliferator-Activated Receptor (PPAR) signaling pathway is mediated by a family of nuclear receptor members (PPARs) and is widely present in animals, regulating various physiological processes such as metabolism, inflammation, immunity, and cell differentiation (57). The PPAR family mainly includes three subtypes: PPAR-α, PPAR-β/δ, and PPAR-γ. PPAR-α and PPAR-γ reduce the production of pro-inflammatory factors by downregulating inflammatory pathways such as NF-κB and AP-1 (58). Additionally, PPAR-γ promotes macrophage polarization from the pro-inflammatory M1 phenotype to the anti-inflammatory M2 phenotype, thereby mitigating inflammation (59). In this study, the VP-vs-BmKn2-7 comparison group showed significant enrichment of PPAR-related terms, which may be attributed to the effects of IsCT in modulating the PPAR signaling pathway to alleviate inflammation, mitigate oxidative stress, and restore metabolic homeostasis.

Liu et al. demonstrated that transcriptome analysis of the hepatopancreas in *Neocaridina denticulata* after *Vibrio parahaemolyticus* infection revealed that numerous DEGs were enriched in immune-related pathways (60). A similar study has also been reported in Sparus macrocephalus (61). The results of this study also revealed significant enrichment of immune-related pathways following *Vibrio parahaemolyticus* infection, but the largest number of DEGs were annotated to metabolic pathways. The PCK2 gene plays a crucial role in regulating gluconeogenesis and energy metabolism, contributing to environmental adaptation, immune defense, oxidative stress alleviation, and reproductive development in the organism (62). PCK2 may help maintain the balance of the host immune system during inflammation and infection by modulating energy metabolism, thereby preventing excessive immune responses from causing damage to the host (63). By enhancing energy supply, PCK2 supports cells in combating oxidative stress, maintaining mitochondrial function, and preserving cellular homeostasis (64). In this study, the VP-vs-BmKn2-7 comparison group revealed that the *PCK2* gene was annotated in numerous significantly enriched pathways, indicating that *PCK2* plays a critical role in immune regulation. The FoxO signaling pathway is involved in the differentiation and functional regulation of immune cells, such as T cells, and mitigates chronic inflammation by suppressing the NF-κB signaling pathway (65). However, under certain conditions, it may also promote the release of inflammatory cytokines. Additionally, FoxO can enhance cellular resistance to oxidative stress by inducing the expression of

antioxidant enzymes, such as superoxide dismutase and catalase (66). AMPK activation can inhibit the transcriptional activity of NF-κB, reduce the production of pro-inflammatory cytokines such as TNF-α and IL-6, and downregulate inflammation mediated by Toll-like receptors (67). In macrophages, AMPK modulates the activity of the NLRP3 inflammasome, thereby suppressing caspase-1-dependent pyroptosis and the release of IL-1β (68). Leukocyte transendothelial migration is a central process in immune responses, regulating the migration of leukocytes from the vascular lumen to inflamed or infected tissues, thereby coordinating innate and adaptive immunity. Its functions span multiple aspects, including immune defense, inflammation regulation, and tissue repair (69). The three immune-related signaling pathways were significantly enriched in the VP-vs-BmKn2-7 comparison group in this study. This enrichment may result from the combined effects of antimicrobial peptides in enhancing immune regulation, alleviating inflammation and oxidative stress, optimizing metabolism, and supporting immune cell migration.

In summary, the *in vitro* mechanisms of membrane permeabilization and ROS elevation induced by the three peptides likely underpin their *in vivo* antibacterial efficacy and immunomodulatory effects. Enhanced membrane permeability directly compromises bacterial membrane integrity, thereby reducing pathogen load and infection severity. Concurrently, elevated ROS levels not only mediate oxidative damage to pathogens but also modulate innate immune responses through the activation of pro-inflammatory signaling pathways and by influencing mitochondrial function, which may promote antigen presentation and immune cell activation.

5 Conclusions

In conclusion, the functional characterization of BmKn1 has been successfully elucidated. The properties and test results of BmKn1, BmKn2, and BmKn2-7, derived from scorpion venom, demonstrate significant potential as antimicrobial agents against *Vibrio parahaemolyticus* (VP) and as immune enhancers for *Litopenaeus vannamei*. The application of these peptides is expected to promote the development and advancement of the *L. vannamei* aquaculture industry.

Data availability statement

The datasets presented in this study can be found in online repositories. The names of the repository/repositories and accession number(s) can be found in the article/Supplementary Material.

Ethics statement

Ethical approval was not required for the study involving animals in accordance with the local legislation and institutional requirements because The manuscript presents research on animals that do not require ethical approval for their study.

Author contributions

LZ: Conceptualization, Funding acquisition, Investigation, Methodology, Software, Supervision, Writing – original draft, Writing – review & editing. YS: Resources, Validation, Writing – review & editing. HZ: Conceptualization, Writing – review & editing. XY: Investigation, Writing – review & editing. RD: Writing – review & editing, Resources. ZC: Supervision, Writing – review & editing. QW: Writing – review & editing, Conceptualization, Investigation, Methodology, Software, Supervision.

Funding

The author(s) declare that financial support was received for the research and/or publication of this article. The research was supported by the Foundation of Guangxi Key Laboratory of Marine Drugs (LMD2024-3), Key Research Projects of Ordinary Universities in Guangdong Province (2024ZDZX2085), Natural Science Foundation of Shenzhen (JCYJ20240813111700002), and the Research on breeding technology of candidate species for Guangdong modern marine ranching (2024-MRB-00-001).

Conflict of interest

The authors declare that the research was conducted in the absence of any commercial or financial relationships that could be construed as a potential conflict of interest.

Generative AI statement

The author(s) declare that no Generative AI was used in the creation of this manuscript.

Publisher's note

Supplementary material

The Supplementary Material for this article can be found online at: https://www.frontiersin.org/articles/10.3389/fimmu.2025.1551816/full#supplementary-material

References

1. Li XY, Pang LR, Chen YG, Weng SP, Yue HT, Zhang ZZ, et al. Activating transcription factor 4 and X box binding protein 1 of Litopenaeus vannamei transcriptional regulated white spot syndrome virus genes Wsv023 and Wsv083. *PloS One*. (2013) 8:e62603. doi: 10.1371/journal.pone.0062603

2. Li F, Huang J, Wang M, Chen MZ, Xiao YH. Sources, distribution and dynamics of antibiotics in Litopenaeus vannamei farming environment. *Aquaculture*. (2021) 545:737200. doi: 10.1016/j.aquaculture.2021.737200

3. Rungrassamee W, Klanchui A, Maibunkaew S, Karoonuthaisiri N. Bacterial dynamics in intestines of the black tiger shrimp and the Pacific white shrimp during Vibrio harveyi exposure. *J invertebrate pathol*. (2016) 133:12–9. doi: 10.1016/j.jip.2015.11.004

4. Fan J, Chen L, Mai G, Zhang H, Yang J, Deng D. Dynamics of the gut microbiota in developmental stages of Litopenaeus vannamei reveal its association with body weight. *Sci Rep*. (2019) 9:734. doi: 10.1038/s41598-018-37042-3

5. Wang Q, Fan DP, Hu YD, Liu HY, Tan BP, Xie SW. Supplementation of clostridium butyricum lv1 lyophilised powder to cottonseed protein concentrate basal diets improves growth, intestinal microbiota, and immunity of litopenaeus vannamei. *Aquaculture*. (2024), 593. doi: 10.1016/j.aquaculture.2024.741334

6. Wang Q, Fan DP, Hu YD, Liu HY, Tan BP, Xie SW. Effects of supplementation with freeze-dried clostridium butyricum powder after replacement of fishmeal with cottonseed protein concentrate on growth performance, immune response, and intestinal microbiota of litopenaeus vannamei. *BMC Veterinary Res*. (2024) 20 (1):519. doi: 10.1186/s12917-024-04372-6

7. Giri SS, Sen SS, Chi C, Kim HJ, Yun S, Park SC, et al. Effect of guava leaves on the growth performance and cytokine gene expression of Labeo rohita and its susceptibility to Aeromonas hydrophila infection. *Fish shellfish Immunol*. (2015) 46:217–24. doi: 10.1016/j.fsi.2015.05.051

8. Brown KL, Hancock REW. Cationic host defense (antimicrobial) peptides. *Curr Opin Immunol*. (2006) 18:24–30. doi: 10.1016/j.coi.2005.11.004

9. Zasloff M. Antimicrobial peptides of multicellular organisms: my perspective. *Adv Exp Med Biol*. (2019) 1117:3–6. doi: 10.1007/978-981-13-3588-4_1

10. Zhu X, Dong N, Wang Z, Ma Z, Zhang L, Ma Q, et al. Design of imperfectly amphipathic alpha-helical antimicrobial peptides with enhanced cell selectivity. *Acta Biomater*. (2014) 10:244–57. doi: 10.1016/j.actbio.2013.08.043

11. Dai Z, Shang L, Wang F, Zeng X, Yu H, Liu L, et al. Effects of antimicrobial peptide microcin C7 on growth performance, immune and intestinal barrier functions, and cecal microbiota of broilers. *Front veterinary sci*. (2022) 8:813629. doi: 10.3389/fvets.2021.813629

12. Zhang X, Zhao Q, Wen L, Wu C, Yao Z, Yan Z, et al. The effect of the antimicrobial peptide plectasin on the growth performance, intestinal health, and immune function of yellow-feathered chickens. *Front Veterinary Sci*. (2021) 8:688611. doi: 10.3389/fvets.2021.688611

13. Dong XQ, Zhang DM, Chen YK, Wang QJ, Yang YY. Effects of antimicrobial peptides (AMPs) on blood biochemical parameters, antioxidase activity, and immune function in the common carp (Cyprinus carpio). *Fish shellfish Immunol*. (2015) 47:429–34. doi: 10.1016/j.fsi.2015.09.030

14. Wang J, Wilson AE, Su B, Dunham RA. Functionality of dietary antimicrobial peptides in aquatic animal health: Multiple meta-analyses. *Anim Nutr*. (2023) 12:200–14. doi: 10.1016/j.aninu.2022.10.001

15. Cervera L, Chaves-Pozo E, Cuesta A. Synthetic Antimicrobial Peptides Fail to Induce Leucocyte Innate Immune Functions but Elicit Opposing Transcriptomic Profiles in European Sea Bass and Gilthead Sea bream. *Mar Drugs*. (2024) 22:86. doi: 10.3390/md22020086

16. Zeng L, Zhang C, Yang M, Sun JF, Lu JG, Zhang HX, et al. Unveiling the Diversity and Modifications of Short Peptides in Buthus martensii Scorpion Venom through Liquid Chromatography-High Resolution Mass Spectrometry. *Toxins*. (2024) 16:155. doi: 10.3390/toxins16030155

17. Cao L, Dai C, Li Z, Fan Z, Song Y, Wu Y, et al. Antibacterial activity and mechanism of a scorpion venom peptide derivative *in vitro* and *in vivo*. *PloS One*. (2012) 7:e40135. doi: 10.1371/journal.pone.0040135

18. GianFranceschi GL, GianFranceschi G, Quassinti L, Bramucci M. Biochemical requirements of bioactive peptides for nutraceutical efficacy. *J Funct Foods*. (2018) 47:252–63. doi: 10.1016/j.jff.2018.05.034

19. Chekmenev EY, Vollmar BS, Forseth KT, Manion MKN, Jones SM, Wagner TJ. Investigating molecular recognition and biological function at interfaces using piscidins, antimicrobial peptides from fish. *Biochim Biophys Acta (BBA)-Biomembranes*. (2006) 1758:1359–72. doi: 10.1016/j.bbamem.2006.03.034

20. Arpornsuwan T, Buasakul B, Jaresitthikunchai J, Roytrakul S. Potent and rapid antigonococcal activity of the venom peptide BmKn2 and its derivatives against different Maldi biotype of multidrug-resistant Neisseria gonorrhoeae. *Peptides*. (2014) 53:315–20. doi: 10.1016/j.peptides.2013.10.020

21. Rosenfeld Y, Lev N, Shai Y. Effect of the hydrophobicity to net positive charge ratio on antibacterial and anti-endotoxin activities of structurally similar antimicrobial peptides. *Biochemistry*. (2010) 49:853–61. doi: 10.1021/bi900724x

22. Yin LM, Edwards MA, Li J, Yip CM, Deber CM. Roles of hydrophobicity and charge distribution of cationic antimicrobial peptides in peptide-membrane interactions. *J Biol Chem*. (2012) 287:7738–45. https://www.jbc.org/article/S0021-9258(20)61086-9/fulltext (Accessed December, 2024).

23. Ong ZY, Cheng J, Huang Y, Xu K, Ji Z, Fan W, et al. Effect of stereochemistry, chain length and sequence pattern on antimicrobial properties of short synthetic β-sheet forming peptide amphiphiles. *Biomaterials*. (2014) 35:1315–25. doi: 10.1016/j.biomaterials.2013.10.053

24. Gagat P, Ostrówka M, Duda-Madej A, Mackiewicz P. Enhancing antimicrobial peptide activity through modifications of charge, hydrophobicity, and structure. *Int J Mol Sci*. (2024) 25:10821. doi: 10.3390/ijms251910821

25. Ringstad L, Andersson Nordahl E, Schmidtchen A, Malmsten M. Composition effect on peptide interaction with lipids and bacteria: variants of C3a peptide CNY21. *Bophys J*. (2007) 92:87–98. https://www.cell.com/fulltext/S0006-3495(07)70807-X (Accessed December, 2024).

26. Sharma P, Ayappa KG. A molecular dynamics study of antimicrobial peptide interactions with the lipopolysaccharides of the outer bacterial membrane. *J Membrane Biol*. (2022) 255:665–75. doi: 10.1007/s00232-022-00258-6

27. Yang H, Wang L, Yuan L, Du H, Pan B, Lu K. Antimicrobial peptides with rigid linkers against gram-negative bacteria by targeting lipopolysaccharide. *J Agric Food Chem*. (2022) 70:15903–16. doi: 10.1021/acs.jafc.2c05921

28. Nayab S, Aslam MA, Rahman S, Sindhu ZD, Sajid S, Zafar N, et al. A review of antimicrobial peptides: its function, mode of action and therapeutic potential. *Int J Pept Res Ther*. (2022) 28:46. doi: 10.1007/s10989-021-10325-6

29. Gostaviceanu A, Gavrilaş S, Copolovici L, Copolovici MD. Membrane-active peptides and their potential biomedical application. *Pharmaceutics*. (2023) 15:2091. doi: 10.3390/pharmaceutics15082091

30. Dharmaraja AT. Role of reactive oxygen species (ROS) in therapeutics and drug resistance in cancer and bacteria. *J Medicinal Chem*. (2017) 60:3221–40. doi: 10.1021/acs.jmedchem.6b01243

31. Juan CA, Pérez de la Lastra JM, Plou FJ, Pérez-Lebeña E. The chemistry of reactive oxygen species (ROS) revisited: outlining their role in biological macromolecules (DNA, lipids and proteins) and induced pathologies. *Int J Mol Sci*. (2021) 22:4642. doi: 10.3390/ijms22094642

32. Zeng XC, Wang SX, Zhu Y, Zhu SY, Li WX. Identification and functional characterization of novel scorpion venom peptides with no disulfide bridge from *Buthus martensii* Karsch. *Peptides*. (2004) 25:143–50. doi: 10.1016/j.peptides.2003.12.003

33. De la Salud Bea R, Petraglia AF, Ascuitto MR, Buck QM. Antibacterial activity and toxicity of analogs of scorpion venom IsCT peptides. *Antibiotics*. (2017) 6:13. doi: 10.3390/antibiotics6030013

34. Bechinger B, Gorr SU. Antimicrobial peptides: Mechanisms of action and resistance. *J Dental Res*. (2017) 96:254–60. doi: 10.1177/0022034516679973

35. Datta S, Roy A. Antimicrobial peptides as potential therapeutic agents: A review. *Int J Pept Res Ther*. (2021) 27:555–77. doi: 10.1007/s10989-020-10110-x

36. Seyfi R, Kahaki FA, Ebrahimi T, Montazersaheb S, Eyvazi S, Babaeipour V, et al. Antimicrobial peptides (amps): Roles, functions and mechanism of action. *Int J Pept Res Ther*. (2020) 26:1451–63. doi: 10.1007/s10989-019-09946-9

37. Wang YD, Kung CW, Chen JY. Antiviral activity by fish antimicrobial peptides of epinecidin-1 and hepcidin 1-5 against nervous necrosis virus in medaka. *Peptides*. (2010) 31:1026–33. doi: 10.1016/j.peptides.2010.02.025

38. Phuket TRN, Charoensapsri W, Amparyup P, Imjongjirak C. Antibacterial activity and immunomodulatory role of a proline-rich antimicrobial peptide sppr-amp1 against vibrio campbellii infection in shrimp litopenaeus vannamei. *Fish Shellfish Immunol*. (2023) 132:108479. doi: 10.1016/j.fsi.2022.108479

39. Chettri JK, Mehrdana F, Hansen EB, Ebbensgaard A, Overgaard MT, Lauritsen AH, et al. Antimicrobial peptide cap18 and its effect on yersinia ruckeri infections in rainbow trout oncorhynchus mykiss (walbaum): Comparing administration by injection and oral routes. *J Fish Diseases*. (2017) 40:97–104. doi: 10.1111/jfd.12497

40. Wang Q, Li W, Liu H, Tan B, Dong X, Chi S, et al. The isolation, identification, whole-genome sequencing of clostridium butyricum lv1 and its effects on growth performance, immune response, and disease-resistance of litopenaeus vannamei. *Microbiological Res*. (2023) 272:127384. doi: 10.1016/j.micres.2023.127384

41. Duan YF, Zhong GW, Nan YX, Yang YK, Xiao M, Li H. Effects of nitrite stress on the antioxidant, immunity, energy metabolism, and microbial community status in the intestine of litopenaeus vannamei. *Antioxidants*. (2024) 13(11):1318. doi: 10.3390/antiox13111318

42. Hu F, Chen G, Hu JJ, Bao ZM, Wang MQ. Transcriptome and micrornaome elucidate the mechanism underlying the immunomodulatory effects of dietary cpg oligodeoxynucleotides (cpg odns) in litopenaeus vannamei. *Aquaculture*. (2024) 593:741275. doi: 10.1016/j.aquaculture.2024.741275

43. Hu F, Wang S, Hu JJ, Bao ZM, Wang MQ. Comprehensive evaluation of dietary tandem cpg oligodeoxynucleotides on enhancement of antioxidant capacity, immunological parameters, and intestinal microbiota in white shrimp

(litopenaeus vannamei). *Aquaculture*. (2024) 579:740250. doi: 10.1016/j.aquaculture.2023.740250

44. Nguyen HT, Huang HT, Lin YR, Chen YY, Nan FH, Hu YF. Dietary galla chinensis on white shrimp penaeus vannamei: Promotes growth, nonspecific immunity, and disease resistance against vibrio parahaemolyticus. *Aquacult Rep*. (2024) 35:102012. doi: 10.1016/j.aqrep.2024.102012

45. Xiao M, Nan YX, Yang YK, Li H, Duan YF. Changes in physiological homeostasis in the gills of litopenaeus vannamei under carbonate alkalinity stress and recovery conditions. *Fishes*. (2024) 9(11):463. doi: 10.3390/fishes9110463

46. Yin XL, Zhuang XQ, Liao MQ, Cui QQ, Yan CX, Huang JY, et al. Andrographis paniculata improves growth and non-specific immunity of shrimp litopenaeus vannamei, and protects it from vibrio alginolyticus by reducing oxidative stress and apoptosis. *Dev Comp Immunol*. (2023) 139:104542. doi: 10.1016/j.dci.2022.104542

47. Li YF, Tong RX, Li ZY, Zhang X, Pan LQ, Li YB, et al. Toxicological mechanism of ammonia-n on haematopoiesis and apoptosis of haemocytes in litopenaeus vannamei. *Sci Total Environment*. (2023) 879:163039. doi: 10.1016/j.scitotenv.2023.163039

48. Tong RX, Li YB, Yu X, Zhang N, Liao QL, Pan LQ. The mechanism of reactive oxygen species generation, DNA damage and apoptosis in hemocytes of litopenaeus vannamei under ammonia nitrogen exposure. *Aquat Toxicol*. (2024) 272:106958. doi: 10.1016/j.aquatox.2024.106958

49. Yu XW, Liu WB, Chen KK, Liu Y, Deng Y, Chi C. Feeding lycium barbarum polysaccharides (lbp) alleviates apoptotic, inflammatory hepatopancreas atrophy and injury in chinese mitten crab (eriocheir sinensis) poisoned by t-2 toxin. *Aquacult Rep*. (2023) 33:101819. doi: 10.1016/j.aqrep.2023.101819

50. Yin XL, Zhuang XQ, Luo WT, Liao MQ, Huang L, Cui QQ, et al. Andrographolide promote the growth and immunity of litopenaeus vannamei, and protects shrimps against vibrio alginolyticus by regulating inflammation and apoptosis via a ros-jnk dependent pathway. *Front Immunol*. (2022) 13:990297. doi: 10.3389/fimmu.2022.990297

51. Paria P, Chakraborty HJ, Pakhira A, Devi MS, Mohapatra PKD, Behera BK. Identification of virulence-associated factors in *Vibrio parahaemolyticus* with special reference to moonlighting protein: a secretomics study. *Int Microbiol*. (2024) 27:765–79. doi: 10.1007/s10123-023-00429-y

52. Wang LH, Zeng QF, Hu JJ, Bao ZM, Wang MQ. Proteome analysis of outer membrane vesicles from *Vibrio parahaemolyticus* causing acute hepatopancreatic necrosis disease. *J Invertebrate Pathol*. (2024) 204:108082. doi: 10.1016/j.jip.2024.108082

53. Duan YF, Zhang JS, Dong HB, Wang Y, Liu QS, Li H. Oxidative stress response of the black tiger shrimp Penaeus monodon to *Vibrio parahaemolyticus* challenge. *Fish Shellfish Immunol*. (2015) 46:354–65. doi: 10.1016/j.fsi.2015.06.032

54. Wang Q, Fan DP, Hu YD, Liu HY, Tan BP, Xie SW. Supplementation of sodium alginate-coated *Clostridium butyricum* after cottonseed protein concentrate replacement of fishmeal can improve growth, immunity, and intestinal health in Litopenaeus vannamei. *Aquacult Rep*. (2024) 39:102533. doi: 10.1016/j.aqrep.2024.102533

55. Jones M, Kujundzic M, John S, Bismarck A. Crab vs. Mushroom: A review of crustacean and fungal chitin in wound treatment. *Mar Drugs*. (2020) 18(1):64. doi: 10.3390/md18010064

56. Luo SS, Chen XL, Wang AJ, Liu QY, Peng M, Yang CL. Identification, functional analysis of chitin-binding proteins and the association of its single nucleotide polymorphisms with Vibrio parahaemolyticus resistance in Penaeus vannamei. *Fish Shellfish Immunol*. (2024) 154:109966. doi: 10.1016/j.fsi.2024.109966

57. Yang XY, Liu M, Liang QL, Jiang KY, Wang BJ, Wang L. The potential mechanisms for isoliquiritigenin on the growth and immune regulation of Penaeus vannamei revealed by transcriptomic and metabolomic. *Aquaculture*. (2024) 589:740945. doi: 10.1016/j.aquaculture.2024.740945

58. Kuenzli S, Saurat JH. Peroxisome proliferator-activated receptors in cutaneous biology. *Br J Dermatol*. (2003) 149:229–36. doi: 10.1046/j.1365-2133.2003.05532.x

59. Luo WJ, Xu QY, Wang Q, Wu HM, Hua J. Effect of modulation of PPAR-γ activity on Kupffer cells M1/M2 polarization in the development of non-alcoholic fatty liver disease. *Sci Rep*. (2017) 7(1):44612. doi: 10.1038/srep44612

60. Liu YJ, Xing KF, Yan CC, Zhou YZ, Xu XM, Sun YY, et al. Zhang: Transcriptome analysis of Neocaridina denticulate sinensis challenged by Vibrio parahemolyticus. *Fish Shellfish Immunol*. (2022) 121:31–8. doi: 10.1016/j.fsi.2021.10.004

61. Xiang XW, Xiao JX, Zhou YF, Zheng B, Wen ZS. Liver transcriptome analysis of the *Sparus macrocephlus* in response to *Vibrio parahaemolyticus* infection. *Fish Shellfish Immunol*. (2019) 84:825–33. doi: 10.1016/j.fsi.2018.09.057

62. Tang MM, Sun JJ, Cai ZG. *PCK2* inhibits lung adenocarcinoma tumor cell immune escape through oxidative stress-induced senescence as a potential therapeutic target. *J Thorac Disease*. (2023) 15:2601–15. doi: 10.21037/jtd-23-542

63. Vincent EE, Sergushichev A, Griss T, M. Gingras C, Samborska B, Ntimbane T, et al. Mitochondrial phosphoenolpyruvate carboxykinase regulates metabolic adaptation and enables glucose-independent tumor growth. *Mol Cell*. (2015) 60:195–207. doi: 10.1016/j.molcel.2015.08.013

64. Bluemel G, Planque M, Madreiter-Sokolowski CT, Haitzmann T, Hrzenjak A, Graier WF, et al. *PCK2* opposes mitochondrial respiration and maintains the redox balance in starved lung cancer cells. *Free Radical Biol Med*. (2021) 176:34–45. doi: 10.1016/j.freeradbiomed.2021.09.007

65. Eijkelenboom A, Burgering BMT. FOXOs: signalling integrators for homeostasis maintenance. *Nat Rev Mol Cell Biol*. (2013) 14:83–97. doi: 10.1038/nrm3507

66. Zhang XB, Tang NM, Hadden TJ, Rishi AK. Akt, FoxO and regulation of apoptosis. *Biochim Et Biophys Acta-Molecular Cell Res*. (2011) 1813:1978–86. doi: 10.1016/j.bbamcr.2011.03.010

67. Wang J, Li ZY, Gao L, Qi YS, Zhu HB, Qin XM. The regulation effect of AMPK in immune related diseases. *Sci China-Life Sci*. (2018) 61:523–33. doi: 10.1007/s11427-017-9169-6

68. Hardie DG. AMPK-sensing energy while talking to other signaling pathways. *Cell Metab*. (2014) 20:939–52. doi: 10.1016/j.cmet.2014.09.013

69. Muller WA. Mechanisms of Leukocyte Transendothelial Migration. *Annual Review of Pathology: Mechanisms of Disease*. (2011) 6(1):323–44. doi: 10.1146/annurev-pathol-011110-130224

Frontiers in Immunology

Explores novel approaches and diagnoses to treat immune disorders.

The official journal of the International Union of Immunological Societies (IUIS) and the most cited in its field, leading the way for research across basic, translational and clinical immunology.

Discover the latest Research Topics

See more →

Frontiers

Avenue du Tribunal-Fédéral 34
1005 Lausanne, Switzerland
frontiersin.org

Contact us

+41 (0)21 510 17 00
frontiersin.org/about/contact